

THE NATURE AND TIMING OF GRANITOID PLUTONISM
IN THE WABIGOON VOLCANIC-PLUTONIC BELT,
NORTHWESTERN ONTARIO

THE NATURE AND TIMING OF GRANITOID PLUTONISM
IN THE WABIGOON VOLCANIC-PLUTONIC BELT,
NORTHWESTERN ONTARIO

Geochemistry, Rb/Sr Geochronology, Petrography
and Field Investigation

By

W. DIETER BIRK

B.Sc. (Toronto), Hon. B.Sc. (Queen's)

A Thesis

Submitted to the School of Graduate Studies

in Partial Fulfilment of the Requirements

for the Degree

Doctor of Philosophy

McMaster University

Copyright © Dieter Birk (1978)

DOCTOR OF PHILOSOPHY (1978)
(Geology)

McMASTER UNIVERSITY
Hamilton, Ontario

TITLE:

The nature and timing of granitoid
plutonism in the Wabigoon volcanic-
plutonic belt, Northwestern Ontario:
Geochemistry, Rb/Sr geochronology,
Petrography and Field investigation

AUTHOR:

Wolf Dieter Birk
B.Sc. (Toronto), Hon. B.Sc. (Queen's)

SUPERVISOR:

Dr. R. H. McNutt

NUMBER OF PAGES:

xxv; 496

ABSTRACT

Twelve Archean granitoid plutons, intrusive into greenstones of the Wabigoon volcanic-plutonic belt in the Superior Province were investigated as to their nature and time of emplacement evidenced from field mapping, petrography, X-ray fluorescence for major and trace elements, in situ gamma ray spectrometry for radioelements and mass spectrometry for Sr isotopes.

Despite common tectonic setting, these plutons range from "homogeneous" granodiorites and porphyries to concentrically zoned or complex plutons of granite-monzonite-monzodiorite. Homogeneity has been tested in one lithologically monotonous pluton by extensive sampling and trend surface analysis. Tenuous textural and petrochemical phases are defined and attributed to subtle magmatic differentiation overprinted by deuteriic autometasomatism. The genetic model proposed is one of pulsating diapirism followed by fluid infiltration, diffusion and cation exchange.

Lithologically zoned plutons are multiple intrusives with younger, more felsic cores and discontinuous petrochemical trends. Cores exhibit homogeneity, deuteriic metasomatism and felsic dyking similar to the monolithologic plutons. The genetic model proposed is multiple diapiric intrusion from multiple sources through a common conduit.

Quartz-feldspar porphyries show petrographic and geochemical evidence of extensive alteration, cataclasis and metasomatism more indicative of a synvolcanic hypabyssal origin than affinity with phaneritic granitoids.

Binary plots of concentration versus a chemical index compiled for 247 granitoid samples provide rough estimates of element clarkes. Some plutons are anomalous but as a group these granitoids have high Sr, Ba, K/Rb and low Rb/Sr, Th and U. There is no evidence for large scale magma contamination but ubiquitous lensoid mafic enclaves derived from adjacent supercrustals, experienced basification and alkali metasomatism with enrichment in Rb, Nb, Ce and Y and growth of megacrysts.

There is also no chemical evidence in this study to support either a model of secular evolution of Archean granitoids or to demonstrate a chemical distinction between high level and low level plutons.

Seven stocks and a portion of a batholithic complex have been dated by Rb/Sr whole-rock isochrons sensu stricto (York 1, $\lambda_{\beta} = 1.39 \times 10^{-11} \text{y}^{-1}$ 2 σ errors):

Pluton	No.		Lithology	Age (m.y.)	Initial
	Samples				Ratio
Burditt Lake	(9)		Granodiorite	2598 \pm 45	.7009 \pm 6
Bears Passage	(6)		Granodiorite	2702 \pm 158	.7002 \pm 17
Esox Lake	(4)		Porphyry	2572 \pm 42	.7003 \pm 5

Flora Lake	(5)	Granite-Monzodiorite	2636 ± 63	.7017 ± 6
Ottertajl Lake	(10)	Granite-Monzodiorite	2514 ± 78	.7016 ± 5
Taylor Lake	(5)	Granodiorite-Monzonite	2640 ± 31	.7005 ± 3
Ryckman Lake	(7)	Granodiorite-Monzodiorite	2609 ± 63	.7001 ± 5
Rainy Lake Batholith	(10)	Monzogranite-Tonalite	2616 ± 66	.7012 ± 5

Student's-T tests show only Ottertail is distinct. Weighted pooling of isochrons gives: 2616 ± 43 m.y. for seven stocks while a composite 39 point regression yields 2623 ± 35 m.y. These estimates lie median to the Algoman Orogeny (2400 - 2750 m.y.) and are younger than the proposed Kenoran Orogeny (mean age: 2690 m.y.) and suggest coeval vulcanism, batholithic and intra-belt granitic magmatism spanning less than 35 m.y. (68% confidence). A possible southward juvenescence is beyond Rb/Sr resolution. Initial Sr ratios straddle the single-stage, linear mantle growth and suggest a low ($^{87}\text{Sr}/^{86}\text{Sr}$)_i provenance.

Aeromagnetic maps suggest that these stocks are upper crust features with dimensions approximated by their surficial exposures.

Regional distribution and emplacement was controlled by diapirism or polydiapirism from a lower crust or upper mantle source layer. Upwelling was initiated by deep extensions of faults and superbelt interfaces or by downwarping and crustal thinning at paleobasin centers.

"... Think of it? I think it is nothing but a lot of granite rubbish and nasty glittering mica that isn't worth 10¢ an acre! ..."

Mark Twain (1872) Roughing It,
1st Edition, Hartford, p. 204.

ACKNOWLEDGEMENTS

The author acknowledges his indebtedness to Dr. R. H. McNutt for thesis supervision, review and moral support. Research grants to Dr. R. H. McNutt, from the National Research Council and the Department of Energy, Mines and Resources financed the bulk of the work. Other members of the McMaster University faculty, including: Dr. W. B. Clarke, Dr. P. M. Clifford, Dr. J. H. Crocket and Dr. D. M. Shaw participated in committee supervision and individually made numerous contributions of ideas or technical resources.

A generation of comrades-in-arms including graduate students P. Fung, F. Longstaffe, C. Westerman, M. Wolff, etc. and undergraduates K. Garner and R. Pichette shared the frolic of the field, the labyrinth of the lab and the complications of the computer. An army of technical support was enlisted, including outstanding contributions by W. Dolan (typing) H. Elliott (typing), F. Graef (electronics), J. Muysson (chemistry), J. Whorwood (photography), etc.

The scientific community at large donated considerable talent and technology. Appreciation is extended to Mr. C. E. Blackburn (O.D.M., Toronto), Dr. B. W. Charbonneau (G.S.C., Ottawa), Dr. C. S. Hutchison (Malaysia), Dr. A. Turek (Windsor, Ontario) as well as Geometrics Services Ltd. (Downsview, Ontario) and Philips Electronics Ltd. (Don Mills, Ontario).

I owe most to my wife Margret and my daughter Cassie for tolerating my obsession and oppression when economic realities had long ago dictated the prudence of a different path.

TABLE OF CONTENTS

	<u>Page</u>
<u>CHAPTER 1: INTRODUCTION</u>	
1.1 WABIGOON VOLCANIC-PLUTONIC BELT	1
1.2 THESIS SCOPE	3
1.3 HISTORICAL REVIEW	7
 <u>CHAPTER 2: THE NATURE OF GRANITOID PLUTONISM</u>	
2.1 HOMOGENEOUS PLUTONS	
2.1.1 Introduction	13
2.1.2 Burditt Lake Stock	15
Previous Work	15
Field Observations	18
Structural Features	23
Petrography	26
Geochemistry: Major Elements	48
Geochemistry: Trace Elements	57
Geochemistry: Radioelements	73
Trend Surface Analysis	83
Autometasomatism	107
2.1.3 Scattergood Lake Stock	116
Field Observations	116
Petrography	119
Geochemistry	120
2.2 HETEROGENEOUS PLUTONS	
2.2.1 Introduction	126
2.2.2 Ryckman Lake Stock	128
Field Observations	128
Petrography	134
Geochemistry: Major Elements	140
Geochemistry: Trace Elements	143
Geochemistry: Radioelements	154
2.2.3 Flora Lake Stock	158
Field Observations	158
Petrography	161
Geochemistry: Major Elements	164
Geochemistry: Trace Elements	168
2.2.4 Concentrically Zoned Plutons	
Previous Models	177
2.2.5 General Models	178

	<u>Page</u>
2.3 QUARTZ-FELDSPAR PORPHYRIES	
2.3.1 Introduction	182
2.3.2 Esos Lake: Field Observations	185
2.3.3 Petrography	189
2.3.4 Chemistry	192
2.3.5 Petrogenesis of Porphyries	194
2.4 RECONNAISSANCE INVESTIGATIONS	
2.4.1 Introduction	198
2.4.2 Rainy Lake "Algoman" Plutons	198
Rest Island Stock	199
Bears Passage Stock	202
Ottertail Lake Pluton	205
Aeromagnetic Flux	206
2.4.3 Wabigoon Plutons	209
Froghead Bay Stock	209
Regina Bay Stock	210
Stormy Lake Stock	212
Taylor Lake Pluton	214
2.4.4 Chemistry	217
 <u>CHAPTER 3: REGIONAL SYNTHESSES</u>	
3.1 VARIATION TRENDS AND AVERAGE COMPOSITIONS	
3.1.1 Introduction	221
3.1.2 Major Elements: Trace Elements; Element Ratios	223 223
3.2 Na-K-Ca TERNARY RELATIONSHIPS	239
3.3 MAFIC ENCLAVES	
3.3.1 Introduction	244
3.3.2 Mafic Lensoid Enclaves	246
3.4 AEROMAGNETIC FLUX	
3.4.1 Introduction	250
3.4.2 Discussion	252
 <u>CHAPTER 4: CHRONOLOGY OF GRANITOID PLUTONISM</u>	
4.1 NON-RADIOMETRIC CHRONOMETRY	
4.1.1 Stratigraphy	255
4.1.2 Petrography	258
4.2 ISOTOPIC GEOCHRONOLOGY: PREVIOUS WORK	
4.2.1 Introduction	260
4.2.2 Wabigoon Belt Chronology	262

	<u>Page</u>
4.3 Rb/Sr ISOCHRONS'	
4.3.1 Introduction	272
4.3.2 Wabigoon Late-To-Post Tectonic Stocks	
A. Wabigoon Internal Plutons	276
B. Wabigoon-Quetico Interface	285
C. Composite Isochrons	293
4.3.3 Syntectonic Batholithic Complexes	
Introduction	303
Lake Despair Area	305
Ancient Granitoids	312
4.4 STATISTICAL EVALUATION OF ISOCHRONS	
4.4.1 Testing Differences Between Isochrons	316
4.4.2 Pooling of Isochrons	320
4.5 PROBLEMATICAL PLOTS	
4.5.1 Errorchrons	325
4.5.2 Pseudoisochrons	334
4.6 ISOTOPIC CONCLUSIONS	
4.6.1 Geochronological Conclusions	341
4.6.2 Initial Strontium Ratios	346
 <u>CHAPTER 5: SYNOPSIS</u>	
5.1 CHEMISTRY OF ARCHEAN GRANITOIDS	354
5.2 REGIONAL DISTRIBUTION AND EMPLACEMENT	357
 <u>REFERENCES</u>	 364
 <u>APPENDICES</u>	 403
A. PLATES	404
B. MODAL ANALYSES	
Introduction	416
Tables	418
C. MAJOR ELEMENTS	
Introduction	423
FeO and Fe ₂ O ₃	426
Precision	427
Accuracy	430
Tables	434
D. TRACE ELEMENTS	
Introduction	441
Precision	444
Accuracy	447
Detection Limits	451
Tables	453

	<u>Page</u>
E. ELEMENT RATIOS Tables	460
F. MESONORM CALCULATIONS Introduction Tables	467 469
G. RADIOELEMENTS Introduction Field Procedures Precision and Accuracy	476 477 477
H. ISOTOPIC DETERMINATIONS Introduction Wet Chemistry Contamination Levels Filament Preparation Mass Spectrometry Data Processing Precision and Accuracy Isochron Calculation	481 481 481 484 484 485 487 489
I. BURDITT LAKE SAMPLE LOCATIONS	494

LIST OF TABLES

1.1	Subdivisions of the Western Superior Province: terminology	2
1.2	Lithologic analyses	5
2.1	Tests for statistical evaluation of the "fit" of a trend surface, by the method of Agterberg and Chung (1975): Burditt Lake Stock	93
2.2	Chemical analyses for the Scattergood Lake Stock	124
2.3	Agpaitic coefficients for the Flora Lake Stock and Ryckman Lake Stock	176
3.1	Lithologies plotting in the "megacryst field" of the Na-K-Ca plot: correlation of mineral modes and megacryst development	241
3.2	Aeromagnetic flux (unfiltered) over lithologic units and its correlation with total iron content of surface samples	251
4.1	Whole rock trace element and isotopic Rb/Sr data	273
4.2	Isochron parameters from REGROSS of Brooks <u>et al.</u> (1972) for granitoid plutons intrusive into the Wabigoon Belt	274
4.3	Isochron parameters (REGROSS of Brooks <u>et al.</u> , 1972), Rainy Lake batholithic complex, Lake Despair area	306
4.4	Wabigoon internal granitoid plutons: pooled variance test for isochron differences using students-T; York I parameters	318
4.5	Rainy Lake batholithic complex: pooled variance test for isochron differences using students-T; York I parameters	321

4.6	Pooled ages and initial ratios	323
4.7	Errorchrons and pseudoisochrons	329
4.8	Cause of outliers	333
4.9	Ryckman model rotated isochrons	337
4.10	Regression models for the Icarus Pluton	340
4.11	Whole-rock isochron ages	344
5.1	Geochemical comparison of Archean "deep level" and "higher level" granitoids of the Canadian Shield	356B

LIST OF FIGURES

1.1	Western portion of the Wabigoon volcanic plutonic belt showing granitoid distribution	4
2.1	Lithology and structure of the Burditt Lake Stock, Northwestern Ontario	17
2.2	Sample location map, Burditt Lake Stock	19
2.3	Mafic enclave distribution over the Burditt Lake Stock	21
2.4	Burditt Lake Stock: modes on a IUGS (1973) Q-A-P plot.	28
2.5	Burditt Lake Stock: modes on quartz-feldspar-mafic diagram	28
2.6	Burditt Lake Stock mineral modes - biotite	29
2.7	Burditt Lake Stock mineral modes - epidote	29
2.8	Burditt Lake Stock mineral modes - muscovite	32
2.9	Burditt Lake Stock mineral modes - glomerogranular quartz	32
2.10	Grain size distribution over the Burditt Lake Stock based on identity change numbers	41
2.11	Modal variation diagrams for the Burditt Lake Stock	47
2.12	Binary plots of major cations <u>vs</u> modified Larsen Index of Nockolds and Allen (1953) for the Burditt Lake Stock samples	54
2.13	Ca-Na-K plot of Green and Poldervaart (1958) for the Burditt Lake Stock	56
2.14	Felsic index <u>vs</u> mafic index plot of Simpson (1954) for the Burditt Lake Stock	56

2.15	Linear variation diagram for Rb <u>vs</u> the modified Larsen Index of Nockolds and Allen (1953), Burditt Lake Stock	61
2.16	Linear variation diagram for Sr <u>vs</u> the modified Larsen Index of Nockolds and Allen (1953), Burditt Lake Stock	61
2.17	Linear variation diagram for Zr <u>vs</u> the modified Larsen Index of Nockolds and Allen (1953), Burditt Lake Stock	62
2.18	Linear variation diagram for Ba <u>vs</u> the modified Larsen Index of Nockolds and Allen (1953), Burditt Lake Stock	62
2.19	Linear variation diagram for Ce <u>vs</u> the modified Larsen Index of Nockolds and Allen (1953), Burditt Lake Stock	63
2.20	Linear variation diagram for Y <u>vs</u> the modified Larsen Index of Nockolds and Allen (1953), Burditt Lake Stock	63
2.21	Linear variation diagram for Nb <u>vs</u> the modified Larsen Index of Nockolds and Allen (1953), Burditt Lake Stock	64
2.22	Burditt Lake Stock analyses on a Ba-Rb-Sr plot of Bouseily and Sokkary (1975)	70
2.23	Zr element distribution over the Burditt Lake Stock	72
2.24	Ba element distribution over the Burditt Lake Stock	72
2.25	<u>In situ</u> analyses of eU by differential gamma-ray spectrometry over the Burditt Lake Stock	78
2.26	<u>In situ</u> analyses of eTh by differential gamma-ray spectrometry over the Burditt Lake Stock	78
2.27	U, Th and Th/U variation with the modified Larsen Index for the Burditt Lake Stock	79

2.28	<u>In situ</u> analysis of eTh/eU in the Burditt Lake Stock	82
2.29	Polynomial trend surfaces from linear to quartic order for SiO ₂ content in the Burditt Lake Stock	91
2.30	Half-confidence interval maps for the polynomial trend surfaces of Figure 2.29	92
2.31	"Best-fit" polynomial contour map for Al ₂ O ₃ in the Burditt Lake Stock	99
2.32	"Best-fit" polynomial contour map for CaO in the Burditt Lake Stock	99
2.33	"Best-fit" polynomial contour map for Fe ₂ O ₃ in the Burditt Lake Stock	99
2.34	"Best-fit" polynomial contour map for MgO in the Burditt Lake Stock	99
2.35	"Best-fit" polynomial contour map for K ₂ O in the Burditt Lake Stock	101
2.36	"Best-fit" polynomial contour map for Rb in the Burditt Lake Stock	101
2.37	"Best-fit" polynomial contour map for Ce in the Burditt Lake Stock	104
2.38	"Best-fit" polynomial contour map for Sr in the Burditt Lake Stock	104
2.39	"Best-fit" polynomial contour map for Zr in the Burditt Lake Stock	104
2.40	"Best-fit" polynomial contour map for Ba in the Burditt Lake Stock	104
2.41	Model of the Burditt Lake Stock as a prototype silicate ion exchange column, involving pulsating diapirism, infiltration, diffusion and cation exchange	112
2.42	Lithology and structure of the Scattergood Lake Stock	117

2.43	Scattergood Lake Stock mineral modes plotted on Q-A-P diagram of IUGS (1973)	122
2.44	Scattergood Lake Stock analyses on a Ba-Rb-Sr plot of Bouseily and Sokkary (1975)	122
2.45	Ca-Na-K plot of Green and Poldervaart (1958) for the Scattergood Lake Stock	123
2.46	Lithology and structure of the Ryckman Lake Stock	129
2.47	Ryckman Lake stock modes on an IUGS (1973) ternard Q-A-P diagram	135
2.48	Ca-Na-K plot of Green and Poldervaart (1958) for Ryckman Lake Stock	141
2.49	Si <u>vs</u> modified Larsen Index for Ryckman Lake Stock	146
2.50	Al <u>vs</u> modified Larsen Index for Ryckman Lake Stock	146
2.51	Fe <u>vs</u> modified Larsen Index for Ryckman Lake Stock	147
2.52	Mg <u>vs</u> modified Larsen Index for Ryckman Lake Stock	147
2.53	Na <u>vs</u> modified Larsen Index for Ryckman Lake Stock	148
2.54	K <u>vs</u> modified Larsen Index for Ryckman Lake Stock	148
2.55	Ca <u>vs</u> modified Larsen Index for Ryckman Lake Stock	149
2.56	P <u>vs</u> modified Larsen Index for Ryckman Lake Stock	149
2.57	Ti <u>vs</u> modified Larsen Index for Ryckman Lake Stock	150
2.58	Zr <u>vs</u> modified Larsen Index for Ryckman Lake Stock	150

2.59	Rb <u>vs</u> modified Larsen Index for Ryckman Lake Stock	151
2.60	Sr <u>vs</u> modified Larsen Index for Ryckman Lake Stock	151
2.61	Ba <u>vs</u> modified Larsen Index for Ryckman Lake Stock	152
2.62	Ce <u>vs</u> modified Larsen Index for Ryckman Lake Stock	152
2.63	Ryckman Lake Stock - analyses on ternary Rb-Ba-Sr plot of Bouseily and Sokkary (1975)	153
2.64	<u>In situ</u> analysis of eU in Ryckman Lake Stock by portable differential gamma-ray spectrometry	156
2.65	<u>In situ</u> analysis of eTh in Ryckman Lake Stock by portable differential gamma-ray spectrometry	156
2.66	<u>In situ</u> eU and eTh analyses <u>vs</u> modified Larsen Index of near-equivalent samples	157
2.67	Lithology and structure of the Flora Lake Stock	159
2.68	Ca-Na-K ternary plot of Green and Poldervaart (1958) for Flora Lake Stock	167
2.69	Felsic index <u>vs</u> mafic index plot of Simpson (1954) for the Flora Lake Stock	167
2.70	Si <u>vs</u> modified Larsen Index for the Flora Lake Stock	170
2.71	Al <u>vs</u> modified Larsen Index for the Flora Lake Stock	170
2.72	Fe <u>vs</u> modified Larsen Index for the Flora Lake Stock	170
2.73	Mg <u>vs</u> modified Larsen Index for the Flora Lake Stock	170

2.74	Na <u>vs</u> modified Larsen Index for the Flora Lake Stock	171
2.75	K <u>vs</u> modified Larsen Index for the Flora Lake Stock	171
2.76	Ca <u>vs</u> modified Larsen Index for the Flora Lake Stock	171
2.77	P <u>vs</u> modified Larsen Index for the Flora Lake Stock	171
2.78	Ti <u>vs</u> modified Larsen Index for the Flora Lake Stock	172
2.79	Zr <u>vs</u> modified Larsen Index for the Flora Lake Stock	172
2.80	Rb <u>vs</u> modified Larsen Index for the Flora Lake Stock	172
2.81	Sr <u>vs</u> modified Larsen Index for the Flora Lake Stock	172
2.82	Y <u>vs</u> modified Larsen Index for the Flora Lake Stock	173
2.83	Nb <u>vs</u> modified Larsen Index for the Flora Lake Stock	173
2.84	Ba <u>vs</u> modified Larsen Index for the Flora Lake Stock	173
2.85	Ce <u>vs</u> modified Larsen Index for the Flora Lake Stock	173
2.86	Flora Lake Stock phases on ternary Rb-Ba-Sr plot of Bouseily and Sokkary (1975)	175
2.87	Esox Lake granitoids	184
2.88	Esox Lake granitoids plotted on Na-K-Ca diagram of Green and Poldervaart (1958)	193
2.89	Esox Lake granitoids on Ba-Sr-Rb ternary plot of Bouseily and Sokkary (1975)	195

2.90	Rest Island Stock	201
2.91	Bears Passage Stock - sample locations	204
2.92	Ottertail Lake Pluton - lithology	207
2.93	Froghead Bay Stock - sample locations	213
2.94	Regina Bay Stock - sample locations	213
2.95	Stormy Lake Stock - sample locations	213
2.96	Taylor Lake Stock - sample locations	215
2.97	Na-Ca-K plot of Green and Poldervaart (1958) for Wabigoon and Rainy Lake plutons	218
2.98	Na-Ca-K plot of Green and Poldervaart (1958) for the Taylor Lake Stock	218
2.99	Ternary Rb-Sr-Ba plot of Bouseily and Sokkary (1975) for Wabigoon and Rainy Lake plutons	220
3.1	Linear correlation compilations for 247 granitoids of the Wabigoon Belt: Si <u>vs</u> modified Larsen Index	225
3.2	Linear correlation compilations for 247 granitoids of the Wabigoon Belt: Al <u>vs</u> modified Larsen Index	225
3.3	Linear correlation compilations for 247 granitoids of the Wabigoon Belt: Fe <u>vs</u> modified Larsen Index	226
3.4	Linear correlation compilations for 247 granitoids of the Wabigoon Belt: Mg <u>vs</u> modified Larsen Index	226
3.5	Linear correlation compilations for 247 granitoids of the Wabigoon Belt: Na <u>vs</u> modified Larsen Index	227

3.6	Linear correlation compilations for 247 granitoids of the Wabigoon Belt: K <u>vs</u> modified Larsen Index	227
3.7	Linear correlation compilations for 247 granitoids of the Wabigoon Belt: Ca <u>vs</u> modified Larsen Index	228
3.8	Linear correlation compilations for 247 granitoids of the Wabigoon Belt: Mn <u>vs</u> modified Larsen Index	228
3.9	Linear correlation compilations for 247 granitoids of the Wabigoon Belt: Ti <u>vs</u> modified Larsen Index	229
3.10	Linear correlation compilations for 247 granitoids of the Wabigoon Belt: P <u>vs</u> modified Larsen Index	229
3.11	Linear correlation compilations for 247 granitoids of the Wabigoon Belt: Rb <u>vs</u> modified Larsen Index	231
3.12	Linear correlation compilations for 247 granitoids of the Wabigoon Belt: Sr <u>vs</u> modified Larsen Index	231
3.13	Linear correlation compilations for 247 granitoids of the Wabigoon Belt: Ba <u>vs</u> modified Larsen Index	232
3.14	Linear correlation compilations for 247 granitoids of the Wabigoon Belt: Y <u>vs</u> modified Larsen Index	232
3.15	Linear correlation compilations for 247 granitoids of the Wabigoon Belt: Zr <u>vs</u> modified Larsen Index	233
3.16	Linear correlation compilations for 247 granitoids of the Wabigoon Belt: Ce <u>vs</u> modified Larsen Index	233
3.17	Na/K <u>vs</u> modified Larsen Index for 247 granitoids of the Wabigoon Belt	235

3.18	Rb/Sr vs modified Larsen Index for 247 granitoids of the Wabigoon Belt	235
3.19	Sr/Ba vs modified Larsen Index for 247 granitoids of the Wabigoon Belt	236
3.20	Ca/Sr vs modified Larsen Index for 247 granitoids of the Wabigoon Belt	236
3.21	K/Rb vs modified Larsen Index for 247 granitoids of the Wabigoon Belt	237
3.22	Ti/Zr vs modified Larsen Index for 247 granitoids of the Wabigoon Belt	237
3.23	Na-K-Ca fields for major lithologies, Wabigoon plutons	240
3.24	Proposed chemical budget between enclave and host	249
4.1	Wabigoon Belt chronology	264
4.2	Whole-rock 9 point Rb/Sr isochron (York I) for Burditt Lake Stock	278
4.3	Whole-rock 7 point Rb/Sr isochron (York I) for Ryckman Lake Stock	279
4.4	Whole-rock 5 point Rb/Sr isochron (York I) for Taylor Lake Stock	281
4.5	Whole-rock 5 point Rb/Sr isochron (York I) for Flora Lake Stock: phanerites only	283
4.6	Whole-rock 6 point Rb/Sr isochron (York I) for Flora Lake Stock	284
4.7	Whole-rock 4 point Rb/Sr isochron (York I) for Esos Lake quartz-feldspar porphyry	286
4.8	Whole-rock Rb/Sr isochron (York I) for Bears Passage Stock	291
4.9	Mineral:whole-rock Rb/Sr isochron (York I) for Bears Passage Stock	291

4.10	Whole-rock 10 point Rb/Sr isochron (York I) for Ottertail Lake Stock	294
4.11	Composite whole-rock Rb/Sr "isochron" plot (York I) based on 39 granitoid samples from 7 plutons of the Wabigoon Belt	297
4.12	Composite whole-rock Rb/Sr "isochron" plot (York I) similar to Figure 4.11, but with 2 highest points removed	297
4.13	Composite whole-rock Rb/Sr "isochron" plot (York I) based on 7 aplite and aplite-pegmatite samples from 3 plutons within the Wabigoon Belt	301
4.14	Composite whole-rock Rb/Sr "isochron" plot for aplites and aplite-pegmatites from Wabigoon Belt. Samples for Figure 4.13 excluding F27	302
4.15	Composite whole-rock Rb/Sr isochron (York I) for 3 phases of the Rainy Lake batholithic complex	307
4.16	Whole-rock Rb/Sr York I plot for Northwest Bay granitic complex of the Rainy Lake batholith	309
4.17	Whole-rock 3 point Rb/Sr isochron (York I) for Jackfish Lake granitoid complex of the Rainy Lake batholith	309
4.18	Whole-rock 4 point Rb/Sr isochron (York I) for Footprint Lake gneiss of the Rainy Lake batholith	311
4.19	Composite 7 point whole-rock Rb/Sr isochron (York I) for Footprint and Jackfish phases of the Rainy Lake batholithic complex	311
4.20	Whole-rock 5 point Rb/Sr pseudoisochron (York I) for Ryckman Lake Stock	339
4.21	Initial $^{87}\text{Sr}/^{86}\text{Sr}$ ratios from this study in relation to Sr evolution models	349

LIST OF PLATES

1.1	Feldspathized mafic enclave (location RY10)	405
1.2	Feldspathized mafic enclave (location 80)	405
1.3	Feldspathized mafic enclave (location 49)	405
1.4	Feldspathized and silicified mafic enclave (location F2)	405
1.5	Pyritized quartz porphyry (location EX5)	405
2.1	Mafic schlieren of biotite and hornblende in association with chloritic enclaves (location RY93)	407
2.2	"Double enclaves" of intrusion breccia (location F18)	407
2.3	Aligned inclusions in microcline-perthite megacrysts (location 118)	407
2.4	Inclusions in biotite of mafic enclave (location S11)	407
3.1	Several generations of pink aplite dykes in granodiorite (location 64)	409
3.2	Granodiorite dyke in metapyroclastics microcline-perthite megacrysts at dyke-host interface (location 69)	409
3.3	Aplitic dyke with felsic reaction rim, in granodiorite (location 24)	409
3.4	Aplite veinlet in corrosive contact with microcline-perthite grain (location 35)	409
4.1	Glomerogranular quartz surrounded by plagioclase (location 1)	411
4.2	Elongated quartz "eyes" in pink aplite dyke (location 64)	411

4.3	Euhedral quartz "eyes", massive pink aplite	411
4.4	Euhedral quartz inclusion in microcline-perthite megacryst (location 118)	411
5.1	Synneusis cluster of plagioclase shown by composite zoning and misfit (location 27)	413
5.2	Synneusis twins of plagioclase (location S6)	413
5.3	Subhedral epidote with optical zoning (location 61)	413
5.4	Euhedral metamict allanite in microcline-perthite (location 60)	413
5.5	Granoblastic plagioclase, microcline, quartz (location RY37)	413
6.1	Plagioclase embayed by albite (location 35)	415
6.2	Sawtooth contact between quartz and plagioclase (location 70)	415
6.3	Synneusis twins of plagioclase with secondary epidote-sericite in cores (location: Burditt Lake Stock)	415
6.4	Myrmekitized plagioclase partly surrounded and corroded by microcline (location 58)	415
6.5	Plagioclase with myrmekitized marginal zone against microcline (location 102)	415

CHAPTER 1

1.1 WABIGOON VOLCANIC-PLUTONIC BELT

The Superior Province is one of seven tectonic divisions of the Canadian Shield and represents the world's largest crustal exposure of Archean age rocks. The western portion of this Province is characterized by an east-west trending striped pattern of alternating volcanic plutonic and metasedimentary-gneiss terrain. This banded tectonic style was recognized by the earliest workers (Van Hise, 1893) and has generated a variety of terminology (Table 1.1).

Because of the economic incentive provided by gold and base metal exploration, the best understood and most comprehensively mapped portion of the Superior Province corresponds to the volcanic-plutonic belts. Of these, the Wabigoon Volcanic-Plutonic Belt is one of the better defined linear regimes, being flanked on either side by distinctively contrasting metasedimentary-gneiss lithology of the English River Belt (to the north) and the Quetico Belt (to the south).

The Wabigoon Belt consists of thick vertically dipping piles of metavolcanics and metasediments forming curvilinear and stellate arrays, embayed and separated by amoeboid clusters of granitoid batholiths. The dimensions attributed to this

Table 1.1 Subdivisions* of the Western Superior Province:
Terminology

Stockwell (1970)	Wilson (1971)	Goodwin (1968)	Goodwin & West (1974); Goodwin (1977)
Cross Lake Belt	Gods Lake Block	LaRonge Volcanic Belt	Pikwitonei Belt
		Amisk Volcanic Belt	
		Windigo Volcanic Belt	Sachigo Volcanic Belt
Cat Lake Belt	Berens River Block Red Lake Block	Uchi Volcanic Belt	Berens Plutonic Belt Uchi Volcanic Belt
English River Belt	English River Block		English River Gneiss Belt
Wabigoon Belt	Kenora Block	Keewatin Volcanic Belt	Wabigoon Volcanic- Plutonic Belt
Quetico Belt	Quetico Block		Quetico Gneiss Belt
Wawa Belt	Algoma Block	Abitibi Volcanic Belt	Shebandowan Volcanic- Plutonic Belt

*Regions are only roughly equivalent; boundaries differ with authors

Belt are dependent on contact interpretations by the various investigators, but are probably in excess of 200 km (width) by 800 km (length).

Figure 1.1 is a sketch of the western portion of the Wabigoon Volcanic-Plutonic Belt showing only granitoid distribution. This region roughly matches Figure 6 of Clifford (1972), Figure 1 of Wilson et al. (1974) and Figure 3 of Langford and Morin (1976) and is derived from Map 2115 of the Ontario Division of Mines with modifications based on the author's own mapping. This western portion best illustrates the tectonic framework that characterizes the Wabigoon Belt from the other Subprovinces: "gregarious" granitoid batholithic complexes flanking synformal supracrustals, with epizonal to mesozonal late-kinematic stocks emplaced into the supracrustals.

Goodwin (1965) employed a planimeter survey over regional maps to arrive at percentage lithology estimates (Table 1.2).

1.2 THESIS SCOPE

The granitoid plutons lying internal to the supracrustals of the Wabigoon Belt are the focus of attention for this thesis. On the basis of Goodwin's (1965) estimate, they represent only 3.7% of the region, but because of the sharp contacts against contrasting lithology and because these small plutons are

WABIGOON BELT GRANITOIDS

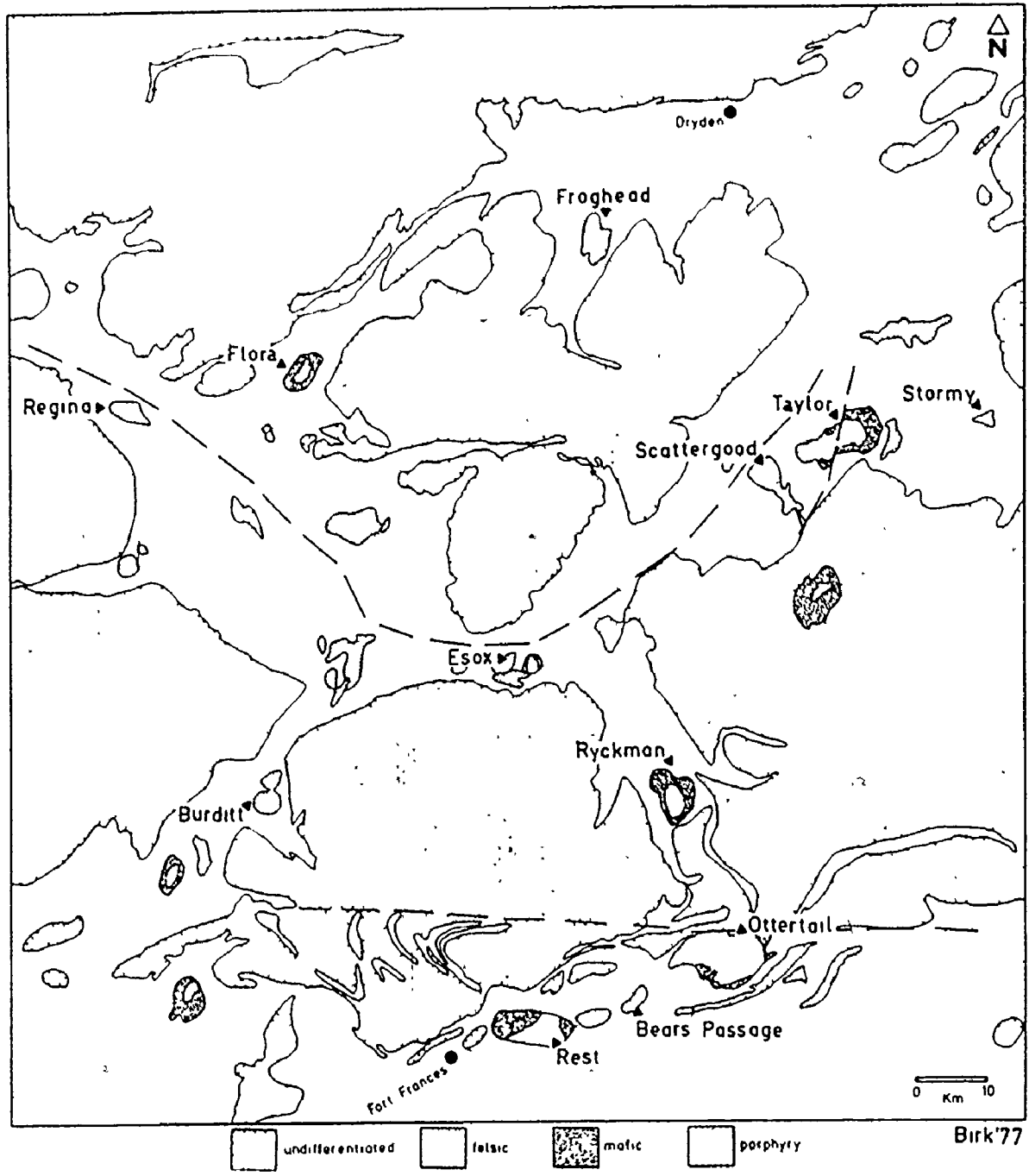


FIGURE 1.1 WESTERN PORTION OF THE WABIGOON VOLCANIC PLUTONIC BELT SHOWING GRANITOID DISTRIBUTION. PLUTON NAMES ARE ABBREVIATED AND CORRESPOND TO PLUTONS INCLUDED IN THIS STUDY.

Table 1.2 Lithologic Analyses

A. Lake-of-the-Woods - Manitou Lakes - Wabigoon Lake Region:

Planimeter survey (modified from Goodwin, 1965, Table 3):

<u>Lithology</u>	<u>Area (sq. mi.)</u>	<u>Percent</u>
Granitoid batholithic complexes	2,790	46.8
Basic volcanics	1,938	32.5
Acid volcanics	459.3	7.7
Sediments	459.1	7.7
Granitoid intrusions	218	3.7
Mafic intrusions	<u>95.2</u>	<u>1.6</u>
	<u>5,959.6</u>	<u>100.0</u>

B. Wabigoon Volcanic-Plutonic Belt: Internal Granitoid Plutons:

Ratios of areal abundances (based on Map 2115):

Types:	$\frac{\Sigma \text{zoned plutons}}{\Sigma \text{homogeneous plutons}} = \frac{2.59}{1}$
Lithology:	$\frac{\Sigma \text{granodiorite-granite}}{\Sigma \text{diorite-monzonite}} = \frac{1.67}{1}$
Zoned pluton: lithology:	$\frac{\Sigma \text{granodiorite-granite}}{\Sigma \text{monzonite-diorite}} = \frac{1.35}{1}$

located in areas that have undergone extensive mapping and exploration activity, these plutons represent the only portion of the granitoid terrain for which good field control is available. Although at the time of writing, several reconnaissance mapping projects have been conducted on batholithic complexes (Alneau Dome, Wilson et al., 1974; Irene-Eltrut Lakes Complex, Sowden-Wabakimi Lakes Complex, Sage et al., 1975) when this study was initiated, the batholithic areas represented unmapped "pink" on government maps.

A study of the geochronology and geochemistry of granitoids is best confined to those granitic units for which contact relationships and lithologic distribution has been established in the field. Figure 1.1 locates twelve granitoid plutons within the Wabigoon Belt that were visited and sampled by the author over a two summer period (1973, 1974). A third summer of field work (1976) involved a reconnaissance survey of eight metavolcanic regions concentrating on field visits to felsic metavolcanics and hypabyssal synvolcanic plutons. Many of the regional concepts presented in this dissertation are based on experience gained by this reconnaissance overview.

All twelve of the plutons (Figure 1.1) comprising this study lie internal to metavolcanics or metasediments. A consideration of lithologic distribution (Table 1.2B) shows that granodiorite-granite forms the bulk of the granitoids, with granite sensu stricto confined to aplitic dykes and minor

patches; diorite to monzonite is confined to border phases of zoned plutons. The multiphase plutons are more than twice as voluminous as single phase "homogeneous" bodies.

1.3 HISTORICAL REVIEW: GRANITOID STUDIES IN THE WESTERN SUPERIOR PROVINCE

Work by Lawson (1887, 1913) in the Rainy Lake region laid the foundation for Precambrian granitoid geology and nomenclature. Prior to Lawson's (1887) report, all granitic rocks in the Canadian Precambrian Shield were called "Laurentian" and were considered to form Archean basement for Huronian sediments and volcanic rocks (Van Hise, 1893). Lawson defined three series of supracrustals, in stratigraphic order: Couthiching sediments, Keewatin volcanics, and Seine Series sediments. The "Laurentian" granitoids proved to intrude and therefore post-date both the Couthiching and the Keewatin. Lawson found evidence (specifically at Shoal Lake) that these granitoids were overlain by the Seine Series sediments which he considered to be Huronian in age. Down strike Lawson located granitoids that intruded the Seine Series (at Sabaw Lake) and for these he coined the term "Algoman". Lawson's "type" localities for Laurentian granitoids included the Bad Vermilion granite and the sheared granite of Grassy Island. Type localities for the post-Seine Algoman granitoids included: Rocky Islet Bay mica-syenite gneiss, Pukamo Island mica-syenite

gneiss, sheared porphyroid gneiss (Quetico Fault zone augen gneiss of Harris, 1974), Grassy Island granite-gneiss, Nowhere Island granite-gneiss, Knuckle Island granite, Bear Passage granite and the Redgut Bay granite (Lawson, 1913). Some of these type localities will be discussed in following chapters of this thesis.

Considerable controversy was generated in the literature by Lawson's dual granitoid classification. Much subsequent effort was spent in either affirming or denying the "Laurentian" or "Algonian" nature of individual granitoid bodies (see J.K. Frye, 1959, for a summary). Many of Lawson's type localities were revisited and reclassified (Grout, 1929). Lawson's key evidence that Seine sediments overlie some granitoids was an outcrop of the Bad Vermilion granite at the Foley Mine, on Shoal Lake. Intrusive relationships between this granitoid and the Seine conglomerate were questioned and reclassified in the literature no less than five times (Frye, 1959, Table 2). The present author also made the "trek to mecca" but found relationships obscured by overgrowth.

Lawson's dual granitoid classification in the Rainy Lake region was extended to Minnesota by correlation of the Seine Series with the Ogishke conglomerate and the Knife Lake slates of Vermilion (Grout, 1929). By 1929 F.F. Grout was forced to conclude that:

"The batholithic activity along this boundary (Minnesota-Ontario) seems to have been more complex than that indicated by the simple terminology, Laurentian and Algoman In order to emphasize the complexity of the series of intrusions their sequence may be tabulated as follows:-

Keweenawan	}	(Dike intrusions (Probable batholithic invasion (Basic extrusions and intrusions (Sedimentation probable unconformity
Animikian	}	Sedimentation unconformity Late Algoman batholithic invasion Early Algoman batholithic invasion
Ogishke (Seine Series).....	}	Sedimentation unconformity Late Laurentian batholithic invasions Early Laurentian batholithic invasions
Keewatin		Flows and sedimentation"

F.F. Grout (1929, p.799)

On Grout's (1929) regional sketch map, the Laurentian batholithic areas included: the Northern Light Lake gneiss, Saganaga granite and the Lake-of-the-Woods area (Aulneau Dome). Algoman or later batholiths included the Giants Range granite, Burntside Lake gneiss, Vermilion granite and the Rainy Lake masses (Manitou Dome).

With more detailed mapping, most granitoid bodies were assigned to the later Algoman granites (Bass, 1961): including Lawson's type Laurentian localities at Grassy Island (Grout, 1929) and at Shoal Lake (Tanton, 1936). The remaining evidence of pre-Seine granitoid plutonism and a major unconformity, rested with granitoid pebbles found in the Seine conglomerates and other stratigraphically equivalent conglomerates (Timiskaming series, Ogishke series, etc.). Bass (1961) made a detailed petrographic investigation of such granitoid clasts and concluded that with few exceptions, they could be attributed to erosion of Keewatin-type hypabyssal porphyries and porphyry dikes associated with volcanism. The term "Laurentian" fell into disuse except in the vicinity of the Minnesota-Ontario border.

The complexity of granitoid intrusive relationships in any one field area led to the adoption of alternate classification schemes. Purdy and York (1966) cite that in the Red Lake region the sequence of igneous activity was assigned to "early pre-Algoman, late pre-Algoman, and Algoman intrusive phases, the Algoman itself being subdivided into four distinct major periods and several minor periods of intrusion". Many field geologists have opted out for a simpler "synkinematic; late-kinematic; postkinematic" or "syntectonic; late-tectonic; post-tectonic" categorization (e.g. Morey and Sims, 1976).

Although several authors have called for the abolition of both the terms Algoman and Laurentian (e.g. Walker, 1971),

this two-fold classification regained its popularity in recent publications of radiometric chronology studies (Heimlich, 1963; Hart and Davis, 1969; Peterman et al., 1972). To present their plethora of radiometric ages in a digestible format, geochronologists found the dual granitoid classification a helpful starting point. Unfortunately this stance occasionally ignored the 50 years of controversy over intrusive relationships. Thus both Hart and Davis (1969) and Peterman et al. (1972) adopted Lawson's assumption that:

"Algonian intrusives (at Rainy Lake) are demonstrably younger than the (Laurentian) Bad Vermilion intrusive".

Hart and Davis (1969, p.609)

Radiometric dating extended the number of granitoid intrusive events until Goldich (1968) could quote five for the Precambrian in Minnesota:

<u>Event</u>	<u>Intrusive Rocks</u>
Keweenawan igneous activity (1,000-1,200 m.y.)	Duluth Gabbro complex
Penokean orogeny (1,600-1,900 m.y.)	Granites in east-central Minnesota; small intrusions in Minnesota River Valley
Algonian orogeny (2,400-2,750 m.y.)	Vermilion and Giants Range granitic complexes; granite and gneiss in Minnesota River Valley
Laurentian orogeny (age?)	Granite at Saganaga Lake
? (3,300-3,550 m.y.)	Gneiss, Minnesota River Valley

In contrast Ayres et al. (1972) wrote the viewpoint more prevalent among Canadian geologists:

"This two-fold subdivision into Laurentian and Algonian is an oversimplification because granitic plutonism appears to span most of Archean time". (p.577)

CHAPTER 2

THE NATURE OF GRANITOID PLUTONISM IN THE WABIGOON VOLCANIC-PLUTONIC BELT

2.1 HOMOGENEOUS PLUTONS

2.1.1 Introduction

The distinction between homogeneous and heterogeneous is a function of the intensity of the observations. For a given pluton the total variability of an attribute (chemical, physical or modal) is the sum of analytical variance plus the components of variance at all local and regional scales. Rogers (1964) considered a pluton to be homogeneous with respect to some measured attribute if the value varies randomly throughout the volume within predetermined precision. He proposed testing homogeneity by comparing actual frequency distribution of the measured parameter against the theoretical distribution expected if the property varies randomly. But mathematically random distributions depend on abundances: for example, major elements show arithmetically normal distributions while trace elements are distributed logarithmically normal (Rogers and Adams, 1963). Furthermore, while non-random frequency distribution cannot be obtained from a homogeneous

body by random sampling, random distribution could be obtained from a body showing areal trends.

Whitten (1961) suggested trend surface analysis to obtain quantitative estimates of variability of granitic complexes. Other techniques that have been proposed include: correspondence analysis (David and Woussen, 1973), variograms and variance component analysis (Miesch, 1975), cluster and discriminatory analysis (Rhodes, 1969) and grid deviation maps (Saha, 1964). In studies that successfully applied these techniques to selected granitoid bodies, several authors were able to demonstrate that granitic bodies field-mapped as "homogeneous" did in fact carry distinct physical, modal and chemical zones that could support models of multiple intrusion (Joyce, 1973); magmatic differentiation; assimilation and contamination (Rhodes, 1969; Falkum, 1976).

Granitoid bodies have been traditionally mapped on the basis of megascopic field criteria: mineral modes; colour index; textures, etc., and subsequently categorized as zoned or composite versus massive or homogeneous. The heading to this section is based on such field criteria. Such categories carry significant petrogenetic implications which may be erroneous if the scale of investigation is not realistic. For example, by erroneously assuming homogeneity and coevality for the "gregarious batholiths" of Rhodesia, Talbot (1968) formulated an untenable thermal convection model (Bliss, 1969).

Scales of homogeneity have rarely been tested for granitoids of Northwestern Ontario: government mapping surveys traditionally widen their traverse spacings over granitoid terrain (e.g. Blackburn, 1976). Ayres (1972, 1974) stimulated a change in attitude by subdividing the North Trout Lake Batholith into 23 phases on the basis of field observations of composition, texture and structure. Paulus and Turnock (1971) carried out a two-traverse study of the relatively homogeneous Ross River quartz-diorite pluton. Their limited study outlined regional homogeneity of mineral modes, specific gravities and oxides disturbed by local irregular fluctuations. Although they also proposed the presence of mild zonal patterns, the author did not recognize them in the published results.

The lack of such statistical studies for granitoids of Northwestern Ontario make discussions on homogeneity and variance extremely imprecise. To rectify this for all plutons investigated in this study would be a monumental task - instead the author has selected the Burditt Lake Stock for detailed testing of homogeneity. Other plutons have been investigated at various scales of intensity and have been broadly categorized as to "homogeneous" or "composite" with recognized imprecision.

2.1.2 The Burditt Lake Stock

Previous Work

Burditt Lake, locally called Clearwater Lake is situated in Senn Township, 45 km northwest of Fort Frances, Ontario.

Lawson (1887) mapped the east shore of Burditt Lake as "Laurentian biotite-granite gneiss", continuous with the Manitou Dome to the east. He recognized two phases: a "distinctly foliated variety at Gloomy Cove in contrast to a more granitoid aspect at Sunny Cove". Reconnaissance mapping by J.C. Davies generated the stock boundaries shown on Map 2115 (Davies and Pryslak, 1967). In 1971 Blackburn carried out 1"/0.25 mi. mapping resulting in two preliminary maps and a final 1"/0.5 mi. map and report (Blackburn, 1972a,b, 1976).

Blackburn (1972) defined a twin lobed medium-grained to porphyritic granodiorite body roughly 3 miles in diameter emplaced in a vertically dipping wedge of felsic pyroclastics. The distribution of coarse-grained felsic pyroclastics around the stock suggested to Blackburn that the stock may be occupying a former volcanic vent.

Since traverse spacings were considerably wider over granitoids than over metavolcanic terrain, Blackburn's granitoid mapping was still of a reconnaissance nature. During the summers of 1973 and 1974, the author carried out an outcrop-by-outcrop investigation of the stock including a gamma-ray spectrometric survey. Field data was compiled regarding distribution and orientation of mafic enclaves, aplitic and pegmatitic dykes; distribution of textural and colour variations of lithology and megacrysts. These field observations and follow-up petrography allowed internal subdivision of the stock (Figure 2.1).

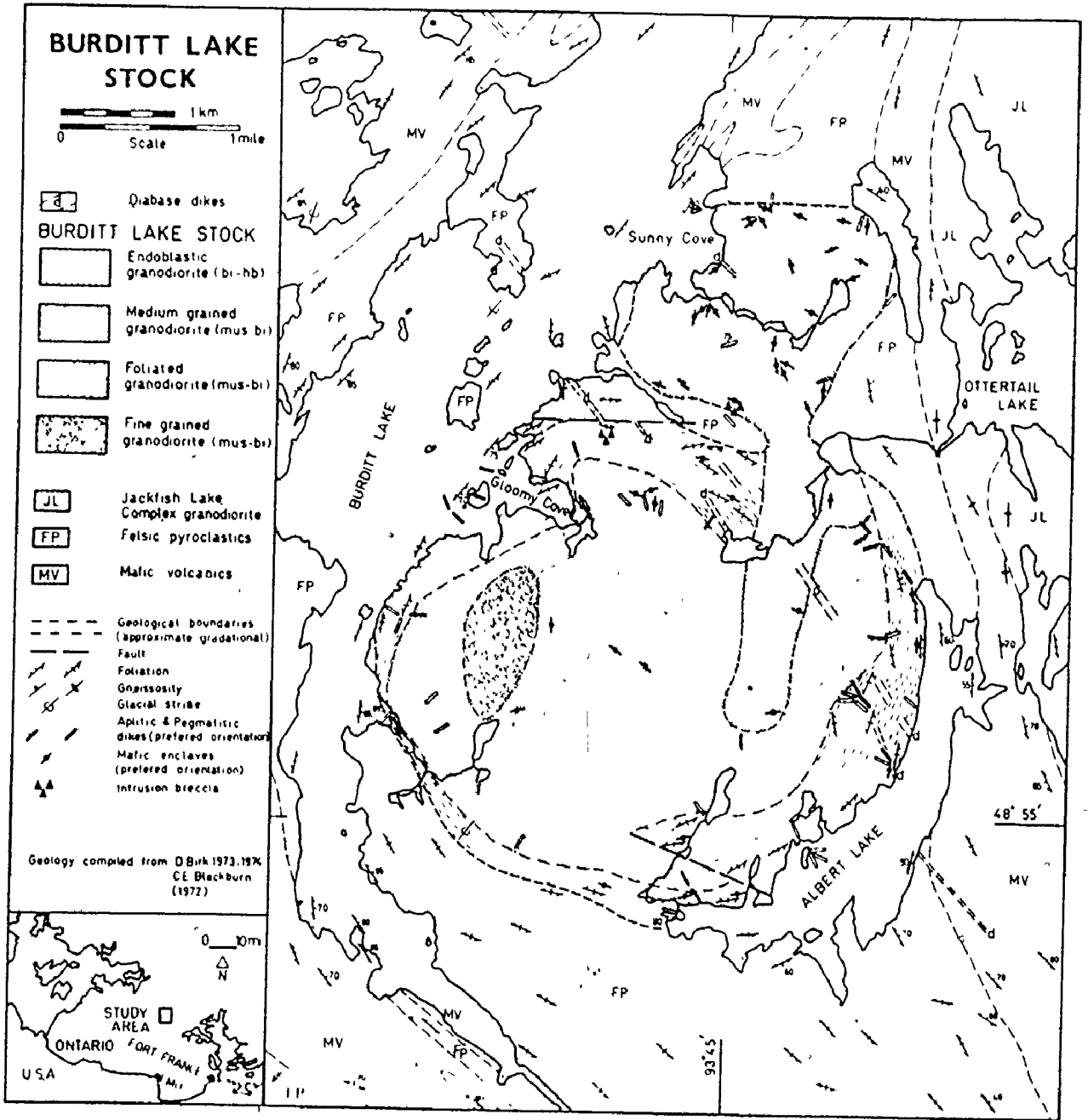


FIGURE 2.1 LITHOLOGY AND STRUCTURE OF THE BURDITT LAKE STOCK, NORTHWESTERN ONTARIO.

Subsequent discussions of internal features will refer to sample locations shown on Figure 2.2.

Of historical interest regarding the Burditt Lake Stock, a cliff exposure south of Gloomy Cove carries ancient Indian pictographs (Dewdney and Kidd, 1967).

Field Observations

Field observations recognize two mineral assemblages and four textural regions within the stock (Figure 2.1). A grey hornblende-granodiorite bearing microcline megacrysts dominates the northern lobe. Medium-grained pink biotite-granodiorite with glomerogranular quartz "eyes" makes up the bulk of the larger southern lobe.

The margin of the southern lobe carries strong lineation of biotite and occasionally lensoid quartz "eyes" (location 4); this lineation weakens then disappears towards the interior. The peripheral lineation is concordant to the foliation in the enclosing pyroclastics which appear to wrap around the stock. Off-center but well interior to the southern lobe is a region of finer grained granodiorite with sharp contacts (location 81) against the medium-grained phase.

Integral to the foliated margin are patches and dykes of pink aplite and occasional zoned dykes of aplite-pegmatite. Locally the aplite has brecciated the foliated granodiorite to form an agmatitic patchwork (locations 10; 131). At least two generations of aplite are recognized from cross-cutting

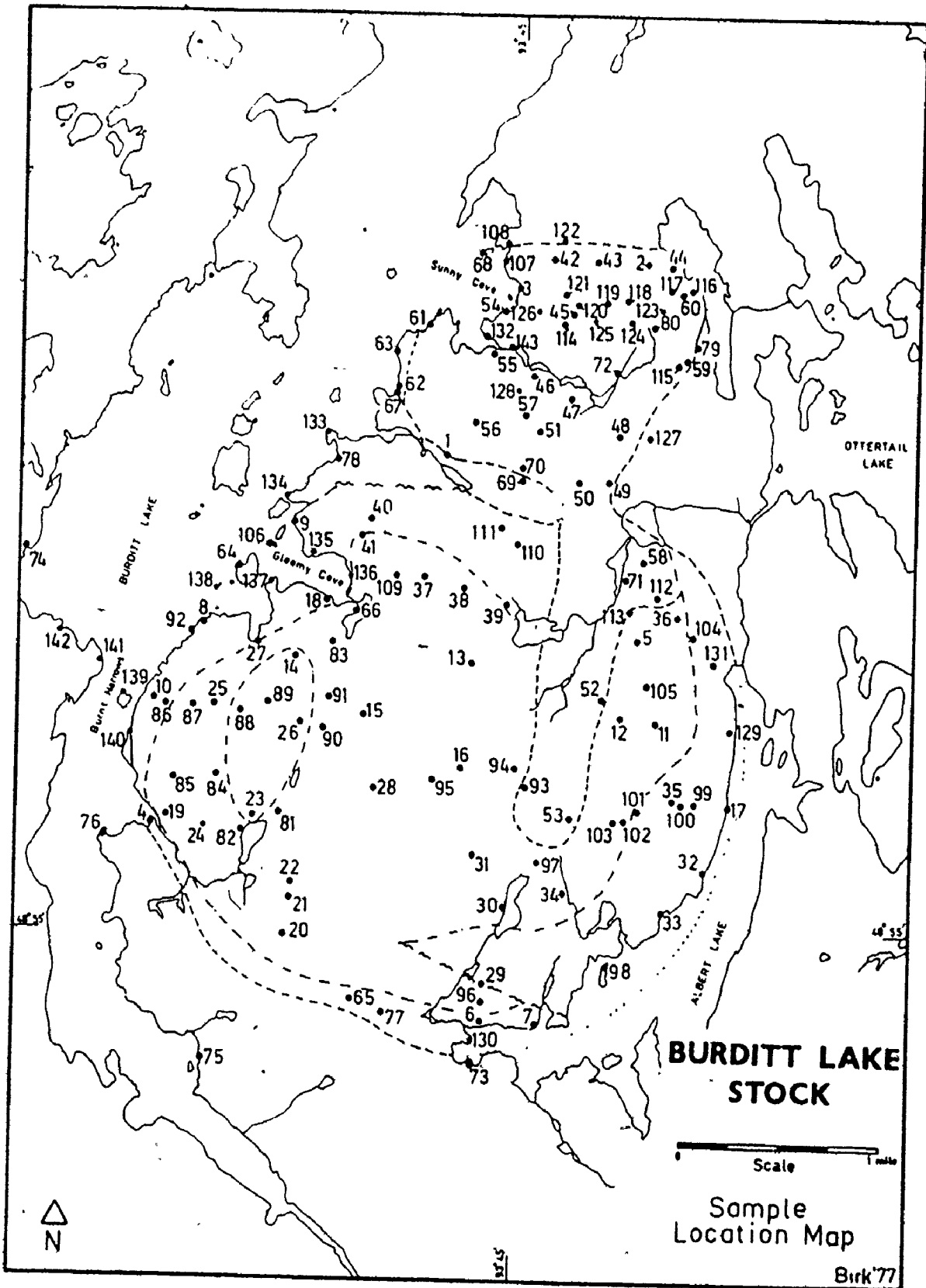


FIGURE 2.2

REFER TO APPENDIX I
FOR SAMPLE NUMBERS

relationships (Plate A3.1; locations 7, 10, 64, 96); these in turn are cut by rare dykes of quartz, usually filling tension fractures (location 7).

In contrast, the porphyric¹ north lobe is free of foliation and carries only rare felsic dykes. A tongue of the porphyric hornblende-granodiorite penetrates deep into the south lobe core, but poor outcrop exposure masks the contact relationships. Likewise the contact relationships are obscure for a small patch of biotite-granodiorite that hugs the rim of the northern lobe, just south of Sunny Cove.

Dense melanic lensoid enclaves, generally surmicaceous, are distributed throughout the stock but appear larger and more frequently in the northern lobe (Figure 2.3). In the southern margin the enclaves have their long axes oriented coincident with foliation. At two localities within the foliation zone were recorded biotite schlieren smeared subparallel to foliation (locations 17, 64). Occasional felsic enclaves (pink, saccharoidal) were located within the northern porphyric lobe (locations 47, 72, 114). The geological map shows two locations of "intrusion breccia" marginal to the north and south lobe, respectively. The two localities are markedly different, though both straddle the contact with metavolcanics. The northern locale shows swarms of subangular to nebulous mafic enclaves in granodiorite grading into feldspathized amphibolite. The southern locale (location 40) presents a dense network of granitic veinlets cut in turn by aplitic veinlets in a metatuff.

¹ porphyric: bearing inlets or megacrysts (Sylvester, 1964)

Distribution of mafic Enclaves

Legend

abundance	size (longest dimension)
○ absent over 100 sq m outcrop	● <10 cm
○ rare <3	● <30 cm
● abundant >3	● >30 cm

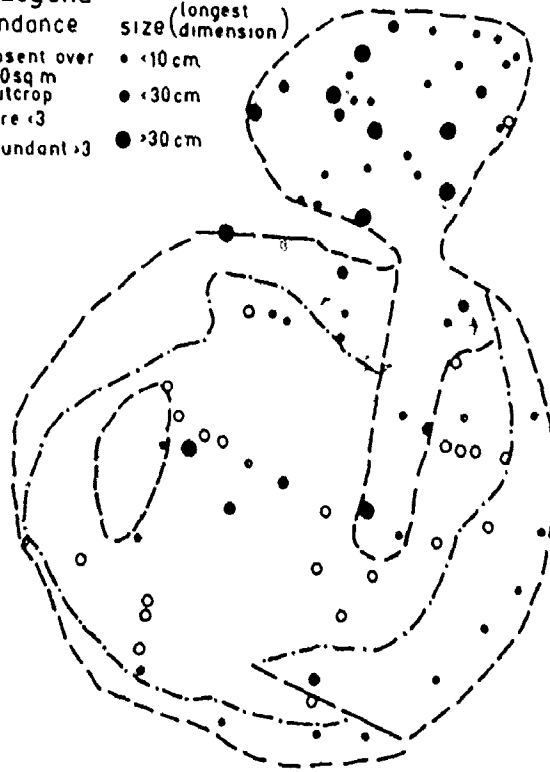


FIGURE 2.3 MAFIC ENCLAVE DISTRIBUTION OVER THE BURDITT LAKE STOCK. NOTE ENLARGEMENT AND PREPONDERANCE TOWARDS NORTH LOBE.

Didier (1973) calls this net-veining. Dyke swarms of aplite-pegmatite occur both within the stock (location 35) and in felsic pyroclastics adjacent to the stock (location 68).

The most prominent field distinction between the north and south lobe are the microcline-perthite megacrysts which weather in relief in the hornblende granodiorite. Even field observations can recognize inclusion zoning of hornblende and biotite within these megacrysts. Most significant are the megacrysts that occur within mafic enclaves or straddling enclave-granodiorite contacts (Plate A1.2; locations 46, 49, 80). These present convincing proof of a deuteric rather than magmatic origin of the megacrysts (see petrographic discussions).

Texturally as significant but less visible in the field are glomerogranular quartz "eyes" in the biotite-granodiorite of the southern lobe. At location 64, aplite dykes in foliated granodiorite carry lensoid quartz grains that straddle the aplite-granodiorite boundaries and are oriented with foliation (Plate A4.2). At one locality (location 4; Plate A4.3) an aplitic patch carries prominent quartz dipyrramids. These field sightings suggest the quartz formed as endoblasts after the emplacement of aplites, roughly contemporaneous in the cooling history with the microcline megacrysts.

A comparison of sample chips from the Burditt Lake Stock reveals subtle color and texture variations defining several

subzones within each lobe. These variations are gradational and not recognizable during field traverses - neither are they shown on geological map - but they add further need for a definition of homogeneity when dealing with granitoid plutons. Blackburn (1976) described the Burditt Lake Stock as:

"In the field, rocks of the stock appear to be homogeneous in composition, with rocks of the northern lobe a little more porphyritic". (p.31)

The fact that commonly used field criteria treat the Burditt Lake Stock as a "homogeneous" pluton must be kept in mind when comparing the lithologic and textural subdivisions of Figure 2.1 with those of other mapped plutons.

Structural Features

The country pyroclastics have been shouldered aside by forceful intrusion of the stock - similar to the case of the Snowbank Stock, described by Balk and Grout (1934). The contacts are sharp and smooth, suggesting that assimilation and stoping of supracrustal units was minimal. Lensoid nature of enclaves has been cited by some authors as evidence of extensive assimilation. However the intrusion breccia found at site 70, carries swarms of lensoid enclaves even adjacent to the tuffaceous units from which they were derived.

The concentration of felsic dykes in the foliated periphery and their orientation tangent to or radial to the

stock (Figure 2.1) attest to late stage fracturing of semi-consolidated magma followed by infiltration of deuteritic fluids. This fracturing may have been by thermal shrinkage or iso-static adjustment. The magma underwent further structural adjustments evidenced by plastic deformation of some of the peripheral aplite dykes (Plate A3.1; location 106). The centre of the south lobe shows no signs of magmatic motion; no foliation, and no aplite or pegmatite veins. Much of this core is occupied by the mineralogy and megacrysts typical of the north lobe. On the other hand, the porphyric north lobe also shows little evidence of magma motion after emplacement: no internal foliation; poor to random alignment of enclaves; only rare aplitic and pegmatitic dykes. The megacrysts of the north lobe and the southern core could have grown by deuteritic metasomatism in a stagnant semiconsolidated magma pool, from pneumatolitic fluids driven inward and northward by inward crystallizing granodiorite of the south lobe.

This model would have the south lobe undergoing internal motion perhaps by slow convection, while the north lobe represented a relatively quiescent environment for porphyroblastic growth. The textural contrast of the porphyric granodiorite with the equigranular foliated south lobe may be analogous to recrystallization of glacial ice. Seligman (1949) reported that active glacial ice shows aligned equigranular fabric while stagnant blocks of ice recrystallize to an

isotropic porphyroblastic texture. Bradley and Lyons (1953) used this glacier model to explain the "non-porphyrific" texture in foliated granodiorite adjacent to a "porphyritic" isotropic granite in the Cathedral Peak Pluton, Sierra Nevada. The same analogy fits well with the field evidence at Burditt Lake.

Minor faulting on the southern extremities of the stock, post-dating consolidation, is indicated by displacement of the foliated border correlating with a negative airphoto lineation. Blackburn (1976) mapped several other faults dissecting the stock based on airphoto interpretation, but many may just reflect glacial scouring. Some evidence is present of displacement of north-west trending diabase dykes which cut the stock and were first recognized by Lawson (1887).

The ODM-GSC aeromagnetic map (ODM , 1971 , Map 1167G) shows that magnetic intensities over the stock lie below 60,360 gammas, and carry a shallow magnetic gradient. The northern lobe shows a slight magnetic depression to 60,310 gammas, compared to 60,340 for the south lobe. These values contrast with a flux greater than 60,500 gammas for both the metavolcanics and the Jackfish Lake complex to the east.

Blackburn (1976) considered the Burditt Lake Stock to be a late-tectonic felsic intrusion. The structural features are, however, equally compatible with the "synkinematic" mesozonal to catazonal diapirs described by Anhaeusser et al. (1969) and Ayres and Ermanovics (1972).

Petrography

Introduction:

The bilobed nature of the stock (Figure 2.1) reflects a bilateral distribution of mineral assemblages. The northern lobe is a biotite-hornblende granodiorite with the assemblage (in order of abundances):

plagioclase + quartz + microcline + epidote + hornblende + biotite
 ± accessories: zircon, sphene, allanite, opaques, calcite
 ± alteration products: chlorite, sericite, etc.

The microcline occurs dominantly as megacrysts with minor amounts as anhedral matrix grains. The southern lobe, with the exception of a central tongue invading from the north (Figure 2.1), is devoid of hornblende and instead carries muscovite as a major constituent. All microcline present occurs as anhedral matrix grains. The south lobe is therefore a muscovite-biotite granodiorite with the assemblage:

plagioclase + quartz + microcline + biotite + epidote + muscovite
 ± accessories and alteration products

Modal analyses based on 1,000-point counts on 54 stained thin sections are listed in the appendix. The large number of analyses were found necessary to distinguish phases in this relatively homogeneous pluton. Figure 2.4 is a Q-A-P plot as recommended by the IUGS Subcommittee on the Systematics of Igneous Rocks (1973). The modal analyses show a restricted

field of modal variation for essential minerals that occupies mainly the granodiorite field. The north-lobe megacrystic samples show a slight alkali feldspar enrichment in relation to the south-lobe granodiorite samples, which in turn are slightly enriched in silica. A similar separation of clusters is evident on a Q-F-M plot (Figure 2.5), with north lobe samples showing enrichment in mafic minerals and south lobe samples showing quartz enrichment.

A plot of regional variations of mineral modes yields visually random distributions for biotite (Figure 2.6), and a bimodal distribution of epidote (Figure 2.7). Muscovite is almost entirely confined to the south lobe (Figure 2.8) with the exception of a small wedge of megacryst-free granodiorite on the west rim of the north lobe which is correspondingly free of hornblende and is considered to be an apophysis of the south phase.

Synneusis Twinning:

Plagioclase dominates the textural fabric of all phases of the stock as embayed and corroded laths partially sericitized and saussurized. The laths carry ubiquitous concentric optical zoning accentuated by sericitization along zonal planes. The zoning allows for the recognition of synneusis twinning: the joining of two or more individual grains generally along the (010) face following the Albite-Carlsbad twinning law (Ross, 1957). Synneusis is attributed to grain coalescence

BURDITT LAKE STOCK
 MODES ON A IUGS (1973)
 Q-A-P PLOT. NORTH LOBE [x]
 SOUTH LOBE [•]

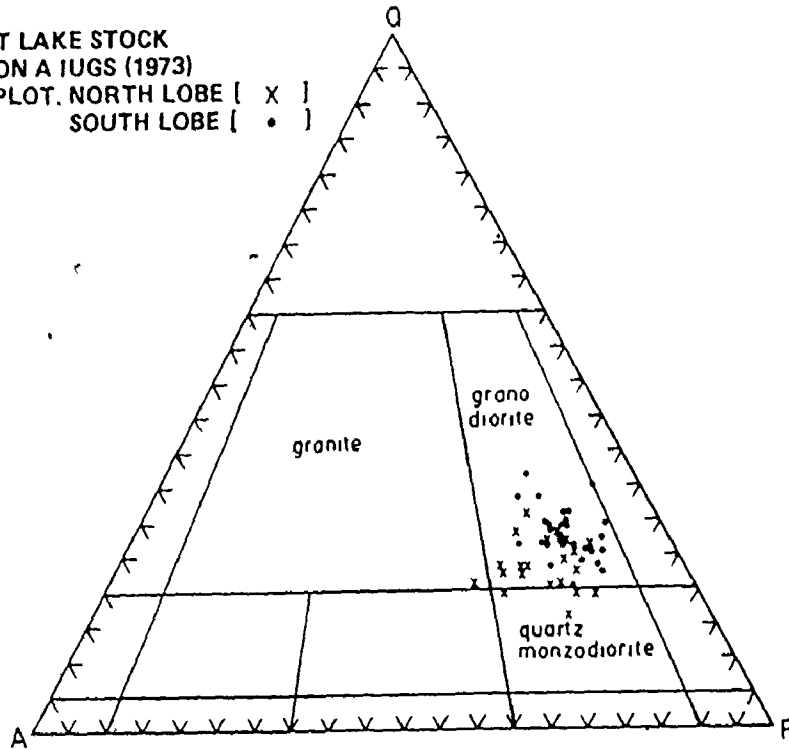
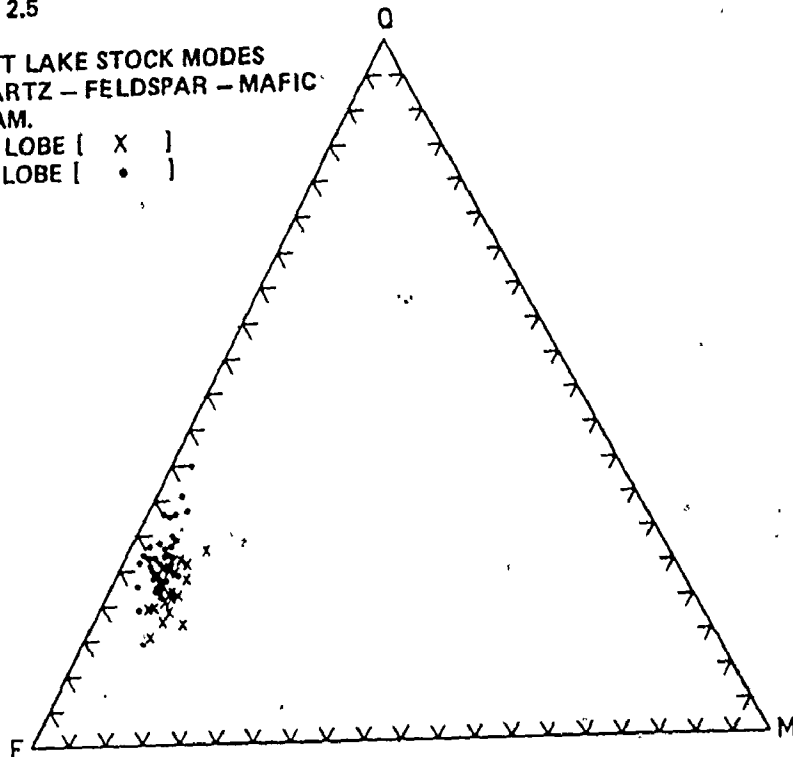
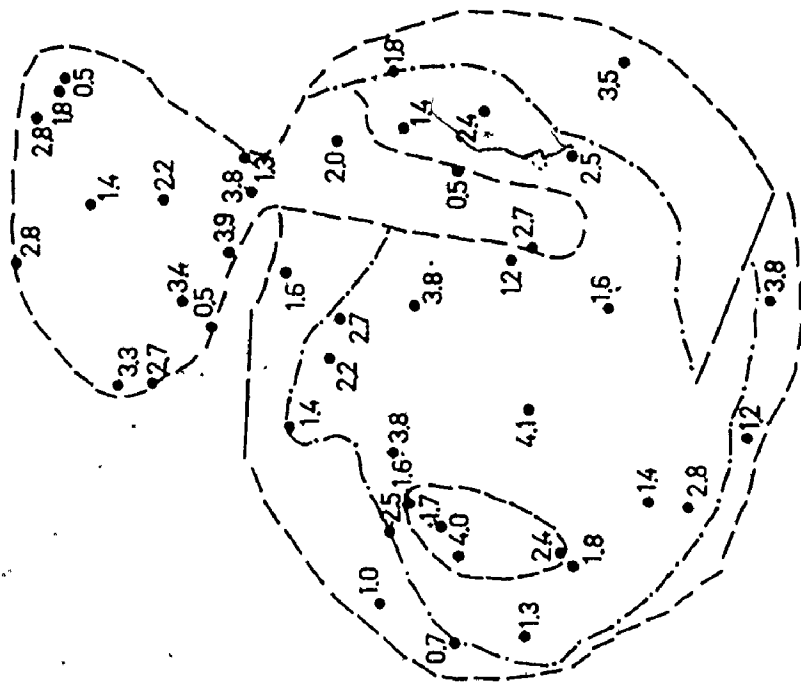


FIGURE 2.5

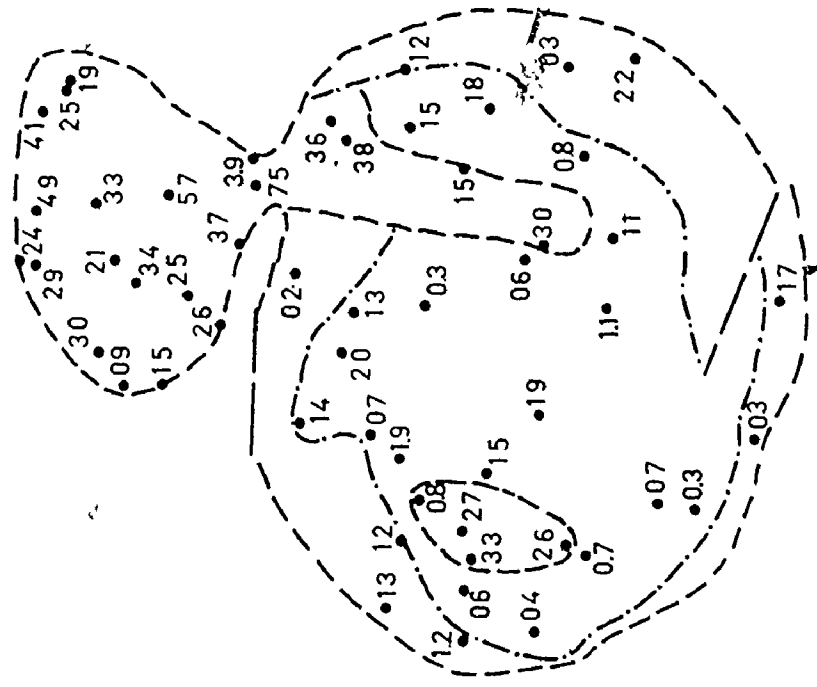
BURDITT LAKE STOCK MODES
 ON QUARTZ - FELDSPAR - MAFIC
 DIAGRAM.
 NORTH LOBE [x]
 SOUTH LOBE [•]





BIOTITE : MODAL %

FIGURE 2.6



EPIDOTE . MODAL %

FIGURE 2.7

BURDITT LAKE STOCK MINERAL MODES.

during growth in a liquid medium possibly due to magmatic turbulence and is strong evidence of magmatic genesis (Ross, 1957; Vance, 1969). It is most easily recognized if coalescence involves two or more concentrically zoned crystals (Plates 5.1 and 5.2).

The geographical distribution of abundant synneusis (defined by one or more well recognizable synneusis twins per thin section), shows it to be more prevalent in the northern lobe of the Burditt Lake Stock - reflecting a greater prevalence of optical zoning in the north. This implies that not only is there a difference in the mineralogy of the two lobes, but there is also a difference in the manner of emplacement. Vance (1969) proposed that synneusis is due to magmatic turbulence corresponding to an episode of emplacement or vigorous convection. Bartlett (1969) has calculated that granitic plutons greater than 15 meters in diameter will experience natural convective mixing of components smaller than 0.5 cm. prior to consolidation. This suggests that synneusis reflects gentle convective mixing in a crystal-liquid mush during emplacement. Synneusis at Burditt Lake is present also to a lesser extent for primary accessory minerals such as sphene.

Glomerogranular Quartz:

A textural phenomenon akin to synneusis is "glomerogranular texture" coined by Hawkes (1929) for the common clumping of like anhedral grains. Related terms are: glomeroporphyritic (Hawkes, 1929), augen, or "eye" texture (Hopwood, 1976). The granodiorite of the south lobe of the Burditt Lake Stock carries quartz in subhedral to rounded glomerogranular clusters a few centimeters in diameter (Plate A4.1). Because of a masking effect from the phaneritic groundmass, the "eyes" of quartz are best seen in stained thin sections viewed by eye. The dimensions of "eyes" are gradational with groundmass quartz grains, but prominent "eyes" are confined exclusively to the south lobe granodiorite (Figure 2.9), again reflecting the textural contrast between the biotite-hornblende granodiorite and the muscovite-biotite granodiorite.

This texture, though less often recognized in phaneritic granitoids, is probably analogous to the quartz-eye texture described for hypabyssal quartz-feldspar porphyries. Vance (1969) attributes glomeroporphyritic habit in quartz porphyries and the clusters of "subhedral dipyrramids of high quartz noted in certain granodiorites" both to be formed by synneusis with subsequent corrosion and overgrowth. Ovoid to subhedral glomerogranular quartz "eyes" in a phaneritic trondhjemite of New Mexico have been interpreted as recrystallizations from

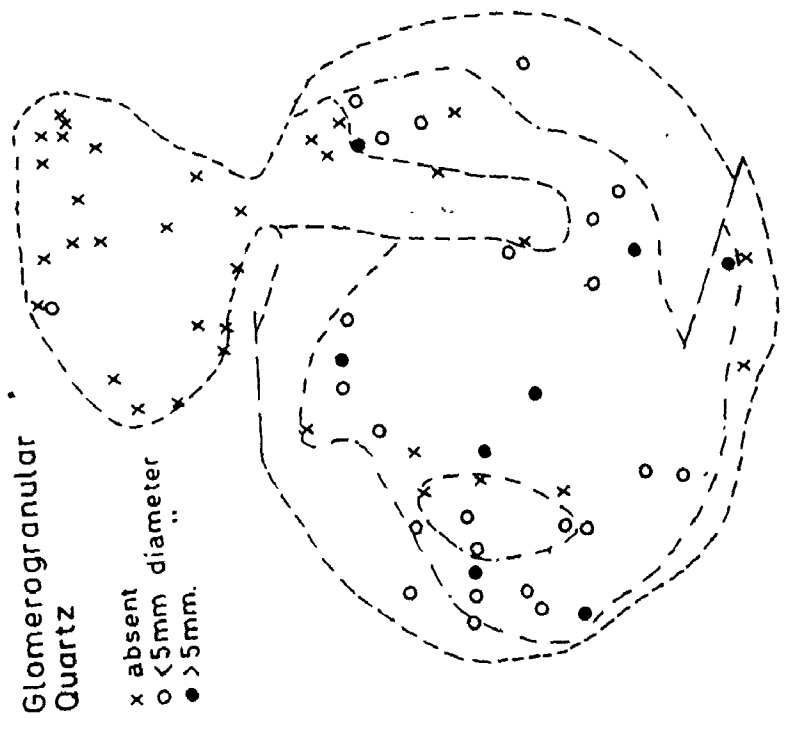


FIGURE 2.9

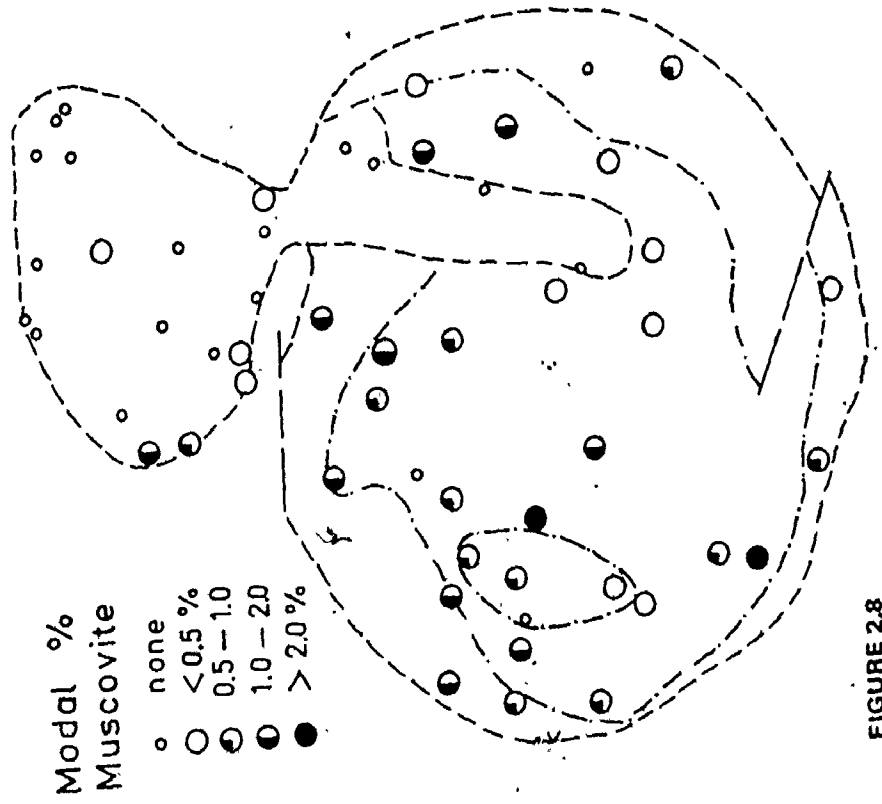


FIGURE 2.8

relict phenocrysts (Barker et al., 1974). On the other hand, for quartz-eyes in hypabyssal porphyries, Hopwood (1976) proposed porphyroblastic growth within an actively deforming matrix. Porphyroblastic or more likely endoblastic¹ growth seems an appropriate explanation for the texture at Burditt Lake, since corrosion textures (Plate A6.2) place quartz late in the crystallization sequence. Field evidence cited previously collaborates this interpretation. If the quartz-eyes from porphyries and the glomerogranular quartz at Burditt Lake are genetically akin, this may provide a criteria for high level emplacement. Glomerogranular quartz may bridge the textural gap between epizonal phaneritic granitoids and hypabyssal felsites.

K-feldspar Megacrysts:

The most striking field feature of the northern lobe is the abundance of 1/2" microcline-perthite megacrysts. Thin section observations reveal a zonal arrangement of plagioclase and hornblende inclusions aligned crystallographically within these megacrysts (Plate A2.3). Several authors (Frasl, 1954; Schermerhorn, 1960; Vance, 1969) have taken these aligned inclusions as definite proof of growth of the megacrysts from magmatic liquids. Probe work by Kerrick (1969) and petrographic work by Hibbard (1965) gives collaborative evidence. However, the recorded occurrence of this texture in porphyroblasts of augen gneisses and within enclaves

¹ endoblastesis: crystalloblastic growth in deuteritic stage of magmatic consolidation.

(Smithson, 1965) suggests the controversy is not resolved.

Two features seen in the Burditt Lake megacrysts favour magmatic origin, the rare occurrence of euhedral quartz inclusions (Plate A4.4) and the single occurrence of a twinned megacryst apparently on the Carlsbad law. Carlsbad twinning has been reported by Schermerhorn (1956, p.76) and Hibbard (1965, p.248). Euhedral quartz in the margins of inlets was reported by Hibbard (1965, p.251).

On the other hand, since the megacrysts at Burditt Lake do not show synneusis relationships, the author concludes that growth occurred after emplacement. Furthermore, the borders of the megacrysts have distinct endoblastic relationships to adjacent matrix grains. The megacrysts disperse at the borders into anhedral groundmass microcline. There is a preponderance of myrmekite at megacryst-plagioclase contacts. This textural evidence along with field evidence of microcline porphyroblasts within lensoid enclaves convinces the author that the megacrysts are either endoblasts or metablasts.

Several textural features reported for such megacrysts and mentioned by other authors were not found by this investigation. Schermerhorn (1958) found less perthite towards the rims of the megacrysts, and concluded that less plagioclase was taken up by the alkali feldspar as crystallization temperatures lowered. The investigation at Burditt Lake suggests more perthite towards the rims. In one recorded case

the perthite forms a thick mantle that is suggestive of rapakivi¹ texture. Schermerhorn (1958) also associates the microcline twinning with the stage of perthite exsolution since twinning seems to concentrate around the perthitic patches. This association was also noted in sections of the Burditt Lake granodiorite, but the twinning was associated as well with plagioclase inclusions.

The author prefers the explanation of Erdmannsdorffer (1950) and Schermerhorn (1958) that attributes the megacrysts to endoblastesis - blastesis from magmatic rest fluids following magmatic crystallization. The megacrysts, therefore, record the transition from a magmatic stage to a metasomatic stage as the fluid phase increases and the granitoid undergoes autometasomatism. This last stage is contemporaneous with the crystallization of groundmass microcline. According to Schermerhorn (1958) it is also contemporaneous with the formation of the enigmatic K-feldspar porphyroblasts in the enclaves.

Corrosion and Replacement Textures:

The prevalence of corrosion and replacement textures in granitoids have been well documented (Augustithis, 1973), although the genetic implications are a continuing debate. Thin sections from all phases of the Burditt Lake Stock yield many examples of mineral embayments, symplectic² intergrowths,

¹rapakivi texture: K-feldspars mantled with Na - plagioclase.

²symplectic: intergrowth of 2 minerals

¹ synantetic reaction rims, etc. Plagioclase appears to record several episodes of corrosion and overgrowth (Plates A6.1 to A6.5), most likely reflecting a sequence of retrograde reactive and metasomatic events since early stages of crystallization.

Worm-like intergrowths of quartz and plagioclase are coined "myrmekite" and form a perplexing problem in granitoid petrography. Theories for their genesis are numerous: replacement of alkali feldspar (Becke, 1908), plagioclase breakdown to quartz and epidote (Sarma and Raja, 1959), metasomatic solutions invading plagioclase along Smekal defects (Drescher-Kaden, 1948), exsolution of albite from orthoclase and recrystallization of cataclastic quartz (Shelley, 1964), exsolution from a high temperature alkali feldspar solid solution (Hubbard, 1967), etc. Many of the classic features mentioned by these authors are evident in the Burditt Lake granitoids. Often cited is the juxtaposition of myrmekite to microcline, in both groundmass and megacryst microcline. Several plagioclase grains were found with myrmekitization only at one end of the lath - the end adjacent to microcline (Plates A6.4, 6.5). Two interesting cases of quartz rhabdites² and blebs encroaching on adjacent K-feldspar were recorded similar to Figure 163 of Augustithis (1973). These imply that myrmekitization preceded the corrosion of the plagioclase by microcline. In several cases, the myrmekite rims around plagioclase were not in direct contact with the microcline

¹ synantetic: produced by reaction of 2 minerals.

² rhabdite: myrmekitic quartz body,
(Augustithis, 1973).

neighbour but were separated by a narrow band of albite overgrowth. This suggests that albitization or decalcification of plagioclase followed myrmekitization.

From the petrographic evidence obtained in this study, no firm support could be established for any of the genetic models. No correlation of myrmekite with abundant cataclastic quartz was seen to support Shelley's idea. In some cases, myrmekite occurred far removed from any K-feldspar; this, however, may just be a cut effect due to the two dimensional nature of the section. What did appear evident is that exsolution from K-feldspar is ruled out. Myrmekite was seen to occur in primary plagioclase unrelated to any overgrowth. The stepped nature of the quartz blebs as recorded by Schermerhorn (1958) was not found.

Another mineral showing frequent symplectic intergrowths with quartz (and feldspar ?) was muscovite. Schermerhorn (1958) reported a similar phenomenon. At Burditt Lake the myrmekite-like habit appears to be a transitional stage in the conversion of biotite to muscovite.

Interesting textures recorded in Plate A6.2 are saw-tooth contacts between quartz and plagioclase compared to more irregular K-feldspar contacts with plagioclase. Schermerhorn (1958) and Augustithis (1973, Figure 594) uncovered similar features. Augustithis (1973) attributed these indentations to invasion by plastically mobilized quartz during tectonic

deformation. The author prefers Schermerhorn's (1958) explanation that: quartz corrosion of plagioclase occurred late stage at low temperature when corrosive powers of invading fluids were less and required adherence to the structural patterns of the host mineral. This provides additional support for late paragenesis of quartz.

Deuteric Minerals:

Most of the muscovite in the southern lobe of the Burditt Lake Stock is secondary, forming shredded fringes around biotite grains or small flakes in sericitized plagioclase, but evidence exists that some flakes are primary. In one thin section, large flakes of muscovite occur mantled by a microcline megacryst. A plot of modal biotite against modal muscovite fails to show a negative correlation - suggesting that alteration from biotite does not account for all of the large flakes.

Epidote has traditionally been considered a late secondary mineral in granites, stemming from the breakdown of plagioclase (Johannsen, 1939, p.181, vol. 2; Schermerhorn, 1961). Such an association with saussurization of plagioclase may be the case at Burditt Lake for a few minor inclusions in plagioclase, but the majority of epidote grains show an association with early formed biotite or its alteration product, chlorite. Furthermore, in some thin sections, epidote shows a definite association with stubby euhedral apatite

grains and zircons. For a similar association of primary accessories with early biotite and hornblende, Schermerhorn (1958, p.97) makes the comment that such minute crystals may serve as convenient crystallization centers. This suggests, therefore, that some of the epidote is magmatic and the textural association with primary accessories is a criterion for the magmatic origin of the granitoid (Schermerhorn, 1958, p.97). More convincing still, however, is the distinct idiomorphic habit and optical zoning exhibited by many epidote grains. Heimlich (1965) reported epidotes from the Flora Lake Stock with "a suggestive hexagonal outline" although he still favoured a secondary origin.

If both muscovite and epidote are considered to be primary phases rather than alteration products, it must be noted that: (muscovite + epidote + microcline + albite) is a low temperature assemblage inconsistent with a magmatic origin and incompatible with the upper amphibolite metamorphic facies assemblages usually attributed to granitoids. The answer lies probably in the "telescoping of mineral facies" of Schermerhorn (1960) or the "mixed facies" concept of Rittmann (1973). Muscovite and epidote represent "low temperature" minerals overprinted on a higher temperature assemblage by retrograde growth during deuteritic autometasomatism (Schermerhorn, 1961). The textural distinction between primary magmatic growth and endoblastic growth may be gradational.

I.C. Numbers:

A semi-quantitative determination of grain size distribution was made by the method of Chayes (1958) employing Identity Change Numbers (I.C.). Chayes defined the I.C. Number as the number of times the mineral species changes over a linear traverse across a thin section. Only essential minerals are counted and the traverse length is preset. For our study, traverses of 100 mm. were carried out and were normalized to 40 mm. to correspond to Chayes' figures. The regional distribution of these values (Figure 2.10) readily distinguishes the fine grained granodiorite phase but shows similar values for the north and south lobe phanerites. There is a concentration of higher I.C. numbers along peripheries of the north and south lobe suggesting a slight chill margin. The range of I.C. numbers (34-130) shows the grain size for the Burditt Lake Stock to be finer than reported for the Ross River quartz-diorite pluton of Manitoba (I.C. Numbers: 16-31; Paulus and Turnock, 1971). This may signify higher emplacement and therefore more rapid cooling, or may just reflect relatively smaller dimensions of the Burditt Lake Stock and therefore more rapid heat loss.

Feldspathized Enclaves:

A megascopic textural feature briefly referred to in the field descriptions of the Burditt Lake Stock is the occurrence of alkali-feldspar megacrysts within mafic enclaves

Identity Change Numbers

40mm traverses
on stained thin sections

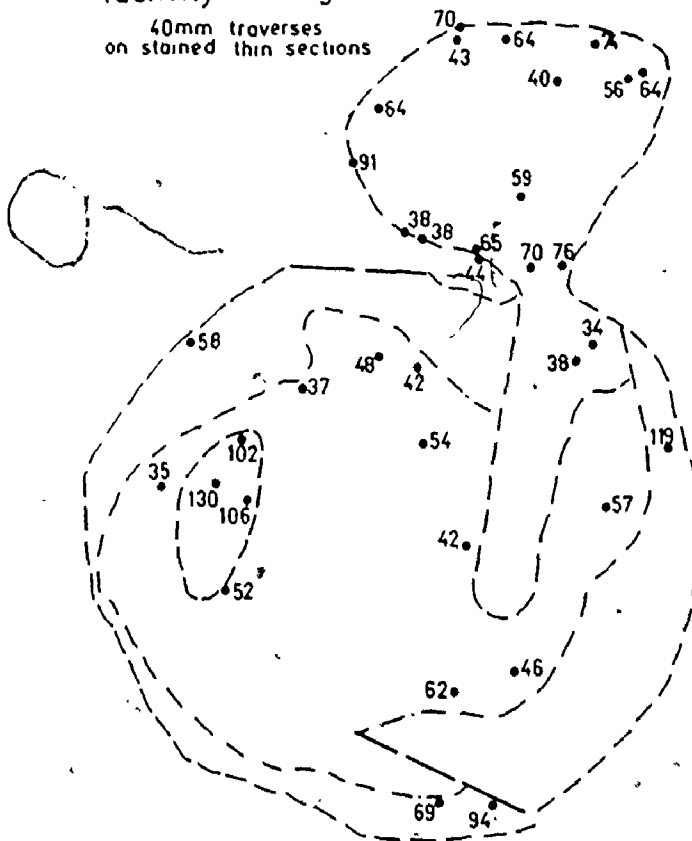


FIGURE 2.10 GRAIN SIZE DISTRIBUTION OVER THE BURDITT LAKE STOCK BASED ON IDENTITY CHANGE NUMBERS. 100 MM TRAVERSES MADE ON STAINED THIN SECTIONS WERE NORMALIZED TO 40 MM TO CORRESPOND TO CHAYES (1958) VALUES. HIGHER NUMBERS SIGNIFY FINER GRAIN SIZE.

(Plate Al.2). The universal occurrence of this texture is evidenced by the number of applicable terms: "porphyry inclusion" (Grout, 1937); "feldspathized enclaves" (Didier, 1973); "dents de cheval" (Read, 1957, p.104); "double inclusions" (Augustithis, 1973, p.16); "double enclave" (Read, 1957, p.187); "filons moniliformes" (Didier, 1973, p.217), and others.

Feldspathized enclaves have been recognized by other Ontario workers (Giblin, 1964, p.14; Pye, 1965; Milne, 1972, p.48), but although a crystalloblastic origin is inferred or stated, it is generally not extended to the textures of the granitoid proper. Pye (1965) reports for a porphyry of the Georgia Lake area:

"... the inclusions commonly exhibit porphyroblasts of feldspar identical to the phenocrysts of the enclosing porphyry". (p.12)

In another report he describes the "porphyritic" Rosspoint granite near Schreiber, Ontario, as having formed by a two-stage crystallization. Feldspar phenocrysts formed slowly at depth while the groundmass crystallized under the chill conditions of emplacement (Pye, 1969, p.69). This explanation, as implied by the term "phenocryst" is routinely applied to insets even when the presence of feldspathized enclaves provides powerful contrary evidence. A more appropriate field term in ambiguous cases would be "porphyric" as coined by Sylvester (1964).

In Archean granitoids the megacrysts enclosed in enclaves are invariably microcline-perthite, including and replacing plagioclase. However, "double enclaves" of plagioclase and/or quartz are not unknown (Grout, 1937, p.1542; Milne, 1972; Joyce, 1973, p.183). For chronologically younger granitoids, authors have even reported zoned plagioclase as "double enclaves" (Pitcher and Berger, 1972, p.105).

Genetic interpretations of the enclave insets argue between endoblastic growth induced by the pneumatolitic activities of the emplaced magma (Schermerhorn, 1958) and true metablastic growth after consolidation (Stone and Austin, 1961, p.466; Augustithis, 1973). Few geologists subscribe to the mechanical emplacement hypothesis of Thomas and Smith (1932, p.289). Erdmannsdorfer (1946) suggested that the insets in the host granitoid began growth as phenocrysts under magmatic conditions, but completed growth metasomatically during the pneumatolitic stage by endoblastesis. The insets of the enclaves grew during this last stage. The "double enclaves" are therefore metablasts, while the insets of the granite proper are endoblasts (Augustithis, 1973).

The megacrysts of the enclaves have been often demonstrated to be analogous in size (Schermerhorn, 1958); texture (Smithson, 1966), and chemistry (Spencer, 1938), to the insets of the host granitoid. A distinct history for the enclave insets different from the granitoid megacrysts is hard to

support. Special attention has been focused on oriented plagioclase and mafic mineral inclusions within the microcline-perthite insets (Schermérhorn, 1956; Sylvester, 1964; Hibbard, 1965; Smithson, 1966; Kerrick, 1969, etc.). Hibbard (1965) claimed that this texture is definitive of magmatic crystallization based on an outward increase in albite content of plagioclase inclusions arranged zonally in a microcline-perthite megacryst. His chemical evidence could as well be interpreted as the product of exsolution of sodic plagioclase from the alkali host. Kerrick's (1969) study showed sodic rims of plagioclase inclusions to be optically distinct.

Regarding the chemistry of feldspar crystalloblasts, Spencer (1938) predicted:

"One would expect such crystals to be less homogeneous than those formed from magmas, owing, firstly to unassimilated non-feldspathic material, and secondly to the lessened mutual solubility of the two feldspars at lower temperatures". (p.112)

Such inhomogeneity has been documented recently by Piwinski (1968, p.216) and Kerrick (1969, p.842) for the insets of the granitoids proper of Sierra Nevada. This chemical evidence plus the works of Marmo (1971, p.43) and Augustithis (1973, p.20) form a powerful argument for a crystalloblastic origin for all the alkali feldspar megacrysts, whether in the enclaves or in the host. Convincing field

evidence to support this notion are the megacrysts straddling enclave-granitoid boundaries (Schermerhorn, 1956, p.343, 1958, p.78; Stone and Austin, 1961, p.470; Marmo, 1971, p.46; Didier, 1973, p.149; Plate Al.1 of this study).

The recognition of "double enclaves" in the Burditt Lake Stock makes a significant contribution towards demonstrating post-magmatic metasomatism and explaining the other textural complexities. The occurrence of megacrysts in the enclaves but not in adjacent country rock attests to the localized nature of the metasomatism, in contrast to the extensive contact metasomatism reported for another region by Sylvester (1964). "Double enclaves" may also be evidence that the mafic lensoid enclaves have an igneous origin (Didier, 1973).

Textural Conclusions:

All the textural evidence points to extensive late-stage autometasomatism: feldspathization of enclaves, myrmekitization, albitization or decalcification of plagioclase, growth of inlets, etc. The difference in mineralogy between the northern hornblende granodiorite and the southern muscovite granodiorite may likewise be due to reactions and overgrowths caused by autometasomatism. Although a complete investigation of reaction paths is beyond the present thesis, there are suggested textural trends:

(1) hornblende → biotite → muscovite

(2) plagioclase → myrmekite → albite → microcline → perthite → quartz

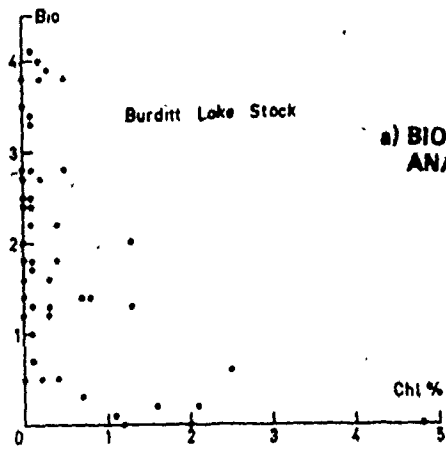
The first suggested reaction path is supported by negative correlations between modal biotite and hornblende and epidote and hornblende (Figures 2.11 b and c) and biotite-epidote pseudomorphs after hornblende. Biotite versus muscovite and biotite versus chlorite show no correlation, suggesting complex derivatives. The second path is a simplified summary of correlative relationships, but may reflect the changing chemistry of metasomatic fluids. Schermerhorn (1958) claims that the crystallization of K-feldspar correlates with the transition:

hornblende gabbro facies → albite-epidote amphibolite facies

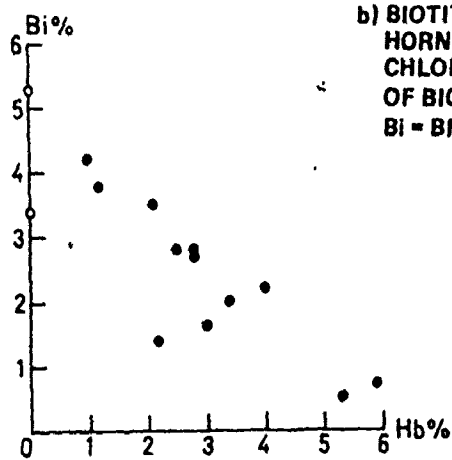
Autometasomatism is therefore auto-retrograde metamorphism.

Schermerhorn (1960) considers quartz bipyramids to form during gabbro facies conditions and if preserved (for example, rarely in megacrysts at Burditt Lake) to represent armoured relics spared from resorption by inclusion in still later minerals.

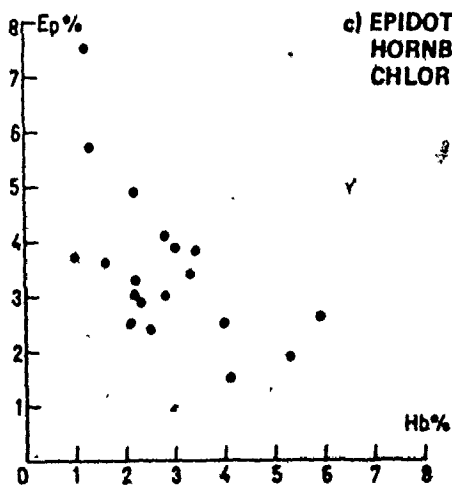
Although he applies the same explanation to quartz-eyes in hypabyssal porphyries, the author prefers to consider the quartz-eyes of Burditt Lake to be second generation endoblasts similar to the feldspar megacrysts.



a) BIOTITE-CHLORITE: BASED ON THIN SECTION 1000 PT. ANALYSES OF NORTH AND SOUTH LOBE SAMPLES.



b) BIOTITE-HORNBLLENDE: POINT COUNTS ON NORTH LOBE HORNBLLENDE GRANODIORITE. SAMPLES WITH HIGH CHLORITE OMITTED (GREATER THAN 40% OF BIOTITE + CHLORITE).
Bi = BIOTITE + CHLORITE



c) EPIDOTE-HORNBLLENDE: POINT COUNTS ON NORTH LOBE HORNBLLENDE GRANODIORITE. SAMPLES WITH HIGH CHLORITE OMITTED i.e. > 2% .

FIGURE 2.11 MODAL VARIATION DIAGRAMS FOR THE BURDITT LAKE STOCK

Geochemistry

Introduction: Major Elements

The best method of displaying whole-rock geochemical data is a continuing controversy with adhesions dependent on which of three problems are being tackled: classification, distinction or genesis. Major elements are traditionally presented as oxide weight percents and have been so listed in the appendix of this study, but other formats such as ionic weight percents (Green and Poldervaart, 1958) or cation and oxide weights per unit volume (Whitten, 1975) may be equally or more appropriate. Genetic interpretations of large numbers of analyses are best made by defining petrochemical fields or trends on two or three dimensional graphical displays. Simple linear variation diagrams such as Harker plots of SiO_2 versus oxides have been discredited on the one hand because of inherent correlation between variables (Tuominen, 1964; Chayes, 1967), because they distort genetic trends by changing their slopes (Pearce, 1968), or because the range and change of a single variable abscissa may not reflect petrogenetic processes (Wager, 1956), but on the other hand they are still promoted elsewhere (Wright, 1974). Many attempts have been made to generate useful multivariate plots:

(A) by summing of components:

1. Larsen Index = $1/3\text{SiO}_2^{\text{wt}} + \text{K}_2\text{O} - \text{MnO} - \text{CaO} - \text{FeO}$

(Larsen, 1938)

2. Modified Larsen Index = $1/3\text{Si} + \text{K} - \text{Ca} - \text{Mg}$

(Nockolds and Allen, 1953)

(B) by ratios:

1. Molar ratios: e.g. $\frac{\text{CaO}}{\text{Al}_2\text{O}_3}$ versus $\frac{\text{FeO}}{\text{Al}_2\text{O}_3}$

(Pearce, 1968)

2. Felsic Index: $\frac{(\text{Na}_2\text{O} + \text{K}_2\text{O}) \times 100}{\text{CaO} + \text{Na}_2\text{O} + \text{K}_2\text{O}}$

(Simpson, 1954)

3. Mafic Index: $\frac{(\text{FeO} + \text{Fe}_2\text{O}_3) \times 100}{\text{MgO} + \text{FeO} + \text{Fe}_2\text{O}_3}$

(Simpson, 1954)

4. Alkalinity Ratio: $\frac{\text{Al}_2\text{O}_3 + \text{CaO} + \text{alkalis}}{\text{Al}_2\text{O}_3 + \text{CaO} - \text{alkalis}}$

(Wright, 1969)

5. Iron Ratio: $\frac{\text{Fe}^{+2} + \text{Mn}}{\text{Fe}^{+2} + \text{Mn} + \text{Mg}}$

(Wager, 1956)

(C) by ternary plots:

1. Ca versus K versus Na

2. Ca versus Fe versus (Na + K) etc. (Green and Poldervaart, 1958)

(D) by recasting analyses into normative mineral ratios:

1. Differentiation Index: weight % normative quartz + orthoclase + albite + nepheline + leucite + Kalsilite (Thornton and Tuttle, 1960)
2. Crystallization Index: weight % normative anorthite + diopside + forsterite + enstatite + spinel (Poldervaart and Parker, 1964)
3. Albite Ratio: $\frac{\text{mol. albite}}{\text{mol. albite} + \text{anorthite}}$ (Wager, 1956)

Formulation of most of these ratios and indices represents attempts to reflect fractional crystallization and assumes that this mechanism is the primary cause of diversity in rock chemistry. Trends on linear variation diagrams employing the indices are usually assumed to represent differentiation based on fractional crystallization, despite that inherent correlation of variables is not entirely absent (Chayes, 1967). Unfortunately the indices and ratios were developed for volcanic suites and most are not strictly applicable to granitoid rocks. The Crystallization Index, Mafic Index, and Iron Ratio were designed to reflect the earliest stages of fractionation series which have little application to the generation of granitoids. The Differentiation Index of Thornton and Tuttle (1960) deals with "petrogeny's residua system", but because it is based on the CIPW norm, it is also not strictly applicable to granitoids.

Hall (1967) partially solved this by adding normative corundum to allow for muscovite granites. A modified differentiation index based on the mesonorm of Barth (1959) would provide a better compromise but the author is loath to add still another "index" to the already cluttered literature.

In the following thesis, a variety of the above mentioned plots is employed, but interpretations are tempered by the following considerations:

- (1) Numerous other plots and indices could be used to obtain the same or similar trends;
- (2) Application of the indices to granitoids may not correlate with original proposals;
- (3) Inherent correlation of variables may have generated part or all of the observed trends;
- (4) The underlying assumption of fractional crystallisation is not proven;
- (5) A major function of the plots is to differentiate between rock types rather than to imply genetic models.

Major Elements: Burditt Lake Stock:

Major element oxides for Burditt Lake listed in the appendix include 68 whole-rock analyses from the pluton proper and 25 analyses from related aplitic and pegmatitic phases, mafic enclaves and surrounding metavolcanics. Three geochemical

phases can be visually separated, correlating with the bi-hb granodiorite; musc-bi granodiorite and pink saccharoidal patches within the foliated border. The distinction between phases is sufficiently subtle to lend credence to Whitten's (1962) argument that limited sampling of "homogeneous" plutons may not yield satisfactory "average" compositions nor reflect variability.

Major Elements: Petrochemical Fields and Trends:

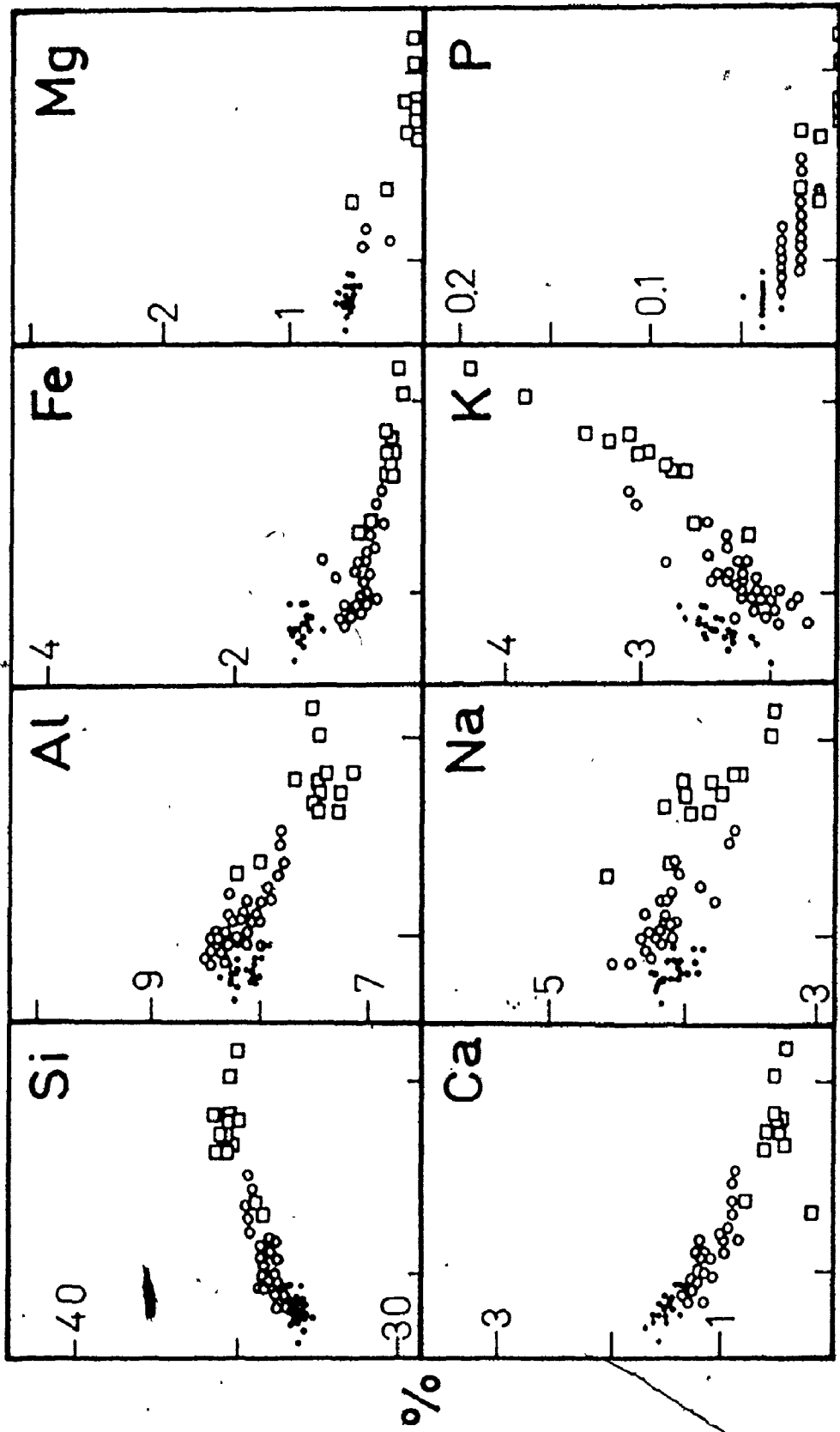
A binary plot of major cations against the modified Larsen Index of Nockolds and Allen (1953) reveals clear separations of the above three petrochemical groups (Figure 2.12). The data clusters could be interpreted as straddling a very limited portion of a fractional crystallization path with the north lobe bi-hb granodiorite representing the most primitive phase.

Trends predicted for calc-alkali series rocks are: a positive correlation of Si and K with the index, negative correlation of Ca, Mg and Fe, and almost horizontal patterns for Al and Na (Larsen, 1938; Nockolds and Allen, 1953). The element abundances between the north and south lobe follow tradition with the exception of K. There is an obvious K-enrichment for the more basic north lobe granodiorite.

The Ca-Na-K system has been proposed as a useful petrochemical plot for granitoids because it reflects feldspar

FIGURE 2.12
BINARY PLOTS OF MAJOR CATIONS VS
MODIFIED LARSEN INDEX OF NOCKOLDS
AND ALLEN (1953), FOR THE BURDITT
LAKE STOCK SAMPLES.
SYMBOLS AS FOLLOWS:

- BI-HB GRANODIORITE
- MUSC. - BI. GRANODIORITE
- APLITIC AND
APLITE-PEGMATITE DYKES
AND PERIPHERAL PATCHES.



MODIFIED LARSEN

FIGURE 2.12

fractionation which in granitoids dominates over fractionation of ferromagnesian (Green and Poldervaart, 1958), and because the plot may be able to distinguish fields of "magmatic granites" from fields for "replacement granites" (Raju and Rao, 1972). Figure 2.13 shows that Burditt Lake phases locate on the Na side of the "igneous trend line" of Green and Poldervaart (1958). The displacement of data from the "igneous trend line" suggest that local processes predominated over processes of fractionation (Green and Poldervaart, 1958), and that the Na/K ratio is higher than predicted from fractionation. On the Ca-Na-K diagram of Raju and Rao (1972) the Burditt Lake phases would overlap with the "magmatic granitic field" but locate partially outside towards the Na apex. Since a "replacement" origin for the Burditt Lake Stock is untenable from petrographic evidence, the "magmatic field" is probably too restrictive and the chemical distinction between "replacement" and "magmatic" granitoids has not been demonstrated.

Another graphic display of the fractionation model is given by Simpson's (1954) plot of Felsic Index versus Mafic Index. This plot should illustrate the competing paths of feldspar fractionation (Felsic Index) versus ferromagnesian fractionation (Mafic Index). Non-selective fractionation should generate a 45° linear gradient (Simpson, 1954), whereas for average igneous rocks Green and Poldervaart (1958) showed the Felsic Index to dominate 2:1. The F-M plot for the Burditt Lake Stock (Figure 2.14) follows the original oxide format of

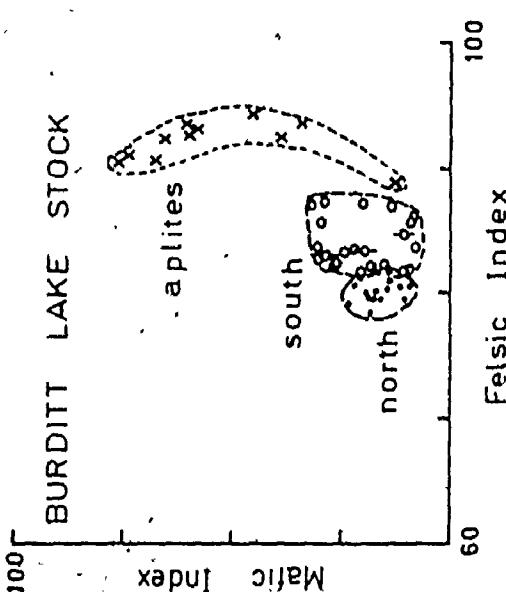


FIGURE 2.14

FELSIC INDEX VERSUS MAFIC INDEX PLOT OF SIMPSON (1954) FOR THE BURDITT LAKE STOCK:
 [•] BI-HB GRANODIORITE
 [o] MUSC.-BI GRANODIORITE
 [x] APLITES, APLITE-PEGMATITES

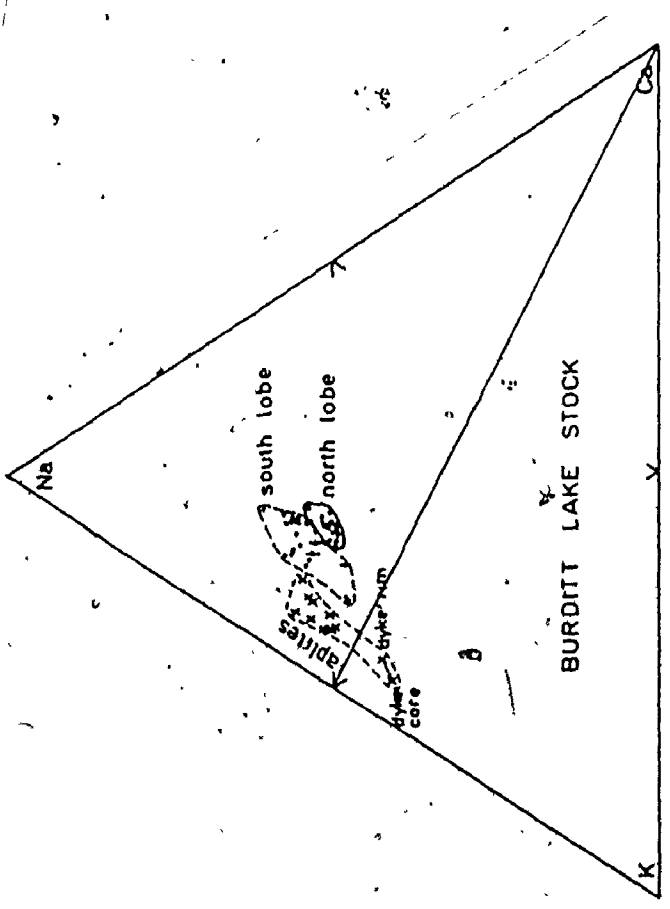


FIGURE 2.13

CA-NA-K PLOT OF GREEN AND POLDERVAART (1958) FOR THE BURDITT LAKE STOCK:
 [•] BI-HB GRANODIORITE
 [o] MUSC.-BI GRANODIORITE
 [x] APLITES, APLITE-PEGMATITES

Simpson (1954) but corresponds roughly to the top right corner of Green and Poldervaart's (1958) Figure 2, which is expressed in ionic weight percents. The Burditt model follows the "igneous trend" (Green and Poldervaart, 1958) with a sharp slope change for aplites, corresponding to a similar curve for "strong sodic granites" on Green and Poldervaart's (1958) plot. This suggests late development for some ferromagnesians - possibly deuteritic growth of epidote or reflects rapid depletion in MgO (driving the mafic index to 100).

Trace Elements:

Introduction:

Treatments of published trace element data show the same diversity of plots, ratios and indices as characterizes major element studies. Petrogenetic fields and trends have been sought on linear variation diagrams, ternary diagrams, etc., generally with the underlying assumption that crystal fractionation dictates distribution. Recent studies have been directed towards quantitative trace element theories using partition coefficient data to model partial melting or fractional crystallization (Ryabchikov, 1962; Arth and Hanson, 1975; Arth, 1976, McCarthy and Hasty, 1976). As with theories of major element differentiation, most of the quantitative trace element modelling has involved volcanic suites. At present, the available models do not incorporate the complexities of metasomatism, endoblastesis, etc., that dominate in granitoid

genesis. Furthermore, Tauson (1967) has argued that trace element distribution in granitic magmas is a function of composition, size, depth and tectonic setting of the intrusive. The influence of depth was confirmed by Shmakin (1971). Because of these complexities as applied to granitoids, no quantitative model was attempted in the current thesis.

Appendix D1 tabulates the following trace elements determined for samples of the Burditt Lake Stock: Rb, Sr, Y, Zr, Nb, Ba, Ce, U, Th. Th and U were obtained in situ by portable gamma-ray spectrometry and only a few field stations corresponded to sample locations. These radioelements will be discussed separately. Rubidium and strontium analyses were not only necessary for the geochronological portion of this thesis (Chapter 4), but Rb has been found a useful tracer of post-magmatic metasomatism (Vlasov, 1966), while the trio Rb-Ba-Sr have been used as a trace element measure of major silicate fractionation in granitoids (McCarthy and Hasty, 1976). Rare earth elements such as Ce and related Y increase with magmatic differentiation and are nearly three times as abundant in granites as in basalts (Koljonen and Rosenberg, 1974). Furthermore, their relative insensitivity to metamorphic or metasomatic disturbances make them useful tracers of original distribution patterns. Zirconium concentration has been used as a measure of magmatic alkalinity. Under alkaline conditions, zirconium will not crystallize wholly as zircon, but will be

mainly incorporated in the lattices of mafic minerals (Bowden, 1966). Both zirconium and niobium form complexes in silicate magma and therefore provide an indication of the role of polymerization in element distribution. A further major consideration in the selection of trace elements for analysis was the relative concentrations. Blackburn (1976) obtained analyses for one sample of the Scattergood Lake Stock for twenty trace elements of which only Ba, Sr and Zr gave values greater than 100 ppm. Many elements (As, Be, Co, Mo, Ni, Sb, Sc, Sn) were present in concentrations near to or below analytical detection, and therefore would not yield petrogenetic information. Similar concentrations were anticipated in rocks of this study.

Linear Variations: Burditt Lake Stock

If fractional crystallization dominates trace element distribution (on a first approximation), the physicochemical factors discussed by Ringwood (1955a,b) and Taylor (1964) predict residual enrichment in Rb, Zr, Y, Nb, Ba and rare earths and residual depletion in Sr. Corresponding ratios that decrease with differentiation are Ba/Sr and K/Rb, while Sr/Ca and U/Th increase.

Linear variation diagrams are plotted for the Burditt Lake Stock using the modified Larsen Index as abscissa (Figures 2.15 to 2.21). The trends with increasing indices are a strong negative correlation of Sr and a weak negative

**FIGURES 2.15 TO 2.21:
LINEAR VARIATION DIAGRAMS FOR TRACE
ELEMENTS IN THE BURDITT LAKE STOCK,
VERSUS THE MODIFIED LARSEN INDEX OF
NOCKOLDS AND ALLEN (1953).**

SYMBOLS AS FOLLOWS:

- BI-HB GRANODIORITE
- MUSC. - BI. GRANODIORITE
- APLITES AND APLITE PEGMATITES.

FIGURE 2.15

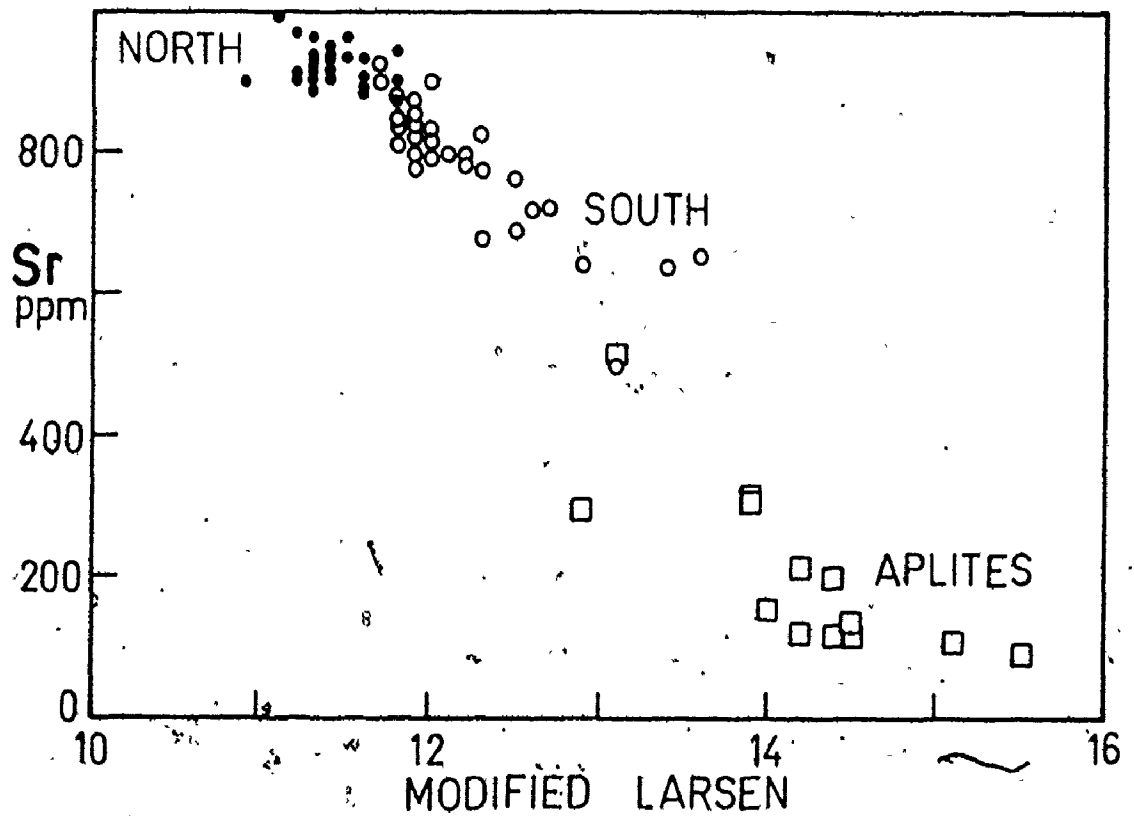
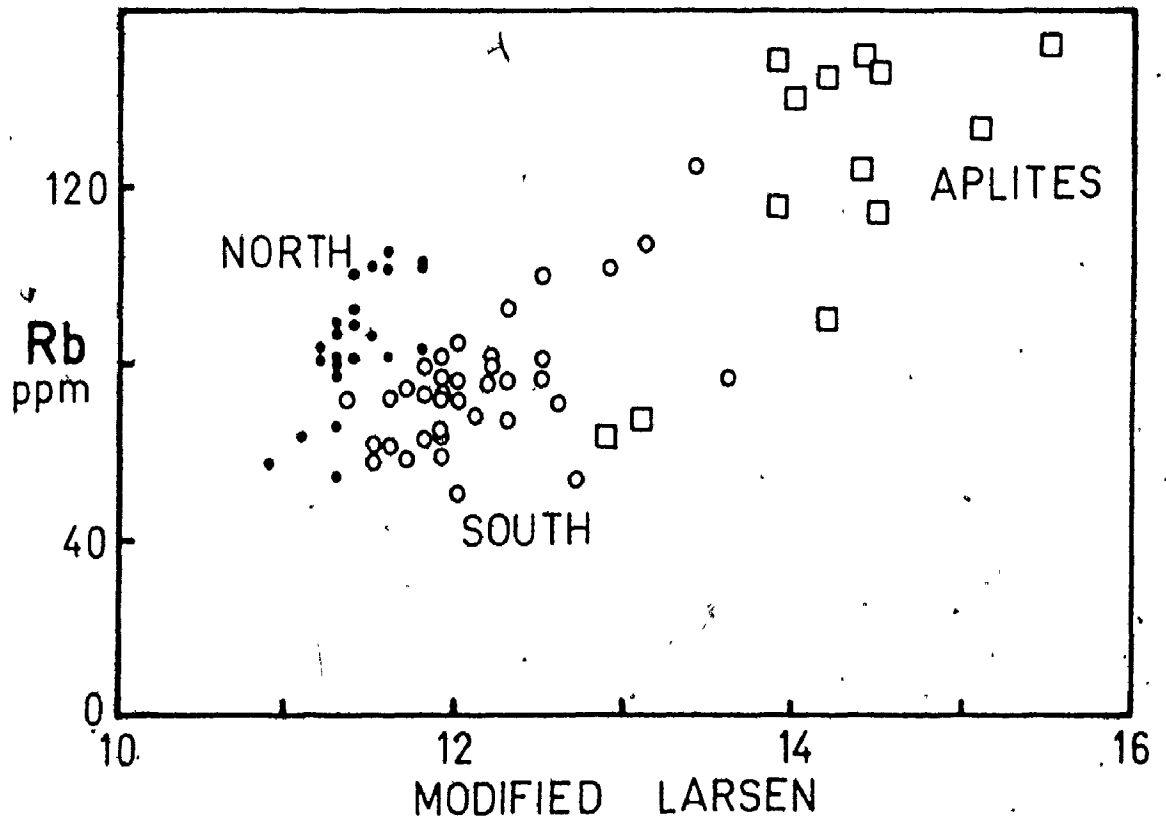


FIGURE 2.16

FIGURE 2.18

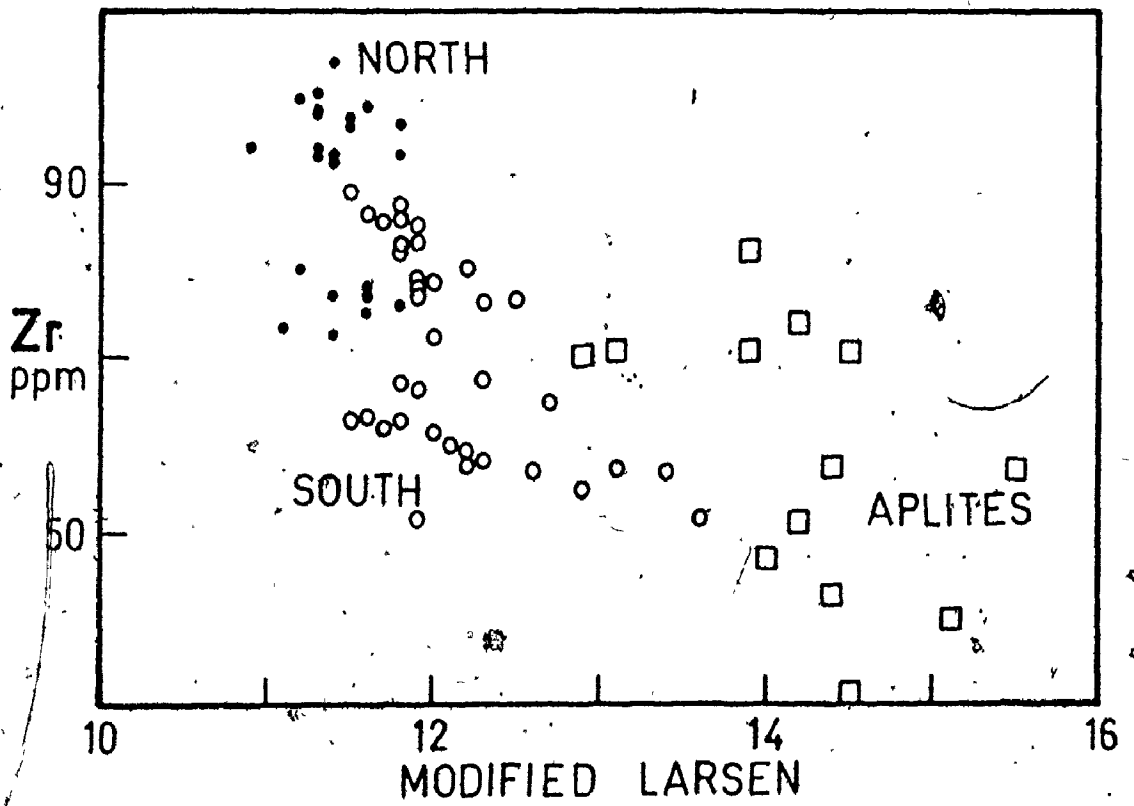
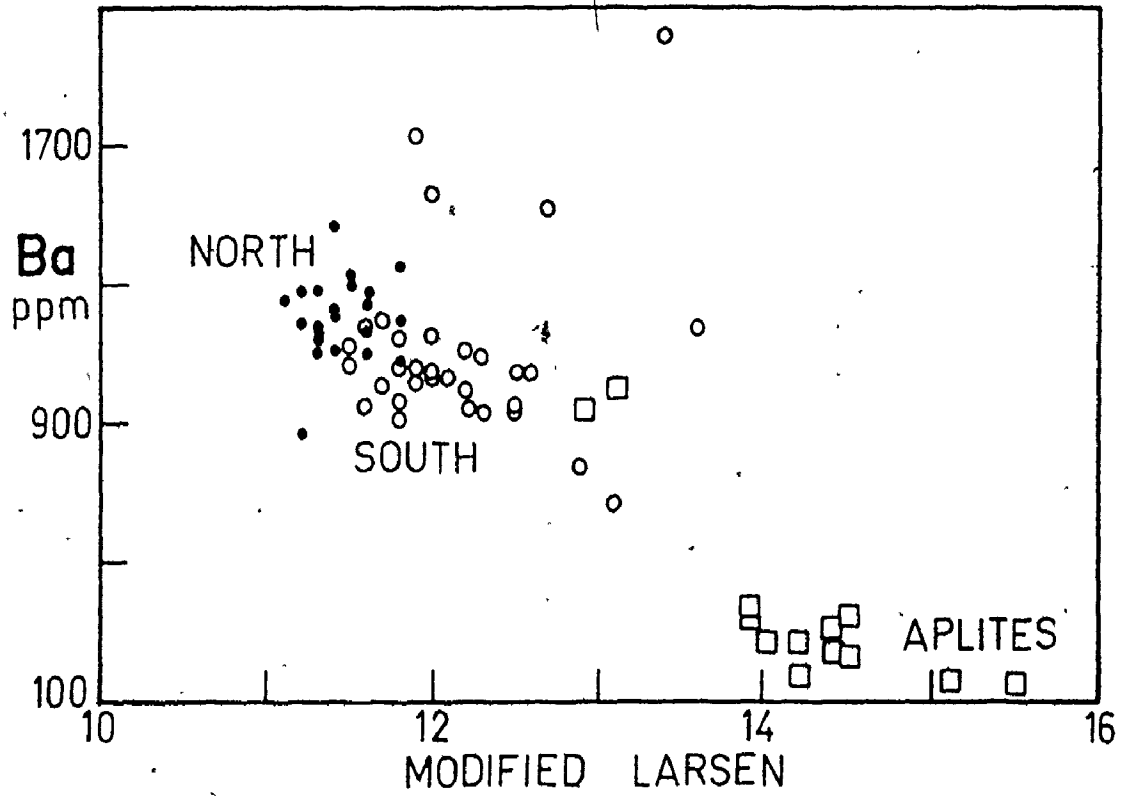


FIGURE 2.17

FIGURE 2.19

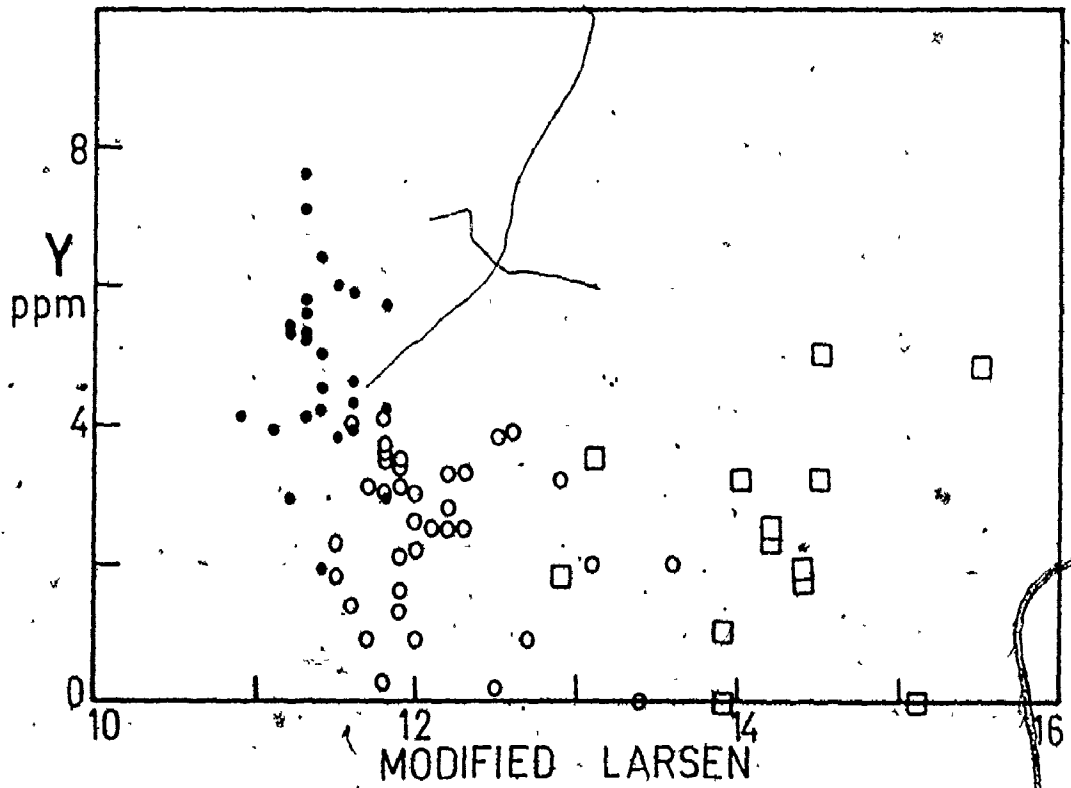
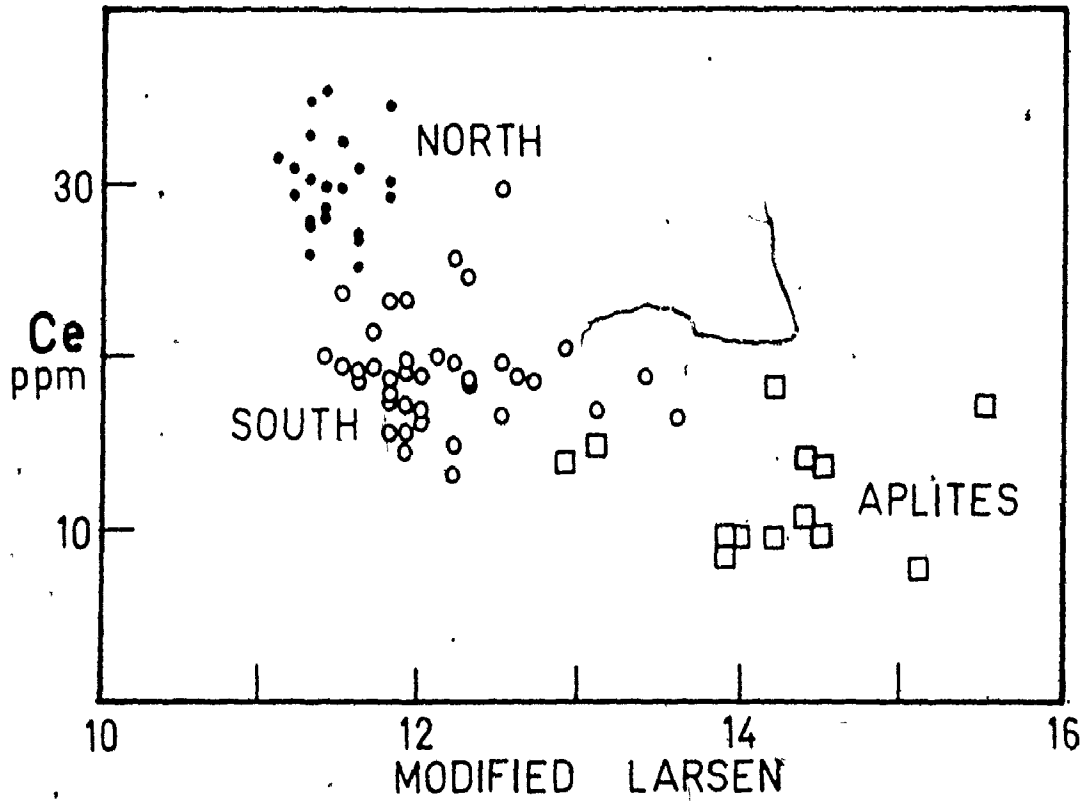


FIGURE 2.20

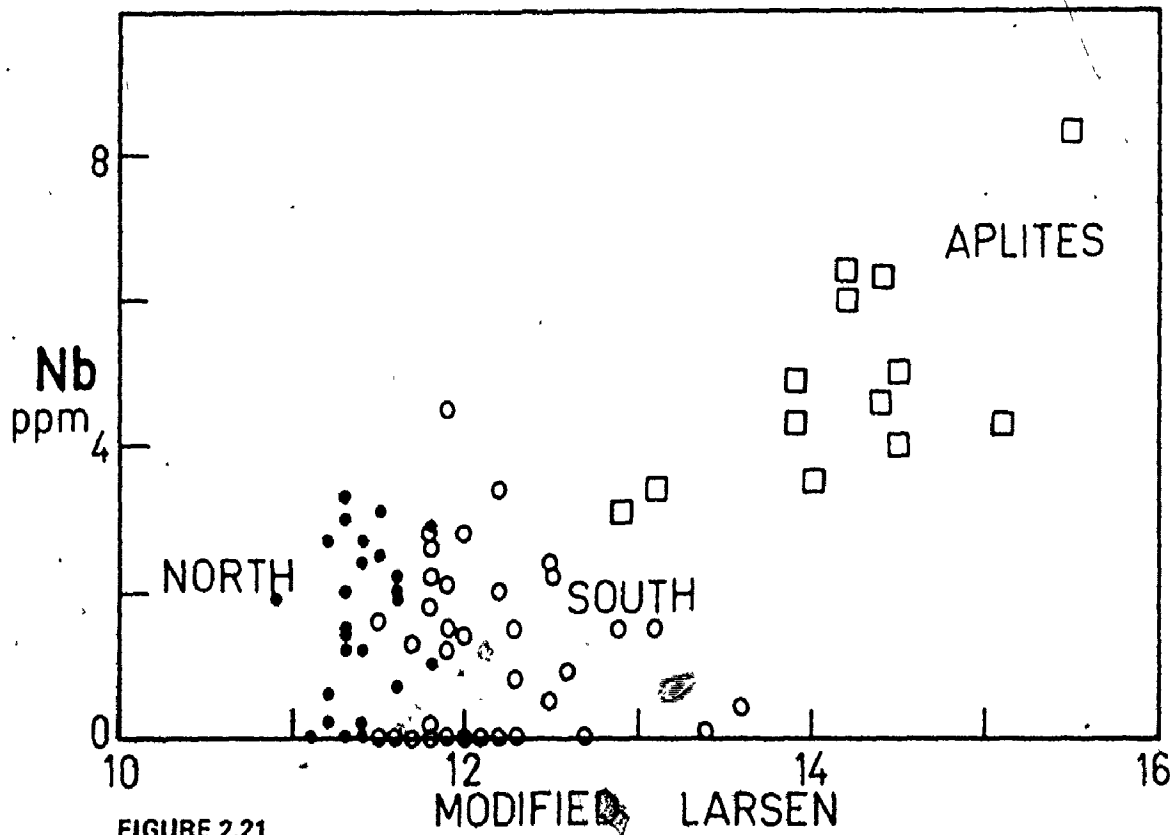


FIGURE 2.21

correlation in Zr and Ce. The dominant pattern for Ba is depletion with index, but this pattern is distorted by five enriched outliers from the south lobe and one depleted outlier from the north cluster. Yttrium shows depletion from the north lobe granodiorite to the south lobe granodiorite, but the trend pattern for higher indices is obscure because of proximity to the detection limit (1.2 ppm, Appendix D). There is a suggestive curvilinear pattern of depletion followed by slight enrichment in aplites. Low concentrations for niobium (detection limit of 2.0 ppm, Appendix D) have also obscured the pattern except for distinct enrichment in aplites.

A sequential depletion-enrichment pattern is apparent for rubidium. Although the concentrations for the north and south lobes are approximately equal, the north lobe granodiorite carries higher Rb for an equivalent index. On the other hand, the aplites also show enrichment. This pattern could be generated by a metasomatic overprint of a primary positive correlation of Rb with index. The north lobe with lower index may have suffered addition of Rb.

The sequential depletion-enrichment phenomenon exhibited by Rb mimicks a similar anomalous pattern uncovered earlier for K. This illustrates the sympathetic behaviour of these two elements, but goes contrary to predictions from the fractional crystallization model. The observations of Vlasov (1966) provide an alternative:

"...In postmagmatic metasomatic formations of the granite series, rubidium is a characteristic element related genetically to (a) greisenized alaskite massifs; (b) greisenized granites (early stage of postmagmatic metasomatism); (c) fluoritization zones in carbonate rocks; (d) vein fillings (quartz-cassiterite and quartz-topaz veins); (e) albitized granites." (p.60)

The recognized mobility of Rb in metasomatic environments suggests that both Rb and K were redistributed by metasomatic processes following initial residual concentration. The redistribution involved migration of Rb and K to the northern lobe to explain the sequential depletion-enrichment pattern. Ringwood (1955b) predicted that the degree of SiO_4^{-4} polymerization in the magma controls the crystallization of accessory minerals and consequently the removal of certain trace elements. Volatile-free acid magmas have a high degree of polymerization and crystallize accessories early, while volatile-rich acid magmas possess a lower degree of polymerization and precipitate late accessories. Both Zr and Nb form complexes in silicate magma that either concentrate in the residual fluids or are scavenged by accessory minerals (Ringwood, 1955b). Nb is commonly taken up by sphene or in lesser amounts by biotite (Parker and Fleischer, 1968). The enrichment of Nb in the aplitic phases suggests the controlling influence of volatile phases in keeping Nb in solution despite the fact that sphene is a ubiquitous phase in the modes (Appendix B.1). On the

other hand, rare earths such as Ce and associated Y should also concentrate in residual liquids (Ringwood, 1955b), yet the plots show a strong negative correlation with index.

Nagasawa and Schnetzler (1971) have demonstrated that mafic mineral rare earth partition coefficients are much larger for acidic magmas than in basic magmas. Crystallization of hornblende, zircon and apatite in the north lobe granodiorite effectively depleted the magma chamber prior to generation of the south lobe granodiorite. The Ce and Y patterns of Figures 2.19 and 2.20, which violate Ringwood's and Taylor's predictions, nevertheless are interpreted as reflecting primary distribution patterns showing the more primitive nature of the north lobe.

Zirconium distribution has been tied to alkalinity conditions with concentrations proportional to the apatitic coefficient: $\frac{Na + K}{Al}$ (Bowden, 1966). This factor could not be significant in distributing the element over a relatively homogeneous pluton such as at Burditt Lake. The distribution of Zr goes contrary to predictions from fractional crystallization, but is compatible with Ringwood's (1955b) observations on complex formation. Some Zr^{4+} probably replaced Ca^{2+} in apatite while the majority precipitated out as zircon. A curiosity is the two concentration clusters shown for the northern lobe of the Burditt Lake stock: the significance of this will be dealt with later.

These petrochemical patterns demonstrate that the relatively homogeneous felsic plutons such as the Burditt Lake

Stock record only the tail-end of differentiation which may not parallel broad trends for the entire melanic-felsic petrogenetic spectrum. These trends may furthermore be overprinted by metasomatic redistributions. A comparison of the Burditt patterns with the trends for the extreme acid end of the Southern California Batholith (Nockolds and Allen, 1953) shows that Sr, Rb and Zr behave likewise, but Y and Ba trends are antipathetic.

Comparisons with the Snowy Mountains granodiorite of Australia (Kolbe and Taylor, 1966), or the Rosses granite complex of Ireland (Hall, 1967), shows similar directions of trend. This supports Tauson's (1967) argument that trace element distribution is not just governed by crystallochemical considerations, but is also a function of the degree of magma degassing and the depth and nature of emplacement. These physical factors would be strongly operative in late-differentiates.

Ternary Ba-Rb-Sr:

The triumvirate of Ba-Rb-Sr has been recommended as a useful model of differentiation because these elements occur only in major silicates and not in accessories (McCarthy and Hasty, 1976). Bouseily and Sokkary (1975) have proposed this ternary relationship as a criterion for distinguishing magmatic from metasomatic or granitized granites.

Figure 2.22 shows the Burditt Lake analyses on a ternary Ba-Rb-Sr plot subdivided by the petrogenetic fields of Bouseily and Sokkary (1975). The author does not fully subscribe to the interpretations of these authors. Especially contentious is the "anomalous granite" field through which these authors draw their "differentiation trend". This diagram however provides a useful comparative study. The following observations are made from the Burditt plot:

- (1) Phanerites plot in the "granodiorite field" as expected.
- (2) The north lobe hornblende granodiorite yields a tight cluster of points, whereas the south lobe muscovite granodiorite field is spread out along the Ba-Sr axis.
- (3) There is no evidence of differentiation between the north and south lobe.
- (4) Aplitic phases do not locate in the "strongly differentiated" field.
- (5) Both the south lobe granodiorite and the aplitic fields overlap with the "anomalous granite" quadrilateral.

Bouseily and Sokkary (1975) concluded that absolute values of Rb, Ba and Sr, or the binary relations between any pairs of these elements, do not reliably trace differentiation in granitic rocks. They proposed that the Ba/Sr ratio dominates distribution in the main differentiation sequence, while late-residual differentiation is better illustrated by Ba/Rb.

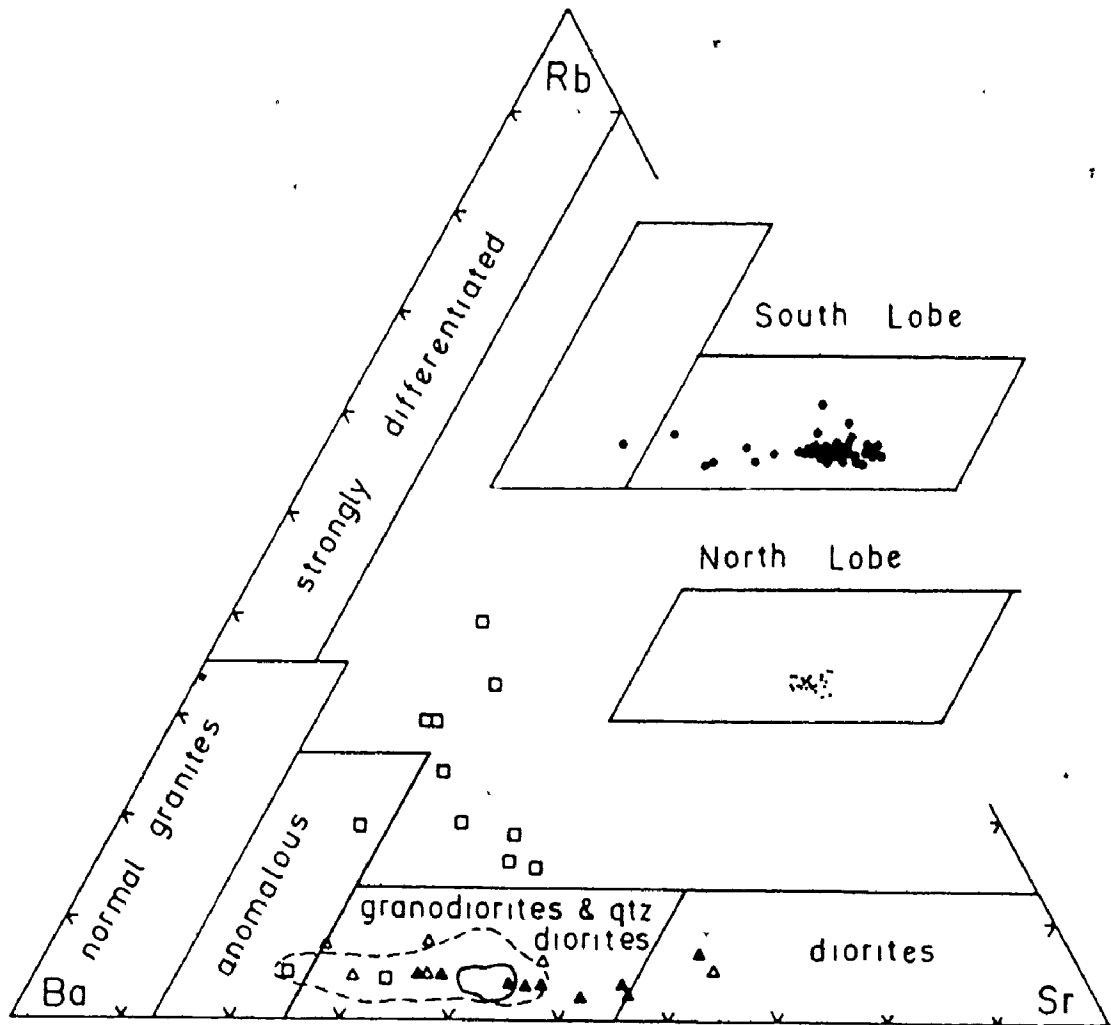


FIGURE 2.22 BURDITT LAKE STOCK ANALYSES ON A BA-RB-SR PLOT OF BOUSEILY AND SOKKARY (1975).
 BI-HB GRANODIORITE: [•] AND SOLID FIELD.
 MUSC-BI GRANODIORITE: [•] AND DASHED FIELD.
 APLITES & PEGMATITES: [□]
 ADJACENT METAVOLCANICS: [▲]
 ENCLOSED MAFIC ENCLAVES: [△]

INSETS ARE ENLARGEMENTS OF GRANODIORITE - QTZ DIORITE FIELD AND ANOMALOUS FIELD.

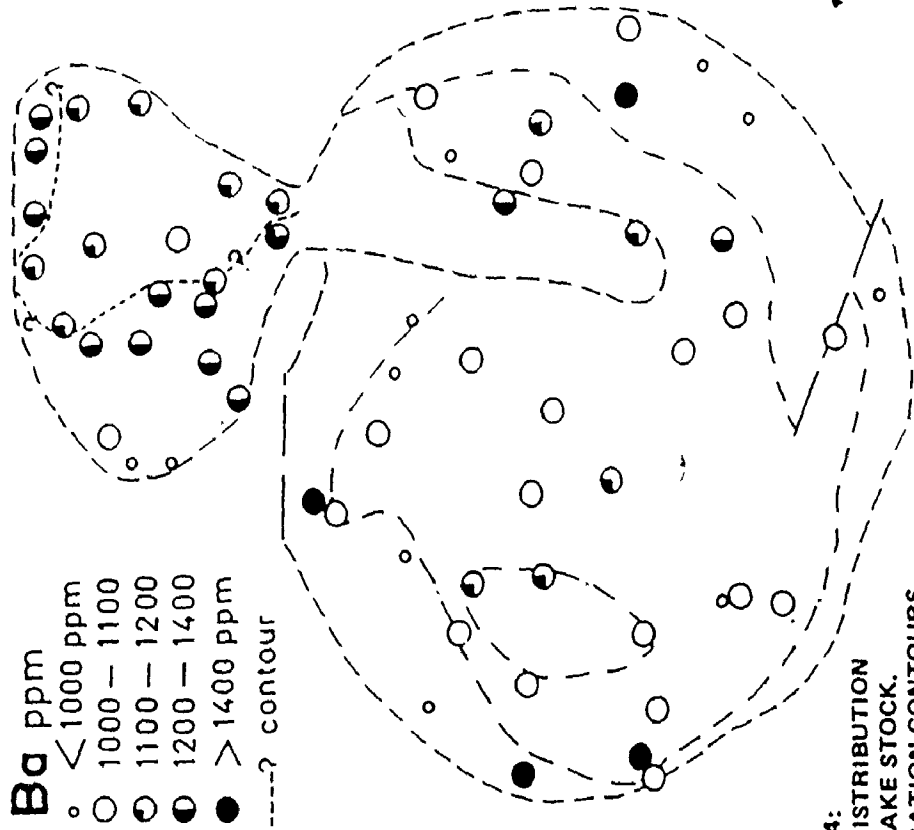
Such observations are less apparent for the subtle differentiation in the Burditt Lake Stock: Rb enrichment appears to have dominated separation of the aplitic field but factors controlling Ba/Sr were ineffectual. The scatter of south lobe points towards the Ba apex and into the "anomalous" field could be interpreted as evidence for a metasomatic overprint. The author prefers to consider this trend as indicating local erratic behaviour of Ba at the margins of the south lobe.

Areal Distribution: Ba and Zr

Two trace elements present in appreciable concentrations and displaying erratic behaviour on the foregoing plots are Ba and Zr. Figures 2.23 and 2.24 give a schematic overview of element distribution over the Burditt Lake Stock. The barium distribution shows clearly the enrichment of the north lobe in contrast to the south. A further revelation is the wide range of values recorded in the foliated marginal phase of the south lobe. Both the highest and lowest values are recorded in this phase. Wolhuter (1973) found erratic Ba values in mafic margins of the Opemisca Lake pluton, Quebec, and attributed them to wall rock contamination and lesser metasomatic mobility for Ba^{+2} compared to competing K^{+} . No evidence for contamination exists at Burditt Lake, but abundant aplitic patches and marginal dykes attest to deuteric metasomatic fluids.

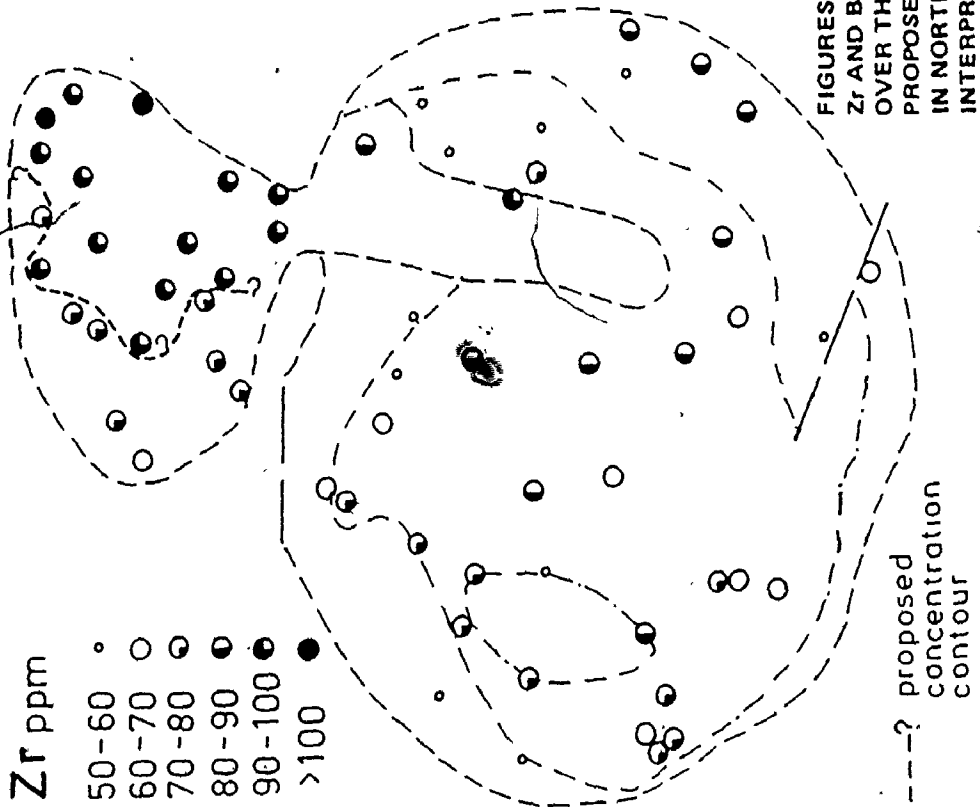
Ba also shows a very vague zonal distribution in the

FIGURE 2.24



FIGURES 2.23 AND 2.24:
Zr and Ba ELEMENT DISTRIBUTION
OVER THE BURDITT LAKE STOCK.
PROPOSED CONCENTRATION CONTOURS
IN NORTH LOBE ARE BASED ON VISUAL
INTERPRETATION.

FIGURE 2.23



hornblende granodiorite of the north lobe. Higher values are located marginally (as illustrated by the visually drawn "contour"), except for the biotite granodiorite apophysis on the western flank.

A similar schematic map for Zr shows enrichment for the north lobe and scattered distribution over the south lobe. Again a visual contour can be drawn for the north lobe showing a semi-concentric distribution with higher central values. This zonal pattern accounts for the bimodal clusters of Zr for the north lobe in Figure 2.17. It is significant to note that the contours drawn for Zr and Ba are not coincident - suggesting that the pattern is very vague.

Radioelements: U and Th

Previous Work:

One of the earliest attempts to obtain radioactivity profiles for Precambrian granitoid plutons was an alpha activity study by Ingham and Keevil (1951) on the Bourlamaque, Elzevir and Cheddar batholiths of Quebec and southern Ontario. Doig (1968) developed a prototype portable differential gamma ray spectrometer that allowed him to obtain contour maps of K, U and Th distribution for the Preissac Granite of north-western Quebec.

Individual laboratory gamma-ray analyses for granitoids

in the vicinity of this thesis area were reported by Whitfield et al. (1959):

Saganaga Granite:	U = 0.14 ppm	Th = 0.75 ppm
Burntside Gneiss:	U = 0.3 ppm	Th = 0.07 ppm
Vermilion Granite:	U = 3.1 ppm	Th = 30.0 ppm

Any published laboratory analyses much prior to this work are suspect of large analytical errors (Clark et al., 1966). More recently, Farquharson (1976) reported laboratory gamma measurements of U, K and Th in six granitoid units of southeastern Manitoba. Airborne gamma ray profiles have been flown across northwestern Ontario by the Resource Geophysics and Geochemistry Division of the Geological Survey of Canada. One such traverse in 1970 cut the Scattergood Lake Stock (Dr. Charbonneau, personal communication).

Petrogenetic implications:

Th and U are known to increase in more felsic granitic rocks (Whitfield et al., 1959), but whether crystal fractionation or deuteritic and postmagmatic metasomatic factors control distribution is not clear. Granitoids are more oxidized than basalts and the ability of uranium to oxidize to soluble uranyl ions suggests that metasomatic and hydrothermal activity can significantly distort the primary differentiation pattern. An autoradiographic study of the mode of occurrence of radioelements

in granitic rocks (Baranov et al., 1962) showed an increase in alpha-tracks with sericitization of feldspars and chloritization of biotites leading to the conclusion that autometasomatism, hydrothermal and supergene processes overprint the primary radioelement distribution by differentiation. Ragland et al. (1967) studied the Enchanted Rock Batholith, Texas, and found that the distribution of thorium and uranium seems to be controlled by autometasomatism: deuteritic allanite crystallization and loss of uranium by oxidation.

Several investigators have found U and Th to concentrate at the periphery of batholiths and stocks regardless of lithologic distributions (Ingham and Keevil, 1961; Labhart and Rybach, 1971). Rybach and Labhart (1973) modelled this pattern on the basis of deuteritic diffusion in a temperature gradient. Buntebarth (1976) ruled out thermodiffusion for peripheral U enrichment, but proposed deuteritic convective flow and diffusion driven by chemical, electrical and pressure gradients. He calculated a velocity for U migration of 0.1-0.3 cm/year over a duration of 0.3-1.0 m.y. for the Mont Blanc granite (Swiss Alps).

Other authors have noted a correlation between high Th and U contents and abundant K-feldspar megacrysts. Killeen and Heier (1975) proposed that the same fluids that deposited the K-feldspar megacrysts at the marginal zones of the Vradal granite (Norway) also controlled migration of Th and U. This

fits well with the long recognized correlation between K abundance and Th and U abundance (Clark, Jr. et al., 1966). On the other hand, a radiometric survey of megacryst-bearing granitoids of S.W. England by Tammemagi and Smith (1975) showed neither peripheral enrichment nor any marked differences between megacrystic phases and megacryst-free phases.

Radioelement distribution over the Burditt Lake Stock:

The possible role of autometasomatism and the link between megacrysts and U and Th distribution make these two trace elements especially useful for the petrogenesis of the Burditt Lake Stock.

U and Th analyses were performed in situ using a four channel differential gamma ray spectrometer, model DISA 400A, loaned to the author by Geometrics Services (Canada) Ltd., Exploranium Division, Downsview, Ontario. A full discussion of analytical technique, instrument calibration and precision is presented in Appendix G and in Birk (1974). Figures 2.25 and 2.26 present counting stations and eU and eTh determinations over the Burditt Lake Stock. These numbers are ppm averages based on four readings of two minute duration, corrected for background (center of Burditt Lake). Figure 2.27 plots some of the field analyses against the modified Larsen index using only those field stations adjacent or coincident with sample stations of Figure 2.2. A direct correlation

FIGURES 2.25 AND 2.26:

**IN-SITU ANALYSES OF ^{238}U AND ^{232}Th
BY DIFFERENTIAL GAMMA-RAY
SPECTROMETRY OVER THE BURDITT LAKE
STOCK. ^{238}U AND ^{232}Th ARE EQUIVALENT
TO U AND Th CONCENTRATIONS IF
PARENT-DAUGHTER EQUILIBRIUM PREVAILED
IN THE RADIOACTIVE SERIES.**

FIGURE 2.27:

**U, Th AND Th/U VARIATION WITH
MODIFIED LARSEN INDEX FOR THE
BURDITT LAKE STOCK. INDEX
CALCULATED FROM WHOLE ROCK XRF
ANALYSES OF HAND SPECIMENS TAKEN
ADJACENT OR COINCIDENT TO DETECTION
AREA OF SPECTROMETER.
PARENT-DAUGHTER EQUILIBRIUM IS
ASSUMED.**

FIGURE 2.25

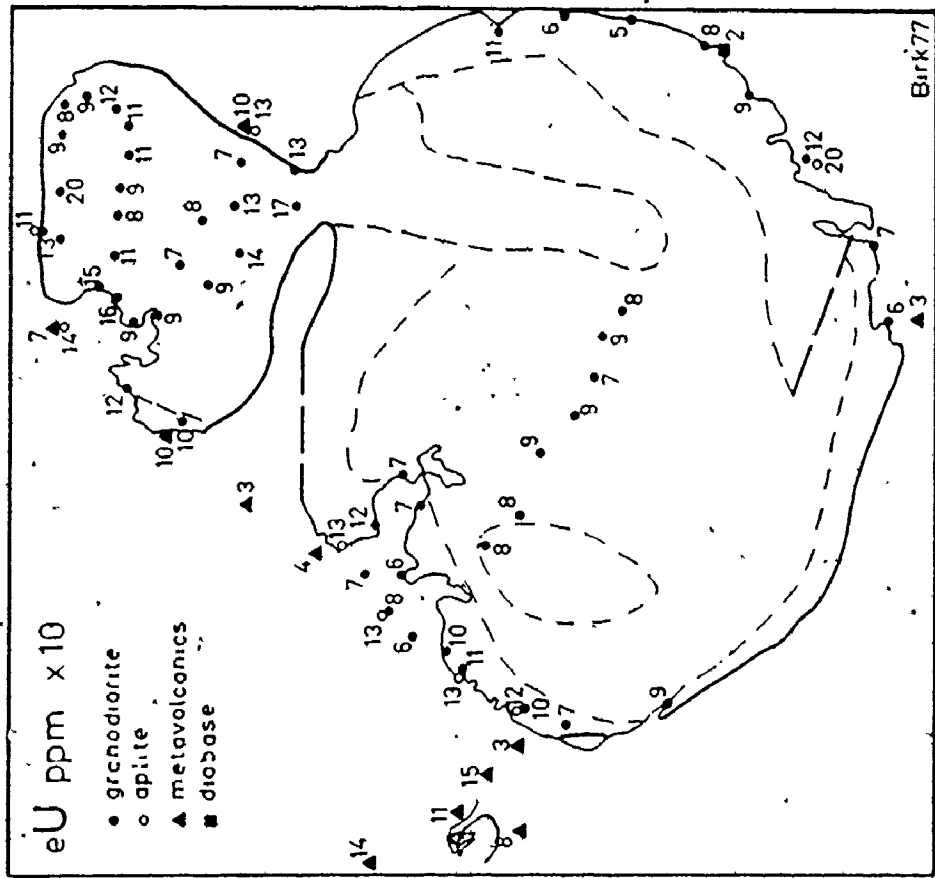
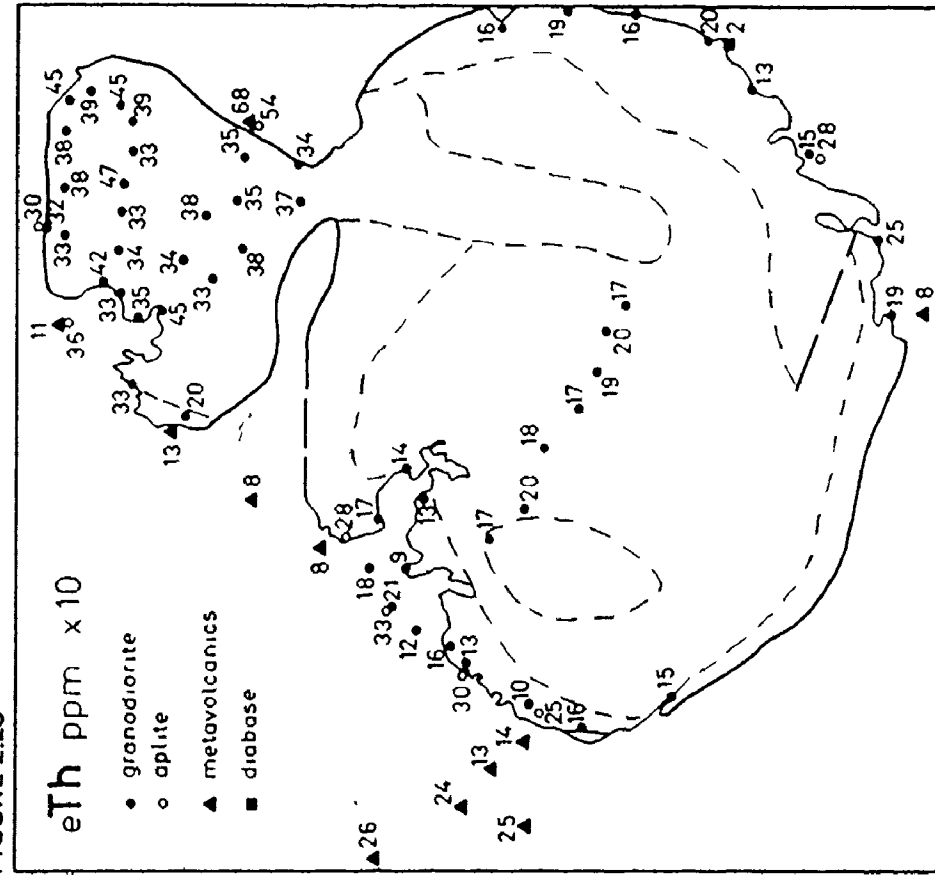


FIGURE 2.26



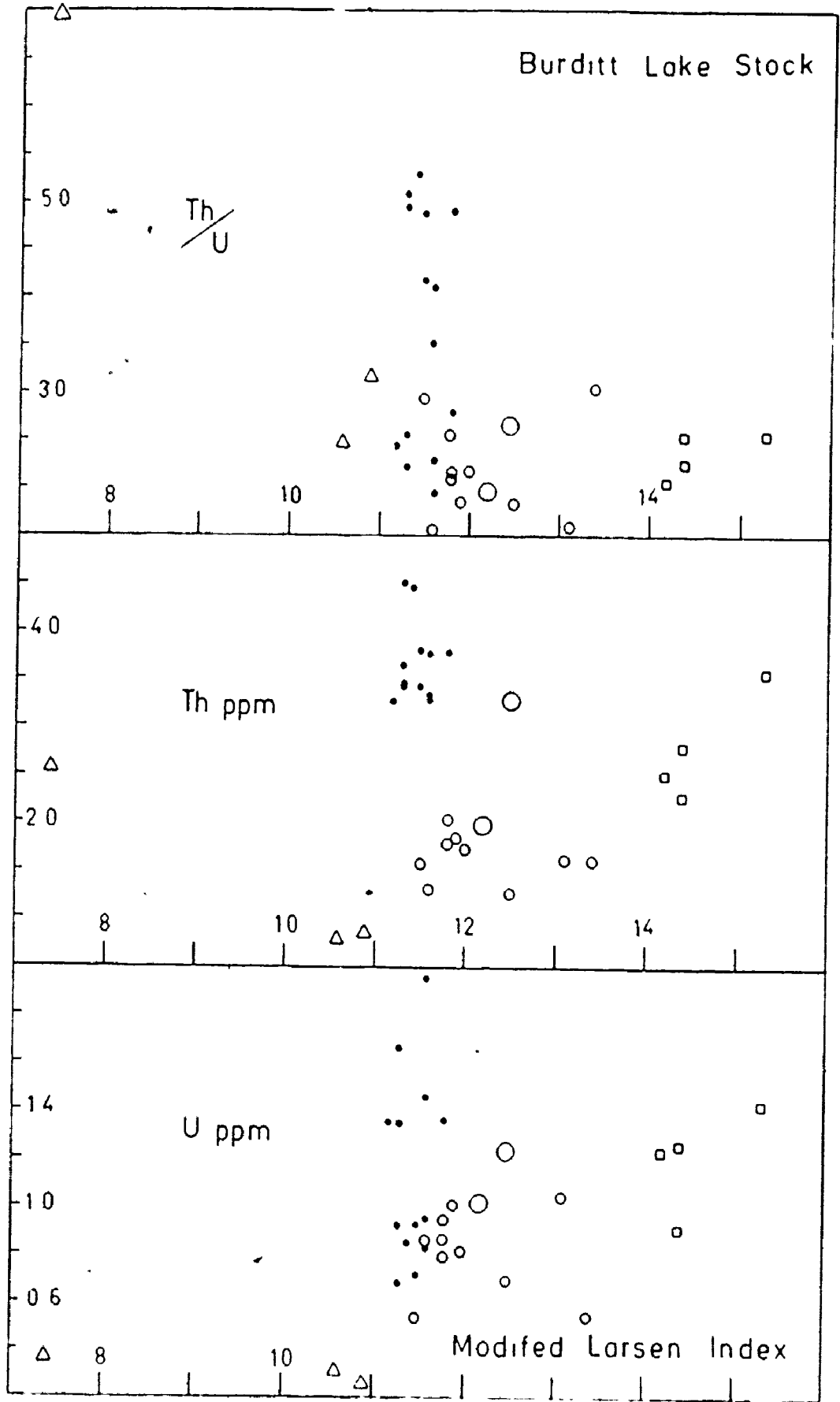


FIGURE 2.27

cannot be expected since hand specimens can rarely be collected for sites within the "effective sample" area beneath the spectrometer detector.

The concentrations of U and Th displayed by the Burditt Lake Stock are low relative to average granodiorites (2.6 ppm U; 9.3 ppm Th: Clark, Jr. et al., 1966), and are low relative to averages estimated for the Canadian Shield (2.45 ppm U; 10.3 ppm Th: Shaw, 1967). The linear variation diagrams show large scatter partially attributable to resolution, but general patterns prevail: a decrease with differentiation index is recorded in the phanerites followed by an increase in the aplitic phase. The north lobe hornblende granodiorite shows a distinct enrichment in Th and an irregular enrichment in U over the south lobe biotite granodiorite. These patterns rule out crystal fractionation as the sole control on distribution. Of significant note is the correlation of higher values with the megacryst-bearing granodiorite.

Figures 2.25 and 2.26 show the areal distribution of values and includes sporadic determinations for country rock intermediate metapyroclastics and a diabase dyke. The diabase dyke is distinctively low in radioelements, but the meta-volcanics carry a range of values similar to the pluton, although U is characteristically lower. There is indistinct evidence that Th and possibly U concentrations increase in the metavolcanics away from the contacts. This may correlate with lithology or may indicate meteoric water interaction. For

mapping purposes, the author concludes that at Burditt Lake the portable gamma ray spectrometer can better differentiate between phases within a granitoid pluton than between the granitoid and country rock.

Within the borders of the pluton there is no clear evidence of marginal enrichment, except for the higher concentrations in peripherally located aplites. However, a plot of eTh/eU ratios (Figure 2.28) shows a vague central increase of values for the hornblende granodiorite as defined by a visual contour. This vague zonal pattern could be dismissed as insignificant, except that it mimicks similar vague patterns uncovered for Ba and Zr distribution. This nebulous pattern may be explained by a model of crystallization from the walls inwards with progressive U depletion relative to Th. On the other hand, the enrichment of Th and U in the more basic phase of the Burditt Lake Stock suggests that auto-metasomatism rather than crystal fractionation controlled radioelement distribution. Both sphene and allanite have been recorded in the mineral modes (Appendix B), of which deuteritic allanite is proposed as a radioelement residence site along with replacement products (sericite, chlorite, etc.) and interstitial pores (Baranov et al., 1962).

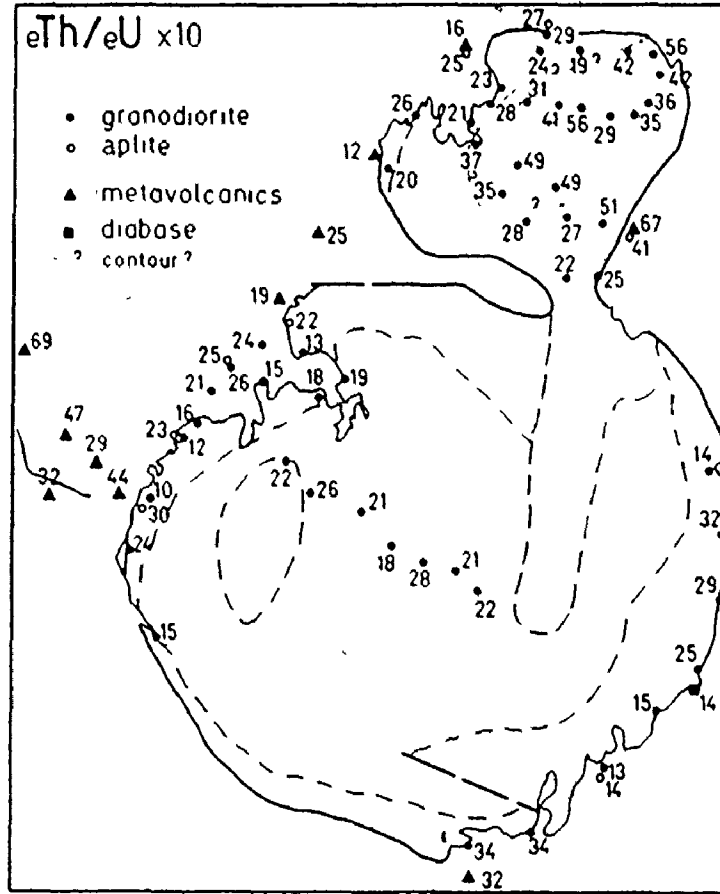


FIGURE 2.28 IN-SITU ANALYSIS OF eTh/eU IN THE BURDITT LAKE STOCK.
 SAME STATIONS AS IN FIGURES 2.25 and 2.26.

TESTING HOMOGENEITY, IN THE BURDITT LAKE STOCK:
TREND SURFACE ANALYSIS:

Introduction: }

Trend surface analysis is the mathematical least-squares fitting of a hypothetical smooth surface to a mapped variable. Two-dimensional trend surface fitting can be used to statistically illustrate geographic variability of data. The application to irregularly spaced (non-orthogonal) data for the two-dimensional erosional surface of granitoid plutons was pioneered by Whitten (1960, 1961, 1962) and Dawson and Whitten (1962). Peikert (1965) and Mathews et al (1975) extended the method to three dimensions for granitoid bodies by including vertical relief as a variable.

For each mapped variable, several trend surfaces can be calculated based on increasingly more complex polynomial expressions. It is commonly recognized that regional trends are best shown by low order polynomial surfaces (linear, quadratic or cubic) , while local variability is best accomodated by surfaces defined

by higher degree polynomial contours (quartic, quintic, sextic, etc.). Considerable controversy surrounds the selection of the "most meaningful" trend surface. While some authors consider that surface fitting should account for most of the data variability (Chayes and Suzuki, 1963; Chayes, 1970), others (Whitten, 1963) argue that low order poor-fit surfaces (accounting for less than 50% of the data variability expressed as a sum of squares) are more meaningful by reflecting geological trends hidden by local variability. A sobering fact is that polynomial trend surfaces with apparent "trends" can be generated even for random data (Howarth, 1967). Although correlation of patterns can be expected between hand-drawn contour maps and polynomial contour maps (see Dawson and Whitten, 1962, Figure 6; Raglund and Butler, 1972, Figure 3), the two techniques are distinctive and not interchangeable: trend surface contouring is mathematical and not necessarily geologically meaningful.

For trend surface fitting to be valid for non-orthogonal data, three criteria should be fulfilled: there should be (1) enough samples, (2) evenly distributed over (3) a square field area.

Baird et al. (1967) pointed out that as the trend surface becomes more complex, the number of coefficients used in the polynomial expression increases and the degrees of freedom decrease. The number of localities must considerably

exceed the number of coefficients.

Tinkler (1969) observed that clustered data generates low angles of trend where data is concentrated and steep gradients where data is sparse. Concentric patterns tend to be displaced towards the centre of gravity of data clusters, and areas of poor data control tend to generate "saddle" patterns (Doveton and Parsley, 1970). Clustering of data may be tolerable if only regional patterns of low order are desired, or if the trend surface has a high percentage of fit.

In elongated map areas, trend surfaces show a tendency toward subparallelism with the long margins. Doveton and Parsley (1970) termed this distortion by linearity, and determined that the elongation distortion induced in the trend surfaces is roughly proportional to the ratio of the major to minor dimensions of the area.

The ideal contour conditions are rarely achieved in geological work because of outcrop limitations. Even when the mathematical model is closely approximated, the trend surface technique suffers criticism. Multivariate data must be reduced to univariate data, which in turn generates a multiplicity of contour maps - any one or all of which may carry no geological significance. Several tests have been developed to determine the best "fit" surfaces:

- (1) Percentage reduction in sum of squares (Whitten, 1961; Howarth, 1967);
- (2) F-ratio of variances (Chayes, 1970);
- (3) Multiple correlation coefficients (see Agterberg and Chung, 1975);
- (4) Half-confidence interval maps (Agterberg and Chung, 1975).

Not only do these various selection procedures not agree (Agterberg and Chung, 1975), but authors have not agreed on how good a fit is desirable. Agterberg and Chung (1975) concluded that:

"... The best test that a trend really exists may be simply its reproducibility from subsets of data or its emergence from polynomial equations of several different degrees".

Parslow (1971) noticed that the precision of the method falls off rapidly when low order polynomials are applied to large geographic areas. Higher order surfaces however are prone to "rippling": for example, a linear array of points is defined as a wave-form curve by the sextic polynomial. On the other hand, real periodic variations in data are masked by surface fitting (Saha, 1964).

All these criticisms are essentially mathematical and do not touch on the geological limitations of the method. To decide on which trends are consistent becomes extremely difficult when dealing with superimposed regional patterns

caused by several petrogenetic processes (Bernotat, 1973). Furthermore, two dimensional surface fitting ignores vertical relief which may make a marked contribution to regional variation (Exley, 1963; Peikert, 1965; Mathews et al., 1975).

Despite these shortcomings, trend surface analysis remains as the most popular technique for testing variation in granitoid plutons. The following types of data have been subjected to surface fitting:

modal mineral analyses (Whitten, 1961; Dawson and Whitten, 1962; Peikert, 1965; Parslow, 1971, etc.);

specific gravity (Dawson and Whitten, 1962; Mathews et al., 1975, etc.);

major element oxides (Parslow, 1971; Ragland and Butler, 1972; Mathews et al., 1975; Falkum, 1976, etc.);

trace elements (Propach and Dopel, 1972, etc.).

Parslow (1971) found that oxide data showed more distinct trends than modal data. Since oxide data represent a "closed number system", oxides as variates are not independent and the trend surfaces for each oxide do not provide completely different information. In order to confirm suspected trends by different sets of data, comparisons are best made not only between different oxides, but also between oxides and some other type of data. For the current study, the author has selected oxides and trace elements.

Burditt Lake Stock:

Method

The exposed vertical relief is negligible over the Burditt Lake Stock, in relation to its horizontal dimensions; therefore two-dimensional trend surface fitting was considered sufficient to outline variability. Major element oxides and trace elements were selected as variates based on 62 data stations distributed over the stock. Sample distribution was not uniform due to ubiquitous smelly beaver ponds; neither did the stock dimensions conform with a square field area. Trend distortions caused by both clustering and linearity were therefore anticipated.

Analyses for each data station are listed in the appendix and localities are shown in Figure 2.2 and by solid points on each contour plot. Only phaneritic granodiorite samples were considered; aplite dykes and aplitic marginal phases were omitted since the objective was to detect trends in visually homogeneous units.

The calculation method of Agterberg and Chung (1975) was adopted because it allowed for calculation of a confidence interval surface for each polynomial trend surface. Polynomial contours and corresponding confidence contours up to quintic order were plotted for each, an analysis of variance including three tests of "fit" were included. Geographical X-Y coordinates were arbitrarily designated by placing a grid over Figure 2.2

with (0,0) coordinates centred at latitude $48^{\circ}55'$, longitude $93^{\circ}45'$ and each coordinate unit equal to 40 feet (12.2 meters).

The proliferation of plots caused by progressively increasing the polynomial order is magnified in the method of Agterberg and Chung (1975) because each level generates two plots: a polynomial contour map and a half-confidence interval map. Since polynomials up to 8th order are possible, up to 16 maps for each variate can be generated. This is not only unwieldy, but also redundant. To illustrate the method, the author plotted contours and confidence intervals up to quartic order for SiO_2 (Figures 2.29 and 2.30), but limited all other plots to "best-fit" polynomial contours. The author does not agree with the approach of Whitten (1963) - that poor-fit surfaces are more meaningful. Such a procedure would require that equal consideration be given to all eight polynomial maps and would lead to more confusion than if the data is simply visually inspected.

Table 2.1 presents results for three statistical tests of "best-fit" based on the procedure of Agterberg and Chung (1975). The surfaces accepted in this study as being most appropriate were selected by compromising between the lowest residual variance and the highest percent probability (based on analysis of variance).



**FIGURE 2.29:
POLYNOMIAL TREND SURFACES FROM
LINEAR TO QUARTIC ORDER FOR SiO_2
CONTENT IN THE BURDITT LAKE STOCK.
DATA LOCATIONS INDICATED BY DOTS.**

**FIGURE 2.30:
HALF-CONFIDENCE INTERVAL MAPS FOR
THE POLYNOMIAL TREND SURFACES OF
FIGURE 2.29 CALCULATION BY METHOD
OF AGTERBERG AND CHUNG (1975).**

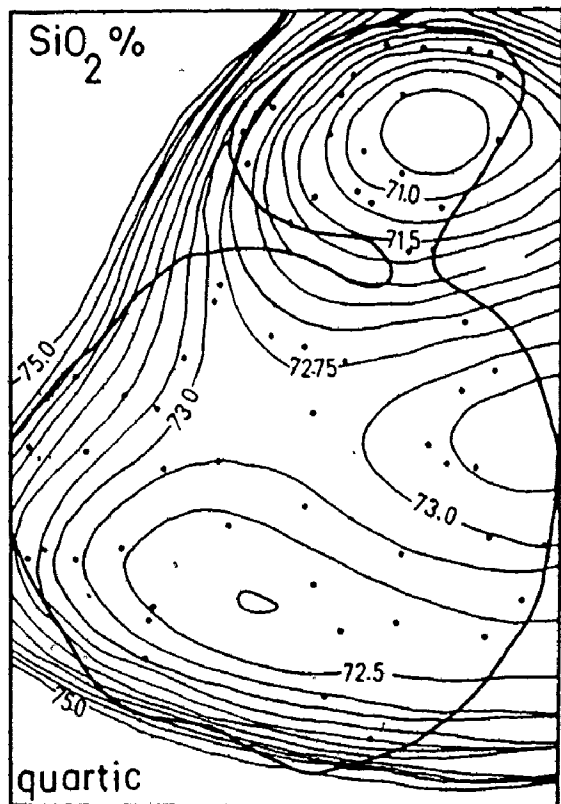
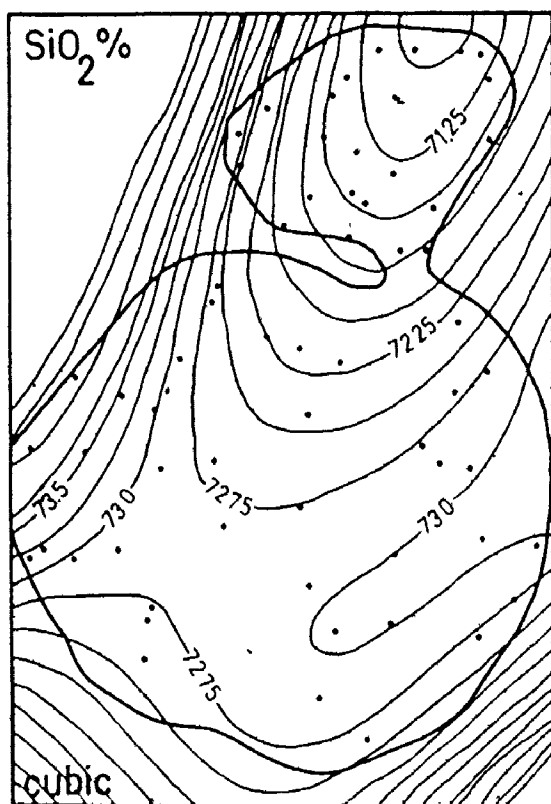
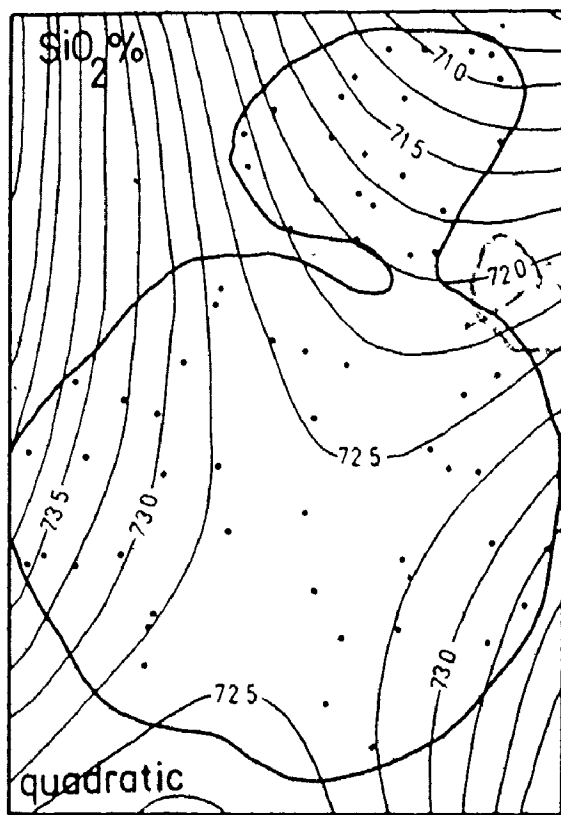
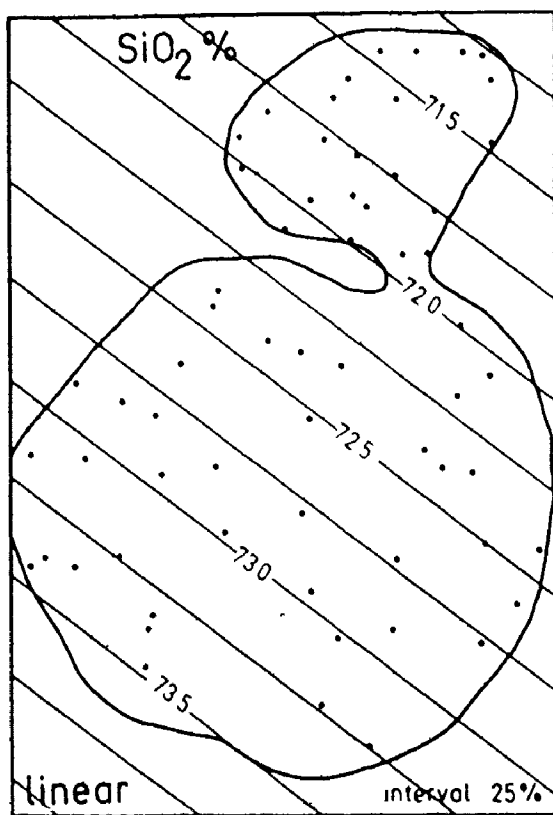


FIGURE 2.29

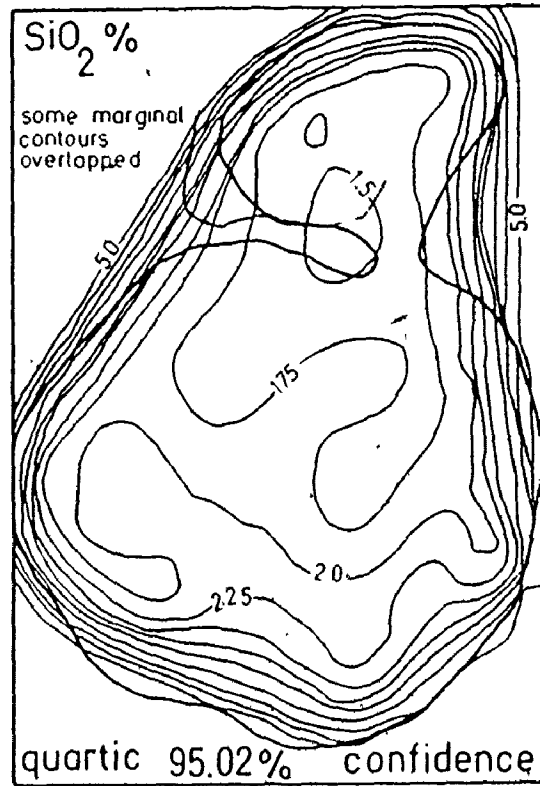
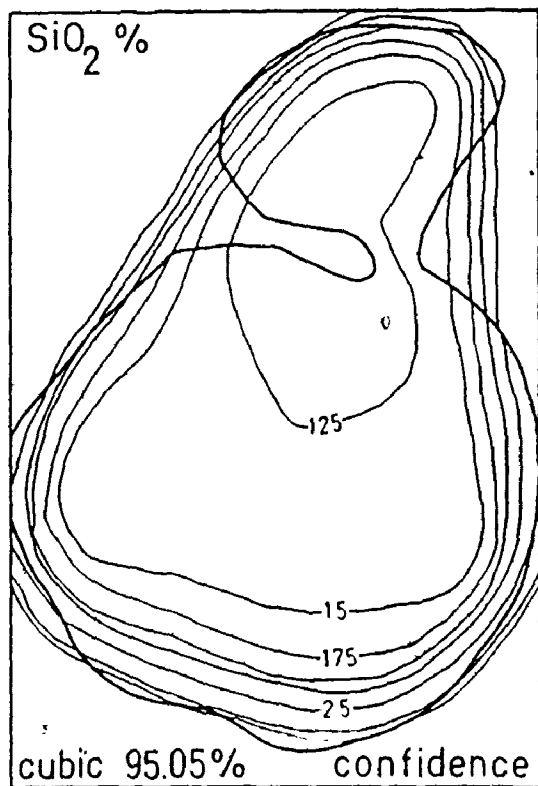
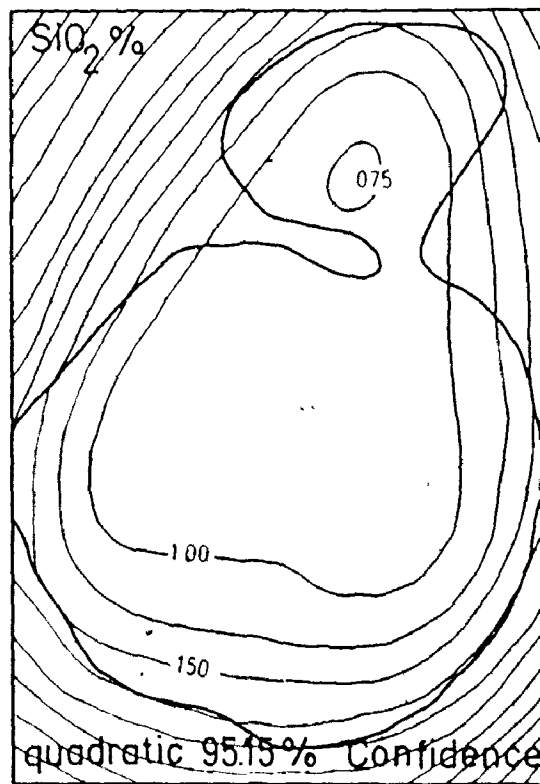
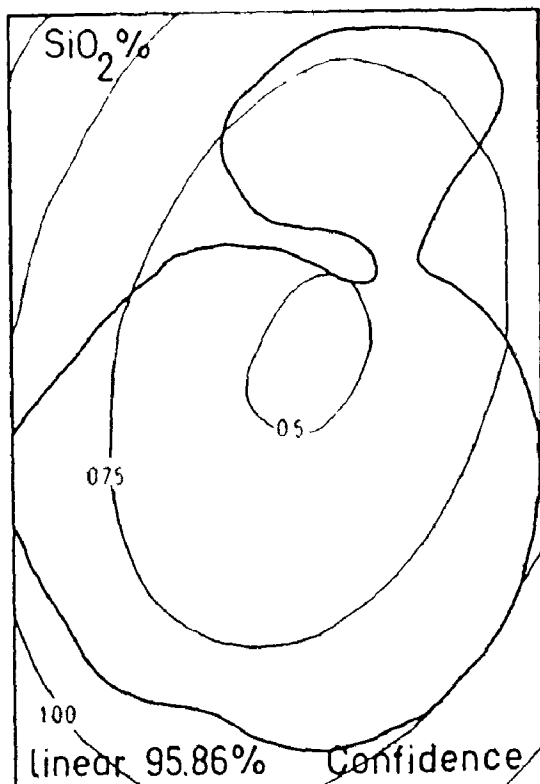


FIGURE 2.30

Table 2.1 Tests for statistical evaluation of the "fit" of a trend surface, by the method of Agterberg and Chung (1975): Burditt Lake Stock

Degree	Residual Variance	R ²	F-ratio	Probability %
SiO ₂				
1	0.834	0.33	14.55	100.0
2	0.743	0.43	3.42	97.7
3	0.709	0.50	1.66	82.7
4*	0.617	0.61	2.58	96.2
5	0.620	0.65	0.94	52.5
Al ₂ O ₃				
1	0.097	0.07	2.37	89.8
2	0.099	0.10	0.59	37.5
3*	0.092	0.23	2.15	91.24
4	0.088	0.33	1.43	76.7
5	0.086	0.43	1.24	69.5
CaO				
1	0.053	0.35	16.20	100.0
2	0.045	0.48	4.62	99.4
3*	0.041	0.56	2.32	93.1
4	0.040	0.61	1.23	68.9
5	0.043	0.64	0.55	23.5
Fe ₂ O ₃				
1	0.087	0.53	32.88	100.0
2	0.075	0.61	4.02	98.8
3	0.071	0.66	1.75	84.8
4*	0.066	0.71	1.91	88.9
5	0.068	0.74	0.77	40.0

Table 2.1/continued

Degree	Residual Variance	R^2	F-ratio	Probability %
MgO				
1	0.035	0.41	20.40	100.0
2	0.029	0.53	4.71	99.5
3	0.027	0.60	2.19	91.7
4*	0.023	0.69	2.88	97.6
5	0.022	0.73	1.12	63.4
K ₂ O				
1	0.074	0.26	10.50	100.0
2	0.077	0.28	0.35	20.8
3*	0.068	0.41	2.85	96.7
4	0.070	0.45	0.74	40.6
5	0.061	0.58	2.12	92.9
Rb				
1	190.7	0.22	8.18	99.9
2	199.5	0.22	0.14	6.3
3	184.4	0.33	2.14	91.1
4*	149.9	0.51	3.39	98.9
5	139.2	0.60	1.60	83.0
Ce				
1*	21.3	0.47	25.31	100.0
2	20.4	0.52	1.91	86.2
3	19.9	0.56	1.33	73.0
4	19.6	0.61	1.12	63.9
5	20.1	0.65	0.83	44.0

Table 2.1/continued

Degree	Residual Variance	R^2	F-ratio	Probability %
Sr				
1	7126	0.22	8.52	99.9
2	6292	0.35	3.61	98.1
3*	5122	0.51	4.20	99.5
4	4544	0.61	2.32	94.2
5	4742	0.64	0.67	32.8
Zr				
1	170.6	0.25	9.81	100.0
2	163.7	0.32	1.81	84.4
3	151.7	0.42	2.09	90.5
4*	128.4	0.55	2.84	97.5
5	123.6	0.63	1.30	72.1
Ba				
1	43554	0.034	1.02	63.3
2	43910	0.076	0.84	52.4
3	41896	0.18	1.66	82.7
4	37394	0.34	2.23	93.3
5*	28333	0.57	3.45	99.2

*Selected surface for contour maps based on compromise between lowest residual variance and highest probability.

Probability = values along the probability axes of (cumulative) F-distributions for appropriate degrees of freedom.

F-ratio = F-ratios computed for successive orders by step-wise analysis of variance, for 95% confidence intervals.

R^2 = multiple correlation coefficient squared.

Polynomial Trend Surfaces: Major Elements

SiO₂:

The linear and quadratic surfaces over the Burditt Lake Stock (Figure 2.29) reflect the bimodal distribution of silica between the north lobe granodiorite and the south lobe. The north carries a mean of $71.28 \pm 0.62\%$ (1σ , 26 samples), compared to $72.98 \pm 0.76\%$ (1σ , 36 samples) for the south lobe granodiorite. No distinction is made here between the mineral assemblages - only the geographical distribution. The lowest residual variance is recorded by the quartic surface which is consequently considered to be the most appropriate. The quartic contours define an inverted cone located off-centre over the north lobe, suggesting a concentric increase of silica towards the margins. A similar marginal increase may be inferred for the south lobe complicated by a central "saddle". In both areas the trends steepen towards the stock margins which suggest distortion due to data clustering (Tinker, 1969; Doveton and Parsley, 1970). This edge effect will be further evaluated from half-confidence maps.

Half-Confidence Interval Maps:

The half-confidence interval map defines a roughly 95% probability that the true trend surface does not anywhere intersect the confidence interval surface placed above or below the calculated polynomial surface. Since the significance of any specified trend surface is questionable, the confidence

interval on this surface is even more difficult to interpret (Agterberg and Chung, 1975). For areas where the computed half-confidence intervals are large, the corresponding trend surfaces are unreliable. On the other hand, polynomial surfaces with poor fit statistics may carry narrower confidence intervals than intervals corresponding to best-fit surfaces (Agterberg and Chung, 1975). Because of this paradox, no attempt was made in this study to compare confidence intervals for different surfaces. The most useful application in this study was the evaluation of edge effects.

The half-confidence maps for all four polynomial surfaces for SiO_2 (Figure 2.30) show a distorted inverted cone over the stock with error limits increasing outwards. The shape of the distortion follows the stock outlines and an increase in gradient towards geological contacts testifies to strong edge effects on reliability, which in turn would influence the polynomial surfaces. The marginal increase recorded by the SiO_2 quartic surface is mimicked by an equivalent increase in confidence limits on the quartic half-confidence map. The marginal increase in silica is therefore partially or entirely an edge effect. There remains however a strong concentric pattern over the northern lobe which lies within low confidence limits. It is also interesting to note that the confidence limits for the linear surface are considerably narrower than the limits for the quartic surface - although

the latter has been selected as the "best fit".

Al_2O_3 and CaO:

In contrast to SiO_2 a lower order cubic surface is more appropriate for both Al_2O_3 and CaO (Figures 2.31, 2.32). This suggests that variation in these two oxides is more subtle and of a regional nature: i.e. a slight increase in CaO and decrease in Al_2O_3 towards the north. Al_2O_3 shows shallow gradients over the entire stock. Similar behaviour of Al_2O_3 was reported for a Norwegian granitoid (Falkum, 1976). The general fabric of trend runs northeast for both oxides, which may be a function of distortion by linearity or may be generated by the tongue of megacryst-bearing granodiorite which has been mapped in the south lobe (Figure 2.1). Both Al_2O_3 and CaO distinguish an aberration on the western edge of the north lobe which corresponds to a phase of megacryst-free granodiorite (see Figure 2.1). Half-confidence interval maps (not shown) carry contours of $\pm 0.36\%$ for CaO and $\pm 0.58\%$ for Al_2O_3 over most of the stock with the exception of extreme margins. The above polynomial maps are therefore considered to carry uniform reliability over the stock except for margin effects.

Fe_2O_3 and MgO:

The quartic polynomial surfaces for total iron (as Fe_2O_3) and MgO (Figures 2.33 and 2.34) display a fabric almost

FIGURE 2.31

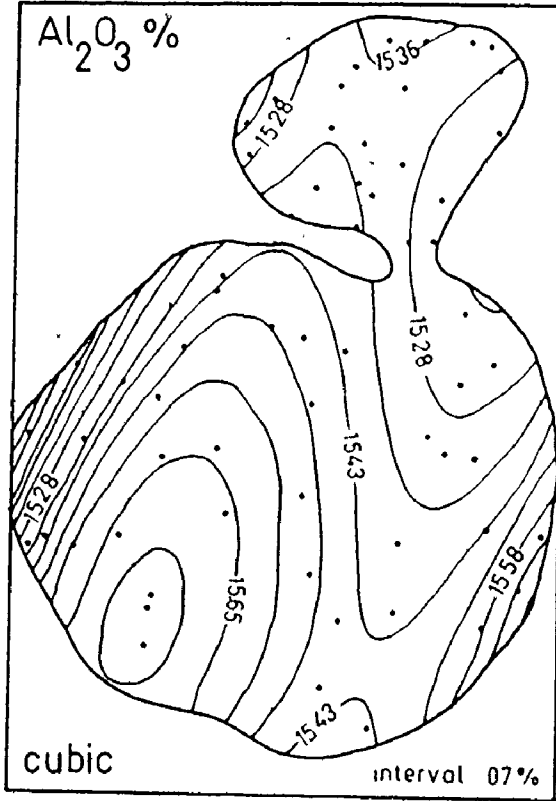


FIGURE 2.32

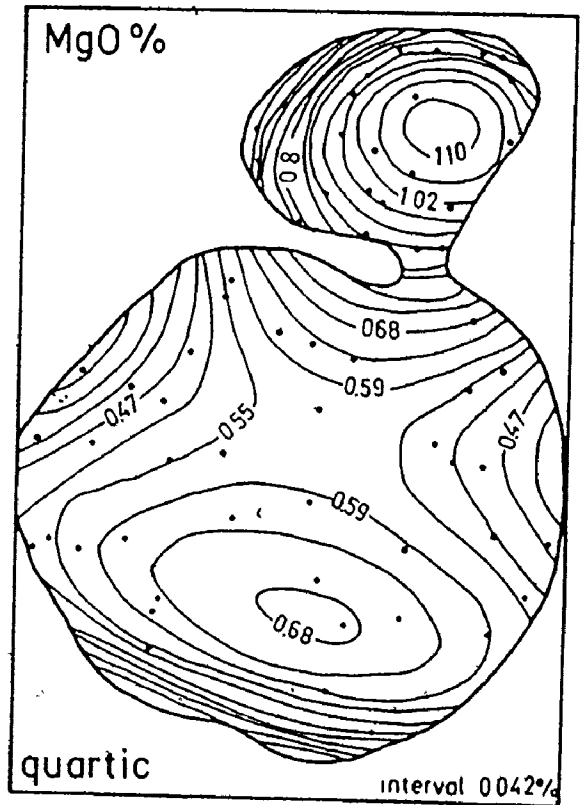
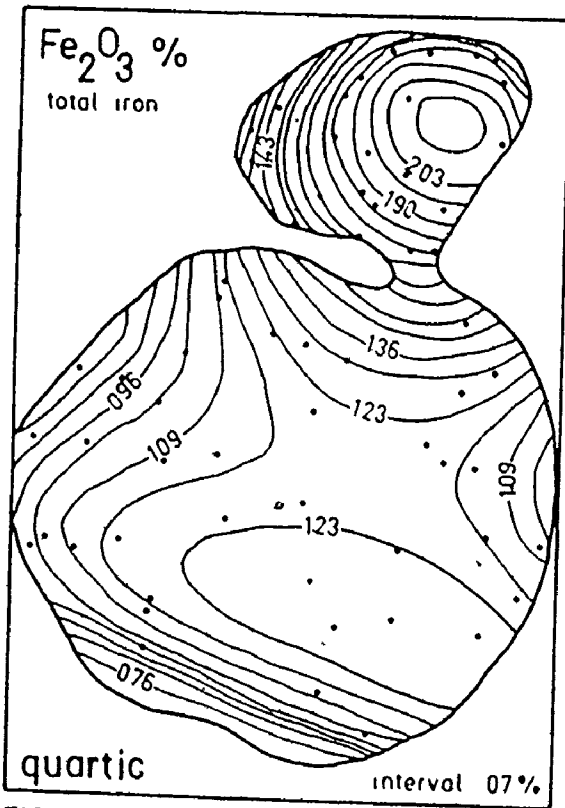
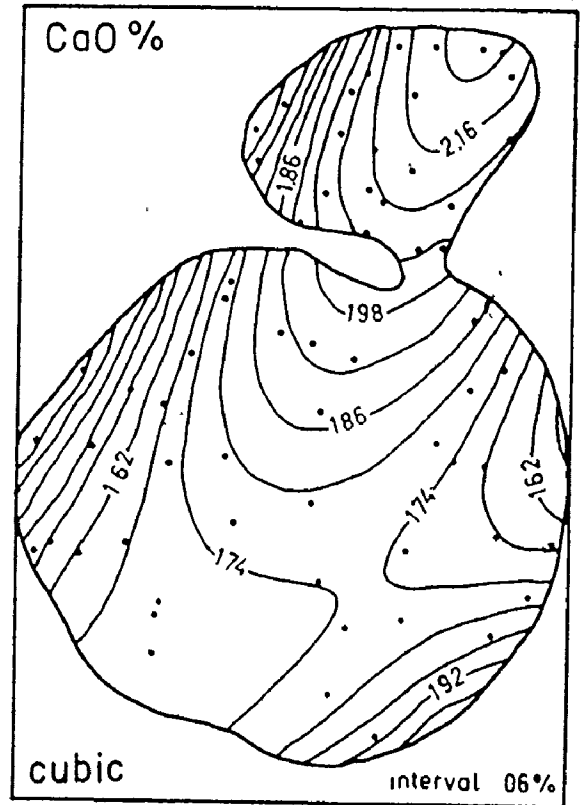


FIGURE 2.33

FIGURE 2.34

FIGURES 2.31 TO 2.35:
"BEST-FIT" POLYNOMIAL CONTOUR MAPS FOR MAJOR ELEMENTS IN THE BURDITT LAKE STOCK.
"BEST-FIT" BASED ON TABLE 2.1.

coincident with that of SiO_2 . This holds true also for the corresponding half-confidence interval maps (not shown). Conclusions are therefore similar, bearing in mind the influence of the "close number system" syndrome. The dominant observations are: strong positive MgO and FeO cones off-centre over the north lobe, with lower values and shallow gradients over the south lobe.

K_2O :

K_2O produces a preferred cubic surface and even shallower gradients than Al_2O_3 , with a mild regional increase northward (Figure 2.35). This shallow gradient is petrogenetically significant since potassium figures prominently in the commonly employed indices of differentiation (Larsen Index, Modified Larsen Index, Differentiation Index, etc.). The corresponding half-confidence map shows $\pm 0.49\%$ contours over most of the stock.

Polynomial Trend Surfaces: Trace Elements

Rb:

In contrast to K_2O , Rb shows greater local variability requiring a quartic order polynomial for best fit (Figure 2.36). The fabric is similar to K_2O but with a more prominent deltaic high encroaching from the northern lobe into the south. The location of this delta matches the tongue of megacrystic granodiorite located in the field.

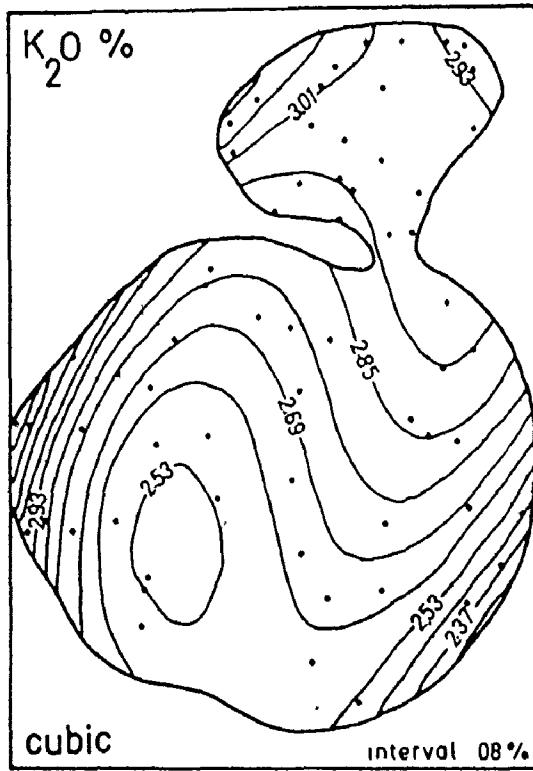


FIGURE 2.35

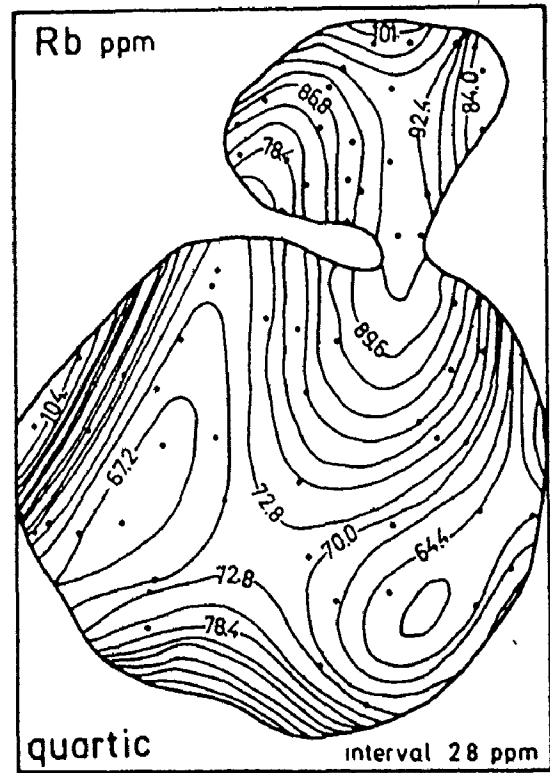


FIGURE 2.36

FIGURES 2.36
 → 2.40

"BEST-FIT" POLYNOMIAL CONTOUR MAPS FOR TRACE ELEMENTS
 IN THE BURDITT LAKE STOCK. "BEST-FIT" BASED ON TABLE 2.1.

Ce:

Cerium is the only element investigated in this study that showed best-fit probabilities of less than 90% for all orders of polynomials except linear. This suggests that only a vague regional trend exists, with higher values northward (Figure 2.37).

Sr:

Both the cubic and quartic surfaces have acceptable best-fit statistics (Table 2.1), although only the cubic surface is depicted (Figure 2.38). The fabric of the cubic surface is significantly different from that of Rb. This difference is even more pronounced when comparing the quartic Sr and quartic Rb surfaces. The quartic Sr surface (not shown) carries a shallow concentric pattern over the north lobe and does not display a tongue embayment into the south. Therefore the antipathetical behaviour between Rb and Sr as predicted from differentiation models (Taylor, 1964) is not supported by the trend surface fabrics. Rb distribution is considered to be a secondary phenomenon.

Zr:

The quartic order surface for zirconium displays a strong positive anomaly off-centre over the north lobe, corresponding in location to the cones described for SiO_2 , MgO and

Fe_2O_3 . As well, the Zr surface over the south lobe is dominated by steep marginal gradients and waveform contours that cannot be entirely attributed to edge effects.

Ba:

Marginal vortices are even more pronounced for the Ba high order quintic polynomial. It is significant that only the high order quartic and quintic surfaces carry percentage probabilities greater than 90%. This suggests that Ba is most strongly influenced by local variability in contrast to Ce, which showed only mild regional variation. The half-confidence interval map is as complex as the polynomial surface, and suggests that unstable conditions prevail where the marginal vortices are located. It is disturbing to note that one of the marginal vortices (southern edge) is controlled by no data point. This may mean that part or all of the marginal patterns are products of the high order polynomial "rippling" that Parslow (1971) encountered.

Conclusions:

The foregoing trend surface analysis leads to the following conclusions:

- (1) The north lobe is concentrated in MgO, Fe_2O_3 , CaO, K_2O , Rb, Zr, Ce, Sr, and depleted in Al_2O_3 and SiO_2 relative to the south lobe.

FIGURE 2.37

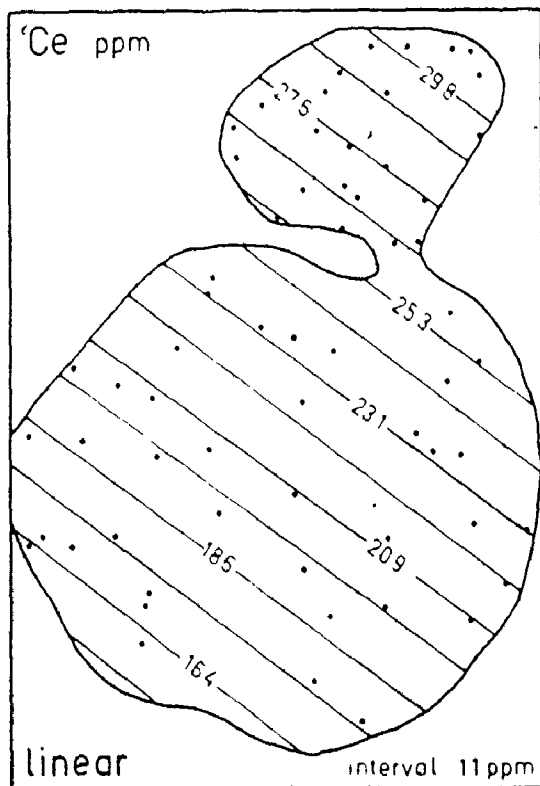


FIGURE 2.38

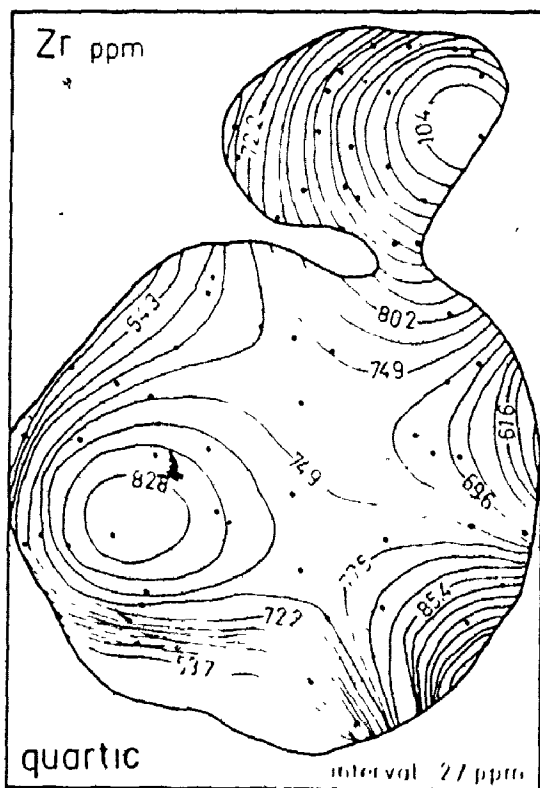
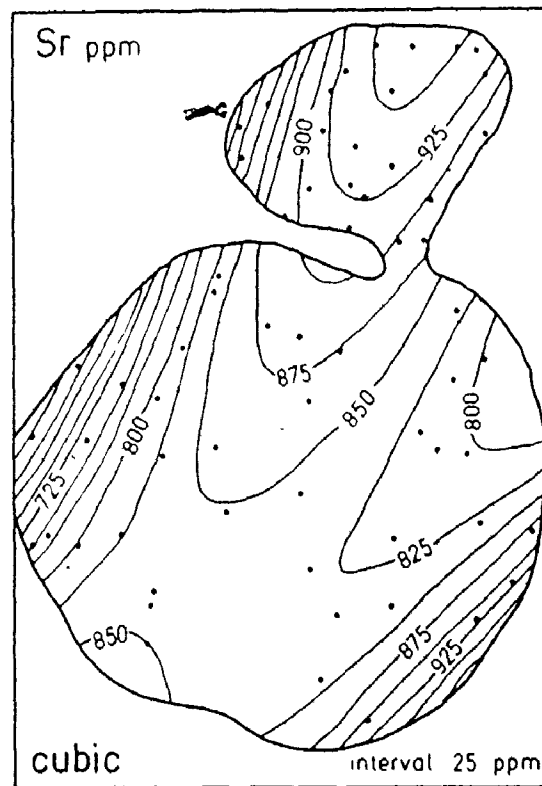


FIGURE 2.39

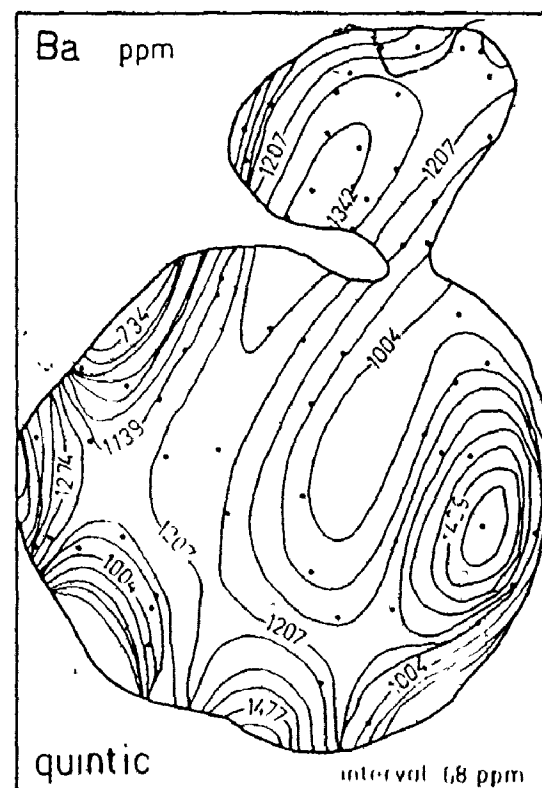


FIGURE 2.40

- (2) The north lobe displays a concentric distribution for some elements with a marginal increase in SiO_2 and a core enrichment in Fe_2O_3 , MgO , Zr , Sr .
- (3) K_2O , Al_2O_3 and Ce carry shallow profiles suggesting only broad regional trends with little local fluctuation in content.
- (4) Rb and Ba trends show steep gradients and fabrics distinct from the other elements.
- (5) Phases defined by field mapping (e.g. the tongue of megacryst-bearing granodiorite in the south, or the megacryst-free granodiorite in the north), are vaguely outlined by some element distributions, but not by all.
- (6) Ba displays the greatest control by local variability, and Ce shows the least control by local variability.

Of the above conclusions, a most significant "find" are the concentric patterns over the north lobe. Two factors, however, rule against this trend being real: first, the presence of a mappable megacryst-free phase on the western edge of the north lobe (Figure 2.1); and second, the smaller dimensions of the north lobe make trends more susceptible to distortion by clustering. In order to test the credibility of the concentric trend, the author subjected the north lobe data to a separate trend surface analysis. To avoid redundancy, the results of this second test are summarized verbally. The

following points emerged:

- (1) Best-fit tests usually selected either a linear polynomial surface (Zr, Ce), or a quintic surface (SiO_2 , Sr, Rb), suggesting either very shallow regional trends or very complex local fluctuations.
- (2) Half-confidence interval maps for the quintic surfaces were also very complex, suggesting that sample distribution and density was insufficient (23 samples) to give good control.
- (3) Most element patterns distinguished between the western margin of the lobe and the main body of the lobe.
- (4) Best-fit tests for Ba selected the quartic surface which carried a concentric low pattern located off-centre on the east side of the lobe. This pattern was distinct from a low on the western flank.

From the above auxiliary study, the author concludes that the concentric patterns reflect a geological feature that is partially masked by data sparsity and trend interference from the distinctive lithological phase on the north-western flank. The concentric patterns are further supported by the visual contours noted for Ba, Zr and eTh/eU distribution (Figures 2.23, 2.24, 2.28). A best-fit linear surface for Zr suggests that the geological feature may be a roughly west-to-east trend rather than a clearly concentric pattern. To

substantiate this further would require additional sample stations.

The uncertainty of the conclusions shows that trend surface analysis has not substantially improved interpretation as opposed to simple visual data contouring.

Autometasomatism:

Introduction:

The earliest workers on granitoids recognized the field and petrographic evidence of transport and crystallization of granitic material from hydrothermal fluids. Lawson (1887) suggested that feldspar inclusions in xenoliths of the Sabaskong Bay granitoids (northwest of Burditt Lake) were absorbed from the enclosing magma "by the agency of the penetrating and watery solutions from the granite magma ..." (p.133). Anderson (1934) studied the origin of microcline megacrysts of the Cassia Batholith of Idaho and suggested that: "... potash rich emanations soaked through the body of the granodiorite itself during or shortly after crystallization ...".

Terzaghi (1935) suggested that the increasingly hydrous residual liquids of a crystallizing pluton may react with already crystallized components to extract orthoclase for deposition elsewhere as potash-rich granite or pegmatite.

Eskola (1956) found that late-kinematic granites (sensu stricto)

of Finland characteristically plot towards the Or apex and away from the eutectoid granite composition of the hydrous Q-Or-Ab ternary system. He attributed this to deuteritic addition of potassium from an unknown crustal source. Although the classic transformistic theory of granitization was based largely on such evidence of alkali metasomatism, neither source nor transport mechanism were agreed upon.

Korzhinskii (1970) summarized the experimental and theoretical work on metasomatism documented previously in the Russian geological literature. Korzhinskii (1970) attributed the phenomenon of metasomatism to a combination of two mechanisms: diffusion and infiltration. Infiltration he considered to be regionally the most effective. In pure diffusion, chemicals are transferred by ionic diffusion through stationary pore solutions and vapours, through crystal lattices and along grain boundaries. Infiltration metasomatism involves a stream of aqueous solutions percolating through rock pores. As hydrated ions are filtered through the pore systems, they experience a "sieve effect" which controls their mobility. Alkali metals are the most mobile, while multivalent metals are the least mobile. Acids are more rapidly filtered than bases. This results in a "metasomatic column" of synchronous zones or "waves" of acidic and basic components as the stream of solutions percolates through.

Much of Korzhinskii's (1970) work involved the derivation of transport equations to describe the development and

motion of the "metasomatic column" and subsequently to apply this theory to explain bimetasomatism (interaction between two contiguous rocks) and granitization. His work explained how multiple metasomatic mineral zones and sequential corrosive or depositional textures could be caused by a single metasomatic event.

Korzhinskii (1970) demonstrated that both diffusion and infiltration can generate the simultaneous growth of several metasomatic zones. However, only infiltration can precipitate new minerals and only infiltration is temperature or pressure dependent. The vertical zones generated by post magmatic metasomatism are products of infiltration because they are a response to pressure and temperature gradients. Korzhinskii (1971) proposed that large-scale regional granitization and metamorphism are generated by infiltration of: "... streams of ascending juvenile transmigmatic solutions ..." of under-crust origin generated by degassing of the mantle.

Hofmann (1972) found Korzhinskii's infiltration transport model to be compatible with chromatographic transport equations for an idealized ion-exchange column under conditions of isothermal equilibrium and transport by pressure. Hofmann (1972) distinguished infiltration by:

- (1) transport in one direction;
- (2) sharp replacement fronts;
- (3) disequilibrium mineral assemblages separated by sharp fronts;

(4) high concentrations of mobile trace elements (Li, Be, B, U, Pb) in the most advanced replacement front.

For an alkali solution passing through a ternary feldspar system, Hofmann (1972) predicted two replacement fronts: a leading front of albitization and a trailing front of alkali feldspar replacing the albitized plagioclase.

Both Korzhinskii (1970) and Hofmann (1972) considered the transport contribution by diffusion to be minor, because the diffusion rate of solutes in solvents is negligible compared to the infiltration rate of fluids through pores. On the other hand, Weare et al. (1976) have argued that the dissolution of silicates by cation exchange results in an altered crystal surface through which subsequent dissolving ions must diffuse. For feldspars, the initial altered layer is probably amorphous $\text{Al}(\text{OH})_3$ with an additional reaction zone of kaolinite. Consequently the infiltration transport equations of Korzhinskii and Hofmann must be supplemented by diffusion equations as modelled by Korzhinskii (1970) and Weare et al. (1976).

Orville (1963) carried out ion exchange and diffusion experiments in the system KAlSi_3O_8 - $\text{NaAlSi}_3\text{O}_8$ - NaCl - KCl - H_2O . He found that the proportion of $\text{K}:(\text{K}+\text{Na})$ in the vapour phase that coexists with two alkali feldspars decreases with falling temperatures. Melt-crystal equilibria and vapour-crystal equilibria are the same for alkali feldspars at a given

temperature. Thus the physical nature of the diffusing medium, hydrothermal (liquid-crystal) or pneumatolitic (vapour-crystal), is not a significant factor. The presence of a thermal gradient in a two-feldspar rock generates compositional gradients with respect to alkalis in the vapour/fluid phase. Alkali ions will tend to diffuse through the vapour or fluid in response to these gradients. Orville (1963) concluded that reciprocal alkali transfer between two portions of such a rock mass at different temperatures will move K to the low temperature and Na to the high temperature portion. He attributed the porphyroblastic growth of K-feldspar "dents de cheval" to this mechanism. The thermal driving force for alkali exchange contrasts with Korzhinskii's (1970) assumption that diffusive transport is independent of temperature.

Model for the Burditt Lake Stock:

The foregoing discussions lead to a model of the Burditt Lake Stock as a prototype silicate ion exchange column involving pulsating diapirism, infiltration, diffusion and cation exchange (Figure 2.41).

A quartz-diorite diapir rose by gravitational instability as a convecting crystal-liquid mush of plagioclase and hornblende rafting wall rock xenoliths. A second pulse from the same magma chamber fractionated slightly towards granodiorite followed up the same conduit. Agglutination of the two pulses

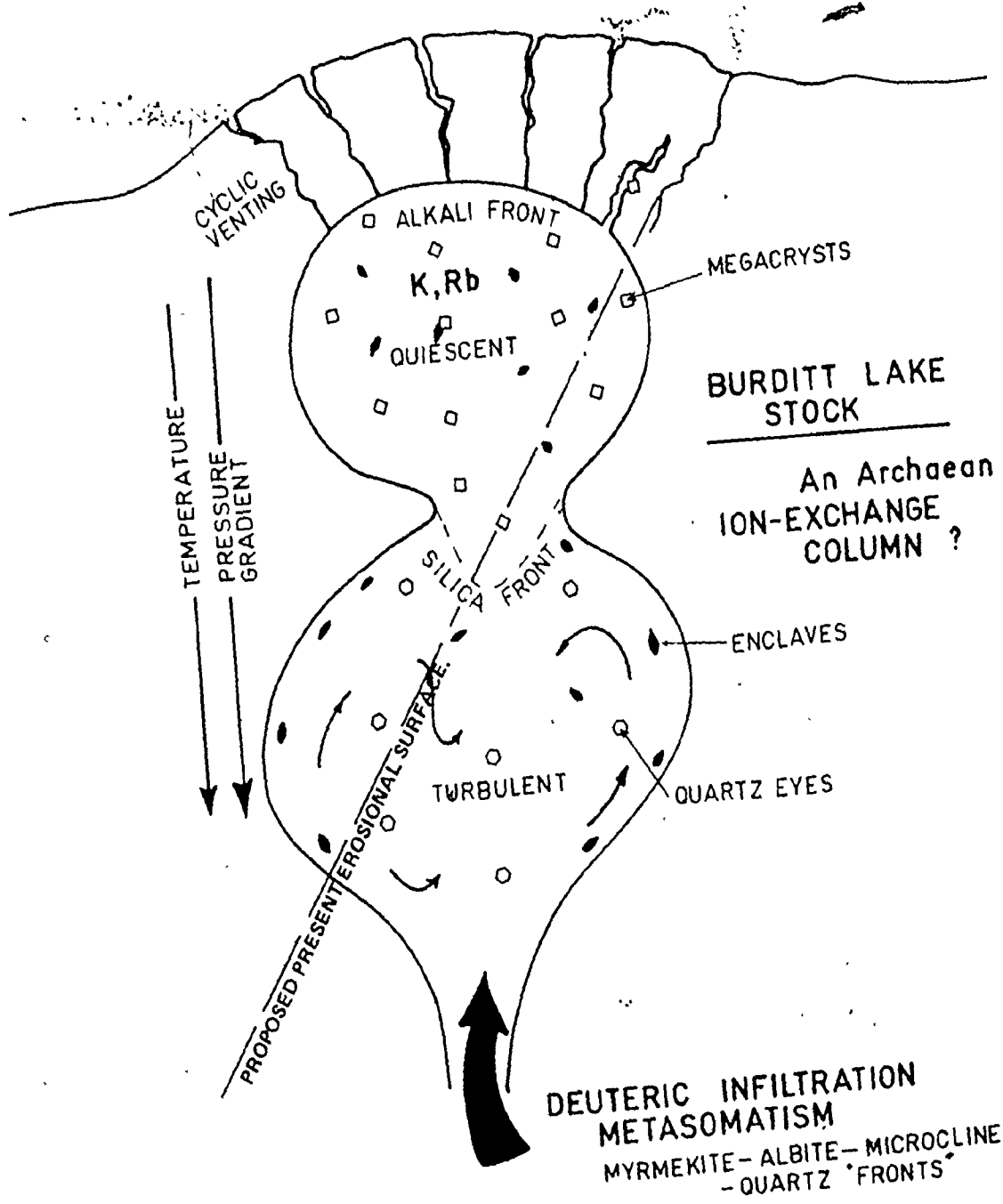


FIGURE 2.41 MODEL OF THE BURDITT LAKE STOCK AS A PROTOTYPE SILICATE ION EXCHANGE COLUMN, INVOLVING PULSATING DIAPYRISM, INFILTRATION, DIFFUSION AND CATION EXCHANGE.

left the first mass at a higher elevation and established a temperature and pressure gradient. Crystallization continued from the walls inward with the top lobe forming a stagnant plastic mass, while the hotter bottom lobe (corresponding to the south lobe of Figure 2.1) continued to convect. A diffuse "tail" of granitic liquid representing residuals was injected along the wallrock contacts of the south lobe and into thermal shrinkage cracks, to form the aplitic patches and dykes.

The diapirs and aplitic liquid graded into a stream of alkalic hydrothermal or pneumatolytic fluids that infiltrated up the P-T gradient to react with the earlier now solid phases. A sequence of ion-exchange fronts travelled through the pluton leaving a sequel of corrosive, overgrowth and endoblastic textures. Major element transport was recorded in myrmekite-albite-microcline-quartz fronts, and in endoblasts of quartz and microcline-perthite. Trace element transport was recorded in endoblasts of allanite and possibly sphene. The entire system was "frozen" at a stage when the alkali fronts dominated the north lobe and a silica front dominated the south lobe. Metasomatism was supplemented by retrograde metamorphism as the system cooled to generate the disequilibrium telescoped mineral facies observable today (Schermerhorn, 1960).

Elements for which transport from south to north lobe has been reasonably established include K, Rb, Ba, Th and U.

Na was likely enriched in the south. Other elements that may have migrated from the south to the north lobe include Zr. Other major elemental distribution reflects the crystal fractionation prior to emplacement. The overall effect was to granodioritize the entire mass, distort the record of mineral paragenesis and confound the trends on traditional differentiation diagrams.

Some difficulties exist with this model. The intrusive sequence of mafic to felsic and anhydrous to hydrous violates physicochemical predictions for tapping of a fractionating magma chamber. More felsic wetter phases should occupy the top of the magma chamber and be drained first. Perhaps diapiric rise of granitoid magma drives fluids towards the lower pressure "tail" end of the diapir. This problem is also encountered in models for zoned plutons (Chapter 2.2).

If glomerogranular quartz "eyes" record high-level emplacement gradational with hypabyssal quartz-eye porphyries, the south lobe should occupy the higher elevation. This evidence is partially offset by enclave enrichment in the north, and migmatitic net-veining in the south, but is supported by the core of megacrystic granodiorite in the south. Since no intrusive contacts between north and south could be established, the author assumes the north lobe to occupy a higher level.

The movement of alkali fluids by thermal gradients

should have resulted in granitization of wall rocks with the growth of "dents de cheval". Although no such extensive granitization of supracrustals was observed, some interaction is suggested by the Th and U values. Perhaps the wall rocks provided a selective geochemical barrier as suggested by Buntebarth (1976) for uranium diffusion, or Emmermann (1968) for K and Ba rich solutions.

The mechanism of differentiation by autometasomatism as described above is somewhat similar to the interpretations of Ragland et al. (1968) for the Enchanted Rock batholith; of Boone (1962) for the Deboullie syenite; Emmermann (1968) for the Albtal granite of the Black Forest and Ermanovics et al. (1967) for the Belleoram Stock of Newfoundland.

An alternative, though related model, is given by Kresten (1974) for the Oro-Hamno-Massiv of south Sweden. He suggested that post-magmatic remobilization occurred in the solid state after renewed burial of the pluton. His photographs of xenoliths, "post-kinematic" feldspar megacrysts and plastically deformed aplites could as well have been taken on outcrops of the Burditt Lake Stock. Such burial could generate a thermal gradient for diffusive transport, but sufficient fluids for infiltration would be lacking. In the absence of infiltration solutions it is difficult to envision megacryst growth in mafic enclaves.

2.1.3 Scattergood Lake Stock

Field Observations

Scattergood Lake lies some 58 km south of Dryden, Ontario, within NTS coordinates 52 F/7. Thomson (1933) first mapped an elongate bulb-shaped granitoid stock wholly confined within supracrustals. Ontario Division of Mines field parties led by C.E. Blackburn remapped the region in 1972 and 1975, resulting in two preliminary maps and a geological report and map (Blackburn, 1973, 1975, 1976). The Scattergood Lake Stock straddles the two preliminary map boundaries and appears partially within the 1976 report area.

For logistical reasons, the author's field investigations were restricted to two days of traverses in the northern bulb. However, a member of Blackburn's field party (R. Pichette) supplied the author with samples covering the southern portion. Figure 2.42 shows the pluton geology as derived from Blackburn's maps with this author's modifications. Sample stations labelled "P" are contributions from R. Pichette.

Blackburn (1975) recognized a homogeneous pink hornblende granodiorite, intrusive into an 8,200 m homoclinal sequence of pillowed metabasalt. Sinistral offsets of metavolcanic units were recorded for either side of the stock, suggesting that the Scattergood Lake Stock was emplaced in a pre-existing northwesterly striking fault. To the south the Scattergood body is separated from granitoids of the Irene-Eltrut Lakes

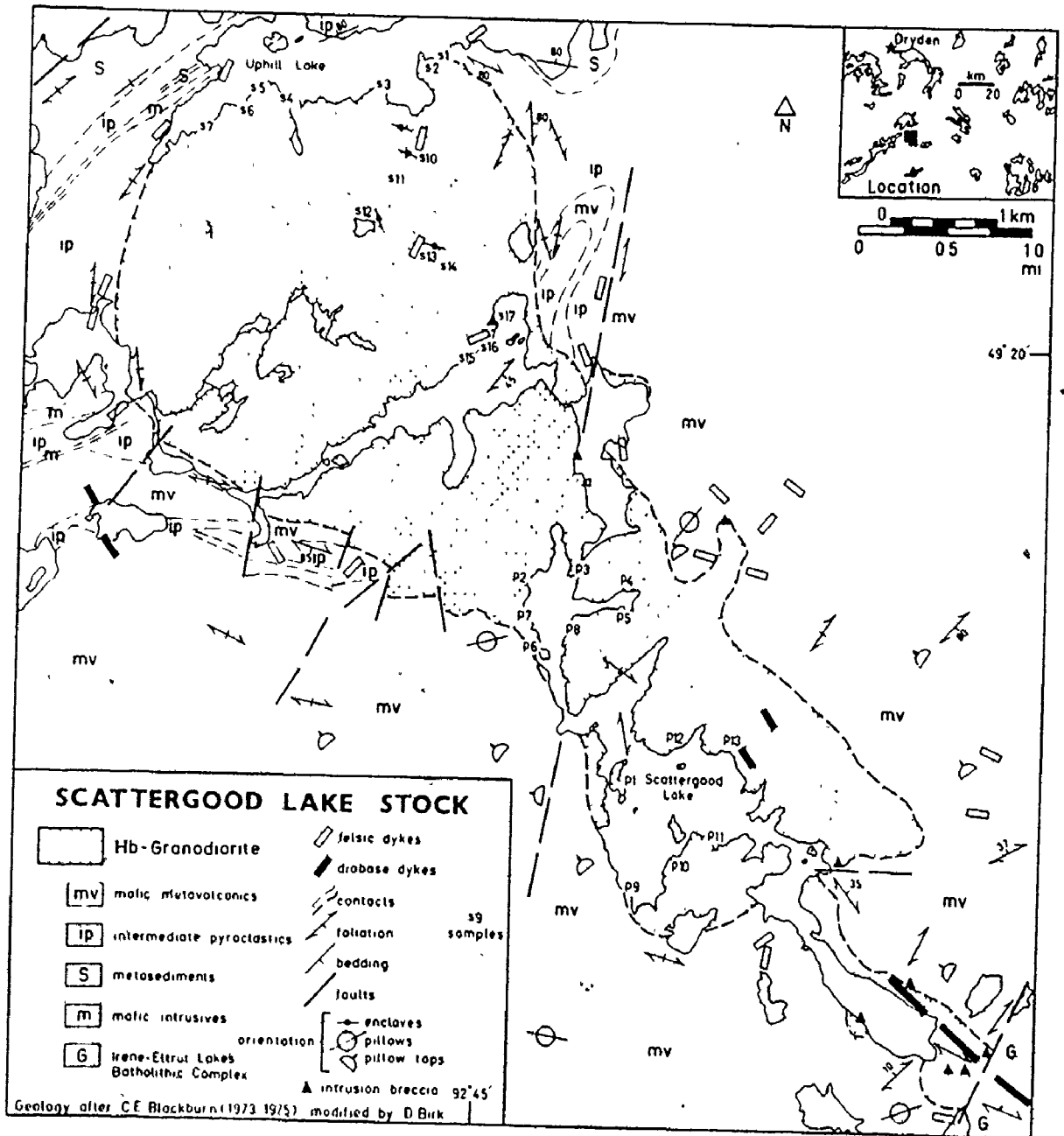


FIGURE 2:42 LITHOLOGY AND STRUCTURE OF THE SCATTERGOOD LAKE STOCK NORTHWESTERN ONTARIO (NTS 52 F/7.)

batholithic complex (Sage et al., 1975) by the northeast trending Taylor Lake Fault.

The margins of the pluton along the south shore of Uphill Lake show faint alignment of surface pits, mafic constituents, lensoid enclaves and microcline megacrysts. The author interprets this as mild late-stage flow foliation, since the strike changes gradually from 135° at S2 to 230° at S7 following the curvature of the contact. This foliation is considerably more subtle than at Burditt Lake and therefore is omitted on Figure 2.42.

Blackburn (1976) found only "small mafic clots rarely larger than 2 or 3 cm", whereas the author's visits encountered several locales with subrounded to mafic lensoid enclaves up to 2 x 1.5 ft. At S17 (Figure 2.42) an intrusion breccia zone or enclave swarm contains a diverse xenolith lithology including blocks of "greenstone" feldspathized by microcline megacrysts and thin aplitic dykelets.

Megacrysts of microcline-perthite are sparsely scattered throughout the stock but do not occur at every outcrop. Aplitic and granitic apophyses have been mapped in adjacent metavolcanics (Figure 2.42) and were encountered by the author within the northern lobe, but are scarce in the southern portion (Pichette, personal communication).

Blackburn (1976) plotted a Rose diagram of 27 joint determinations and located a weak maximum at N55E correlating

with regional fracture patterns and airphoto lineaments. Figure 2.42 furthermore shows several contact offsets that attest to post-consolidation structural activity.

On the 1973 preliminary map, Blackburn plotted a metamorphic isograd near the western flank of the stock, differentiating amphibolite facies metavolcanics near the stock from greenschist facies metavolcanics to the west. This contact aureole is based entirely on field mapping (Blackburn, personal communication) and remains speculative.

The aeromagnetic map for Upper Manitou Lake (ODM 1971, map 1153G) shows a close correlation between isomagnetic lines and the boundaries of the Scattergood Lake Stock. The magnetic flux over the pluton is relatively homogeneous and lies between 60,500 and 60,800 gammas. This is high compared to the granitoids of the Irene-Eltrut Lakes complex, which exhibit readings of 60,320 to 60,400 gammas at Meggisi Lake, southeast of Scattergood Lake.

Petrography

Ten modal analyses (see Appendix B2) show a uniform mineral assemblage of hornblende-granodiorite (Figure 2.43):

plagioclase + quartz + microcline-perthite + hornblende +
 epidote + accessories: biotite ± sphene ± apatite ± zircon ±
 allanite(?) + alteration products: sericite, chlorite

Plagioclase (oligoclase) occurs as strongly zoned and sericitized laths occasionally synneusis twinned. Microcline-perthite shows all gradations between interstitial habit to prominent megacrysts with classic examples of aligned inclusions of plagioclase and hornblende. Compared to the bimodal distinction in microcline habit at Burditt Lake, the dominant Scattergood habit is an incipient megacryst stage, i.e. a few rounded plagioclase laths floating in a local concentration of microcline-perthite without clear megacryst dimensions (e.g. in samples S4, S15). The microcline-perthite intergrowths are strongly perthitic grading into antiperthite.

Compared to the megacrystic granodiorite of Burditt Lake, the Scattergood samples show greater abundance in sphene (to 0.8%), and zircon, and a notable scarcity of myrmekite. Embayment and replacement textures of plagioclase are otherwise similar. Epidote is in altered earthy anhedral patches associated with hornblende-biotite intergrowths. Modal abundances (Appendix B2) show the Scattergood granodiorite to carry lower quartz, lower epidote and higher hornblende than the hornblende granodiorite of Burditt Lake.

Geochemistry

Introduction:

Twenty-five samples of the Scattergood Lake Stock granodiorite have been analysed for major and trace elements

(Appendix C2, D2). Table 2.2 tabulates the mean and standard deviation for these twenty-five samples and compares these with two previously published analyses of the Scattergood Lake Stock. The most obvious feature is the extreme uniformity of values. Much of the data deviation for this study is contributed by one sample (ST9P), while some of the disparity between published values and this study is due to the volatile-free basis of the author's values.

The standard deviations of values for twenty-five field locations separated by as much as 6 miles (10 km) are not substantially different from the quoted analytical precision and accuracy (Appendix C) for this study.

This remarkable homogeneity makes the Scattergood Lake Stock an ideal candidate as an international geochemical granitoid standard. The name "Scattergood" is also appropriate.

Petrochemical Fields:

Figure 2.45 is a ternary Na-K-Ca plot showing the "igneous trend" line of Green and Poldervaart (1958). Scattergood samples plot as a tight cluster on the Na side of the median. In the Ba-Sr-Rb triangle of Bouseily and Sokkary (1975) (Figure 2.44) the Scattergood samples form an exceptionally tight cluster within the granodiorite field. Both plots illustrate the chemical homogeneity of this pluton.

A comparison with the equivalent Burditt Lake Stock

FIGURE 2.43

SCATTERGOOD LAKE STOCK MINERAL
MODES PLOTTED ON Q-A-P DIAGRAM
OF IUGS (1973). TIGHT CLUSTER
DEMONSTRATES HOMOGENEITY.

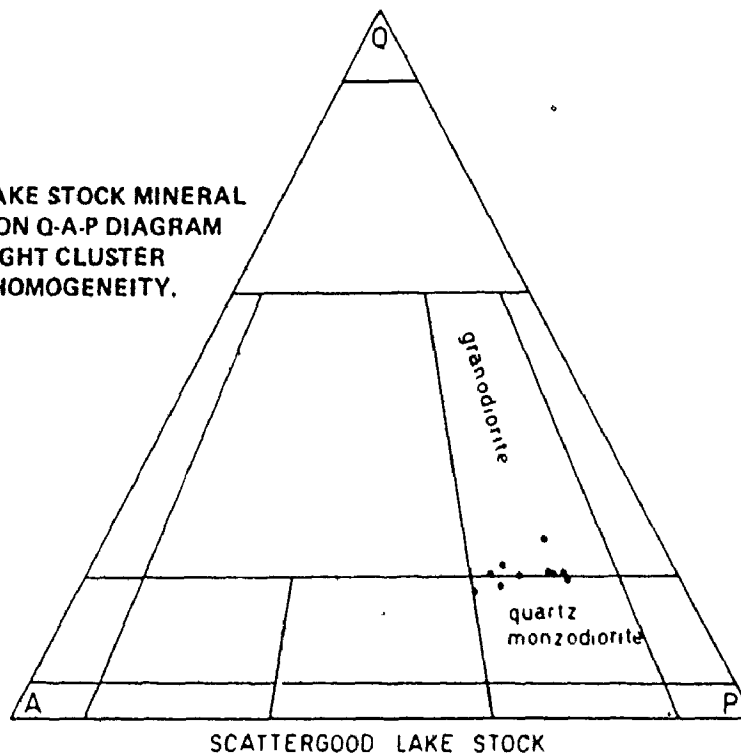
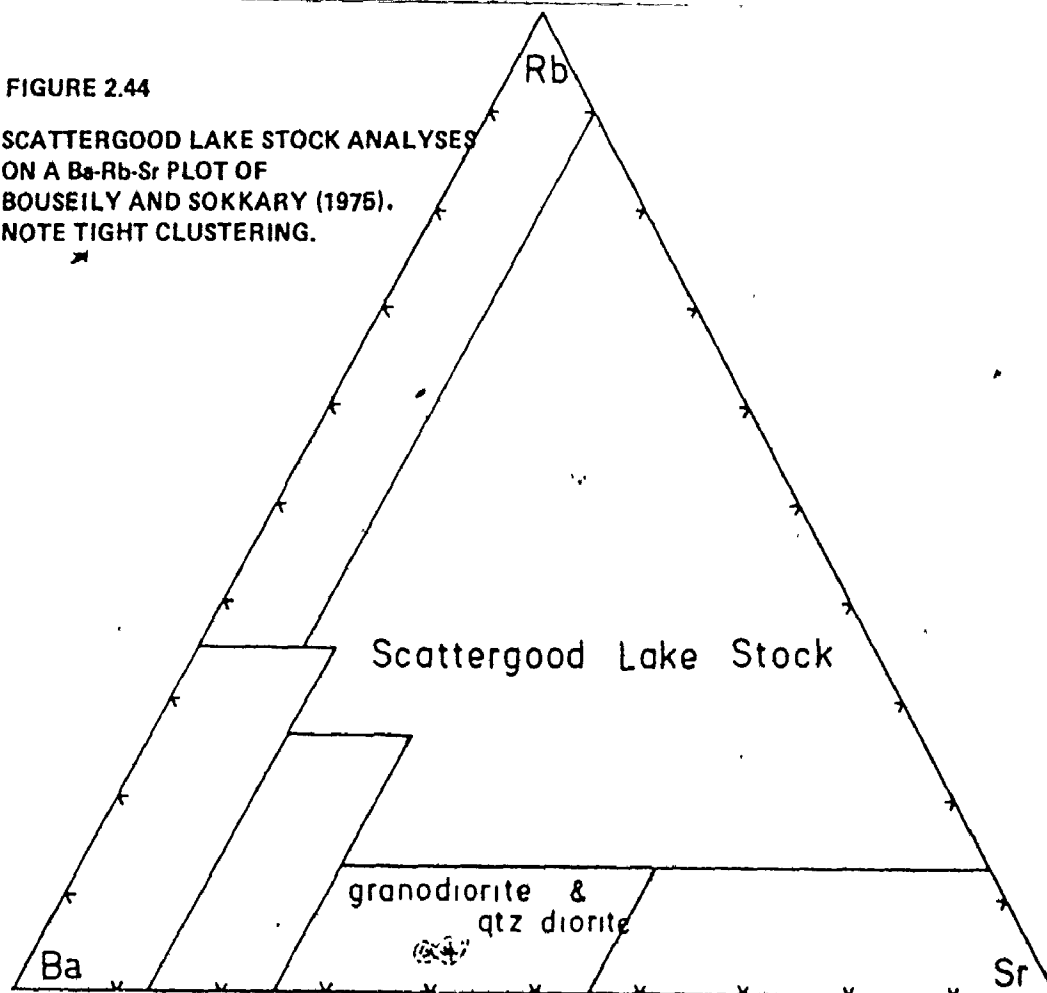


FIGURE 2.44

SCATTERGOOD LAKE STOCK ANALYSES
ON A Ba-Rb-Sr PLOT OF
BOUSEILY AND SOKKARY (1975).
NOTE TIGHT CLUSTERING.



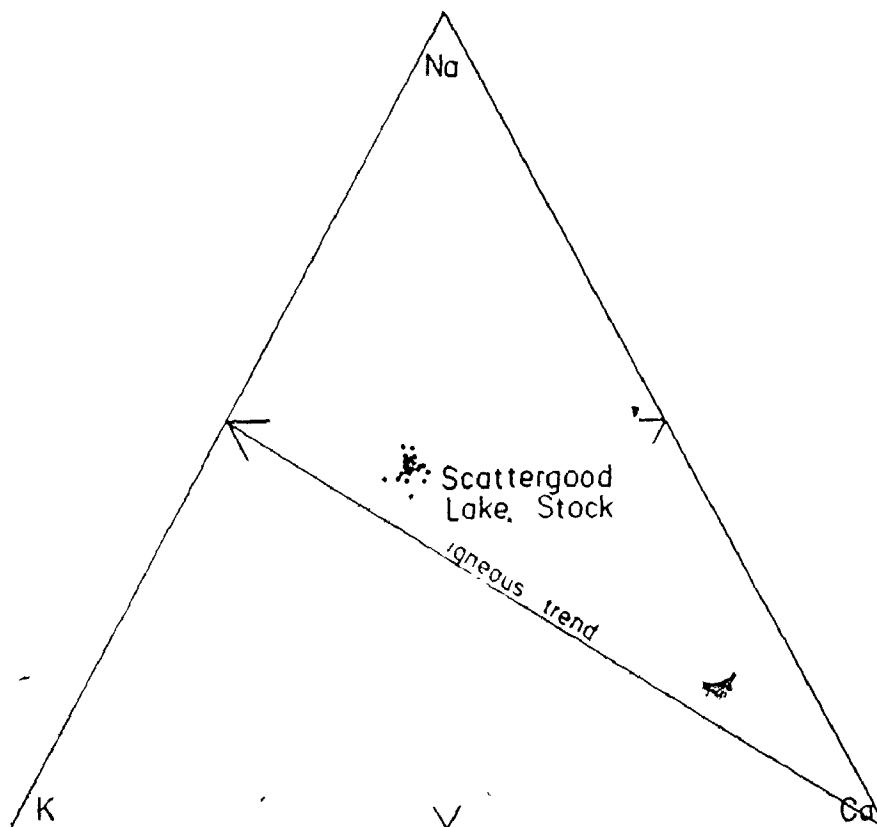


FIGURE 2.45 Ca-Na-K PLOT OF GREEN AND POLDERVAART (1958) FOR THE SCATTERGOOD LAKE STOCK. TIGHT CLUSTERING SHOWS HOMOGENEITY.

Table 2.2 Chemical Analyses for the Scattergood Lake Stock

Oxide	Thomson (1933)* 1 sample	Blackburn (1976) 1 sample	Birk (this study) 25 samples
SiO ₂	66.95	67.50	68.39±0.47' (<u>±1σ</u>)
Al ₂ O ₃	16.53	15.60	15.64±0.22
Fe ₂ O ₃	1.60	1.96)	2.75±0.22
FeO	1.17	1.25)	
MgO	1.36	1.68	1.50±0.13
CaO	2.83	2.49	2.85±0.16
Na ₂ O	5.12	5.13	5.08±0.18
K ₂ O	2.95	3.78	3.27±0.14
TiO ₂	0.39	0.30	0.29±0.02
P ₂ O ₅	0.10	0.15	0.17±0.02
S	0.01	<0.01	
MnO	0.08	0.05	0.05±0.01
CO ₂	0.33	0.10	
H ₂ O ⁺)		0.30	
H ₂ O ⁻)	0.48	0.25	
	<u>99.90</u>	<u>100.50</u>	<u>100</u> (normalized)

*quoted in Blackburn (1976)

plots (Figures 2.13, 2.22) shows that the Scattergood granodiorite is more akin to the north lobe of Burditt than the south - not only because of mutual hornblende and megacrysts, but also because chemical fields for these hornblende granodiorites are more restricted than equivalent plots for the south lobe biotite granodiorite. This suggests a correlation between the degree of homogeneity and megacryst formation. Whether megacryst-bearing granitoids are more homogeneous than megacryst-free granitoids will be investigated for other plutons of this study.

Element Abundances:

A visual comparison of Appendix tables C1, C2 and D1, D2 shows the hornblende granodiorite of Scattergood to carry elemental abundances slightly more primitive, within a fractional crystallization context, than the hornblende granodiorite of Burditt. Of the major oxides, all except SiO_2 and Na_2O are relatively enriched resulting in a slightly lower modified Larsen Index (average 10.4). Of trace elements, Zr, Y and Ce are relatively enriched while Rb, Sr, Ba and Nb abundances are similar.

Conclusions:

The field and petrographic features suggest that the stock was emplaced as a convecting diapiric crystal-liquid

mush. Hydrothermal or pneumatolitic alkali-metasomatism operated locally to develop the megacrysts and the feldspathized enclaves but did not appreciably segregate phases. The shape of the stock may represent an oblique section through a tear-shaped diapir with the northern dyke-rich bulb at the higher elevation.

The uniform hornblende-rich assemblage and incomplete megacryst development suggest that less fluid was available for infiltration metasomatism and therefore for autometasomatic differentiation in situ than was the case for the Burditt Lake Stock. Alternatively, thermal convection may have been more effective in homogenizing the magma pool. The lower quartz content and incipient megacrysts could also be interpreted as illustration that an alkali but not a silica front had traversed the stock in an infiltration cycle at the time the system was "frozen".

2.2 HETEROGENEOUS PLUTONS

2.2.1 Introduction

Middlemost and Romoy (1968) developed a "check-list" of factors which may affect the crystallization history of a magma and thereby contribute to differentiation and heterogeneity. Each of these factors may be operative during magma genesis, transit, emplacement or quiescence, and the extent

of this "check-list" cautions petrologists against trying to apply a few simple models to all igneous provinces. Just a partial list of parameters discussed by Middlemost and Romey (1968) includes: primary magma composition, extraterrestrial impact, tectonic recycling, relay magmas, diffusion, convection, infiltration, polymerization, laminar flow segregation, gravity sinking, gas streaming, seismic sieving, filter pressing, contamination, hydrothermal differentiation, etc. Discussion of these mechanisms is outside the scope of this introduction, except to point out that a model of differentiation by fractional crystallization as implied by phase diagrams, variation graphs and trace element modelling, is not likely to explain all the diversities and lithologic distributions in the heterogeneous plutons of Wabigoon. That certain factors are dominant is, however, apparent in the reoccurring gross similarities between plutons.

One such reoccurring feature is concentric lithologic zoning resulting in mafic borders and felsic cores. This phenomenon will be reviewed in the following section using the Ryckman Lake Stock and Flora Lake Stock as examples. Other plutons in this study that exhibit concentric zoning of various complexities are the Ottertail Lake Stock, Rest Island Stock, Taylor Lake Stock and the eastern granitoid at Esox Lake. These units will be treated briefly in subsequent sections.

2.2.2 The Ryckman Lake Stock

Field Observations

Ryckman Lake lies 50 km northeast of Fort Frances, Ontario, within NTS coordinates 52C/15. The Ryckman Lake Stock was first recognized as a plutonic entity on the map of Lawson (1887) but restricted to the granitoids surrounding Crowrock Bay (Ryckman Lake was called "Sand Lake"). Blackburn mapped the region in 1970 and published a preliminary map at 1" = 0.5 mi. and a final map (1" = 1 mi.) and geological report (Blackburn, 1971, 1973). Mapping was based on traverses at greater than 0.5 mile intervals over granitoids and therefore must be considered reconnaissance. Supplementary mapping was carried out by the author over two weeks in the summer of 1974 along with a gamma ray spectrometer survey and a sampling program. Figure 2.46 represents a compilation of Blackburn's mapping and the 1974 visit. Location numbers in the following discussion match sample stations of Figure 2.46.

Blackburn (1973) recognized an elliptical zoned granodiorite to monzonite stock forming a late-tectonic intrusion into the common limb of the Tupman Lake Antiform-Winkle Lake Syncline. Host supracrustals are dominantly metabasalts, amphibolites and minor intermediate tuff-breccia, metamorphosed to the lower amphibolite facies (Blackburn, 1973).

Field observations and petrography define four mineral assemblages concentrically distributed (Figure 2.46). The

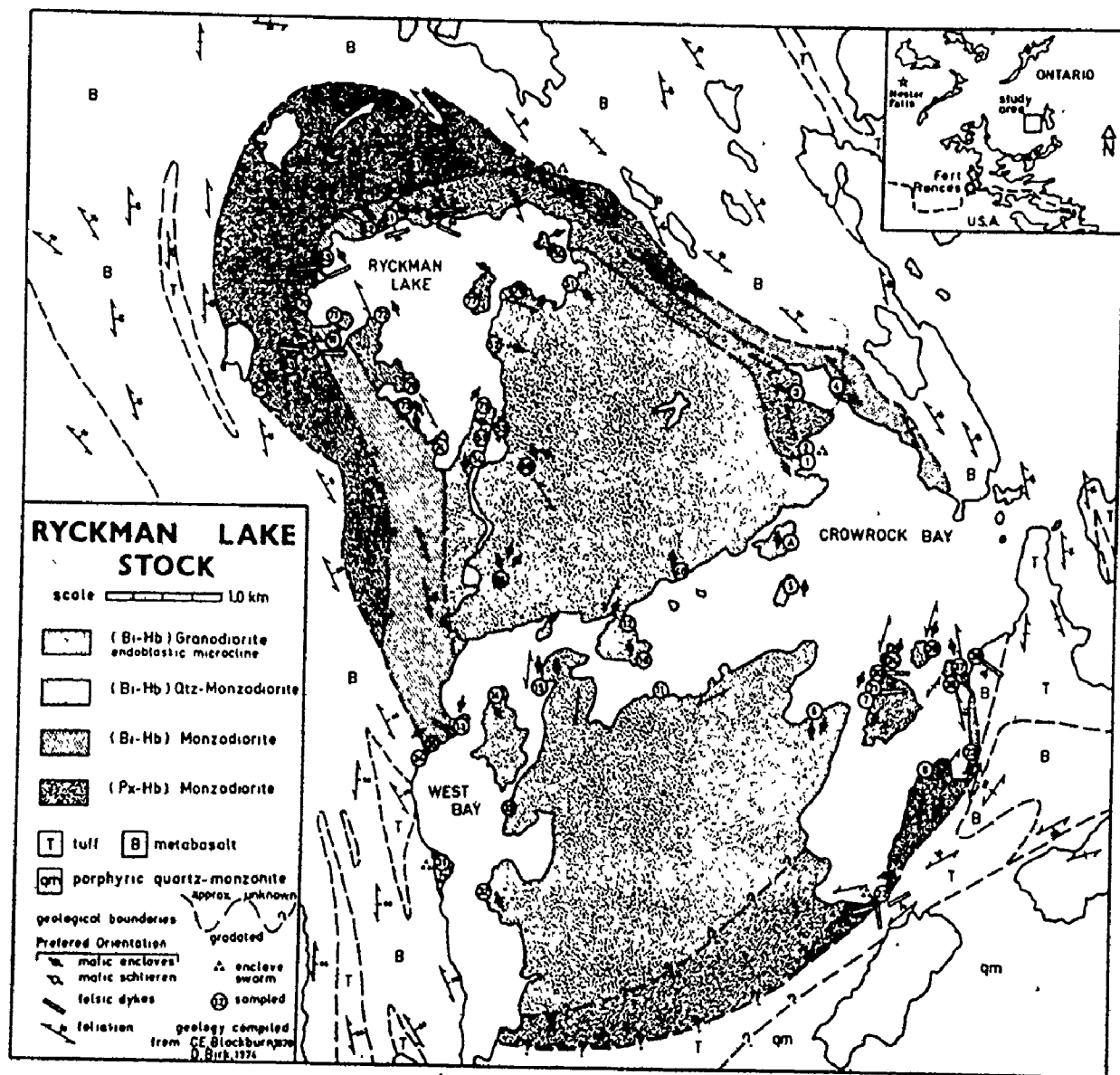


FIGURE 2.46 LITHOLOGY AND STRUCTURE OF THE RYCKMAN LAKE STOCK NORTHWESTERN ONTARIO, (NTS 52 C/15)

NOTE:
CORRESPONDING SAMPLE NUMBERS IN APPENDIX CARRY PREFIX "RY."

core is a microcline-perthite megacryst bearing hornblende granodiorite. Contact with the marginal phases is generally sharp and marked by abundant aplite-pegmatite dykes (location 13) or complex intrusion melange (location 2). At one sample station (76) contact with quartz monzodiorite is gradational over 1.5 m. Contacts between the three marginal phases are gradational and controlled by the mutually exclusive appearance of quartz and pyroxene. At location 70, a 28 cm wide mylonite zone strikes parallel to the quartz monzodiorite-monzodiorite interface displacing several aplite dykes. Further suggestions of post-intrusive movement is supplied by the unusual nature of the core granodiorite: this unit appears intimately shattered and jointed with pervasive micro-slickensides stained with iron oxide. This makes sampling of unweathered specimens difficult.

Mild subparallel alignment of hornblende grains and lensoid mafic enclaves is characteristic of the core granodiorite (location A). Much stronger lineation of enclaves, mafics and megacrysts occurs in the rim phases, locally accented by migmatitic banding (35) or surmicaceous¹ schlieren (20, 93).

Large xenolithic blocks (240 x 90 cm at location 82) of metavolcanics occur within the border zones. Contact between the stock and supracrustals is sharp to complex: at 84 is located a 1.5 m wide swarm of lensoid enclaves; at location 22, concordant gabbroic patches and discordant gabbroic

¹ surmicaceous: biotite-rich (Didier, 1973).

dykes inject into tuff-breccia and subsequently are cut by aplite dykes.

Mafic enclaves pervade all four pluton phases and compositions imply a variety of source lithology: coarse gabbro (50, 55, 62); hornblendite (51, 62); fine chlorite schist (54, 63). At location 92 a heterogeneous swarm of lensoid enclaves, some showing nebulous contacts, appears to merge with the host granitoid (also at 62). As suggested by Blackburn (1973), the outer rim of the stock may be a hybrid zone produced by assimilation of metavolcanics. These observations suggest that the host magma was quartz monzodioritic rather than the later intruded granodiorite.

Blackburn (1973) suggested that:

"...The Ryckman Lake Stock is unique among the felsic plutonic rocks of the Otukamamoan Lake area in that no pegmatite or aplite dykes are present". (p. 25)

Although the granodiorite core is relatively free of felsic dykes, the periphery of the granodiorite and adjacent quartz-monzodiorite is characterized by abundant aplite-pegmatite veins. Dykes are usually composite pegmatite with aplite cores (56 cm wide dykes at location 13; a swarm of 30-90 cm wide dykes at location 92), but reverse zoned dykes of aplite with pegmatite core occur occasionally (locations 61, 2). Unusually large felsic apophyses have also invaded the supracrustals: a 4 ft wide pegmatite dyke is visible near

shore at location 36, while a 2 ft 2 in. wide pink aplite cuts tuff-breccia at location 22. A very spectacular 50 ft wide elongate outcrop of pure milky quartz occupies location 53 near the centre of the granodiorite.

Microcline-perthite megacrysts in the granodiorite resemble those of the Burditt Lake north lobe. Insets of microcline straddling enclave-granodiorite boundaries, or lying within mafic enclaves are even more numerous than at Burditt Lake (locations 3, 13, 15, 10, 12). Field visits observed pink feldspar phenocrysts within the border monzodiorite increasing in concentration towards the rim (at 37, 4, 81). These proved to be cumulate clusters of sericitized plagioclase laths partially replaced by microcline. At locale 37 the pink insets are strongly aligned with mafic mineral foliation and impart a very attractive mottlement.

Blackburn (1973) argued that "... many of the diorites that occur in the contact zone may be recrystallized volcanic rocks ...". The author's visit uncovered several features that rules this out. At location 22, dykes of gabbroic to dioritic material cut the tuffaceous supracrustals, while intrusion breccia at 82, 84 and 31 attest to forceful intrusion. The xenolithic blocks of metavolcanics at 82 have preserved sharp contacts.

The aeromagnetic map for Little Turtle Lake gives rough correlation with lithology (ODM, 1971, Map 1151G).

The granodiorite core of the Ryckman Lake Stock is approximately contained below the 60,500 gamma contour. The quartz monzodiorite and monzodiorite envelope carries a high magnetic flux (greater than 60,500) indistinguishable from the high flux over adjacent supracrustals. Strong anomalies are centred over metavolcanics south of West Bay (62,500 gammas), on the north-east edge (60,900 gammas), and at the mouth of Crowrock Bay (60,900 gammas); the last anomaly correlates with magnetite in thick mafic flows.

The field evidence points to multiple intrusion in a mafic to felsic sequence. Three intrusions are recorded: monzodiorite, quartz-monzodiorite and granodiorite. Some of the mafic components of the monzodiorite were contributed by wall rock assimilation. The monzodiorite rim further differentiated in situ by crystallizing from the rim inward to form a pyroxene-bearing phase and a pyroxene-free phase. A hiatus was recorded between the time of monzodiorite + quartz-monzodiorite intrusion and the emplacement of the granodiorite core. The granodiorite therefore was emplaced into a rigid or semi-rigid subcircular mass which was fractured, mylonized and injected by aplitic residuals of the granodiorite. Subsequent to emplacement came an autometasomatic infiltration front that developed the microcline-perthite megacrysts in the granodiorite.

Petrography

Introduction:

Four lithologic units have been mapped on Figure 2.46 based on the following mineral assemblages (constituents in order of abundance):

1. Biotite-hornblende granodiorite:

plagioclase + quartz + K-feldspar + hornblende + epidote ±
± biotite ± sphene ± apatite ± opaques

2. Biotite-hornblende quartz monzodiorite:

plagioclase + hornblende + K-feldspar + quartz + biotite +
epidote ± allanite ± schorlite ± sphene ± opaques

3. Biotite-hornblende monzodiorite:

plagioclase + hornblende + K-feldspar + epidote ± biotite ±
sphene ± apatite ± opaques

4. Pyroxene-hornblende monzodiorite:

plagioclase + K-feldspar + hornblende + pyroxene + biotite +
epidote + opaques ± schorlite ± sphene ± allanite

Modal analyses for the Ryckman Lake Stock are listed in Appendix B3 and when plotted on the IUGS (1973) ternary Q-A-P diagram (Figure 2.47) they define a broad band ranging from granodiorite to monzodiorite. The following petrographic

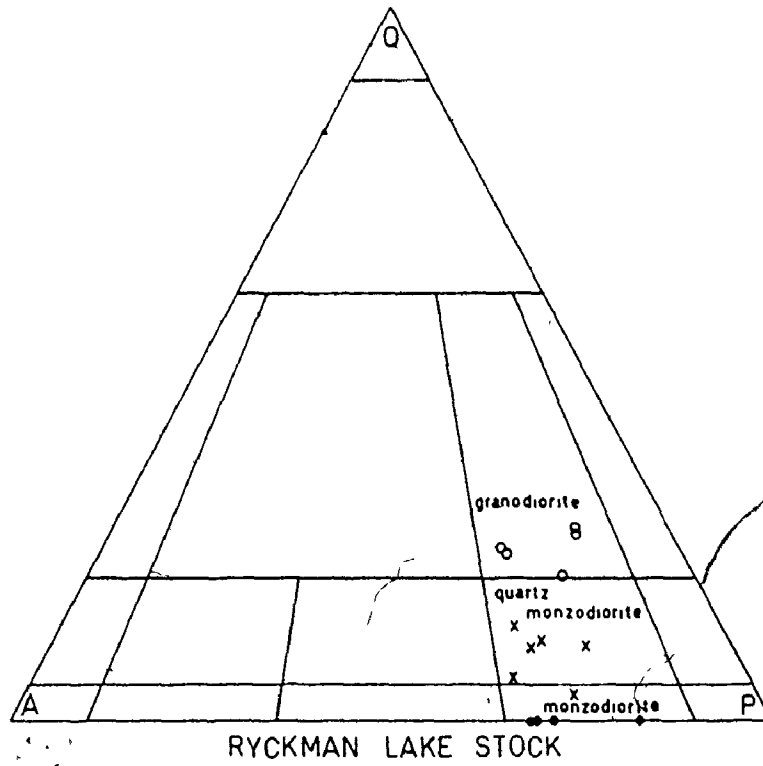


FIGURE 2.47 RYCKMAN LAKE STOCK MODES ON AN IUGS (1973) TERNARY Q-A-P DIAGRAM. SYMBOLS AS FOLLOWS:

- Bi-Hb GRANODIORITE
- X Bi-Hb QTZ-MONZODIORITE
- Bi-Hb OR Px-Hb MONZODIORITE

descriptions concentrate on petrogenetically significant features characteristic for these rocks.

Bi-Hb granodiorite:

The core granodiorite displays microcline-perthite megacrysts similar to Burditt with diffuse borders, bearing crystallographically aligned plagioclase and hornblende inclusions and occasional rim myrmekite. Plagioclase occurs in two generations:

- (1) as highly digested and embayed laths with bent and fractured twin lamellae and concentric sericite alteration;
- (2) as weakly twinned granoblastic equant grains with triple junctions against granoblastic quartz and K-feldspar

Quartz and K-feldspar occur both as irregular interstitial grains and in patches of granoblastic triple-junctioned mosaics (Plate A5.5). Epidote forms granulated anhedral fringes to hornblende.

The petrographic impression is of a complex history of crystallization, autometasomatism, followed by cataclasis and recrystallization. These features confirm the field observations of microslickensides. The author considers these textures to be autometamorphic, i.e. protoclastic, caused by

differential flow of the magma before complete consolidation.

Bi-Hb quartz monzodiorite:

The quartz monzodiorite medial zone carries much greater variety of mineralogy and texture. At station 72, highly sericitized elongate plagioclase laths form subparallel cumulate networks confining smaller subhedral grains of hornblende and interstitial K-feldspar and quartz. The plagioclase shows occasional synneusis twins, myrmekite and alteration zoning. A thin section from location 3 shows an equant mosaic of interlocked anhedral grains of plagioclase and subhedral equidimensional hornblende. K-feldspars occur as interstitial grains carrying the Na-cobaltinitrite stain (see Appendix B) in mottled relief, probably due to microscopic patch perthite. Epidote forms anhedral interstitial aggregates or fringes to hornblende, while sphene forms anhedral aggregates. At station 21, plagioclase shows two generations: mildly sericitized interlocking equant grains and large ragged sericitized phenocrysts. Locally granoblastic texture prevails with triple junctions between polygons of plagioclase, quartz and K-feldspar. Station 7 is further characterized by biotite flake clusters and abundant polygons of K-feldspar, as well as two-generation plagioclase. At station 60 several anhedral grains of brown tourmaline (schorlite) associated with hornblende contribute to the mode. Hornblende in sections from

60, 61 and 71 shows peculiar polysynthetic twinning of lamellar fracture that may be cataclastic. By the Michel Levy test (sections 7, 23), plagioclase is oligoclase.

Bi-Hb monzodiorite:

The quartz monzodiorite grades texturally into, and may in fact be in continuum with biotite-hornblende monzodiorite as quartz disappears. Station 4 shows "phenocrysts" of relict sericitized and digested plagioclase set in a finer matrix of granoblastic K-feldspar and second-generation plagioclase. These large plagioclase relicts were mis-identified by field observations as incipient pink K-feldspar megacrysts. Hornblende forms large subhedral to anhedral stubby plates. At station 35, highly sericitized stubby laths of plagioclase form a tight decussate network with subhedral hornblende and localized polygonal mosaics of K-feldspar and secondary plagioclase interspersed.

Px-Hb monzodiorite:

The Bi-Hb monzodiorite grades into pyroxene-hornblende monzodiorite with the appearance of hornblende-pyroxene intergrowths. The rocks of the Ryckman Lake Stock show a strong antipathy between quartz and pyroxene with mineral modes showing exclusion of one or the other.

Location 84 shows large frayed laths of plagioclase

that have suffered extensive invasion and replacement by grid-iron twinned microcline. Replacement of plagioclase in places shows as amoeboid patches of microcline which coalesce towards margins. These textures are suggestive of incipient microcline megacrysts complete with occasional rounded plagioclase inclusions. The author suggests that further work be done to determine if K-feldspar megacrysts could form by pseudomorphic replacement of plagioclase phenocrysts.

At 94 the monzodiorite displays a very dense intergrowth of plagioclase and hornblende-pyroxene with biotite flake inclusions. The rock is notable for very abundant euhedral apatite that forms inclusions in biotite, hornblende opaques and euhedral sphene. A very fine crystallographic "fencing" of microlitic needles occur in biotite similar to textures recorded for biotite from mafic enclaves (Plate A2.4). Lamellar jointing in hornblende and rare grains of subhedral schorlite were recorded in sample 84.

Textural conclusions:

If the marginal phases of the Ryckman Lake Stock represent separate intrusions, the contacts may have been homogenized by subsequent contact metamorphism from the granodiorite injection. The textures suggest the border phases were emplaced as a plagioclase-hornblende or plagioclase-pyroxene crystal cumulate. Autometasomatism caused microcline

of and of pyroxene. Subsequent ³protoclasmation and recrystallization followed, possibly caused by invasion of the core granodiorite. Alternatively, the entire stock may have suffered a postmagmatic metamorphic event although no other evidence for such an event is available.

Geochemistry: Major Elements

Appendix C5 tabulates major oxides for 41 phanerites and two felsic dykes of the Ryckman Lake Stock as well as several analyses of mafic enclaves and metavolcanics. The lithologic zoning mapped in figure 2.46 is reflected in the large range of chemical concentrations, especially in SiO_2 , FeO , MgO , and CaO .

If fractional crystallization was the dominant differentiating mechanism, this should be better recorded in petrochemical fields and trends than was the case for the "homogeneous" plutons, because of the wider chemical range. On the Na-K-Ca plot of Green and Poldervaart (1958) analyses define three petrochemical fields on the Na side of the "igneous trend" divide (Figure 2.48) while felsic dykes plot on the K side. The granodiorite of the core defines a distinct tight cluster of points. The quartz monzodiorite mantle overlaps with the bi-hb monzodiorite and px-hb monzodiorite, i.e., they are not discriminated on the Na-K-Ca plot. Although the three phanerite units form a continuous sequence compatible with the "igneous trend" for crystal fractionation, individual fields are wide suggesting that other factors contributed to deviation from the ideal trend.

The behaviour of individual elements is better observed on cation versus modified Larsen plots (figure 2.49 to 2.57). At first

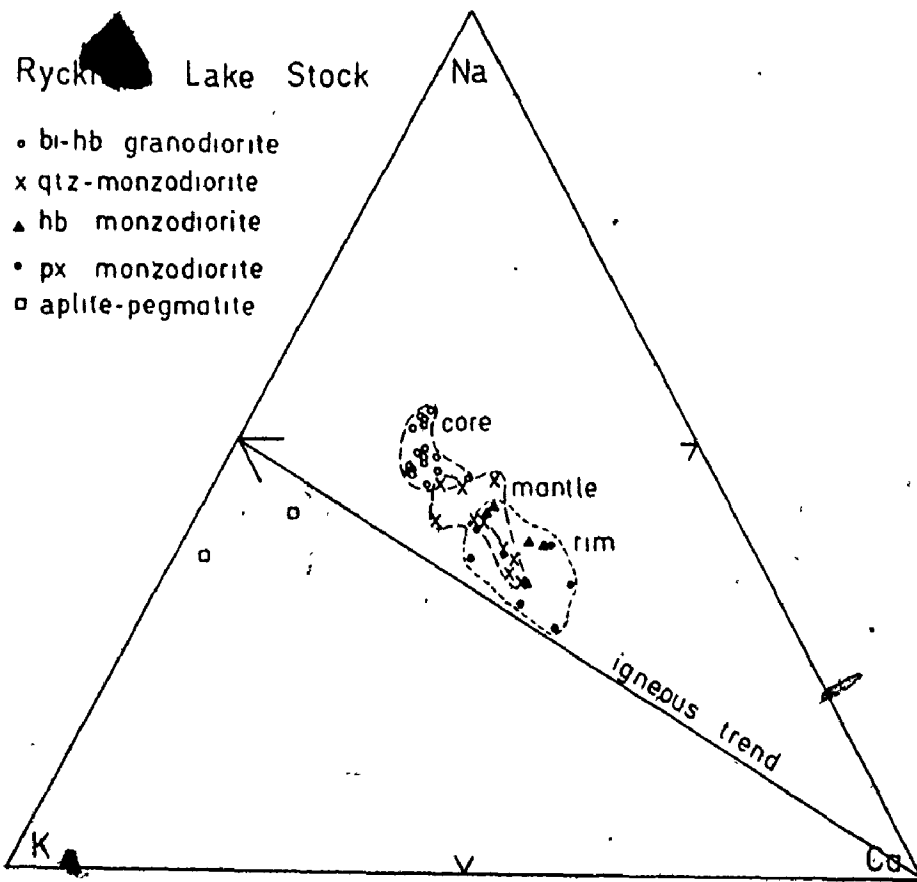


FIGURE 2.48 Ca-Na-K PLOT OF GREEN AND POLDERVAART (1958) FOR RYCKMAN LAKE STOCK.

glance these plots suggest differentiation trends with a strong positive correlation of Si with index and a strong negative correlation of Fe, Mg, Ca, Ti, P, K, Na, and Al are relatively constant with index except for the felsic dykes. Taking into consideration the individual lithologies, the following interesting features emerge:

1. Except for one outlier (RY6), the granodiorite core is represented by a very tight cluster of points for each element. More mafic phases show a progressively wider scatter with lowered index.
2. For several elements (clearly for Si and Al; vaguely for Na, P) the three mafic outer zones - quartz monzodiorite, bi-hb monzodiorite and px-hb monzodiorite - define three distinct linear or curvilinear arrays. Visual best-fit lines through their sample points give different slopes and intercepts. This suggests that the data points do not in fact define a single differentiation trend but instead record three distinct histories of differentiation.
3. Na and K plots display wide scatter. Except for two outliers, Na shows a shallow convex distribution. No pattern is recognizable for K.

Two interpretations of the major element patterns are proposed with selection of the preferred model deferred until other zoned plutons have been considered. The two interpretations correspond to a single magma source model versus multiple source model. Initial fractionation from a single magma source may have been complicated by

continued crystal fractionation in transit or in situ. This is compatible with nebulous gradational contacts between phases and gradations within phases. It is supported by the convergence of the mafic curvilinear arrays on the granodiorite cluster with increasing index. Alternatively, the three mafic phases and the granodiorite core may have been derived from different source regions. The "primitive" ends of the linear variations suggest that earlier marginal intrusions were richer in Al, Na, K and P and depleted in Si relative to the quartz monzodiorite of the same index. A model requiring different source regions does not, however, fit the evidence from the Ca, Fe and Mg plots for which strong negative correlation indicates chemical gradation in a related rock series.

Trace Elements:

Trace element analyses for the Ryckman Lake Stock are tabulated in Appendix D5. Linear variation diagrams using the modified Larsen index as abscissa are presented in figures 2.58 to 2.62. Trends are obscured or obliterated by numerous outliers or critically low concentrations (e.g. Y and Nb) but the following features emerge:

1. Zr, Ba and Ce concentrations appear to violate the physicochemical predictions of Ringwood (1955) and Taylor (1964) for fractional crystallization. These elements should increase with index (i.e., in residual liquids) but all show a decrease.
2. Granodiorite displays a tight cluster of points for all elements (except for outlier 33 in figure 2.58).

3. Ba is remarkably constant in the bi-hb monzodiorite but scatters widely for the px-hb monzodiorite and the quartz monzodiorite. The two felsic dykes differ considerably in Ba content.
4. Rb concentration is constant for all phanerite lithologies, but increases sharply in the felsic dykes. This pattern is analogous to the K distribution.
5. Sr content is widely scattered for the mafic phases which contrasts sharply with the strong negative correlation with index exhibited by Ca.

The ternary Rb-Ba-Sr plot (figure 2.63) shows that phanerite phases locate within the "granodiorite to quartz diorite" rhomboid of Bouseily and Sokkary (1975), as overlapping clusters elongated along the Ba-Sr axis. The granodiorite cluster is the most confined. The aplite and aplite-pegmatite dykes plot marginal to or outside this rhomboid, far removed from "strongly differentiated" trapezoidal field proposed by Bouseily and Sokkary (1975). This reflects the low Rb and high Sr content of even the most highly differentiated phases of this pluton, relative to the granitoids compiled by these authors. Representative samples of contact metavolcanics and internal mafic enclaves have been included in Figure 2.63. Only one enclave sample plots outside the "granodiorite/Qtz diorite rhomboid. This indicates that for the Ryckman Lake area, the Ba-Rb-Sr plot does not effectively distinguish between lithologies.

FIGURES 2.49 TO 2.57:

**MAJOR ELEMENT CATIONS VERSUS
MODIFIED LARSEN INDEX FOR
RYCKMAN LAKE STOCK. OUTLIERS LABELED.**

- o Bi-Hb GRANODIORITE
- X QTZ MONZODIORITE
- ▲ Hb MONZODIORITE
- Px MONZODIORITE
- APLITE-PEGMATITE

FIGURES 2.58 TO 2.62

**TRACE ELEMENTS VERSUS MODIFIED
LARSEN INDEX FOR RYCKMAN
LAKE STOCK. OUTLIERS LABELED
SYMBOLS AS FOR FIGURES 2.49 TO 2.57.**

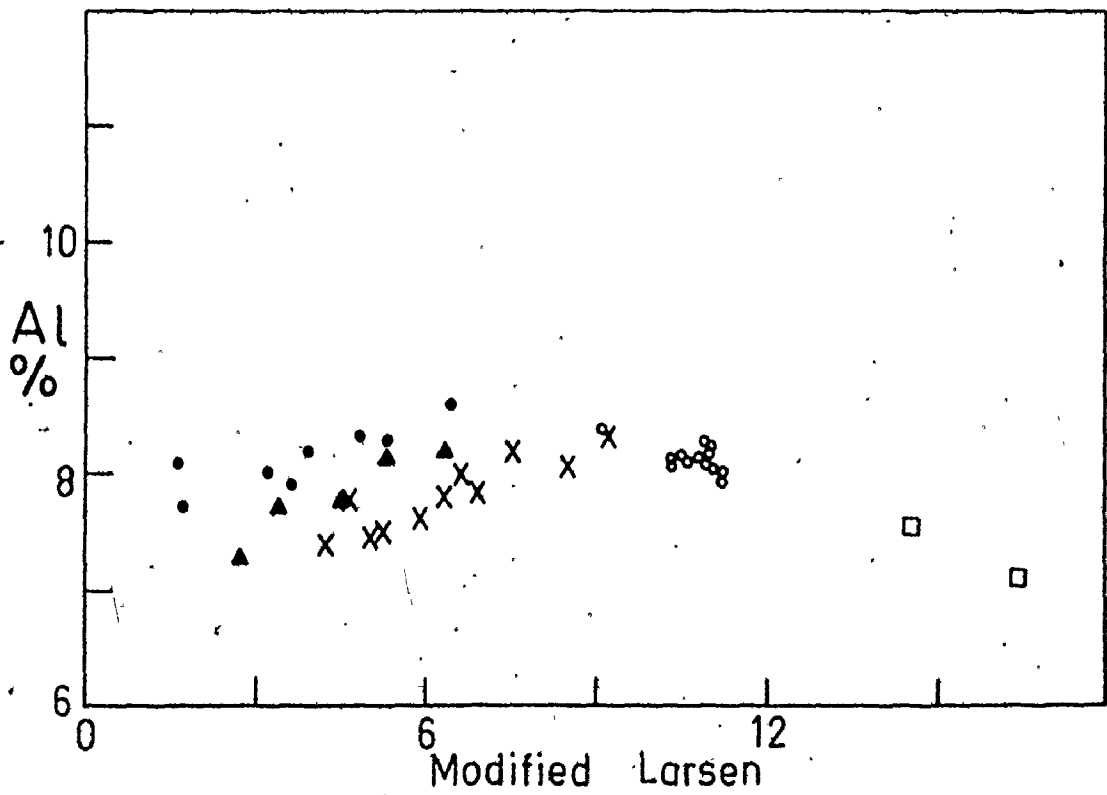
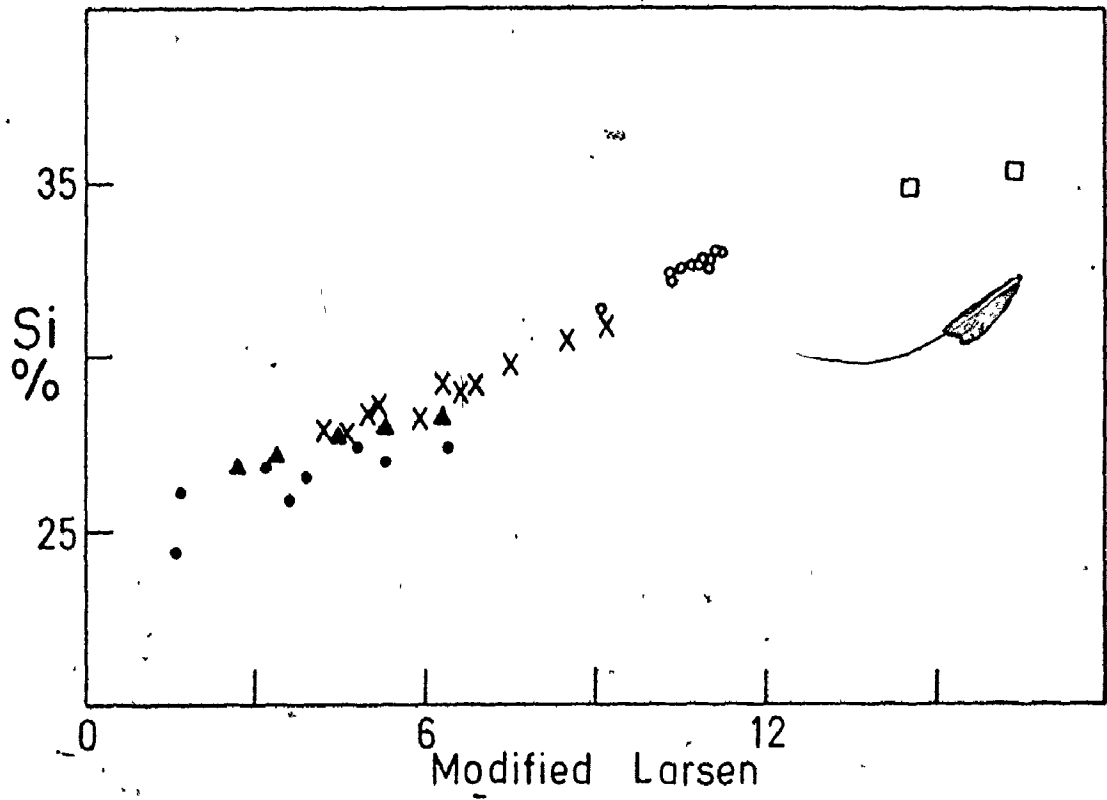


FIGURE 2.50

FIGURE 2.51

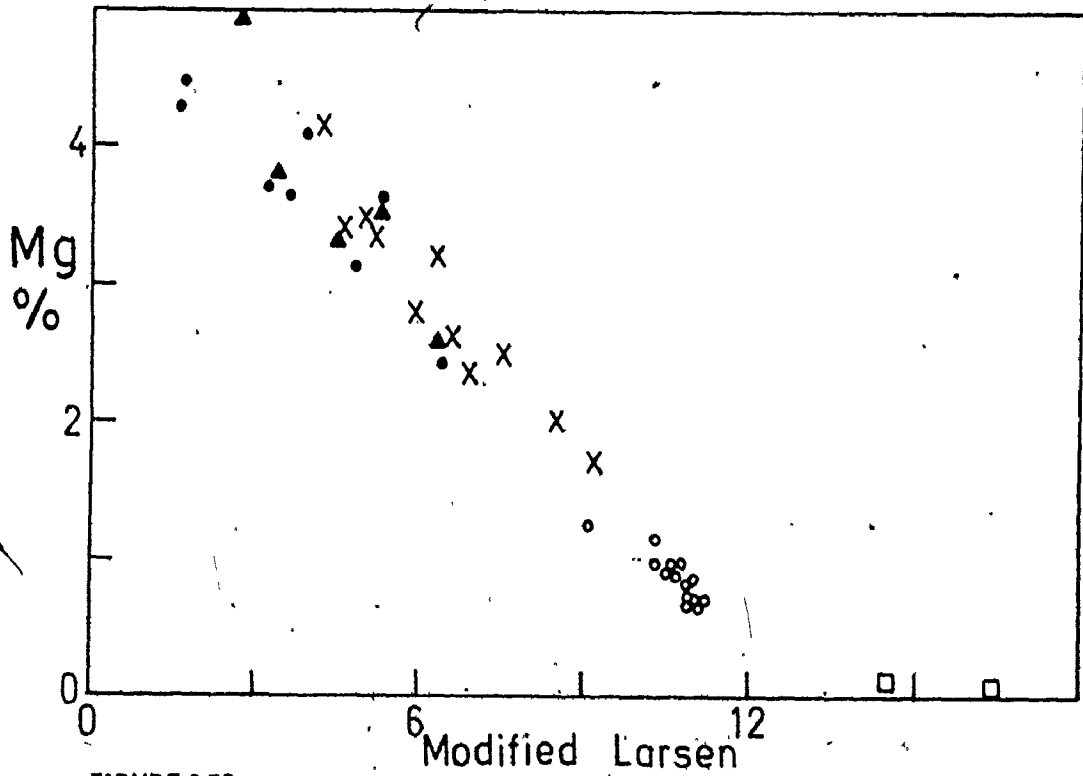
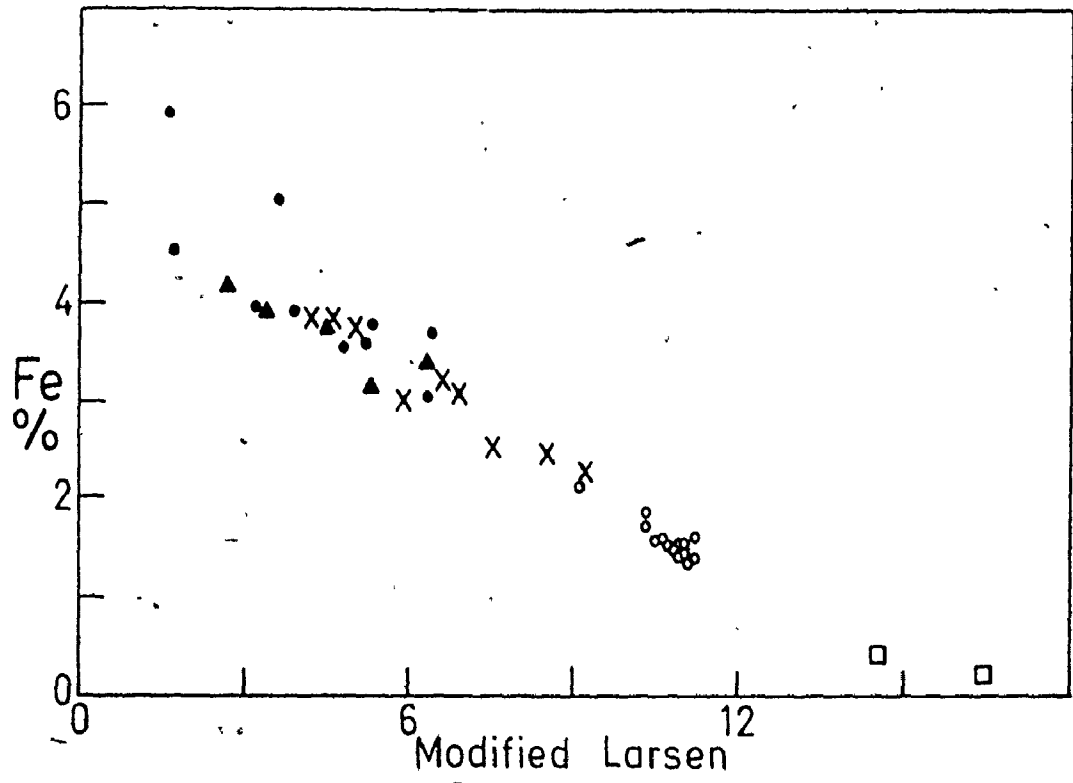


FIGURE 2.52

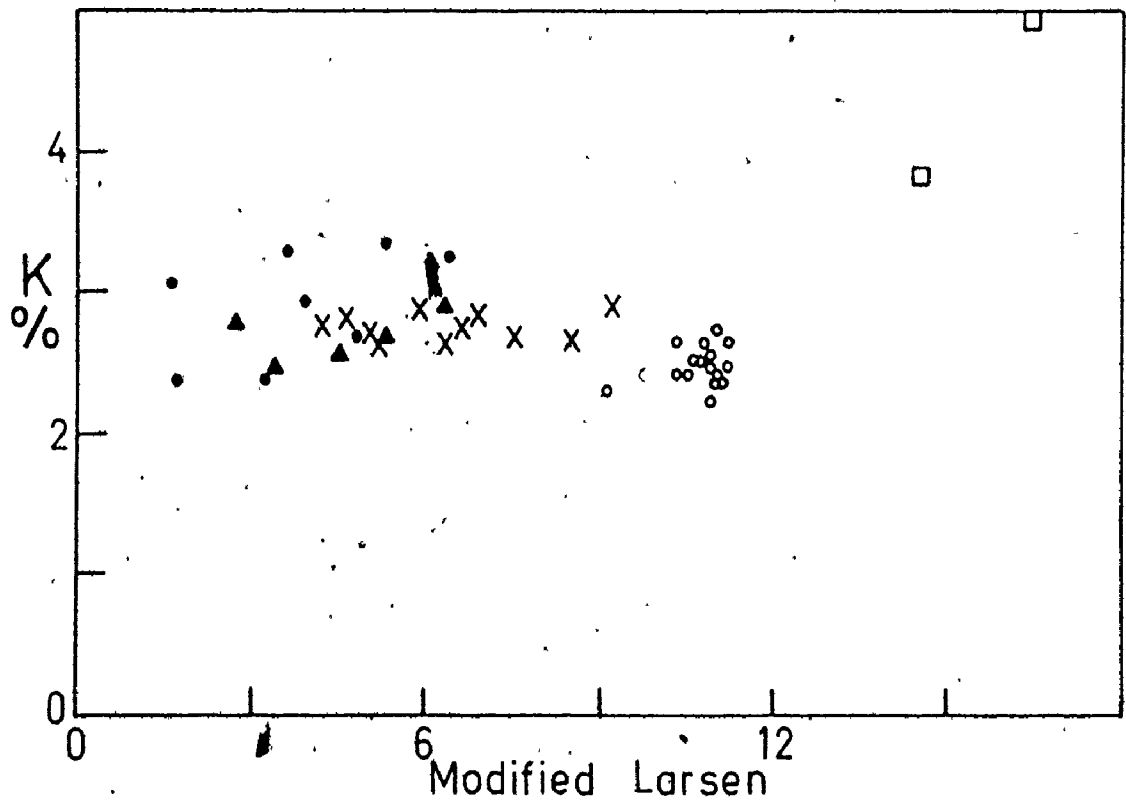
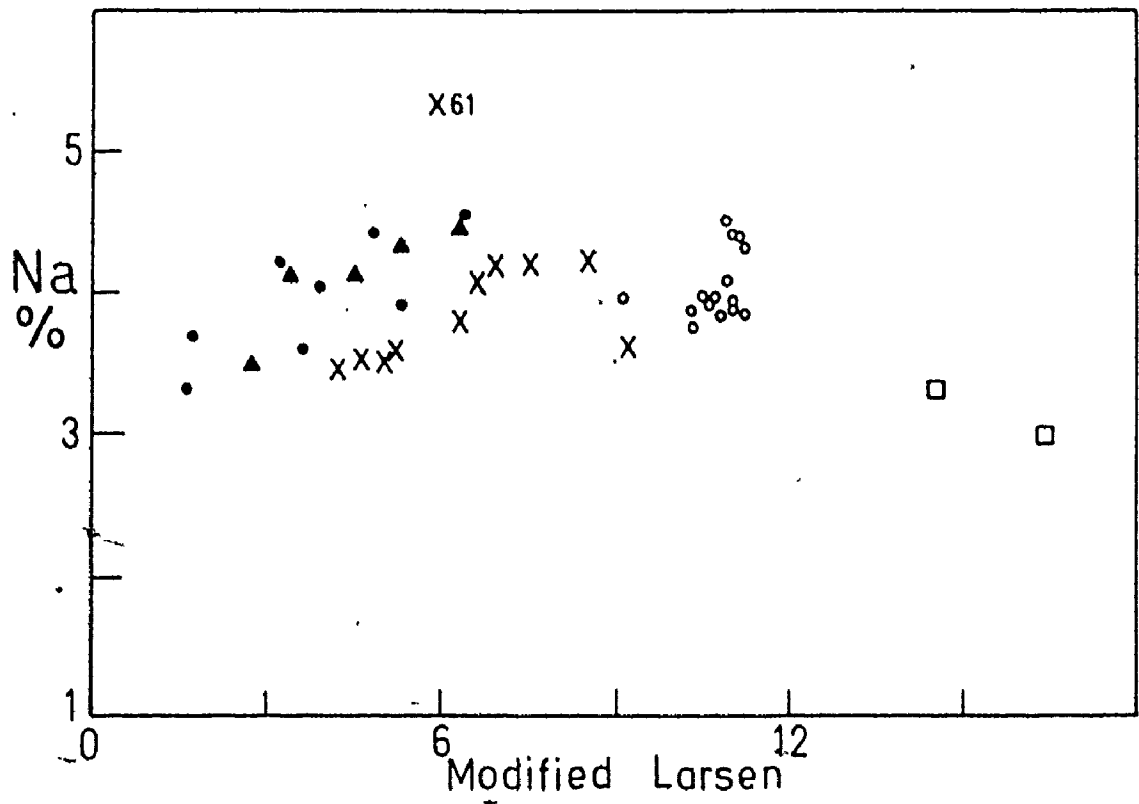


FIGURE 2.54

FIGURE 2.55

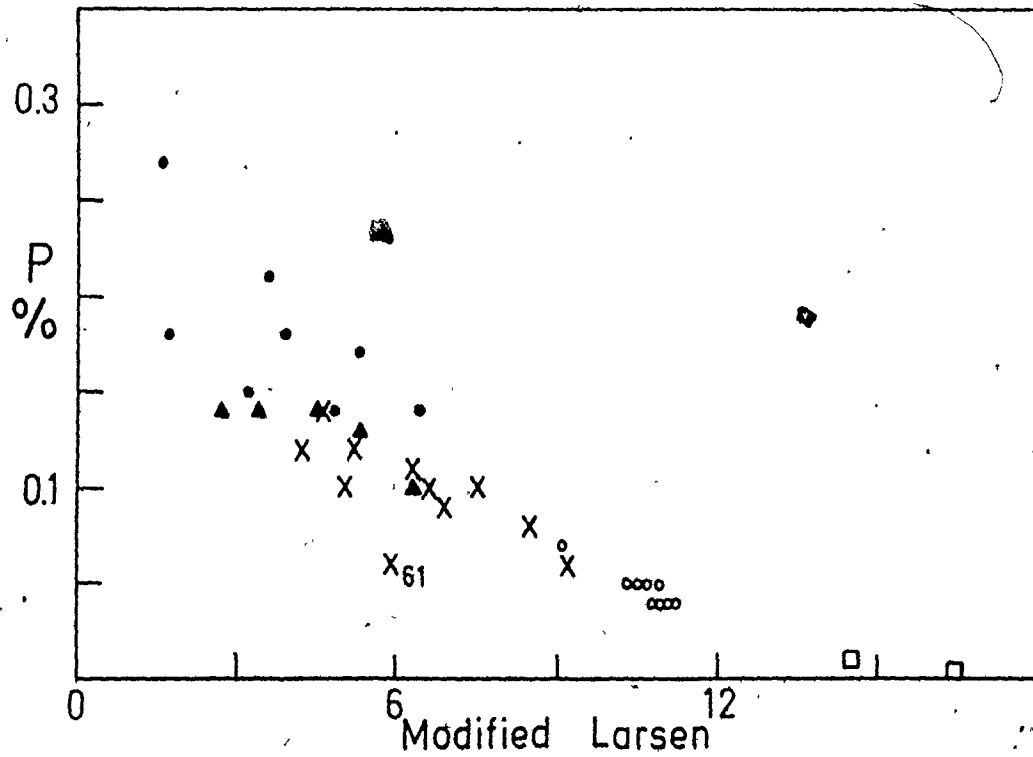
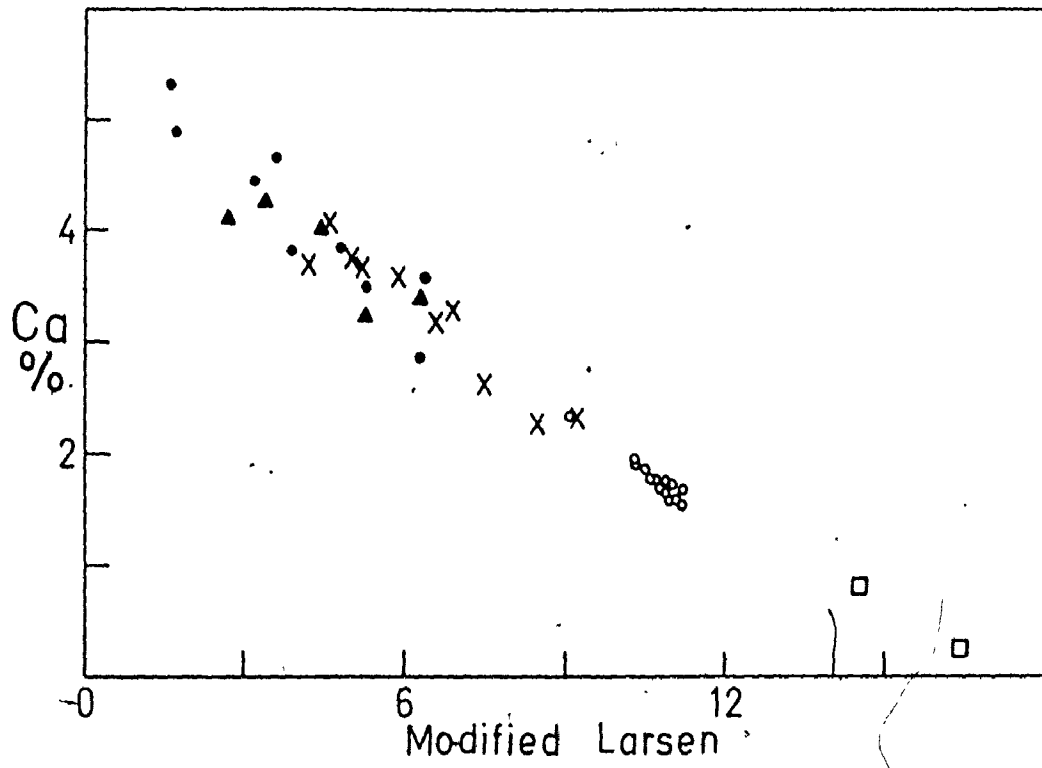


FIGURE 2.56

FIGURE 2.57

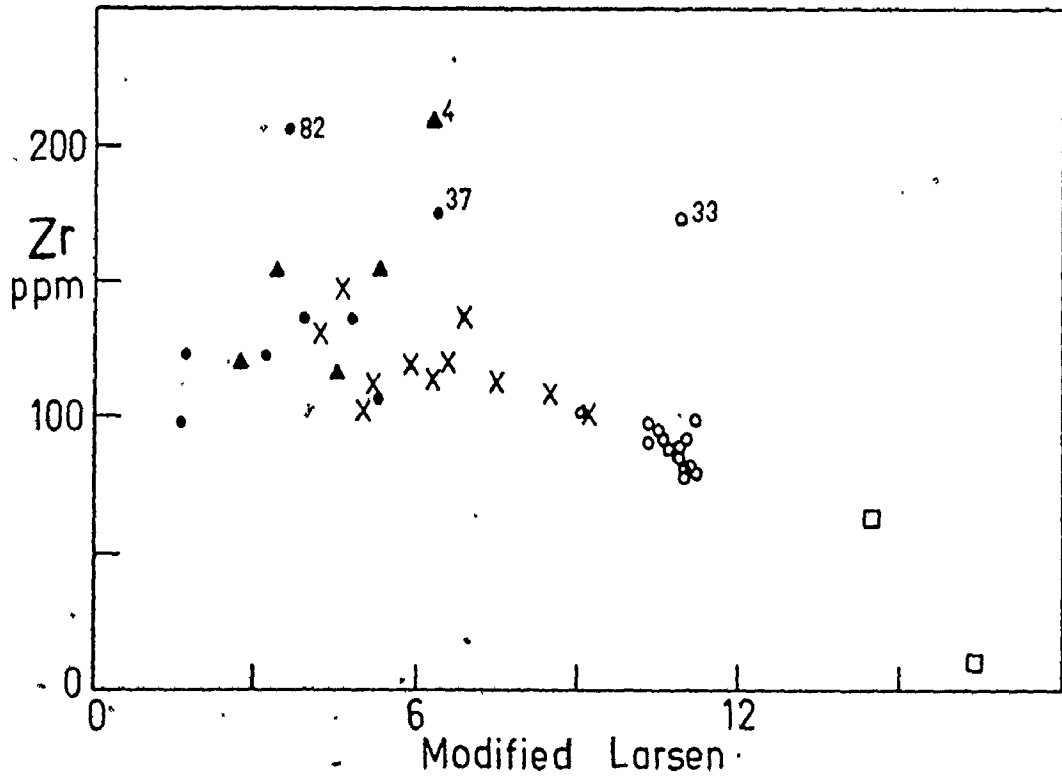
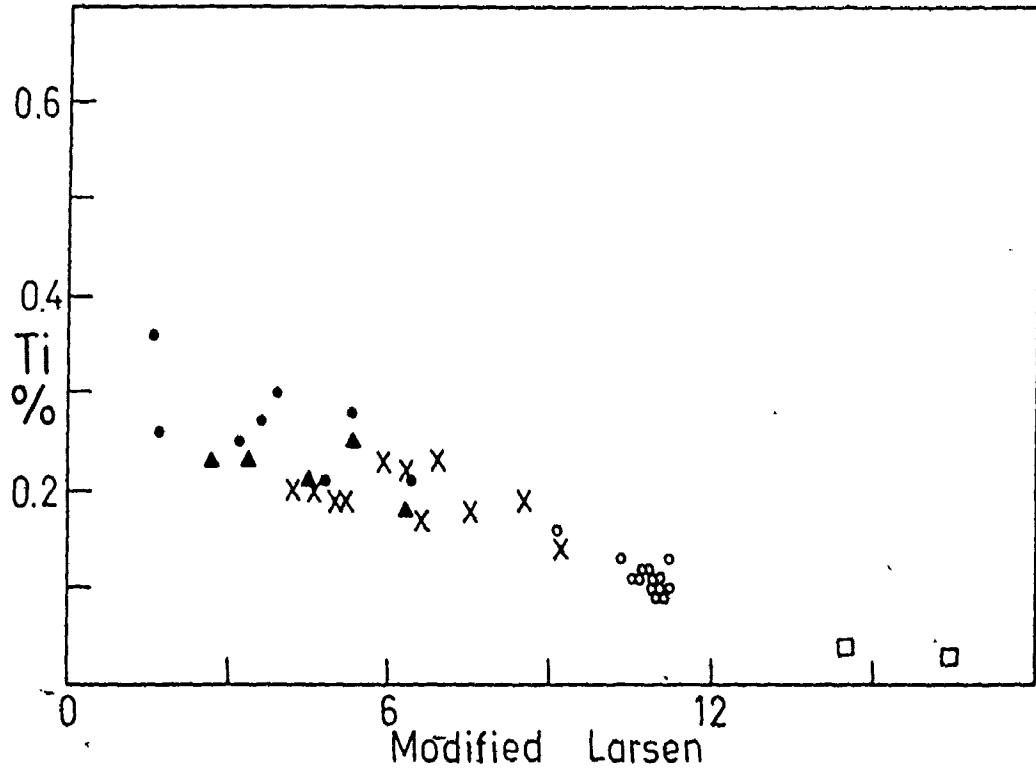


FIGURE 2.58

FIGURE 2.59

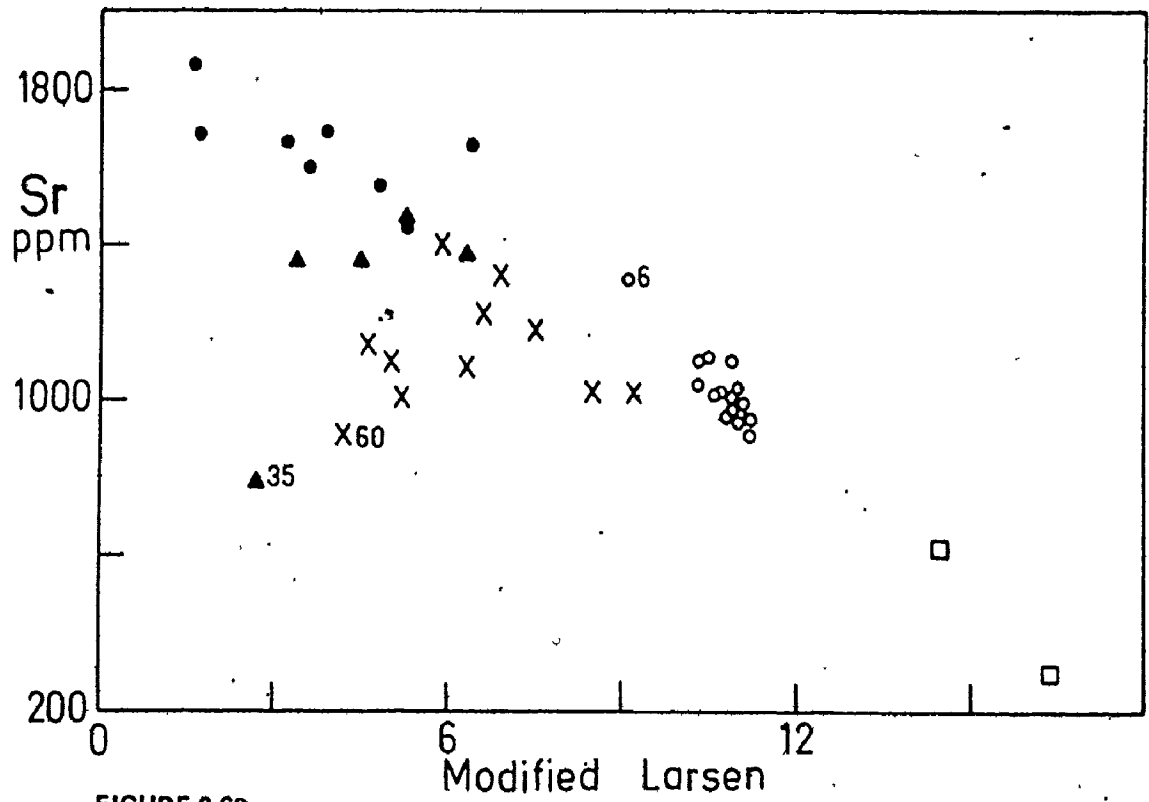
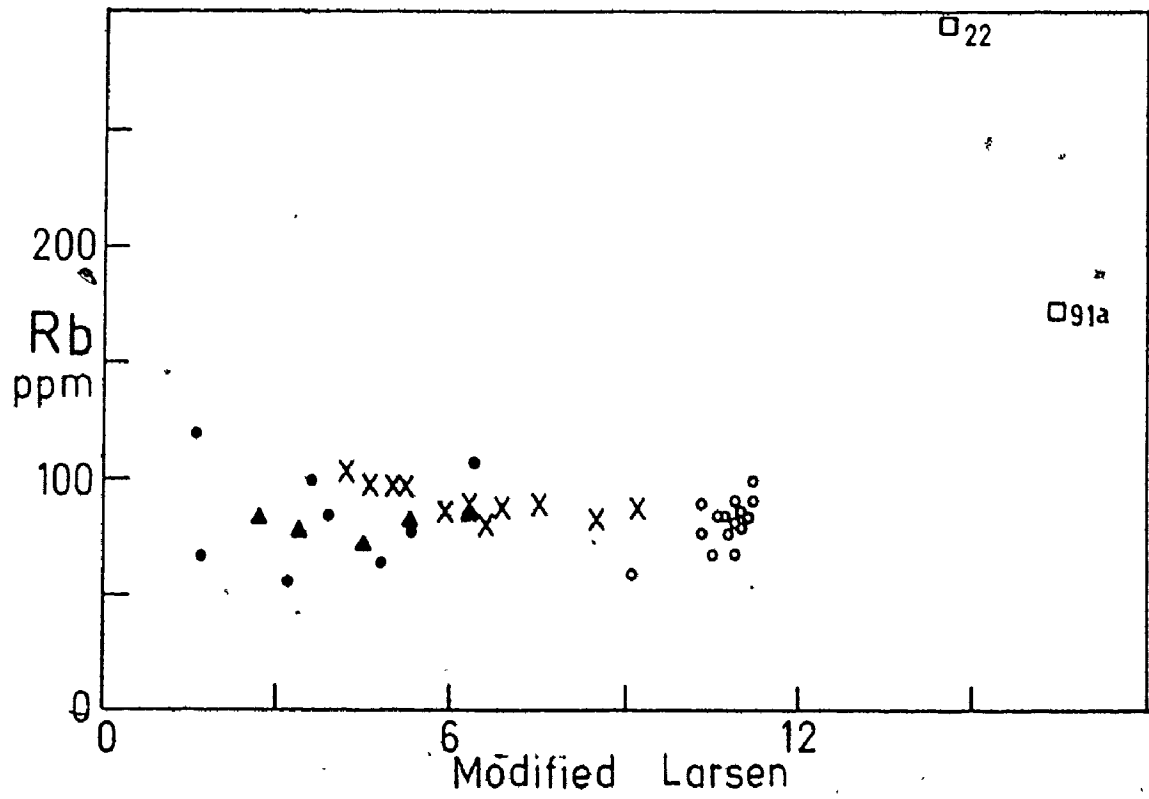


FIGURE 2.60

FIGURE 2.61

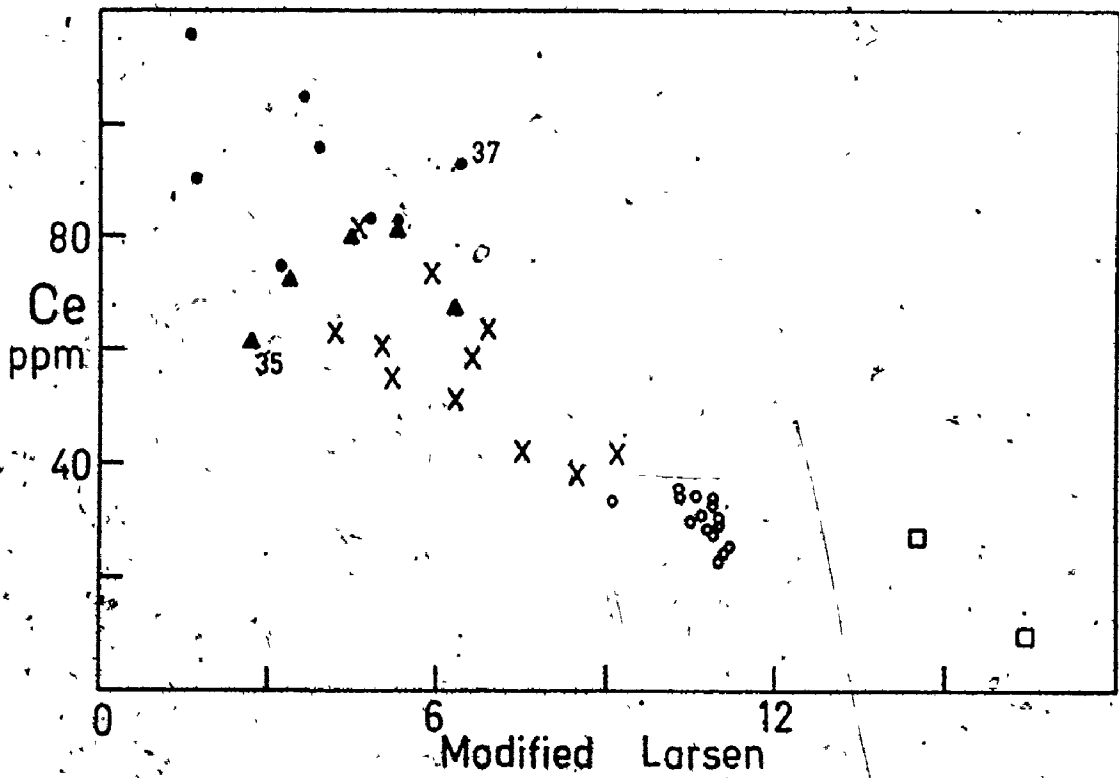
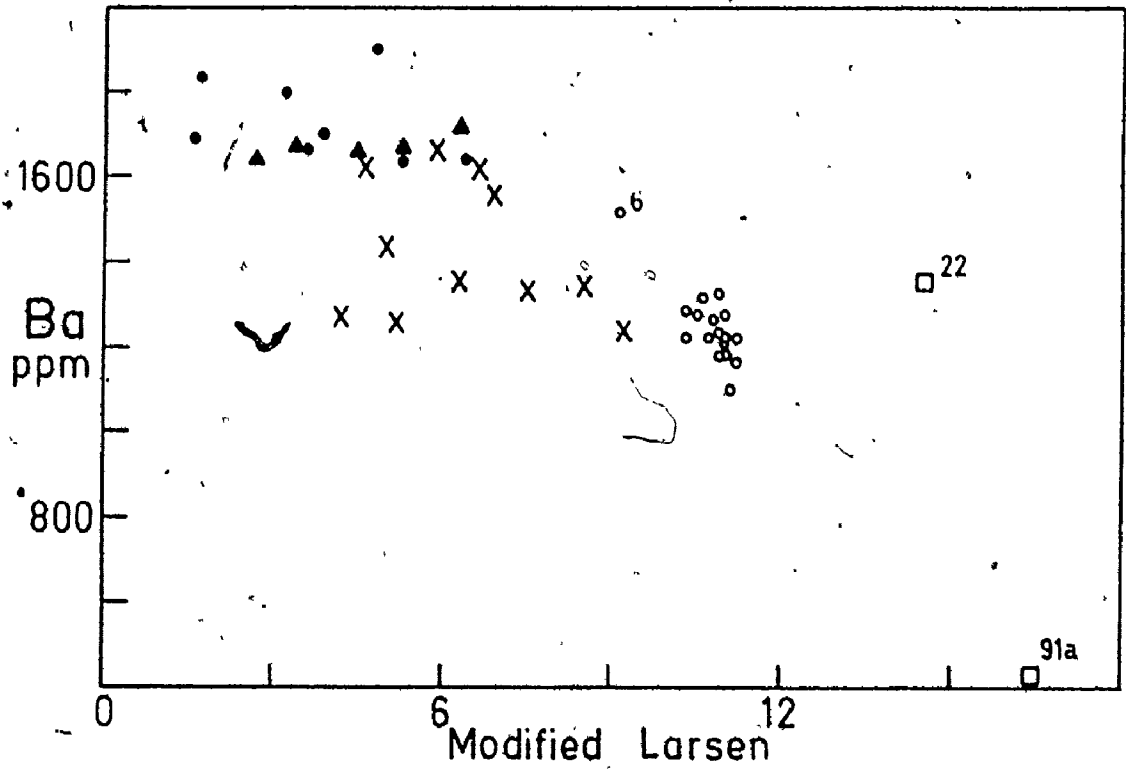
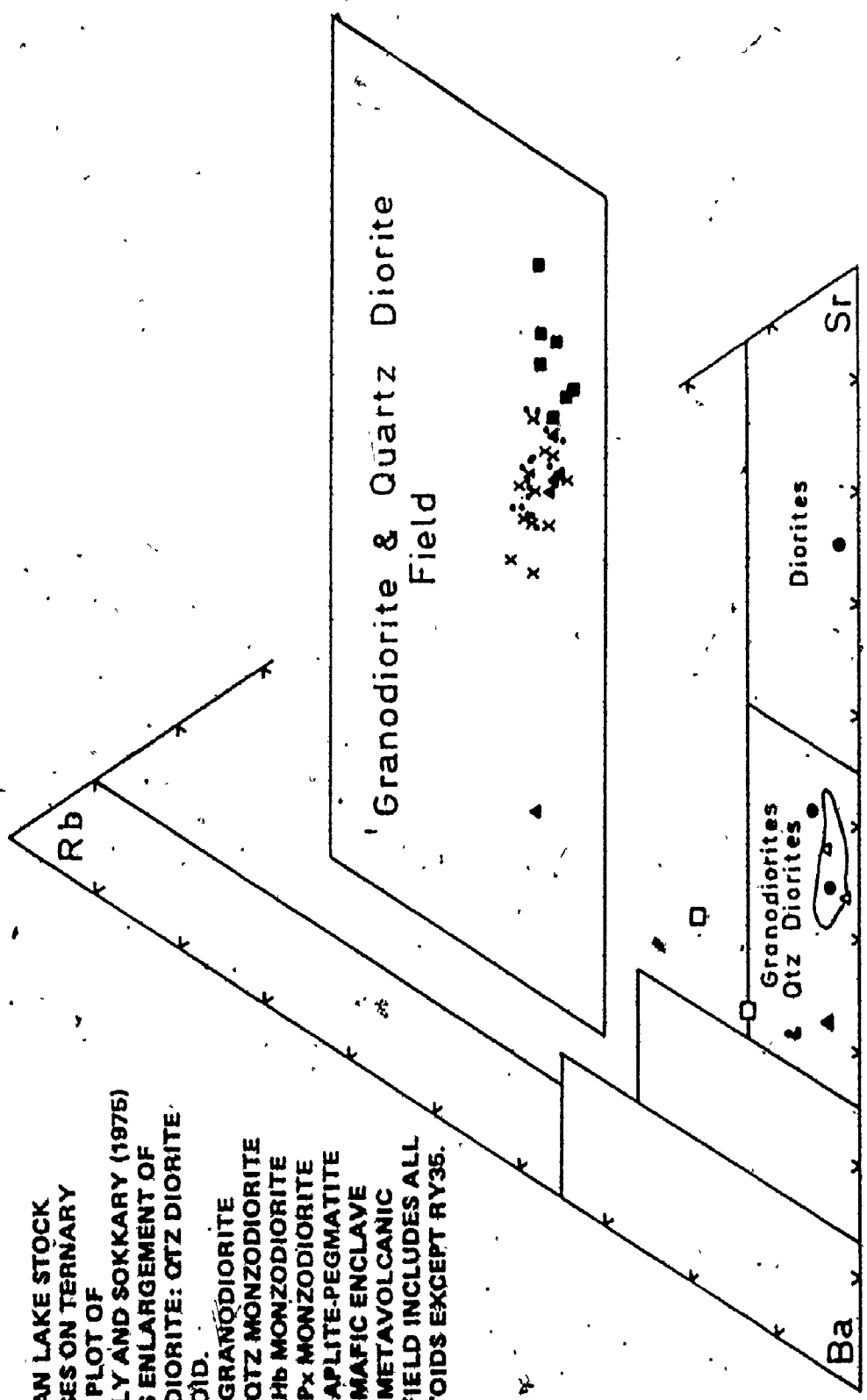


FIGURE 2.62

FIGURE 2.63 RYCKMAN LAKE STOCK ANALYSES ON TERNARY Rb-Ba-Sr PLOT OF BOUSEILY AND SOKKARY (1975) INSET IS ENLARGEMENT OF GRANODIORITE: QTZ DIORITE RHOMBÖID.

- GRANODIORITE
- X QTZ MONZODIORITE
- ▲ Hb MONZODIORITE
- Px MONZODIORITE
- APLITE-PEGMATITE
- MAFIC ENCLAVE
- △ METAVOLCANIC

SOLID FIELD INCLUDES ALL GRANITOIDS EXCEPT RY35.



8

Radioelements: U and Th

Figures 2.64 and 2.65 show eU and eTh determinations for 35 field stations by the same method described for the Burditt Lake Stock. Location A (Figure 2.46) served as a "standard outcrop" and the center of Crowrock Bay provided background values.

All phases of the stock are slightly higher in eU but similar in eTh compared to the Burditt Lake Stock. Marginal mafic phases are enriched in both eU and eTh relative to the core granodiorite. Country metavolcanics carry lower gamma ray flux while intrusion breccia appear to be relatively enriched. Similar radioelement enrichment was detected by the author for large mafic enclaves in the Lake Despair area (data not shown) which indicates possible diffusive enrichment of both enclaves and intrusion breccia at the time of emplacement.

The marginal increase in eU and eTh correlates with change in lithology and cannot be attributed to any diffusive peripheral phenomenon as modeled by Buntebarth (1976). It is significant to note that the megacryst-bearing core granodiorite does not show enrichment in radioelements. Metasomatism causing megacryst growth did not eliminate the primary radioelement pattern controlled by lithology.

Eighteen of the field stations correspond closely with sample locations (Appendix C5) and if in situ analyses are plotted against the modified Larsen, (Figure 2.66) the following additional information emerges:

- No distinction between the three mafic phases.
- A clear separation of the granodiorite core, showing lower eU and eTh.

- Enrichment of aplite dyke over the granodiorite.

The radioelement distribution supports previous evidence that the three mafic phases are related but the core granodiorite has had a different history.

IN-SITU ANALYSES OF eU AND eTh
 IN RYCKMAN LAKE, STOCK BY
 PORTABLE DIFFERENTIAL/GAMMA-RAY
 SPECTROMETRY.

FIGURE 2.64

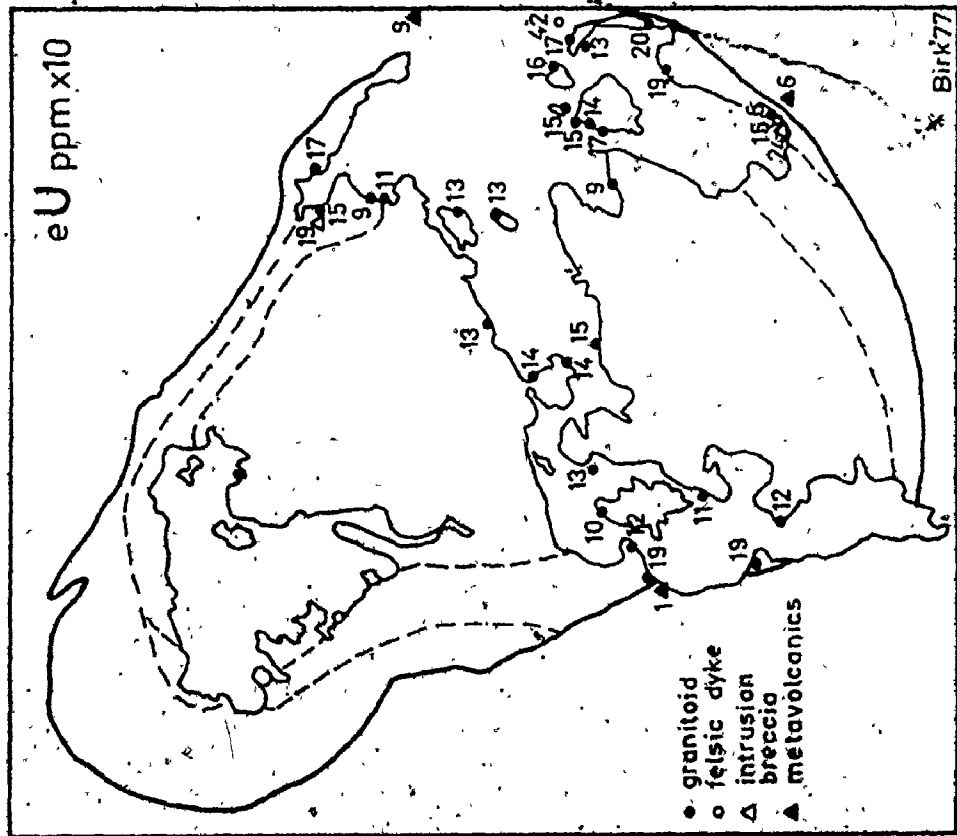
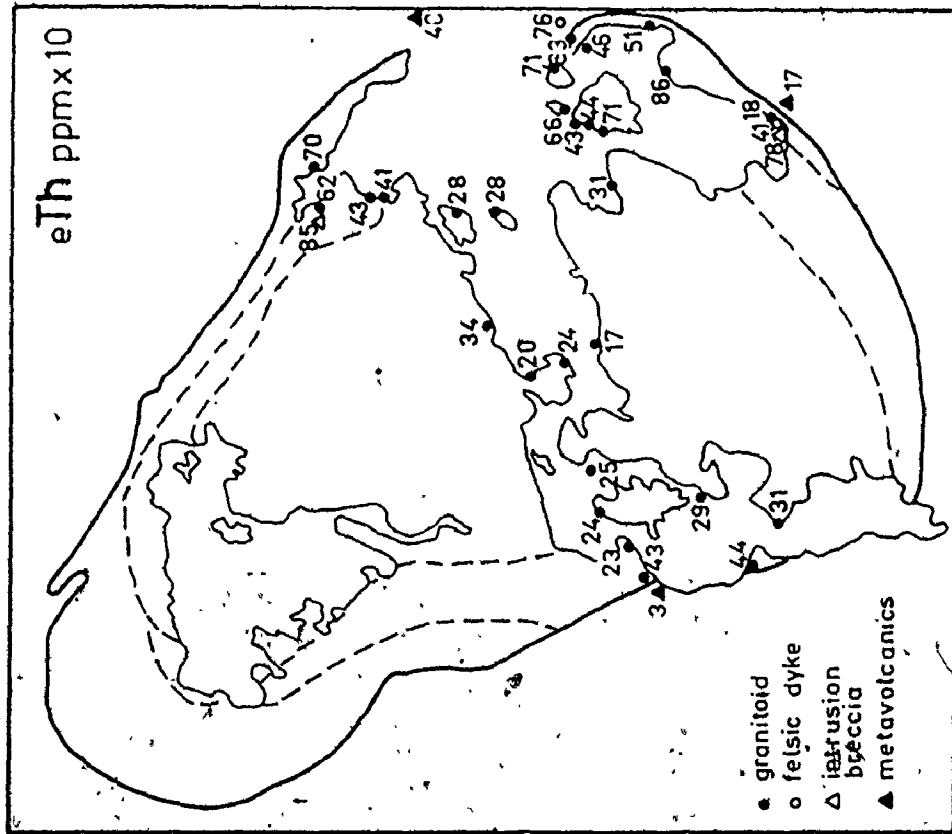


FIGURE 2.65



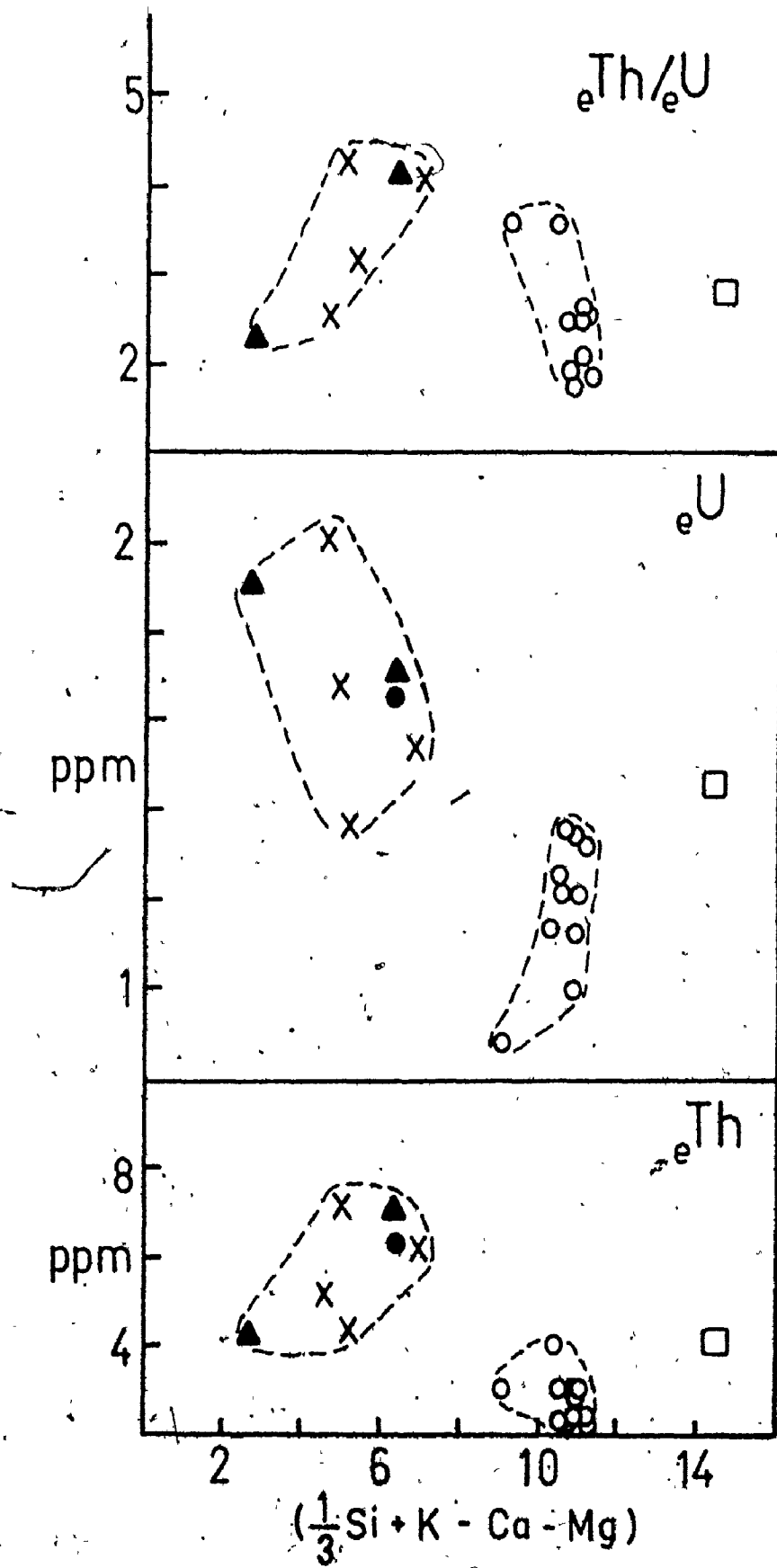


FIGURE 2.66 IN-SITU ${}^e\text{U}$ AND ${}^e\text{Th}$ ANALYSES VERSUS MODIFIED LARSEN INDEX OF NEAR-EQUIVALENT SAMPLES (APPENDIX C5).

- GRANODIORITE
- × QTZ MONZODIORITE
- ▲ Hb MONZODIORITE
- Px MONZODIORITE
- APLITE-PEGMATITE

2.2.3 THE FLORA LAKE STOCK

Field Observations:

Flora Lake lies 30 km north-east of Sioux Narrows, Ontario within the NTS quadrangle 52F/5. The concentrically zoned elliptical granite-monzodiorite pluton, striking north-east from Flora Lake has received considerable attention (Heimlich 1963, 1965, 1968; Davies 1967, 1973; Johnston 1962; 1965, 1968). Figure 2.66 is based on the geological map of Davies (1973) modified by a one week visit by the author in 1974. Location numbers in the following discussion match sample stations on Figure 2.67.

Heimlich (1965) recognized a multiple intrusion of monzodiorite-monzonite-granite (oldest to youngest) forming an ellipse with the long axis subparallel to the north-east regional fabric. Davies (1973) concluded that the stock intruded a point of inflection along an anticlinal axis. Figure 2 of his report shows a major regional shear zone striking north-east and lying on the eastern flank of the pluton. The surrounding supracrustals are pillowed metabasalt at almandine-amphibolite facies grade with schistosity concordant to the pluton and dipping steeply outward from the contacts. Heimlich (op.cit.) described an indistinct contact zone up to 2000' wide marked by coarser granoblastic metabasalt, in places exhibiting felsic "solution soaking", migmatitic zones, pyroxene and retrograde metamorphic textures.

Heimlich (op.cit.) drew attention to greater relative mobility of the granite core compared to the monzodiorite rim or monzonite

CORRESPONDING SAMPLE NUMBERS IN
APPENDIX CARRY PREFIX "FL." OR "FLOR."

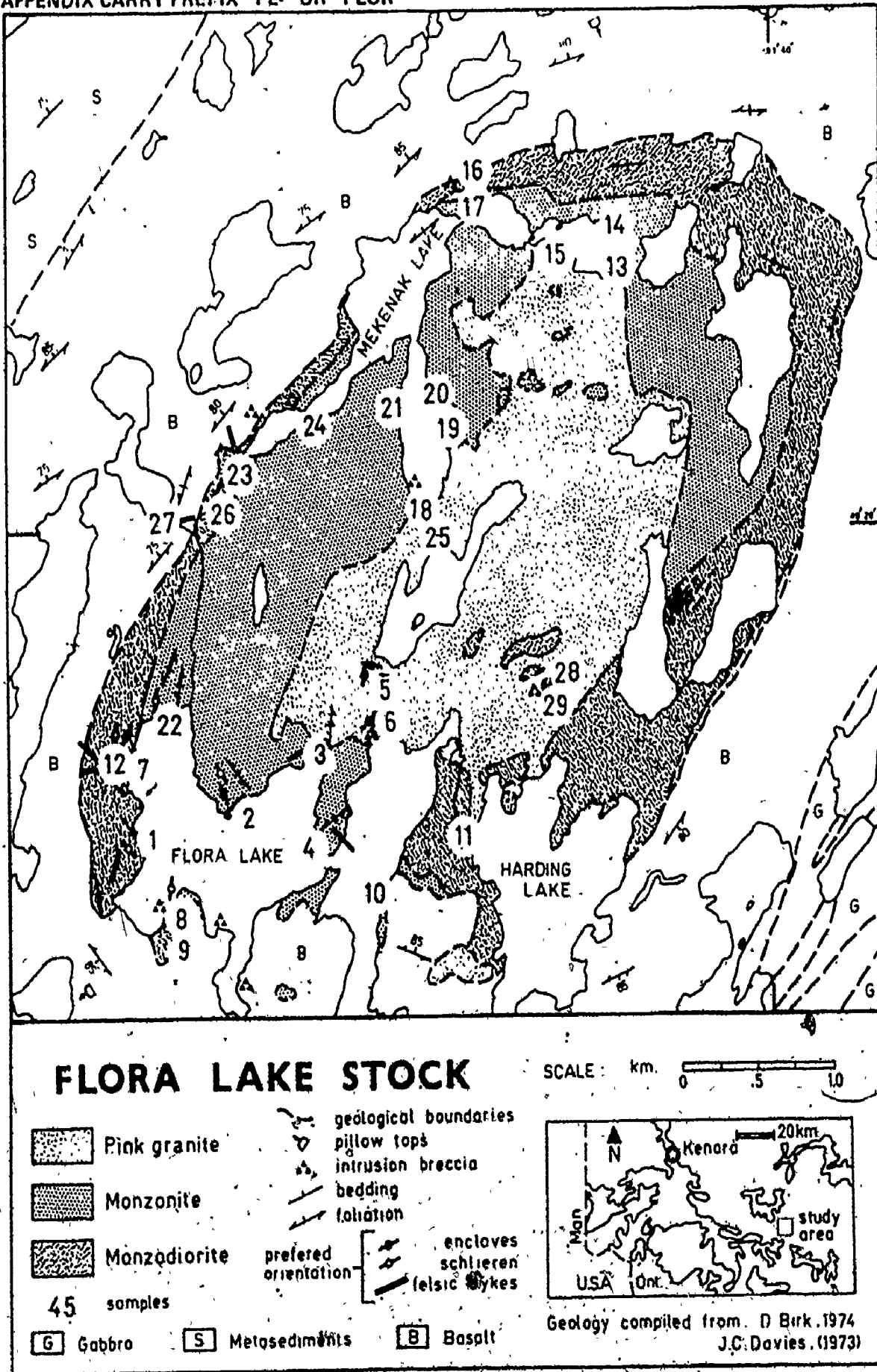


FIGURE 2.67 LITHOLOGY AND STRUCTURE OF THE
FLORA LAKE STOCK, NORTHWESTERN

mantle. This reflects a later intrusion of hot granite into rigid border phases, as evidenced by:

1. Breccia zones at the granite-monzonite and granite-monzodiorite contacts (locations 6,18 and 11,17 respectively).
2. Myriads of granitic dykes, occasionally xenolithic, transgressing the marginal units and metabasalts.
3. Aplite and aplite-pegmatite dykes cutting all units including adjacent metavolcanics (1.5 m. wide aplite at 27).
4. Dykes of monzonite and monzodiorite on the otherhand are rare.
5. Angular blocks of monzodiorite, metabasalt, and less frequently monzonite, form xenoliths within the granite core - occasionally at mappable scale (Figure 2.67).

Davies (1973) concluded that the granite core must have been primarily liquid at time of intrusion while the border phases were emplaced as crystal-liquid mush. Of all the late-kinematic stocks studied in this thesis, the Flora Lake Stock shows the most extensive and most photogenic examples of intrusion breccia, agmatites and xenolith swarms. At location 18, a xenolith swarm includes angular blocks of metabasalt carrying original flow textures; "double enclaves" of monzodiorite-greenstone (Plate 2.2) and feldspathized mafic enclaves. On the otherhand, the small lensoid mafic enclaves so characteristic in other stocks described in this thesis, are virtually absent in the main body of the stock. In their place, the monzodiorite and monzonite phases carry foliate structures in the form of mafic schlieren (location 1,2,7,8), arcuate "rock swirls" (Heimlich, 1965) and bands of amphibole-biotite extending down-strike for several meters (Figure 2 of Heimlich, 1965). Both marginal units also carry strong mineral foliation subparallel to

contacts. Despite the abundant schlieren and xenoliths, both the granite and monzonite present relatively homogeneous field appearance. The rim monzodiorite, however, shows considerable variability in texture and colour.

The aeromagnetic map for Caviar Lake (ODM (1971); map 1169G) shows a strong magnetic response covering the entire pluton with a flux greater than 60,800 gammas. Two anomalies are centered over the monzonite-monzodiorite envelope at Flora Lake (61,500 gammas) and Granny Lake (61,800 gammas). Heimlich (1965) correlates these magnetic highs with 0.3 to 3.5% modal magnetite in the monzodiorite. Davies (1973) on the otherhand correlates the northeastern anomaly with a zone of abundant metapyroxenite enclaves in the monzodiorite (up to 60 meters wide) and the southeastern peak to a granitic dyke swarm at the edge of the stock.

The granite core carries a shallower magnetic flux between 60,830 and 60,940 gammas. Such a high overall magnetic response contrasts sharply with the shallow gradient over granitoids of the Atikwa Lake Complex which rises northeastward from 60,360 at Head Bay to 60,620 gammas at Atikwa Lake. Johnston (1968) postulated a genetic link between the Flora Lake Stock and the Overflow Bay mafic intrusions, partially on the evidence of mutually high magnetic flux.

Petrography:

A detailed petrographic study was not carried out because of the comprehensive discussion and numerous modes published by Heimlich (1965). However, a brief reconnaissance of unstained thin sections was undertaken to give additional

The average modal analyses of Heimlich (1965, Table 2) when plotted on the IUGS (1973) ternary Q-A-P diagram (not shown) do not quite conform with the terminology of Heimlich. The "granite" mode straddles the interface between granite and granodiorite while the "monzonite" falls slightly within the monzodiorite field. The discrepancies in terminology are minor, therefore the author has retained Heimlich's rock names. It must be noted, however, that the lithologies of the Flora Lake Stock are not as different from those of the Ryckman Lake Stock as the terminologies might imply.

Heimlich (op.cit.) recognized three mineral assemblages with constituents listed in order of abundance as follows:

GRANITE (OR GRANODIORITE)

plagioclase + microcline + quartz + biotite + epidote + accessories

MONZONITE (OR MONZODIORITE)

plagioclase + microcline + biotite + hornblende + epidote + quartz
+ accessories

MONZODIORITE

plagioclase + microcline + biotite + hornblende + pyroxene + epidote
+ opaques + accessories

Several petrographic features reported by Heimlich (1965) should be noted for their genetic implications:

1. Concentric zoning in 10% of the granite plagioclase: He noted that "... in some cases, zoning is truncated against twinning..". This is here interpreted as synneusis twinning.
2. Optically homogeneous granite microclines of low soda content ($0.99\text{Ab}_{99}\text{An}_1$). The abundance of microcline in the granite (up to 35.5% of modes) yet the absence of megacrysts is a significant feature.

3. Pyroxene of diopsidic augite variety (36% clinoenstatite, 15% ferrosilite, 49% wollastonite).
4. Mosaic texture of quartz and plagioclase in granite and microfaulted and bent biotite in monzonite (his Plate 3) suggest minor protoclasis and granoblastic recrystallization.
5. Ubiquitous plagioclase corrosion by quartz and microcline and abundant myrmekite, as well as biotite replacement of hornblende and hornblende pseudomorphic after pyroxene attest to deuteritic autometasomatism and autometamorphism.

The author's own observations revealed the following:

- plagioclase synneusis in monzonite
- Pyroxene-biotite intergrowth in monzodiorite
- rare quartz coexisting with pyroxene in the monzodiorite
- muscovite after biotite in granite
- rare local concentrations of microcline with plagioclase inclusions (incipient megacrysts?) in the granite.
- large corroded plagioclase laths in monzodiorite carrying amoeboid patches of microcline which coalesce at margins to form "incipient megacrysts" with swarms of rounded plagioclase inclusions.

The incipient megacrysts in monzodiorite are identical to features reported for the Px-hb monzodiorite of Ryckman Lake. The other petrographic textures are also so similar between Flora and Ryckman that a textural explanation for one should suffice for the other. The greatest differences are recorded for the core units. The granite differs from the Ryckman Lake granodiorite in the absence of megacrysts, microlickensides or hornblende and in finer grain size. These differences can be attributed to more rapid injection of a

Geochemistry: Introduction

Appendix C4 and D4 tabulate major and trace elements (Rb, Sr, Y, Zr, Nb, Ba, Ce) for 21 phanerites, three dykes and two autoliths of the Flora Lake Stock. Heimlich (1965) published whole-rock analyses for 5 singlicate and 3 composite specimens of the Flora Lake stock including the trace elements Ga, Cu, Ni, Cr and V. His trace elements complement this study but his major oxide values are of limited use because:

- K₂O was calculated modally.
- Large discrepancies between singlicate specimens and his composites, indicating insufficient sampling.
- Systematically low Na₂O compared to this study.
- No standards reported, therefore, poor analytical control.

Furthermore, analyses based on composites - i.e., mixtures of several specimens, are less useful than analyses of several specimens since the mixtures mask the chemical variability. The following discussion therefore relies only on major element analyses from this study.

Major Elements:

A comparison of major oxides for the Flora Lake and the Ryckman Lake Stocks (Appendices C4 and C5) reveal that:

1. Flora granite is higher in SiO₂ and K₂O; lower Fe₂O₃T, MgO and CaO than the Ryckman granodi-

2. The mantle and rim zones at Flora (monzonite and monzodiorite respectively) are significantly enriched in Al_2O_3 and K_2O and depleted in MgO relative to corresponding mantle and rim zones at Ryckman (qtz monzodiorite and monzodiorite respectively).
3. Na_2O is very similar for all corresponding phases.

On the Na-K-Ca diagram of Green and Poldervaart (1958), the three main phases at Flora straddle the igneous trend line (Figure 2.68) but form a discontinuous sequence, with no field overlap. Similarly, on the Mafic Index/Felsic Index plot (Simpson, 1954) the three Flora phases define three distinct clusters with no overlap (Figure 2.69). If these units are related by fractional crystallization, then the differentiation could not have occurred in situ because parts of the differentiation sequence are missing. The granite field on the Na-K-Ca plot is elongated perpendicular to the igneous trend, suggesting that factors besides crystal fractionation were operative. It is interesting to note that the direction of elongation of the granite field in both the Na-K-Ca and mafic-felsic plot is almost at right angles to the elongation direction of the monzonite and monzodiorite fields. This feature, together with the unusual Al_2O_3 enrichment in the mafic phases points to a different history for the granite core from that of the mafic marginal granitoids. It is also interesting that the aplite dyke plots very close to the granite fields in contrast to aplitic dykes of other stocks.

FIGURE 2.68

Ca-Na-K TERNARY OF GREEN AND POLDERVAART (1958) FOR FLORA LAKE STOCK.

- GRANITE
- X MONZONITE
- ▲ MONZODIORITE
- APLITE

FIGURE 2.69

FELSIC INDEX VERSUS MAFIC INDEX PLOT OF SIMPSON (1954) FOR THE FLORA LAKE STOCK:

- GRANITE
- X MONZONITE
- ▲ MONZODIORITE
- ⊖ APLITE IN METAVOLCANICS
- ⊗ GRANITE DYKE (g) IN MONZONITE
- ⊗ GRANITE DYKE IN MONZODIORITE
- ⊙ MONZODIORITE (mzd) ENCLAVE IN GRANITE
- ⊗ MONZODIORITE (mzd) ENCLAVE IN MONZONITE
- ▲ C CONTACT MELANGE (c):
MONZODIORITE-METAVOLCANIC.

FIGURE 2.68

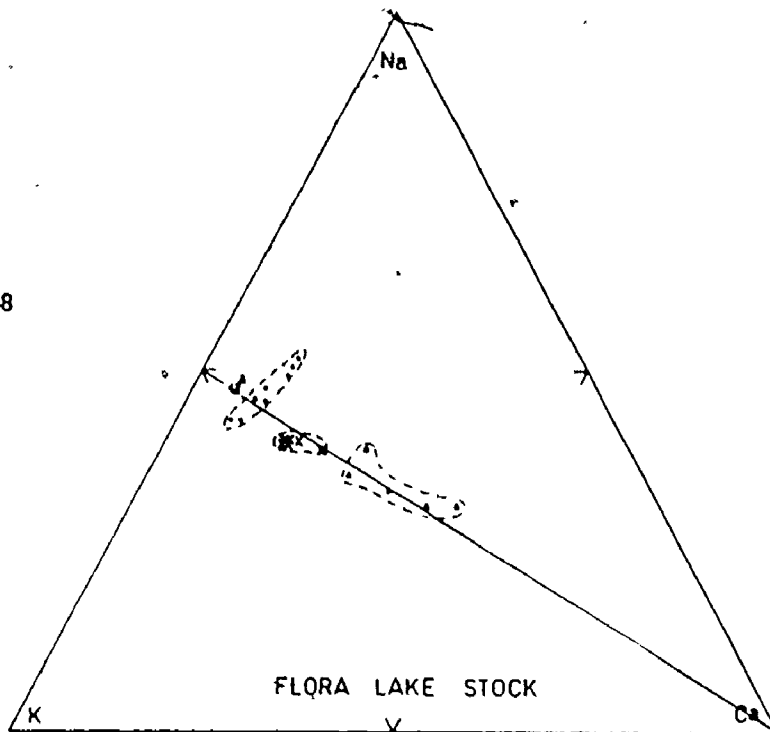
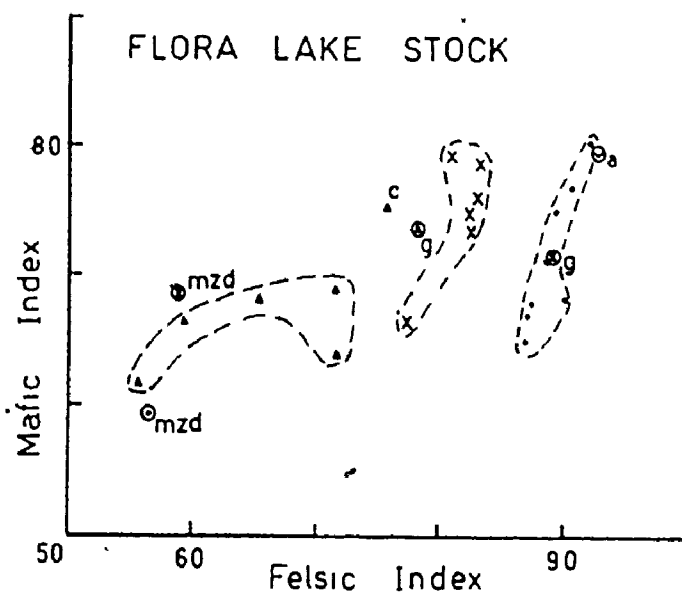


FIGURE 2.69



Figures 2.70 to 2.78 show that Ca, P, Mg, Ti and Fe have strong negative correlations and Si a positive correlation with respect to the modified Larsen index. All plots could be interpreted as differentiation trends. As for the previous plots, the trends show data gaps between the main phases while the aplitic sample plots in sequence with the granite core.

Al and K plots show a two-fold trend. They increase in concentration with index for the border phases but drop significantly in the granite core. A maximum in the Al-curve is common for linear variation diagrams (Tuominen, 1964; Aramaki et al, 1972) but the amount of convex curvature is extreme for Flora. Na shows a much shallower convex curvature.

Trace Elements:

Phases of the Flora Lake Stock are significantly enriched in Rb and depleted in Sr compared to spatially equivalent phases of the Ryckman Lake Stock. The Flora granite is enriched in Zr and Nb over the Ryckman granodiorite. The Flora monzonite is enriched in Y, Zr, Nb and Ce and depleted in Ba relative to the Ryckman quartz monzodiorite. Flora monzodiorite is higher in Y and Nb but carries similar levels of Zr, Ba and Ce to those of the Ryckman monzodiorite. These plutons, therefore, although physically similar (concentrically zoned) and petrographically similar, are distinctive by their trace element "finger prints". Modified Larsen plots (Figures 2.79 to 2.85) reveal these significant patterns:

FIGURES 2.70 TO 2.78:

**MAJOR ELEMENT CATIONS VERSUS
MODIFIED LARSEN INDEX FOR THE
FLORA LAKE STOCK. OUTLIERS
LABELED**

- O GRANITE**
- X MONZONITE**
- MONZODIORITE**
- APLITE**

FIGURES 2.79 TO 2.85

**TRACE ELEMENTS VERSUS MODIFIED
LARSEN INDEX FOR FLORA LAKE
STOCK. OUTLIERS LABELED.
SYMBOLS AS FOR FIGURES 2.70-2.78.**

FIGURE 2.76

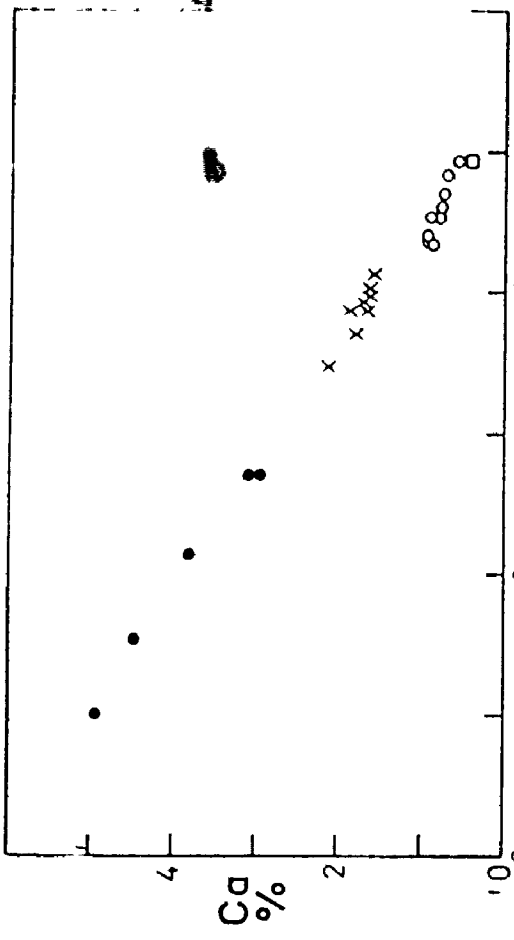


FIGURE 2.77

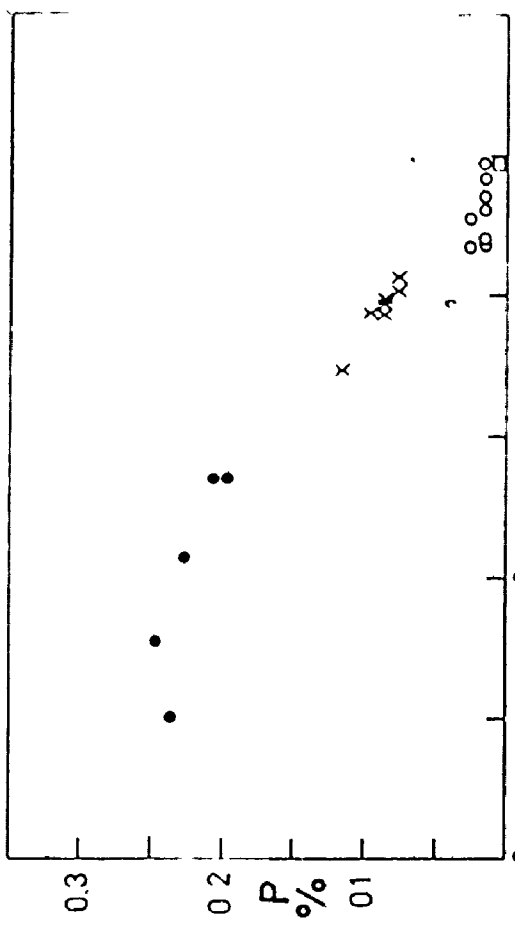


FIGURE 2.74

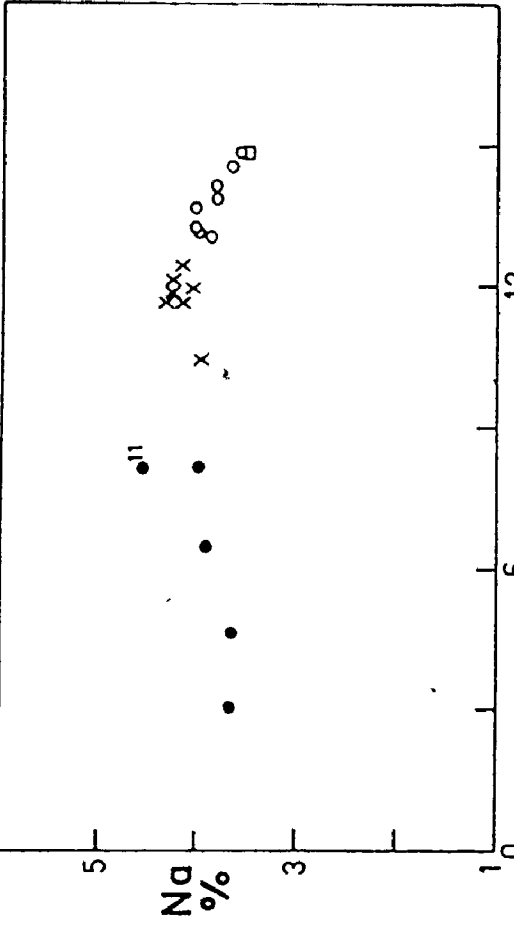


FIGURE 2.75

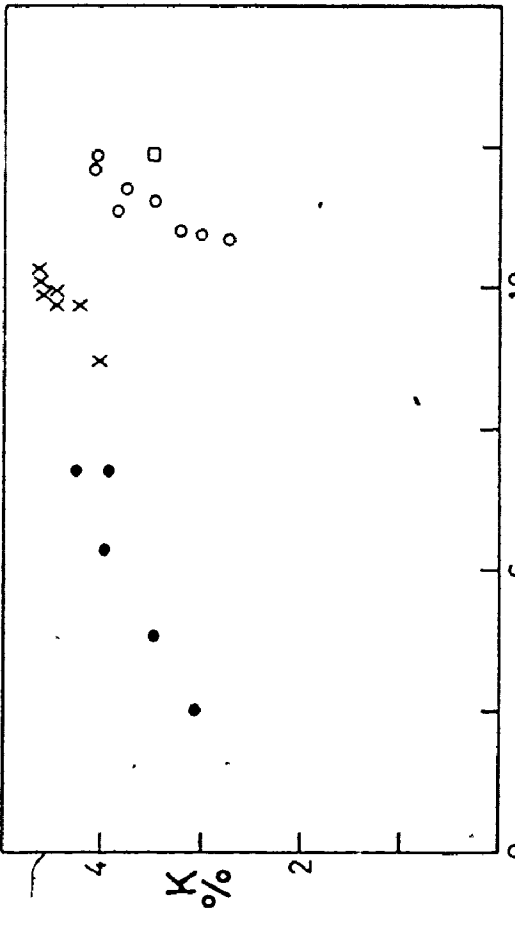


FIGURE 2.78

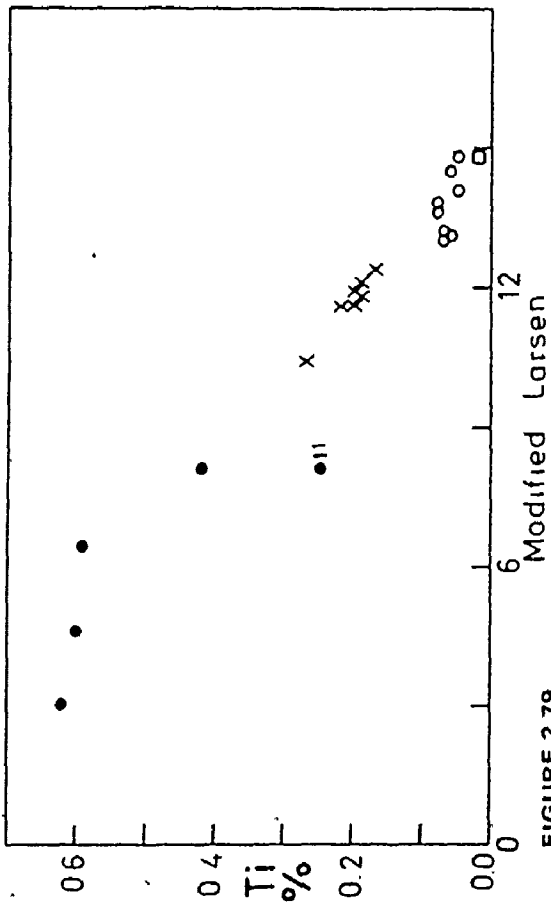


FIGURE 2.80

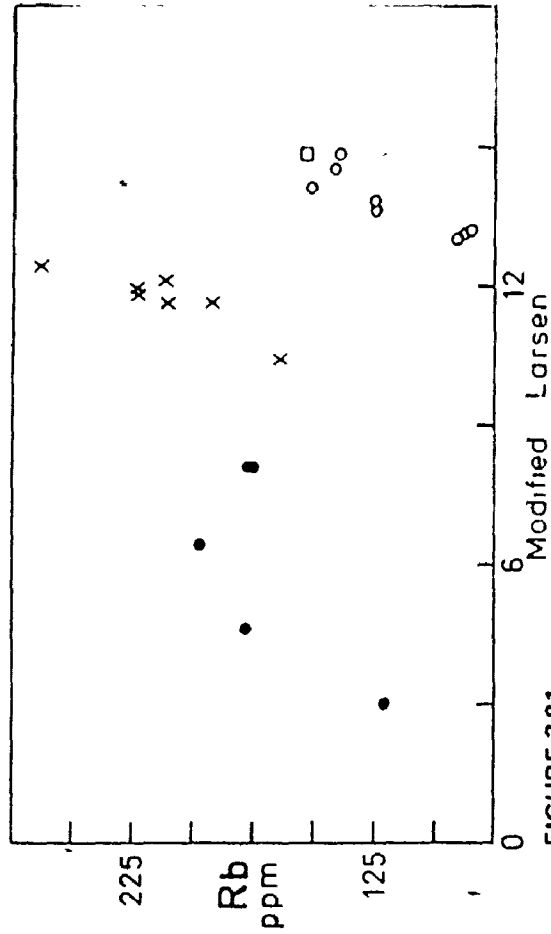


FIGURE 2.79

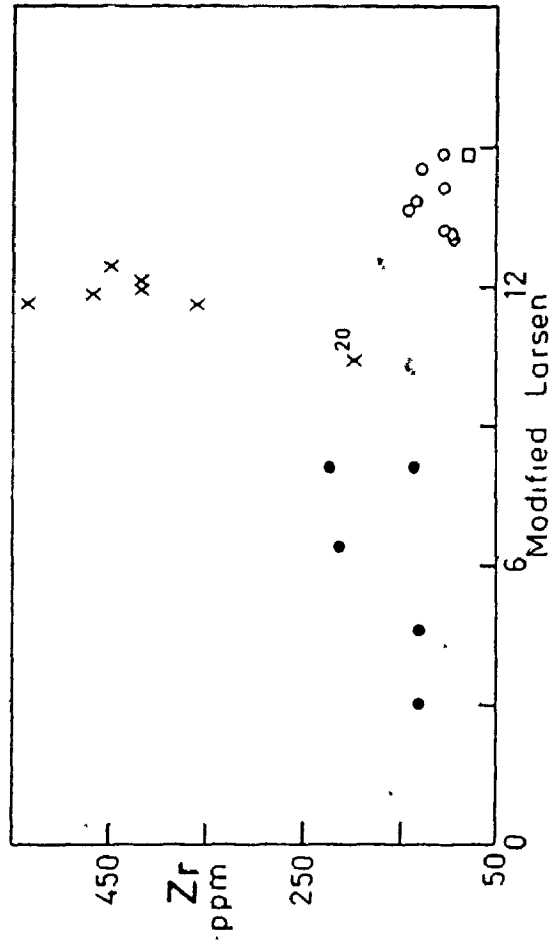


FIGURE 2.81

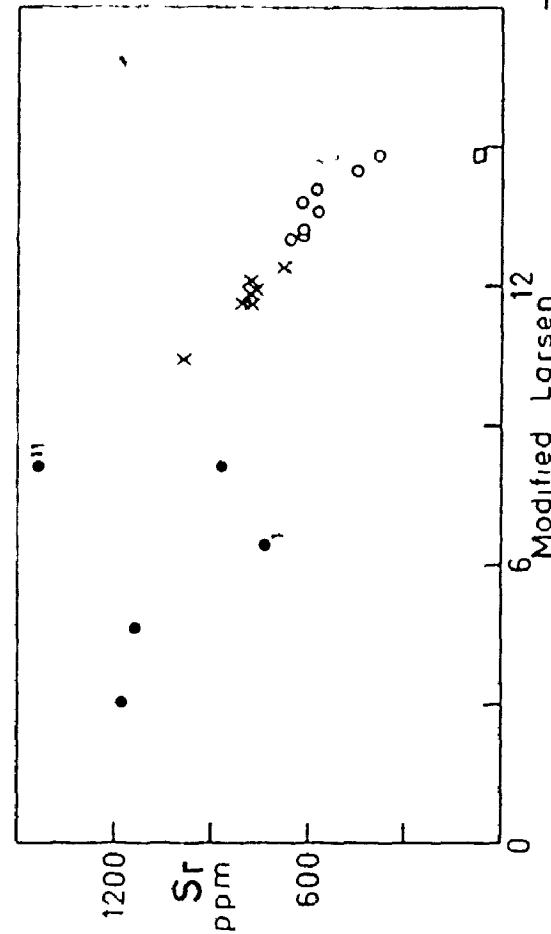


FIGURE 2.84

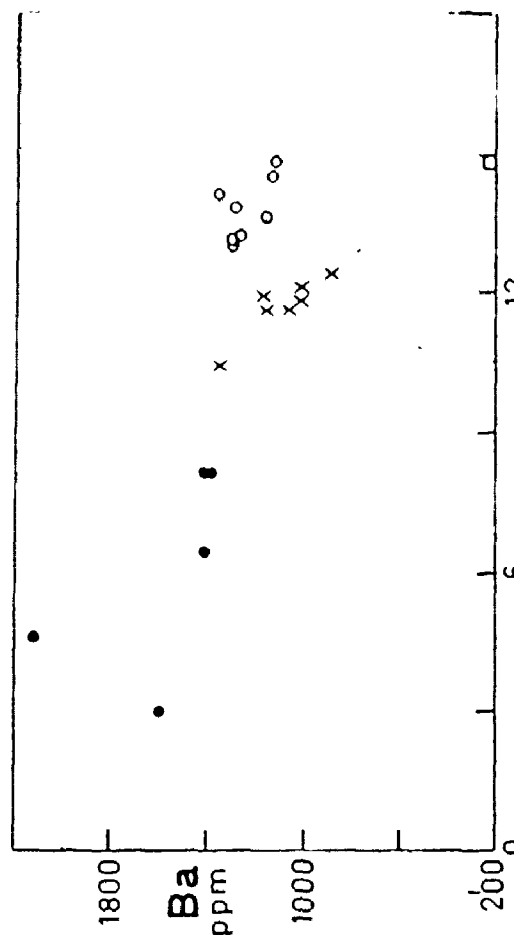


FIGURE 2.85

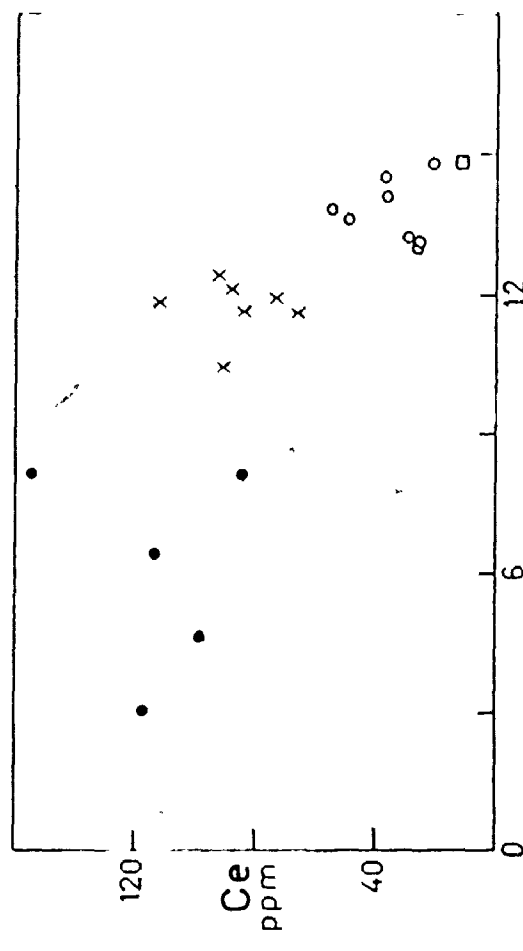


FIGURE 2.82

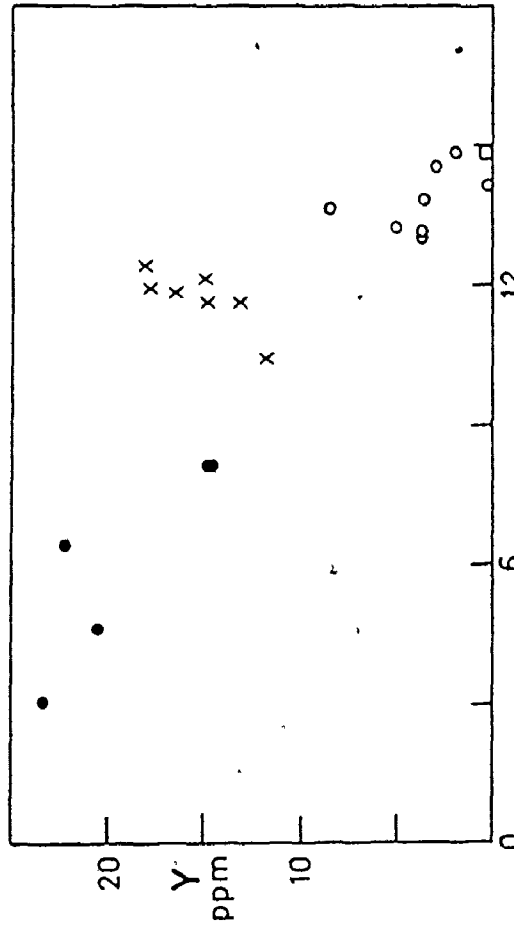
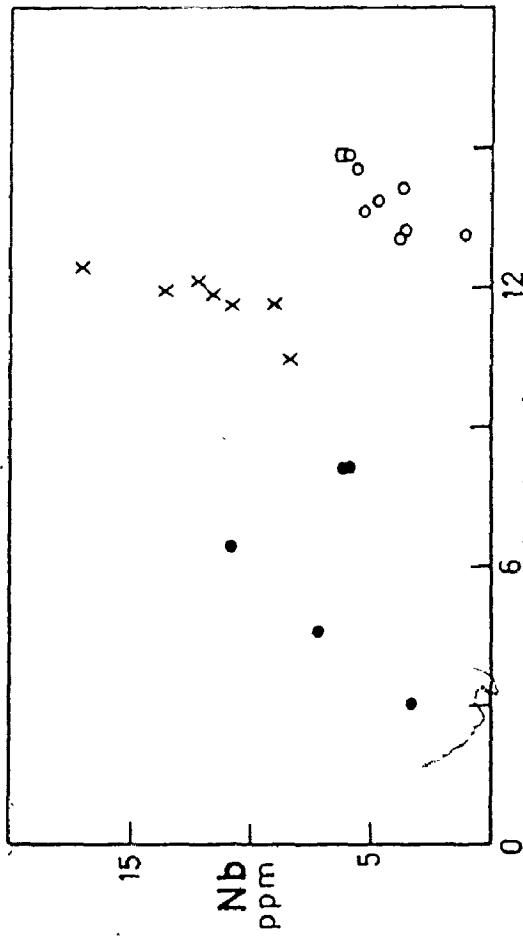


FIGURE 2.83



1. Rb, Zr and Nb show strong enrichment in the monzonite that effectively eliminates curvilinear correlation with index.
2. Y, Ce and Sr show weak negative correlation but have some outliers. The Y analyses deviate from linear correlation towards enrichment in sympathy with the Rb, Zr and Nb trends.
3. Ba shows weak negative correlation in the mafic phases terminating with slight enrichment in the granite.
4. The aplite dyke carries trace element abundances similar to the granite except for Ba and Sr depletion.

On the ternary plot of Bouseily and Sokkary (1975), the Flora phases define separate clusters within the granodiorite-qtz diorite rhomboid (Figure 2.86). The monzonite cluster is located partially outside this rhomboid, towards the Rb apex, attesting to the unusually high Rb content of this stock. As reported for the felsic dykes of Ryckman, the Flora aplite also falls outside any of the proposed fields, including the trapezoid for "highly differentiated granites". The aplite is far removed from the granite cluster, in contrast to the major element similarities previously noted. This accounts for the extremely high Rb/Sr and $^{87}\text{Sr}/^{86}\text{Sr}$ reported for the aplite in Table 4.1 of Chapter 4.

Heimlich (1965) reported that Cu, Ni, V and Cr diminish progressively in the sequence monzodiorite to granite while Ga mimics the curve for alumina, with composite sample values of 18 ppm (monzodiorite), 20 ppm (monzonite) and 15 ppm (granite).

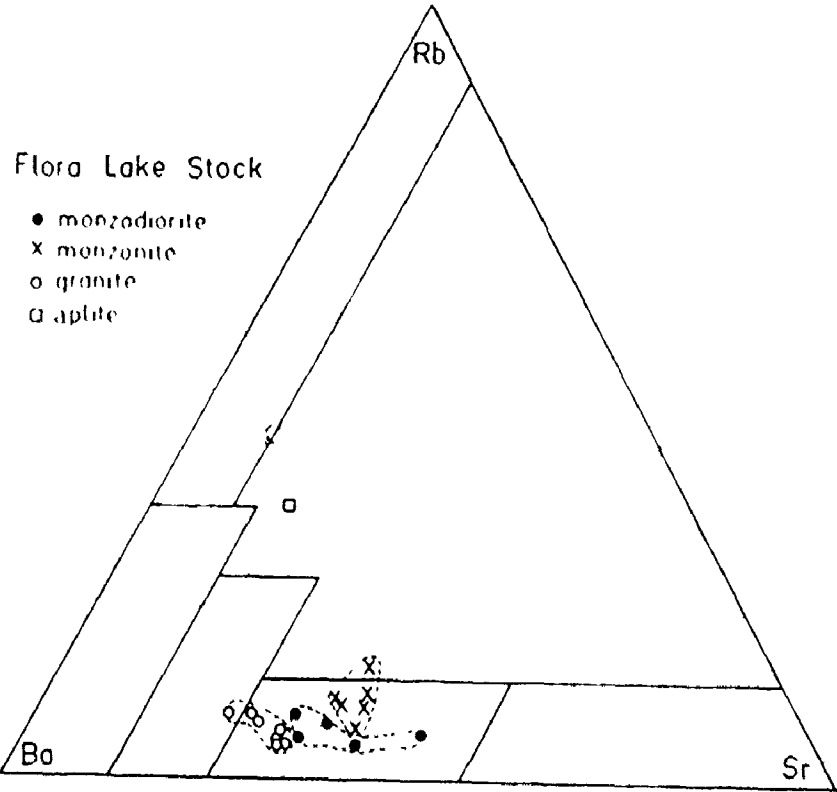


FIGURE 2.86 FLORA LAKE STOCK PHASES ON
TERNARY Rb-Ba-Sr PLOT OF
BOUSEILY AND SOKKARY (1975)

Bowden (1966) reported that magma alkalinity as measured by the agpaitic coefficient $((Na + K)/Al)$ correlates with Zr content in the Nigerian Younger Granites. The enrichment of Rb, Zr, Nb, Ga and Al in the monzonite of Flora suggests a similar pattern here. To test the role of magma alkalinity, Table 2.3 lists the agpaitic coefficients for both the Flora Lake Stock and Ryckman Lake Stock. The coefficients for spatially equivalent phases do not differ appreciably between these two stocks and are only slightly lower than values reported by Bowden (1966). There is a slight increase in average coefficient towards more felsic members at Flora but the range in values at both Flora and Ryckman appear independent of lithology except for aplites. No correlation of agpaitic coefficient and Zr content is apparent, precluding changes in magma alkalinity as a possible mechanism for the chemical patterns observed. Both the Flora and Ryckman phanerites have coefficients near 1 and are, therefore, metaluminous to subaluminous (Carmichael *et al*, 1974, p.31).

Table 2.3

Agpaitic Coefficients* for the Flora Lake Stock and Ryckman Lake Stock:

Flora Lake Stock			Ryckman Lake Stock		
Phase	#	$\frac{Na + K}{Al}$ *	$\frac{Na + K}{Al}$ *	Phase	#
Core Granite	8	.83 - .97 \bar{x} = .90	.75 - .85 \bar{x} = .81	Granodiorite	17
Mantle Monzonite	7	.77 - .89 \bar{x} = .86	.78 - 1.07 \bar{x} = .93	Quartz	11
Rim Monzodiorite	5	.75 - .89 \bar{x} = .82	.85 - .90 \bar{x} = .87	bi-hb Monzodiorite	5
			.79 - .91 \bar{x} = .84	px-bi Monzodiorite	7
Dykes Aplite	1	.97	.95 - 1.12	Aplite & Pegmatite	2

Number of samples

* Values given as range and mean for # samples.

2.2.4 CONCENTRICALLY ZONED PLUTONS OF THE SUPERIOR PROVINCE:

PREVIOUS MODELS

Lawson (1913) considered the "syenite" of Pukamo Island and the "granite" of Nowhere Island (collectively: the Rest Island Stock) to constitute "... a single irruptive mass, differentiated into two petrographic types ...". Cram (1932) proposed differentiation from a primary basalt during transit. Sanders (1929) studied the composite "syenite-granite" at Snowbank Lake (Northeastern Minnesota) and concluded that "... gravitative differentiation in the magmatic reservoir ..." led eventually to autointrusion of interior fluid into consolidated roof and walls of the same magma.

In contrast to these magmatic hypotheses, Gummer (1941) attributed basic borders of the Mackenzie Island pluton (Red Lake, Ontario) to reciprocal reaction between "granite" and metavolcanic xenoliths. In similar fashion, Heimlich (1971) explained a marginal hornblende-tonalite of the Atikwa Lake batholithic complex by piecemeal stoping of greenstone wall-rock. Blackburn (1973) considered the monzodiorite rim of the Ryckman Lake Stock to be a hybridization product of the core granodiorite and mafic volcanics.

For the concentrically zoned Falcon Lake Stock of Manitoba, Gibbins (1971) listed the following published interpretations:

1. Multiple intrusions of crystallization differentiates coupled with metasomatism.
2. Crystallization differentiation in place and subsequent plastic flow.
3. Assimilation.

Gibbins (1971) himself preferred a model of crystallization differentiation from rim to core with thermal convection at the solid-liquid interface and resurgent boiling.

Heimlich (1965) could not decide between two possible mechanisms for the concentric Flora Lake Stock:

1. Multiple intrusion of crystallization differentiates in order of mafic to felsic, from a mafic magma chamber.

or:

2. Partial fusion of basement rocks to yield monzodioritic material which fractionated in transit to monzonite. Both phases rose as crystal-liquid mush and were subsequently invaded by more mobile granitic magma.

In a subsequent discussion, Johnston (1968) countered with a model for the Flora Lake Stock as a synvolcanic structure forming a feeder pipe for adjacent metabasalts and gabbro sheets. Admittedly, he presented very little supportive evidence (Heimlich 1968) but the model is an interesting consideration for all the concentrically zoned plutons.

2.2.5 GENERAL MODELS: CONCENTRIC ZONING

Papers that have dealt primarily with concentric zoning in granitic plutons include Vance (1961); Karner (1970); Mursky (1972).

Vance (1961) proposed a hypothesis involving:

1. Crystallization from the margins inward, sealing in released volatiles which are forced downward with further crystallization.
2. Migration downward of alkalis and silica, with the volatiles, and their enrichment in the magma at depth, leaving behind a more mafic residuum.

Karner (1970) suggested convection, with flow in the magma chamber directed down along the cool margins where early mafic minerals form. Mursky (1972) presented a two-stage model for the White Creek Batholith (British Columbia) involving: mantle source emplacement to form mafic border units intruded later by remobilized granitic crust.

Other contributions to the problem of concentric zoning include:

1. Bald Rock Batholith trondjemite-tonalite: migma-magma from a basaltic source (Larsen and Poldervaart, 1961).
2. El Pinal granodiorite-tonalite (Mexico): root of a ring fracture system (Duffield, 1968).
3. Pikes Peak Batholith: alkali basalt of mantle origin reacted with and partially melted the base of sialic crust (Barker *et al*, 1975) i.e., relay magma model of Middlemost and Romey (1968).

All the foregoing efforts were directed at "normal zonation" characterized by mafic borders and felsic cores. Several authors have dealt with the reverse relationship (Saha, 1959; Ragland *et al*, 1968; Cook and Rogers, 1968; Ermanovics, 1970; etc.), which makes a single comprehensive model for zoning an unlikely prospect. The aplitic patches in the foliated margin of the Burditt Lake Stock could be considered a mild expression of "reverse" zonation.

For composite plutons of the Wabigoon Belt, field relationships eliminate several models. The sharp cross cutting relationships of felsic cores to mafic borders at Flora and Ryckman discount models of contamination, convection, diffusion, infiltration, laminar-flow segregation and crystal differentiation in place. Multiple intrusive pulses are imperative to the formation of these bodies.

The geochemical and petrographic nature of the Ryckman Lake granodiorite core is identical to the "homogeneous" Burditt and Scattergood granodiorites and shows similar evidence for autometasomatism and felsic dyking, exclusive of the surrounding monzodiorite mantle. A genetic model applicable to both the homogeneous granodiorites and the granodiorite cores of zoned stocks is not unreasonable. If these two granodiorite habits are in fact genetically related, any model for zoning at Ryckman Lake would have to account for the absence of mafic rims at Burditt and Scattergood.

The petrographic and petrochemical trends for zoned plutons are discontinuous with the largest breaks between the core granite-granodiorite phases and marginal monzonite-monzodiorite phases. Core units are relatively homogeneous with restricted petrochemical fields while rim units show data scatter. Trace element distribution at Flora shows aberrations at the core-rim interface. These features rule against fractional crystallization from a common parent magma chamber and favour hypotheses that call upon at least two magma sources to derive the core and rim phases. Such models include:

1. Relay magmas (Middlemost and Romey, 1968), i.e., zone melting of Hamilton and Myers (1968) or reaction melting of Barker et al (1975).
2. Polydiapirism from a stratified mantle source through a common conduit (model modified after Stephansson, 1975).
3. Granitoid diapirism into a:
 - a. ring dyke,
 - b. cone sheet swarm
 - c. basaltic feeder pipe

Any of these models can account also for the homogeneous stocks if the common conduit is removed or if the cut effect of the present erosion level eliminates mafic components.

The genetic association of granitic stocks with volcanic ring dyke complexes and cauldron subsidence has been long recognized (Buddington, 1959) but models have been generally based on fractional crystallization. Ring dyke models were suggested for the Lone Grove Pluton (Cook and Rogers, 1968) and the Enchanted Rock Batholith (Ragland et al, 1968) of Texas. A ring-dyke complex in Precambrian terrain of Colorado-Wyoming was recognized by Egger (1968). A zoned granite/quartz-monzonite/diorite pluton was attributed to domal emplacement of granite along old ring fractures.

For the Flora and Ryckman Lake stocks, a model of multiple intrusion from two sources best fits the data. Initial intrusion may have been a dioritic diapir generated by zonal melting, or may have represented the coarse-grained base of a basaltic feeder pipe. This mafic phase may have differentiated in situ to develop the various mineral assemblages on record. Alternatively, a feeder pipe may have repeatedly transferred magma of differing composition, each wave contributing material to the conduit walls. The second major intrusion was a granodiorite or granite diapir which took advantage of the structural passage-way. Therefore; this suggests a closer genetic link between granodiorites of the homogeneous plutons and granodiorites of zoned plutons than between cores and rims of the zoned plutons. Some of the evidence for multiple intrusion from different sources has probably been obliterated by metasomatism and/or metamorphism of mafic rims by the later felsic cores.

2.3 QUARTZ-FELDSPAR PORPHYRIES:

2.3.1 INTRODUCTION:

Figure 1.1 includes quartz-feldspar porphyries among the granitoids of the Wabigoon volcanic-plutonic Belt. The actual origin and association of these porphyritic felsites has been an enigma for several generations of geologists and is universally dubbed as "the Porphyry Problem". At some field localities these units show extensive features and appear consanguineous with felsic volcanics; elsewhere porphyries show kinship with phaneritic granitoids and appear to represent hypabyssal expressions of granitoid plutonism.

Parsons (1912) wrote that:

"... the quartz porphyries or andesite porphyries of the region are contemporaneous with the so called later granites, and are to be grouped with them ..." (p.170)

Likewise, Hurst (1935) considered the quartz porphyries of the Porcupine region of Ontario to be "... related to the Algonian granitic intrusions ...". Blackburn (1976) mapped numerous dykes of porphyry in the vicinity of the Scattergood Lake Stock and found both syn-granitic and ~~syn~~volcanic features. Moorhouse (1959), on the otherhand, pointed out that some porphyry-like rocks are produced by growth of quartz and feldspar metacrysts in metavolcanics and metasediments. Investigation of this "porphyry problem" in Northwestern Ontario is limited in this thesis to one massive porphyry and adjacent phaneritic granitoids at Esox Lake.

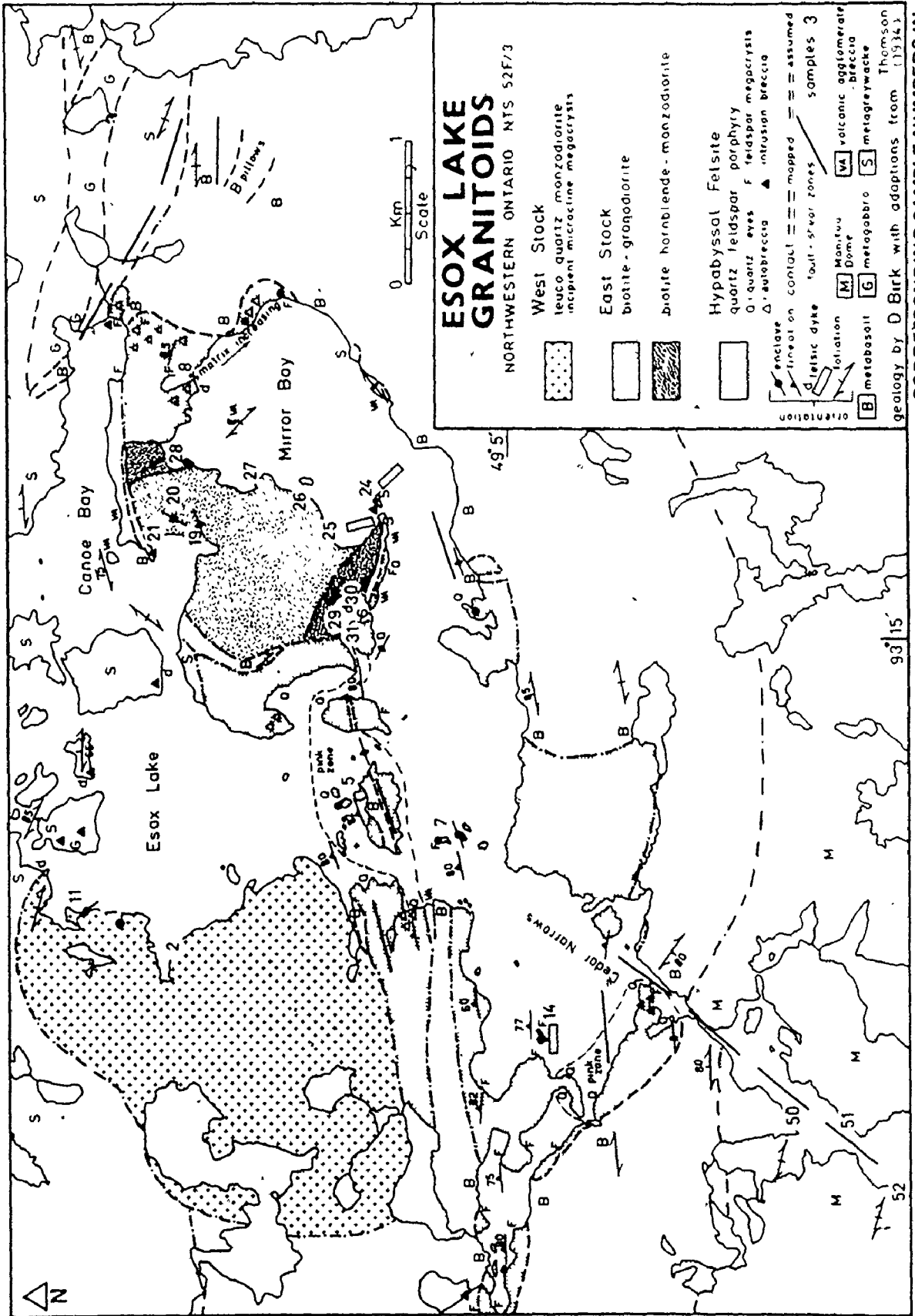
Esox Lake ("Pickere] Lake" of Lawson, 1887) is located 55 km north of Fort Frances, Ontario, within the NTS quadrangle 52 F/3. The

area straddles pillowed metabasalts and metagreywackes bordering the north end of the Manitou Dome (Goodwin, 1965), also termed the Stanjikoming Laurentian area (Lawson, 1887).

Lawson (1887) recognized two distinct bosses of "granite" on either side of the lake cutting Keewatin rocks. On the west side, a granite intrudes "... greenish-gray schistose clastic rocks ..." (north) and "... felsic schists, schistose quartz-porphyrines ..." (south). On the east side, a stock "... presents in its margin the facies of a porphyry ..." (p.145f). J. E. Thomson (1934) remapped the region and interpreted a single "Algoman" granite stock grading into quartz porphyry. Thomson's map lumps all three of Lawson's units (western granite, eastern granite and felsic porphyry schist) into one pluton intrusive into pillowed metabasalt.

Two field weeks were spent for this thesis to unravel the confusion. Figure 2.87 compiles the latest mapping and petrography to subdivide the granitoids as follows:

1. HYPABYSSAL FELSITE:
 - a. massive pink quartz porphyry (+ feldspar megacrysts)
 - b. massive grey feldspar porphyry (+ quartz eyes)
 - c. Grey feldspar porphyry cataclasite
 - d. grey feldspar porphyry agglomerate
 - e. agglomerate/breccia with feldspar porphyry clasts
2. WEST STOCK: leuco-quartz-monzodiorite
3. EAST STOCK:
 - a. biotite-granodiorite core
 - b. bi-hb monzodiorite rim



CORRESPONDING SAMPLE NUMBERS IN APPENDIX CARRY PREFIX "EX."

FIGURE 2.87

4. MANITOU DOME: granitoids (South of Cedar Narrows)

This latest visit confirms Lawson's (1887) subdivisions but favours Thomson's intrusive interpretations for the schistose porphyry.

2.3.2 FIELD OBSERVATIONS:

The quartz-feldspar porphyry occupying the southern half of figure 2.87 is a synvolcanic hypabyssal stock grading vertically in the stratigraphic pile from a hypabyssal quartz porphyry to a partially extrusive, feldspar porphyry breccia/agglomerate. Two "pink zones" are defined by pink (weathering pink) quartz-eye bearing felsite grading locally to saccharoidal texture, free of quartz eyes (location 31). The rest is grey (weathering white) felsite carrying feldspar megacrysts.

Thompson (1934) acknowledged the difficulty in distinguishing between intrusive porphyries and extrusive rhyolites and trachytes. At Esox, the most convincing intrusive relationships can be witnessed at Cedar Narrows, where a hornblende amphibolite is lit-par-lit interfingered with quartz porphyry. Quartz-eye porphyroblasts, identical to eyes within the felsite occur within the amphibolite. Two generations of quartz-eyes are developed near the center of Esox Lake (west shore): quartz lenses, elongated parallel to schistosity and equant porphyroblastic quartz, overprinting schistosity. In the center of the porphyry body (locations 5, 7, 14) outcrops preserve angular chlorite schist enclaves up to several meters wide. These xenoliths are likely of basaltic parentage as is the hornblende amphibolite.

Two generations of quartz-eyes are developed near the center of Esox Lake (west shore): quartz lenses elongated parallel to schistosity and equant porphyroblastic quartz overprinting schistosity. In the center of the porphyry body (locations 5, 7, 14) outcrops preserve angular chlorite schist enclaves up to several meters wide. These xenoliths are likely of basaltic parentage as is the hornblende amphibolite. Porphyroblastic cubes of pyrite have grown along both sides of the xenolith-porphyry contacts (Plate 1.5, Appendix A). These key localities demonstrate magmatic intrusion followed by recrystallization and metasomatic exchange between host volcanics and porphyry.

Beard (1975) noted a rhyolitic appearance and "... vague flow banding ..." in the porphyry. This "flow banding" is the mildest expression of an east-west lineation that caused Lawson (1887) to term the unit a felsitic schist. Goodwin (1965) recognized a regional schist zone that girdles the Atikwa-Niven granitoid mass north of Esox. Part of this carbonization^{it}-shear^{it} girdle is traceable down from Pipestone Lake (Edwards, 1975) and may be responsible for the flow-banding texture within the porphyry.

Going northeast from Cedar Narrows, the lineation grades into strands of chlorite-sericite wrapped around lensoid porphyry clasts. At the east end of Mirror Bay (Figure 2.87) the chloritic matrix darkens and increases in volume. Amphibolite or metabasalt fragments appear interspersed with feldspar porphyry clasts. Thomson (1934) attributed this brecciation of the porphyry to shrinkage adjustments during consolidation. Alternatively it may be autobrecciation caused

by degassing as the hypabyssal intrusive entered the volcanic pile. A later regional east-west shear may have been superimposed, to accentuate the cataclasis.

At the mouth of Mirror Bay and on islands in Mirror Bay and Canoe Bay outcrops a very fresh looking volcanic breccia containing clasts of chert, subangular grey feldspar porphyry, subangular scoria, vesicular basalt and massive pyrite nodules. The matrix is a friable carbonate-chlorite melange. Thomson (op cit) mapped the unit as a basal conglomerate indicating erosional hiatus between Keewatin greenstones and overlying Timiskaming metagreywackes. A similar unit is described by Edwards (1975) for the Pipestone Lake area to the northwest. Here it has also been interpreted as a basal conglomerate marking an unconformity between metasediments and a shallow-level porphyry. The proximity of these clastic rocks to porphyries at both Esos and Pipestone suggests a genetic link. They may represent near-source volcanic breccia, partially derived from unroofing of the porphyries. At Esos the clastic unit represents the end-member of a gradational series of progressively more cataclastic and polygenetic nature, beginning with massive porphyry. The abundance of pyrite cobbles among the clasts makes the basalt-porphyry contact a favorable target for sulphide exploration.

Two lithologically distinct phaneritic granitoid stocks are mapped on Figure 2.87: a homogeneous medium grained leuco-quartz-monozodiorite occupying the western shore of Esos Lake and a small composite stock of biotite-granodiorite and biotite-hornblende-monozodiorite. Neither Lawson (1887: p.145f) nor this author could locate

actual contacts between phanerites and porphyry to confirm Thomson's suggestion of gradation.

Cross-cutting relationships in the zoned pluton (location 25) suggest multiple intrusion with a younger granodiorite core, followed by late aplite and aplite-pegmatite dyking (locations 24, 30). Islands north on Esos Lake show fine laminated cherts and greywackes migmatized and granitized by apophyses from the homogeneous pluton. Both plutons were therefore relatively wet. Thomson (1934) also recognized that the granite intruded Timiskaming sediments. Since the porphyry supplied clasts to the "conglomerate" located basal to these sediments, it follows that the porphyry is stratigraphically older than the Esos West stock.

The Esos West stock and Esos East stock have intruded the stratigraphic pile at the interface between metabasalts and Timiskaming metasediments. Close proximity to the synvolcanic porphyry suggests that the volcanic conduit may have supplied a structural weak point. The volcanic breccia at Mirror Bay and Canoe Bay are likely near the volcanic paleocenter. Goodwin (1965), in contrast, located possible paleocenters north of Esos Lake under the present Atikwa-Niven Dome.

The aeromagnetic map for Esos Lake (ODM, 1971; map 1160G) shows clear magnetic distinction between the three felsic intrusions.

The Esos West stock is outlined by the 60,400 gamma contour and carries a shallow magnetic gradient with a mild depression. In contrast, the Esos East stock is overlain by an off-center positive anomaly up to 60,620 gammas. The contact between phaneritic stocks

and the quartz-feldspar porphyry is demarcated by the 60,400 gamma contour. At Cedar Narrows the pink zone within the porphyry carries a negative anomaly down to 60,290 gammas. Regionally the porphyry is characterized by a magnetic flux below 60,400 gammas. This is also the case for granitoids of the Manitou Dome, south of Cedar Narrows. In summation, the magnetic flux supports the concept of three separate granitoid plugs at Esos Lake.

2.3.3 PETROGRAPHY

Porphyry:

- The grey porphyry is characterized by a microcrystalline quartzo-feldspathic or lepidoblastic chlorite-biotite matrix carrying vague, highly sericitized plagioclase phenocrysts or local concentrations of sericite-carbonate, pseudomorphic after plagioclase. Locally, large muscovite flakes or poikiloblastic muscovite have replaced the sericite-carbonate pods. Quartz-eyes appear as anhedral pods of secondary quartz or quartz and subhedral epidote. Elsewhere the quartz and epidote fill tension gashes. Rough visual modes suggest 30% plagioclase relicts, 35% quartz, 5% epidote, 20% muscovite-sericite, 5% carbonate, and 5% biotite-chlorite. Petrographic textures reveal the following events:

- cataclasis or protoclasia
- extensive sericitization
- metasomatic introduction of carbonate
- growth of porphyroblastic muscovite
- secondary quartz and epidote

The pink felsite carries some 15% well defined megacrysts, of which half are quartz and half are microcline or plagioclase. Muscovite is rare in contrast to its prevalence in the grey felsite. Microcline, however, is much more abundant both as megacrysts and in the quartzo-feldspathic matrix. Staining with Na-cobaltinitrite confirms the high K-feldspar content of the pink felsite matrix.

Quartz "eyes" occur as subhedral corroded and fractured megacrysts embayed by lobes of granular matrix. Moorhouse (1959) has written:

"... The most striking textural feature of the porphyries is the corroded quartz, the phenocrysts of quartz penetrated by lobes of the matrix. This texture is restricted to fine-grained porphyries and porphyritic flows. Feldspar phenocrysts do not show this corrosion ..." p.284

Contrary to this statement, in the Esox porphyry, microcline megacrysts are also invaded by lobes of matrix. The great contrast in petrography between these porphyries and phaneritic granitoids of this study is in the extensive sericitization, carbonatization and silicification of primary textures. Also notable is the abundance of sulphides (pyrite) which rarely appear in phanerite thin sections. Surprising is the great contrast in mineralogy and texture between the grey and pink felsite which in the field appear gradational.

This contrast also emerges in mesonoma calculations (Appendix F3). The pink felsite yields an abnormal amount of normative Or (to 45.3%) and is otherwise distinct from the grey felsite by its higher normative quartz and lower normative Ab, An; Bi, Tn, Mt and AP.

Esox East and Esox West Stocks:

Modal analyses used to classify the phaneritic granitoids by the IUGS (1973) ternary diagram are presented in Appendix B4. Mineral assemblages recorded include:

LEUCO-QUARTZ-MONZODIORITE:

plagioclase + microcline + quartz + epidote + biotite ±
hornblende ± muscovite ± sphene

BIOTITE GRANODIORITE:

plagioclase + microcline + quartz + biotite + epidote + sphene
± chlorite ± muscovite ± opaques

BIOTITE-HORNBLLENDE MONZODIORITE:

plagioclase + microcline + quartz + hornblende + epidote +
biotite + sphene + opaques

Recorded textures and mineral paragenesis are similar to corresponding lithologies of other plutons discussed in this thesis and therefore will not be covered in detail.

The leuco-quartz monzodiorite is unusual in having a high microcline content and very low mafic mineral content in view of only moderate quartz and high plagioclase modes. In mineral modes, except for the low mafic mineral content, the Esox West stock closely resembles the Scattergood Lake stock. This similarity is accentuated by abundant moderately developed incipient microcline megacrysts with plagioclase inclusions. Other observations include saw-tooth corrosion contacts between plagioclase and quartz and the notable lack of myrmekite. The Esox East stock displayed synneusis twinning of

plagioclase in both the granodiorite core and monzodiorite rim. In neither stock was any textural evidence seen for gradation into porphyry.

2.3.4 CHEMISTRY:

Appendix C3 tabulates major oxide analyses for 15 phanerites and 4 porphyry samples. Most notable is the wide range in chemistry displayed by the porphyry in contrast to relatively consistent values for phaneritic lithologies. The pink felsite and grey felsite, despite gradational field appearance show sharp differences. The pink felsite is significantly enriched in SiO_2 and K_2O and depleted in Al_2O_3 , Fe_2O_3 , MgO and CaO and Na_2O .

On the Na-K-Ca plot (Figure 2.88) phanerites plot as tight clusters on the Na side of the igneous trend line. The porphyry samples scatter widely and extend far towards the K apex. Previously cited petrographic evidence of microcline megacrysts, muscovite porphyroblasts, sericitization and carbonatization suggests that the chemical heterogeneity was caused by deuteric or post-magmatic metasomatism.

Trace elements for Esos granitoids are tabulated in Appendix D3. Porphyry samples differ sharply from phanerites in lower Rb, Sr and Zr although Ba, Y, Nb and Ce are present in similar concentrations. On the Ba-Rb-Sr ternary, the phanerites form tight clusters within the granodiorite/quartz diorite field but porphyry samples scatter in a linear array near the Sr-Ba axis (Figure 2.89).

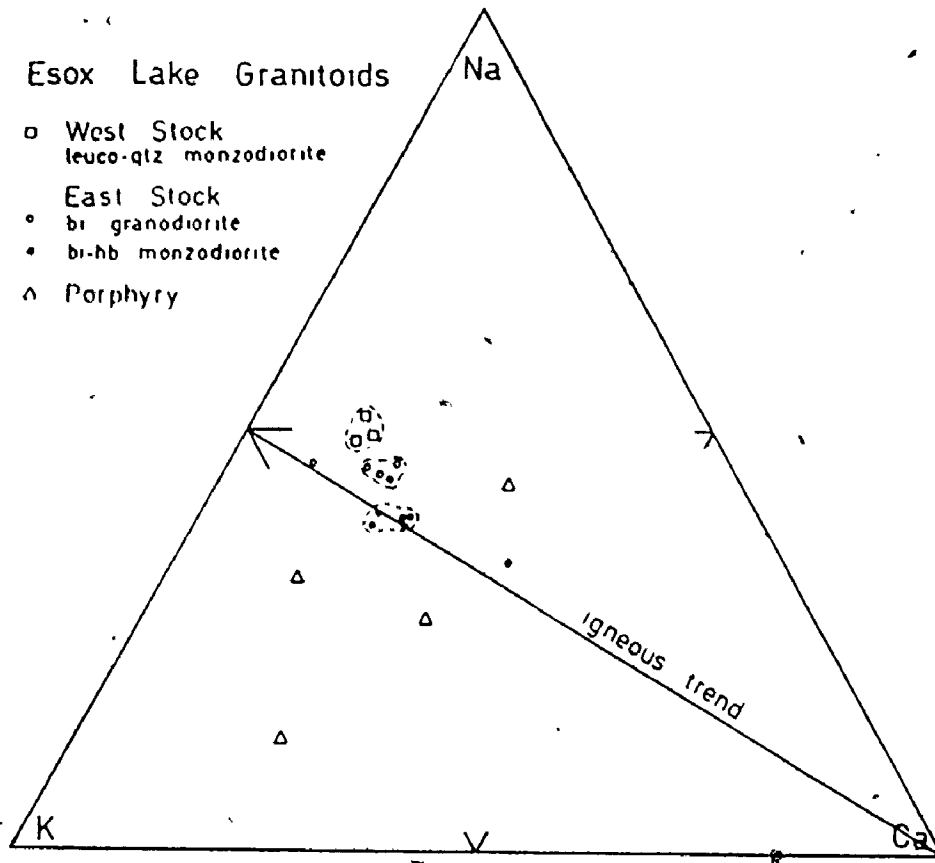


FIGURE 2.88 ESOX LAKE GRANITOIDS PLOTTED ON Na-K-Ca DIAGRAM OF GREEN AND POLDERVAART (1958). NOTE WIDE SCATTER FOR PORPHYRY SAMPLES

As for the major elements, the chemical spread is attributable to deuteric or post-magmatic metasomatism more extensive in the porphyry than in phanerites.

2.3.5 PETROGENESIS OF PORPHYRIES:

Hopwood (1976) presented a detailed investigation of "quartz-eye" porphyroidal rocks from 12 Canadian volcanogenic massive sulphide deposits. The structural relationships and textures, as documented by numerous sketches and photomicrographs show these porphyries to be similar to the body at Esox. Hopwood (1976) arrived at the following conclusions:

1. The combined association of pyritic-rich units and quartz-eye bearing porphyroidal acid rocks appears closely related to the occurrence of volcanogenic massive pyritic Cu-Zn sulphide deposits.
2. The quartz eyes formed by porphyroblastic growth within a matrix which was actively deforming during development of regional schistosity.
3. The quartz-eye porphyry represents a melt of former quartz monzonitic composition which has been syntectonically intruded during the development of a regional schistosity.

Although the Esox area cannot boast of an economic sulphide deposit, the association with massive pyrite has been previously noted, as has the porphyroblastic nature of some quartz eyes.

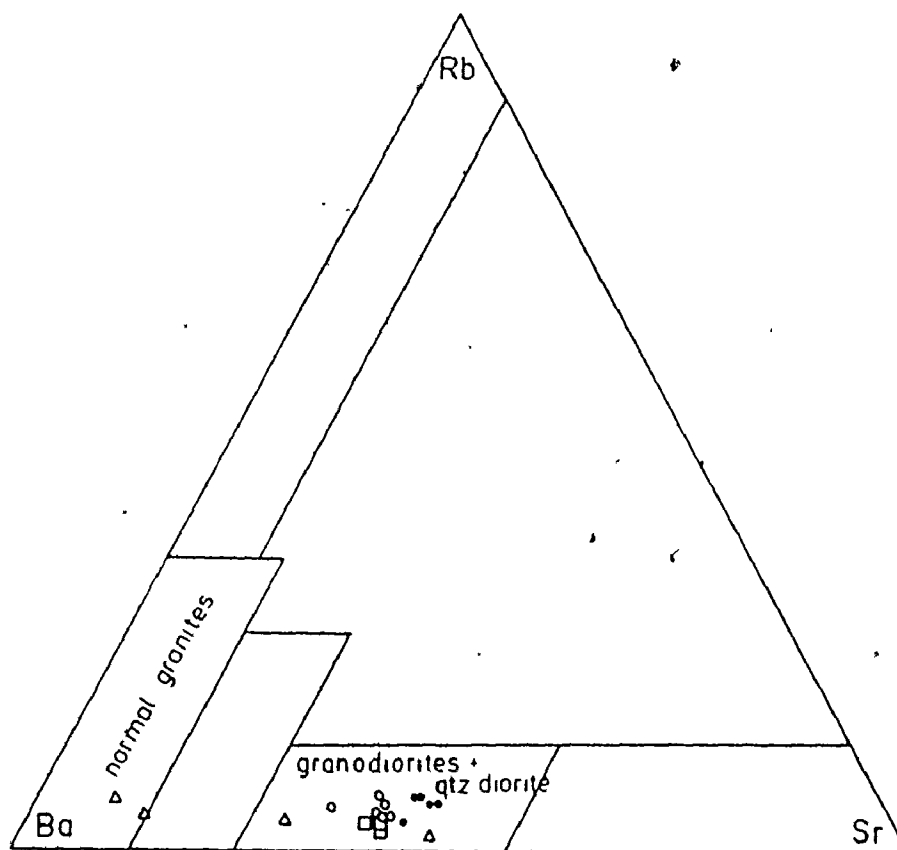


FIGURE 2.89 ESOX LAKE GRANITOIDS ON
Ba-Sr-Rb TERNARY OF BOUSEILY
AND SOKKARY (1975)

- LEUCO-QTZ-MONZODIORITE
- Bi-GRANODIORITE
- ◆ Bi-Hb MONZODIORITE
- △ PORPHYRY

Hopwood's third conclusion has not been demonstrated for the Esox Lake porphyry but has also not been dismissed. If the porphyry originated as a quartz monzonite magma yet was emplaced in association with volcanics, this solution neatly straddles both sides of the "Porphyry Problem".

The scatter of chemical data has led the author to suggest deuteric or post-magmatic metasomatism. Kochhar (1977) studied a comagmatic calc-alkaline suite of felsite, quartz porphyry, ash beds and muscovite granite forming a ring complex in the Indian Shield. He concluded that rapidly cooled acid volcanic rocks undergo post-emplacment modification in alkali contents by devitrification, hydrothermal alterations, alkali ion exchange and ground water leaching. He considered that quartz porphyry is less susceptible to hydrothermal alteration and therefore more likely to retain primary compositions. If this is true for the Esox Lake porphyry, then the heterogeneity must be attributed to deuteric autometasomatism rather than post-emplacment leaching.

Tauson (1967) has written that:

"... Degassing of the hypabyssal granitic intrusives with high content of volatiles causes migration of the rare elements into the upper parts of the magma chamber, not only during the magmatic stage but also during autometasomatic and high temperature metasomatic activity. As a result, areas strongly enriched in some rare elements, especially Li, Rb, Be, Sn and W may occur in the apical parts of such intrusives ...".

If such a mechanism accounts for the chemical disparity between the grey and pink phases at Esox, the pink porphyry with its higher Rb, Nb, Y, Ba, Si and K must represent the higher elevation. This, however, contradicts the field observations which trace the grey

porphyry gradationally into volcanic breccia. The very local nature of the pink and grey differentiation may be beyond the resolution of Tauson's model although the general principles still apply to explain the total chemistry of the porphyry.

Boone (1969) dealt at length with the petrogenesis of red and grey phases in a granitic porphyry of Eastern Canada. He attributed the difference in colouration to hematiferous albite, pseudomorphic after plagioclase. Plagioclase had reacted with vapour plus Fe and Mg released during decomposition oxidation of primary mafic phases. Unfortunately, the chemical and mineralogical trends in Boone's porphyry do not match trends at Esox. His red porphyry carries lower SiO_2 , K_2O and higher Al_2O_3 than the grey phase. Formation of pink porphyry at Esox is therefore more likely a product of deuteritic volatile migration and introduction of microcline.

Of interest is the juxtaposition of the Esox porphyry against both a homogeneous phanerite and a concentrically zoned stock. A similar trio of porphyry/homogeneous stock/zoned stock has been documented at Hope Lake (Heimlich, 1966). He considered the porphyry to be younger than the phanerites and chemically distinct with higher Cu, Cr and Ni.

This brief study of the Esox porphyry has not solved the "Porphyry Problem" but has shown that the genetic link between porphyries and Algoman granitoids as assumed by the earlier workers (Parsons, 1912; Hurst, 1935) has not been proven. Therefore the following chapter on regional chemical compilations do not include Esox porphyry samples.

2.4 RECONNAISSANCE INVESTIGATIONS:

2.4.1 INTRODUCTION

Seven other granitoid plutons located on Figure 1.1 and lying within or adjacent to the Wabigoon Belt received only cursory field visits and sampling. Some of these plutons have been included in the geochronological study (Chapter 4) but all these plutons are included in major and trace element tables of Appendices C to F. Two or more modal analyses were carried out for each of these plutons to allow classification by the Q-A-P ternary of IUGS (1973) with modes tabulated in Appendix B5. For clarity, the plutons investigated in reconnaissance fashion have been grouped into:

- Wabigoon Plutons
- Rainy Lake Algonian Plutons

These groupings are arbitrary since all granitoids of this study are considered to be located within or peripheral to the Wabigoon Belt. The "Rainy Lake Algonian" distinction is useful to emphasize their role in the classic Precambrian studies of Lawson and others. The Taylor Lake Pluton is listed separately because of the many phases and detailed descriptions provided by Pichette (1976).

2.4.2 RAINY LAKE "ALGOMAN" PLUTONS:

Four of Lawson's (1913) type Algonian plutons (Nowhere Island Granite, Knuckle Island Granite, Bears Passage Granite and Redgut Bay

Granite) have been the subject of intensive radiometric dating (see Chapter 4.3.2) and are structurally significant because of their distribution along the Wabigoon-Quetico Belt interface (Mackasey et al, 1976). Their geometric centers form a linear array striking northeast along the north shore of Swell Bay. Similar linear alignments of stocks emplaced into supracrustals have been recognized in other Archean terrain (Goodwin, 1965; Glikson, 1972). Three of these stocks have been included in the present reconnaissance survey.

Rest Island Stock (Nowhere Island Granite)

The Nowhere Island granite of Lawson (1913) was renamed and treated in detail by I.H. Cram (1932). This "Algonian batholith" straddles the U.S.A.-Canada border some 15 km northeast of Fort Frances, Ontario, with outcrops almost entirely restricted to islands on Rainy Lake. Cram (1932) described a core phase of "... gray somewhat gneissic granite with abundant pale-blue quartz ..." and a border phase of gneissic hornblende "shonkinite" (mica-syenite-gneiss of Lawson, 1913). Harris (1974) disagreed with both Lawson (1913) and Cram (1932) and mapped the border phase as a separate intrusive complex forming part of the "Rocky Islet Bay Complex". His map shows lithology ranging from hornblendite to porphyritic quartz monzonite. While Cram (1932) uncovered a gradation of "granite" to "shonkinite" on Grassy Island, Harris (1974) countered with an outcrop on Pukamo Island where porphyritic quartz monzonite cuts granite.

A reconnaissance visit was made to the Rest Island stock but observations were not sufficient to resolve the relationship between the syenitic border and the core. At sample station 4 (Figure 2.90), the syenitic border phase is shattered by an agmatitic network of granitic dykes carrying iridescent blue quartz. At least at this station, there is no doubt that the granitoid core intruded the syenitic phase and is not gradational with it. Harris (1974) marked off a "blue-quartz area" in the center of the granitoid phase. Blue quartz can be observed well beyond Harris's boundary, though less prominent. Iridescent blue quartz porphyroblasts are carried within mafic enclaves at stations 2 and 3, demonstrating a deuteritic origin for the blue quartz. The felsic core of the Rest Island stock carries a preponderance of subangular to subrounded mafic enclaves, occasionally with dimensions up to 5'.

General lineation is faint to well developed, and where strong, the mafic enclaves also show a dominant long-axis orientation. At station 5, a single truncated half-moon shaped mafic enclave attests to post-placement movement. There is a notable lack of aplitic or pegmatitic dykes within the core of the Rest Island stock.

Lawson (1913) described the structure of this pluton as follows:

"... in regard to the relation of the Coutchiching to the combined Nowhere Island and Pukamo Island plutonic mass, ... where the plutonic mass widens out to the westward, we have a belt of schist extending for at least 3 miles from Last Island to Nowhere Island, sunk down into the granite. This indicates that the arch of sedimentary rocks over the plutonic mass in this section was not disposed in a simple curve, but was a double arch, with a medial synclinal sag which sank into the molten mass and became congealed in it as a roof pendant as defined by Daly." p. 100

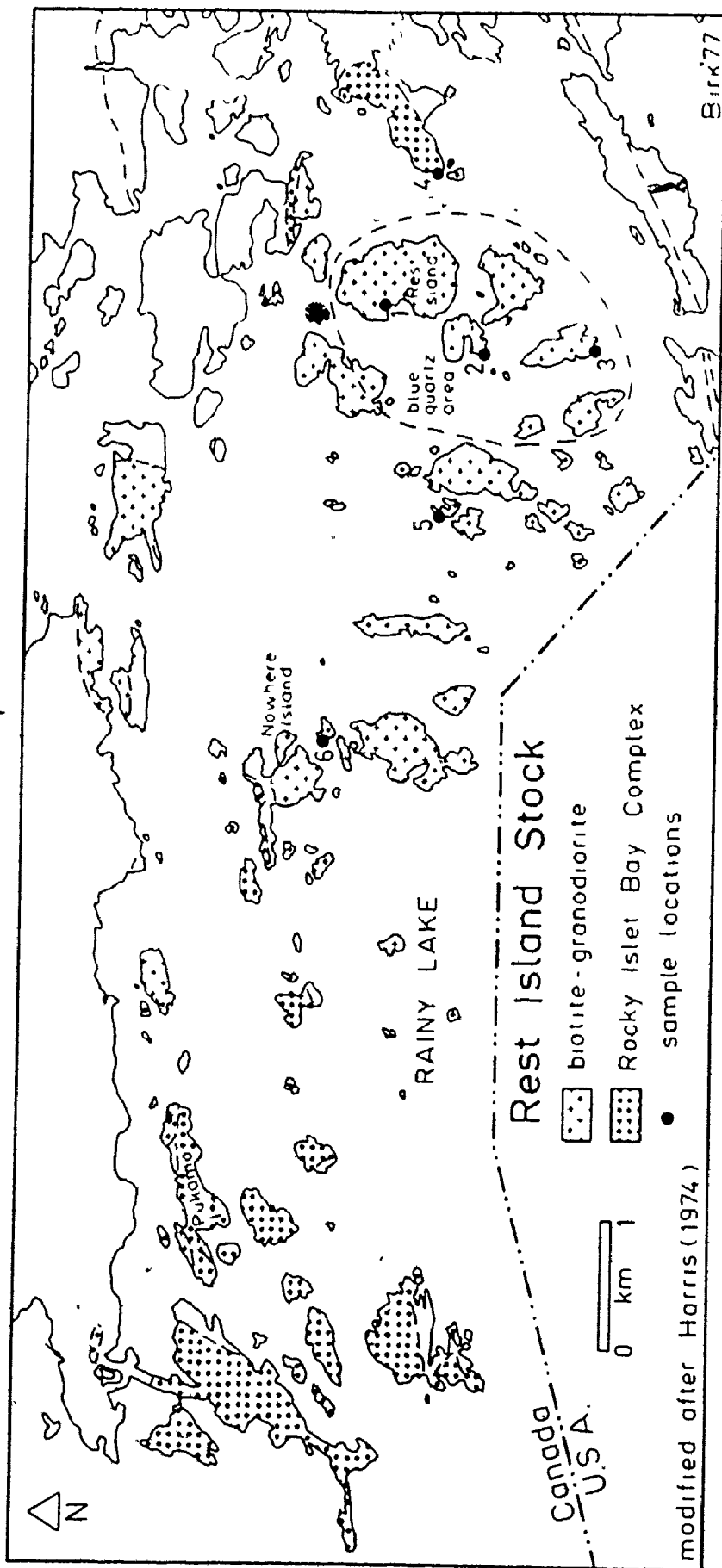


FIGURE 2.90

NOTE:
 CORRESPONDING SAMPLE NUMBERS IN
 APPENDIX CARRY PREFIX "REST."

Two modal analyses of the core unit (Appendix B5) define a biotite granodiorite (IUGS, 1973). Petrographic features include:

- zoned and sericitized plagioclase in synneis twinning.
- highly disseminated interstitial microcline
- polygonal quartz mosaics or large plates of quartz

surrounded by polygonal quartz

No explanation for the opalescent blue nature of the quartz was found. Allison (1925) attributed blue quartz in the Giants Range Batholith to inclusions of zircon, apatite and fluid inclusions.

Opalescent blue quartz can be observed in the following other lithologies of northwestern Ontario:

1. As rounded quartz megacrysts in mafic enclaves of the Froghead Bay Stock and Esos West Stock.
2. As pale blue quartz-eye porphyroblasts in strongly sheared intermediate volcanics or metagreywackes along the Quetico Fault (south end of Shoal Lake and south end of Calm Lake).
3. In rhyolites, dacite porphyries, andesites, lapilli tuff, gabbro and batholithic granitoids of the Eagle Lake - Wabigoon Lake region, commonly associated with sulphide mineralization (at Hardrock Bay, Fornieri Bay and Contact Bay).

All these environments suggest that blue quartz is²a product of metasomatism or metamorphism in places cogenetic with sulphide mineralization.

Bears Passage Stock

Highway 11 cuts the Bears Passage stock 28 km east of Fort Frances, Ontario. Lawson (1913) recognized a medium grained homogeneous "biotite granite" free of felsic dykes and encased by contact metamorphosed Couthiching schists. The Bears Passage contact where the Couthiching series dips away from the granitoid and beneath the Keewatin metavolcanics was Lawson's type locality for defining the Couthiching. Harris (1974) confirmed the metamorphic aureole around the stock by locating garnets and altered staurolite in the schists and phyllites. The structure was described by Lawson (1913) as:

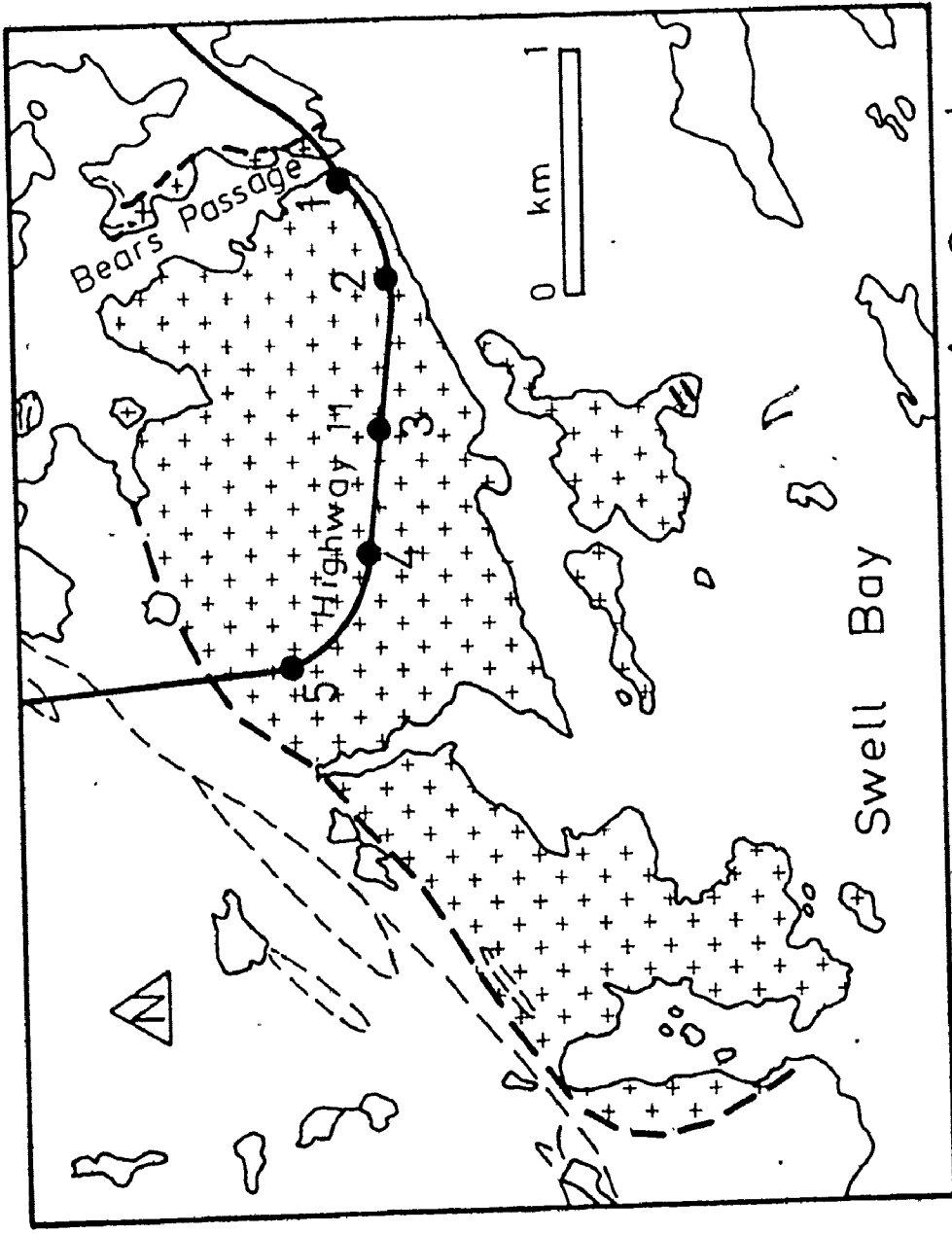
"... that of a truncated dome, the encasing rocks having once arched the granite in the fashion of a laccolith roof ..." p. 100.

Six representative samples were collected on a traverse following Highway 11. The stock appears strikingly white and homogeneous, grading to pale pink (Figure 2.91, stations 4,5) with unusual sulphide and molybdenite mineralization in and adjacent to the stock. Harris (1974) reports:

"... The best exposed molybdenum mineralization is at the northeastern contact between the Bears Passage granite stock and the Bears Passage metasediments; just east of the bridge at Bears Passage The molybdenite (allied with pyrite) is in or closely associated with narrow discontinuous quartz veins in the granite... (or) is concentrated in paper-thin fractures in the granite and biotite-feldspar-quartz schist. These molybdenite-coated fractures commonly have slickensides indicating fault movement ..." p.81

Mineral modes (Appendix B5) define a leuco-muscovite-granodiorite (IUGS, 1973). Petrographic features worth noting include:

- fresh appearance of interstitial microcline
- primary appearance of muscovite as large flakes or muscovite-biotite intergrowths.
- biotite as highly altered chloritized ragged remnants
- veinlets of quartz and sulphides or sulphide grains as rare inclusions in plagioclase
- triple junctioned polygonal quartz or globules of quartz as inclusions in poikilitic plagioclase.



Bears Passage Stock Sample Locations

FIGURE 2.91

NOTE:
CORRESPONDING SAMPLE NUMBERS IN
APPENDIX CARRY PREFIX "TR."

Two modal analyses of the core unit (Appendix B5) define a biotite granodiorite (IUGS, 1973). Petrographic features include:

- zoned and sericitized plagioclase in synneusis twinning.
- highly disseminated interstitial microcline
- polygonal quartz mosaics or large plates of quartz

surrounded by polygonal quartz

No explanation for the opalescent blue nature of the quartz was found. Allison (1925) attributed blue quartz in the Giants Range Batholith to inclusions of zircon, apatite and fluid inclusions.

Opalescent blue quartz can be observed in the following other lithologies of northwestern Ontario:

1. As rounded quartz megacrysts in mafic enclaves of the Froghead Bay Stock and Esos West Stock.
2. As pale blue quartz-eye porphyroblasts in strongly sheared intermediate volcanics or metagreywackes along the Quetico Fault (south end of Shoal Lake and south end of Calm Lake).
3. In rhyolites, dacite porphyries, andesites, lapilli tuff, gabbro and batholithic granitoids of the Eagle Lake - Wabigoon Lake region, commonly associated with sulphide mineralization (at Hardrock Bay, Fornieri Bay and Contact Bay).

All these environments suggest that blue quartz is a product of metasomatism or metamorphism in places cogenetic with sulphide mineralization.

Ottertail Lake Pluton (Redgut Bay Granite of Lawson 1913)

Lawson (1913) mapped an asymmetric pluton of medium grained "biotite granite", intrusive into both the Keewatin and Coutchiching, in a series of obtuse lobes. To the north the pluton is cut and terminated by a band of porphyroid gneiss (Quetico Fault zone). Of the structure he wrote:

"... where the tongues of schist project out into the granite terrain ... they are roof pendants that are still connected with the margin of the roof. ... The disposition of the roof pendants, whether connected or detached in the Redgut Bay region, and particularly the one at Moose Point, indicates that the present surface of the granite is not much below its original surface as it lay under its roof when the latter was intact." p.100 - 102.

More recent mapping by Harris (1974) separated Lawson's pluton boundaries into two stocks, centered at Redgut Bay and Ottertail Lake. The author's field visit was restricted to the highway 11 traverse across the Ottertail Lake body (Figure 2.92). The stock is concentrically zoned with three modal phases (Appendix B5) classed as muscovite granite, biotite granodiorite and a heterogeneous mafic rim reported as hornblende diorite to quartz monzodiorite. The dominant biotite granodiorite unit grades from pink to grey and carries prominent microcline megacrysts in 1.5 cm laths. Biotite clots and mafic enclaves up to 30 cm were located in both the granodiorite and quartz monzodiorite (stations OT1, OT6, OT7) and an extensive breccia zone has been mapped south of Ottertail Lake. The centrally located muscovite granite represents the last intrusion, having sent granitic dykes into the granodiorite (OT4) and possibly supplied a myriad of felsic dykelets to the mafic rim (OT1).

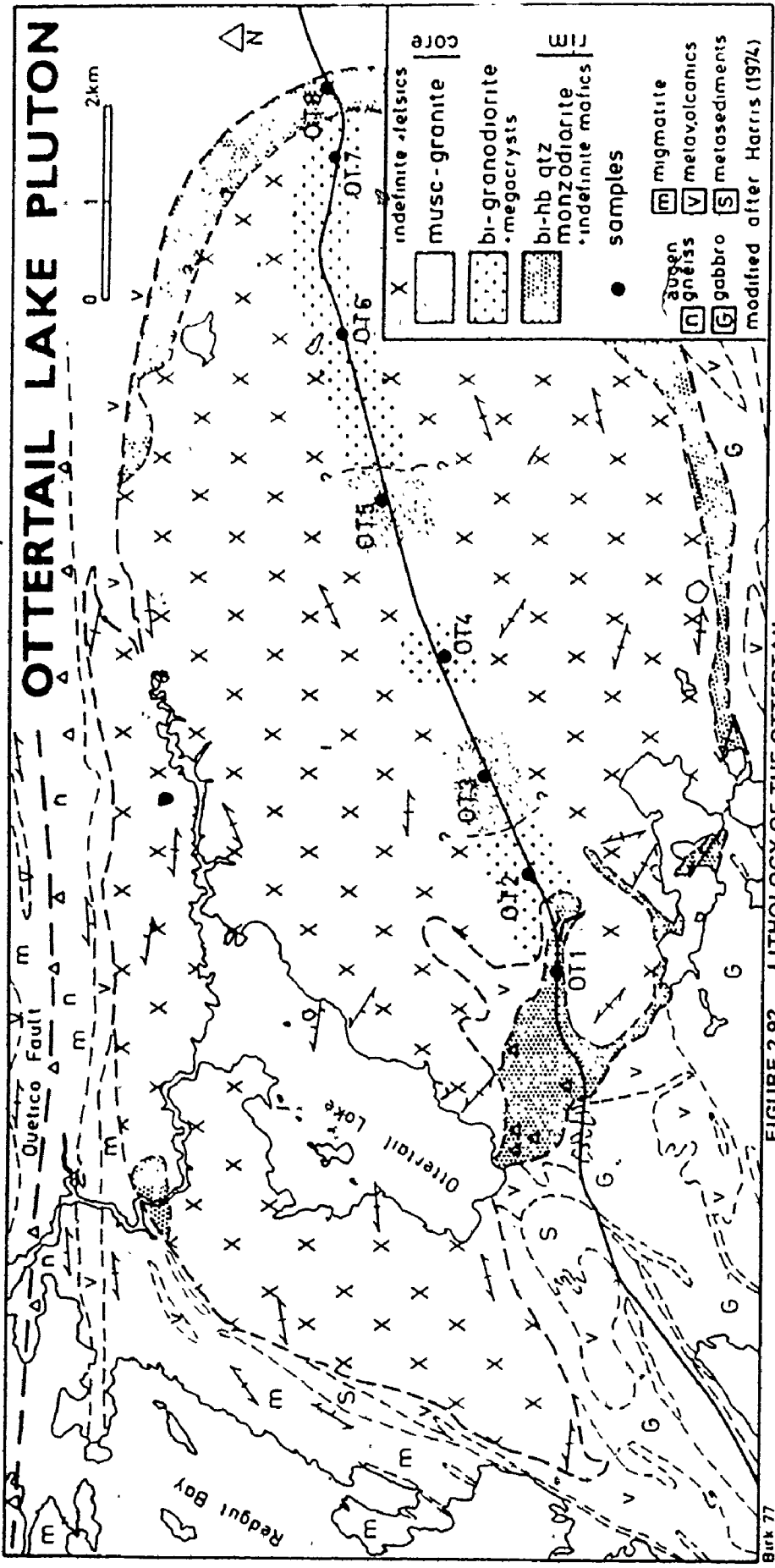


FIGURE 2.92 LITHOLOGY OF THE OTTERTAIL LAKE PLUTON. ONLY THE HIGHWAY TRAVERSE (BLACK) WAS VISITED BY AUTHOR THUS PHASE CONTACTS ARE UNCERTAIN.


BRK 77

The muscovite granite is modally and texturally very similar to the muscovite granodiorite of the Bears Passage stock, carrying the same fresh appearance to interstitial microcline and prominent primary muscovite flakes. A model of ~~co~~genesis or subsurface connection is not unreasonable but needs to account for the zoned nature at Ottertail in contrast to the homogeneous nature at Bears Passage. Differences in erosional level are not likely since both stocks were considered by Lawson (1913) to show near-roof structures.

Aeromagnetic Flux - Rainy Lake:

The Fort Frances sheet of the ODM-GSC Aeromagnetic series (ODM 1971; Map 1158G, 52C/11) shows a continuous band of shallow gradient low magnetic flux, striking northeast along Swell Bay, coinciding with the linear array of Algonian granitoids. The felsic granitoids are contained below the 60,300 gamma contour while slightly higher (60,400) flux corresponds to the syenitic border of the Rest Island stock. Outchiching metasediments and Keewatin metavolcanics display much steeper gradients and magnetic flux above the 60,400 contour, hitting a maximum of 62,500 gammas over the gabbroic sill at Grassy Portage Bay.

On the otherhand, the Ottertail Lake stock is characterized by a concentric magnetic pattern grading from 60,300 gammas at the core to 60,500 gammas at the margins (Map 1150G, Sein Bay sheet 52 C/10).



2.4.3 WABIGOON PLUTONS

Plutons lying internal to the Wabigoon Belt and studied in reconnaissance fashion include three relatively homogeneous bodies, (Froghead Bay Stock, Regina Bay Stock and Stormy Lake Stock) and one complex zoned pluton (Taylor Lake Stock).

Froghead Bay Stock

Froghead Bay drains into Eagle Lake, 25 kilometers southwest of Dryden, Ontario (NTS 52 F/11). The earliest geological map showing the Froghead Bay Stock is that of Parsons (1912). Detailed mapping of the stock and vicinity was conducted by Moorhouse (1939) who wrote:

"... an elliptical cupola or stock of granite surrounds Froghead Bay ... the massive light coloured ... granite intrudes the Keewatin without any noticeable effect on the massive pillow lavas except recrystallization ..."

A reconnaissance visit (Figure 2.93) revealed a "salt-and-pepper" textured homogeneous tonalite carrying mild foliation of mafic minerals; surface pits and quartz lenses. Abundant quartz takes on a blue opalescence locally similar to that of the Rest Island Stock (Harris, 1974). Mafic round to lensoid enclaves are ubiquitous and frequently carry megacrysts of feldspar and opalescent blue quartz ("double enclaves"). Dykes of aplite and quartz are abundant but small (less than 5" in width).

At the north and south extremities of the stock are numerous quartz and porphyry dykes which Moorhouse classed as "Algoman" and contemporaneous with the stock.

Petrographically (Appendix B5) the stock is unusually poor in K-feldspar, giving a modal classification of biotite tonalite (IUGS, 1973). One sample, however, pink in hand specimen, carries abundant interstitial microcline and straddles the granite-granodiorite modal field boundary. This sample may represent a separate intrusion or an apical localization of alkalis.

Aeromagnetic contours for the Froghead Bay Stock are shown on the Eagle Lake Sheet (Map 1162G, sheet 52 F/11): The magnetic contours, concordant with the stock boundaries, show a magnetic low on the west side of Froghead Bay (down to 60,510 gammas) and a shallow gradient (60,510 - 60,560 gammas). The Froghead Bay Stock carries a distinctively lower magnetic flux than the felsic volcanics of Buchan Bay to the north (>60,700 gammas) or the granitoids of Osbourne Bay to the southeast (<60,600 gammas). On the otherhand, the granitoids west of Meridian Bay show a lower flux (<60,500 gammas).

Regina Bay Stock

The Regina Bay Stock (Figure 2.94) is an elliptical body forming the shore of Regina Bay, immediately east of the town of Sioux Narrows, Ontario (NTS 52E/8).

Not long after Lawson (1913) introduced his "Algoman-Laurentian" bimodal classification, prospectors concluded that gold deposits are:

"... genetically connected with granites to which the name Algoman is applied..." (Miller and Knight 1915, p.245).

The Regina Bay Stock became a type locality for this association because of a producing gold mine within its southern

margin (Regina Gold Mine, alias: Kenland Mine, Black Eagle Mine, Horse-Shoe Mine). Coleman (1897) reported that 80% of the gold was disseminated in a quartz vein (up to 8'; up to 15' quoted by later authors) in a free but very fine state, associated with accessory pyrite and molybdenite. Kwong's (1975) study of background gold distribution attributed gold mineralization to alkali autometasomatism adjacent to the quartz vein resulting in gold and sulphide precipitation from residual magmatic fluids. The background gold content of the host stock (.10 - 4.88 ppb) is similar to gold content in the nearby unmineralized Stephen Lake Stock.

The present study was limited to reconnaissance sampling at six stations. The most recent published map of Regina Bay geology is Fraser (1943) who characterized the stock as quartz diorite. The earlier visit of Coleman (1897) described the lithology as:

"a small boss of plagioclase granite, much of which has the greenish look of protogine" p.91

The aeromagnetic map for the Sioux Narrows quadrangle (ODM, 1971; map 1177G) shows a complex double vortex pattern over the Regina Bay Stock. A magnetic high (to 60,780 gammas) sits over the north shore while a magnetic low defines the centre of Regina Bay (down to 60,650 gammas). The strong zonal pattern contrasts with a much shallower magnetic gradient (60,440 to 60,700 gammas, generally 60,500) for the Aulneau Dome (Whitefish Bay to Miles Bay area).

Modes from the Regina Bay Stock (Appendix B5) plot on the Q-A-P diagram (IUGS, 1973) nearly coincident with samples from the Froghead Bay Stock and therefore define a tonalite, but texturally the rocks are remarkably different. The Regina Bay thin sections show

1
protogine: gneissic granitoid from Alps formed by recrystallization under stress.

complete sericitization of plagioclase, leaving only pseudomorphs. Calcite mosaics and veinlets of calcite and quartz are abundant while K-feldspar is totally lacking. Biotite appears rarely as very altered green remnants, some bearing networks of acicular inclusions (sillimanite?). Most of the mafic component is a fine chlorite-uralite mat. The textures and alterations at Regina Bay are more akin to porphyries than to previously discussed phaneritic granitoids. The evidence suggests extreme alteration and metasomatism possibly related to the gold mineralization.

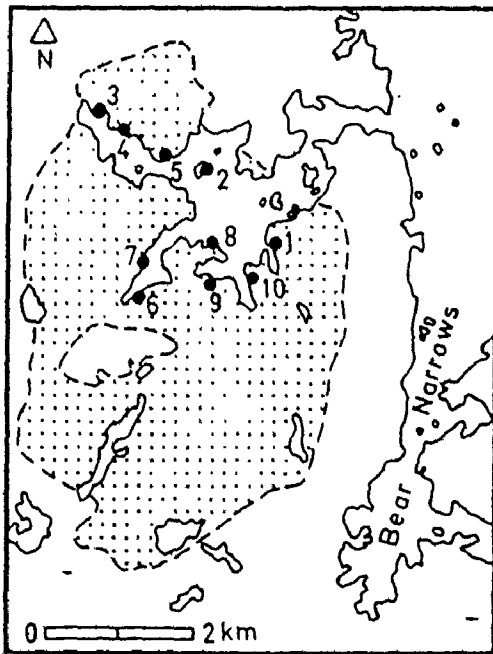
Stormy Lake Stock

This stock is poorly exposed on a peninsula in Stormy Lake, some 58 Km southeast of Dryden, Ontario. Thomson (1933) mapped it as an Algonian "granite" and noted the extensive drift cover. The stock is entirely surrounded by a pyroclastic and epiclastic sequence forming part of the Manitou Series in fault contact with thick mafic flows to the north. Sampling (Figure 2.95) was carried out to determine if intrusion into a sedimentary sequence has affected the nature of mafic enclaves in contrast to the more common intrusion into mafic or intermediate flows. Field exposure was, however, too sparse to allow a judgement.

Two modal analyses (Appendix B5) define a biotite granodiorite (IUGS, 1973) with prominent synneusis clusters of well zoned plagioclase and interstitial microcline.

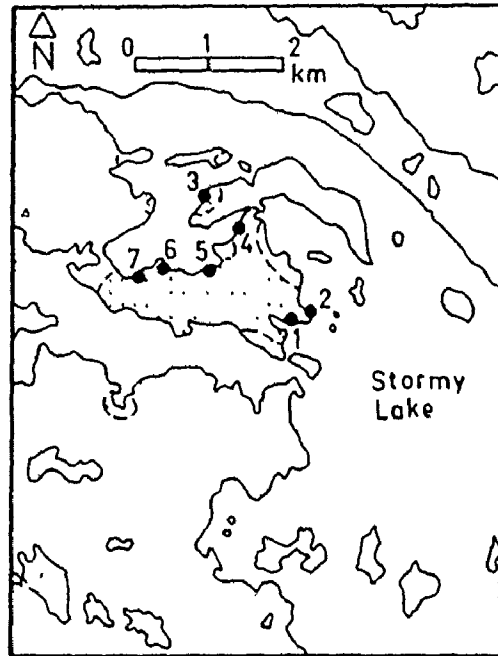
NOTE:
 SAMPLE LOCATIONS ARE ABBREVIATIONS
 OF SAMPLE NUMBERS IN APPENDIX.
 FOR FULL NUMBERS USE PREFIX:
 FH - FROGHEAD
 ST - STORMY
 REG - REGINA

FIGURE 2.93

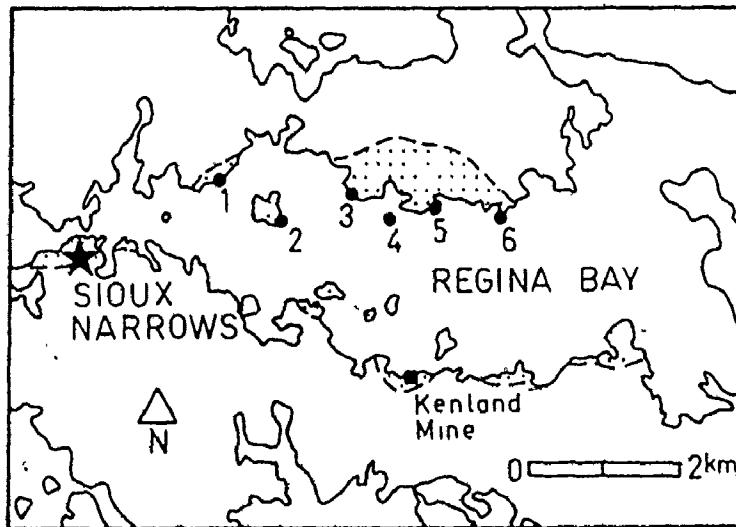


Froghead Bay Stock
 Sample Locations

FIGURE 2.95



Stormy Lake Stock
 Sample Locations



Regina Bay Stock sample locations

FIGURE 2.94

Taylor Lake Pluton

The Taylor Lake stock is a 10 x 6 km elliptical pluton located 48 km southeast of Dryden, Ontario (NTS 52 F/7). Previous mapping was by Thomson (1933) and Blackburn (1976). A detailed field petrographic, and geochemical description was carried out by Pichette (1976). The Taylor Lake stock is the only pluton included in this thesis that was not personally visited by the author. Pichette's study in 1975 followed field work with the author while surveying the other plutons of this study. His field techniques and geochemical procedures are considered compatible with this study. The samples and field descriptions utilized here were supplied by Pichette, and his original sample numbers have been retained (Figure 2.96).

Figure 2.96 is a summarized version of Pichette's (1976) map. Nine lithologic phases form a multiple granitoid intrusive into the apex of a north plunging antiform of mafic pillowed metavolcanics. The main mass is a hornblende-granodiorite characterized by microcline-perthite megacrysts. A small boss of finer grained biotite granodiorite intrudes the core of endoblastic granodiorite in the vicinity of Taylor Lake. These granodiorite units are partially mantled by a complex of: quartz monzonite, monzonite, monzodiorite carrying variable proportions of hornblende, biotite, and pyroxene. The eastern extremity is rimmed by a thin wedge of leucocratic microgranite. Pichette (1976) worked out an age sequence (oldest to youngest) of:

1. monzodiorite
2. monzonite/quartz monzonite
3. granodiorite

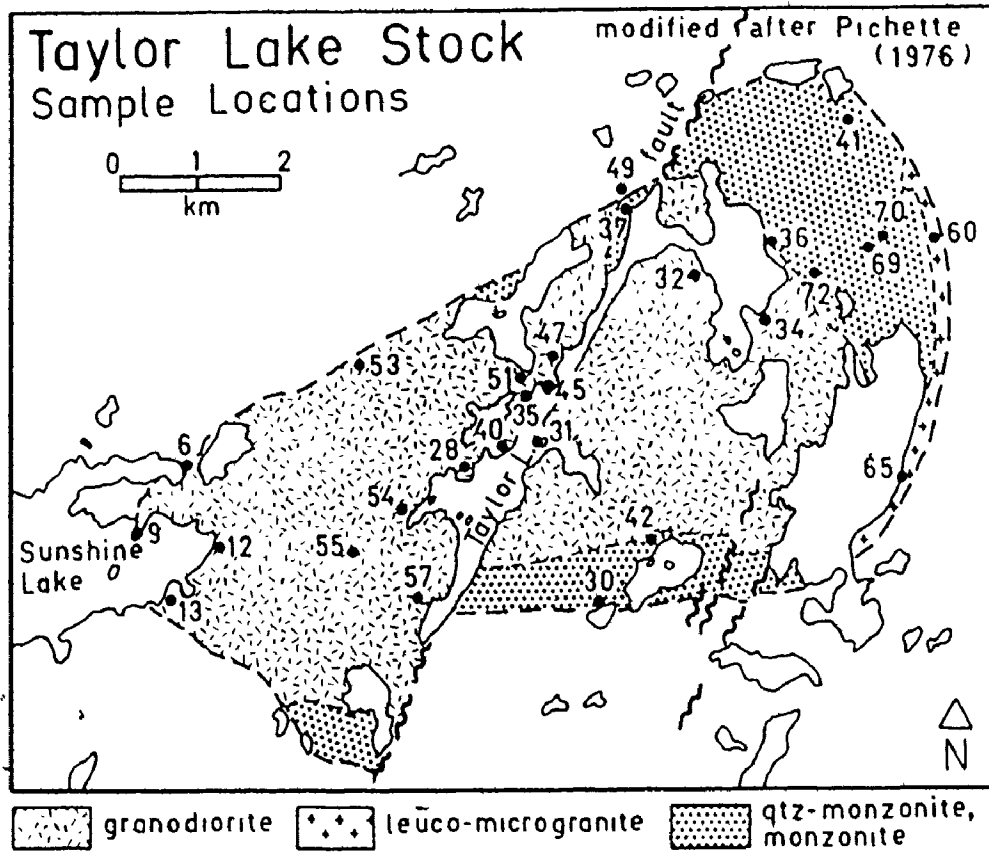


**FIGURE 2.96 TAYLOR LAKE STOCK (NTS 52F/7)
MODIFIED AFTER PICHETTE (1976).
APPENDIX SAMPLE NUMBERS
CARRY PREFIX "T."**

4. leucocratic microgranite
5. aplite; pegmatite
6. fine granodiorite

The aeromagnetic map for the Upper Manitou Lake quadrangle (ODM, 1971; Map 1153G) shows the Taylor Lake stock bounded by the 60,500 gamma contour. The magnetic flux correlates closely with lithology: The mantle of quartz-monzonite/monzonite on the eastern flank is defined by a concordant magnetic high grading from 61,000 to 61,400 gammas. A similar magnetic high defines the southern flank, rising to 62,000 gammas immediately above a small boss of monzodiorite.

In contrast, the main granodiorite mass carries shallow magnetic gradients straddling the 60,600 gamma contour. The core of fine grained granodiorite is outlined by a magnetic low down to 60,460 gammas.

The magnetic contours show deflection corresponding to the 1800 meter displacement of lithologies along the north-northeast trending Taylor Lake Fault which bisects the pluton along the length of Taylor Lake.

The magnetic flux over the Taylor Lake pluton is comparable to the flux over the Scattergood Lake stock to the west (>60,500 gammas) but is distinctly different from the magnetic field over granitoids of the Irene-Eltrut Lakes complex to the south (60,320 to 60,400 gammas near Meggisi Lake).

2.4.4 CHEMISTRY:

The foregoing plutons investigated in reconnaissance fashion are included in the chemical tabulations of appendices C, D and E. Previously published major and trace analyses include Grout (1929), Cram (1932) and Peterman et al (1972) for Rainy Lake plutons and Pichette (1976) for the Taylor Lake stock. A sample from the Bears Passage stock was included in one of the earliest trace element analyses of silicate rocks (Harcourt, 1934). Qualitative quartz spectrograph analyses were obtained for Ba, Sr, Cr, V, Sn, Pb and Ag.

Figures 2.97 and 2.98 are composite Na-K-Ca plots for the reconnoitred plutons. All plutons except the Ottertail Lake body define clusters on the Na side of the igneous divide. The Froghead Bay and Regina Bay stocks both show extreme K depletion. Despite petrographic evidence of alteration by sericitization and carbonatization, the Regina Bay stock fails to show the wide data scatter characteristic for the petrographically similar Esos Lake porphyry. This homogeneity in the Regina Bay tonalite shows that alteration was autochthonous.

Ottertail Lake samples straddle the igneous trend line in fields that do not overlap with the less potassic Bears Passage and Rest Island stocks. This chemical disparity contradicts the notion that these Rainy Lake plutons are subsurface apophyses from one batholith.

The more complex Taylor Lake pluton (Figure 2.98) shows as much chemical diversity as the other six plutons combined. Interestingly, the Taylor lithologies occupy a section of the Na-K-Ca plot

Na-Ca-K PLOT OF GREEN AND POLDERVAART (1958) FOR WABIGOOON PLUTONS, RAINY LAKE PLUTONS AND THE TAYLOR LAKE STOCK.

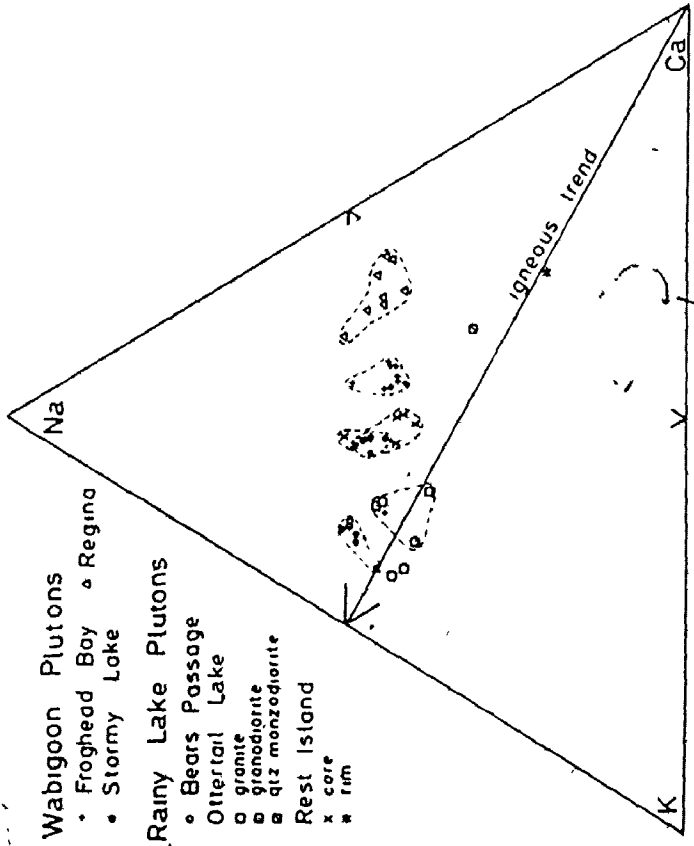


FIGURE 2.97

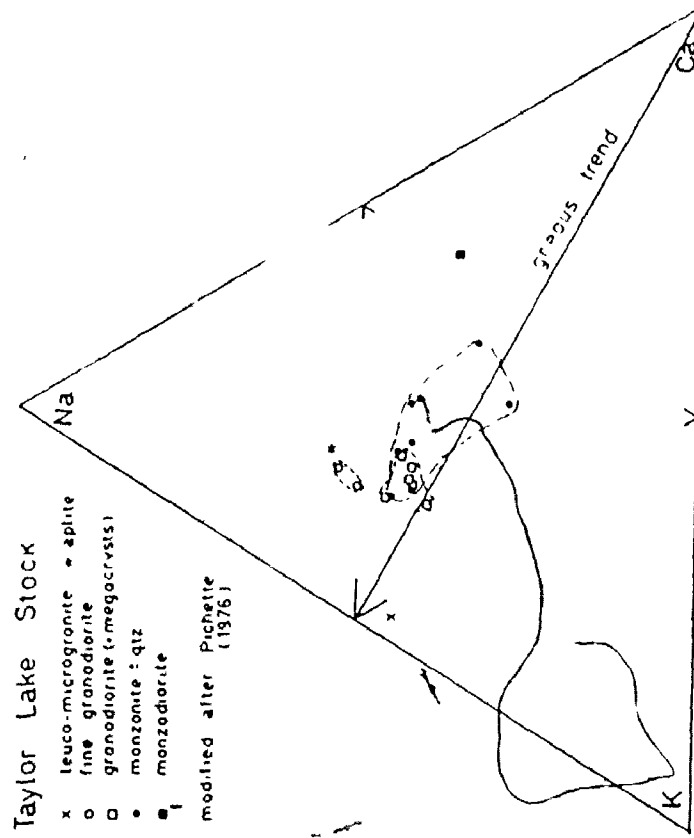
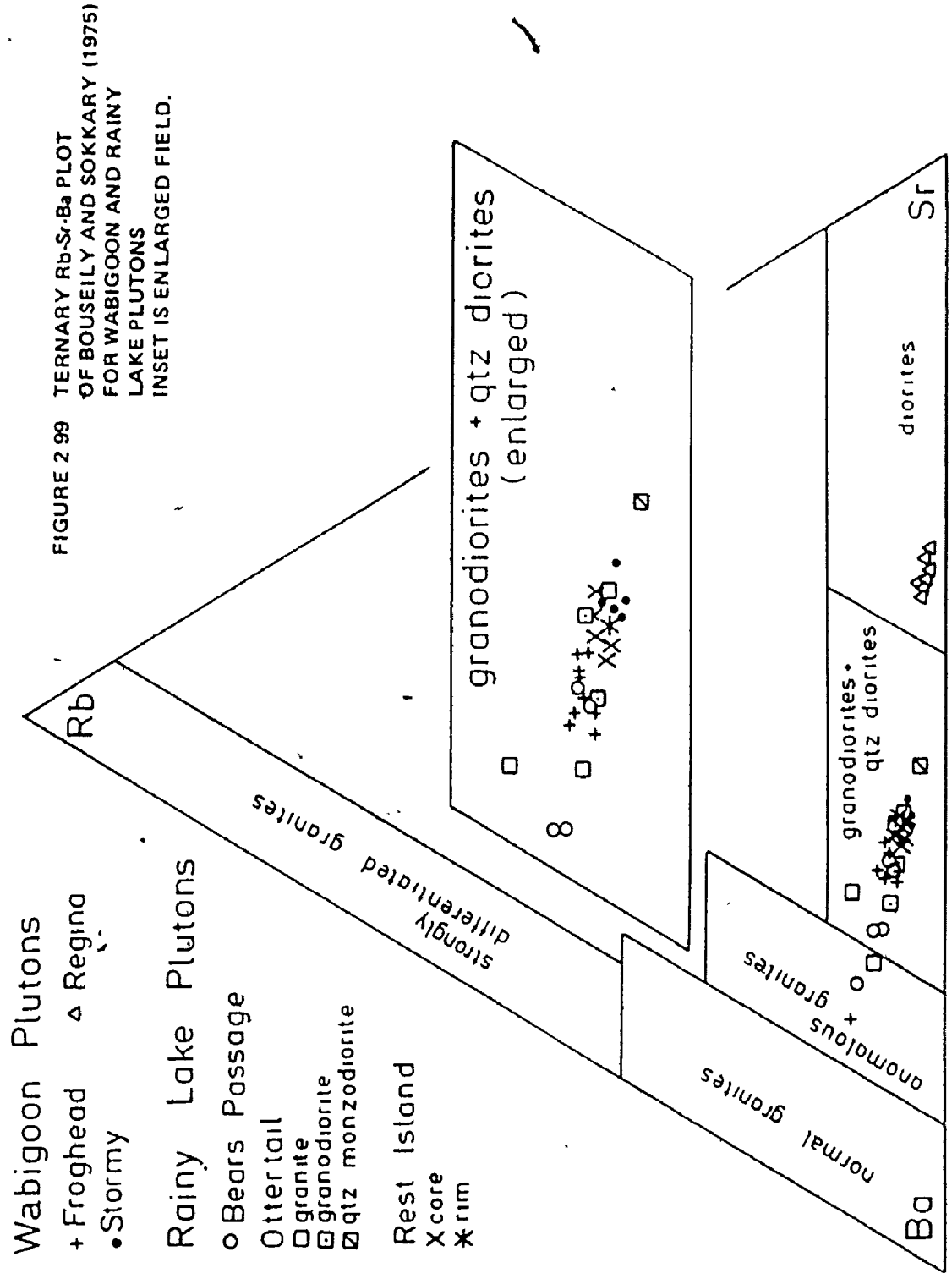


FIGURE 2.98

near coincident to the area occupied by the other plutons (Figure 2.97). This leaves room for the hypothesis that composite plutons are produced by superposition of the same magma pulses that generate the single phase plutons.

Figure 2.99 summarizes the Rb-Sr-Ba ternary for reconnoitred plutons omitting the complex Taylor body. All plutons except Regina lie dominantly in the granodiorite/quartz diorite rhomb. The Regina Bay tonalite is notably distinct from the Froghead Bay tonalite by occupying the diorite field. Bears Passage samples show an unexpected spread of values, not in keeping with the homogeneous lithology, while Rest Island, Froghead and Stormy samples form tight data clusters. These chemical peculiarities should be further investigated and a link be sought with molybdenite mineralization at Bears Passage and gold mineralization at Regina Bay.



CHAPTER 3

REGIONAL SYNTHESSES:

3.1 VARIATION, TRENDS AND AVERAGE COMPOSITIONS FOR 247 GRANITOIDS

3.1.1 Introduction

The chemical and petrographic portion of this study has been strongly influenced by the work of Whitten (1962) and Peikert (1965) on the variability of plutonic bodies. The following statements have been taken to heart:

Whitten (1962): "... virtually nothing is known about the average composition of igneous rock masses ..."
"... For igneous masses it is ideally necessary to determine the average composition on the basis of the three dimensional variability ..."

Peikert (1965): "... the mineralogical composition of each exposed level of a pluton is unique. Thus one must be cautious in applying observations of a two dimensional exposed surface to the determination of the genesis of a three dimensional pluton ..."

Other students of the Precambrian do not acknowledge this complexity and prefer to speculate on limited samplings. Viljoen and Viljoen (1969) calculate chemical "averages" for Barberton region granitoids based on as few as three and at most eighteen samples. These "averages" are repeated in Glikson (1971) for genetic speculations supplemented with 25 samples defining granitoid "averages" for all of Western Australia. In Glikson and Sheraton (1972) these granitoid averages are compared with Lewisian gneisses of Scotland for which 339 samples are available.

Even chemical averages based on large compilations such as the classic paper by Nockolds (1954) have limited usefulness. Rock classification is ambiguous. IUGS (1973) have commented on the diversity of classification schemes and overlapping rock names. Nockolds (1954) used a "... semiquantitative mineralogical ..." classification. Chemical averages furthermore mask chemical variability within each group and ignore the spectrum nature of petrogenetic provinces.

For comparative purposes and discussions of "averages", the author favours the use of petrochemical fields and trends. Such a technique has been applied by Aramaki et al (1972) to Japanese granitoids. Based on 1189 analyses and the linear correlation of oxides against D.I. of Thornton and Tuttle (1960), they calculated average oxide concentrations for a D.I. range of 50 to 100 at class intervals of 5.

Although over 247 granitoid samples were analysed in this study, (Appendix C to E) the quantitative procedure of Aramaki et al (1972) is not practical because:

1. The Differentiation Index of Thornton and Tuttle (1960) has been rejected (Section 2.1.2).

2. These analyses do not reflect volumetric abundance.

Sampling was biased in favour of homogenous granodiorites resulting in unequal sample densities over the range of variables. This thwarts attempts to draw least-squares regression lines.

A similar but more qualitative approach was adopted to compile the 247 analyses and to illustrate the range in chemistry for all 12

Wabigoon Belt granitoids. In following diagrams, appendix analyses are plotted as cations against the modified Larsen Index. Subsequent discussions of normality, averages and outliers are based on visual inspections of these compilations. The quartz-feldspar porphyry of Essex was omitted for reasons discussed previously. Likewise, Aramaki et al (1972) excluded porphyries from their compilations.

3.1.2 Major Elements; Trace Elements; Element Ratios:

Figures 3.1 to 3.10 present trend compilations for major cations. Three plutons locate consistently on the fringes or outside the main cluster: the Regina Bay Stock, Froghead Bay Stock and the monzonite and monzodiorite of the Flora Lake Stock. If these "outliers" are removed, the remaining trends include:

1. Strong positive correlation of Si.
2. Strong negative correlation of Fe, Mg, Ti, Ca.
3. Weak negative correlation of Mn and P.
4. Relatively constant Na and K.
5. Mild convex curvature for Al.

These trends are similar to those reported for 80 Egyptian granitoids (El-Gaby, 1975) except for stronger Al curvature, more scatter for K and less scatter for Si in this study. The trends are also similar to those reported for the Southern California Batholith (Nockolds and Allen, 1953) except that this study recorded an Al curvature.

The anomalous plutons are characterized as follows:

Flora Lake Stock (border phases)	:	enriched in Al, Fe, Ti, P, K depleted in Si
-------------------------------------	---	--

FIGURES 3.1 TO 3.10

LINEAR CORRELATION COMPILATIONS
FOR 247 GRANITOIDS OF THE
WABIGOON BELT: MAJOR CATIONS
VERSUS MODIFIED LARSEN INDEX.
THESE COMPILATIONS INCLUDE PHANERITES
AND APLITES BUT EXCLUDE THE
PORPHYRY OF ESOX LAKE. VALUES
CALCULATED FROM APPENDIX C1 TO C7
SAMPLES FROM FROGHEAD BAY STOCK (FR)
REGINA BAY STOCK AND FLORA LAKE
STOCK (SOLID CIRCLES) CLUSTER OUTSIDE
THE MAIN QUASI LINEAR TRENDS
(CROSSES).

NOTE: SYSTEMATIC VALUES AT HIGH
MODIFIED LARSEN INDEX FOR Mn, TI AND
P IS FUNCTION OF PROXIMITY TO XRF
DETECTION LIMIT.

FIGURES 3.11 TO 3.16

LINEAR CORRELATION COMPILATIONS
FOR 247 GRANITOIDS OF THE
WABIGOON BELT: TRACE ELEMENTS
VERSUS MODIFIED LARSEN INDEX.
PORPHYRIES EXCLUDED. OUTLIERS
FROM MAIN QUASI-LINEAR TRENDS
(DATA CROSSES) SHOWN AS SOLID DOTS.

FR = FROGHEAD
RI = RESTISLAND
RG = REGINA

SAMPLE NUMBERS MATCH APPENDIX LIST.
DATA FROM APPENDIX D1 TO D7.

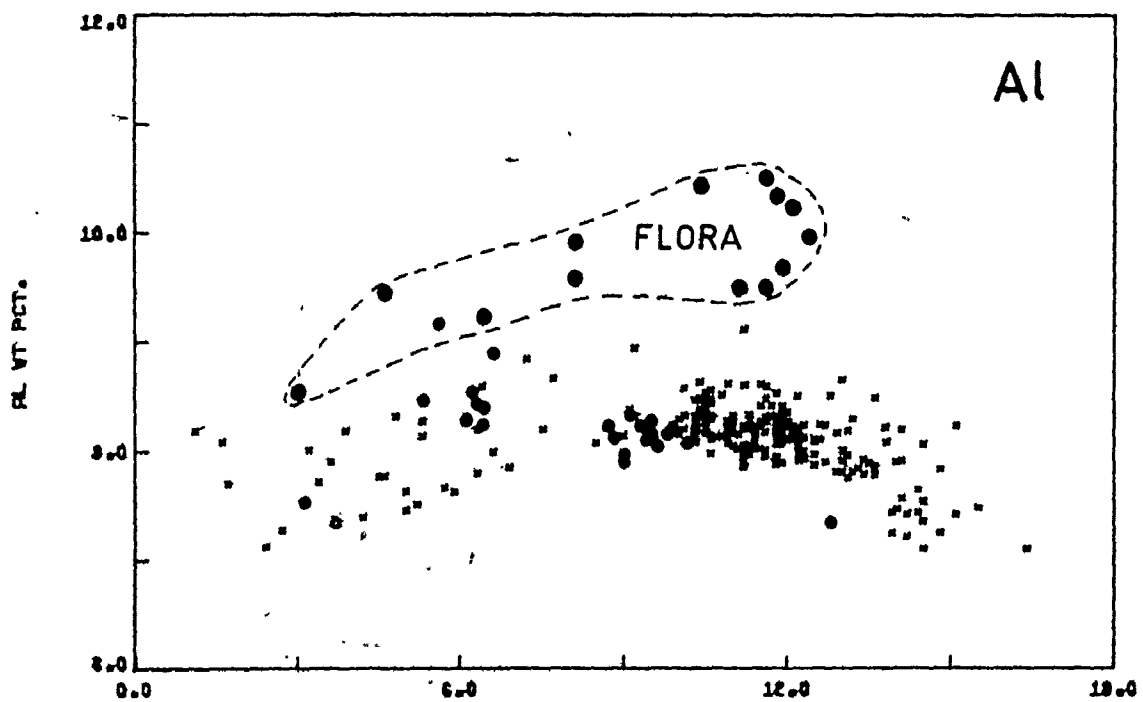
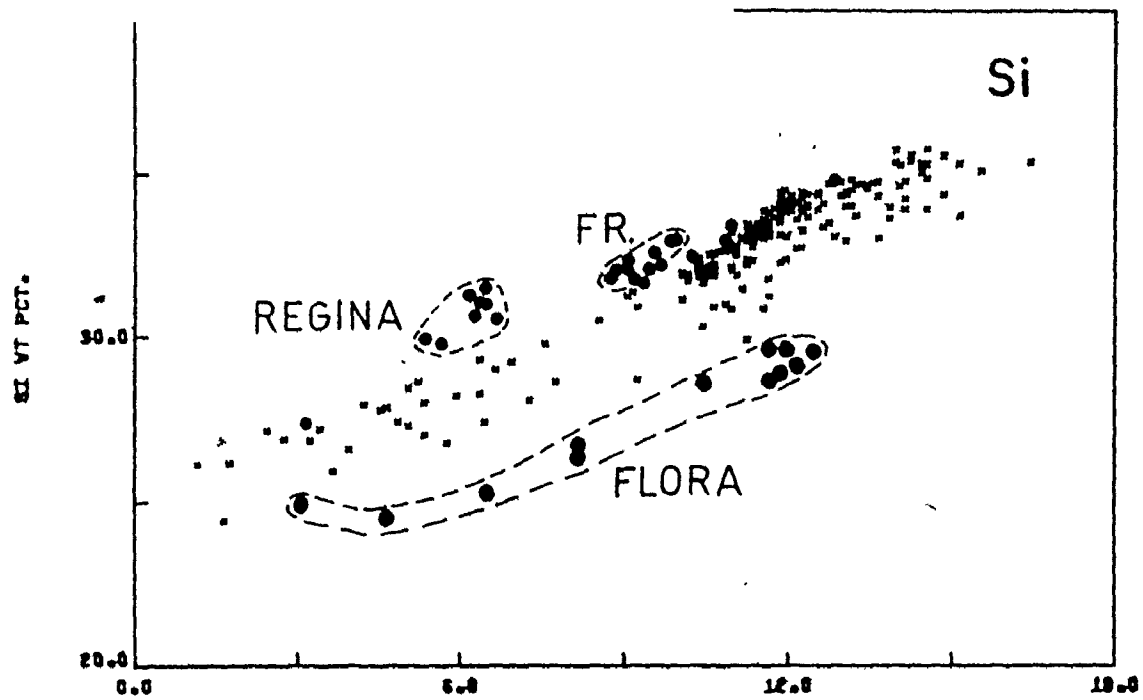


FIGURE 3.2

MODIFIED LARSEN

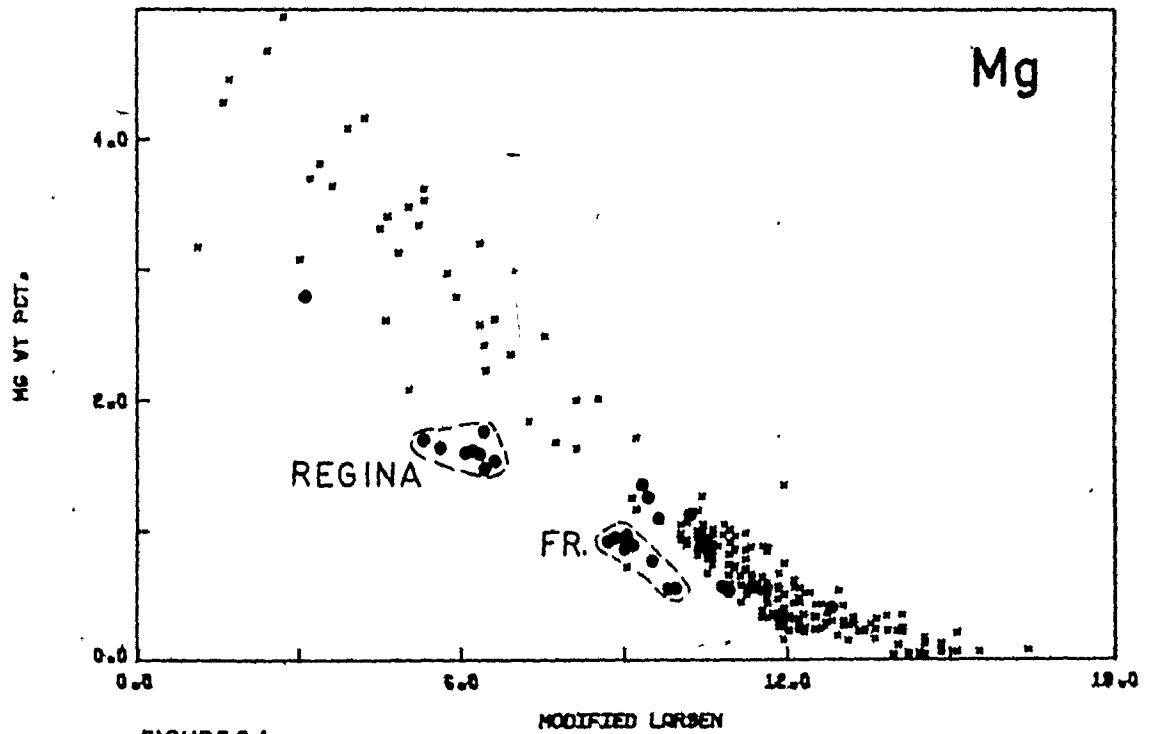
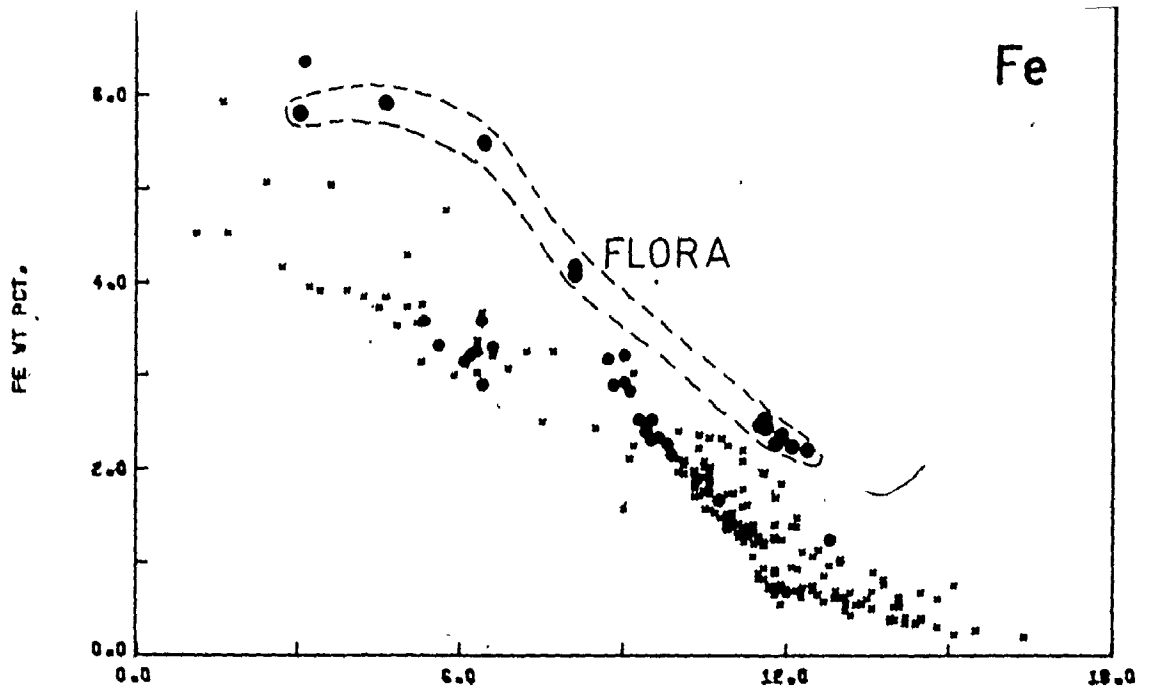


FIGURE 3.4

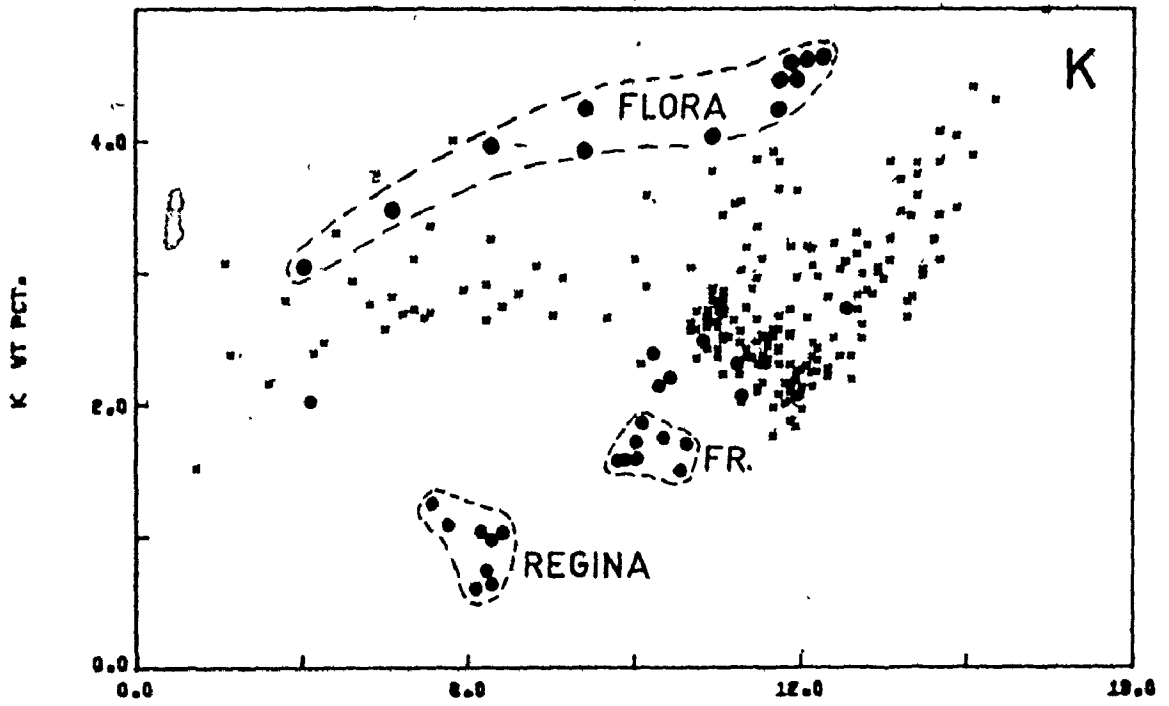
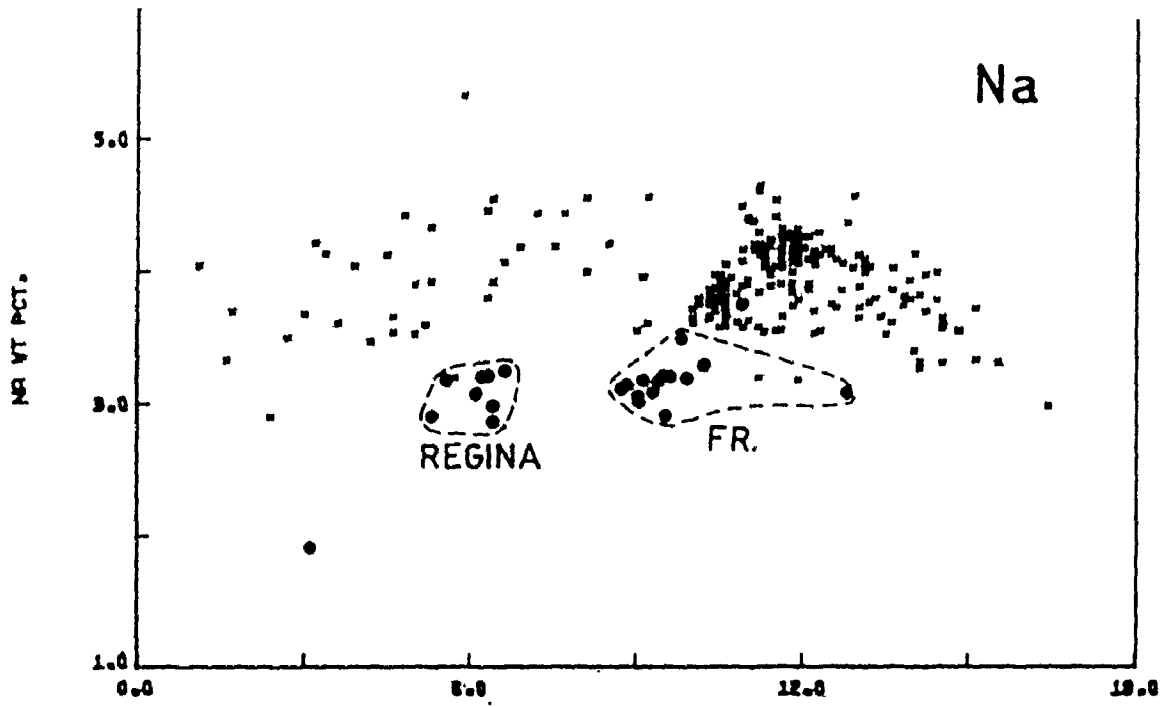
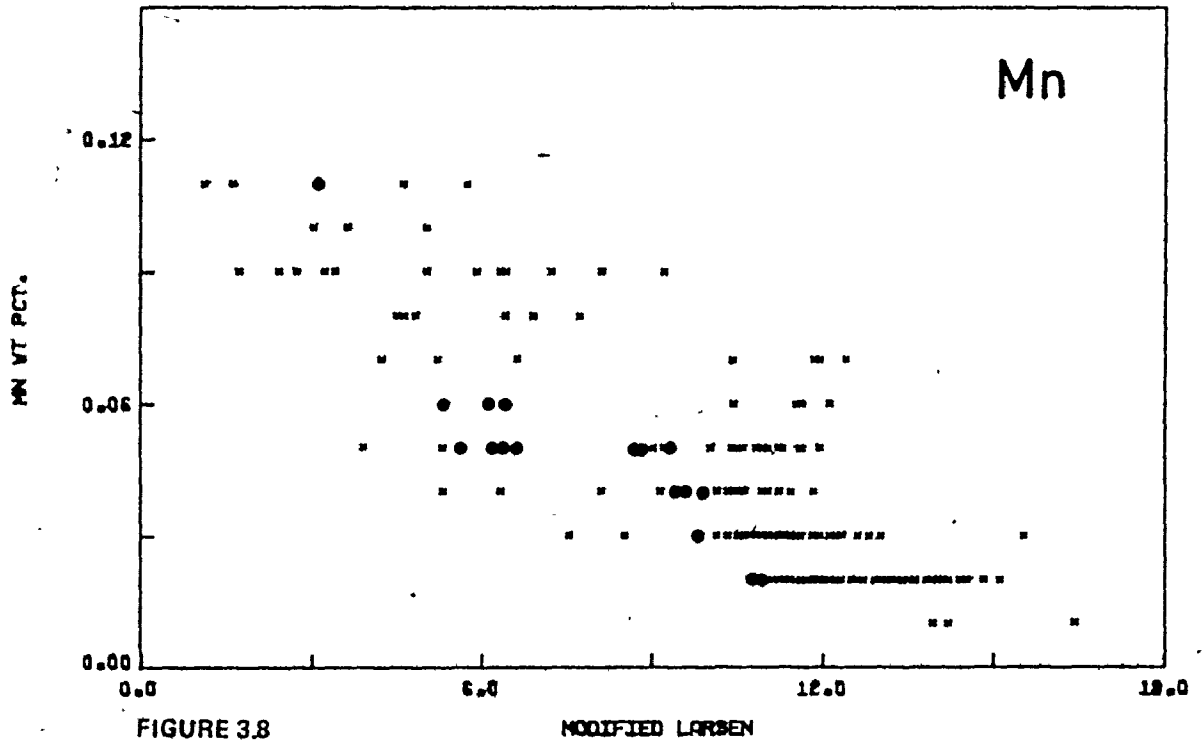
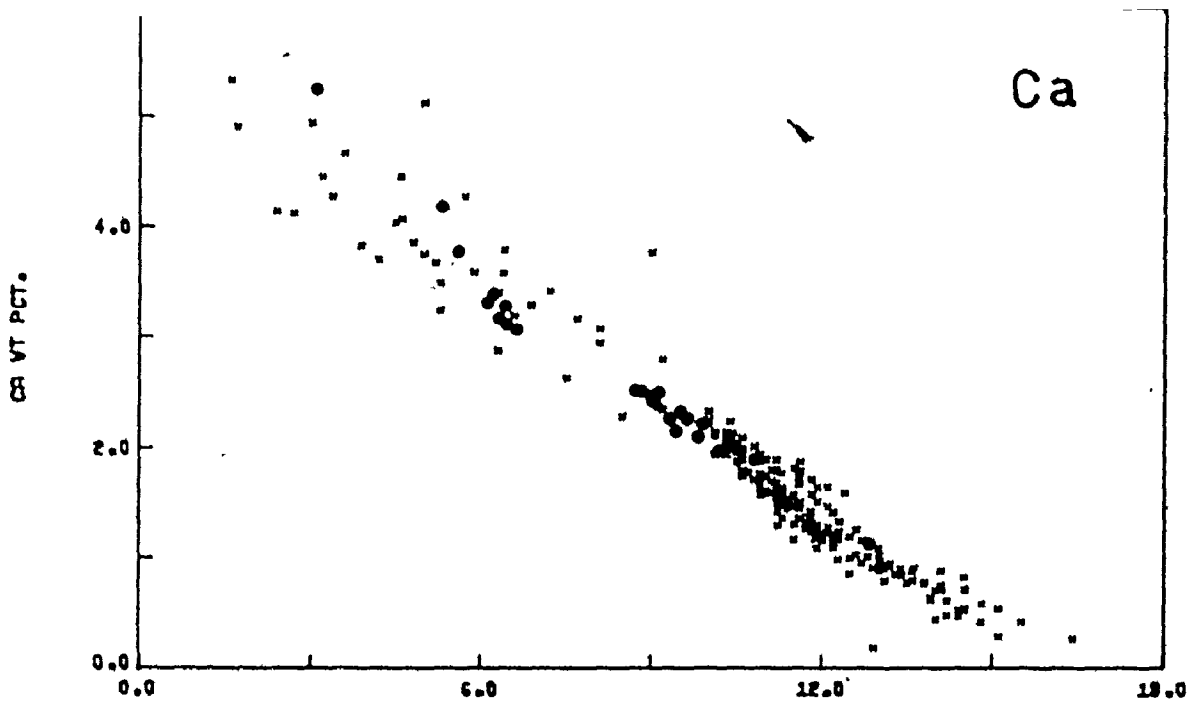


FIGURE 3.6

MODIFIED LARSEN



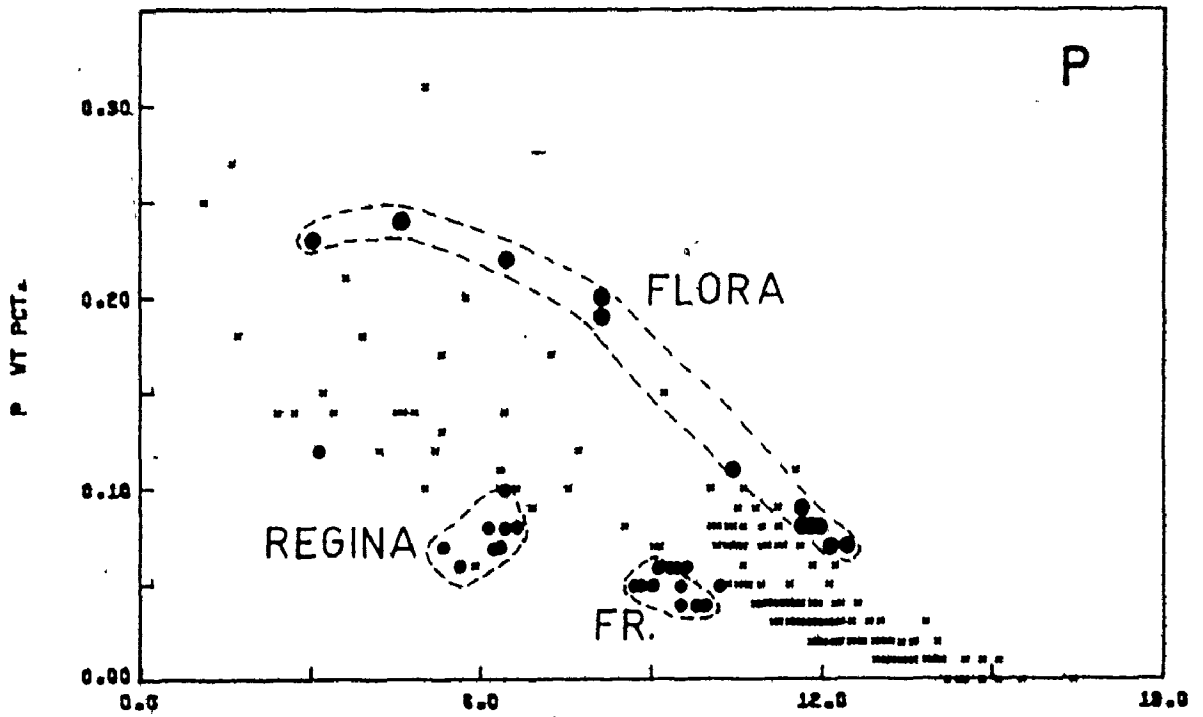
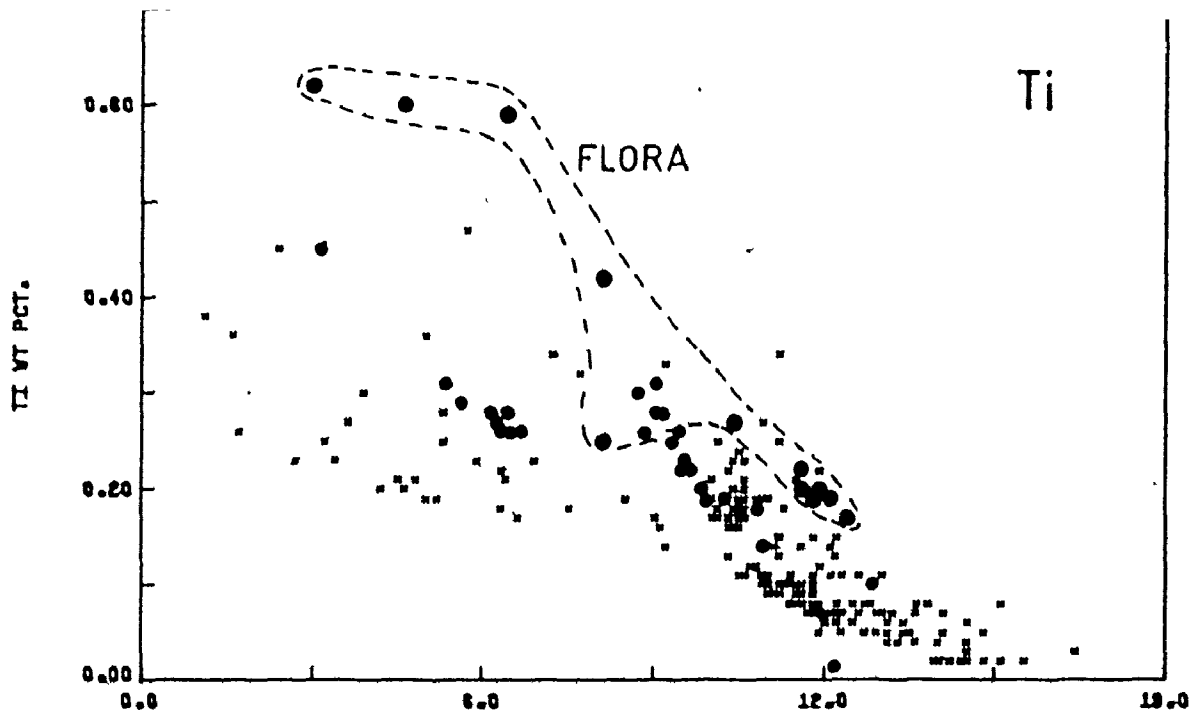


FIGURE 3.10

MODIFIED LARSEN

Regina Bay Stock	:	enriched in Si. depleted in Mg, P, Na, K.
Froghead Bay Stock	:	enriched in Si. depleted in Mg, P, Na, K.

The geochemical similarity between the Regina Bay and Froghead Bay Stocks is remarkable in view of their petrographic differences. Either these stocks are related by source region or they have suffered identical post-emplacement factors. The gold mineralization at Regina Bay suggests that Froghead Bay should also be explored for gold.

Figures 3.11 to 3.16 show trend compilations for trace elements. As for the major elements, three plutons (Flora, Regina, Froghead) carry concentrations consistently at variance with the majority of samples of equivalent index. As well, Rest Island and Esox West samples carry abnormal Ba and Sr while numerous individual outliers are also indicated.

With outliers removed, the trace element trends with increasing index include:

1. Decreasing Sr Ba and Ce for indices greater than 12.
2. Increasing Rb for indices greater than 12.
3. Slightly convex trend of Zr for entire range of indices.

These trends are admittedly vague in view of the number of outliers. No trend is apparent in the Y diagram, (Figure 3.14). Lithologies with indices below about 12 show no clear-cut correlations. Crude estimates of "averages" can therefore be made for this index range of 0 to 12 by considering the range of concentrations and visually drawing median lines to the ordinates. More sophisticated statistical derivation of "averages" is not promoted because of the lithologic variety and volumetric disparities previously

FIGURE 3.11

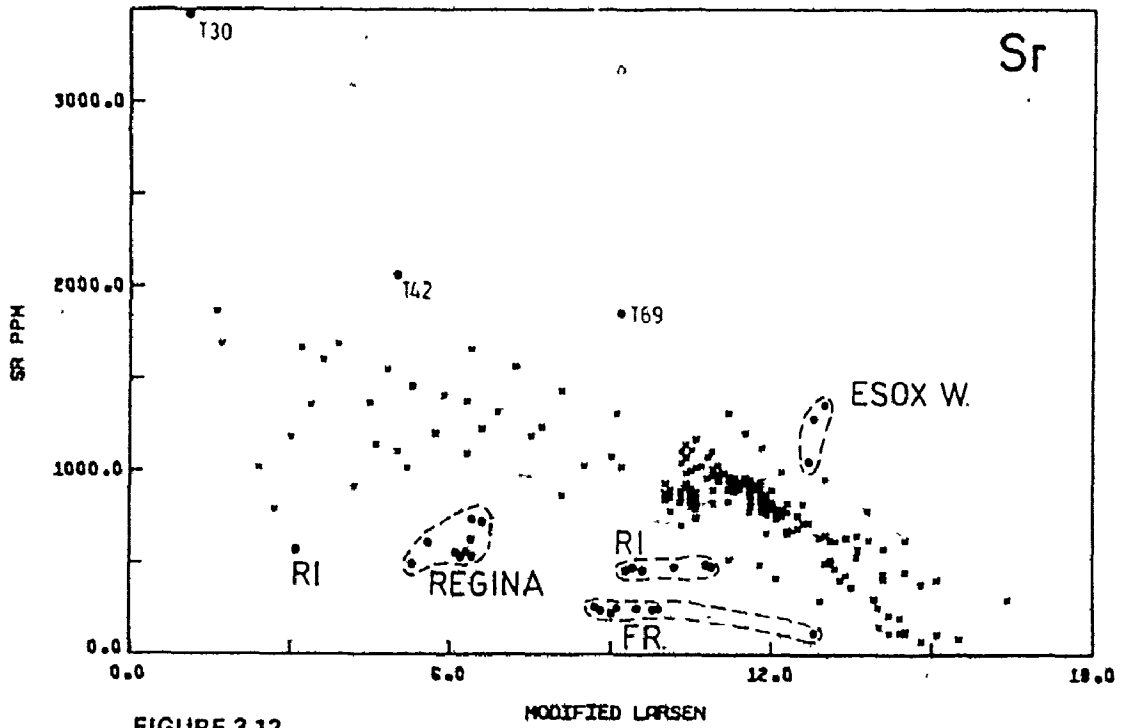
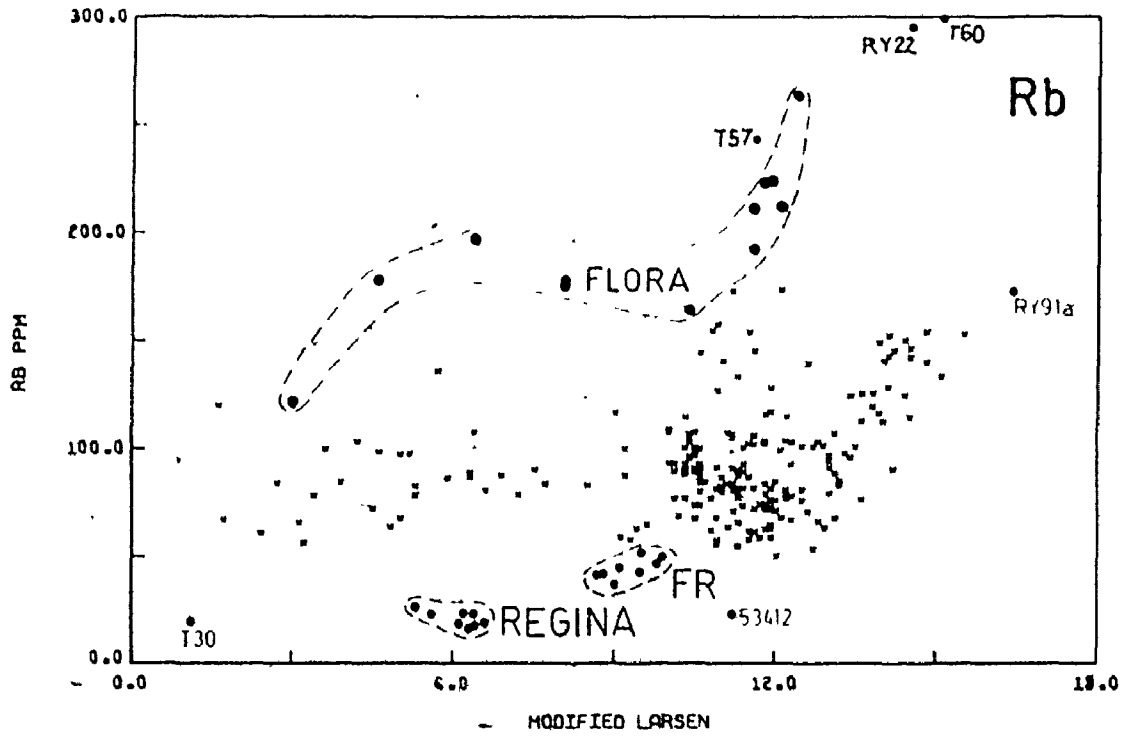


FIGURE 3.12

FIGURE 3.13

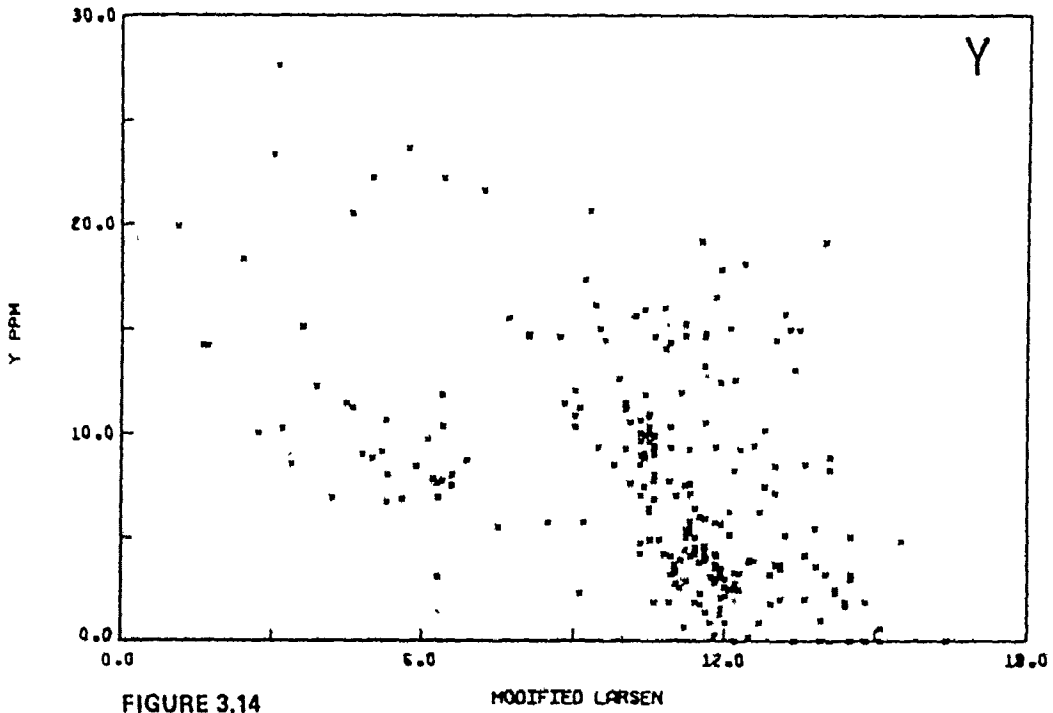
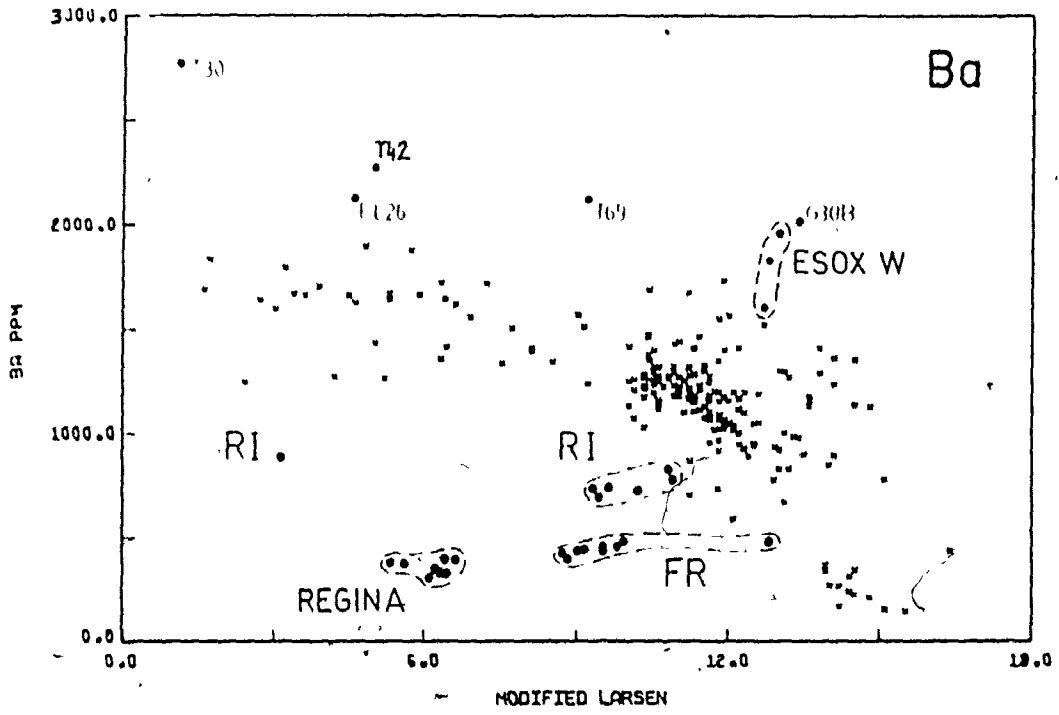


FIGURE 3.14

FIGURE 3.15

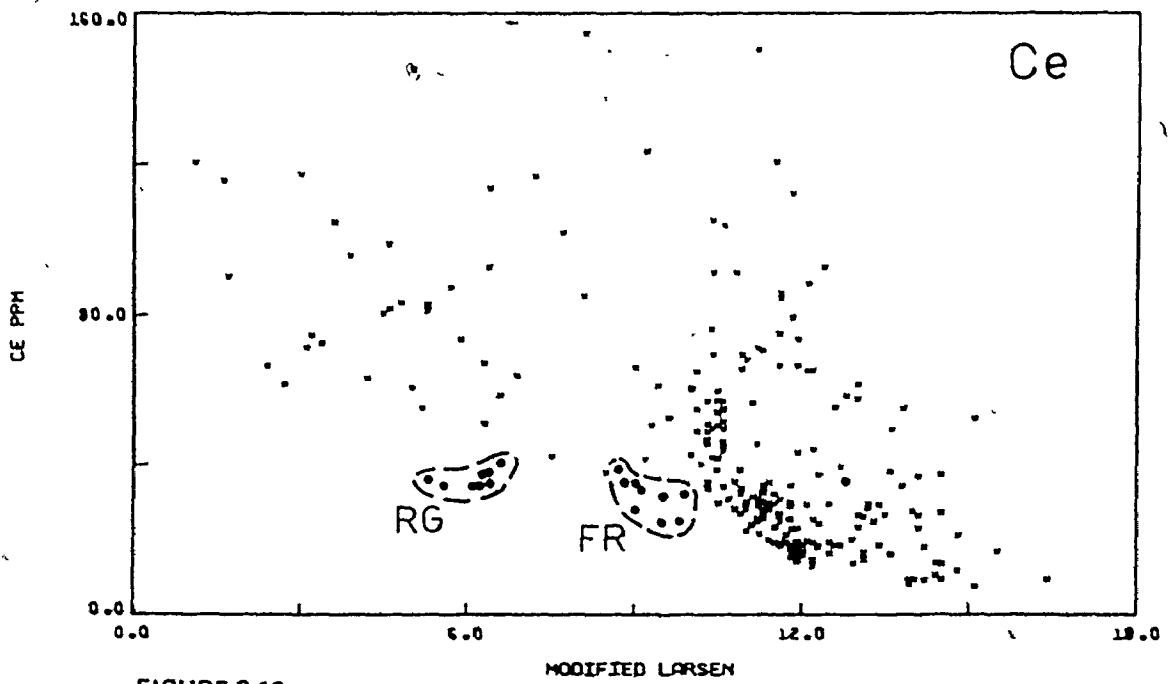
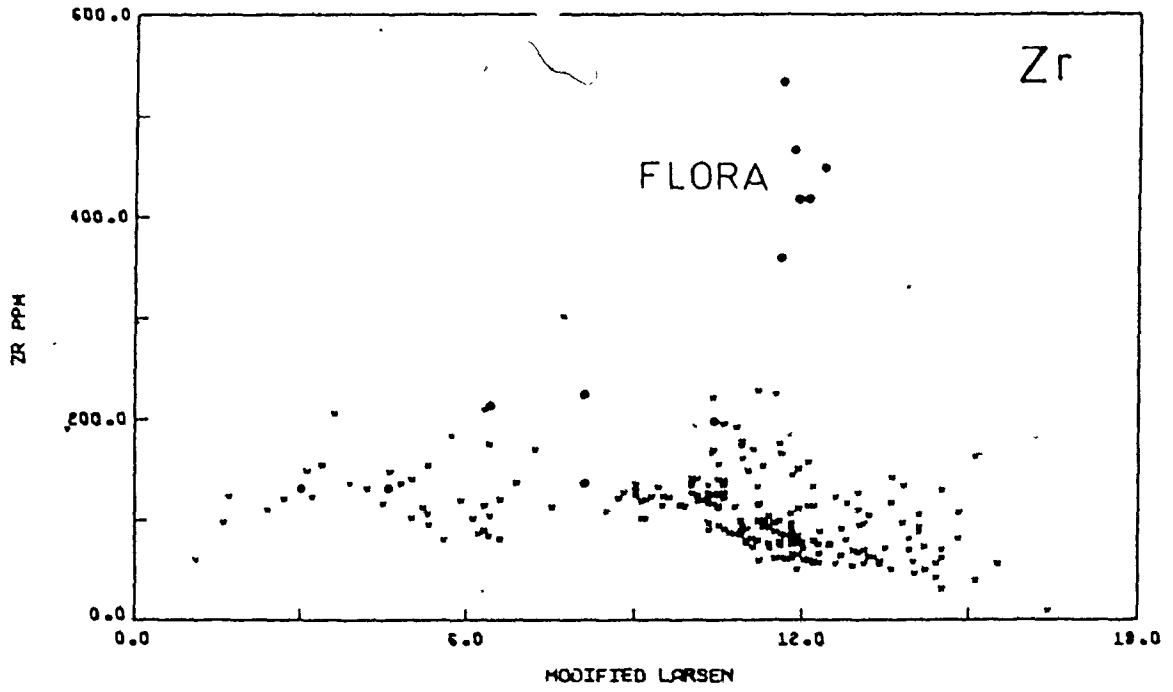


FIGURE 3.16

mentioned. The approximate trace element clarkes in Wabigoon granitoid stocks are as follows:

Rb 90 \pm 50 ppm

Sr 1200 \pm 600 ppm

Zr 150 \pm 70 ppm

Ba 1500 \pm 400 ppm

Ce 90 \pm 70 ppm

Y 15 \pm 15 ppm

Of equal interest are the compilations of element ratios shown in Figures 3.17 to 3.22. As for previous diagrams, the values for samples from Regina, Froghead, Flora and Rest Island could be considered anomalous. The Rb/Sr ratio shows the most persistent pattern; very low values up to an index of about 12 and then very rapid increase in the high index phases. Na/K ratios show a remarkable "floor" at approximately 1.0, thereby categorizing these plutons as sodic rather than potassic. The Regina Bay tonalite shows a dramatic deviation from the main cluster while interestingly, the Froghead tonalite carries Na/K ratios buried within the main cluster. Both tonalites, on the otherhand, record abnormally high Ca/Sr ratios, while on the Sr/Ba diagram the Regina and Froghead samples represent outliers of opposite nature.

With outliers removed, the main data clusters show the following correlations:

1. Negative correlation of Ti/Zr with index, especially for indices above 9.

FIGURES 3.17 TO 3.22
ELEMENT RATIOS VERSUS MODIFIED
LARSEN INDEX FR 247 GRANITOIDES
OF THE WABIGOON BELT: SYMBOLS
AS FOR FIGURES 3.1 TO 3.16
DATA FROM APPENDIX E1 TO E7

FIGURE 3.17

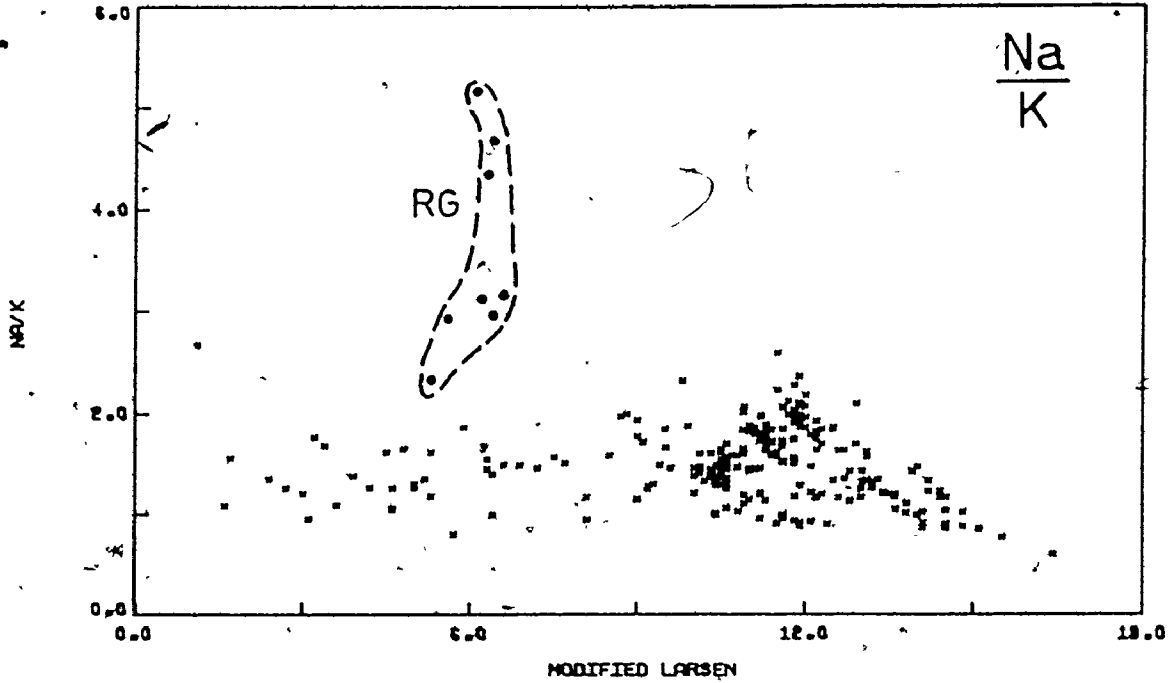


FIGURE 3.18

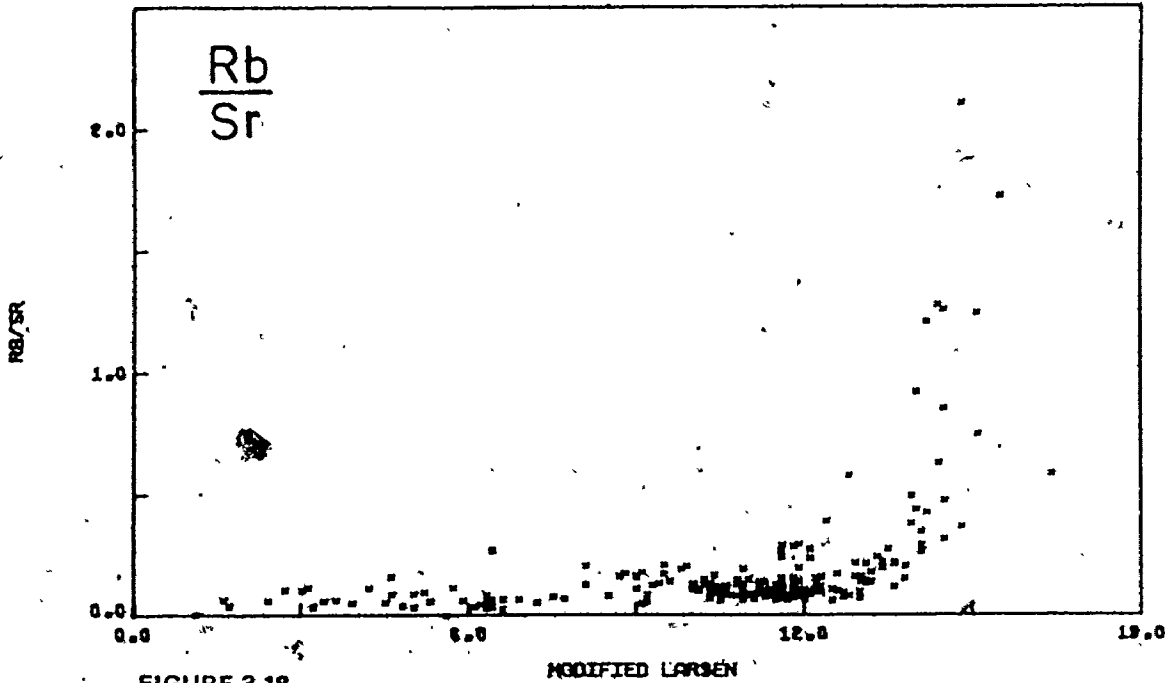


FIGURE 3.19

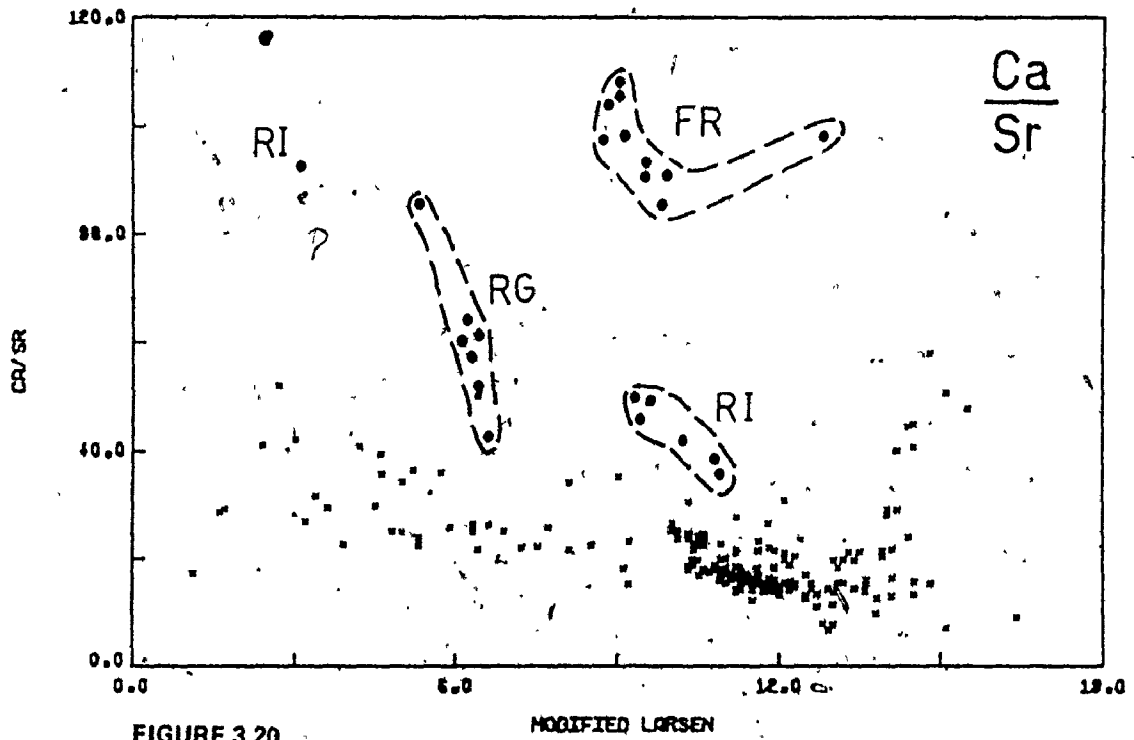
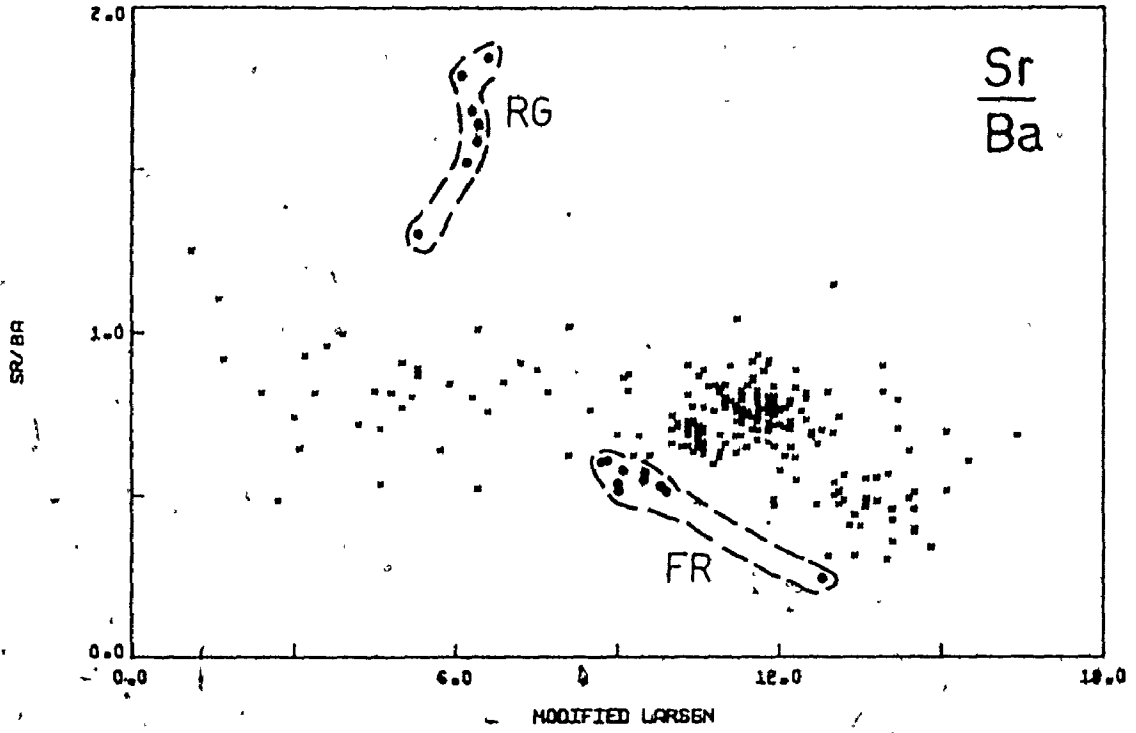


FIGURE 3.20

FIGURE 3.21

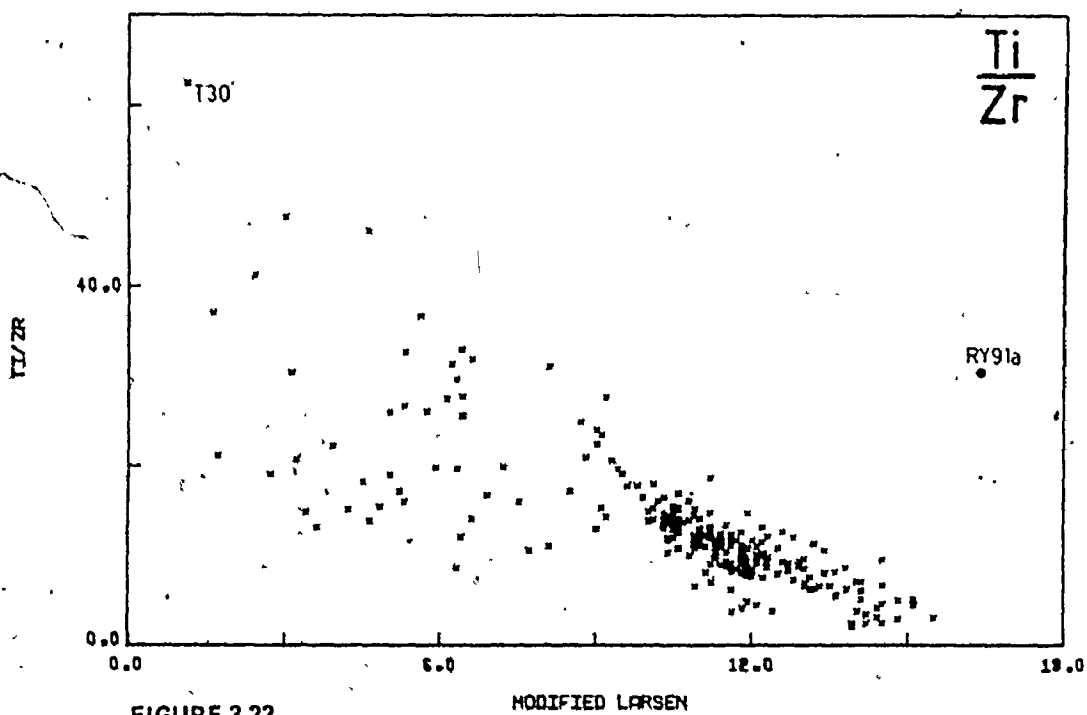
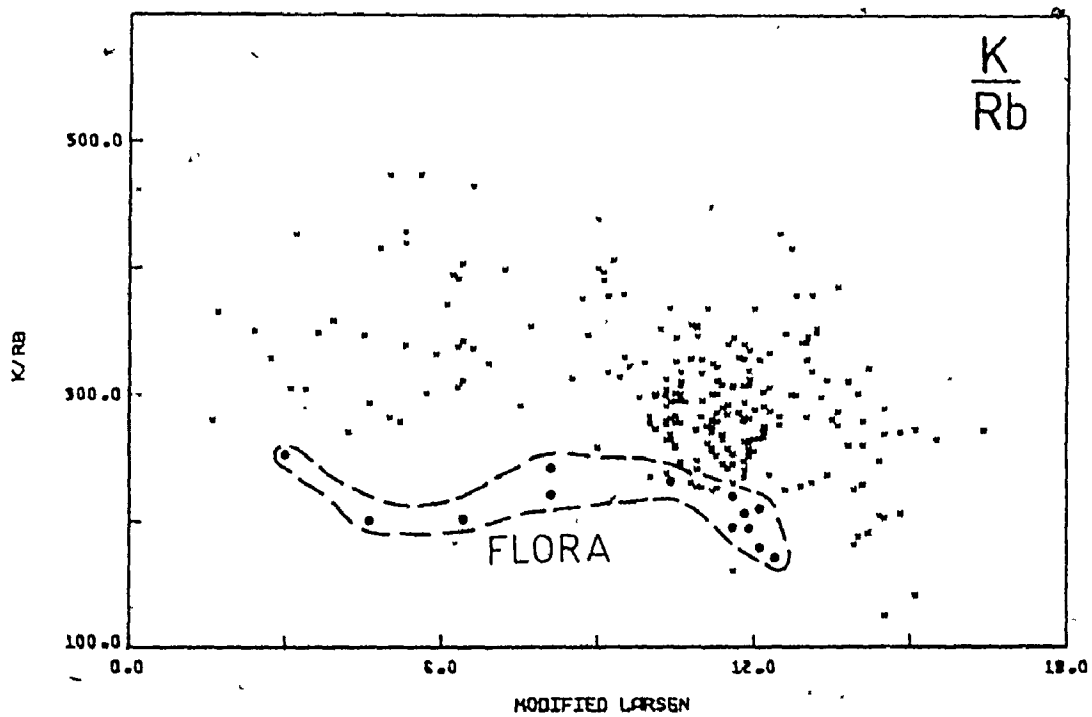


FIGURE 3.22

2. Positive correlation of Rb/Sr with index for indices above 12. This trend is vague and could also be interpreted as a bimodal distribution of values: high Rb/Sr for indices above 13; low Rb/Sr for indices 13.
3. Weak negative correlation of Ca/Sr up to index 14, then sharp increase in Ca/Sr, in some samples.

No apparent correlation is evident in the data clusters for Na/K, Sr/Ba or K/Rb. "Average" values are approximated from visualized median lines as follows:

Na/K	1.5 ± 0.6
Rb/Sr	0.1 ± 0.1 (up to index 13)
Sr/Ba	0.8 ± 0.4 (up to index 13)
Ca/Sr	30 ± 20 (up to index 13)
K/Rb	320 ± 150

No "averages" are estimated for Ti/Zr due to the strong negative correlation with index.

The K/Rb ratio has been proposed as an indicator of metamorphic grade (Lambert and Heier, 1968) or metasomatism (Shaw, 1968). The estimated "average" K/Rb for Wabigoon Belt plutons locates on the high side of Shaw's "main trend" for igneous rocks. This "average" is probably controlled by the median ratio of 300 in plagioclase (Shaw, 1968) and the modal proportions of biotite and hornblende. The relatively wide range of K/Rb may reflect the deuteric autometasomatism proposed for several stocks on the basis of field criteria (Chapter 2).

3.2 Na-K-Ca TERNARY RELATIONSHIPS: THE "MEGACRYST FIELD"

In Figure 3.23 are superimposed the major lithologic fields from previous Na-K-Ca diagrams. Almost all fields plot on the Na side of the "igneous trend" divide. The Wabigoon Belt plutons are therefore sodic granitoids although the "center of gravity" is not much displaced from the center of the Na-K-Ca plot. The two tonalitic stocks, Regina and Froghead show the greatest deviation. The greatest data density corresponds to overlapping granodiorite fields. The granodiorites and related felsites show smaller spreads but wider deviations from the trend line than the more mafic members.

Microcline megacryst bearing lithologies cluster about a point at Na:K:Ca = 45:35:20. For the following discussion this area of cluster will be designated the "megacryst field". Several mafic fields of Figure 3.23 show a high K concentration but fail to carry insets. On the otherhand, several equigranular lithologies plot within the "megacryst field". This demonstrates that other factors besides bulk chemistry must dictate textural types. It is significant that high K concentrations alone do not generate microcline megacrysts and likewise, the presence of megacrysts does not necessarily show high K.

Table 3.1 compiles lithologic types which have Na:K:Ca fields lying within the "megacryst field". Modal analyses are averaged from Appendix B or taken from published sources. Table 3.1 shows that modal microcline has no correlation with megacryst development. Rocks as rich as 29.5% modal microcline (Flora Lake monzonite) fail to

Na-K-Ca Fields
for major lithologies:
Wabigoon Plutons

microcline megacrysts:
 ——— abundant
 - - - - - incipient
 _____ absent

- | | |
|------------|----------------|
| Plutons | 6 Ottertail |
| 1 Bears | 7 Regina |
| 2 Burditt | 8 Rest |
| 3 Esox | 9 Ryckman |
| 4 Flora | 10 Taylor |
| 5 Froghead | 11 Scattergood |
| | 12 Stormy |

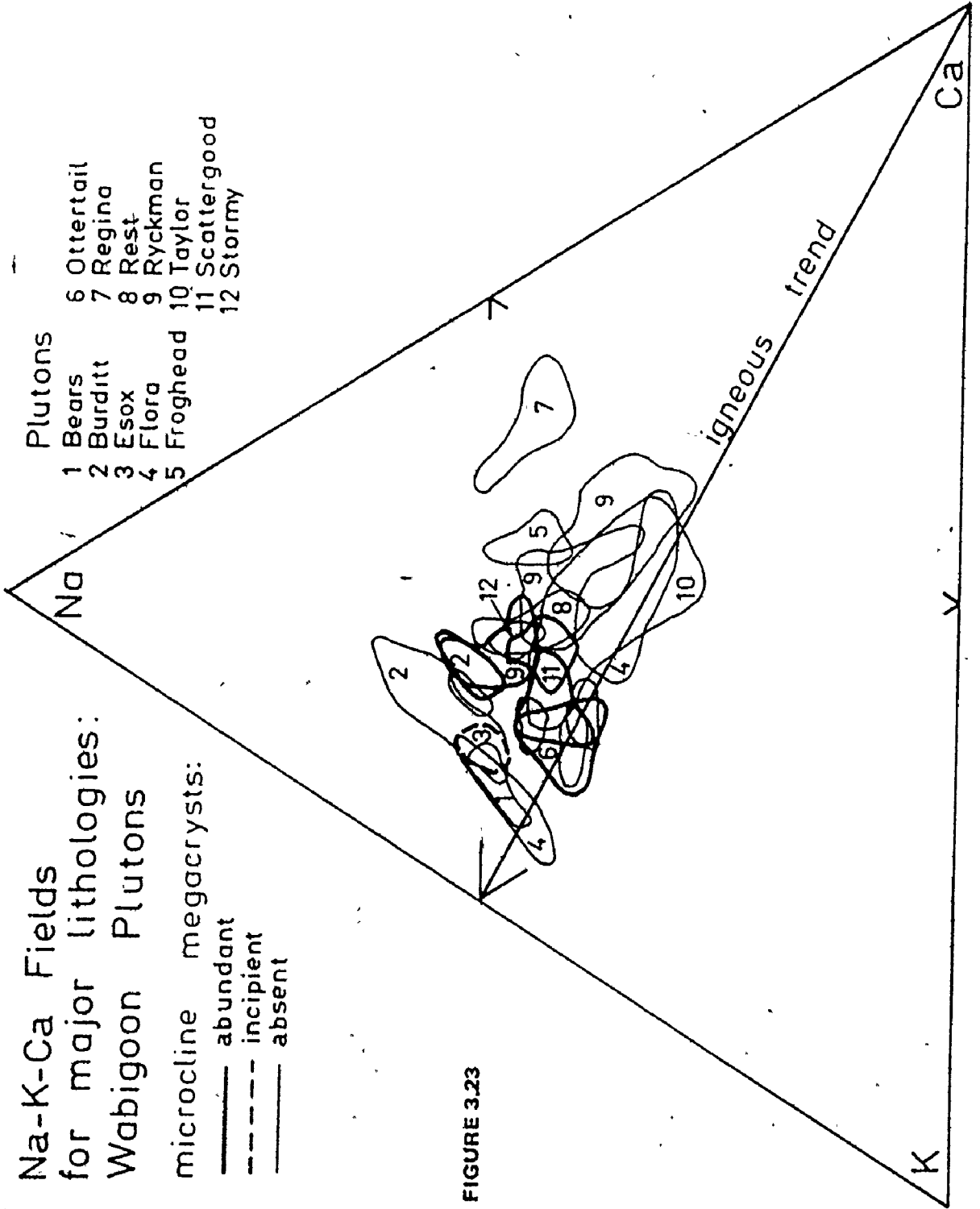


FIGURE 3.23

develop megacrysts yet some megacryst-rich rocks contain as little as 15.9% K-feldspar. Microcline megacrysts are largely confined to hornblende-rich granodiorites. Granodiorites with biotite as the dominant mafic mineral fail to develop megacrysts. The absence of hornblende correlates with an absence of microcline megacrysts.

Among the equigranular lithologies, the monzodiorite of Esos East carries high hornblende yet no megacrysts. This granitoid is also unusually mafic for the "megacryst field" which is otherwise dominated by granodiorites. This exception detracts only slightly from the strong correlation between megacryst development and hornblende content.

A brief literature search revealed that the association of microcline-perthite megacrysts with hornblende granodiorites is not universal, and can be generalized only for the plutons of this study. Whitfield et al (1959) correlated megacrysts of potassium feldspar with granitoids having high K-feldspar and lower plagioclase in the modes. They furthermore found a strong negative correlation between % modal potassium feldspar and % modal plagioclase and attributed this to magmatic differentiation. For Table 3.1 the megacryst-bearing lithologies do carry somewhat lower plagioclase but the correlation between megacrysts and modal K-feldspar can be ruled out. The correlation between K-feldspar content and modal plagioclase is likely a product of inherent correlation of variables i.e., the closed number syndrome common to linear variation trends (Chayes, 1967). This is especially likely in view of the metasomatic origin demonstrated for many occurrences of microcline-perthite megacrysts.

Peikert (1963) noted that the disappearance of potash feldspar megacrysts in foliated granitoids of northeastern Alberta did not signal any abrupt change in K-feldspar modal percentages. He attributed the growth of megacrysts in contrast to interstitial potash feldspar to relaxation of shear stresses in a regional metamorphic regime. This mechanism is not applicable to the Wabigoon plutons, first because no tectonic distinctions occur between the megacryst-bearing lithologies and the equigranular lithologies, and secondly because in Peikert's (1963) rocks, the presence of megacrysts correlate with high modal biotite.

The conditions under which megacrysts have developed in the plutons of the Wabigoon Belt can be summarized as follows:

1. Bulk chemistry of granodiorite
2. Na:K:Ca = 45:35:20 approximately
3. Conditions compatible with hornblende stability (and less compatible with biotite stability?).

The correlation of megacrysts with hornblende granodiorites may simply reflect the chronological sequence of magmatic emplacement. For several of the composite plutons, the megacryst-bearing phase was not the last intrusive pulse. Megacrystic granodiorite of Taylor Lake was intruded by a circular plug of fine-grained megacryst-free biotite granodiorite (Pichette, 1976). The Ottertail Lake stock (Figure 2.92) carries central outcrops of muscovite granite which may post-date the megacryst-bearing granodiorite. The Burditt Lake hornblende granodiorite is adjacent to megacryst-free biotite granodiorite. If the infiltration metasomatic model proposed for the Burditt Lake stock

... is universally applicable, each of the megacryst bearing lithologies may have provided quiescent semi-consolidated environments that were infiltrated by deuteritic fluids associated with chronologically younger intrusive pulses. The lack of evidence for younger units at Scattergood Lake and Ryckman Lake may be simply a function of exposure.

3.3 MAFIC ENCLAVES: XENOLITHS, AUTOLITHS AND SCHLIEREN¹

3.3.1 Introduction

The ubiquitous mafic enclaves within granitoid plutons of this region have been recognized by the first geologists (Lawson, 1887). F. F. Grout (1937) reviewed the geology of enclaves with his observations based mainly on the Ontario-Minnesota region. Mafic enclaves are significant as field mapping criteria (Chapter 2), as indicators of contamination and for their possible role as remnant oceanic crust (Viljoen and Viljoen, 1969; Glikson, 1976).

Four types of enclaves were recognized in this study: small lensoid hornblende-biotite enclaves; rare saccharoidal felsic enclaves; autoliths and mafic schlieren. Autoliths² at Flora Lake represent marginal monzodiorite fragments rafted by subsequent monzonite and granite intrusions. These monzodiorite enclaves have preserved the texture and much of the chemistry (Appendix C and D) of their plutonic source. Rare felsic enclaves likewise may be autoliths of aplitic parentage but are too scarce to sample. Mafic schlieren of biotite and hornblende are prevalent only in the more mafic phases of zoned or complex stocks such as Ryckman and Flora. Heimlich (1965) observed that schlieren are never found near enclaves and therefore have no relationship. Plate 2.1 in contrast, shows chloritic enclaves forming pseudo-slump structures with schlieren in the Ryckman Lake monzodiorite. This suggests that schlieren are enclave remnants signaling assimilation and contamination. Whether they are remnants of autoliths or xenoliths is not clear.

¹ as defined by Didier (1973)

² autolith: enclave congeneric with host rock (Didier, 1973)

The lensoid mafic enclaves on the otherhand are of questionable ancestry and play a prominent role in published models of Archean crustal evolution. Glikson and Lambert (1976) consider mafic enclaves in the diorites and granodiorites of Rice Lake, Manitoba to represent relicts of 3 b.y. old greenstones and therefore to indicate multiple greenstone cycles. Glikson (1976) however, uses ultramafic and mafic enclaves in "early Na-granites" (quartz diorites) of the Berens River and Sachigo areas of northwestern Ontario as evidence for a primitive ultramafic-mafic oceanic crust antecedent to granitoid plutonism.

3.3.2 Mafic Lensoid Enclaves:

Petrographically, these lensoid mafic enclaves are clusters of biotite and/or hornblende and/or chlorite with dimensions gradational from some tens of centimeters down to the prevailing granitoid texture. Contacts with the granitoids appear sharp in the field but prove to be gradational in thin section. Textures are varied from fine altered aggregates to "fresh" poikiloblasts to concentrically zoned mixtures of the two. One distinctive feature is the common occurrence of acicular inclusions (sillimanite?) forming crystallographic networks within the larger biotite flakes.

Field evidence suggests derivation from the supercrustals surrounding each stock (Section 2.1.2) shown by the peripheral concentrations of enclave swarms and the proximity of lensoid enclaves to feldspathized host rocks. Conversely, the enclaves are generally more mafic than either the host granitoid or possible source supercrustals.

A comparison of major element chemistry for Burditt and Scattergood enclaves (Appendix C1, C2) with surrounding metavolcanics shows the enclaves to be consistently lower in SiO_2 , Al_2O_3 , Na_2O and higher in CaO , MnO , MgO , Fe_2O_3 , TiO_2 , K_2O and P_2O_5 . Trace element chemistry is more complex (Appendix D1, D2). Enclaves show generally higher Rb, Nb, Ce, Y and lower Sr than either the host granitoids or proposed source metavolcanics. Zr is higher than host or source for Burditt enclaves but lower than host or source for Scattergood. Ba behaviour is inconsistent. Data for enclaves in the Taylor Lake or Ryckman Lake stocks (Appendix D5, D7) is too scarce for conclusions except to note abnormally low Ba in some Ryckman enclaves and unusually high Rb (299 ppm) and Ba (1584 ppm) in the single Taylor Lake enclave analysis.

The lensoid mafic enclaves have most likely undergone an extensive "reciprocal reaction process" (Didier, 1973) with the enclosing magma, involving both basification and alkali metasomatism. Field evidence for metasomatic exchange is documented in the feldspathized enclaves of Plates 1.1, 1.2, 1.3 and 1.4 and in the pyritized quartz porphyry of Plate 1.5. At Froghead Bay, megacrysts of opalescent blue quartz within lensoid enclaves match blue quartz in the tonalite. Didier (1973) reports a similar phenomenon.

Since basification, silicification and feldspathization (Figure 3.24) are opposing chemical trends, enclave chemistry reflects the chemical budget for element exchange and may no longer reflect the source rock. Abnormally high concentrations of some trace elements (Rb, Nb, Ce) may signal preferential diffusion into the enclave from

the host or may represent restite elements. The diverse enclave petrography is the pooled effect of difference in source and different physicochemical conditions leading to different mineral facies and textures (Didier, 1973).

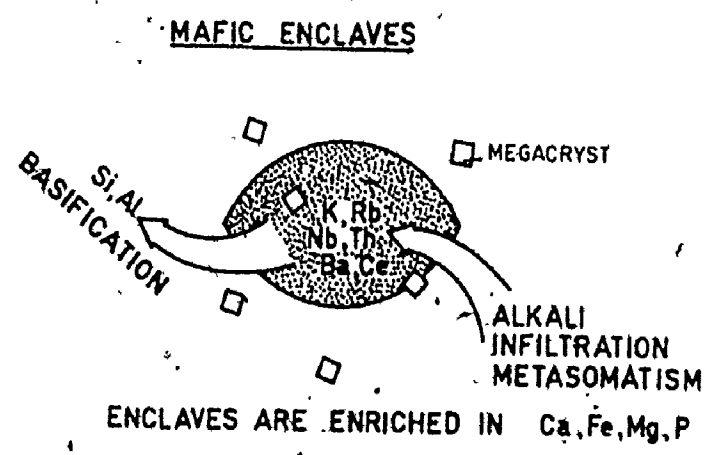
A detailed treatment of enclave chemistry was reported by De Albuquerque (1973) for granitoids of Northern Portugal. Here the enclaves are quartz-plagioclase-biotite with higher Modified Larsen indices than reported in this study. Zr and Rb are higher than either host or adjacent supercrustals. SiO_2 , K_2O , Na_2O and CaO are higher and Al_2O_3 is lower than for adjacent metasediments. De Albuquerque interprets these enclaves as restites within anatectic granitoid bodies. Such an interpretation for Wabigoon Belt enclaves is ruled out by previously discussed field evidence.

In any case, the ultramafic or mafic nature of enclaves cannot be adopted as indicative of an ultramafic or mafic source and therefore cannot be used to hypothesize an Archean oceanic crust. Appendices C1- C2 and D1-D2 give the chemistry for host (G), enclave (X) and source (T) for an intrusion breccia at Burditt and enclave (SXTN) and bordering granodiorite (SXTNG) for a hand specimen from Scattergood. In either case, the granodiorite does not differ noticeably from the average chemistry for that phase. No serious contamination is evident. These conclusions may, however, not be valid where mafic schlieren are prevalent.

Despite chemical exchange, there is no evidence for large scale contamination of the host granitoids by assimilation of enclaves. Areal distribution of mafic enclaves at Burditt and

Scattergood has not disturbed the homogeneity of the granodiorites. Neither do the Sr isotopes indicate large scale crustal contamination (Chapter 4). The chemical characteristics of the Wabigoon Belt plutons can therefore be accepted as indicative of the source material.

Figure 3.24 Proposed chemical budget between enclave and host:



3.4. AEROMAGNETIC FLUX:

3.4.1 Introduction

Previous pluton descriptions included the aeromagnetic flux as reported by the ODM (1971) geophysical map series. Table 3.2 compares previous quoted gamma values, corresponding surface lithologies and average iron content of surface samples (from Appendix C). Comparative magnetization over adjacent supercrustals or batholithic granitoids is also included.

Homogeneous plutons show a positive correlation of surface iron with the aeromagnetic flux. This demonstrates the causality of surface lithology and magnetization which in turn explains the concordance of magnetic contours and stock boundaries. Of the homogeneous stocks, the Scattergood body shows an unusually high magnetic flux in relation to iron content and compared to adjacent batholithic granitoids. Metavolcanics are generally more magnetized than the homogeneous stocks whereas batholithic granitoids carry both stronger and weaker patterns.

The Esos Lake hypabyssal porphyry is characterized by a relatively low flux in comparison to average iron content. This may be a cut effect since pink felsite carries only 1.03% Fe_2O_3 and may be proportionally more significant at depth relative to the iron-rich grey felsite.

The cores of composite plutons carry relatively shallow magnetic gradients similar to the homogeneous bodies and in contrast to sharper gradients over marginal phases. For most of the zoned stocks, the marginal mafic phases have dimensions smaller than the

Table 3.2
Aeromagnetic Flux (unfiltered) Over Lithologic Units and its Correlation With Total Iron Content
of Surface Samples.

Stock	Phase	Magnetic Flux (In Gammas)	% Fe ₂ O ₃ *#	Magnetic Flux of Adjacent Rocks (Flux in Gammas) (Lithology)
<u>Homogeneous Plutons:</u>				
Bears Passage Burditt	Granodiorite	<60,300	0.80 (6)	60,400 - 62,500 Metavolcanics
	Granodiorite	60,310 - 60,360	1.36 (64)	>60,500 Metavolcanics 60,500 Granitoids
Essex West	Quartz	<60,400	1.38 (3)	
	Monzodiorite			
Scattergood Froghead Bay	Granodiorite	60,500 - 60,800	2.74 (25)	60,320 - 60,400 Granitoids
	Tonalite	60,510 - 60,560	3.90 (9)	>60,700 Felsic Volcanics <60,600 Osbourne Granitoids <60,500 Meridian Granitoids 60,440 - 60,700 Aulneau Granitoids
Regina Bay	Tonalite	60,650 - 60,780	4.67 (7)	
<u>Zoned Plutons:</u>				
Flora	Granite Core	60,830 - 60,940	0.98 (8)	60,360 - 60,620 Atikwa Granitoids
	Mafic Rim	60,800 - 61,800	5.01 (12)	
Taylor	Fine			
	Granodiorite	60,460 - 60,600	1.36 (2)	60,320 - 60,400 Granitoids
Essex East	Granodiorite	60,600	2.49 (6)	60,320 - 60,400 Granitoids
	Mafic Rim	61,000 - 62,000	4.79 (9)	60,320 - 60,400 Granitoids
Ottertail	Core & Rim	60,400 - 60,620	1.79 (7)	
	Core & Rim	60,400 - 60,620	3.27 (5)	60,400 - 62,500 Metavolcanics & Metasediments
Ryckman	Granodiorite	60,500	2.24 (17)	60,500 - 62,500 Metavolcanics
	Mafic Rim	60,500 - 60,900	5.43 (23)	60,400 - 62,500 Metavolcanics & Metasediments
Rest Island	Core	<60,300	2.81 (5)	
	Granodiorite	60,400	9.12 (1)	
<u>Hypabyssal Plutons:</u>				
Essex Porphyry pink & grey felsite		60,290 - 60,400	2.09 (4)	

* Total iron expressed as Fe₂O₃ in analysed surface samples of stock phases.
Number of samples analysed and averaged (from Appendix C).

resolution of the aeromagnetic maps, therefore an unambiguous match of surface lithology with characteristic magnetization is not expected. Likewise the correlation of gamma flux with iron content is not consistent. The granite core of Flora is the most highly magnetized felsic granitoid in this study despite low iron content. This unusually high flux may signal a mafic root contribution or may mean that Flora is located on a regional high of deep-seated origin.

3.4.2 Discussion

Hall (1968) defined regional magnetic anomalies and magnetic units over the western half of the study area by filtering out short wavelength anomalies (<5 mi.) from the aeromagnetic maps of the Geological Survey of Canada. Regional magnetic anomalies correlate with granitoid-greenstone lithology with lows centered over greenstone belts and magnetic highs located over granitoid batholithic complexes. McGrath and Hall (1969) expanded this study using a 12 km wavelength cut-off and contoured an area including the eastern half of figure 1.1 of this study. Their work recognized regional lows over the English River Gneiss Belt and confirmed the anomalous lows over greenstone belts and highs over granitoid batholiths. This contrasts with findings of Krutikhovskaya et al (1973), that most granitoids within Precambrian shields are either non-magnetic or weakly magnetic.

Comparisons of regional magnetic patterns with seismic sounding suggested to Hall (op.cit) that the principal magnetization causing regional patterns lies below a few kilometers in depth and extends downwards to the Intermediate Discontinuity (at 16 km). Krutikhovskaya et al (1973) likewise concluded that long-wavelength

components of the magnetic field cannot be explained by the effect of the near-surface geological bodies. Conversely, local magnetic anomalies of the shields are readily explained in terms of geological structures of the upper crust at less than 10 km depth. The magnetic patterns over granitoid stocks of this study therefore contribute to the residual anomaly map (Hall, 1968, Figure No. 8) but not to the regional anomaly map (Hall, op.cit., Figure No. 1).

Hall's (1968) conclusion that granitoids are more magnetic than greenstones is not apparent when unfiltered short-wavelength anomalies are considered. The magnetic flux over stocks at Burditt Lake, Bears Passage, Froghead Bay, Ottertail Lake and Rest Island in each case is less than the prevailing magnetic field over adjacent metavolcanics (Table 3.2). On the otherhand, small stocks carrying intensities greater than adjacent batholithic granitoids include Scattergood, Froghead, Regina, Flora and Taylor. For upper crust sources the magnetic flux appears greater over metavolcanics than over granitoids. This distinction disappears with the most mafic border phases of composite stocks.

The local magnetic anomalies over the small stocks of this study represent fields due to geological structures of the upper crust, down to a few kilometers in depth. In most cases, anomaly contours are concentric to the mapped borders of the plutons and are largely contained within these lithologic borders. This leads to the conclusion that the present surficial exposures are representative of the total dimensions of the plutons. The stocks do not substantially widen at depth. The distinctive character of the magnetic profiles compared to adjacent granitoid batholithic complexes suggests that the

stocks are not subsurface apophyses of these batholithic areas.

Further work needs to be done to explain the magnetic flux over the batholithic areas and to reconcile this flux with the multiphase lithology.

CHAPTER 4

CHRONOLOGY OF GRANITOID PLUTONISM

4.1 NON-RADIOMETRIC CHRONOMETRY: PREVIOUS WORK

4.1.1 Stratigraphy

Lawson's (1913) Algoman-Laurentian granitoid classification was essentially stratigraphic, dependant on intrusive relationships with the Seine conglomerate. Correlation of the Seine series with the Ogishke conglomerate and the Knife Lake slates expanded the Algoman-Laurentian terminology to the Vermilion District in Minnesota. Attempts at correlation with other sediments led to the use of Lawson's terms over the entire Superior Province. Since Archean metasediments are commonly bordered by metavolcanics and fault contacts, such correlation is usually difficult even within a single depositional basin (McGlynn, 1970; Goodwin et al., 1972). As a consequence recent detailed mapping has based chronological classification of granitoids on intrusive relationships to all supracrustals rather than correlation with any particular stratigraphic horizon.

Modern emphasis is on tectonic position, or level of intrusion, resulting in three-fold subdivisions:

synkinematic, late-kinematic, post-kinematic (Blackburn, 1976);
syntectonic, late-tectonic, post-tectonic (Morey and Sims, 1976);
catazonal, mesozonal, epizonal (Ayres and Ermanovics, 1972).

In discussing the tectonic grouping of granitoids, Marmo (1971) writes:

"...tectonic classification has been adopted in very many countries, including Brazil, India, and some African countries The groups established on a tectonic basis have, however, distinct petrological and mineralogical characteristics. These are so obvious that one may comparatively safely construct a petrological classification of granites which runs parallel to e.g. Eskola's syn-, late-, and post-kinematic granites." (p-30)

Recent mapping, over complex batholithic granitoid terrain in Northwest Ontario, lends support to correlation of tectonics and the nature of granitoids. Sage et al. (1975) subdivided the Irene-Eltrut Lakes granitoid complex (south-east quadrant of this study region) into two contrasting suites:

- (1) highly foliated trondhjemite-granodiorite containing:
- (2) "younger" massive, homogeneous or concentrically zoned granodiorite ± syenodiorite plutons.

The western edge of the Rainy Lake Batholithic Complex ("Stanjikoming Laurentian area" of Lawson, 1888; "Manitou Dome" of Goodwin, 1965) was mapped by Blackburn (1976) and

Longstaffe et al. (1977) with the following subdivisions:

(1) Early Syntectonic Plutonic Rocks -

Jackfish Lake Complex - foliated granodiorite +
syenodiorite;

Northwest Bay Complex - foliated trondhjemites,
monzogranites;

Footprint Lake Gneiss - gneisses + migmatites.

(2) Late-tectonic massive granitic stocks, internal to the
greenstones.

Such a tectonic field classification implies a hiatus of unknown duration between the "syntectonic" complexes and the "post or late" tectonic plutons, although in the Superior Province this has never been radiometrically tested. The belief in a significant chronologic break between the batholithic complexes and the "high level late-tectonic" plugs is implicit in several popular models of Archean crustal evolution (Anhaeusser et al., 1969; Sutton, 1973; Glikson and Lambert, 1976).

Other investigators recognize the multi-phase nature of the batholithic terrain but do not support the two-fold tectonic classification and the inherent hiatus concept. The Aulneau Batholith to the west of our study area, covers 1,250 sq. km. and has been subdivided into eleven lithologic phases, yet marginal foliation and its elliptical shape suggest

to Wilson et al. (1974) that a single emplacement event is responsible. In a similar investigation far to the north of the thesis area, Ayres (1974) mapped 20 discrete intrusive phases to the North Trout Lake Batholith but postulated a series of magmatic pulses over a short time span. Even several of the high-level late-tectonic stocks are composite intrusives with cross-cutting relationships between the various lithologies. An important consideration is whether the time span of multiple intrusion is significantly different from the hiatus suggested by a syntectonic : late-tectonic categorization. Ayres and Ermanovics (1972) embraced both concepts of contemporaneity and temporal break when they summarized their observations:

"Intrusive activity reached a peak during the Kenoran Orogeny when the batholithic complexes and many of the smaller plutons were emplaced, but intrusion continued well into post-kinematic time with emplacement of late stocks, dykes and sheets in both batholithic complexes and supracrustal sequences. Some of the latest intrusions may be post-Archean." (p.578)

4.1.2 Petrography

Grout (1929) attempted to find petrographic criteria to compliment Lawson's Laurentian-Algoman granitoid sequence. After investigating several plutons along the Minnesota-Ontario border with respect to nature of enclaves; microcline

distribution; alkalinity; degree of metamorphism or foliation; contact effects; composition range; petrographic uniformity and alkali ratios, he was left with this conclusion:

"Even in the few batholiths whose ages have been determined, the petrographic variation is so great that it is hard to find any feature not represented in masses of very different ages ... there is more variation in a single batholith than between the main mass of Laurentian and the main mass of Algomian."

Tyler, Marsden, Grout and Thiel (1940) carried out a comprehensive study of heavy minerals and their ratios in meta-sediments and plutonic masses of the Lake Superior region with the view of correlating masses of the same age or distinguishing those of different ages. Zircons provide the best criteria:

"... there is in several districts a relation between distinguishable types of zircon and the geologic ages of the granite masses. The hyacinth variety of zircon [pink to brown-purple, pleochroic, zones, prismatic, indices of refraction: 1.900-1.945] ... can be found in nearly every sample of known early pre-Huronian granite in Michigan and Wisconsin, and nearly every known pre-Animikie granite in Minnesota. On the south side of Lake Superior some late pre-Huronian granites and some Huronian granites show a dominance of malacon [cloudy, altered, etched, indices: 1.795-1.850] over other zircons, and Keweenaw rocks all around the west end of the lake show a dominance of

simple forms, the "normal" zircon [euhedral, clear colourless to pale yellow, strong birefringence, indices: 1.915-1.955]." (p.1522)

On the other hand, they were not able to distinguish on the basis of zircons between Algonian and Laurentian masses. Both the Giants Range Granite ("Algonian") and the Saganaga Batholith ("Laurentian") are dominated by hyacinth zircons. None of the granitoids sampled between Morton, Ortonville and Rainy Lake carried zircons of the "normal" type. "Normal" zircons may therefore distinguish post-Archean granitoids from hyacinth bearing Archean granitoids.

4.2 ISOTOPIC GEOCHRONOLOGY: PREVIOUS WORK

4.2.1 Introduction: Superior Province

Compilations of radiometric geochronology in the Superior Province have been presented by Goldich (1968), Burwash (1969) and Stockwell (1970). On the basis of a histogram plot of biotite and muscovite K-Ar ages, Stockwell (1970) defined a major orogeny centered at 2,480 m.y. This "Kenoran Orogeny" spans various phases of vulcanism, sedimentation, granitoid intrusion and basic intrusion previously referred to respectively as the Keewatin, Temiskaming (or Seine), Algonian and Haileyburian events. When limitations to mineral dates became better known, Stockwell (1972)

relocated the Kenoran Orogeny at 2,690 m.y. based on the mean of Rb/Sr whole-rock isochron dates ($\lambda_{\beta} = 1.39 \times 10^{-11} \text{y}^{-1}$). For the Minnesota region, Goldich (1968) defined an equivalent plutonic event: the Algoman Orogeny spanning 2,400-2,750 m.y. but based his considerations on the concordance of dates by several isotopic methods. Goldich (1968) proposed four other plutonic orogenies for the region: Keweenawan (1,000-1,200 m.y.); Penokeyan (1,600-1,900 m.y.); Laurentian (?) and an event (3,300-3,550 m.y.) accounting for gneisses in the Minnesota River Valley.

A synopsis of isotopic ages for granitoids of the Superior Province was presented by Ayres and Ermanovics (1972). After considering more than one hundred published isotopic ages, they concluded:

"There is as yet no recognizable pattern to the distribution of age dates ... most of the granitic plutons were probably emplaced between 2,700 and 2,550 m.y. In most areas where both supracrustal sequences and synkinematic plutons have been dated by similar methods, there are only slight age differences between volcanism, sedimentation and granite emplacement ..." (p.578)

4.2.2 Wabigoon Belt Chronology

Compilation

Previous radiometric dating in Northwestern Ontario has been largely confined to samples collected along the major roads: Highways 11, 17, 71 and Red Lake Road 105. This is evident from Figure 4.1 which compiles essentially all published geochronology for the region intruded by the granitoids of this study.

Missing from this compilation are lead-alpha dates of Pollock (1960) because the technique used has been discredited (Goldich, 1968). Also omitted are published ages that have been subsequently refined or discredited. The data of Hart and Davis (1969) for example, for the Rainy Lake area have been largely revised and augmented by Peterman et al. (1972). A few published dates (by Wasserburg et al., 1956, Peterman et al., 1972; Heimlich, 1963) have been recalculated by the author to standardize the compilation with respect to half-lives and regression models. Included in the compilation map are Rb/Sr whole-rock isochrons from this study which will be discussed in subsequent chapters.

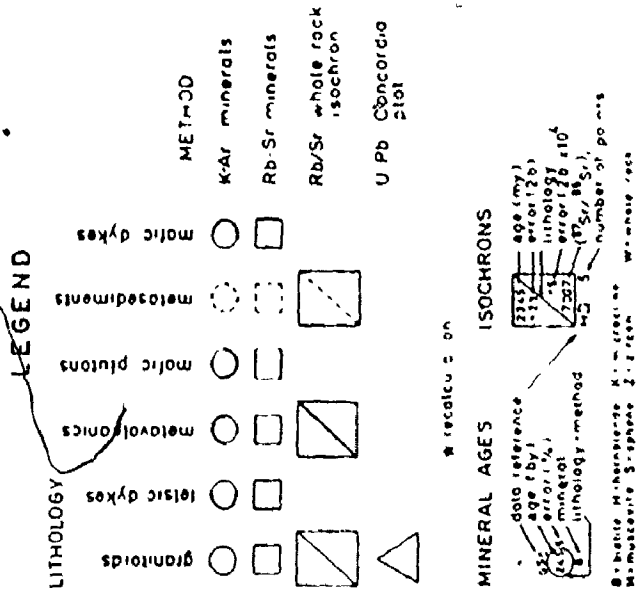
Mineral Dates: Cautionary Note

Most of the mineral dates available for this region were obtained by the total degassing K-Ar method with analytical uncertainties estimated at $\pm 5\%$. Apparent ages from minerals are now considered to record time of cooling to a thermal

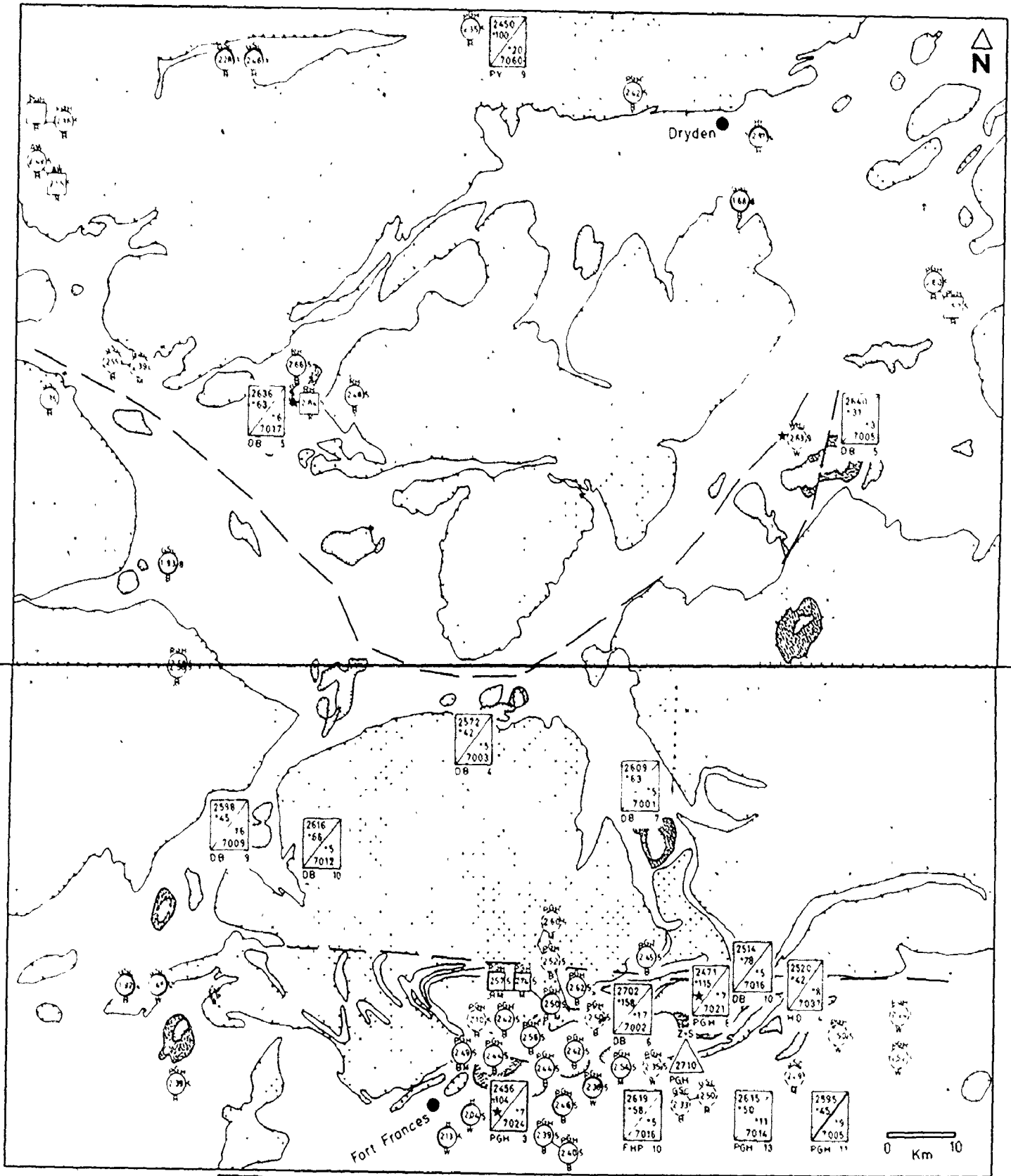
Figure 4.1

Wabigoon Belt Chronology

Map Symbol	Data Reference
AW	Aldrich and Wetherill (1960)
DB	Birk (this study)
FHP	Fairbairn, Hurley and Pinson (1967)
GSC	Geological Survey of Canada (for reference listing see: Wanless, Stevens, Lanchance and Delabio, 1974)
H	Hanson (1968)
Ht	Hart (1961)
HD	Hart and Davis (1969)
RH	Heimlich (1963)
PGH	Peterman, Goldich, Hedge and Yardley (1972)
PY	Purdy and York (1966)
WHJ	Wasserburg, Hayden and Jensen (1956)



WABIGOON BELT CHRONOLOGY



GRANITOIDS undifferentiated felsic mafic porphyry

D Birk 77

threshold below which radiogenic daughters are effectively locked into the mineral lattice. As such the spread in mineral "ages" may reflect various blocking temperatures for different minerals or the mix products of metamorphic overprint. Comparative studies of apparent ages of coexisting minerals suggests a sequence:

Rb/Sr(K-feldspar) > K/Ar(hornblende) > Rb/Sr(muscovite) >
Rb/Sr(biotite) \geq K/Ar(biotite) > K/Ar(K-feldspar) (Moorbath, 1967).

The highest apparent age for an assemblage of coexisting minerals has generally been interpreted as dating the minimum age of metamorphism or crystallization. On the other hand, unacceptably high K-Ar apparent ages have been reported especially from the lowest potassium minerals such as pyroxene (Roddick and Farra, 1971). This leads to considerations of extraneous radiogenic argon. Hayatsu (1972) suggests the possibility that primordial Ar^{36} still resides in the earth and that a variable $(^{40}Ar/^{36}Ar)_i$ must be accounted for. Therefore a multi-sample isochron plot such as $^{40}Ar/^{36}Ar$ versus $^{40}K/^{36}Ar$ yields a better age estimate than any single K-Ar mineral date. Hayatsu and Palmer (1975) concluded from K-Ar studies in the Grenville Province that:

"... even in Precambrian samples, where initial argon contribution might be expected to be negligible, it is in fact not negligible and the isochron method must be applied."

Only one K-Ar isochron plot is available for Northwestern Ontario: a $2,706 \pm 23$ m.y. slope for the Poohbah Lake alkaline complex intrusive into Coutchiching metasediments of the Quetico Belt (Mitchell, 1976). The mineral apparent ages of Figure 4.1 must therefore be treated as of reconnaissance value only.

Metasediments

On Figure 4.1, the oldest K-Ar dates for metasedimentary units are:

Sioux Narrows	- biotite:	2.55 b.y. $\pm 5\%$
Manitou	- total rock:	2.63
Rainy Lake	- muscovite:	2.60
Bad Vermilion Lake	- total rock:	2.52

These mineral dates do not discriminate between the Coutchiching ~~sediments which~~ Lawson (1913) mapped underlying the Keewatin and the Seine Series that overlie the Keewatin. These dates are compatible with a Rb/Sr isochron of pooled Northwestern Ontario metasediments reported by Fairbairn et al. (1967) as $2,617 \pm 58$ m.y. This isochron in turn agrees with a $2,615 \pm 50$ m.y. Rb/Sr isochron for Coutchiching metasediments (Peterman et al., 1972).

The significance of metasedimentary isochrons is questionable (Goldich, 1972). Fairbairn et al. (1967) argued

that the low initial $^{87}\text{Sr}/^{86}\text{Sr}$ ratio on their plot signifies isotopic equilibration between sediment and sea water and therefore the apparent age reflects time of deposition. Alternatively the isochron could reflect the age of provenance or post-depositional metasomatism. Spears (1974) found that Carboniferous shales show reduction in $^{87}\text{Sr}/^{86}\text{Sr}$ relative to $^{87}\text{Rb}/^{86}\text{Sr}$ compared to source granitoids and credits this to weathering reactions producing clay minerals. The effect of weathering is equivalent to incomplete homogenization between detrital sediment and sea water. Isochron plots may represent mixing lines between resistate (muscovite) and hydrolyzate (clay) fractions of the sediment.

Metavolcanics

Only four mineral dates are available from metavolcanic suites within our compilation map area, and of these a 2.46 b.y. hornblende from Highway 17 carries the oldest date. A more convincing estimate of timing of Keewatin volcanism is given by a Rb/Sr pooled isochron age of $2,595 \pm 45$ m.y. from the Rainy Lake region (Peterman et al., 1972). This pooled isochron carries points of diverse lithology - including an anorthosite at Bad Vermilion Lake that clearly intrudes Keewatin metabasalts.

Mafic Flows, Sills and Dykes

A gabbro sill at Kakagi Lake has yielded a biotite K-Ar age of 1.93 b.y. while a gabbro-harzburgite intrusion at Wabigoon Lake gives biotite K-Ar ages of 1.68 b.y. (Figure 4.1). These dates are among the lowest encountered in the map region and indicate either an analytical problem or they indicate that some mafic plutons are post-Archean. Diabase dykes west of Fort Frances give biotite K-Ar and whole rock K-Ar dates of 1.92 b.y. and 1.46 b.y., respectively. These dates are somewhat older than the 1.22 b.y. (biotite, whole rock K-Ar) reported by Fahrig and Wanless (1963) for the north-west trending diabase dyke swarm of the Superior Province.

Granitoids

K-Ar mineral dates for granitoids within the compilation map area range from 2.35-2.66 b.y. Rb-Sr biotite dates range from 2.50-2.57 b.y., while one Rb-Sr microcline date of 2.84 b.y. has been obtained for the Flora Lake Stock (recalculated by the author from Heimlich, 1963). Felsic dykes in the Rainy Lake area have yielded a Rb-Sr muscovite age of 2.74 b.y.

Of interest are the mineral dates from the granitoid batholith complexes: biotite K-Ar 2.35 b.y. for the Aulneau Dome; biotite K-Ar 2.58 b.y. for the Sabaskong Batholith. These values do not differ appreciably from mineral dates obtained for the late-kinematic "Algoman" plutons intrusive into Wabigoon supracrustals: (biotite, K-Ar) 2.66 b.y. for

Flora Lake stock; (biotite, K-Ar) 2.44 b.y. for the Rest Island stock.

Purdy and York (1966) presented a 9 point whole-rock Rb/Sr isochron for granitic gneisses covering 125 miles of the English River Gneiss Belt; going north from the top of our compilation map area. The isochron parameters were:

$2,450 \pm 100$ m.y., $R_0 = 0.706 \pm 0.002$. Wanless and Loveridge (1972)

produced a 4 point Rb/Sr whole rock isochron for the Quetico Belt south of our study region by pooling granitoid and pegmatite samples from a 300 mile traverse. Linear regression

(recalculated by this author to $\lambda_{\beta} = 1.39 \times 10^{-11} \text{y}^{-1}$) yielded an apparent age of $2,763 \pm 81$ m.y. with an intercept at $0.6991 \pm$

0.0037 . The diversity of lithology, the geographical scatter and the large error limits make interpretation of these pooled plots difficult. A regionally more restricted and therefore

a geologically more acceptable "pooled" isochron was produced

by Peterman et al. (1972) for the "Algoman" granitoids of Rainy

Lake. Thirteen whole rock samples from four granitoid plutons

define an isochron age of $2,540 \pm 90$ m.y. ($R_0 = 0.7015 \pm 0.0009$).

Prior to this study, only two Rb/Sr isochrons had been published utilizing demonstrably cogenetic samples from within

the compilation map area. Peterman et al. (1972) reported

that six of their "Algoman" samples came from the Ottetail

Lake Stock, and when regressed alone gave isochron parameters

of: $2,520 \pm 140$ m.y. Hart and Davis (1969) obtained a four

point whole rock Rb/Sr isochron for the Bad Vermilion Lake "Laurentian Tonalite" yielding an age of: $2,520 \pm 42$ m.y.

Available U-Th-Pb dating from within the compilation map area has been summarized by Peterman *et al.* (1972) and updated by them in a single Concordia diagram for zircons and sphene from the Rainy Lake area. On the basis of this Concordia plot, these authors proposed that "Algoman" plutonism spanned the interval of 2,750-2,700 m.y. and that the younger Rb/Sr isochron ages reflect disturbance of the isotopic systems. The zircon data is difficult to evaluate since sample source is reported for only one "Algoman" zircon (from a granitic boudin in schist). Two of three other granitoid zircons were excluded from linear regression by the original authors (Hart and Davis, 1969).

Conclusions

From the above literature survey of isotopic data, and from the geographical distribution of this data, the following conclusions are warranted:

- (1) There is no pattern to isotopic ages within our study area, either by lithology, or geographical distribution, with the exception of anomalously young mineral ages on mafic intrusives;
- (2) Age dates do not correlate with or reflect known field stratigraphic chronology;

- (3) The scatter of isotopic ages (except for mafic intrusions) is largely confined by the limits of the "ALGOMAN OROGENY": 2,400-2,750 m.y. of Goldich (1968).

As Moorbath (1967) points out:

"For the purposes of defining episodes of crystallization in a basement complex ... a single Rb/Sr whole rock isochron date, may be far more significant than any number of K/Ar and Rb/Sr dates on fine grained micas. Though the latter may form a convincing peak on a date histogram, this may signify no more than the termination of a radiogenic Ar or Sr diffusion episode. In contrast, a considerable spread in dates on a histogram may often be due, not to continuous plutonic activity but to the inclusion of a large number of apparent, "overprinted" dates - particularly in a polymetamorphic terrain." (p.123)

To eliminate ambiguities caused by comparing isotopic ages obtained by different analytical methods with different error components and possibly different "overprint" contributions, the author restricts further geochronological discussion to whole-rock Rb/Sr isochrons. Such isochrons will be furthermore standardized to the York (1966) linear regression model; with 95% confidence error estimates and using

$${}^{87}\text{Rb}\lambda_{\beta} = 1.39 \times 10^{-11} \text{y}^{-1} \text{ (unless otherwise stated).}$$

4.3 Rb/Sr ISOCHRONS FOR GRANITOIDS OF THE WABIGOON VOLCANIC-PLUTONIC BELT

4.3.1 Introduction

Isotopic and trace element data necessary to calculate Rb/Sr isochrons have been obtained for seven granitoid stocks and one batholithic granitoid complex within the Wabigoon Belt (Table 4.1). Only seven out of the twelve granitoid stocks of this study carried sufficient variation in ^{87}Rb and ^{87}Sr to be suitable for the isochron method. The difficulty in obtaining a sufficient spread in Rb/Sr and thereby generate a linear array has been reported for numerous areas (Fullagar, 1971; Hills et al, 1972). The problem is accentuated in these granitoids because of high Sr and low Rb concentrations.

Discussion on mass spectrometry and XRF techniques; accuracy and precision; data processing and selection, is reserved for the appendix. All sets of data were treated by the multiple-model regression package of Brooks et al. (1972) resulting in four sets of isochron parameters for every colinear suite, corresponding to four linear regression models common to Rb/Sr literature. Data processing assumed blanket error estimates for $^{87}\text{Rb}/^{86}\text{Sr}$ and $^{87}\text{Sr}/^{86}\text{Sr}$ and no correlation of errors. All errors quoted are for 2σ taken as 95% confidence. The acceptability of each linear array as an isochron sensu stricto was tested by the indices calculated in each regression model. Isochron parameters and indices for seven stocks are listed in Table 4.2 while regressions for the batholithic

TABLE 4.1 WHOLE ROCK TRACE ELEMENT AND ISOTOPIC Rb/Sr DATA

SAMPLE #	PB	SR	Rb/Sr ¹	LITHOLOGY	ANALYST D. GIEK	
					87Rb/86Sr ²	87Sr/86Sr ³
BUNDITT LAKE STOCK						
S1424	1	63.3	991.3	0.06344	BI-MB GRANODIORITE	.18149 .73709
G9	2	102.1	881.3	0.1052	BI-MB GRANODIORITE	.18149 .71220
G72	3	101.4	938.6	0.1099	BI-MB GRANODIORITE	.31529 .71142
GAC	4	67.6	912.8	0.1315	MASSIVE APLITE	.38156 .71547
44221	5	101.1	637.4	0.1501	MUSC-BI GRANODIORITE	.45464 .71710
4141	6	149.6	982.0	0.4935	RPO SPOTTED APLITE DYKE	1.42291 .72449
G42A	7	124.1	199.8	0.6272	MASSIVE APLITE	1.82292 .74771
G31	8	146.2	118.8	1.241	RPO SPOTTED APLITE DYKE	1.67679 .74617
G74	9	149.9	117.5	1.261	MASSIVE APLITE	1.76143 .74876
FLORA LAKE STOCK						
FL-P		186.9	1093.0	0.1806	GRANITIC DYKE	.29139 .71275
FL-R		123.1	969.7	0.2174	DICTITE GRANITE	.41056 .71275
FL-22		211.9	778.6	0.2675	MB-BI MONZONITE	.77599 .71077
FL-13		161.9	648.7	0.3121	BI GRANITE	.90567 .71545
FL-26		262.9	674.7	0.3831	MB-BI MONZONITE	1.11275 .72201
FL-7AD		153.6	71.0	2.091	APLITE DYKE	6.17880 .92277
RYCKMAN LAKE STOCK						
RY40		56.2	1664.1	0.01363	PX-MB MONZODIORITE	.39730 .70411
RY6		78.9	1389.9	0.04482	BI-MB GRANODIORITE	.18769 .72710
RY5		97.0	1182.1	0.08128	BI-MB GRANODIORITE	.82918 .72670
RY21		102.1	1082.9	0.09610	BI-MB QTZ MONZODIORITE	.27420 .71947
RY60		102.1	918.1	0.1124	BI-MB QTZ MONZODIORITE	.32544 .71140
RY22		292.4	282.7	0.3124	APLITE DYKE	1.32544 .75074
RY91A		172.5	296.1	0.3759	APLITE-ECHEMITE	1.67510 .78233
TAYLOR LAKE STOCK						
T42		67.5	2056.4	0.03244	BI-MB-PX MONZONITE	.09186 .72411
T11		126.5	979.7	0.1280	BI-MB GRANODIORITE	.17170 .71410
T16		157.0	821.1	0.1897	BI-MB-PX MONZONITE	.54366 .72114
T40		98.4	114.4	1.3382	MB-BI GRANODIORITE (FINC)	.68207 .72791
T77		242.3	832.7	0.2890	BI-MB GRANODIORITE	.83249 .71134
T60		299.0	482.1	0.7170	MUSC-BI MICROGRANITE	2.18855 .76093
ESOX LAKE QUARTZ-FELDSPAR PORPHYRY						
EX7		34.4	906.0	0.03910	GREY QTZ-FELDSPAR PORPHYRY	.11314 .72629
EX6		71.3	439.0	0.1362	GREY FLOSPR PORPHYRY	.39434 .71471
EX8		71.7	224.7	0.3211	PINK QTZ-FELDSPAR PORPHYRY	.33176 .71444
EX11		107.7	149.9	0.7181	PINK QTZ-FELDSPAR PORPHYRY	2.39237 .77411
BEARS PASSAGE STOCK						
B27		79.2	496.1	0.1577	BI-MUSC GRANODIORITE	.45697 .71969
B10		82.8	467.1	0.1751	BI-MUSC GRANODIORITE	.58736 .71904
B4A		95.3	431.9	0.2181	BI-MUSC GRANODIORITE	.63236 .72615
B01		97.5	481.7	0.2482	BI-MUSC GRANODIORITE	.69460 .72784
B4B		180.4	784.4	0.2271	BI-MUSC GRANODIORITE	.78931 .73081
B01		111.8	256.1	0.4330	BI-MUSC GRANODIORITE	1.25420 .76771
OTTERTAIL LAKE STOCK						
OT1		60.6	1014.3	0.05882	BI-MB QTZ MONZODIORITE	.17024 .70739
OT2		104.5	894.4	0.1152	BI GRANODIORITE	.33360 .71406
OT4		182.3	682.8	0.1551	BI GRANODIORITE	.44953 .71974
OT1		128.0	438.8	0.2890	MUSC GRANITE	.9346 .73051
OT5		142.6	480.9	0.3447	MUSC GRANITE	1.00060 .71741
RAINY LAKE BATHOLITH						
F74	J	13.5	2310.	0.08620	MB LEUCO QTZ DIORITE	.01793 .70174
F112	J	71.7	1243.	0.05749	GRANODIORITE	.16438 .70679
F25	J	82.7	760.	0.1085	GRANODIORITE	.31422 .71245
F103	J	32.3	711.	0.04487	BI TONALITE GNEISS	.12754 .73679
F5	F	94.9	843.	0.09264	BI TROCHMITE	.26822 .71116
F5	F	97.9	523.	0.1889	BI TROCHMITE	.31525 .71252
F7	F	76.2	475.	0.1629	BI TONALITE GNEISS	.47201 .71833
F110	F	98.2	461.	0.1936	GRANODIORITE	.56115 .72294
F29	M	65.8	702.	0.09138	BI-MUSC MONZODIORITE	.26428 .71152
F66	M	167.0	332.	0.5018	BI LEUCO MONZOGRAHITE	1.4566 .75919
F179	M	223.9	437.	0.5067	BI-MUSC MONZOGRAHITE	1.4754 .75619

LEGEND

- FROM XRF UNKNOWN/STANDARD COUNT RATIOS BY LINEAR REGRESSION
- $87Rb/86Sr = Pb/Sr \cdot X + .2055$ ($S = .430 + .87SR/86SR$)
ANALYTICAL ERROR +/- 1.8 PCT. (1 SIGMA)
- NORMALIZED TO $86SR/89SR = 0.1194$
ANALYTICAL ERROR +/- .065 PCT. (1 SIGMA)
- SAMPLE NUMBERS ON ISOCHEM PLOT AND LOCATION MAP.
- SAMPLES FROM PICHELLE (1976)
- SAMPLES AND Pb/Sr ANALYSES FROM F. LONGSTAFFE.
- UNITS J=JACKFISH, F=FOOTPRINT, M=NORTHWEST BAY
- SAMPLE NUMBERS ON ISOCHEM PLOTS ARE ABBREVIATED.
- ISOCHEM OUTLIER.

Table 4.2

ISOTOPE PARAMETERS FOR REGRESS OF BROOKS ET AL (1972) FOR GRANITOID PLUTONS INTRUSIVE INTO THE MARIPOSA BELT

MODEL	TEST	AGE	ERROR 2 SIGMA	INITIAL RATIO	ERROR 2 SIGMA
BURNETT LAKE STOCK (SAMPLES - 1,2,3,4,5,6,7,8,9)					
MCINTYRE I	MSWD	1.30	2889	38 MY	.7889
YORK I			2841	48 MY	.7889
YORK II	S	1.19	2640	38 MY	.7889
WENDT I	SCSD	0.91	2594	34 MY	.7889
WENDT II	SCSD	1.19	2680	37 MY	.7889
BLANKET ERROR (87Rb/86Sr) = 0.81 , (87Sr/86Sr) = 0.865 (PCT)					
FLODA LAKE STOCK (PHANERITES + APLITE DYKE - 0,5,22,13,24,??)					
MCINTYRE I	MSWD	0.81	2534	56 MY	.7877
YORK I			2534	82 MY	.7876
YORK II	S	1.31	2539	82 MY	.7876
WENDT I	SCSD	0.88	2539	82 MY	.7876
WENDT II	SCSD	1.01	2539	82 MY	.7876
BLANKET ERROR (87Rb/86Sr) = 0.81 , (87Sr/86Sr) = 0.865 (PCT)					
FLODA LAKE STOCK (PHANERITES - 0,5,22,13,24)					
MCINTYRE I	MSWD	0.25	2636	126 MY	.7817
YORK I			2636	67 MY	.7817
YORK II	S	0.50	2637	125 MY	.7817
WENDT I	SCSD	0.38	2542	127 MY	.7816
WENDT II	SCSD	0.50	2542	122 MY	.7817
BLANKET ERROR (87Rb/86Sr) = 0.81 , (87Sr/86Sr) = 0.865 (PCT)					
DYCKMAN LAKE STOCK (PHANERITES + DYKES - 30,6,5,21,68,22,91A)					
MCINTYRE I	MSWD	1.32	2689	63 MY	.7801
YORK I			2689	67 MY	.7801
YORK II	S	1.84	2689	68 MY	.7801
WENDT I	SCSD	0.88	2687	61 MY	.7802
WENDT II	SCSD	1.34	2684	51 MY	.7801
BLANKET ERROR (87Rb/86Sr) = 0.81 , (87Sr/86Sr) = 0.865 (PCT)					
TAYLOR LAKE STOCK (SAMPLES - 42,13,38,57,61)					
MCINTYRE I	MSWD	0.19	2640	78 MY	.7805
YORK I			2640	31 MY	.7805
YORK II	S	0.44	2639	78 MY	.7805
WENDT I	SCSD	0.15	2637	78 MY	.7805
WENDT II	SCSD	0.44	2639	67 MY	.7805
BLANKET ERROR (87Rb/86Sr) = 0.81 , (87Sr/86Sr) = 0.865 (PCT)					
ESSEX LAKE QUARTZ-FELDSPAR PORPHYRY (SAMPLES - 7,9,5,11)					
MCINTYRE I	MSWD	0.87	2572	78 MY	.7803
YORK I			2572	48 MY	.7803
YORK II	S	0.51	2571	78 MY	.7803
WENDT I	SCSD	0.45	2575	71 MY	.7803
WENDT II	SCSD	0.61	2575	64 MY	.7803
BLANKET ERROR (87Rb/86Sr) = 0.81 , (87Sr/86Sr) = 0.865 (PCT)					
BEARS PASSAGE STOCK (SAMPLES - 19,4A,3,4B,5, AND KA350)					
MCINTYRE I	MSWD	1.94	2781	155 MY	.7802
YORK I			2782	150 MY	.7802
YORK II	S	1.32	2785	157 MY	.7802
WENDT I	SCSD	0.75	2713	157 MY	.7801
WENDT II	SCSD	1.02	2786	141 MY	.7802
BLANKET ERROR (87Rb/86Sr) = 0.81 , (87Sr/86Sr) = 0.865 (PCT)					
BEARS PASSAGE STOCK MINERALS AND WHOLE ROCK (SAMPLES PL40,19,4A,3,4B,KA350,5,KSPAR,MUSC)					
MCINTYRE I	MSWD	1.23	2861	48 MY	.7819
YORK I			2864	102 MY	.7820
YORK II	S	1.33	2864	75 MY	.7820
WENDT I	SCSD	0.39	2867	75 MY	.7820
WENDT II	SCSD	1.33	2855	75 MY	.7820
BLANKET ERROR (87Rb/86Sr) = 0.87 , (87Sr/86Sr) = 0.865 (PCT)					
BEARS PASSAGE STOCK MINERALS (PL40, KA350, KSPAR, MUSC)					
MCINTYRE I	MSWD	1.59	2830	81 MY	.7820
YORK I			2834	137 MY	.7820
YORK II	S	1.35	2833	78 MY	.7820
WENDT I	SCSD	1.15	2846	88 MY	.7820
WENDT II	SCSD	1.35	2834	84 MY	.7820
BLANKET ERROR (87Rb/86Sr) = 0.87 , (87Sr/86Sr) = 0.865 (PCT)					
DUFFERIN LAKE STOCK (SAMPLES - 1,2,3,5)					
MCINTYRE I	MSWD	0.97	2889	111 MY	.7811
YORK I			2859	105 MY	.7811
YORK II	S	0.33	2829	111 MY	.7811
WENDT I	SCSD	0.68	2855	111 MY	.7811
WENDT II	SCSD	1.33	2859	107 MY	.7811
BLANKET ERROR (87Rb/86Sr) = 0.81 , (87Sr/86Sr) = 0.865 (PCT)					

TABLE 4.2 CONTINUED

MODEL	TEST	AGE	ERROR Σ SIGMA	INITIAL LATIC	ERROR Σ SIGMA
OTTERTAIL LAKE STOCK (1,2,3,5,RL4 ² ,RL4 ³ ,PL4 ² ,PL4 ³ ,KAT5 ²)					
MCINTYRE I	MSMD= 0.65	2514	95 MY	.7816	.0007
YORK I		2514	78 MY	.7816	.0005
YORK II	S= 0.92	2512	94 MY	.7816	.0010
WENDT I	SCSD= 0.65	2509	96 MY	.7817	.0007
WENDT II	SCSD= 0.52	2513	98 MY	.7816	.0007
BLANKET ERROR (87RP/86SR)= 0.02 , (87SP/86SD)= 0.065 (PCT)					
APLITES (22,6,918,7,8,9,27)					
MCINTYRE I	MSMD= 1.21	2547	52 MY	.7822	.0016
YORK I		2549	50 MY	.7822	.0014
YORK II	S= 1.14	2545	57 MY	.7822	.0021
WENDT I	SCSD= 0.94	2545	52 MY	.7821	.0015
WENDT II	SCSD= 1.14	2547	58 MY	.7822	.0015
BLANKET ERROR (87RB/86SP)= 0.01 , (87SB/86SD)= 0.065 (PCT)					
APLITES (22,6,918,7,8,3)					
MCINTYRE I	MSMD= 1.22	2577	71 MY	.7815	.0019
YORK I		2577	68 MY	.7815	.0022
YORK II	S= 1.11	2576	71 MY	.7815	.0025
WENDT I	SCSD= 0.90	2577	71 MY	.7815	.0019
WENDT II	SCSD= 1.13	2576	69 MY	.7815	.0019
BLANKET ERROR (87RP/86SR)= 0.01 , (87SB/86SD)= 0.065 (PCT)					
POOLET MABIGOOM GRANITOIDS (19 SAMPLES)					
MCINTYRE I	MSMD= 1.77	2614	25 MY	.7807	.0004
YORK I		2621	35 MY	.7807	.0004
YORK II	S= 1.39	2628	28 MY	.7807	.0004
WENDT I	SCSD= 1.07	2622	24 MY	.7806	.0004
WENDT II	SCSD= 1.39	2628	26 MY	.7807	.0004
BLANKET ERROR (87RP/86SP)= 0.01 , (87SR/86SD)= 0.065 (PCT)					

LEGEND

MSMD = MEAN SQUARE OF WEIGHTED DEVIATES
 S = SQUARE ROOT OF W. WEIGHTED SUM RESIDUALS SQUARED/(N-2)
 SCSD = SUM OF CHISQUARE
 1 SAMPLE NUMBERS ABBREVIATED FROM TABLE 4.1
 2 PETERMAN ET AL (1972) TABLE 5, NUMBERS ABBREVIATED.
 * BEST ESTIMATE OF ISOCRON SENSU STRICTO.

complex are tabulated in Table 4.3.

Actual isochron plots presented in the subsequent discussion are based on the York I model (Brooks et al., 1972). The selection of York I was arbitrary; based partially on the prevalence of York (1966) regressions among published isochrons of the region. For isochrons sensu stricto the various models give near identical parameters.

All age estimates are based on the ^{87}Rb decay constant of: $\lambda_{\beta} = 1.39 \times 10^{-11} \text{y}^{-1}$. Calculations using the higher value of $\lambda_{\beta} = 1.42 \times 10^{-11} \text{y}^{-1}$ recommended by Neumann and Huster (1976) and Davis, Gray and Baadsgaard (1977) would yield 2.1% younger ages.

4.3.2 Wapigoon Late- to Post-Tectonic Stocks

A. Wapigoon Internal Plutons

Previous Work:

Whole rock Rb/Sr isochrons from this study have been previously reported in Birk and McNutt (1977a,b). The only other radiometric ages available are a microcline Rb/Sr apparent age of $2,840 \pm 142$ m.y. (adjusted by the author to $\lambda_{\beta} = 1.39 \times 10^{-11} \text{y}^{-1}$) and a biotite K-Ar age of $2,660 \pm 133$ m.y., from the granite and monzodiorite of Flora Lake (Heimlich, 1963).

Phaneritic Granitoid Stocks:

A 9 point isochron for the Burditt Lake Stock was

published in Birk and McNutt (1977a) and is reproduced in Figure 4.2. Because of a narrow Rb/Sr spread, the four granodiorite samples, if regressed alone, generate a poorly defined isochron of $2,341 \pm 292$ m.y. with an intercept¹ at 0.7019 ± 0.0013 (MSWD = 0.69 ²). To draw out the plot and give better control on the slope, the isochron of Figure 4.2 relies on massive aplite samples from the peripheral zone of the south lobe. The five aplitic samples control the isochron parameters. When regressed as a set they generate parameters of $2,578 \pm 47$ m.y., $R_0 = 0.7017 \pm 0.0011$ (MSWD = 0.98). Since these aplitic patches are of probable late-deuteric parentage, the isochron age of Figure 4.2 is a minimum age for emplacement. The duration of magmatic consolidation was almost certainly much shorter than the isochron error limits; therefore this minimum age can be accepted as the time of magmatic emplacement, provided that closed systems prevailed.

Likewise^a the isotopic samples from the Ryckman Lake Stock (Table 4.1) can be grouped into phanerites and felsic dykes. The two felsic dykes come from locations internal and marginal to the stock and are also of likely deuteric parentage. Figure 4.3 (Table 4.2) is a regression of phanerites and felsic dykes to yield a York I age of $2,609 \pm 63$ m.y. A second plot can be generated confined to phanerite samples only to yield a younger age by 379 m.y. (Table 4.4) with conflicting error estimates between the various regression models. This

1. Isochron intercept henceforth

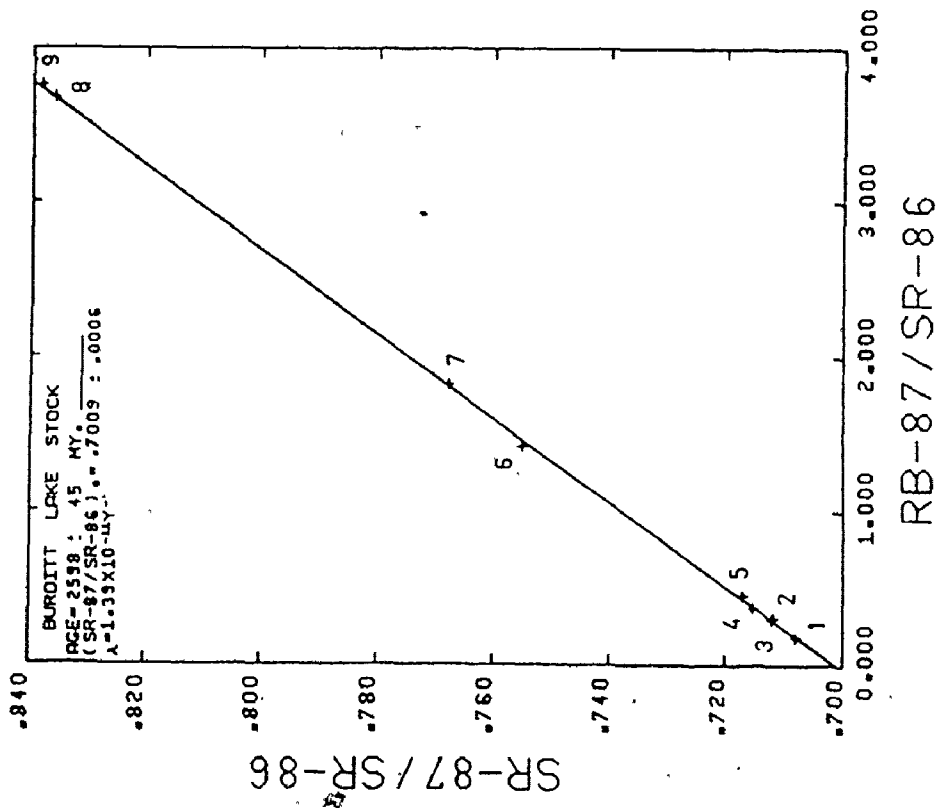


FIGURE 4.2 WHOLE-ROCK 9 POINT Rb/Sr ISOCHRON (YORK 1) FOR BURDITT LAKE STOCK SAMPLES 4,6,7,8 AND 9 ARE APLITES AND GIVE MINIMUM EMPACEMENT AGE

A

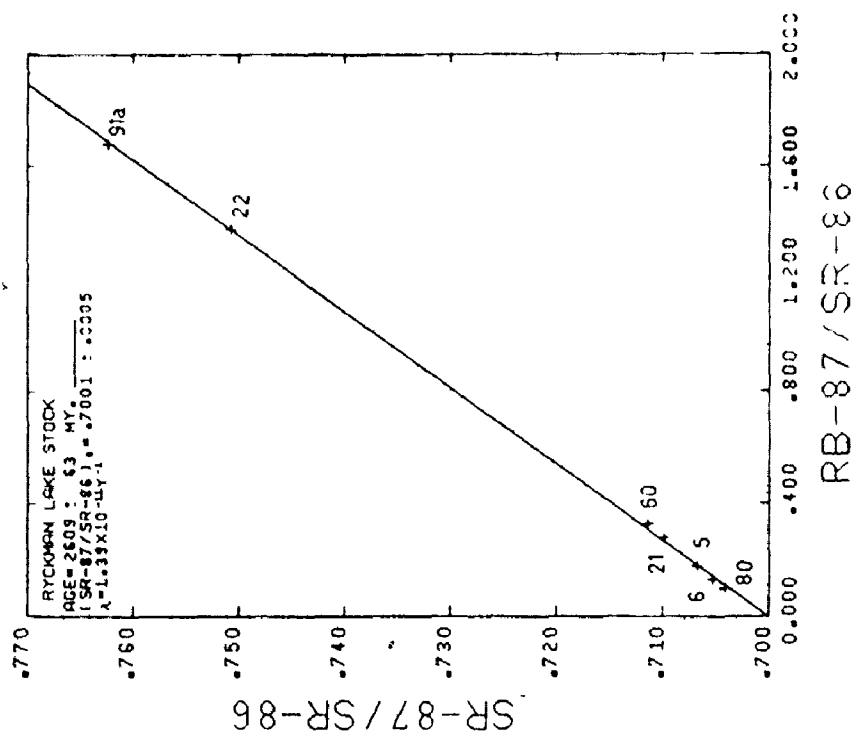


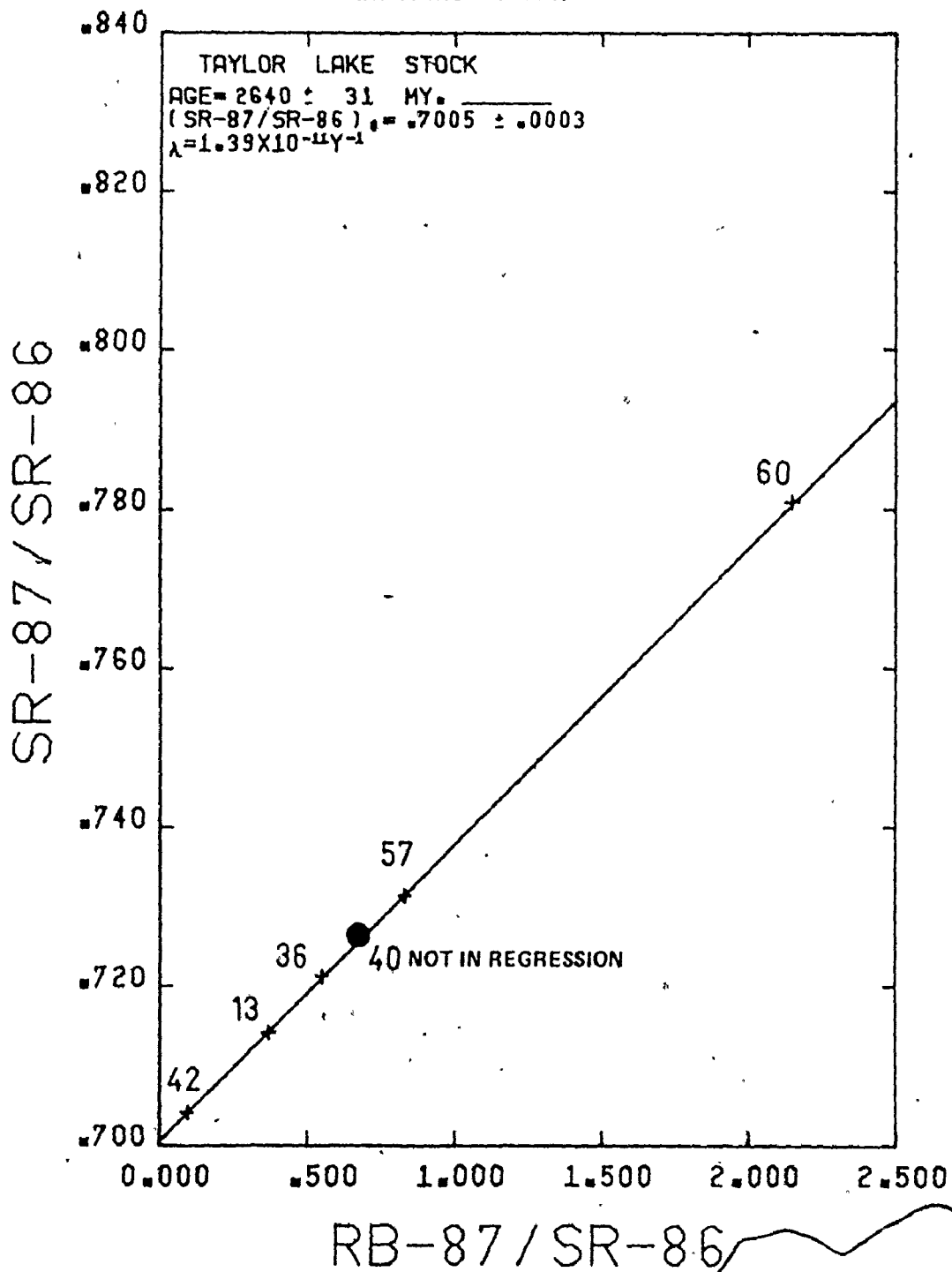
FIGURE 4.3 WHOLE-ROCK 7 POINT Rb/Sr ISOCHRON (YORK 1) FOR RYCKMAN LAKE STOCK SAMPLES 22 AND 91A ARE APLITE AND APLITE-PEGMATITE AND DICTATE MINIMUM EMPLOYMENT AGE.

paradox will be discussed in detail in section 4.5.2.

A 5 point linear regression for the Taylor Lake Stock was published by Birk and McNutt (1977a) and is repeated in Figure 4.4. The slope of this isochron ($2,640 \pm 31$ m.y.) relies heavily on a single sample from marginal microgranite bearing a high Rb/Sr ratio. Eliminating this felsite from the regression yields a slightly younger age of $2,617 \pm 64$ m.y. ($R_0 = 0.7006 \pm 0.0004$), MSWD = 0.22) with somewhat wider error limits. As reported in Birk and McNutt (1977a) some geological disturbance is suspected in sample T40 which was therefore omitted from the regression. Although colinearity with the accepted points is only slightly outside the limits of an isochron sensu stricto according to the definition of Brooks et al. (1972), slight fault induced disturbance of the Rb/Sr systematics is postulated. Sample T40 was collected from a site straddling the Taylor Lake Fault which strikes north-northeast with a displacement of 1,800 m., postdating all intrusive activity (Pichette, 1976). A detailed discussion on outliers and errorchrons is presented in section 4.5.1. The best estimate of age for the Taylor Lake Stock is therefore the 5 point $2,640 \pm 31$ m.y. regression. The time required to accommodate the six intrusive phases postulated by Pichette (1976) is considered to fall within the age error limits.

Birk and McNutt (1977a) published a 5 point whole-rock isochron for Flora Lake stock which has been slightly revised

FIGURE 4.4 WHOLE-ROCK 5 POINT Rb/Sr ISOCHRON
(YORK I) FOR TAYLOR LAKE STOCK.
SAMPLE 40 NOT INCLUDED IN
REGRESSION. SAMPLE 60 IS
MICROGRANITE AND STRONGLY
INFLUENCES SLOPE.



in Figure 4.5 (Table 4.2). Sample EL 22 was reanalysed to give $^{87}\text{Sr}/^{86}\text{Sr} = 0.7308$, which consequently modified the regression parameters but not the interpretation. Despite a diverse lithology (monzodiorite to granite) the range in Rb/Sr is restricted. To improve control on the slope an aplitic apophysis intruding metavolcanics was analysed. The resultant 6 point regression (Figure 4.6) is essentially a two-cluster plot with the slope affected strongly by the position of the aplite. The isochron age ($2,534 \pm 55$ m.y., $R_0 = 0.7026 \pm 0.0008$, MSWD = 0.83) is notably lower than the isochron age obtained from phaneritic samples only ($2,636 \pm 63$ m.y., $R_0 = 0.7017 \pm 0.0006$, MSWD = 0.25). Dykes bearing high Rb/Sr commonly plot below the isochron defined by lower points (Brooks *et al.*, 1972). The older isochron age is therefore considered the better time estimate for magmatic emplacement. Cross-cutting field relationships demonstrate that the Flora Lake Stock was the product of multiple intrusion - yet samples from all three major lithologic phases are colinear in the isochron regression. This demonstrates that any hiatus between successive intrusions is accommodated by the error limits.

Hypabyssals: Esox Lake Quartz-Feldspar Porphyry:

Various phases of the hypabyssal felsite at Esox Lake were isotopically analysed in the hope of chronologically differentiating the hypabyssal porphyry from the phaneritic granitoids. The granitoids proved to have an extremely narrow

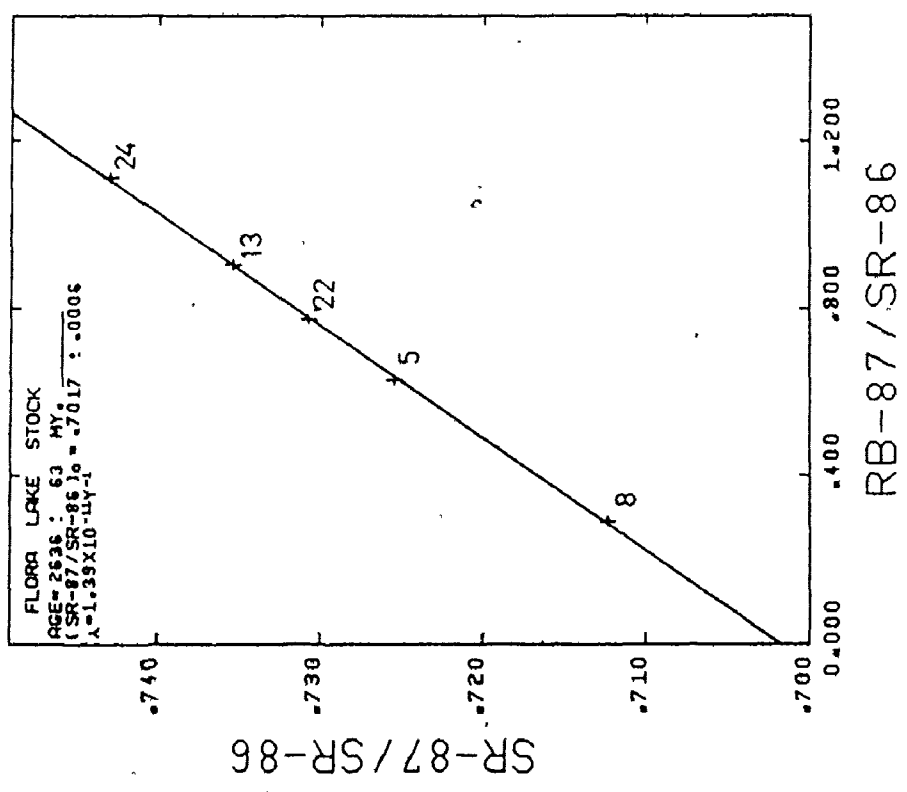


FIGURE 4.5 WHOLE-ROCK 5 POINT Rb/Sr ISOCHRON (YORK II) FOR FLORA LAKE STOCK: PHANERITES ONLY.

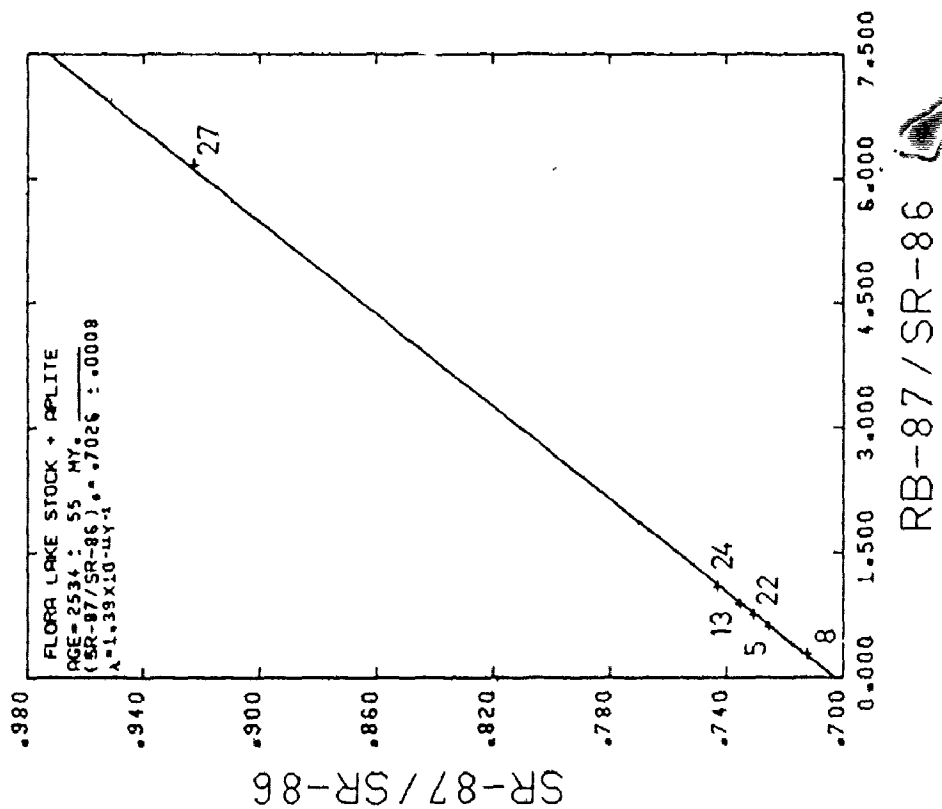


FIGURE 4.6
 WHOLE-ROCK 6 POINT Rb/Sr
 ISOCHRON (YORK 1). SAMPLES
 AS IN FIGURE 4.5 PLUS APLITE
 APOPHYSIS (F22). THE
 APLITE HAS SUFFERED A
 "DROPPING OFF" EFFECT
 AND GENERATES A YOUNGER
 "AGE" THAN FIGURE 4.5

range in Rb/Sr - unsuitable for isochron work. On the other hand, an excellent spread in the hypabyssal body allowed for a well-defined isochron from only four samples. Figure 4.7 shows a four point York I regression utilizing samples from the pink, grey and cataclastite phases of the porphyry. The York I age estimate of $2,572 \pm 42$ m.y. ($R_0 = 0.7003 \pm 0.0005$) is not significantly different from isochron ages for phaneritic granitoids of the region (Burditt Lake Stock and Ryckman Lake Stock, as discussed above). If the Esos East Stock and the Esos West Stock (discussed in section 2) are both younger than the hypabyssal porphyry, and if the porphyry represents a near-surface expression of vulcanism - the above isochron age suggests that vulcanism and granitoid emplacement occurred over a time span accommodated by the isochron error limits. However, the experience of some investigators (Fairbairn and Hurley, 1969; Page, 1976) of a "dropping off" effect in acid volcanics of high Rb/Sr ratio, cautions us to consider the isochron a minimum age estimate.

B. Wabigoon-Quetico Interface: Rainy Lake "Algoman" Plutons

Previous Work:

The first Rb/Sr isochron reported for the Rainy Lake plutons was a six point whole-rock reconnaissance plot for grey to pink medium grained granites from Rainy Lake reported in Hedge and Walthall (1963). Their 2,400 m.y. ($R_0 = 0.7012$) age

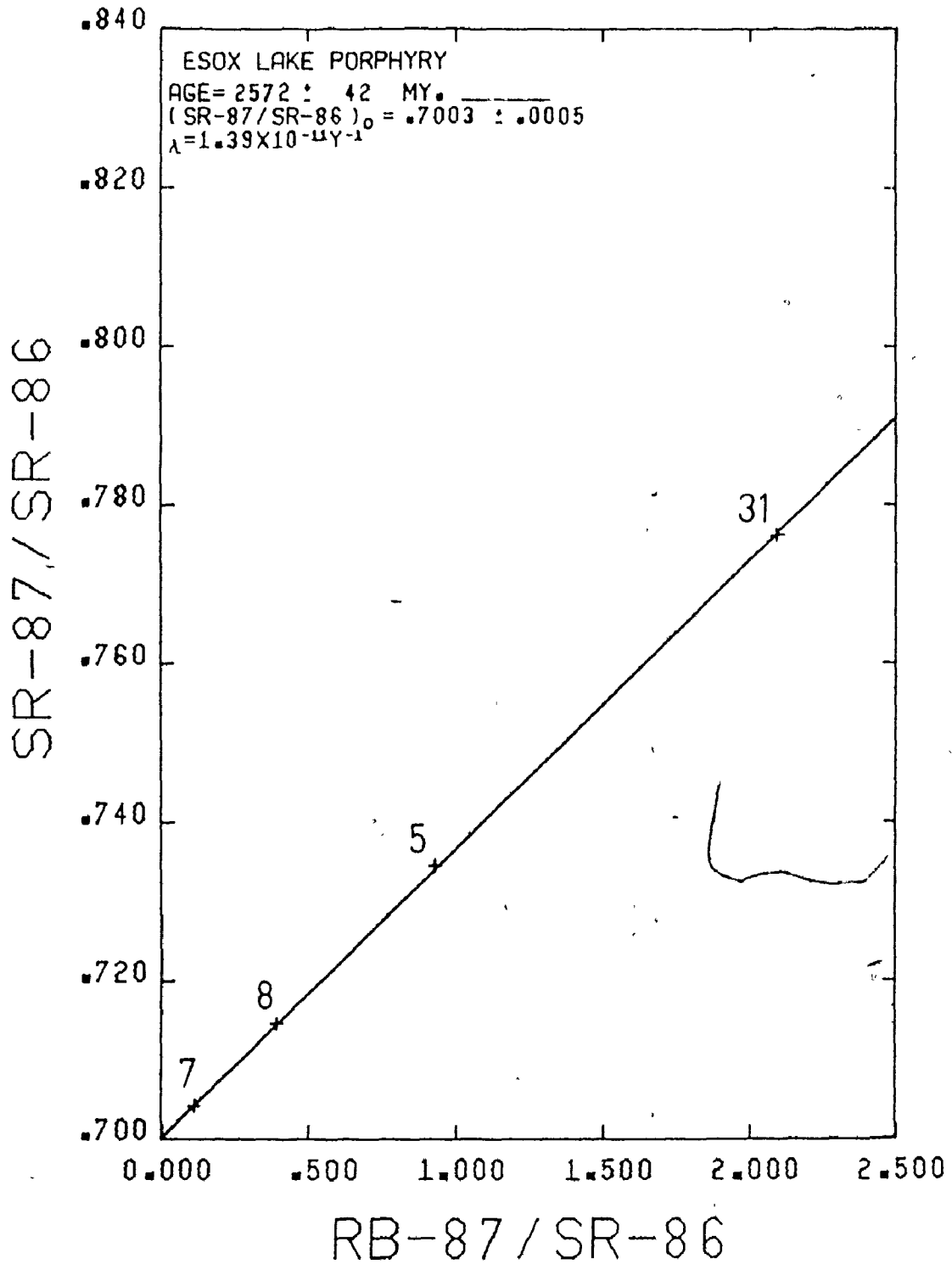


FIGURE 4.7

WHOLE-ROCK 4 POINT Rb/Sr
 ISOCHRON (YORK I) FOR
 ESOX LAKE QUARTZ-FELDSPAR
 PORPHYRY, GIVING MINIMUM AGE
 FOR NEAR-SURFACE VULCANISM.

estimate was recalculated to 2.55 b.y. (for $\lambda_{\text{Rb}87} = 1.39 \times 10^{-11} \text{y}^{-1}$) in Hart and Davis (1969). Hart and Davis (1969) noted that this isochron age was not significantly different from mica ages for the same units.

Peterman et al. (1972) summarized all geochronological work for the Rainy Lake region and provided new Rb/Sr isotopic analyses for the Algoman plutons. A 13 point isochron was presented containing samples from four distinct granitoid plutons whose geometric centres show a colinear trend north-northeast: the Rest Island Stock (3 samples); Bears Passage Stock (1 sample); Knuckle Island Stock (2 samples); and the Ottertail Lake Stock (7 samples). By separating cogenetic suites, Birk and McNutt (1977a) recalculated this data to generate separate York I age estimates. Six points for the Ottertail Lake Stock give $2,471 \pm 115$ m.y. ($R_0 = 0.7021 \pm 0.0007$) while the three points for the Rest Island Stock lie on a $2,455$ m.y. reference isochron (within ± 104 m.y. and with $R_0 = 0.7024 \pm 0.0007$).

These age estimates led Birk and McNutt (1977a) to postulate that the Rainy Lake "Algoman" plutons are younger than the granitoid plutons from within the Wabigoon Belt, which may be attributable to their location along the Wabigoon-Quetico interface. To test this theory further, the author carried out isotopic analyses on two of the plutons treated by Peterman et al. (1972): the Bears Passage Stock and Ottertail

Lake Stock.

Bears Passage Stock:

Peterman et al. (1972) analysed minerals and whole-rock from one specimen of the Bears Passage Stock (KA-350) yielding the following age estimates:

Muscovite	K-Ar: 2.540 b.y.
Muscovite - total rock isochron	Rb/Sr: 2.600 b.y.
Biotite - total rock isochron	Rb/Sr: 2.150 b.y.

Plagioclase and microcline from the same specimen plotted on a $2,520 \pm 60$ m.y. isochron which included whole-rock and mineral specimens from the Knuckle Island Stock. The whole-rock analysis was included on the pooled Algoman granite total-rock isochron of $2,540 \pm 90$ m.y. Peterman et al. (1972) suggested that weathering lowered the Rb/Sr ages of biotite. Three modal analyses (Table B5, Appendix I) for samples from the Bears Passage Stock show the following range in mineral modes:

Muscovite	-	2.7 to 6.0%
Biotite	-	0.0 to 1.1
Chlorite	-	0.0 to 0.6

Muscovite is present in large fresh laths while biotite appears as dark brown shreaded and chloritized flakes. This confirms that the low biotite age may reflect strong weathering.

Five new whole-rock specimens from the Bears Passage Stock have been analysed (Table 4.1) and when regressed with the mean value for sample KA-350 (whole rock) of Peterman et al. (1972), the resultant York I isochron parameters are (Figure 4.8):

$$2,702 \pm 158 \text{ m.y.}, R_0 = 0.7002 \pm 0.0017 \quad (\text{MSWD} = 1.04)$$

This isochron age agrees with the muscovite total-rock age and furthermore agrees with the 2.7 b.y. zircon age of Peterman et al. (1972). The large error is a function of the narrow range in Rb/Sr. A sixth sample was analysed (Table 4.1), but not included in the regression due to discordancy, and will be discussed in section 4.5.1 (Errorchrons).

In an attempt to better define the Bears Passage isochron age, the author combined the available whole-rock analyses and the mineral analyses for sample KA-350 quoted in Peterman et al. (1972), omitting biotite. As indicated from petrography, biotite is the most altered and least abundant of the minerals separated by Peterman et al. (1972) and deviates considerably from colinearity (Table 4.7). Because of an extremely high Rb/Sr ratio, muscovite dominates the slope of the mineral: whole-rock regression to produce an essentially two-point plot (Figure 4.9) with a reference age of $2,555 \pm 102$ m.y. (Table 4.2). A regression of coexisting minerals and whole-rock (KA-350) alone yields an even younger age of $2,534 \pm 107$ m.y. (Table 4.2). The reduction in slope from whole-rock to coexisting mineral

FIGURES 4.8 AND 4.9:

**WHOLE-ROCK AND MINERAL: WHOLE
ROCK Rb/Sr ISOCHRONS (YORK I)
FOR BEARS PASSAGE STOCK.
DATA POOLED FROM AUTHOR'S
TABLE 4.1 AND PETERMAN ET AL
(1972). LARGE ERROR
LIMITS REFLECT POOR
CONFIDENCE IN EITHER
AGE OR INTERCEPT.**

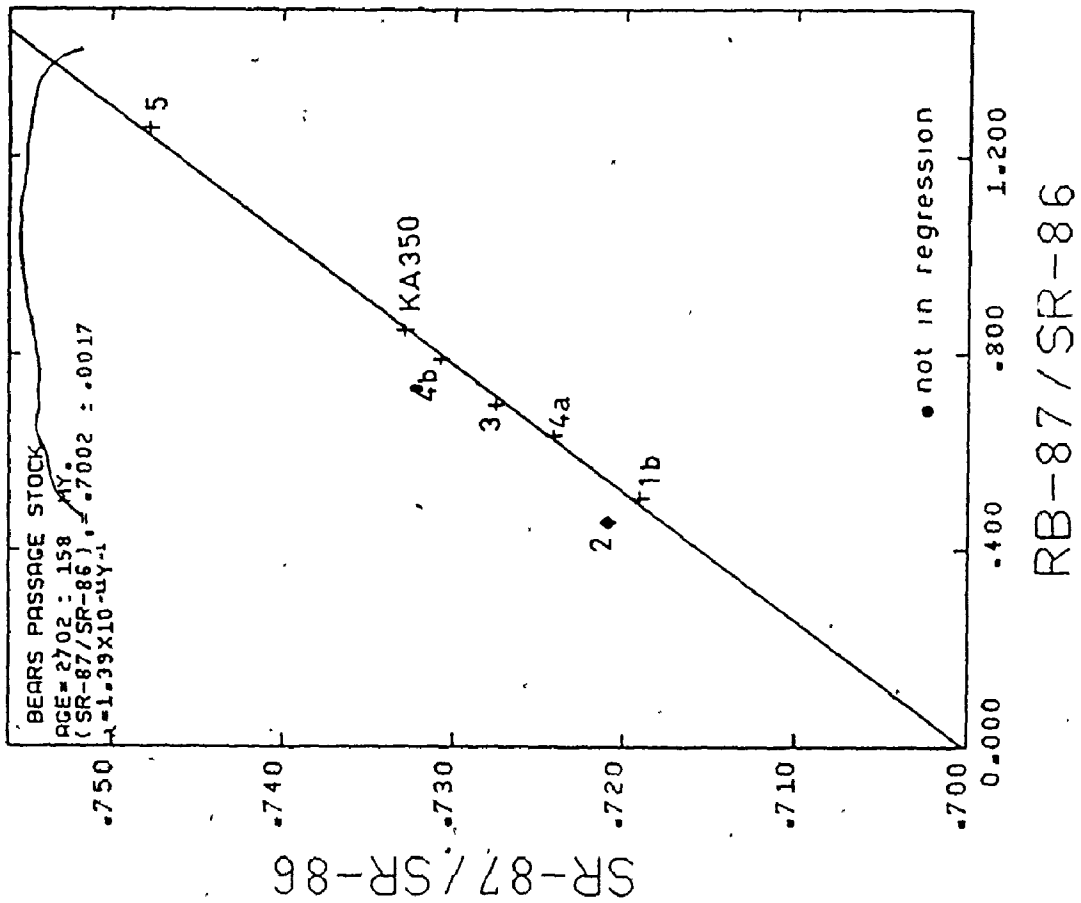


FIGURE 4.8

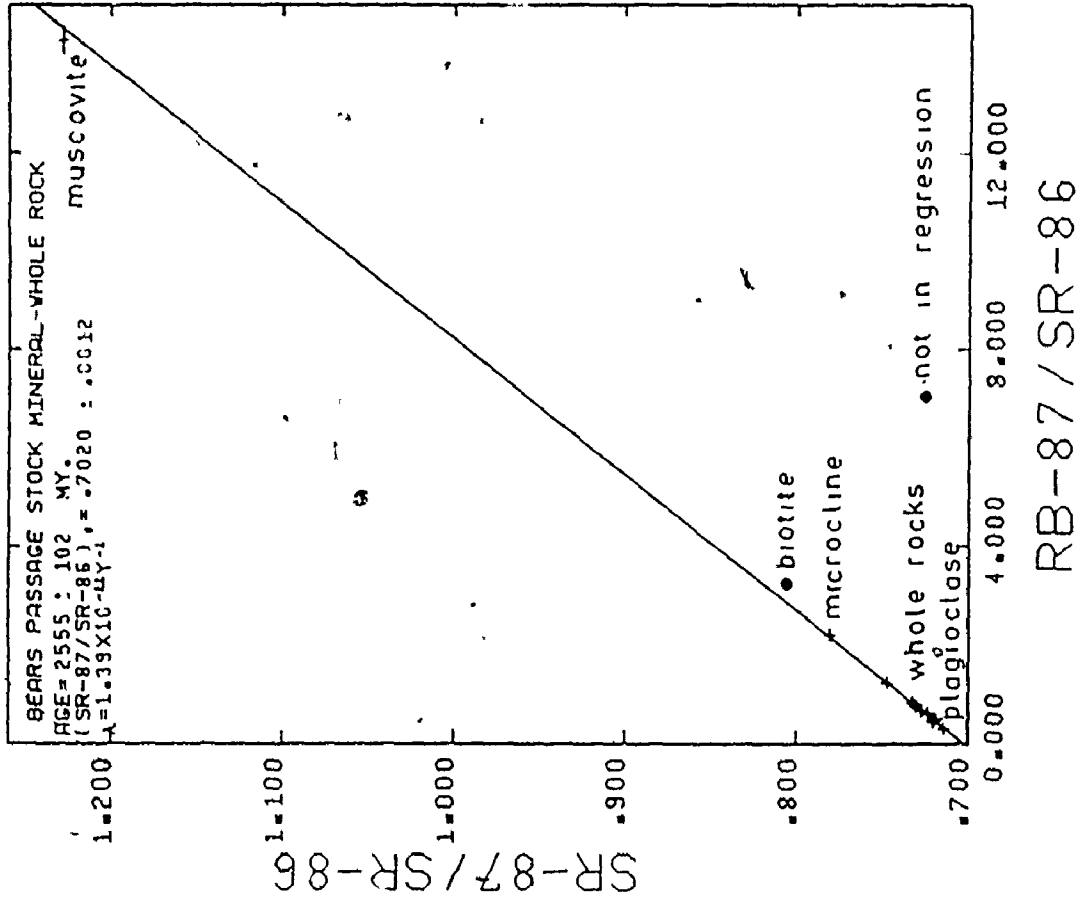


FIGURE 4.9

analyses coincides with an increase in the initial $^{87}\text{Sr}/^{86}\text{Sr}$ ratio; this suggests that the pooled mineral:whole-rock isochron represents two superimposed linear arrays with the mineral isochron reflecting metamorphic re-equilibration causing rotation of the plot. This cannot in fact be demonstrated. A pooled variance test (see section 4.4.1) between the whole-rock and mineral isochron shows that the intercepts are statistically distinct (at 95% confidence) but the gradients are not distinct. The larger error limits on the whole-rock regression therefore better reflect the poor confidence in the apparent age and intercept.

Ottertail Lake Stock:

Peterman et al. (1972) presented seven whole-rock analyses from six locations traversing the Ottertail Lake Stock and reported an age of $2,520 \pm 140$ m.y. Birk and McNutt (1977a) recalculated these isotopic data, found one discordant point (RL3766) and came up with York I parameters of:

$$2,471 \pm 115 \text{ m.y.}, \quad R_0 = 0.7021 \pm 0.0007 \quad (\text{MSWD} = 0.96).$$

Five new samples have been collected and analysed in this study to test the validity of these ages and perhaps narrow the error limits. The new samples do not widen the Rb/Sr range, but they remove the emphasis of the previous one high point on the slope. A regression of the new analyses

(Table 4.1) with the published data yields not only new isochron parameters (Table 4.2), but also a check on the accuracy of my analyses. The colinearity of my data points with those from Peterman et al. (1972) demonstrates interlaboratory consistency.

The new whole-rock regression includes 10 points to give an MSWD of 0.65 and York I parameters of $2,514 \pm 78$ m.y., $R_0 = 0.7016 \pm 0.0005$. Two samples had to be eliminated from the regression treatment to preserve colinearity (RL3766 from Peterman et al., 1972; OT4 from my Table 4.1). A full accounting of the treatment of such outliers is presented in section 4.5.1. In view of the fact that the 10 point regression pools analyses from two laboratories - the colinearity (Figure 4.10) is considered excellent. The new isochron confirms the young apparent age obtained by Peterman et al., (1972).

C. Composite Isochrons

Wabigoon Pooled Granitoid Isochron:

Individual plutons for which whole-rock isochrons are presented in Table 4.2 are scattered over a 3,400 square mile area and separated individually by as much as 60 miles. It would not be unreasonable to suppose that the individual plutons represent discrete granitic episodes unconnected in time and space.

When 39 granitoid samples from the stocks intrusive

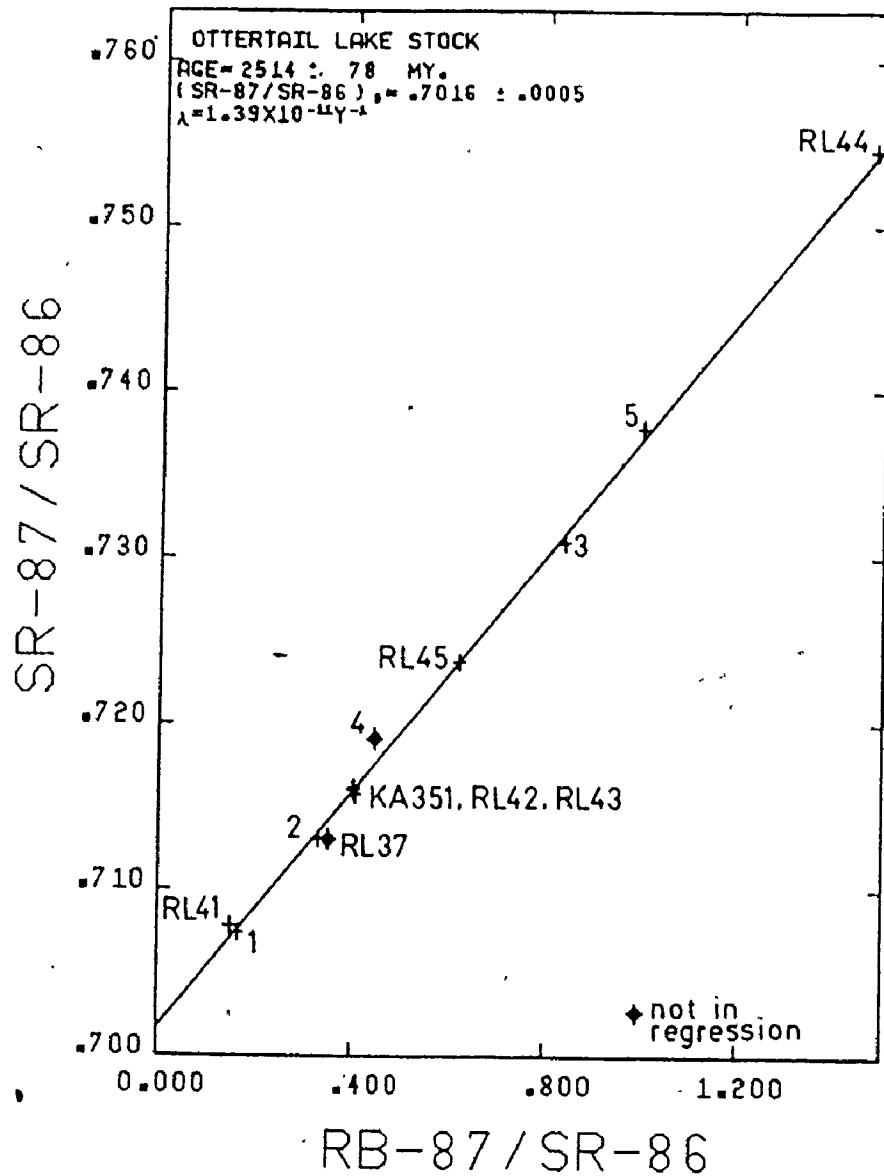


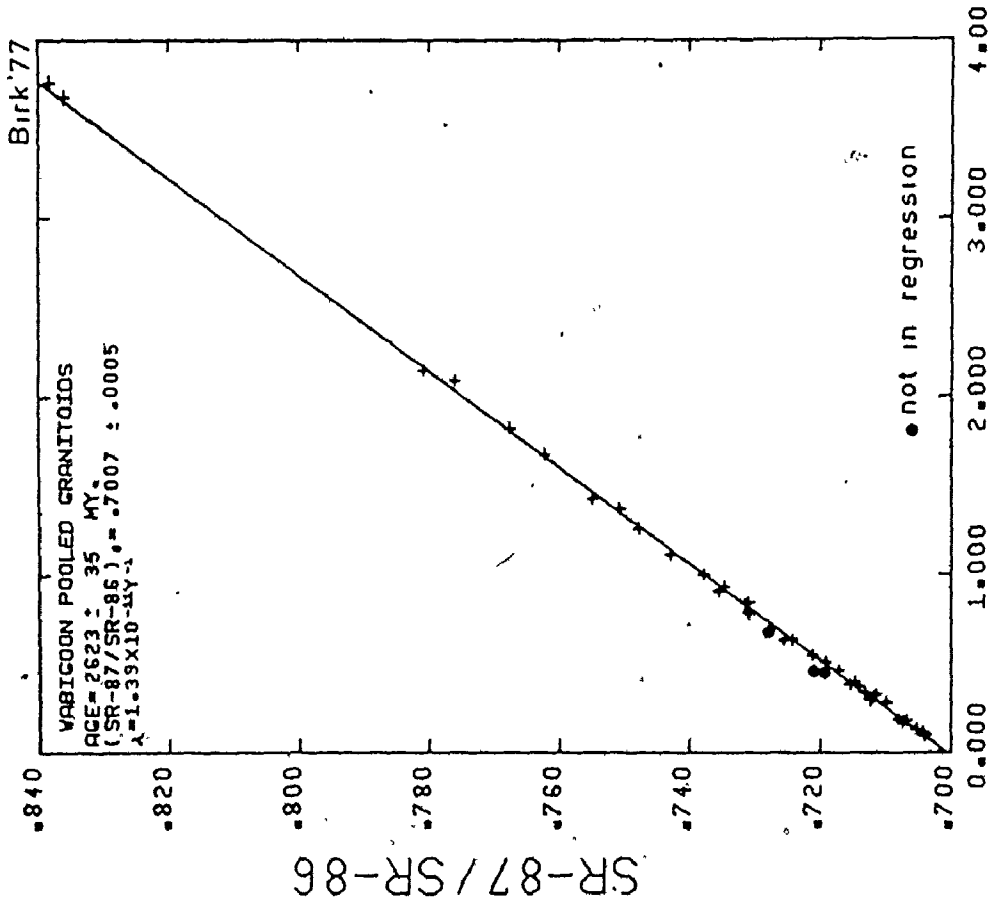
FIGURE 4.10 WHOLE-ROCK 10 POINT Rb/Sr ISOCHRON (YORK 1) FOR OTTERTAIL LAKE STOCK BASED ON POOLED DATA FROM AUTHOR'S TABLE 4.1 AND PETERMAN ET AL (1972). SAMPLE NUMBERS FROM OP. CIT. ABBREVIATED.

into supracrustals, and with isotopic ratios compatible with the previous linear regressions are pooled and treated as cogenetic, the resultant plot (Figure 4.11) shows remarkable colinearity and acceptable isochron characteristics. It should be noted that the 95% confidence levels for this regression do not bracket all the individual age and intercept estimates for the component isochrons. If the two highest Rb/Sr points are removed, the resultant linear regression is only slightly modified (Figure 4.12).

Is the Wabigoon Pooled Granitoid "isochron" an average background "age" for a series of discrete isochrons representing individual episodes or do individual pluton isochrons represent a statistical sampling of a population whose mean is closely approximated by the pooled isochron? In other words, by pooling all samples on to one plot - are we removing analytical and geological "noise" to obtain a clear geochronological "signal" - or are we ironing out meaningful episodes in the record to arrive at a less meaningful average? The former possibility suggests that all granitoid plutons intrusive into the supracrustals of the Wabigoon Belt are coeval with the same initial $^{87}\text{Sr}/^{86}\text{Sr}$ ratio and the same radiometric age. The individual isochron estimates presented previously would then represent samplings from a normally distributed population of an infinite number of potential isochrons whose mean is the true time of emplacement and whose deviation is the sum of: geological error; analytical error and the actual duration of

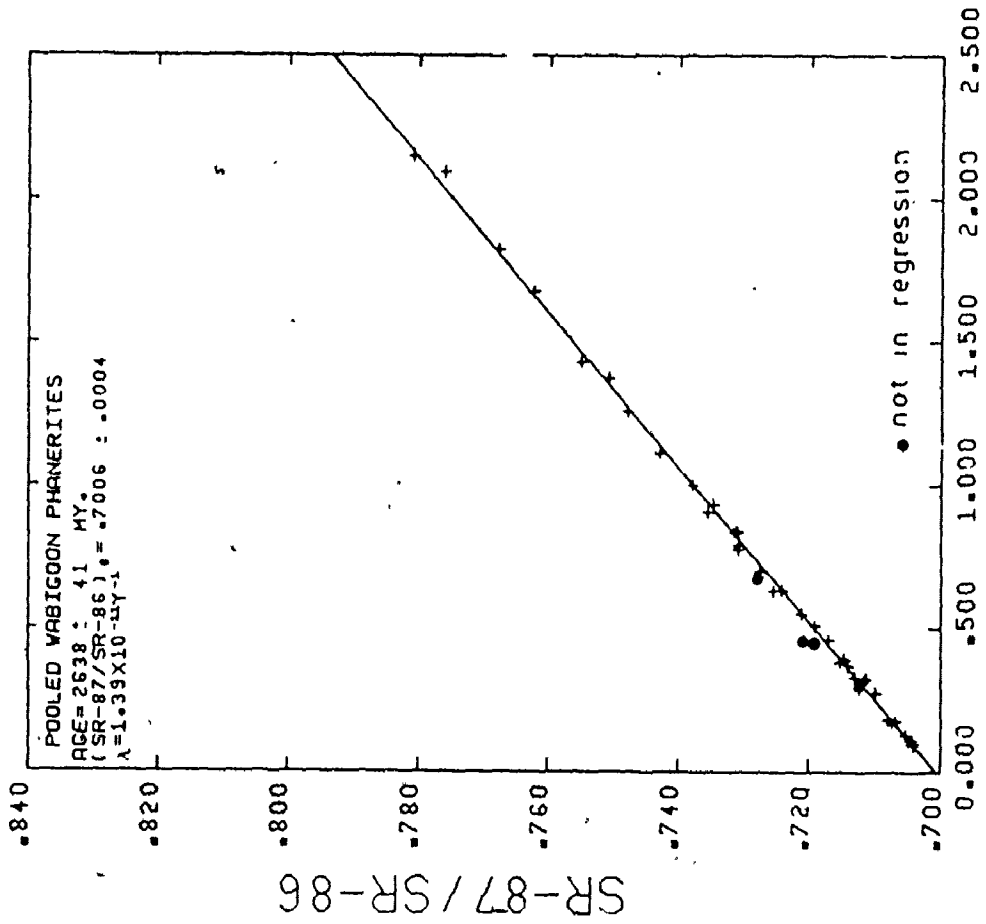
FIGURE 4.11 COMPOSITE WHOLE-ROCK Rb/Sr
"ISOCRON" PLOT (YORK I) BASED
ON 39 GRANITOID SAMPLES
FROM 7 PLUTONS OF THE
WABIGOON BELT. SAMPLES
NOT NECESSARILY COGENETIC
THUS NOT AN ISOCRON
SENSU STRICTO. 95%
CONFIDENCE LEVELS FOR
REGRESSION DO NOT BRACKET
ALL AGE AND INTERCEPT
ESTIMATES OF INDIVIDUAL
PLUTON ISOCHRONS.

FIGURE 4.12 COMPOSITE WHOLE-ROCK Rb/Sr
"ISOCRON" PLOT (YORK I)
SIMILAR TO FIGURE 4.11
BUT WITH 2 HIGHEST POINTS
REMOVED. LINEAR REGRESSION
HAS BEEN ONLY SLIGHTLY
MODIFIED.



RB-87/SR-86

FIGURE 4.11



RB-87/SR-86

FIGURE 4.12

the event. The error estimates for the pooled isochron should bracket the time of this event.

Fairbairn and Hurley (1969) presented a similar pooled plot for 200 granitoid whole-rock Rb/Sr analyses from the Northern Appalachian. Their data produced a scatter diagram enveloped by reference isochrons of 227 m.y. and 608 m.y. Two possible sources for the scatter were proposed: later migrations of Rb and/or Sr, or discrete episodes of plutonism and metamorphism over a span of time. They preferred to conclude that the granitoids of the Northern Appalachian were emplaced as a series of episodes each generating its own isochron. The bounding isochrons for the scatter diagram then bracket the beginning and end of orogenic activity in this ancient orogenic belt. A similar scatter diagram was presented for the Western Liberia Province (northern Guayana Shield and Western Liberia) with data enveloped by reference isochrons of 3,400 m.y. and 2,700 m.y.

A comparison of the above published scatter diagrams with our pooled Wabigoon plot suggests that individual episodes of granitoid magmatism cannot be distinguished in Wabigoon. The Wabigoon plot shows a much greater colinearity of points than either the Appalachian or the Liberian scatterchron, although the areal representation is of the same magnitude. This suggests that the Wabigoon plot is a pooling from coeval or near coeval plutons with similar low $(^{87}\text{Sr}/^{86}\text{Sr})_i$ provenance.

A composite isochron with strong linear correlation similar to the Wabigoon plot was generated by Van Schmus, Thurman and Peterman (1975) for diverse lithologies from Wisconsin. The composite regression yielded an apparent age of: $1,653 \pm 20$ m.y. ($R_0 = 0.7039 \pm 0.0011$) (York I of Brooks et al., 1972) which conflicted with $1,800 \pm 30$ m.y. zircon ages for the same units. These authors considered that low-grade regional metamorphism had reset the Rb/Sr systematics. No such metamorphic overprint is evident for the Wabigoon - and furthermore, the author cannot envisage how such whole-scale resetting could generate strong linear arrays on composite isochrons. The Wabigoon composite plot is considered to reflect primary Rb/Sr "clocks". The estimated age is considered to reflect a single granitoid episode spanning a duration contained within the error limits.

Aplites, Felsites and Pegmatites:

Aplite and felsite samples with high Rb/Sr ratios have often been reported to plot below an isochron defined by cogenetic phanerites bearing lower Rb/Sr ratios (Brooks et al., 1972). A "dropping off" in the age trend for high Rb/Sr rocks has also been reported for felsic volcanics (Fairbairn and Hurley, 1969; Page, 1976). The Coldbrook group of volcanics in New Brunswick "shows a plot of points that has a marked curvature and which could be interpreted as ranging in age

from 405 to 777 m.y. depending on which part of the plot is used" (Fairbairn and Hurley, 1969).

Likewise, Page (1976) found that rhyodacites and dacites from Leichardt metavolcanics carry apparent Rb/Sr isochron ages from $1,840 \pm 36$ m.y. to 1,690 m.y. with younger isochrons showing higher initial ratios. U-Pb concordia plots of zircons carry an upper intercept at $1,865 \pm 5$ m.y. compatible with the oldest Rb/Sr isochron. The validity of using high Rb/Sr samples on any isochron plot must be tested in view of this "dropping off" effect.

In the case of the granitoid isochrons presented in the previous pages, several of the plutons (Burditt Lake Stock, Ryckman Lake Stock, Taylor Lake Stock) carry a narrow range in Rb/Sr necessitating the use of high Rb/Sr deuteritic phases of aplite or felsite to define the slope.

Aplites and aplite-pegmatites from the Burditt, Ryckman and Flora Lake Stocks give a pooled isochron with MSWD = 1.21, and York I parameters significantly lower in age and higher in intercept from that of the phanerite-aplite plots (Table 4.2, Figure 4.13).

The higher initial ratio is predicted from the reported trend for high Rb/Sr volcanics (Fairbairn and Hurley, 1969) if we accept the conclusion that the aplitic isochron has been rotated towards a lower age. In Figure 4.14 however the elimination of Flora Lake sample 27 yields a regression with

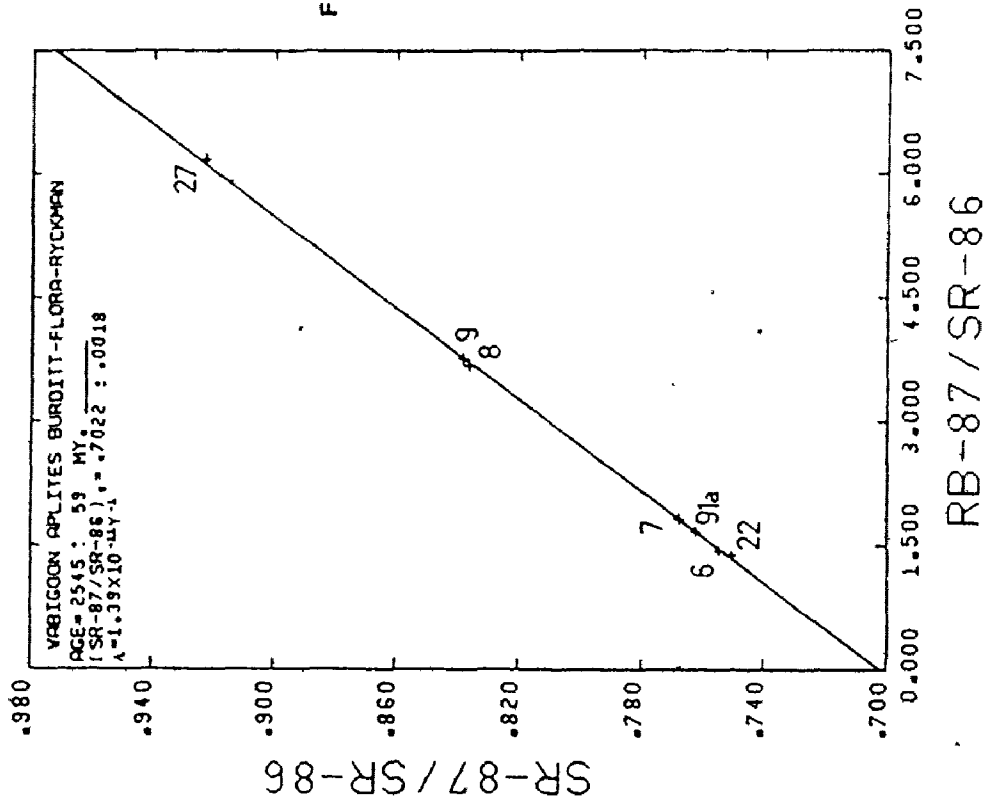


FIGURE 4.13

COMPOSITE WHOLE-ROCK Rb/Sr
 "ISOCRON" PLOT (YORK 1) BASED
 ON 7 APLITE AND APLITE-PEGMATITE
 SAMPLES FROM THREE PLUTONS
 WITHIN THE WABIGOOON BELT.
 NOT NECESSARILY COGENETIC THUS
 NOT AN ISOCRON SENSU STRICTO.
 SAMPLES FROM:

- RYCKMAN LAKE STOCK (22,91a)
- FLORA LAKE STOCK (27)
- BURDITT LAKE STOCK (6,7,8,9)

R

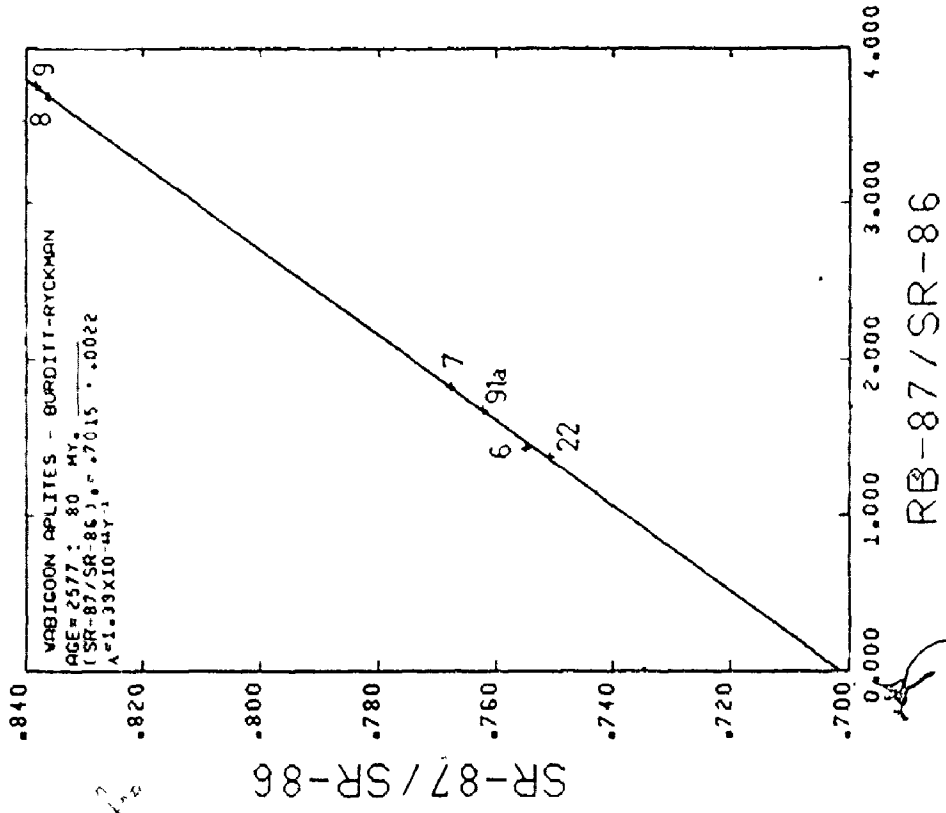


FIGURE 4.14 COMPOSITE WHOLE-ROCK Rb/Sr "ISOCHRON" PLOT FOR APLITES AND APLITE-PEGMATITES FROM WABIGOOON BELT. SAMPLES AS FOR FIGURE 4.13 EXCLUDING F27. SAMPLES NOT NECESSARILY COGENETIC THUS NOT AN ISOCHRON SENSU STRICTO. COMPARISON WITH FIGURE 4.13 SHOWS F27 SUFFERED "DROPPING OFF" EFFECT.

age and intercept closer to the estimate given by the aplite-phanerite plots. Sample F27 appears to illustrate the "dropping off" effect at the high end of the isochron - but the remaining aplitic and pegmatitic samples show no serious deviation. This conclusion confirms our previous comparisons of the Flora Lake aplite and aplite-phanerite regressions.

The author concludes that high Rb/Sr samples are useful for expanding the isochron plot, but are best used in pairs or more and nevertheless remain suspect of open system behaviour. Resultant isochrons are minimum age estimates, but rotation can be considered minimal or absent if intercepts are low.

4.3.3 Syntectonic Batholithic Complexes: The Rainy Lake Dome

Introduction

The narrow range of Rb/Sr isochron ages reported here for the late- to post-tectonic granitoids of the Wabigoon Belt, prompted the author to compare these with ages from batholithic terrain mapped as "syntectonic". The implied hiatus between formation of the stocks intrusive into supracrustals and the syntectonic complexes has never been isotopically tested for the Wabigoon Belt. No Rb/Sr isochrons are available for the batholithic regions.

The region selected for this comparative study is the western edge of the Rainy Lake batholithic complex, which was mapped by Blackburn (1976) and is currently under detailed study

by Longstaffe et al. (1977) and Sutcliffe (1977). Isotopic analyses are presented in Table 4.1 from each of three subdivisions of the batholithic complex as reported by Longstaffe et al. (1977): the Footprint Gneiss, the Northwest Bay Complex and the Jackfish Lake Complex. Rock powders and elemental Rb/Sr analyses were supplied by F. Longstaffe (personal communication) and therefore the sample numbers of Table 4.1 match the location numbers of Figure 34.1 of Longstaffe et al. (1977). These authors should be consulted for information on the lithology and chemistry of the units.

Blackburn (1976) considered the gneisses and migmatites of the Footprint Lake area to be gradational and coeval with syenodioritic rocks of the Jackfish Lake Complex. Longstaffe et al. (1977) found contact breccias and dioritic apophyses that demonstrate the Jackfish Lake Complex to be younger. Sutcliffe (1977) agreed and proposed that a crescent shaped syenodioritic sheet wedged its way along the greenstone-gneiss interface. The intrusive position of the Northwest Bay Complex could not be determined due to masking by the Quetico Fault. Regardless of the stratigraphic relationships, the batholithic complex as a whole is considered by Blackburn (1976) to be the product of a plutonic and deformational event that predated the emplacement of late-Kinematic stocks such as the Burditt Lake body.

Rb/Sr Whole-Rock Isochrons: Lake Despair Area

Ten samples representative of all three phases of the Rainy Lake Batholithic Complex are colinear (Figure 4.15) to yield York I parameters of:

$$2,616 \pm 66 \text{ m.y. } (R_0 = 0.7012 \pm 0.0005) \text{ with MSWD} = 1.15$$

(Table 4.3)

One sample (F103) deviates from linearity only slightly beyond expected analytical error. Regressions employing this sample are discussed in section 4.5 on errorochrons and pseudoisochrons. Two high Rb/Sr samples from Northwest Bay control the slope for the Rainy Lake plot. Separate regressions for each phase result in much larger error estimates due to narrow Rb/Sr spread or few samples (Table 4.3, Figures 4.16 to 4.18). The resultant York I age estimates show a progressive increase:

2,572 ± 113 m.y.	Northwest Bay Complex
2,646 ± 291 m.y.	Jackfish Lake Complex
2,805 ± 362 m.y.	Footprint Lake Gneiss

This progressive increase in model age is compatible with field observations, but in view of the large error overlap, and in view of colinearity on the pooled Rainy Lake plot, the progression is not considered significant.

If the high Rb/Sr samples from the Northwest Bay Complex have suffered a "dropping off" effect as reported for the aplite of Flora Lake, then the pooled isochron for the Rainy

TABLE 4.3 ISOCRON PARAMETERS (REGRESS OF BPOOKS ET AL 1972)
 RAINY LAKE BATHOLITHIC COMPLEX, LAKE OSPAIR AREA

MODEL	TEST	AGE	ERROR 2 SIGMA	INITIAL RATIO	ERROR 2 SIGMA
* RAINY LAKE BATHOLITH (24,110,29,9,26,5,7,110,66,129)					
MCINTYRE I	MSWD= 1.15	2617	61 MY	.7012	.0005
YORK I		2616	66 MY	.7012	.0005
YORK II	S= 1.38	2614	67 MY	.7012	.0006
WENDT I	SCSO= 0.85	2623	61 MY	.7012	.0009
WENDT II	SCSO= 1.00	2614	59 MY	.7012	.0005
NORTHWEST BAY COMPLEX (29,66,129)					
MCINTYRE I	MSWD= 1.44	2572	44 MY	.7019	.0012
YORK I		2577	111 MY	.7019	.0016
YORK II	S= 1.15	2574	44 MY	.7019	.0014
WENDT I	SCSO= 0.96	2571	41 MY	.7019	.0012
WENDT II	SCSO= 1.36	2572	41 MY	.7019	.0012
JACKFISH LAKE COMPLEX (24,26,110)					
MCINTYRE I	MSWD= 0.83	2646	313 MY	.7009	.0009
YORK I		2646	291 MY	.7009	.0008
YORK II	S= 0.91	2645	320 MY	.7009	.0009
WENDT I	SCSO= 0.01	2631	320 MY	.7009	.0009
WENDT II	SCSO= 0.91	2645	308 MY	.7009	.0009
FOOTPRINT LAKE GNEISS (3,5,7,110)					
MCINTYRE I	MSWD= 1.43	2801	303 MY	.7002	.0017
YORK I		2805	167 MY	.7002	.0021
YORK II	S= 1.19	2801	101 MY	.7002	.0019
WENDT I	SCSO= 0.93	2791	301 MY	.7002	.0017
WENDT II	SCSO= 1.19	2801	290 MY	.7002	.0017
POOLED FOOTPRINT + JACKFISH (24,110,9,26,5,7,110)					
MCINTYRE I	MSWD= 0.66	2715	157 MY	.7007	.0007
YORK I		2715	145 MY	.7007	.0007
YORK II	S= 0.92	2713	156 MY	.7007	.0008
WENDT I	SCSO= 0.74	2698	154 MY	.7007	.0007
WENDT II	SCSO= 0.92	2713	150 MY	.7007	.0007

LEGEND AS FOR TABLE 4.2 SAMPLE NUMBERS ABBREVIATED.

BLANKET ERROR (8JRB/86SR)= 0.01 , (87SR/86SR)= 0.065 (PCT)

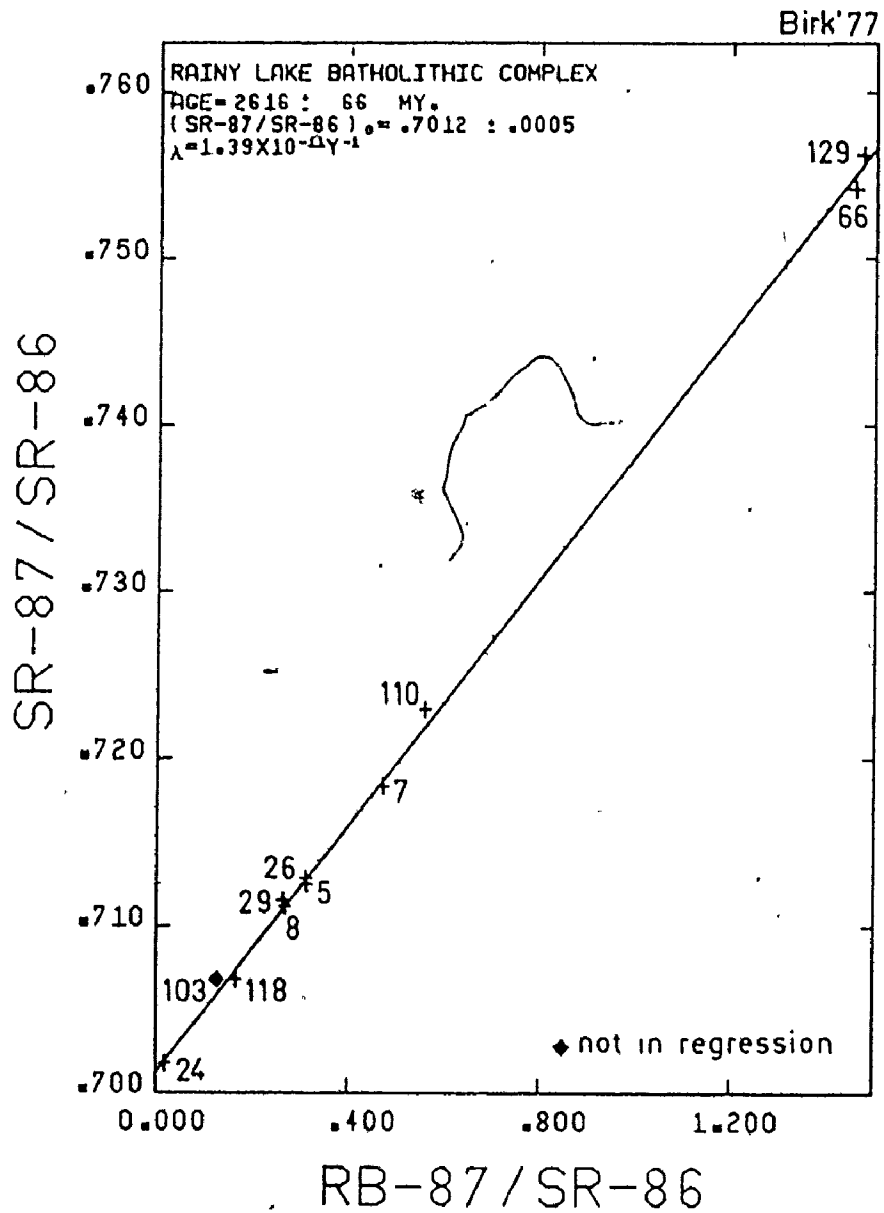


FIGURE 4.15 COMPOSITE WHOLE-ROCK Rb/Sr ISOCHRON (YORK I) FOR THREE PHASES OF THE RAINY LAKE BATHOLITHIC COMPLEX. HIGH Rb/Sr SAMPLES FROM NORTHWEST BAY (66, 129) DOMINATE THE SLOPE OF THIS 10 POINT REGRESSION AND DICTATE A MINIMUM EMPLACEMENT AGE.

FIGURE 4.16 WHOLE-ROCK Rb/Sr YORK I PLOT
FOR NORTHWEST BAY GRANITIC COMPLEX
OF THE RAINY LAKE BATHOLITH.
THE THREE SAMPLES DEFINE A
TWO CLUSTER AGE REFERENCE
LINE (NOT AN ISOCHRON SENSU STRICTO)



FIGURE 4.17 WHOLE-ROCK 3 POINT Rb/Sr
ISOCHRON (YORK I) FOR
JACKFISH LAKE GRANITOID COMPLEX
OF THE RAINY LAKE BATHOLITH.
LARGE ERROR ESTIMATES
REFLECT SPARSE DATA AND
NARROW Rb/Sr RANGE.

S

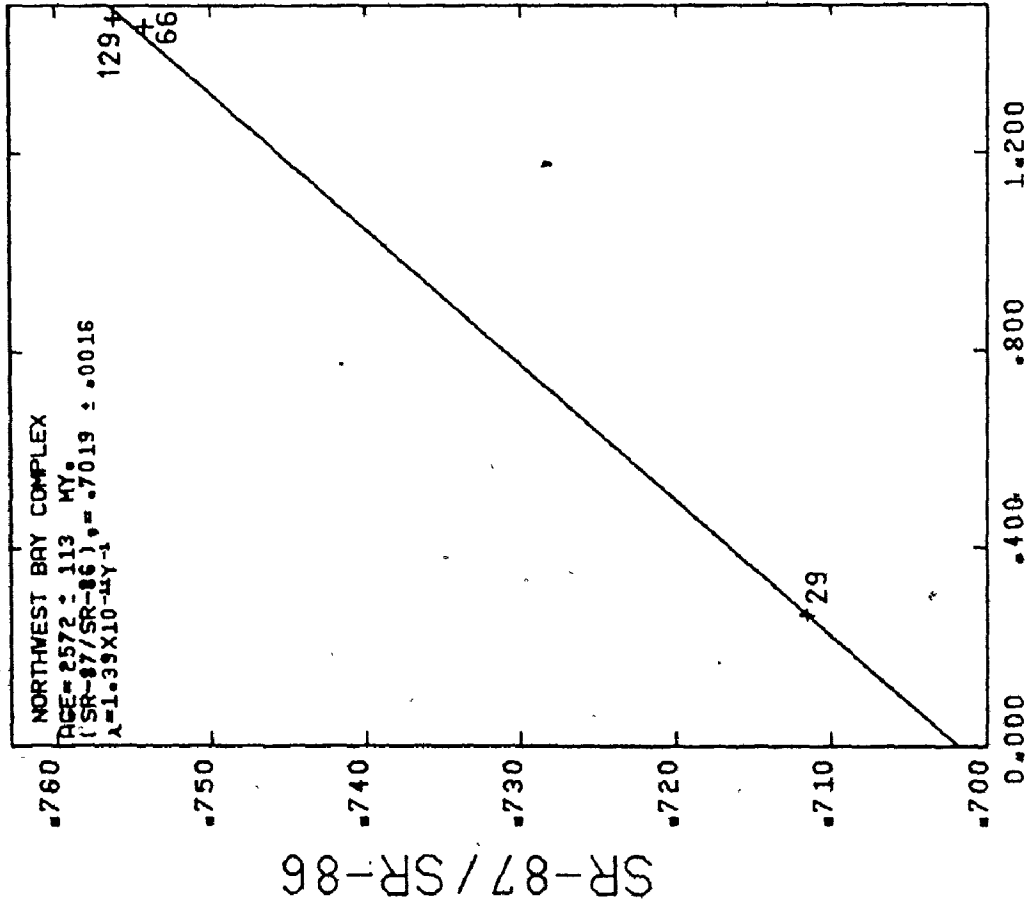


FIGURE 4.16

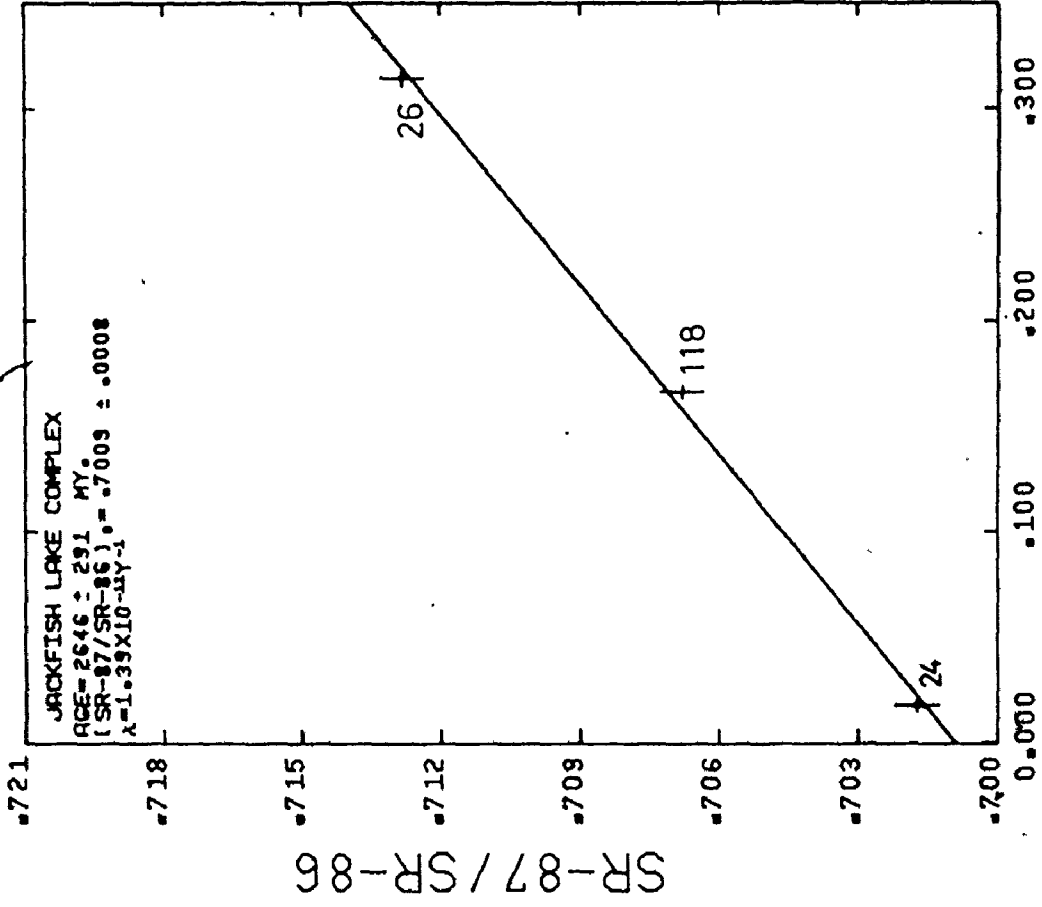


FIGURE 4.17

RB-87 / SR-86

RB-87 / SR-86

FIGURE 4.18 WHOLE-ROCK 4 POINT Rb/Sr
ISOCHRON (YORK I) FOR
FOOTPRINT LAKE GNEISS
OF THE RAINY LAKE BATHOLITH.
LARGE ERROR ESTIMATES
REFLECT NARROW Rb/Sr RANGE

FIGURE 4.19 COMPOSITE 7 POINT WHOLE-ROCK
Rb/Sr ISOCHRON (YORK I) FOR
FOOTPRINT AND JACKFISH
PHASES OF THE RAINY LAKE
BATHOLITHIC COMPLEX. SIMILAR
TO FIGURE 4.15 BUT OMITTING
NORTHWEST BAY SAMPLES (66, 129, 29)
DEMONSTRATES THAT HIGH Rb/Sr
SAMPLES HAVE NOT SUFFERED
NOTICABLE "DROPPING OFF".

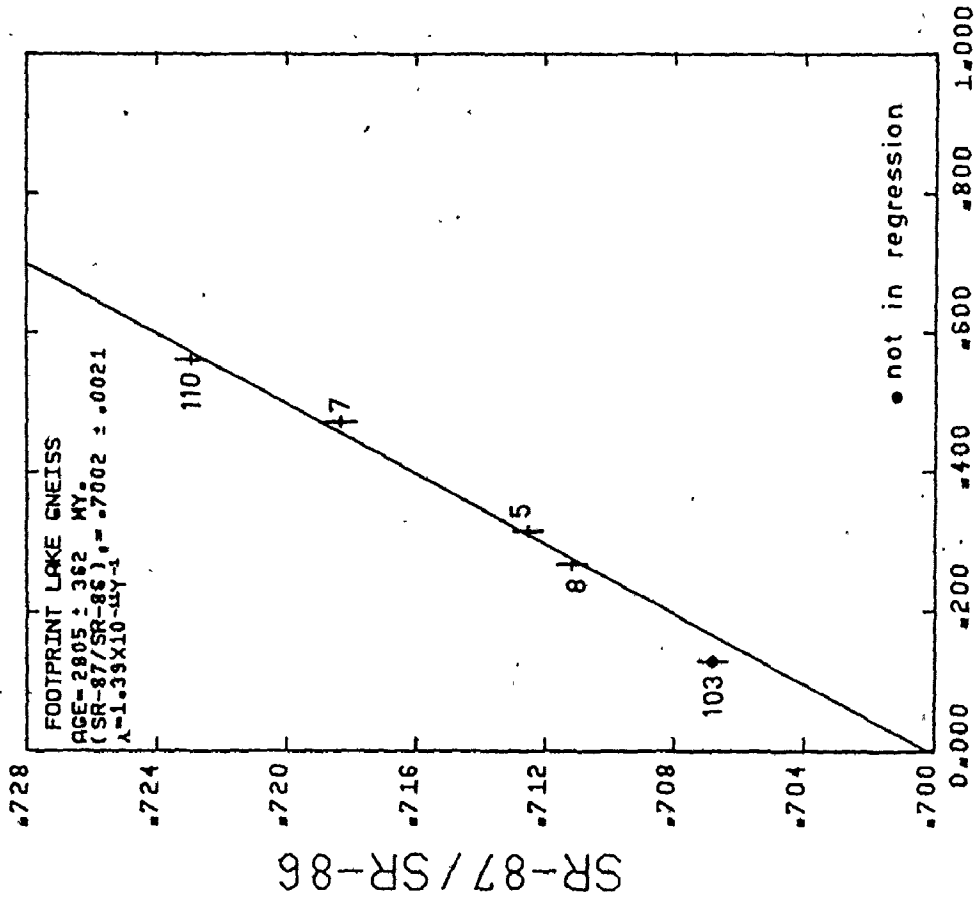


FIGURE 4.18

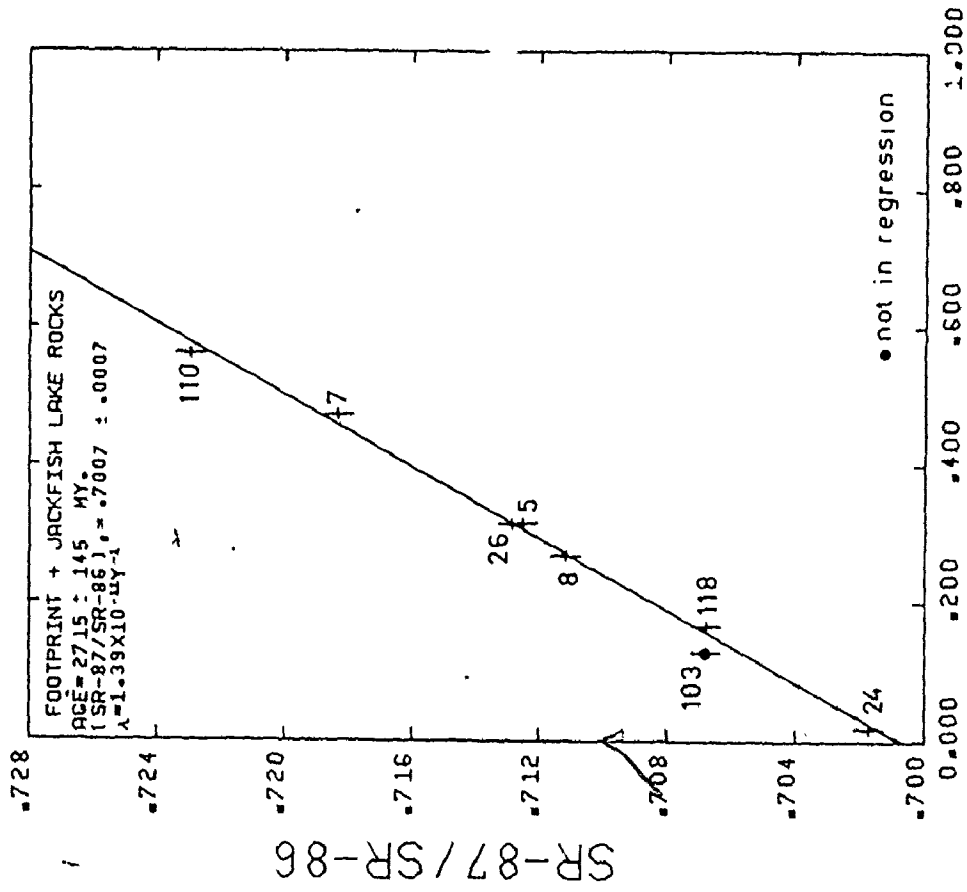


FIGURE 4.19

RB-87/SR-86

RB-87/SR-86

Lake Batholithic Complex sets a minimum age. Pooling of samples from Jackfish Lake and Footprint Lake results in a good fit (MSWD = 0.86) York I isochron of:

2,715±145 m.y. (Table 4.3, Figure 4.19).

Overlap of error limits between the Jackfish-Footprint-Northwest Bay pooled regression and the Jackfish-Footprint pooled regression suggests that any "dropping off" effect on Northwest Bay samples could not have been severe. The author therefore concludes that the Rb/Sr isochron age of the synkinematic Rainy Lake Batholith which flanks the Wabigoon Belt, is similar to the Rb/Sr isochron ages of the late- or post-kinematic stocks intrusive into the Wabigoon Belt.

Ancient Granitoids of Minnesota and Ontario

The gneissic and migmatitic nature of phases of the Rainy Lake Batholithic Complex (Blackburn, 1976) suggest a comparison with gneissic rocks to the south for which remarkably older radiometric ages have been proposed. Goldich et al. (1970) presented a series of Rb/Sr plots for the Morton and Montevideo Gneisses of Southwestern Minnesota carrying reference isochrons ranging in age from 3,800 m.y. to 2,650 m.y. The oldest slope was based on one sample each from the Morton and Montevideo Gneiss (taken 54 km. apart) and an assumed initial ratio of 0.700. Goldich and Hedge (1974) reported

seven whole-rock analyses for the Montevideo Gneiss of which five gave a least squares calculation of: $3,950 \pm 70$ m.y. (2σ) $R_0 = 0.698 \pm 0.004$. Since no evidence was available to justify removal of the two remaining data points, Farhat and Wetherill (1975) recalculated this data to yield a best fit: $3,460 \pm 370$ m.y. (2σ) for the Montevideo Gneiss (7 points). The author carried out his own recalculation using REGROSS and obtained York I parameters of: $3,475 \pm 275$ m.y. (2σ) $R_0 = 0.7042 \pm 0.0026$ (7 points): however, an MSWD of 14.64 clearly demonstrates the incompatibility of this data for linear regression.

In their interpretation, Farhat and Wetherill (1975) pointed out:

"...In conditions of partial re-equilibration it is possible to obtain apparent ages which could be either too old or too young ... there is no reason to believe that widely separated samples represent anything more than individual points on different local metamorphic isochrons, and that their colinearity may well be fortuitous and the age so indicated erroneous." (p.721)

To demonstrate their points, Farhat and Wetherill (1975) analysed multiple samples from individual outcrops (2 m. size). Seven whole-rock analyses from one grey and red banded outcrop of the Montevideo Gneiss yielded an isochron with parameters:

$2,472 \pm 44$ m.y. (2σ) $R_0 = 0.7121 \pm 0.0008$ (2σ)

In reply to this criticism, Goldich and Hedge (1975) revised their previous data to a 10 point pooled whole-rock isochron for the Montevideo Gneiss with estimates (but no published analyses):

$$3,000 \pm 90 \text{ m.y.} \quad \text{and} \quad R_0 = 0.7065 \pm 0.0016 \text{ (95\% confidence)}$$

This is an 800 m.y. reduction from previous age estimates - but without the raw data to evaluate - even this isochron cannot be taken sensu stricto.

Based on zircon data (Goldich et al., 1970) and the high initial ratio of their 2,472 m.y. isochron, Farhat and Wetherill (1975) concluded that the rocks are of uncertain age, probably greater than 3,100 m.y., and have suffered metamorphic re-equilibration at 2,472 \pm 44 m.y.

Hedge (1976) suggested that the Montevideo Gneiss is a hybrid rock composed of volcanogenic biotite gneiss 3,700 \pm 100 m.y. old (grey bands) injected lit-par-lit by a 3,000 m.y. old leucogranite (red bands). The hybrid Rb/Sr systematics were further complicated by metamorphic resetting by a 2,600 m.y. granitic event.

Whether such a complex hypothesis is necessary to account for the Rb/Sr isotopic pattern is questionable. The fact remains that for the Morton and Montevideo Gneisses, none of the published "age" lines with slopes greater than 2,650 m.y. can qualify as an isochron sensu stricto. Zircon data alone remains

to suggest 3,000 m.y. or older ages.

Although the evidence is no longer convincing that the Minnesota River Valley rocks are equivalent in age to the 3.7 b.y. gneisses of Greenland, there is sufficient zircon and Rb/Sr evidence to suspect ages older than obtained in this study for the Rainy Lake Batholithic Complex. The Minnesota Valley units may form a southern equivalent to the English River Gneiss Belt. Krogh et al. (1976) have obtained a U/Pb zircon age of $2,660 \pm 20$ m.y. from a granitic diapir intruding gneisses of the Belt which yielded $3,008 \pm 5$ m.y. zircons. If the Minnesota River Valley gneisses also originated at 3.0 b.y. this has important implications for the origin of the alternating greenstone-gneiss belt tectonics of the Superior Province. Morey and Sims (1976) proposed that the Wawa Belt greenstones accumulated adjacent to a pre-existing sialic protocontinent now exposed as granulite gneisses at Montevideo. The 2.6 b.y. Wabigoon Belt may likewise have accumulated next to 3.0 b.y. protocontinent towards the north. Significant for this model is the fact that gneissic and migmatitic terrain occurs in both the "older" gneissic belts and in the batholithic complexes of the "younger" belts.

4.4 STATISTICAL EVALUATION OF ISOCHRONS

4.4.1 Testing Differences Between Isochrons

Introduction

Although the confidence limits of two isochrons may overlap, it is still possible for the ages and initial ratios to be statistically distinct (Turek, 1966). Significant differences between the gradients or intercepts of the two isochrons must be demonstrated by a pooled variance calculation.

If S_1 and S_2 are two sample statistics with approximately normal sampling distributions, confidence limits for the differences of the sample parameters are given by:

$$S_1 - S_2 \pm z_c \sqrt{\delta_{s_1}^2 + \delta_{s_2}^2} \quad (\text{Spiegel, 1961})$$

where, S_1, S_2 : sample or population parameters;

$\delta_{s_1}, \delta_{s_2}$: standard deviations;

z_c : confidence coefficient

(assuming samples are independent).

For this study, if S_1 and S_2 are slope or intercept of isochron 1 and 2, respectively, then the best available estimate of standard deviation are the confidence intervals from the REGROSS regression models. Rb/Sr work relies on small sample size, therefore the approximation to normal sample distribution is poor and a better estimate is a "Students-T" distribution.

For isochron comparison a confidence coefficient T_c is calculated

such that:

$$z_c \approx T_c = \frac{{}^*s_1 - {}^*s_2}{\sqrt{{}^*\delta_{s_1}^2 + {}^*\delta_{s_2}^2}}$$

where, ${}^*s_1, {}^*s_2$: slope or intercept of isochron 1 and 2
(REGROSS models)

${}^*\delta_{s_1}^2, {}^*\delta_{s_2}^2$: estimated standard deviations (REGROSS
models)

T_c has a "Students-T" distribution with K degrees of freedom given by the relation:

$$\frac{[{}^*\delta_{s_1}^2 + {}^*\delta_{s_2}^2]^2}{K} = \frac{{}^*\delta_{s_1}^4}{N_1 - 2} + \frac{{}^*\delta_{s_2}^4}{N_2 - 2}$$

(modified after McIntyre et al., 1966)

where, N_1, N_2 : number of data points for isochrons 1 and 2.

Differences: Wabigoon Isochrons

Table 4.4 compiles student-T tests on the slopes and intercepts for pairs of York I regressions from Table 4.2. Only the best estimates of isochrons sensu stricto were taken for each sample population. Included in the testing are the

Table 4.4
 Wabigoon internal granitoid plutons: Pooled variance test for isochron differences using student's-T; York 1 parameters.

	Rurditt Lake Stock (9)	Flora Lake Stock (5)	Ryckman Lake Stock (7)	Taylor Lake Stock (5)	Saax Lake Porphyry (4)	Bears Passage Stock (6)	Ottertail Lake Stock (10)	Aplites (6)	Wabigoon Pooled (39)
Rurditt Lake Stock (9)	2.31 (1.73) 7.9	2.43 (0.99) 6.2	2.24 (0.22) 9.6	2.23 (1.49) 10.0	2.39 (0.89) 6.7	2.63 (1.34) 4.7	2.17 (2.00) 12.7	2.40 (0.53) 6.6	2.12 (0.75) 16.4
Flora Lake Stock (5)		2.33 (0.67) 7.5	2.68 (0.07) 4.4	2.68 (0.07) 4.4	2.60 (1.74) 4.8	2.54 (0.84) 5.2	2.22 (2.57) 10.2	2.37 (1.23) 6.9	2.56 (0.48) 5.0
Ryckman Lake Stock (7)			2.36 (0.92) 7.0	2.36 (0.92) 7.0	2.37 (0.95) 7.0	2.53 (1.19) 5.5	2.16 (1.96) 13.0	2.30 (0.64) 8.1	2.29 (0.36) 8.3
Taylor Lake Stock (5)				2.33 (1.19) 7.6	2.79 (2.61) 4.0	2.70 (0.85) 4.5	2.23 (3.13) 10.1	2.55 (1.52) 5.1	2.16 (0.85) 13.3
Saax Lake Porphyry (4)					2.58 (3.33) 4.9	2.65 (1.68) 4.6	2.23 (2.27) 6.0	2.48 (1.79) 5.7	2.52 (1.10) 4.4
Bears Passage Stock (6)					2.56 (1.64) 5.1	2.61 (0.84) 4.3	2.45 (2.27) 6.0	2.45 (1.51) 5.9	2.68 (1.10) 4.4
Ottertail Lake Stock (10)					2.34 (0.12) 7.4	2.71 (0.34) 4.3	2.60 (1.67) 4.8	2.22 (1.18) 10.5	2.19 (2.62) 11.4
Aplites (6)					2.63 (0.51) 4.6	2.73 (0.92) 4.2	2.33 (0.94) 7.6	2.65 (0.15) 4.5	2.49 (1.05) 5.6
Wabigoon Pooled (39)					2.17 (0.69) 12.7	2.14 (0.81) 14.2	2.69 (0.56) 4.4	2.72 (0.74) 4.2	

intercept

Legend:

significant difference at 95% confidence
 student's-T
 calculated students T
 degrees of freedom

* samples not independent; test not strictly valid.

39 point Wabigoon pooled regression and the 6 point aplite pooled regression.

The Ottertail Lake pluton shows an isochron gradient significantly different from that for the Flora Lake, Taylor Lake and Wabigoon pooled regression. This supports the suggestion by Birk and McNutt (1977) that the granitoids along the Quetico-Wabigoon interface may post-date the Wabigoon plutonism. On the other hand, the initial ratio for Ottertail is also statistically different at 95% confidence from the Wabigoon pooled regression and Ryckman, Taylor and Esch plots. This higher ratio allows support for the suggestion from Peterman et al. (1972) that the total rock system suffered moderate metamorphic isotopic equilibration.

The slopes of all other isochron pairs appear to be coincident. Initial ratios also are indistinct except for Flora Lake samples. Table 4.2 shows that for Flora Lake regressions, the models show a disparity in error estimates. Regression models estimating error from analytical uncertainty show twice the error spread of the York I model which relies on data scatter for error estimation. If larger uncertainties are considered the differences in initial ratios become statistically indistinct for Flora tests.

Differences: Rainy Lake Batholithic Complex

Student-T tests on York I pairs are presented in Table 4.5 for samples from the Lake Despair area. Parameters for the Wabigoon pooled regression are included in the test for comparison. No significant differences were detected at 95% confidence except for Northwest Bay and Jackfish Lake regressions for which statistical control is poor.

4.4.2 Pooling of Isochrons

Introduction

Linear regression of analyses pooled from several distinct sample populations is not valid if gradients and intercepts of the isochrons are statistically distinct. Even if the isochron parameters are coincident, the pooling of samples, not demonstrably cogenetic, hazards violating a basic axiom of the Rb/Sr method. The Wabigoon pooled granitoid isochron (Figure 4.11) should therefore not be taken as an isochron sensu stricto. An alternative estimate of mean age and intercept for several sample populations is provided by pooling individual isochron parameters after weighting for confidence (Turek, 1966). The equations are as follows (modified after Turek, 1966):

Table 45 Rainy Lake Batholithic Complex: Pooled variance test for isochron differences using Students - T ; York I parameters.

	Northwest Bay Complex (3)	Jackfish Lake Complex (3)	Footprint Lake Complex (4)	Jackfish & Footprint (7)	Rainy Lake Pooled (10)	Wabigoon Pooled (39)
	slope					
Northwest Bay Complex (3)	6.41 (4.84) 1.3	3.73 (1.26) 2.4	2.65 (1.60) 4.5	4.86 (0.73) 1.8*	5.22 (0.85) 1.2	
Jackfish Lake Complex (3)	5.89 (1.10) 1.5		3.21 (0.70) 3.0	5.69 (0.44) 1.5*	-1.30 (0.19) 1.1*	-31.0 (0.17) 1.0
Footprint Lake Complex (4)	3.19 (1.29) 3.0	3.53 (0.64) 2.5		3.42 (0.47) 2.7*	4.05 (1.03) 2.1*	4.23 (1.03) 2.0
Jackfish & Footprint (7)	6.31 (1.35) 1.4	3.50 (0.36) 2.6*	3.65 (0.48) 2.4*		2.36 (1.25) 2.1*	2.49 (1.30) 5.6
Rainy Lake Pooled (10)	5.62 (0.86) 1.2*	4.57 (0.34) 1.9*	3.89 (0.91) 2.2*	2.22 (1.07) 10.2*		2.17 (0.07) 12.8
Wabigoon Pooled (39)	-1.06 (1.50) 1.1	6.11 (0.55) 1.4	4.07 (0.44) 2.1	2.29 (0.15) 8.3	2.11 (1.63) 17.4	
	intercept					

at 95 % confidence
 students-T $\xrightarrow{\quad}$ T
 Legend: calculated students T $\xrightarrow{\quad}$ (T_c)
 degrees of freedom $\xrightarrow{\quad}$ K^c

* samples not independent; test not strictly valid.

mean slope or intercept:

$$\bar{s} = \frac{\sum \left(\frac{1}{\sigma_i^2} \cdot s_i \right)}{\sum \left(\frac{1}{\sigma_i^2} \right)}$$

estimated standard deviation for \bar{s} :

$$\sigma_{\bar{s}} = \left[\frac{1}{\sum \frac{1}{\sigma_i^2}} \right]^{1/2}$$

The approximate degrees of freedom K of the pooled mean \bar{s} are given by:

$$K = \frac{\bar{s} \sum \left(\frac{1}{\sigma_i^2} \right)^2}{\frac{\sum \left[s_i \left(\frac{1}{\sigma_i^2} \right) \right]^2}{\sum N_i - 2}}$$

where: $i = 1, 2, 3, \dots$ number of isochrons

\bar{s} = mean slope or intercept

$\sigma_{\bar{s}}$ = mean estimated standard deviation for \bar{s}

s_i = slope or intercept of isochron i

N_i = number of points on isochron i

σ_i = estimated standard deviation for s_i

Pooled Ages and Intercepts

Using the above weighting technique, and York I parameters from REGROSS as tabulated in Tables 4.2 and 4.3, the following pooled ages and initial ratios are obtained:

Table 4.6

Group	Component isochrons (number of points)	Age (2 σ)	Initial Ratio (2 σ)
Rainy Lake Batholithic Complex:	Northwest Bay (3)	2598 \pm 573 m.y.	.7010 \pm .0032
	Jackfish Lake (3)		
	Footprint Lake (4)		
Wabigoon Internal Plutons:	Bears Passage (6)	2616 \pm 43 m.y.	.7006 \pm .0005
	Burditt Lake (9)		
	Esox Lake (4)		
	Flora Lake (5)		
	Ryckman Lake (7)		
	Taylor Lake (5)		
Wabigoon Internal Plutons Including:	Ottertail Lake (10)	2610 \pm 41 m.y.	.7007 \pm .0004
All Granitoids:	Rainy Lake Composite (10)	2620 \pm 62 m.y.	.7008 \pm .0006
	Wabigoon Composite (39)		

For the granitoid plutons intrusive into the Wabigoon Belt, there is no significant difference between results from linear regression of pooled samples (York I: 2,623 \pm 35 m.y., .7007 \pm .0004, Table 4.2) or the pooling of isochrons. The

inclusion or exclusion of the low age Ottertail Lake isochron has little effect on the results of pooling of isochrons.

The pooled results from the Rainy Lake area isochrons carry large errors, reflecting the large errors attached to the 3 point regressions. This points to the need for further work in the Rainy Lake area to develop well defined individual isochrons for the three major phases. A better estimate for average age and intercept is given by the pooled regression (Table 4.3: York I: $2,616 \pm 66$ m.y., $.7012 \pm .0005$).

The pooled age and intercepts obtained from the two composite regressions cannot qualify as a true "average" because the Wabigoon composite regression violates the definition of an isochron sensu stricto (i.e. samples cogenetic). Nevertheless, the data is consistent: whether we pool regressions or regress pooled samples, the isotopic systems suggest that less than about 60 m.y. (68% confidence) were required to produce both the synkinematic batholithic complexes and the late-kinematic granitoid stocks of the Wabigoon Belt. This conclusion coincides with Jahn and Murthy (1975) who suggested for the Vermilion District of the Wawa Belt that volcanic extrusion, granitic intrusion and metamorphism were near-contemporaneous within a time span of 50 million years.

4.5 PROBLEMATICAL PLOTS

4.5.1 Errorchrons

Introduction

Since the earliest application of the isochron method in Rb/Sr geochronology, investigators have been plagued by data points that deviate from colinearity with cogenetic samples. The source of deviation can be attributed to one or more of: analytical error; contamination; sampling error; geological error (metasomatism, endomorphism, metamorphism, non-uniform initial $^{87}\text{Sr}/^{86}\text{Sr}$, etc.). Summaries on this problem include Riley and Compston (1962) - laboratory contamination; Heier and Compston (1969) - metamorphism; Brooks et al. (1972) - analytical error. The treatment of aberrant data has differed with investigator and has depended on the number and degree of deviations.

Data scatter severe enough to hamper linear regression has been reported from several metamorphic complexes (Heier and Compston, 1969; Brueckner, 1973; Pankhurst et al., 1973; Grauert et al., 1974). Under these conditions extensive "geological error" is evoked and metamorphic models replace chronological discussions.

Minor deviations from colinearity have received more varied approaches. Some authors have taken aberrant points to define exclusive isochrons distinct from the main trend (e.g. Goldich et al., 1970; Noiret, Montigny and Allegre, 1972).

U This alternative is eliminated if detailed field work precedes sampling. Other authors have increased the 2σ isochron error estimates to 3σ estimates to accommodate minor geological error (Black et al., 1971). Brooks et al. (1972) summarized the methods by which isochrons can be tested for data scatter in excess of analytical uncertainty. Each of the two-error regression models included in REGROSS (data processing procedure of Brooks et al., 1972) calculate an index by which excess scatter can be measured. The McIntyre I model calculates the mean square of weighted deviates (MSWD); York II calculates a $\frac{\text{residual sum}}{\sqrt{n - 2}}$ (hereafter S); the Wendt I and II models define a sum of chi square (hereafter SCSQ). Under ideal conditions all these indices have an expectation of unity or less for a scatter of data points within experimental error. All three indices have been calculated for the regressions presented in Tables 4.2, 4.3, 4.7 of this study.

As pointed out by Brooks et al. (1972), these indices are expected to be ≤ 1 only if the regression analysis and the assigned experimental errors are based on an infinite number of samples. Some authors define isochrons sensu stricto assuming such ideal statistics (Coleman, 1970; Bidgeon and Hopgood, 1975). This condition is never achieved in Rb/Sr isochron work and therefore the cut-off level defining an "errorchron" (Brooks et al., 1972) from an isochron sensu stricto must be an index somewhat greater than unity. To

compensate for the small-sample statistics, Brooks et al. (1972) proposed use of F-distribution tables and a minimum of 8 Rb/Sr data points with assigned experimental errors based on 25 or more duplicates. The cut-off index would then be 2.50. In practice these procedures are too restrictive. Constant modifications in technique and instrumentation in many laboratories precludes obtaining 25 or more duplicates for every study. Sampling limitations often prevent gathering 8 or more data points per isochron.

del Many authors have opted ~~out~~ for a less rigorous approach to isochrons. Bell and Blenkinsop (1975) considered that for their results: "... any MSWD less than about 5 probably represents a suitable fit of the points to a straight line ...". Farquharson and Richards (1970) treated McIntyre III regressions (geological error recognized in $^{87}\text{Sr}/^{86}\text{Sr}$) as "isochrons", but acknowledged "... some heterogeneity in initial ratio among (their) samples ...". Reed and Zartman (1973) considered McIntyre IV solutions (geological error in both $^{87}\text{Rb}/^{86}\text{Sr}$ and $^{87}\text{Sr}/^{86}\text{Sr}$) as "... probably meaningful to within the stated uncertainty ...". Roddick and Compston (1977) even considered data with an MSWD = 14.5 to be "reasonably well fitted".

In many cases, deviation from linear fit is attributable to one or two aberrant points, while the several remaining data points show good linear correlation. Rather than demote the entire data set to an "errorchron", most investigators have

elected to eliminate the offending points from regression calculations. Improvement of the isochron parameters has been sufficient justification for some investigators (Coleman, 1970; Yanagi et al., 1971; Clemons and Long, 1971; Brooks and Leggo, 1972), while others have blamed the outliers on geological contamination (Baadsgaard and Mueller, 1973), differing $^{87}\text{Sr}/^{86}\text{Sr}$ (Heier et al., 1972, DeLaeter and Blockley, 1972), alteration (Coleman, 1970), inclusion of enclaves (Yanagi et al., 1971), unusually large analytical error (Hurst et al., 1975), etc. Andresen and Heier (1975) dismissed a discordant sample simply for being "petrographically different".

Errorchrons: This Study

Out of 54 samples isotopically analysed in this study, four samples show possible discordancy with their cogenetic suite (Table 4.1). A further two aberrant points were discovered in the published analyses of Peterman et al. (1972) when data from these two studies were pooled. In several cases the deviation from linearity was insufficient to define an errorchron by the method of Brooks et al. (1972), yet removal of the questionable data points improved the isochron parameters significantly.

Table 4.7 presents the output from REGROSS for several of the data sets of Table 4.2 and 4.3, but including outliers. Parameters are included for the geological error models of the

TABLE 4.7 ERRORCHRONS AND PSEUDOISOTHERMS

PARAMETERS FROM REGRESS OF BROOKS ET AL (1972)
 ERROR ESTIMATES DO NOT REFLECT 95 PCT CONFIDENCE
 DUE TO POSSIBLE ANALYTICAL OR GEOLOGICAL ERROR.
 PROPOSED OUTLIERS MARKED BY *
 LEGEND AS FOR TABLE 4.2

ERRORCHRONS

MCINTYRE II = ERROR IN X, MCINTYRE III = ERROR IN Y.
 * = PREFERRED MODEL ACCORDING TO MCINTYRE REGRESSION.

MODEL	TEST	AGE	ERROR > SIGMA	INITIAL RATIO	ERROR > SIGMA
WABIGOOY POOLED GRANITIODS (INCLUDING T40,OT4,TR2)					
MCINTYRE I	MSWD= 3.13	2615	25 MY	.7009	.0073
MCINTYRE II	MSWD= 1.30	2655	65 MY	.7005	.0074
MCINTYRE III *	MSWD= 1.00	2501	36 MY	.7010	.0075
YORK I		2618	45 MY	.7009	.0076
YORK II	S= 1.87	2617	25 MY	.7009	.0073
WENDT I	SCSO= 1.45	2623	25 MY	.7008	.0073
WENDT II	SCSO= 1.47	2618	24 MY	.7009	.0073
BLANKET ERROR (87RB/P6SP) = 0.01 , (87SR/P6SP) = 0.065 (PCT)					
REARS PASSAGE STOCK (2,1B,4A,3,43,KA35B,5)					
MCINTYRE I	MSWD= 2.79	2591	132 MY	.7017	.0014
MCINTYRE II	MSWD= 1.00	2566	297 MY	.7019	.0020
MCINTYRE III *	MSWD= 1.00	2592	201 MY	.7017	.0021
YORK I		2592	224 MY	.7017	.0023
YORK II	S= 1.70	2591	132 MY	.7017	.0016
WENDT I	SCSO= 1.31	2541	132 MY	.7017	.0013
WENDT II	SCSO= 1.70	2591	127 MY	.7017	.0013
BLANKET ERROR (87RB/P6SP) = 0.01 , (87SP/P6SP) = 0.065 (PCT)					
REARS PASSAGE STOCK MINERAL-ROCK (PLAG,KA35B,KSPAR,BI,MUSC)					
MCINTYRE I	MSWD= 9.63	2453	64 MY	.7033	.0011
MCINTYRE II	MSWD= 1.30	2433	193 MY	.7036	.0020
MCINTYRE III *	MSWD= 1.00	2591	145 MY	.6984	.0091
YORK I		2445	203 MY	.7034	.0024
YORK II	S= 3.12	2446	65 MY	.7034	.0017
WENDT I	SCSO= 2.76	2450	66 MY	.7032	.0009
WENDT II	SCSO= 3.12	2447	63 MY	.7034	.0019
BLANKET ERROR (87RB/P6SR) = 0.02 , (87SR/P6SP) = 0.050 (PCT)					
OTTERTAIL LAKE STOCK (1,2,4,3,5)					
MCINTYRE I	MSWD= 4.32	2543	111 MY	.7016	.0019
MCINTYRE II	MSWD= 1.30	2596	266 MY	.7013	.0015
MCINTYRE III *	MSWD= 1.00	2537	229 MY	.7016	.0019
YORK I		2544	230 MY	.7016	.0019
YORK II	S= 2.08	2546	111 MY	.7016	.0011
WENDT I	SOSO= 1.63	2557	113 MY	.7015	.0009
WENDT II	SOSO= 2.08	2544	108 MY	.7016	.0009
BLANKET ERROR (87RB/P6SP) = 0.01 , (87SP/P6SP) = 0.065 (PCT)					
TAYLOR LAKE STOCK (42,13,36,40,57,61)					
MCINTYRE I	MSWD= 2.78	2653	71 MY	.7007	.0007
MCINTYRE II	MSWD= 1.00	2671	133 MY	.7005	.0010
MCINTYRE III *	MSWD= 1.00	2644	98 MY	.7008	.0012
YORK I		2654	116 MY	.7007	.0012
YORK II	S= 1.69	2654	71 MY	.7007	.0010
WENDT I	SCSO= 1.26	2654	63 MY	.7007	.0007
WENDT II	SCSO= 1.69	2654	62 MY	.7007	.0007
BLANKET ERROR (87RB/P6SR) = 0.01 , (87SP/P6SP) = 0.065 (PCT)					
FOOTPRINT GNEISS (SAMPLES 103,8,6,7,110)					
MCINTYRE I	MSWD= 2.30	2593	204 MY	.7015	.0011
MCINTYRE II *	MSWD= 1.00	2611	296 MY	.7019	.0013
MCINTYRE III	MSWD= 1.00	2592	311 MY	.7015	.0016
YORK I		2590	310 MY	.7016	.0016
YORK II	S= 1.51	2590	202 MY	.7015	.0012
WENDT I	SCSO= 1.23	2567	202 MY	.7017	.0010
WENDT II	SCSO= 1.51	2590	195 MY	.7015	.0010
BLANKET ERROR (87RB/P6SR) = 0.01 , (87SP/P6SP) = 0.065 (PCT)					

2 PETERMAN ET AL (1972) TABLE 5. MINERALS FROM KA353.

TABLE 4.7 CONTINUED

PSEUDOISOTHERMS

MODEL	TEST	AGE	ERROR 2 SIGMA	INITIAL RATIO	ERROR 2 SIGMA
RYCKMAN LAKE STOCK ¹ (PHANERITES - 80,6,5,21,60)					
MCINTYRE I	MSWD= 0.02	2230	345 MY	.7012	.0010
YORK I		2230	55 MY	.7012	.0002
YORK II	S= 0.16	2230	345 MY	.7012	.0011
WENDT I	SCSQ= 0.15	2232	346 MY	.7011	.0010
WENDT II	SCSQ= 0.16	2231	335 MY	.7012	.0010

RAINY LAKE BATHOLITHIC COMPLEX (SAMPLES F24 + F103)

MCINTYRE I	MSWD= N/A	3241	851 MY	.7009	.0011
------------	-----------	------	--------	-------	-------

BEARS PASSAGE STOCK (TR2 AND ASSUMED INTERCEPT .7002)

MCINTYRE I	MSWD= N/A	3194	216 MY	.7002	.0009
------------	-----------	------	--------	-------	-------

BLANKET ERROR (87RB/86SR)= 0.01 , (87SR/86SR)= 0.065 (PCT)

1 ONLY YORK I MODEL GIVES PSEUDOCISOTHERM.

McIntyre linear regression method. Since some or all of these regressions may be errorchrons, the associated error estimates carry none of the predictive aspects that characterise confidence intervals of isochrons sensu stricto (Brooks et al., 1972).

A survey of Tables 4.2, 4.3 and 4.7 leads to the following conclusions concerning REGROSS:

- (1) Indices testing colinearity are reduced for their respective regressions when the suspect points are omitted;
- (2) Regressions considered as isochrons sensu stricto (Tables 4.2, 4.3) yield identical or near-identical isochron parameters for the regression models. Addition of the suspect points generates greater disparity between models;
- (3) The indices do not respond to data scatter equally or proportionately. They generally follow the sequence -

$$\text{MSWD (model I)} > S = \text{SCSQ (model II)} > \text{SCSQ (model I)}$$

The third conclusion signifies that a static cut-off level for the indices as recommended by Brooks et al. (1972) is not good discrimination between errorchrons and isochrons. Furthermore, confidence in any cut-off level is dependent on the confidence in the experimental error estimate. Calculation

of indices assumes that all data points carry equal responsibility for the possible geological error, which in practice is rarely the case. Each data set must be independently evaluated and if the indices can be drastically lowered by removal of a small percentage of data, this data must be considered suspect and omitted. An isochron sensu stricto should be insensitive to the removal or addition of a point. This does not mean approval of the extreme approach of Gulson (1972) who rejected 5 out of 10 samples to arrive at an MSWD of 5.9 for perthite granites of Northern Sweden. The discrimination between isochrons and errorchrons has not yet been automated: it is still subject to interpretation.

In the case of the Wabigoon composite regression, the Ottertail Lake Stock and the Taylor Lake Stock, suspect samples do not modify the regression parameters sufficiently to change conclusions - except as to the uncertainty intervals. For the Bears Passage and the Footprint Gneiss regressions, omission of suspect points causes severe modification of isochron parameters. Conclusions based on the regressions are therefore very dependent on the validity of the omissions.

For both the Bears Passage Stock and the Footprint Lake Gneiss, the aberrant whole-rock analyses plot above the preferred isochron. Geological models that have been used to explain high outliers include: "inherited isochrons" (Roddick and Compston, 1977); a different initial $^{87}\text{Sr}/^{86}\text{Sr}$ (Heier et al.,

1972; DeLaeter and Blockley, 1972); geological enrichment in Sr^{87} by contamination or metasomatism (Armstrong and Hills, 1967; Allsopp et al., 1968; Gulson, 1972; Baadsgaard and Muller, 1973). Mafic xenoliths have been reported to plot above the host granitoid isochron (Van Breeman and Dodson, 1972), therefore granitoid samples that contain such xenolithic material may carry high $^{87}Sr/^{86}Sr$ (Yanagi et al., 1971).

A posteriori considerations suggest to the author the following possible reasons for sample discordancies (Table 4.8):

Table 4.8 Cause of Outliers

Sample	Proposed Reason	Evidence
T40	Minor metasomatism	Location on Taylor Lake Fault
TR2	?	
OT4	?	
F103	Metasomatism, loss of Rb	Absence of K-feldspar in mode
RL3766*	?	
Biotite (KA350)*	Alteration, weathering	Chloritized, <1% in mode

*From Peterman et al. (1972), Table 5

4.5.2 Pseudoisochrons

Introduction

A linear array of Rb/Sr isotopic analyses that define an apparent age with no geological significance can be termed a pseudoisochron. Several mechanisms can contribute to the generation of such false plots. Partial metamorphic re-equilibration of isotopes over a region can cause apparent ages that are either too old or too young. Individual points from different local metamorphic isochrons may show fortuitous colinearity and yield a meaningless pseudoisochron (Farhat and Wetherill, 1975; Roddick and Compston, 1977). Lunar chronology on whole-rock and mineral separates has shown that pseudoisochrons can be generated by mixing of end-members. Straight arrays in the Rb/Sr diagram may be simply mixing lines between plagioclase and K-rich phase if mineral separation is incomplete (Birck, Fourcade and Allegre, 1975). Similar mixing lines are recognized in K-Ar isochron work as products of atmospheric argon contamination (Hayatsu and Carmichael, 1977). Brooks and Leggo (1970) suggest that mixing of xenolithic and magmatic Sr could generate a pseudoisochron. Matsuda (1974) discussed the possibility of "virtual isochrons" being generated by constant leaching in an open system.

As the number of samples included in the regression is reduced, the possibility of generating a fortuitous linear array is increased. Likewise the probability for a pseudoisochron improves as the field control during sample collection

diminishes. A plot such as the 4 point Quetico Belt "isochron" of Wanless and Loveridge (1972) may be a pseudoisochron because of the 300 mile sampling traverse. If the number of points used to define the line is reduced to two - or if samples cluster at either extreme of the plot - then colinearity has not been demonstrated and the plot is a reference line which may or may not coincide with a geologically meaningful "age". Several authors have speculated on such reference lines (Goldich, et al., 1970; Noiret et al., 1972; Van Schmus et al., 1977).

Apparent "Old" Ages: This Study

Two point reference lines have been calculated for the outliers from the Bears Passage Stock and the Footprint Lake Gneiss (Table 4.7). Sample TR2 for the Bears Passage Stock was fitted to a line from an assumed intercept of 0.7002. A McIntyre I regression fitted a slope of $3,194 \pm 216$ m.y. This reference age is at variance with the regional chronology and the stratigraphic position of the stock (Late-kinematic). The outlier nature of sample TR2 is confirmed.

A similar speculative regression was performed using outlier F103 and the lowest Rb/Sr sample (F24) from the Rainy Lake Batholithic Complex. McIntyre I defines an apparent age of: $3,241 \pm 851$ m.y. This age is less easily dismissed as a pseudoisochron because of the complex lithologies included in

1124
the Rainy Lake study. In the absence of supportive^{ing} evidence and because of the excellent colinearity of other Rainy Lake samples on a 2.6 b.y. slope, sample F103 is considered an outlier, and the 3,241 m.y. reference line is considered a pseudoisochron.

The author wishes to emphasise however, that these apparent old ages obtained by regression of spurious data are no less founded on fact than the 3.7 b.y. speculations of Goldich et al. (1970) or Van Schmus et al. (1977). The current popularity of "old" rocks should not influence data processing.

Apparent "Young" Ages: This Study.

Brooks et al. (1972) and Gibbins and McNutt (1975) observed that the regression models of REGROSS give essentially the same slope, intercept and error parameters if all data scatter is attributable to experimental error. Brooks et al. (1972) concentrated their study on the identification of errorchrons by data scatter that exceeds experimental error. They did not explore the effect of data showing colinearity better than predicted from known analytical error.

As data scatter approaches zero, the isochron errors estimated by York I tend towards zero, while errors estimated by the other regression models continue to reflect analytical uncertainty. This results in disparities between the model parameters and may produce a pseudoisochron. Figure 4.20;

Table 4.7 shows a 5 point data regression for the Ryckman Lake Stock - identical to that of Table 4.2, but omitting two high Rb/Sr dyke samples. The indices calculated by the regression models are extremely low - reflecting the excellent linear fit, but the age estimates differ by 379 m.y. from the Table 4.2 estimate. The felsic dyke samples did not suffer a "dropping off" effect since they plot above rather than below the phanerite isochron.

Compared to the other models, the 95% confidence intervals for the York I model are remarkably narrow: especially in view of the narrow Rb/Sr spread represented. To test the validity of these error estimates, the isochron was rotated towards the highest apparent age within 1σ limits by adding $+1\sigma$ errors to the two high Rb/Sr points and -1σ error to the two low points. An even greater distortion would be induced if 2σ rotation were allowed. The resultant hypothetical models are:

Table 4.9: Ryckman model rotated isochrons:

McIntyre I	MSWD = 0.08	2,550±346 m.y.	0.7002±0.0010
York I		2,550± 97 m.y.	0.7002±0.0003
York II	S = 0.28	2,548±347 m.y.	0.7002±0.0010
Wendt I	SCSQ = 0.25	2,555±348 m.y.	0.7002±0.0010
Wendt II	SCSQ = 0.28	2,550±335 m.y.	0.7002±0.0010

This test illustrates that the 2σ error estimates given by York I are not realistic for the 5 point phanerite plot in view of known analytical uncertainties. The analytical precision estimated for this study and the narrow Rb/Sr spread shown by the phanerites should result in an isochron with a large potential "wobble", as reflected by the size of 10 data crosses on Figure 4.20. The 5 data points show a fortuitous alignment within these error limits that results in unrealistically low York I confidence limits and therefore a pseudoisochron.

Published Pseudoisochrons

Such pseudoisochrons have appeared in the literature. Jahn and Murthy (1975) converted a published McIntyre et al (1966) regression for the Icarus Pluton of Northern Minnesota (Hanson et al., 1971) to the York (1966) model, but in doing so inadvertently generated a pseudoisochron with false error limits. The author has recalculated the original data through REGROSS to allow a model comparison as follows:

D

(YORK I) FOR RYCKMAN LAKE STOCK.
 EXCELLENT LINEAR DATA FIT BUT
 AGE ESTIMATE IS 379 M.Y. YOUNGER
 THAN FIGURE 4.3. DATA FIT DOES
 NOT PROPERLY REFLECT ANALYTICAL
 ERROR THUS YORK I ERROR
 ESTIMATES UNREALISTIC.

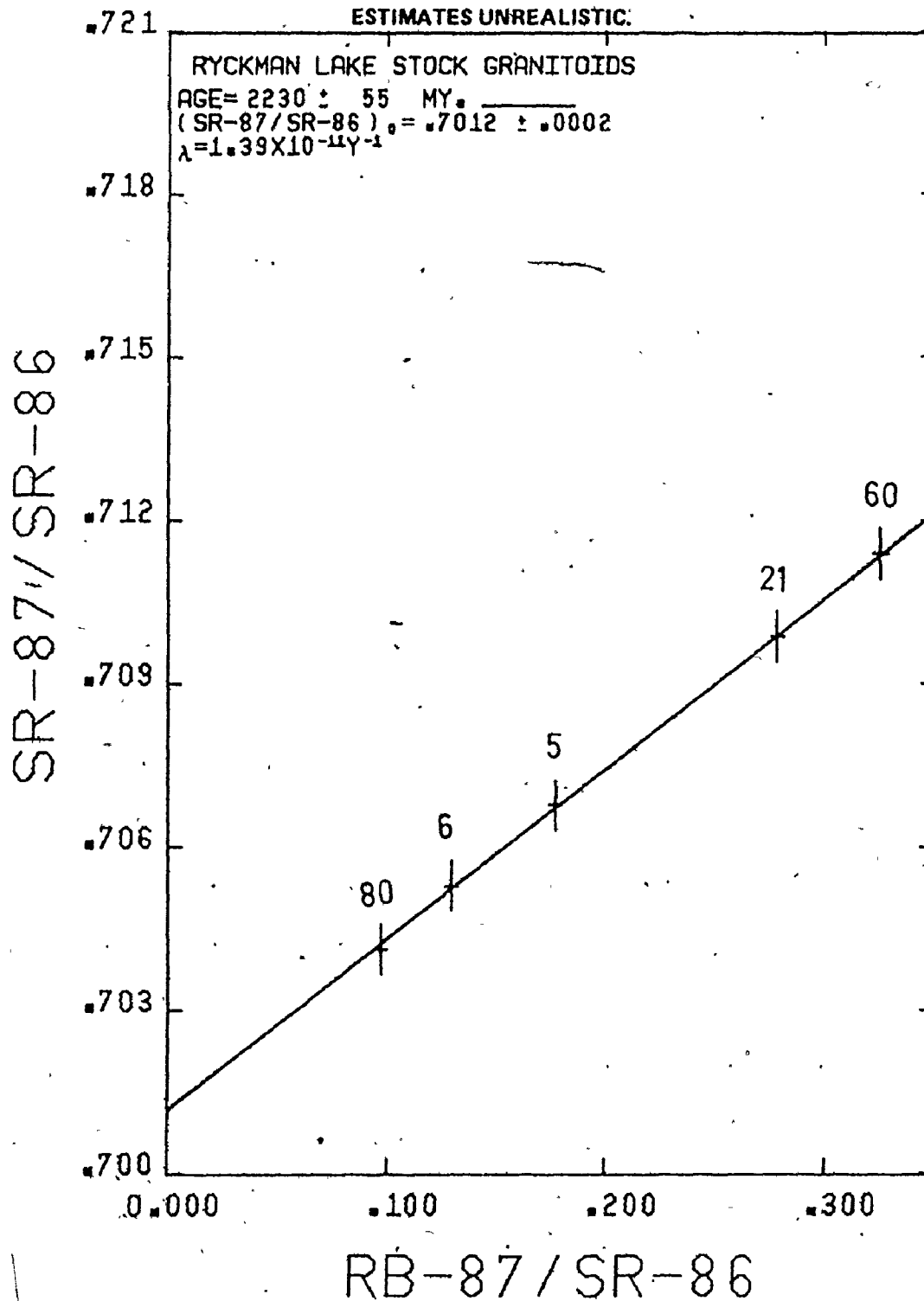


Table 4.10 Regression Models for the Icarus Pluton
(4 analyses from Hanson et al., 1971)

Model	Index	Age. (2σ)	Intercept (2σ)
¹ McIntyre <u>et al.</u> (1966)		2,690±480 m.y.	0.7009±0.0014
² York (1966)		2,690± 21 m.y.	0.7008±0.0001
³ McIntyre I	MSWD=0.02	2,690±215 m.y.	0.7008±0.0006
³ York I	/	2,690± 26 m.y.	0.7008±0.0001
³ York II	S=0.12	2,690±215 m.y.	0.7008±0.0008
³ Wendt I	SCSQ=0.09	2,691±216 m.y.	0.7008±0.0006
³ Wendt II	SCSQ=0.12	2,690±207 m.y.	0.7008±0.0006

1. Model presented by original investigators:
Hanson et al. (1971)
2. Recalculation by Jahn and Murthy (1975)
3. Recalculation through REGROSS using blanket errors of
2% for $^{87}\text{Rb}/^{86}\text{Sr}$ and 0.03% for $^{87}\text{Sr}/^{86}\text{Sr}$

Some discrepancies between models can be attributed to data handling: whereas the McIntyre et al. (1966) and York (1966) models assign error estimates to each data point, the Brooks et al. (1972) versions apply a "blanket error". Nevertheless, both the York (1966) and the near equivalent York I models give unusually low isochron error parameters when compared to

regression treatments that employ analytical error for estimation in place of data scatter. The author interprets the narrow York I and York (1966) model error estimates to indicate fortuitous colinearity beyond expectation in view of analytical uncertainties. The larger error intervals obtained by the other regression models are probably more realistic. Since an age estimate should never be divorced from its reliability estimate, the York I and York (1966) model apparent ages must be considered as pseudoisochrons.

The possibility of generating pseudoisochrons by optimistic fit lends support to the multiple regression method of Brooks et al., (1972). Only when data is regressed by more than one of the available linear regression techniques can the distinction between errorchron, isochron and pseudoisochron be made. An isochron sensu stricto is then defined only if isochron parameters including error intervals are nearly identical between the various regression models.

4.6 ISOTOPIC CONCLUSIONS

4.6.1 Geochronological Conclusions

The survey of published radiometric studies in the Wabigoon Belt (Section 4.2.2, Figure 4.1) can now be supplemented with the Rb/Sr isochron age estimates of the foregoing thesis. As with the published data, the new age estimates

span the interval of the Algonian Orogeny (2,400 to 2,750 m.y.) as defined by Goldich (1968). However, large confidence intervals for a few of the regressions (Tables 4.2, 4.3) account for much of the scatter. The effect of these "noisy" isochrons has been minimized for the Wabigoon late-kinematic plutons by either pooling the ages and intercepts:

$$2,616 \pm 43 \text{ m.y. } R_0 = 0.7006 \pm 0.0005 \text{ (Section 4.4.2)}$$

or by regressing composite populations:

$$2,623 \pm 35 \text{ m.y. } R_0 = 0.7007 \pm 0.0004$$

For the Rainy Lake Batholithic Complex, the "noise" is best eliminated in the composite regression:

$$2,616 \pm 66 \text{ m.y. } R_0 = 0.7012 \pm 0.0005$$

These ages and intercepts have been demonstrated to be statistically indistinguishable. Such coincidence for synkinematic granitoids and late-kinematic granitoids lends credence to a tectonic model for production of the Wabigoon Belt by near-synchronous vulcanism and magmatism spanning less than 35 m.y. (i.e. ~68% confidence from above error estimates). Such a narrow time span is not resolvable by Rb-Sr methods for rocks of such antiquity. That the age estimates for synkinematic and late-kinematic granitoid magmatism fall intermediate to the limits of the Algonian Orogeny assigned by Goldich (1968) is probably not fortuitous. The wider limits assigned to the Orogeny may reflect analytical "noise" as well as discrepancies between various radiometric techniques. The author considers that the Rb/Sr whole-rock isochrons of this study give a

better regional picture of primary ages than all the published mineral dates compiled on Figure 4.1.

Krogh and Davis (1971) and Langford and Morin (1976) recognized that radiometric ages from the Superior Province appear to decrease sequentially southward from the Berens River Block to the Quetico Belt. In an east-west direction radiometric ages appear synchronous even where greenstone belts are not continuous. Goodwin and West (1974) and Langford and Morin (1976) proposed accretion of island arcs as a model for formation of the Uchi, Wabigoon and Wawa Belts, analogous to the plate-tectonic model of Monger et al. (1972) for the Canadian Cordillera. For the Wabigoon Belt, the proposed arc of Langford and Morin (1976) faced away from the Berens River craton. Eagle Lake-Wabigoon Lake formed the back-arc portion, while Kakagi Lake-Manitou Lake formed the fore-arc. Intrusion of granitic plutons occurred in conjunction with coalescence of the island arcs and as a subsurface continuation of vulcanism. Such a model accounts for both the apparent southward juvenescence of belts and the near-synchronous chronology within belts.

An inspection of the compiled Rb/Sr chronology for the western Wabigoon Belt (Figure 4.1) reveals an apparent juvenescence of granitoids southward within the belt (Birk and McNutt, 1977b). Only the poorly defined Bears Passage Stock violates this trend (Table 4.11):

Table 4.11

Approximate Latitude	Whole-Rock Isochron Ages	Plutons
49°25'	2,636± 63 m.y.; 2,640± 31 m.y.	Flora Lake; Taylor Lake
49° 5'	2,572± 42 m.y.	Esox Porphyry
48°55'	2,598± 45 m.y.; 2,609± 63 m.y.	Burditt Lake; Ryckman Lake
48°45'	2,514± 78 m.y.; 2,520± 42 m.y.	Ottertail Lake; Bad Vermilion Lake
48°40'	2,702±158 m.y.; 2,455±104 m.y.	Bears Passage; Rest Island

For plutons internal to the Wabigoon Belt, this apparent juvenescence is probably coincidental since the pooled variance analysis of Section 4.4.1 shows the isochrons to be statistically indistinct. The trend may be real but not clearly resolvable by Rb/Sr chronology. Van Breemen et al. (1975) found a southerly decreasing age trend (of 20 m.y. duration) for Mesozoic granitoids of Nigeria. They proposed a progressive igneous chain formed by local melting of a crustal plate as it migrated over a mantle hot spot. Such a "plume" model is awkward to accommodate in a Wabigoon island arc setting and does not account for the area scatter of the Wabigoon plutons.

Alternatively, the significantly younger pluton apparent

ages of the Wabigoon-Quetico interface may record a single episode post-dating the Wabigoon arc system. This younger episode may be plutonic (Birk and McNutt, 1977a) or may be metamorphic (Peterman et al., 1972). Although metamorphic resetting of minerals is indicated by the Bears Passage mineral isochron, the older whole-rock isochron suggests that total-rock systems remained undisturbed. A metamorphic event capable of resetting the entire Ottetail Lake Stock as suggested by Peterman et al. (1972) casts doubt on the primary nature of all the isochrons obtained in this study.

Goldich (1972) and Van Schmus et al. (1975) proposed that widespread low grade metamorphism could reset Rb/Sr systems while preserving colinear arrays. In a comparative U-Pb:Rb/Sr regional study of Wisconsin, Van Schmus et al. (1975) found apparent Rb/Sr whole-rock isochrons of $1,650 \pm 50$ m.y. for units dated at $1,800 \pm 30$ m.y. by U-Pb. This study is directly analogous to the comparative Rb/Sr:U-Pb study Peterman et al. (1972) carried out in the Rainy Lake region where Rb/Sr isochrons were also incompatible with zircon data. Krogh and Davis (1973) made a significant contribution towards this problem by generating two distinct Rb/Sr isochrons for one lit-par-lit banded paragneiss outcrop. They demonstrated that during regional amphibolite facies metamorphism, isotopic and chemical equilibrium was not attained even over a few centimeters. They concluded that: "The lack of local isotopic

equilibrium precludes the possibility of attainment of isotopic equilibrium on a regional scale, sometimes evoked by geochronologists". The problem of incompatible Rb/Sr isochrons and zircons may be with the zircons rather than with a metamorphic overprint. Krogh and Davis (1973b) suggest that inherited zircons may occur not only in young intrusives in older crust, but also in some Precambrian intrusives. In view of these findings, the author rejects the regional isotopic resetting hypothesis and considers all the whole-rock isochrons sensu stricto of this study to be primary.

4.6.2 Initial Strontium Ratios: Petrogenesis

Introduction

"Algonian" granitoids from Rainy Lake were among samples Hedge and Walthall (1963) used to demonstrate that $^{87}\text{Sr}/^{86}\text{Sr}$ of the earth's crust has changed 1.1% in 3000 million years, while the ratio in the mantle has changed no more than 0.5%. These different rates of Sr^{87} enrichment in two important petrogenetic source regions led Faure and Hurley (1963) to propose that the value of $^{87}\text{Sr}/^{86}\text{Sr}$ ratio of igneous rocks at the time of crystallisation can act as a tracer. The most reliable estimate of this initial $^{87}\text{Sr}/^{86}\text{Sr}$ ratio is given by the intercept of a whole-rock isochron sensu stricto. Calculated initial ratios are generally discussed in relation to model growth lines (Figure 4.21) for potential source regions on a

$^{87}\text{Sr}/^{86}\text{Sr}$ versus time plot. A recent summary of the use of Sr isotopes as petrogenetic tracers is given by Faure and Powell (1972). Several assumptions have been inherent to the early applications but have come under closer scrutiny in the most recent works:

- (1) $^{87}\text{Sr}/^{86}\text{Sr}$ has experienced a linear growth with time in both source regions and "offspring";
- (2) the source regions (especially the mantle) are isotopically homogeneous;
- (3) processes of partial melting, fractional crystallisation, etc. preserve isotopic equilibrium between parent and daughter material;
- (4) whole-rock Rb/Sr isochrons are primary and have not been metamorphically rotated: the "initial ratio" is primary.

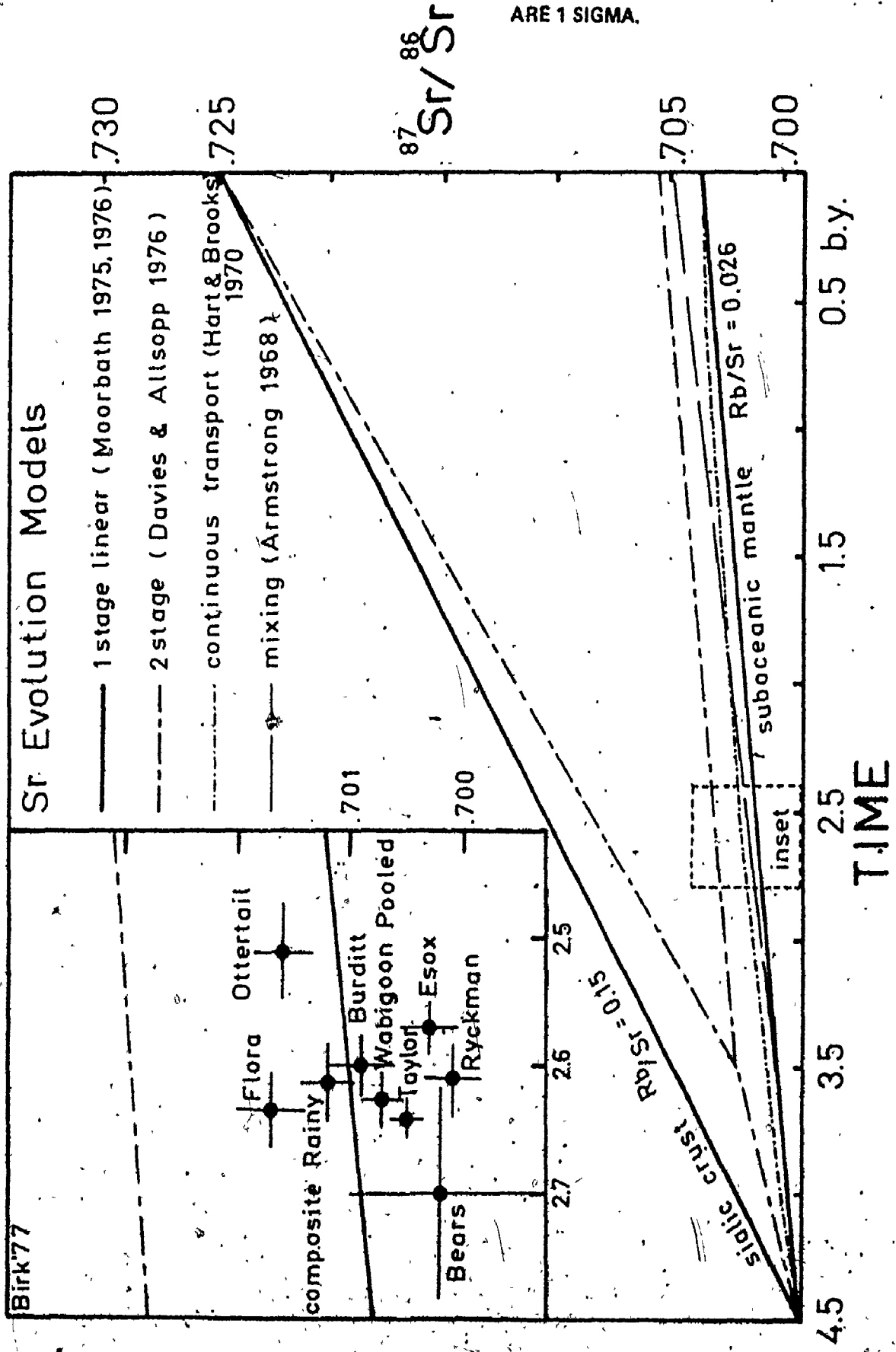
The assumption of linear growth of $^{87}\text{Sr}/^{86}\text{Sr}$ in the mantle implies an infinite reservoir model: the mantle is not depleted in Rb despite constant transfer of magma to the crust. Strontium evolution in the mantle is then represented by an end-member line based on $(^{87}\text{Sr}/^{86}\text{Sr})_i$ in Rb-poor meteorites (4.5 b.y.) and modern volcanics (Faure and Hurley, 1963; Faure and Powell, 1972; Moorbath, 1975, 1976). Hart and Brooks (1970) proposed instead a multi-stage evolution model approximated by a convex "continuous transport" growth curve.

Periodic extractions of material would leave the mantle successively depleted in Rb relative to Sr. Armstrong (1968) proposed an early differentiation of the earth into core-mantle-crust phases coupled with isotopic re-equilibration of crust and upper mantle by repeated mixing in a trench-arc-cordillera system. Davies and Allsopp (1976) preferred a two-stage model with sialic crust: mantle differentiation occurring early in earth history with younger granitic rocks formed largely by anatexis of the primitive crust. Moorbath (1975, 1976) used the simple single-stage mantle evolution model to argue that the consistently low initial ratios for Precambrian units preclude derivation by crustal reworking. The lack of consensus as to the correct growth trend for potential source regions puts any discussion concerning initial $^{87}\text{Sr}/^{86}\text{Sr}$ ratios on a weak footing. Figure 4.21 summarizes the above models.

The assumption of homogeneity of the mantle has now been strongly challenged by isotopic comparisons between modern ocean island basalts and ocean-ridge basalts (Hart and Brooks, 1970; Hedge and Peterman, 1970; Peterman and Hedge, 1971; O'Nions and Pankhurst, 1973; Hofmann and Hart, 1975, etc.). Brooks et al. (1976) used ratios from oceanic island tholeiites and alkali basalts to generate a rough "mantle isochron". The apparent age of 1.6 ± 0.2 b.y. was then proposed as dating a major event of mantle differentiation, such as the segregation of an unradiogenic asthenosphere from a relatively radiogenic

FIGURE 4.21

INITIAL $^{87}\text{Sr}/^{86}\text{Sr}$ RATIOS FROM THIS STUDY IN RELATION TO Sr EVOLUTION MODELS. ERROR BARS ARE 1 SIGMA.



mesosphere. Other workers have tried to trace mantle heterogeneities back into Archean times. Brooks et al. (1970) obtained initial ratios for two series of Archean metavolcanics at Michipicoten, Ontario, and proposed that respective ratios of 0.7028 and 0.7012 were significantly different and illustrated Archean mantle heterogeneity. In a subsequent report, Hart and Brooks (1974) analysed Archean pyroxenites yielding lower ratios (0.7011) with less scatter. The apparent Archean heterogeneities may only reflect metamorphism or weathering. The possibility that apparent isotope heterogeneities could be generated by disequilibrium melting (O'Nions and Pankhurst, 1973) was rejected by Nelson and Dasch (1976) on the basis of diffusion rate data. They concluded that the time required for Sr to move on a regional scale probably results in persistence of mantle isotopic inhomogeneities over distances greater than 0.1 to 1 km.

At the same time that the models on which the growth lines have been based have been criticized, the quality and significance of the initial $^{87}\text{Sr}/^{86}\text{Sr}$ ratio determinations have been questioned. The discrepancies between various isochron linear regression treatments affect not only the age determinations, but also the initial ratio determinations. All cautions on error treatment, errorochrons, pseudoisochrons, etc. as presented in previous chapters (see also Brooks et al., 1972) apply equally to the initial ratio. Kagami, Shuto and

Gorai (1975) demonstrated that the three granitoid fields that Faure and Powell (1972) recognized on their strontium evolution diagram ("granites with initial ratios within the basalt field ... granites with intermediate initial ratios ... granites with high initial $^{87}\text{Sr}/^{86}\text{Sr}$ ratios ...") correlate with the standard deviation on the initial ratio determinations. Points based on data having narrow error limits, plot within a narrow region above the Sr evolution zone for oceanic tholeiites. The same trend is evident for published initial ratios for the Lac du Bonnet Quartz Monzonite pluton of Manitoba. Penner and Clark (1971) published a 5 point isochron of $2,495 \pm 180$ m.y. with an intercept at 0.7088 ± 0.0094 . Farquharson (1975) revised the isochron to a 7 point regression with parameters of: $2,680 \pm 91$ m.y. and an initial ratio of 0.6998 ± 0.0032 . Obviously high initial ratios with large errors must be treated with caution.

Whether an isochron intercept is accepted as an initial ratio with petrogenetic significance has in the past depended on each author's opinion regarding the possibility of rotated whole-rock metamorphic linear arrays. Farhat and Wetherill (1975) used a high intercept as evidence for metamorphic rotation. Reed and Zartman (1973) considered the linear array on an isochron as proof that a high intercept was not the product of metamorphic rotation. Moorbath et al. (1976) obtained a high intercept (0.711 ± 0.002) for extremely old rocks

(3,420±120 m.y.) and preferred a model of crustal reworking to metamorphic rotation. Van Schmus and Anderson (1977) have confused the picture even further by using a poorly defined 0.711 intercept from a 2.1 b.y. scatterchron to extrapolate a 3.4 to 3.7 b.y. "age" on the Sr evolution diagram.

The problems of interpretation appear therefore to be most severe for isochron intercepts that are unusually high for a given age. Relatively low initial ratios carry significance dependent on source heterogeneity and the evolution model adopted.

Initial Ratios: This Study

Section 4.4.1 presented a students-T test to show that all intercepts for isochrons sensu stricto of this study are statistically indistinct with the exception of the Flora Lake and Ottertail Lake intercepts. Figure 4.21 shows the initial ratios relative to the strontium isotope evolution diagram: crosses reflect 1 sigma error. Although the controversies outlined previously, put serious limitations on interpretation, some conclusions are still warranted.

The initial ratios straddle the single-stage linear growth model for the upper mantle. Most of the scatter about this line is accommodated by the intercept uncertainties. The two distinct ratios (Flora and Ottertail) do not deviate sufficiently to warrant separate interpretation. All values

lie significantly below the two-stage subcontinental mantle line of Davies and Allsopp (1976) and are in agreement with the range of 0.700 to 0.702 that Moorbath (1975,1976) considered definitive for upper mantle at that age.

The initial ratios of this study are too low to represent rotated isochrons or crustal contamination. Archean mantle inhomogeneity, if present, was at a scale below detection at the precision quoted in this report. The simple one-stage Sr evolution model for the mantle reservoir, or the plate-tectonic crust-mantle mixing model of Armstrong (1968) are compatible with the data. The curvature on the Hart and Brooks (1970) multi-stage model lies above the data and is therefore rejected.

Orthodox interpretation concludes that the granitoids of the Wabigoon Belt were derived from upper mantle loci rather than by anatexis of pre-existing older crust. This upper mantle material may however have contained recycled sialics in a plate-tectonic mixing regime. Alternatively, the isotopic data allows derivation from low Rb/Sr material residing in the lower crust if such material originated from the mantle less than 50 m.y. prior. A third alternative is derivation from lower crustal material if isotopic equilibrium prevailed between the lower crust and upper mantle.

CHAPTER 5:

SYNOPSIS

5.1 CHEMISTRY OF ARCHEAN GRANITOIDS:

Investigators of Archean rock chemistry have proposed regional scale lateral trends (Langford and Morin, 1976), vertical trends (Lambert and Heier, 1968; Fahrig and Eade, 1968; Eade and Fahrig, 1971, 1973; Engel et al 1974; etc.) and secular trends (Fahrig and Eade 1968; Glikson, 1971, 1972; Engel et al 1974; Cloud, 1976; etc.).

Vertical zonation of the crust has been attributed to metamorphic fractionation leading to chemical distinction between amphibolite facies and granulite facies terrain. Granite facies rocks represent deeper crustal levels and have suffered basification and volatile loss resulting in enrichment in Ti, V, Y, Sc, Co, Cu and Zn and depletion in Pb, U, Th, K, and H₂O relative to rock equivalents under amphibolite facies conditions (Eade and Fahrig, 1971; Holland and Lambert, 1972).

Secular chemical trends were proposed by Eade and Fahrig (1971, 1973) and Fahrig and Eade (1968) based on reconnaissance geochemistry of large segments of the Canadian Shield. These authors reported higher Na₂O, Cr, Ni and lower K₂O, TiO₂, Pb, Zn, U and Th for Archean crystalline rocks compared to Proterozoic rocks. Holland and Lambert (1972) challenged the statistical significance of these trends but accepted the evidence for K₂O enrichment. These secular chemical trends have been variously attributed to compositional

change in mantle source, vertical crustal zonation exposed by differential erosion (Fahrig and Eade, 1968), sedimentary recycling (Holland and Lambert, 1972) or anatectic recycling (Glikson, 1971, 1972).

Secular evolution of granitoids has been proposed by several of the cited authors. Engel et al (1974) claim a three fold increase in the abundance ratio of quartz-monzonite to quartz-diorite from Archean to Proterozoic. Glikson (1971, 1972) and Glikson and Lambert (1976) have proposed secular evolution from sodic to potassic granitoids within the Archean interval. Glikson and Lambert (1976) suggest three Archean granitoid events in Western Australia: the first two being Na-rich granitoids intruded at 3.1 - 2.9 and 2.8 - 2.7 b.y. while the last event was intrusion of K-rich granitoids at 2.6 b.y. They picture the K-rich granitoids to be derived from the underlying older Na-rich granitoids by "... ensialic anatexis ...". Extrapolating their model to the Canadian Shield, Glikson and Lambert (1976) propose that the "Kenoran" plutons are Canadian equivalents to the high-level K-rich granitoids.

All twelve stocks studied in this thesis are compatible with the tectonic classification of Glikson (1971) for:

"... relatively small, high level intrusions of adamellite, calcalkaline granite, and associated aplite and pegmatite ... emplaced into the Swaziland System, the Rhodesian belts and the Kalgoorlie Systems ...".

Furthermore, the geochronology of Chapter 4 confirms classification as "Kenoran" plutons as discussed by Glikson and Lambert (1976). The two-fold division into "early Sodic" versus "late Potassic" (Glikson,

LEAF 356 OMITTED IN PAGE NUMBERING.

monzonite/monzonite) of Eade and Fahrig (1971). It follows therefore that Glikson's and Lambert's model of granitoid evolution can be tested for the Superior Province by chemical comparisons between plutons of this study and granitoid compilations of Eade and Fahrig (1971, 1973) and a companion paper by Reilly and Shaw (1967).

Alkali and trace element averages of Table 5.1 show no systematic differences in chemistry between presumed higher level and deep level Archean granitoids. The range in Na/K for Wabigoon Belt plutons accommodates the average values proposed for both higher level and deep level plutons. Wabigoon Belt plutons differ, however, in significantly higher Ba and Sr than either of the tectonic groupings.

This suggests either that high level plutonism within the Wabigoon Belt was chemically distinct from structurally similar plutonism elsewhere in the Shield or the "higher level" classification of Eade and Fahrig (1971) is not compatible with Kenoran plutonism sampled by this study.

Glikson (1971, 1972) proposed a secular decrease in Na/K, K/Rb and increase in Rb, Sr, Zr, Rb/Sr and $(^{87}\text{Sr}/^{86}\text{Sr})_i$ with Archean granitoid evolution. Table 5.1 rules against secular change in Na/K, Sr and Zr. Chapter 4 has demonstrated that $(^{87}\text{Sr}/^{86}\text{Sr})_i$ is consistently low for Wabigoon Belt granitoids and close to proposed mantle values. Likewise Rb/Sr has been shown to be consistently low except for aplite-pegmatite phases while K/Rb ratios are relatively high for igneous rocks. The evidence therefore does not support the model of secular granitoid evolution, within the Archean interval.

Table 5.1

Geochemical Comparison of Archean "Deep Level" and "Higher Level" Granitoids of the Canadian Shield:

Unit 10 (Higher Level)

Area	Na ₂ O	K ₂ O	Ba	Sr	Y*	Zr*	Na/K	Sr/Ba	No of Samples	Source
New Quebec Fort	4.5	3.26	.063	.042	15	100	1.23	0.67	12	1,2
Enterprise Red L.--	3.6	2.89	.074	.022			1.11	0.30	34	1,2
Lansdowne H. (LGR)	3.9	3.79	.057 ^Δ	.046	<30	102 ^Δ	0.92	0.54	Composites	3
Red L.--										
Lansdowne H. (PGR)	4.1	3.65	.079 ^Δ	.079	<30	108 ^Δ	1.0.	0.66	Composites	3
This Study	3.8 (+.7)	3.0 (+.7)	.15 (+.04)	.12 (+.06)	15 (+15)	150 (+ 70)	1.5 (+ .6)	0.8 (+.4)	247	4

Unit 9 (Deep Level)

Area	Na ₂ O	K ₂ O	Ba	Sr	Y*	Zr*	Na/K	Sr/Ba	No of Samples	Source
New Quebec	3.9	3.54	.084	.041	17	159	0.98	0.49	637	1,2
Keewatin	4.0	3.82	.085	.034	21	211	0.94	0.40	102	1,2
Snowbird L. Red L.--	4.4	3.99	.008	.024			0.98	3.0	18	1,2
Lansdowne H. (GD)	4.4	1.96	.040 ^Δ	.065	<30	119 ^Δ	1.99	1.07	Composites	3
Red L.--										
Lansdowne H. (MGR)	4.3	2.78	.012 ^Δ	.054	<30	100 ^Δ	1.38	0.70	Composites	3

Data Source:

1. Eade and Fahrig (1971)
2. Eade and Fahrig (1973)
3. Reilly and Shaw (1967) quoted in 1.
4. Estimates from compilation Figure Nos. 3.5 to 3.19

* in p.p.m.
others in %

Δ normalized to G-1 standard.

The Wabigoon Belt plutons share a common tectonic setting but range in lithology from homogeneous granodiorites to concentrically zoned plutons or complexes of granite-monzodiorite. The range in chemistry is not restricted to descriptions of Glikson's "late K granite". Each pluton carries a distinctive "fingerprint" of major and trace element abundances but as a group these granitoids carry high Sr, Ba, K/Rb and low Rb/Sr, Th and U (Birk, 1976).

5.2 REGIONAL DISTRIBUTION AND EMPLACEMENT OF GRANITOID PLUTONS:

Sorgenfrei (1971) demonstrated structural similarities between granitoid stocks and salt diapirs and suggested similar modes of emplacement. Diapiric emplacement by bulk creep could occur for various states of melt, crystal mush or crystalline solid. Field evidence mentioned in this thesis that supports granitoid transport in the molten state includes granitic apophyses, and migmatized or rafted country rock. Movement of Wabigoon Belt granitoids in a partially solid state has been indicated by sharp contacts, aligned enclaves, truncated enclaves, plastically deformed aplite dykes and internal faulting.

The geometry and growth pattern of diapiric structures is controlled by the areal extent and shape of the source region, by viscosity differences and by irregularities of overburden and substratum. Stephansson (1972) used centrifuged models of clay and putty to study initiation of diapirism by discontinuities in

contacts to source strata. Stephansson demonstrated that although diapirism initiates at the contact, the piercing movement of diapirs is vertical and does not follow the structural weakness provided by the fault plane.

If the Wabigoon - Quetico interface represents a geological analogy to the overburden discontinuity of Stephansson's model, the linear array of granitoid plutons at Rainy Lake may have been generated as diapirs initiated by the interface, although not necessarily spatially coincident with this interface. Shklanka (1972) concluded from field mapping that the Quetico Fault system remained active over a period spanning pre-Kenoran to early Paleozoic. The fault system may have initiated diapirism, but the irregularities of lithology and tectonics at the interface were equally capable according to Stephansson's (1972) models.

Likewise Kehlenbeck (1977) recognized a linear array of four granitoid plutons parallel to the Quetico Belt - Shebandowan Belt interface. Such regional linear discontinuities in the Archean crust may have been widely responsible for initiating linear arrays of granitic diapirs. Goodwin (1965) summarized the tectonics of northwestern Ontario as "...superposition of dome patterns upon pre-existing east to northeast trending linear fold patterns ...". In the Lake-of-the-Woods region he recognized a curvilinear distribution of small granitoid stocks along east-trending axes. Glikson (1971) mentions subparallel alignments of batholiths within the structural trends in the Kalgoorlie system. Glikson (1976) wrote that:

"... The well pronounced parallel linear pattern of greenstone belts in the Superior Province, Slave Province, south India, Yilgarn

craton and to a lesser extent Kaapvaal craton, yields a vital clue for Archean tectonic models. In these terrains, the long axes of the granitic plutons mostly parallel fold axes, major faults and metamorphic foliations ... the linear structures ante-dated the intrusion of granites. Thus lateral flexures clearly related to granite emplacement are superposed on isoclinal folds coaxial with the greenstone belts ...".

Schwerdtner and Goodwin (1977) concluded that superbelt boundaries such as the Wabigoon-Quetico interface or the Wabigoon - English River boundary represent long-lived tectonic anomalies dating back to supercrustal accumulation prior to granitoid diapiric invasion. Subsurface extensions of tectonic discontinuities recorded by the superbelt interfaces could have initiated and partially controlled the distribution of diapiric upwelling at a lower crust or upper mantle source layer. The diapir distribution at the erosional surface need not match the surface expression of belt discontinuities but reflects the vertical tectonics of diapir transport and the lower crust or mantle source contact with the discontinuity.

The orientation of deep crustal extensions of belt interfaces may be deduced from the relative density of plutons along the interfaces. Whereas the Shebandowan - Quetico boundary and the Wabigoon - Quetico boundary are well defined by volcanic-sedimentary, migmatitic and strike-slip fault contacts, the Wabigoon - English River interface is poorly known because of granitic diapir overprint (Mackasey et al 1974; Schwerdtner and Goodwin, 1977). The Wabigoon - English River interface may intersect the granitic source layer at a higher angle and in the path of vertical diapir transport.

The distribution pattern of felsic volcanics, iron formation, conglomerates and mineral deposits shows a concentration at belt interfaces which may indicate paleobasin margins now occupied by the superbelt boundaries (Schwerdtner and Goodwin, 1977). Any area of decreased thickness of overburden translates into decreased pressure on the source layer and can initiate diapiric uprise (Stephansson, 1972). This suggests that the present distribution of stocks and batholithic complexes within the superbelts may record paleobasin centers where granitic diapirism was initiated by downwarping and crustal thinning.

If the granitoid diapirs rose into a relatively uniform supracrustal blanket of lava, as Wilson et al (1974) suggest for northwestern Ontario, such a uniform overburden should dictate similar diapir dimensions. Some distortion of dimensions is expected from near-surface lateral expansion and differential erosion but the great disparity between dimensions of batholithic complexes and the small stocks intrusive into greenstones cannot be accommodated. Wilson et al (1974) propose a single emplacement event for the multi-phase Aulneau Dome. Schwerdtner and Goodwin (1977) agree that the elliptical shape of this batholith suggests transport in bulk but for other batholiths of more lobate shape they propose piecemeal intrusion.

Stephansson (1975) proposed a mechanism of diapirism within diapirs, i.e. "polydiapirism", for the complex batholiths of central Sweden. His map for the Vdala-Uppland Massif looks similar to the illustration for the Aulneau Batholith given by Wilson et al (1974). The mechanism of polydiapirism is attractive in view of previously

discussed evidence for multiple intrusion in concentrically zoned or lithologically complex stocks (Chapter 2).

The spacing of diapirism is controlled by the thickness, density and viscosity of the source layer (Stephansson, 1972); a multiple strata source could supply multiple diapirs of different wavelength and chemistry. Stephansson (1975) proposed a stratified granitic layer in the upper mantle to explain the spacial and secular trends of lithology in the polydiapirs. Wilson et al (1974) suggested that felsic volcanism in northwestern Ontario left a residual quartz-diorite layer in the upper mantle which after cumulate stratification upwelled as granitic diapirs. If diapirism was initiated by deep extensions of faults and belt interfaces, the lithology being tapped could be a function of the depth of the irregularity. Areas of complex granitoid plutonism could have their origins in multiple faults or lithologic discontinuities of differing depth, intersecting the granitic source layers at different horizons.

This model fails to account for the secular trends characteristic within multiple intrusives: younger more felsic units towards the cores (Chapter 2; Stephansson, 1975). In either a differentiated magma chamber or in a stratified granitic layer, the most felsic units should occupy the top and be drained first. Upwelling en masse of a stratified source as suggested by Sorgenfrei (1971) is ruled out by field observations of intrusion and viscosity differentials. Furthermore, such a multi-strata diapir should still carry the deepest, most mafic layer, in the core. The answer to this enigma may be approached by a model combining polydiapirism with volcanic conduits and ring-dyke complexes (Chapter 2).

The location of a stratified granitic source layer as required by the models of Sorgenfrei (1971), Wilson et al (1974) and Stephansson (1975) remains speculative. The heterogeneity of the Archean mantle was recently discussed by Sun and Nesbitt (1977) who concluded that:

"... Three different mantle evolution models are examined and each suggests that the mantle is stratified with respect to abundances of incompatible trace elements. We suggest that no satisfactory model is available to fully explain the spectrum of geochemical and geophysical data ...".

The nature of the Archean crust is equally enigmatic. Advocates for a relatively thin Archean crust with a steep geothermal gradient (Bridgewater and Fyfe, 1974) are confronted by evidence for a 60 km thick lithosphere (Cloud, 1976; Langford and Morin, 1976). Condie (1973) in contrast considers the Archean crust to have approached the present day average thickness of 38 km by the time of extensive Archean granitoid plutonism at 3.0 to 2.5 b.y.

Smithson and Brown (1977) summarized available geological, geophysical and geochemical data to develop a model for the present lower crust as a metamorphic melange of granitic gneiss, syenite gneiss, anorthosite, granite and gabbro. Based on seismic evidence for ten or more reflectors and multiple reflections, they suggest that the lower crust contains numerous interfaces and small scale layering analogous to exposed granulitic terrain. Such a stratified lower crust could provide numerous loci for diapirism.

Isotopic evidence of section 4.6.2 favours a mantle source for the Wabigoon Belt plutons based on orthodox interpretations for low

($^{87}\text{Sr}/^{86}\text{Sr}$). Objections to low initial ratios in a lower crust source have been countered by suggestions of isotopic equilibration across the lower crust - mantle interface (Baragar and McGlynn, 1976) or Rb depletion of a lower crust (Bridgewater and Fyfe, 1974). The debate goes on.


(The vantage point for this thesis has now telescoped from the petrographic scale to the shield scale. Further speculations on the nature of Archean evolution and the role of granitoids are not warranted within the confines of the thesis data. Megalomodels proposed by more inspired authors have described Wabigoon Belt type terrain as island arc accretions (Langford and Morin, 1976) or ocean sutures (Burke et al., 1976) in an Archean plate tectonic system; as terrestrial equivalents to lunar maria and highlands (Green, 1972) or even as sialic additions to the earth by impact of a swarm of sialic asteroids (Donn et al., 1965; Birk, 1976). The reader is invited to take up the pen of geopoetry where these authors leave off.

REFERENCES

- ABBEY, S. (1975)
Studies in "Standard Samples" of silicate rocks and minerals.
Part 4: 1974 Edition of "usable values".
Geological Survey Canada, Paper 74-41, 23p.
- ABBEY, S., GILLIESON, A.H. AND PERRAULT, G. (1975)
Canadian Reference rock samples Sy-2, Sy-3, MRG-1;
Canadian J. Spectroscopy, V.20, No. 5 pp. 113-115.
- AGTERBERG, F.P. AND CHUNG, C.F. (1975)
A computer program for polynomial trend-surface analysis;
Geological Survey Canada, Paper 75-21.
- ALDRICH, L.T. AND WETHERILL, G.W. (1960)
Rb-Sr and K-Ar ages of rocks in Ontario and Northern Minnesota;
J. Geophys. Res. V.65 No. 1, pp. 337-340.
- ALLISON, I.S. (1925)
The Giants Range batholith of Minnesota;
J. Geol., V.33, No. 5 pp. 488-509.
- ALLSOPP, H.L., ULRYCH, T.J. AND NICOLAYSEN, L.O. (1968)
Dating some significant events in the history of the Swaziland
System by the Rb-Sr isochron method;
Can. J. Earth Sci., V.5 pp. 605-619.
- AL-SAADY, N.A. AND AL-DERZI, N.W. (1975)
Determination of some trace elements in geochemical standards by
x-ray fluorescence;
Chem. Geol., V.15, pp. 229-234.
- ANDERSON, A.L. (1934)
Contact phenomena associated with the Cassia Batholith, Idaho;
J. Geology, V.42, pp. 376-392.
- ANDRESEN, A. AND HEIER, K.S. (1975)
A Rb-Sr whole rock isochron date on an igneous rock body from the
Stavanger area, South Norway; Geol. Rundschau, V.64, No. 1, pp
260-265.
- ANHAEUSSER, C.R., MASON R. VILJOEN, M.J. AND VILJOEN, R.P. (1969)
A reappraisal of some aspects of Precambrian shield geology;
Geol. Soc. Amer., Bull. V.80 pp. 2175-2200.

- ARAMAKI, H. AND NOZAWA, T. (1972)
Chemical composition of Japanese granites,
Part II: Variation trends and average composition of 1200
analyses;
J. Geol. Soc. Japan, V.78, No. 1, pp. 39-49.
- ARMSTRONG, R.L. (1968)
A model for the evolution of strontium and lead isotopes in a
dynamic earth;
Rev. Geophysics, V.6, No. 2, pp. 175-199.
- ARMSTRONG, R.L. AND HILLS, F.A. (1967)
Rb-Sr and K-Ar geochronologic studies of mantled gneiss domes,
Albion Range, S. Idaho, U.S.A.;
Earth, Planet. Sci. Letters, V.3, pp. 114-124.
- ARTH, J.G. AND HANSON, G.N. (1975)
Geochemistry and origin of the early Precambrian crust of
Northeastern Minnesota;
Geochim. Cosmochim. Acta, V.39, pp. 325-362.
- AUGUSTITHIS, S.S. (1973)
Atlas of the Textural Patterns of Granites, Gneisses and Associated
Rock Types;
Elsevier Sci. Publ. Co., New York, 378 p.
- AYRES, L.D. (1972)
Guide to granitic rock nomenclature used in reports of the Ontario
Division of Mines;
Ont. Div. Mines, Miscellaneous Paper 52, 14 p.
- AYRES, L.D. (1974)
Geology of the Trout Lakes area, District of Kenora (Patricia
Portion);
Ont. Div. Mines, GR113, 197 p., incl. map 2270, scale 1" to 1/2
mile.
- AYRES, L.D. AND ERMANOVICS, I.F. (1972)
Granitic plutons; in Variations in Tectonic Styles in Canada, R.A.
Price and R.J.W. Douglas, editors;
Geol. Ass. Canada, Sp. Paper 11, pp. 575-585.
- BAADSGAARD, H. AND MUELLER, P.A. (1973)
K-Ar and Rb-Sr ages of intrusive Precambrian mafic rocks, Southern
Beartooth Mountains, Montana and Wyoming;
Geol. Soc. Amer., Bull. V.84, pp. 3635-3644.
- BAIRD, A.K., McINTYRE, D.B. AND WELDAY, E.E. (1967)
Geochemical and structural studies in batholithic rocks of Southern
California:
Part II, Sampling of the Rattlesnake Mountain pluton for chemical
composition, variability and trend analysis;
Geol. Soc. Amer., Bull. V.78, pp. 191-222.

- BALK, R. AND GROUT, F.F. (1934)
Structural study of the Snowbank Stock;
Geol. Soc. Amer., Bull. V.45, pp. 621-636.
- BALYKIN, P.A., BURBYEV, V.I. AND KRENDELEV, F.P. (1971)
Gamma spectrometric measurements of Clarks of radioactive elements
in gold deposits of the schist zone;
Geochemistry 189 p.
Translated from: Doklady Akademii Nauk SSSR, V209, pp. 190-192.
- BARAGAR, W.R.A. AND McGLYNN, J.C. (1976)
Early Archean basement in the Canadian Shield; A review of the
evidence;
Geol. Survey Canada, Paper 76-14, p.21.
- BARANOV, V.I. TU LE-TIEN AND KOROBKOV, V.I. (1962)
Geochemistry of U and Th in the granitic rocks of the Kyzyltau
Massiv (Central Kazakhstan),
Part 2: Modes of occurrence of radioactive elements in granitic
rocks; Geochemistry, V.5, pp. 469-483.
- BARKER, F., PETERMAN, Z.E., HENDERSON, W.T. AND HILDRETH, R.E. (1974)
Rb-Sr dating of the trondhjemite of Rio Brazos, New Mexico and of
the Kroenke granodiorite, Colorado;
U.S.G.S., Journal of Research, V.2, No. 6, pp. 705-709.
- BARKER, F., WONES, D.R., SHARP, W.N. AND DESBOROUGH, G.A. (1975)
The Pike Peak batholith, Colorado Front Range, and a model for the
origin of the gabbro-anorthosite - syenite - potassic granite
suite;
Precambrian Research, V.2, pp. 97-160.
- BARTH, T.F.W. (1959)
Principles of classification and norm calculations of metamorphic
rocks;
J. Geol., V.67, pp. 135-152.
- BARTH, T.F.W. (1962)
A final proposal for calculating the mesonorm of metamorphic
rocks;
J. Geol., V.70, pp. 497-498.
- BARTLETT, R.W. (1969)
Magma convection, temperature distribution and differentiation;
Amer. J. Sci., V.267, pp. 1067-1082.

- BASS, M.N. (1961)
Regional tectonics of part of the southern Canadian Shield;
J. Geol., V.69, pp. 668-702.
- BEARD, R. (1975)
In: Ontario Div Mines, Report of Activities, Miscellaneous Paper
63.
- BECKE, F. (1908)
Über Myrmekit;
Tschemaks Min. Petro. Mitt., V.27, pp. 377-390.
- BELL, K. AND BLENKINSOP, J. (1975)
Geochronology of eastern Newfoundland;
Nature, V.254, pp. 410-411.
- BERNOTAT, W.H. (1973)
Principal component maps instead of trend surface maps for modal
and chemical data of granitoid rock bodies;
Tschemaks Min. Petr. Mitt., V.19, pp. 185-207.
- BIRCK, J.L., FOURCADE, S. AND ALLEGRE, C.J. (1975)
Rb⁸⁷/Sr⁸⁶ age of rocks from the Apollo 15 landing site and
significance of internal isochrons;
Earth, Planet. Sci. Lett., V.26, pp. 29-35.
- BIRK, W.D. (1974)
Portable gamma ray spectrometry for in situ sample selection in
Rb/Sr geochronometry;
Tech. Memo. 75-3, Dept. of Geology, McMaster University, Hamilton.
- BIRK, D. (1976) a
Trace elements in the Archean granitoid diapirs piercing the
Wabigoon Greenstone Belt;
Proceedings, 22nd Annual Inst. Lake Superior Geology, St. Paul,
Minnesota, p.9.
- BIRK, D. (1976) b
Lake Superior geology;
Geoscience Canada, V.3, No. 3, pp. 231-232.
- BIRK, D. AND McNUTT, R.H. (1976)
Autometasomatism as a mechanism of differentiation in Archean
granitoid diapirs;
Geol. Ass. Canada, Program, 29th Annual Meeting, May 19-21,
Edmonton, p. 74.
- 

- BIRK, D. AND McNUTT, R.H. (1977)a
Rb/Sr isochrons for Archean granitoid plutons within the Wabigoon Greenstone Belt, Northwestern Ontario: A preliminary evaluation; Geol. Survey Can., Report of Activities, Part A, Paper 77-1A, pp. 161-167.
- BIRK, D. AND McNUTT, R.H. (1977)b
Rb/Sr geochronology of Wabigoon Belt granitoids, Northwestern Ontario; Inst. on Lake Superior Geology, Proceedings, 23rd Annual, Thunder Bay, Ontario, p.6.
- BLACK, L.P., GALE, N.H., MOORBATH, S., PANKHURST, R.J. AND MCGREGOR, V.R. (1971)
Isotopic dating of very early Precambrian amphibolite facies gneisses from the Godthaab District, West Greenland; Earth Planet. Sci. Lett., V.12, pp. 245-259.
- BLACKBURN, C.E. (1972)a
Off Lake - Burditt Lake area, (Western Part), District of Rainy River;
Ontario Div. Mines, Prelim. Map P741, 1" = 1/2 mile.
- BLACKBURN, C.E. (1972)b
Off Lake - Burditt Lake area, (eastern part), District of Rainy River;
Ontario Div. Mines, Prelim. map P742, 1" = 1/2 mile.
- BLACKBURN, C.E. (1973)
Geology of the Otukamamoan Lake Area, Districts of Rainy River and Kenora;
Ontario Div. Mines, GR.109/42 p., incl. map 2266, 1" = 1 mile.
- BLACKBURN, C.E. (1976)a
Geology of the OffLake - Burditt Lake Area, District of Rainy River;
Ontario Div. Mines, G.R. 140, 62 p., incl. map 2325, 1:63,360.
- BLACKBURN, C.E. (1976)b
Geology of the Lower Manitou - Uphill Lakes Area; District of Kenora;
Ontario Div. Mines, G.R. 142, 81 p., incl. map 2320, 1" = 1/2 mile.
- BLACKBURN, C.E. (1976)c
Boyer Lake Area, District of Kenora
Ontario Div. Mines, Prelim. map P1187, 1:15,840.

- BLACKBURN, C.E. (1976)d
Meggisi Lake Area, District of Kenora;
Ontario Div. Mines, preliminary map P1188, 1:15,840.
- BLISS, N.W. (1969)
Thermal convection in the Archean Crust?
Nature, V. 222, pp. 972-974.
- BOONE, G.M. (1962)
Potassic feldspar enrichment in magma: Origin of syenite in
Deboullie district, Northern Maine;
Geol. Soc. Amer., Bull. V.73, pp. 1451-1476.
- BOONE, G.M. (1969)
Origin of clouded red feldspars: petrologic contrasts in a
granitic porphyry intrusion;
Amer. J. Sci. V.267, pp. 633-668.
- BOWDEN, P. (1966)
Zirconium in younger granites of northern Nigeria;
Geochim. Cosmochim. Acta, V. 30, pp. 985-993.
- BOUSEILY, E.A.M. AND SOKKARY, E.A.A. (1975)
The relationship between Rb, Ba and Sr in granitic rocks; Chem.
Geol., V.16, pp. 207-219.
- BRADLEY, C. AND LYONS, E.J. (1953)
A mode of evolution of a granitic texture; in R.C. Emmons, ed.,
Selected Petrogenic Relationships of Plagioclase;
Geol. Soc. Amer. Memoir 52, pp. 101-121.
- BRIDGEWATER, D. AND FYFE, W.S. (1974)
The Pre 3 b.y. crust: Fact - Fiction - Fantasy;
Geoscience Canada, V.1, pp. 7-11
- BROOKS, C., HART, S.R., HOFMANN, A. AND JAMES, D.E. (1976)
Rb-Sr mantle isochrons from oceanic regions;
Earth, Planet, Sci. Let., V.32, pp. 51-61.
- BROOKS, C., HART, S.R. AND WENDT, I. (1972)
Realistic use of two error regression treatments as applied to
Rb-Sr data;
Reviews, geophys. Space Phys., V.10, No. 2, pp. 551-577.
- BROOKS C. KROGH, T.E., HART, S.R. AND DAVIS, G.L. (1970)
The Initial $^{87}\text{Sr}/^{86}\text{Sr}$ ratios of the Upper and Lower Series,
Michipicoten Metavolcanics, Ontario, Canada;
Carnegie Inst. Yearbook, Dept. of Terrestrial Magnetism, V.68,
pp. 422-425.

- BROOKS, C. AND LEGGO, M.D. (1972)
The local chronology and regional implications of a Rb-Sr investigation of granitic rocks from the Corryong District, S.E. Australia;
J. Geol. Soc. Australia, V.19; No. 1, pp. 1-19.
- BROWN, G.C., HUGHES, D.J. AND ESSON, J. (1973)
New XRF data retrieval techniques and their application to U.S.G.S. standard Rocks;
Chem. Geol., V.11, pp. 223-229.
- BRUECKNER, H.K. (1973)
Reconnaissance Rb-Sr investigation of salic, mafic and ultramafic rocks in the Oksfjord Area, Seiland Province, N. Norway;
Nord Geol. Tidssk., V.53, pp. 11-23.
- BUDDINGTON, A.F. (1959)
Granite emplacement, with special reference to North America;
Geol. Soc. Amer., Bull. V.70, pp. 671-747.
- BUNTEBARTH, G. (1976)
Distribution of U. in intrusive bodies due to combined migration and diffusion;
Earth, Planet. Sci. Lett., V.32, pp. 84-90.
- BURKE, K., DEWEY, J.F. AND KIDD, W.S. (1976)
Dominance of horizontal movements, arc and microcontinental collisions during the later permobile regime;
In: Windley B.F. (Editor), The Early History of the Earth; John Wiley and Sons, Toronto, pp. 113-129
- BURWASH, R.A. (1969)
Comparative Precambrian geochronology of the North American, European and Siberian Shields;
Can. J. Earth Sci., V.6 pp. 357 - 365.
- CARMICHAEL, I.S.E., TURNER, F.J. AND VERHOOGEN, J. (1974)
Igneous Petrology;
McGraw-Hill, Toronto, 739 p.
- CHAYES, F. (1958)
Petrographic Modal Analysis;
Wiley and Sons, New York, 113 p.
- CHAYES, F. (1967)
On the graphical appraisal of the strength of associations in petrographic variation diagrams; in
Researches in Geochemistry, V.2, P.H. Abelson, Editor; J. Wiley and Sons, New York, pp. 322-339.

- CHAYES, F. (1970)
On deciding whether trend surfaces of progressively higher order
are meaningful;
Geol. Soc. Amer., Bull. V.81, pp. 1273-1278.
- CHAYES, F. AND SUZUKI, Y. (1963)
Geologic contours and trend surfaces (a discussion);
J. Petrol., V.4, pp. 307-312.
- CLARK, S.P., PETERMAN, Z.E. AND HEIER, K.S. (1966)
Abundances of uranium, thorium and potassium;
Handbook of Physical Constants,
Geol. Soc. Amer. Memoir 97, Sect. 24, pp. 521-541.
- CLEMONS, R.E. AND LONG, L.E. (1971)
Petrologic and Rb-Sr isotopic study of the Chiquimula Pluton, S.E.
Guatemala;
Geol. Soc. Amer., Bull. V.82, pp. 2729-2740.
- CLIFFORD, P.M. (1972)
The Superior Province: geological structure;
R.A. Price and R.J.W. Douglas, editors, Variations in Tectonic
'Styles' in Canada;
Geol. Ass. Canada, Sp. Paper_11, pp. 540-553.
- CLOUD, P. (1976)
Major features of crustal evolution;
Alex L. Du Toit Memorial Lecture Series,
Geol. Soc. South Africa, pp. 1-33.
- COLEMAN, A.P. (1897)
Third report on the west Ontario gold region;
Bureau of Mines, 6th Annual Report, Section 2, pp. 71-124.
- COLEMAN, L.C. (1970)
Rb/Sr isochrons for some Precambrian rocks in the Hanson Lake area,
Saskatchewan;
Can. J. Earth Sci., V.7, No. 2., pp. 338-345.
- CONDIE, K.C. (1973)
Archean magmatism and crustal thickening;
Geol. Soc. Amer., Bull. V.84, pp. 2981-2992.
- COOK, B.G. AND ROGERS, J.J.W. (1968)
Radiometry and crystallization history of the Buchanan Granite
massif, Texas, U.S.A.;
Lithos, V.1, pp. 305-314.

- CRAM, I.H. (1932)
The Rest Island Granite of Minnesota and Ontario;
J. Geol., V.40, pp. 270-278.
- DAVID, M. AND WOUSSEN, G. (1973)
Correspondence analysis, a new tool for geologists;
Proc. Min. Pribram., V.1, pp. 41-65
- DAVIES, J.C. (1967)
Atkiwa Lake area;
Ontario Div. Mines, Prelim. Map P338
- DAVIES, J.C. (1973)
Geology of the Atikwa Lake area, District of Kenora;
Ontario Div. Mines, GR111, 58 p., incl. map 2273, 1" = 0.5 mi.
- DAVIES, J.C. AND PRYSLAK, A.P. (1967)
Kenora-Fort Frances Sheet, Districts of Kenora and Rainy River;
Ontario Div. Mines,
Geol. Compilation Series, Map 2115, 1" = 4 mi.
- DAVIES, R.D. AND ALLSOPP, H.L. (1976)
Strontium isotopic evidence relating to the evolution of the lower
Precambrian granitic crust in Swaziland;
Geology, V.4, pp. 553-556.
- DAVIS, D.W., GRAY, J., CUMMING, G.L. AND BAADSGAARD, H. (1977)
Determination of the ^{87}Rb decay constant;
Geol. Ass. Canada, Program With Abstracts, V.2., 15 p.
- DAWSON, K.R. AND CRAWLEY, W.D. (1963)
An improved technique for staining K-feldspars;
Can. Min., pp. 805-808.
- DAWSON, K.R. AND WHITTEN, E.H.T., (1962)
The quantitative mineralogical composition and variation of the
Lacorne, Le Motte and Preissac granitic complex, Quebec, Canada;
J. Petrol., V.3, pp. 1-37
- DE ALBUQUERQUE, C.A.R. (1973)
The origin of enclaves in granitic rocks from northern Portugal;
Geol. Soc. S. Africa, Spec. Publ. 3, pp. 479-493.
- DE LAETER, J.R. AND ABERCROMBIE, I.D. (1970)
Mass spectrometric isotope dilution analyses of rubidium and
strontium in standard rocks;
Earth, Planet. Sci. Letters, V.9, pp. 327-330

- DE LAETER, J.R. AND BLOCKLEY, J.G. (1972) -
Granite ages within the archaean Pilbara Block, W. Australia;
J. Geol. Soc. Australia, V.19, pt3, pp. 363-370
- DEWDNEY, S. AND KIDD, K.E. (1967)
Indian Rock Paintings of the Great Lakes;
U. Toronto Press, 2nd edition.
- DIDIER, J. (1973)
Granites and Their Enclaves;
Elsevier, New York, 393 p.
- DOERING, W.P. (1968)
A rapid method for measuring the Rb/Sr ratio in silicate rocks;
U.S. Geol. Survey, Prof. Paper 600-C, pp. C164-C168.
- DOIG, R. (1968)
The natural gamma ray flux; in situ analysis;
Geophysics, V.33, No. 2, pp. 311-328
- DONN, W.L., DONN, B.D. AND VALENTINE, W.G. (1965)
On the early history of the earth;
Geol. Soc. Amer., Bull. V.76, pp. 287-306.
- DOVETON, J.H. AND PARSLEY, A.J. (1970)
Experimental evaluation of trend surface distortions induced by
inadequate data-point distributions;
Inst. Min. Mett. Bull., Section B, pp. B197-B207.
- DRESCHER-KADEN, F.K. (1948)
Die Feldspat - Quarz - Reaktionsgefüge der Granite and Gneise, und
ihre genetische Bedeutung;
Springer, Heidelberg, 259 p.
- DUFFIELD, W.A. (1968)
The petrology and structure of the El Pinal Tonalite, Baja
California, Mexico;
Geol. Soc. Amer., Bull. 79, pp. 1351-1374
- EADE, K.E. AND FAHRIG, W.F. (1971)
Geochemical evolutionary trends of continental plates
A preliminary study of the Canadian Shield;
Geol. Survey Canada, Bulletin 179, 51 p.
- EADE, K.E. AND FAHRIG, W.F. (1973)
Regional lithological and temporal variation in the abundances of
some trace elements in the Canadian Shield;
Geol. Survey Canada, Paper 72-46, 46 p.

- EDWARDS, G.R. (1975)
Pipestone Lake Area;
Ontario Div. Mines, Prelim. Map P1000, 1" = 1/4 mi.
- EGGLER, D.H. (1968)
Virginia Dale Precambrian ring-dike complex, Colorado-Wyoming;
Geol. Soc. Amer. Bull. V.79, pp. 1545-1564.
- EL-GABY, S. (1975)
Petrochemistry and geochemistry of some granites from Egypt;
Jb. Miner. Abh., V.124, No. 2, pp. 147-189.
- EMMERMANN, R. (1968)
Differentiation and metasomatose des Albtalgranits,
(Südschwarzwald);
N.Jb. Miner. Abh., V.109, pp. 94-130.
- ENGEL, A.E.J., ITSON, S.P., ENGEL, C.G., STICKNEY, D.M. AND CRAY, E.J.
(1974)
Crustal evolution and global tectonics: A petrogenic view;
Geol. Soc. Amer., Bull., V.85, pp. 843-858.
- ERDMANNSDORFFER, O.H. (1946)
Magmatische und metasomatische Prozesse in Graniten, insbesondere
zweigliedergraniten;
Heidelb. Beiträge Mineral. Petrogr., V.1, pp. 213-250.
- ERDMANNSDORFFER, O.H. (1950)
Die Rolle der Endblastese in Granit;
Fortschr. Mineral., V.28, pp. 22-25.
- ERMANOVICS, I.F., (1970)
Zonal structure of the Perth road monzonite, Grenville Province,
Ontario;
Can. J., Earth. Sci., V.7, No. 2 pp. 414-434.
- ERMANOVICS, I.F., EDGAR, A.D. AND CURRIE, K.L. (1967)
Evidence bearing on the origin of the Belleoram stock, southeastern
Newfoundland;
Can. J. Earth Sci., 4, pp. 413-431.
- ESKOLA, P. (1956)
Postmagmatic potash metasomatism of granite;
C.R. Soc. Geol. Finl., V.172, pp. 85-100.

- EXLEY, C.S. (1963)
Quantitative areal modal analysis of granitic complexes: A further contribution;
Geol. Soc. Amer., Bull. V.74, pp. 649-654.
- FABBI, B.P. (1972)
A refined fusion XRF technique and determination of major and minor elements in silicate standards;
Amer. Min., V.57, pp. 237-245.
- FAHRIG, W.F. AND EADE, K.E. (1968)
The chemical evolution of the Canadian Shield;
Can. J. Earth Sci., V.5, pp. 1247-1252.
- FAHRIG, W.F. AND WANLESS, R.K. (1963)
Age and significance of diabase dyke swarms of the Canadian Shield;
Nature, V.200, No. 4910, pp. 934-937.
- FAIRBAIRN, H.W., HURLEY, P.M. AND PINSON, W.H. (1967)
Rb-Sr isochron ages of metasediments in the Canadian Shield;
M.I.T. 15th Ann. Report to U.S. Atomic Energy Com. pp. 61-63.
- FAIRBAIRN, H.W. AND HURLEY, P.M. (1969)
Northern Appalachian geochronology as a model for interpreting ages in older orogens;
Massachusetts Institute of Technology, 17th Annual Report, pp. 11-17.
- FALKUM, T. (1976)
Some aspects of the geochemistry and petrology of the Precambrian Homme granite in the Flekkefjord area, southern Norway;
Geol. For. Stockholm Forh., V.98, pp. 133-144.
- FARHAT, J.S. AND WETHERILL, G.W. (1975)
Interpretation of apparent ages in Minnesota;
Nature, V.257, pp. 721-722.
- FARQUHARSON, R.B. (1975)
Revised Rb-Sr age of the Lac du Bonnet quartz monzonite, southeastern Manitoba;
Can. J. Earth Sci., V.12, pp. 115-118.
- FARQUHARSON, R.B. (1976)
Radioelement content and variation in some granitoid units of southeastern Manitoba and adjacent Ontario;
Can. J. Earth Sci., V.13, pp. 993-997.

- FARQUHARSON, R.B. AND CLARK, G.S. (1971)
Rb/Sr geochronology of some granitic rocks in southeastern
Manitoba;
Geol. Ass. Canada, Sp. Paper 9, pp. 111-117.
- FARQUHARSON, R.B. AND RICHARDS, J.R. (1970)
Whole rock U-Th-Pb and Rb/Sr ages of the Sybella microgranite and
pegmatite, Mount Isa, Queensland;
J. Geol. Soc. Australia, V.17, pp. 53-58.
- FAURE, G. AND HURLEY, P.M. (1963)
The isotopic composition of Sr in oceanic and continental basalts;
application to the origin of igneous rocks;
J. Petrol., V.4, No. 1, pp. 31-50.
- FAURE, G. AND POWELL, J.L. (1972)
Strontium Isotope Geology;
Springer-Verlag, Berlin, 188 p.
- FRASER, N.H.C. (1943)
Whitefish Bay area, Lake of the Woods, District of Kenora,
Ontario;
Ontario Dept. Mines, Annual report, V.52, No. 4, Map 52c.
- FRASL, G. (1954)
Anzeichen schmelzflüssigen und hochtemperierten Wachstums an den
grossen Kalifeldspaten einiger Porphyrgranite, Porphyrgranitgneise
und Augengneise, Osterreichs;
Jb. Geol. Bundesanstalt, V.97, pp. 71-132.
- FRYE, J.K. (1959)
The petrography of the ancient granites of the Minnesota-Ontario
boundary region; unpublished M.Sc. thesis, U. of Minnesota, 55 p.
- FULLAGAR, P.D. (1971)
Age and origin of plutonic intrusions in the Piedmont of the S.E.
Appalachians;
Geol. Soc. Amer., Bull. V.82, pp. 2845-2862.
- GIBBINS, W. (1971)
Geology of the Falcon Lake Stock, southeastern Manitoba;
Geol. Ass. Canada, Sp. Paper 9, pp. 129-135.
- GIBBINS, W. (1972)
Experimental procedures for Rb-Sr age determinations;
Tech. Memo 72-4, Dept of Geology, McMaster University, Hamilton,
Ontario.

- GIBBINS, W.A. (1973)
Rubidium-strontium mineral and rock ages at Sudbury, Ontario;
Unpubl. PhD thesis, McMaster Univ., Hamilton, Ontario.
- GIBBINS, W.A. AND McNUTT, R.H. (1975)
The age of the Sudbury nickel irruptive and the Murray granite;
Can. J. Earth Sci., V.12, pp. 1970-1989.
- GIBLIN, P.E. (1964)
Burchell Lake Area;
Ontario Dept. Mines, Geol. Report 19, 14 p.
- GLIKSON, A.Y. (1971)
Primitive Archaean element distribution patterns: chemical
evidence and geotectonic significance;
Earth, Planet. Sci. Lett., V.12, pp. 309-320.
- GLIKSON, A.Y. (1972)
Early Precambrian evidence of a primitive ocean crust and island
nuclei of sodic granite;
Geol. Soc. Amer., Bull. V.83, pp. 3323-3344.
- GLIKSON, A.Y. (1976)
Archean to early proterozoic shield elements:
Relevance of plate tectonics;
In: Strong, D.F. (Editor), Metallogeny and Plate Tectonics;
Geol. Ass. Canada, Sp. Paper 14, pp. 489-516.
- GLIKSON, A.Y. AND SHERATON, J.W. (1972)
Early Precambrian trondhjemitic suites in western Australia and
N.W. Scotland and the geochemical evolution of shields;
Earth, Planet. Sci. Lett., V.17, pp. 227-242.
- GLIKSON, A.Y. AND LAMBERT, I.B. (1976)
Vertical zonation and petrogenesis of the early Precambrian crust
in western Australia;
Tectonophysics, V.30, pp. 50-89.
- GOLDICH, S.S. (1968)
Geochronology in the Lake Superior region;
Can. J. Earth Sci., V.5, pp. 715-724.
- GOLDICH, S.S. (1972)
Fallacious isochrons and wrong numbers;
Geol. Soc. Amer., Abstracts, V.4, No. 5, 322 p.

- GOLDICH, S.S. AND HEDGE, C.E. (1974)
3800 Myr granitic gneiss in southwestern Minnesota;
Nature, V.252, pp. 467-468.
- GOLDICH, S.S. AND HEDGE, C.E. (1975)
Interpretation of apparent ages in Minnesota: reply;
Nature, V.257, 722 p.
- GOLDICH, S.S., HEDGE, C.E. AND STERN, T.W. (1970)
Age of the Morton and Montevideo gneisses and related rocks, S.W.
Minnesota;
Geol. Soc. Amer., Bull. V.81, pp. 3671-3696.
- GOODWIN, A.M. (1965)
Preliminary report on volcanism and mineralization in the Lake of
the Woods - Manitou Lake - Wabigoon Lake region of Northwestern
Ontario;
Ontario Dept. Mines, PR 1965-2, 63 p.
- GOODWIN, A.M. (1968)
Archean protocontinental growth and early crustal history of the
Canadian Shield;
XXIII Int. Geol. Congress, V.1, pp. 68-89.
- GOODWIN, A.M. (1977)
Bookjacket of: Proceedings, 1977 Geotraverse Conference;
University of Toronto, 234 p.
- GOODWIN, A.M., PETTIJOHN, F.J. AND NORRIS, A.W. (1972)
Stratigraphic analysis of supercrustal rocks;
In: R.A. Price and R.J.W. Douglas, Editors, Variations in Tectonic
Styles in Canada,
Geol. Ass. Canada, Special Paper 11, pp. 529-540.
- GOODWIN, A.M. AND WEST, G.F. (1974)
The Superior Geotraverse project;
Geoscience Canada, V.1, No. 3, pp. 21-29.
- GRANT, N.K. (1970)
Geochronology of Precambrian basement rocks from Ibadan,
southwestern Nigeria;
Earth, Planet. Sci. Lett., V.10, pp. 29-38.
- GRASTY, R.L. AND DARNLEY, A.G. (1971)
The calibration of gamma ray spectrometers for ground and airborne
use;
Geol. Survey of Canada, Paper 71-17, 27 p.

- GRAUERT, B., HANNY, R. AND SOPTRAJANOVA, G. (1974)
Geochronology of a polymetamorphic and anatectic gneiss region:
the moldanubicum of the area Lam-Deggendorf, East Bavaria,
Germany;
Contr. Min. Petrol., V.45, pp. 37-63.
- GREEN, D.H. (1972)
Magmatic activity as the major process in the chemical evolution of
the earth's crust and mantle;
In: Ritsema, A.R. (Editor), The Upper Mantle, Tectonophysics,
V.13, pp. 47-71.
- GREEN, J. AND POLDERVAART, A. (1958)
Petrochemical fields and trends;
Geochim. Cosmochim. Acta, V.13, pp. 87-122.
- GROUT, F.F. (1929)
Ages and differentiation series of the batholiths near the
Minnesota - Ontario boundary;
Geol. Soc. Amer., Bull. V.40, pp. 791-809.
- GROUT, F.F. (1937)
Criteria of origin of inclusions in plutonic rocks;
Geol. Soc. Amer., Bull. V.48, pp. 1521-1572.
- GULSON, B.L. (1972)
The Precambrian geochronology of granitic rocks from northeastern
Sweden;
Geol. For. Stockholm Forh., V.94, pp. 229-244.
- GUMMER, W.K. (1941)
Border rocks of a granite batholith, Red Lake, Ontario;
J. Geol., V.49, No. 6, pp. 641-656.
- GUNN, B.M. (1967)
Matrix corrections for x-ray fluorescence spectrometry by digital
computer;
Can. J. Spectroscopy, V.12, No. 2, pp. 41-46, 64.
- GUNN, B.M. (1969)
The determination of barium in silicate samples by x-ray
fluorescence analysis;
Can. J. Spectroscopy, V.14, pp. 164-170.
- HALL, D.H. (1968)
Regional magnetic anomalies, magnetic units, and crustal structure
in the Kenora district of Ontario;
Can. J. Earth Sci., V.5, No. 5, pp. 1277-1296.

- HALL, A. (1967)
The variation of some trace elements in the Rosses granite complex,
Donegal;
Geol. Mag., V.104, No. 2, pp. 99-109.
- HAMILTON, W. AND MYERS, W.B. (1967)
The nature of batholiths;
U.S. Geol. Survey, Prof. Paper 554.c. C1 p.
- HANSON, G.N. (1968)
K-Ar ages for hornblende from granites and gneisses and for
basaltic intrusives in Minnesota;
Minnesota Geol. Survey, Report on Investigations 8, 20 p.
- HANSON, G.N. GOLDICH, S.S., ARTH, J.G. AND YARDLEY, D.H. (1971)
Age of the early Precambrian rocks of the Saganaga Lake - Northern
Light Lake area, Ontario-Minnesota;
Can. J. Earth Sci., V.8, pp. 1110-1124.
- HARCOURT, G.A. (1934)
The minor chemical constituents of some igneous rocks;
J. Geology, V.42, pp. 585-601.
- HARRIS, F.R. (1974)
Geology of the Rainy Lake area, District of Rainy River;
Ontario Div. Mines, GR115, 94 p.
Maps 2278 and 2279, scale 1" = 1/2 mile.
- HART, S.R. (1961)
The use of hornblendes and pyroxenes for K-Ar dating;
J. Geophys. Research, V.66, No. 9, pp. 2995-3001.
- HART, S.R. AND BROOKS, C. (1970)
Rb-Sr mantle evolution models;
Carnegie Inst. Yearbook 68, pp. 426-429.
- HART, S.R. AND DAVIS, G.L. (1969)
Zircon, U-Pb and whole-rock Rb/Sr ages and early crustal
development near Rainy Lake, Ontario;
Geol. Soc. Amer., Bull. V.80, pp. 595-616.
- HAWKES, L. (1929)
On a partially fused quartz-feldspar rock and on glomero-granular
texture;
Min. Mag., V.22, No. 127, pp. 163-173.
- HAYATSU, A. (1972)
On the basic assumptions in K-Ar dating methods;
Comments on Earth Sciences, Geophysics, V.3, pp. 69-75.

- HAYATSU, A. AND CARMICHAEL, C.M. (1977)
Removal of atmospheric argon contamination and the use and misuse
of the K-Ar isochron method;
Can. J. Earth Sci., V.14, pp. 337-345.
- HAYATSU, A. AND PALMER, H.C. (1975)
K-Ar isochron study of the Tudor Gabbro, Grenville Province,
Ontario;
Earth, Planet. Sci. Lett., V.25, No. 2, pp. 208-212.
- HEDGE, C.E. AND PETERMAN, Z.E. (1970)
The Sr isotopic composition of basalts from the Gordo and Juan de
Fuca Rises, northeastern Pacific Ocean;
Contr. Min. Petrol., V.27, pp. 114-120.
- HEDGE, C.E. AND WALTHALL, F.G. (1963)
Radiogenic strontium 87 as an index of geologic processes;
Science, V.140, pp. 1214-1217.
- HEIER, K. AND COMPSTON, W. (1969)
Interpretation of Rb-Sr age patterns in high-grade metamorphic
rocks, North Norway;
Norsk Geol. Tidsskrift, V.49, No. 3, pp. 257-283.
- HEIER, K.S., NATERSTAD, J. AND BRYHNI, I. (1972)
A Rb-Sr whole rock isochron date from the Stavanger area, S.
Norway;
Norsk. Geol. Tids., V.52, pp. 377-382.
- HEIMLICH, R.A. (1963)
Geochronology of some granitic plutons, Lake of the woods region,
Ontario;
Mass. Inst. Techn., 11th Ann. Report, pp. 113-116.
- HEIMLICH, R.A. (1965)
Petrology of the Flora Lake Stock, Lake of the Woods, Canada;
Geol. Soc. Amer., Bull. V.76, pp. 1-26.
- HEIMLICH, R.A. (1966)
The Hope Lake Stock, Lake of the Woods Region, Ontario;
Can. Min., V.8, 5 p., pp. 620-637.
- HEIMLICH, R.A. (1968)
Petrology of the Flora Lake Stock, Lake of the Woods region,
Ontario, Canada: Reply;
Geol. Soc. Amer., Bull. V.79, pp. 1251-1258.

- HEIMLICH, R.A. (1971)
Greenstone assimilation by tonalite magma, Atikwa Lake, Ontario;
Geol. Mag., V.108, pp. 1-12.
- HIBBARD, M.J. (1965)
Origin of some alkali feldspar phenocrysts and their bearing on
petrogenesis;
Amer. J. Sci., V.263, pp. 245-261.
- HILLS, F.A. AND DASCH, E.J. (1972)
Rb/Sr study of the Stony Creek granite, Southern Connecticut: a
case for limited remobilization;
Geol. Soc. Amer., Bull. 83, pp. 3457-3464.
- HOFMANN, A. (1972)
Chromatographic theory of infiltration metasomatism and its
application to feldspars;
Amer. J. Sci., V.272, pp. 69-90.
- HOFMANN, A.W. AND HART, S.R. (1975)
An assessment of local and regional isotopic equilibrium in a
partially molten mantle;
Carnegie Inst. Yearbook V.74, pp. 195-210.
- HOLLAND, J.G. AND LAMBERT, R. St. J. (1972)
Major element chemical composition of shields and the continental
crust;
Geochim et Cosmochim. Acta, V.36, pp. 673-683.
- HOPWOOD, T.P. (1976)
Quartz-eye bearing porphyroidal rocks and volcanogenic massive
sulphide deposits;
Econ. Geol., V.71, pp. 589-612.
- HOWARTH, R.J. (1967)
Trend-surface fitting to random data - an experimental test;
Amer. J. Sci., V. 265, pp. 619-625.
- HUBBARD, F.H. (1967)
Exsolution myrmekite;
Geol. For. Stockholm Forh., V.89, pp. 410-422.
- HUGHES, C.J. AND HUSSEY, E.M. (1976)
M + Mg values in igneous rocks: proposed usage and a comment on
currently employed Fe₂O₃ corrections;
Geochim. Cosmochim. Acta, V.40, pp. 485-486.

- HURST, M.E. (1935)
Vein formation at Porcupine, Ontario;
Econ. Geol., V.30, 125 p.
- HURST, R.W., BRIDGEWATER, D. AND COLLERSON, K.D. (1975)
3600 M.Y. Rb-Sr ages from very early Archean gneisses from Saglek Bay, Labrador;
Earth, Planet. Sci. Lett., V.27, pp. 393-403.
- HUTCHISON, C.S. (1974)
Laboratory Handbook of Petrographic Techniques;
John Wiley and Sons, Toronto, 527 p.
- HUTCHISON, C.S. AND Jeacocke, J.E. (1971)
Fortran IV computer programme for calculation of the Niggli Molecular Norm;
Geol. Soc. Malaysia, Bull. 4, pp. 91-95.
- INGHAM, W.N. AND KEEVIL, N.B. (1951)
Radioactivity of the Bourlamaque, Elzevir and Cheddar batholiths, Canada;
Geol. Soc. Amer., Bull. V.62, pp. 131-148.
- I.U.G.S. (1973)
Classification and nomenclature of plutonic rocks, recommendations;
International Union of Geological Sciences, Subcommittee on the Systematics of Igneous Rocks; N. Jb. Miner. Mh., H4, pp. 149-164.
- JAHN, B. AND MURTHY, V.R. (1975)
Rb-Sr ages of the Archean rocks from the Vermilion district, N.E. Minnesota;
Geochim. Cosmochim. Acta, V.39, pp. 1679-1689.
- JOHANSEN, A. (1939)
A descriptive petrography of the igneous rocks;
V.2, U. Chicago Press, Chicago.
- JOHNSTON, W.G.Q. (1960)
Atikwa Caviar Lakes area;
Ontario Dept. Mines, Prelim. map, P84.
- JOHNSTON, W.G.Q. (1965)
Geology and Mineral Prospects, Atikwa (Deer) - Populus Lakes area, Kenora District, Ontario;
J.L. Perkins Bookbinder Ltd., Regina, 130 p.

- JOHNSTON, W.G.Q. (1968)
Petrology of the Flora Lake Stock, Lake of the Woods region,
Ontario, Canada; Discussion;
Geol. Soc. Amer. Bull. 79, pp. 1247 - 1250.
- JOYCE, A.S. (1973)
Application of cluster analysis to detection of subtle variation in
a granitic intrusion;
Chem. Geol., V.11, pp. 297-306.
- KAGAMI, H., SHUTO, K. AND GORAI, M. (1975)
Reexamination of the source material of acid igneous rocks based on
the selected Sr isotopic data;
J. Geol. Soc. Japan, V.81, No. 5, pp. 319-330.
- KARNER, F.R. (1970)
Evidence for convection as a cause of zoning in granitic plutons;
Geol. Soc. Amer., Abstracts, V.2, No. 7, 590 p.
- KEHLENBECK, M.M. (1977)
The Barnum Lake Pluton, Thunder Bay, Ontario;
Can. J. Earth Sci., V.14, pp. 2157-2167.
- KERRICK, D.M. (1969)
K feldspar megacrysts from a porphyritic quartz monzonite, central
Sierra Nevada, California;
Amer. Min., V.54, pp. 839-848.
- KILLEEN, P.G. AND HEIER, K.S. (1975)
Th, U, K and heat production measurements in ten Precambrian
granites of the Telemark Area, Norway;
Norges Geol. Under. V.319, pp. 59-83.
- KOCHHAR, N. (1977)
Post-emplacment alkali modifications in rapidly cooled acid
volcanic rocks;
Amer. Min., V.62, pp. 333-335.
- KOLBE, P. AND TAYLOR, S.R. (1966)
Major and trace element relationships in granodiorites and granites
from Australia and S. Africa;
Contr. Min. Petrol, V.12, pp. 202-222.
- KOLJONEN, T. AND ROSENBERG, R.J. (1974)
Rare earth elements in granitic rocks;
Lithos, V.7, pp. 249-261.

- KURZHINSKII, D.S. (1949)
Theory of Metasomatic Zoning; (English Trans.), Oxford, Clarendon Press, 162 p.
- KRESTEN, P. (1974)
Postmagmatische differentiation eines präkambrischen Granitenintrusivs:
Das Örö-Hamnö-Massiv in Südostschweden;
Geol. For. Stockholm Forh., V.96 pp. 67-124.
- KROGH, T.E. AND DAVIS, G.L. (1971)
The effect of regional metamorphism on U-Pb systems in zircons and a comparison with Rb-Sr systems in the same whole rock;
Carnegie Inst. Yearbook 71, pp. 564-571.
- KROGH, T.E. AND DAVIS, G.L. (1973)a
The effect of regional metamorphism on U-Pb systems in zircon and a comparison with Rb-Sr systems in the same whole rock and its constituent minerals;
Carnegie Inst. Yearbook, V.72, pp. 601-610.
- KROGH, T.E. AND DAVIS, G.L. (1973)b
The significance of inherited zircons on the age and origin of igneous rocks - an investigation of the ages of the Labrador Adamellites;
Carnegie Inst. Yearbook, V.72, pp. 610-613.
- KROGH, T.E., HARRIS, N.B.W. AND DAVIS, G.L. (1976)
Archean rocks from the eastern Lac Seul region of the English River gneiss belt, northwestern Ontario: part 2, geochronology;
Can. J. Earth Sci., V.13, pp. 1212-1215.
- KRUFIKHOVSKAYA, Z.A., PASHKEVICH, I.K. AND SIMONENKO, T.N. (1973)
Magnetic anomalies of Precambrian shields and some problems of their geological interpretation;
Can. J. Earth Sci., V.10, pp. 629-636.
- KWONG, Y.T.J. (1975)
Distribution of gold in an Archean greenstone belt, as exemplified by the Kakagi Lake area, northwestern Ontario;
MSc thesis, Dept. Geology, McMaster Univer. Hamilton.
- LABHART, T.P. AND RYBACH, L. (1971)
Abundance and distribution of U and Th in the Syenite of Piz Giuv (Aar-Massif, Switzerland);
Chem. Geol., V.7, pp. 237-251.

- LAMBERT, I.B. AND HEIER, K.S. (1968)
Geochemical investigations of deep-seated rocks in the Australian Shield;
Lithos, V.1, pp. 30-53.
- LANGFORD, F.F. AND MORIN, J.A. (1976)
The development of the Superior Province of northwestern Ontario by merging island arcs;
Amer. J. Sci., V.276, pp. 1023-1034.
- LARSEN, E.S. (1938)
Some new variation diagrams for groups of igneous rocks;
J. Geol., V.46, pp. 505 - 520.
- LARSEN, L.H. AND POLDERVAART, A. (1961)
Petrologic study of Bald Rock Batholith, near Bidwell Bar, California;
Geol. Soc. Amer., Bull. V.72, pp. 69 - 92.
- LAWSON, A.C. (1887)
Report on the Geology of the Rainy Lake Region;
Geol. Natural History Survey of Canada, Ann. Report, V.3, pt.1, pp. 1F - 182F, incl. map: District of Rainy River, Rainy Lake Sheet, 1" = 4 Miles.
- LAWSON, A.C. (1913)
The Archaean geology of Rainy Lake re-studied;
Can. Dept. Mines, Memoir 40, Geol. Series No. 24, 115 p, incl. map 98A (1914), 1" = 1 Mile.
- LEAKE, B.E., HENDRY G.L., KEMP, A., PLANT, A.G., HARREY, P.K., WILSON, J.R., COATS, J.S., AUCOTT, J.W., LUNEL, T. AND HOWARTH, R.J. (1969)
The chemical analysis of rock powders by automatic x-ray fluorescence;
Chem. Geol., V.5, pp. 7 - 86.
- LONGSTAFFE, F.J., McNUTT, R.H. AND SCHWARCZ, H.P. (1977)
Geochemistry of Archean Rocks from the Lake Despair area, Ontario: A preliminary report;
Geol. Surv. Can., Report of Activities, A, paper 77 - 1A, pp. 169 - 178.
- LOYBORG, L., WOLLENBERG, H., SORENSEN, P. AND HANSEN, J. (1971)
Field determination of U and Th by gamma ray spectrometry, exemplified by measurements in the Ilimaussaq alkaline intrusion, S. Greenland;
Econ. Geol., V.66, pp. 368 - 384.

- MACKASEY, W.O., BLACKBURN, C.E., TROWELL, N.F. (1974)
A regional approach to the Wabigoon-Quetico Belts and its bearing
on exploration in northwestern Ontario;
Ont. Div. Mines, Miscellaneous paper 58, 29 p.
- MARCHAND, M. (1973)
Determination of Rb, Sr and Rb/Sr by XRF;
Tech. Memo 73-2, Dept. of Geology McMaster Univ., Hamilton,
Ontario.
- MARCHAND, M. (1976)
A Geochemical and Geochronological Investigation of Meteoritic
Impact Melts at Mistastin Lake, Labrador and Sudbury, Ontario;
Unpublished PhD thesis, McMaster University, Hamilton, Ontario
142 p.
- MARMO, V. (1971)
Granite Petrology and the Granite Problem;
Elsevier, Amsterdam, 244 p.
- MATHEWS, G.W., CAIN, J.A. AND BANKS, P.O. (1975)
Three dimensional polynomial trend analysis applied to igneous
petrogenesis;
Geol. Soc. Amer., Memoir 142, pp. 239 - 256.
- MATSUDA, J. (1974)
A virtual Rb-Sr isochron for an open system;
Geochem. Jour., V.8, pp. 153 - 155.
- MATTINSON, J.M. (1969)
Preparation of HF, HCl, Nitric acid at ultralow lead levels;
Anal. Chem. V.41, pp. 2088 - 2089.
- MCCARTHY, T.S. AND HASTY, R.A. (1976)
Trace element distribution patterns and their relationship to the
crystallization of granitic melts;
Geochim. Cosmochim. Acta, V.40, pp. 1351 - 1358.
- MCGLYNN, J.C. (1970)
Superior Province;
In: R.J.W. Douglas, ed., Geology and Economic Minerals of Canada;
Geol. Survey Canada, Econ. Geol. Report No. 1, 838 p.
- MCGRATH, P.H. AND HALL, D.H. (1969)
Crustal structure in northwestern Ontario: Regional magnetic
anomalies;
Can. J. Earth Sci., V.6, No. 1, pp. 101 - 107.

- McINTYRE, G.A., BROOKS, C., COMPSTON, W. AND TUREK, A. (1966)
The statistical assessment of Rb-Sr isochrons;
J. Geophys. Research, V.71, No. 22, pp. 5450 - 5468.
- MIDDLEMOST, E.A.K. AND ROMEY, W.D. (1968)
A graphic story of magmatic differentiation;
Lithos, V.1, pp. 242 - 263.
- MIESCH, A.T. (1975)
Variograms and variance components in geochemistry and ore
evaluation; Geol. Soc. Amer., Memoir 142, pp. 333 - 340.
- MILLER, W.G. AND KNIGHT, C.W. (1915)
Metallogenetic epochs in the Precambrian of Ontario;
Ontario Bureau of Mines, 24th annual report, Vol. 24, Part 1,
pp. 243 - 248.
- MILNE, V.G. (1972)
Geology of the Kukatush - Sewell Lake area, District of Sudbury;
Ontario Div. Mines, GR97, 48 p.
- MITCHELL, R.H. (1969)
The isotopic composition of strontium in South African Kimberlites
and in alkaline rocks of the Fen area, South Norway;
Unpubl. PhD thesis, McMaster Univ., Hamilton.
- MITCHELL, R.H. (1976)
K-Ar geochronology of the Poohbah Lake alkaline complex,
northwestern Ontario;
Can. J. Earth Sci., V.13, pp. 1456 - 1459.
- MONGER, J.W.H., SOUTHER, J.G. AND GABRIELSE, H. (1972)
Evolution of the Canadian cordillera: a plate-tectonic model;
Amer. J. Sci., V. 272, pp. 577 - 602.
- MOORBATH, S. (1967)
Recent advances in the application and interpretation of
radiometric age data;
Earth Sci. Review, V.3, pp. 111 - 133.
- MOORBATH, S. (1975)
Constraints for the evolution of Precambrian crust from strontium
isotopic evidence;
Nature, V.254, pp. 395 - 398.
- MOORBATH, S. (1976)
Age and isotope constraints for the evolution of Archean crust;
In: B.F. Windley ed., The Early History of the Earth,
pp. 351 - 360.

- MOORHOUSE, W.W. (1939)
Eagle Lake area, District of Kenora;
Ontario Department of Mines, Ann. Report V.48, pt. 4.
- MOORHOUSE, W.W. (1959)
The Study of Rocks in Thin Section;
Harper and Row Publishers, New York, 514 p.
- MOREY, G.B. AND SIMS, P.K. (1976)
Boundary between two Precambrian W. terrains in Minnesota and its
geologic significance;
Geol. Soc. Amer., Bull., V.87, pp. 141 - 152.
- MURAD, E. (1975)
Determination of barium in geological samples by x-ray
spectrometry;
Spectrochimica Acta, V.30 B, pp. 433 - 439.
- MURSKY, G. (1972)
Origin and significance of zonation in a granitic intrusion;
Inter: Geol. Congress, 24th, Sect. 2, p. 181 - 190.
- NAGASAWA, H. AND SCHNETZLER, C. (1971)
Partitioning of rare earth, alkali and alkaline earth elements
between phenocrysts and acidic igneous magma;
Geochim. Cosmochim. Acta, V.35, pp. 953 - 968.
- NATIONAL Bureau of Standards (1972).
Standard reference material 988, Strontium - 84 spike;
U.S. Dept. Commerce, certificate of analysis, Office of Standard
Reference Materials, Oct. 5, 1972.
- NELSON, D.O. AND DASCH, E.J. (1976)
Disequilibrium of Sr isotopes between mineral phases of parental
rocks during magma genesis, a discussion;
J. Volc. Geotherm. Research, V.1, pp. 183 - 191.
- NEUMANN, W. AND HUSTER, E. (1976).
Discussion of the Rb^{87} half-life determined by absolute
counting;
Earth, Planet. Sci. Letters, V.33, pp. 277 - 288.
- NOCKOLDS, S.R. (1954)
Average chemical compositions of some igneous rocks;
Geol. Soc. Amer., Bull. V.65, pp. 1007 - 1032.

- NOCKOLDS, S.R. AND ALLEN, R. (1953)
The geochemistry of some igneous rock series;
Geochim. Cosmochim. Acta, V.4, pp. 105 - 142.
- NOIRET, G., MONTIGNY, R. AND ALLEGRE, C.J. (1972)
 Rb^{87}/Sr^{86} systematics in Basin de Paris basement complex
rocks;
Geol. Soc. Amer., Bull. 83, pp. 3003 - 3006.
- NORMAN II, M.B. (1974)
Improved techniques for selective staining of feldspar and other
minerals using Amaranth;
J. Research, U.S.G.S., V.2, No.1, pp. 73 - 79.
- ODM (1971)
Joint Ontario Div. Mines and Geol. Survey of Canada aeromagnetic
survey, including maps 1150G, 1151G, 1153G, 1158G, 1160G, 1162G,
1167G, 1169G and 1177G as indexed in:
Aeromagnetic Index of Ontario; Ontario Div. Mines, Map 2229,
1:900,800, 1971.
- O'NIONS, R.K. AND PANKHURST, R.J. (1973)
Secular variation in the Sr-isotope composition of Icelandic
volcanic rocks;
Earth, Planet. Sci. Lett., V.21, pp. 13 - 21.
- ORVILLE, P.M. (1963)
Alkali ion exchange between vapor and feldspar phases;
Amer. J. Sci., V.261, pp. 201 - 237.
- PAGE, R.W. (1976)
Response of U-Pb, zircon and Rb/Sr total rock systems to low grade
regional metamorphism in Proterozoic igneous rocks, Mount Isa,
Australia;
Carnegie Inst. Yearbook, V.75, pp. 813 - 821.
- PANKHURST, R.J. AND O'NIONS, R.K. (1973)
Determination of Rb/Sr and $^{87}Sr/^{86}Sr$ ratios of some
standard rocks and evaluation of x-ray fluorescence spectrometry in
Rb/Sr geochemistry;
Chem. Geol., V.12, pp. 127 - 136.
- PARKER, R.L. AND FLEISCHER, M. (1968)
Geochemistry of Niobium and Tantalum;
U.S. Geol. Survey, Prof. paper 612, 43 p.
- PARSLOW, G.R. (1969)
Mesonorms of granitic rock analyses;
Min. Mag., V.37, No. 286, pp. 262 - 269.

- PARSLOW, G.R. (1971)
Variations in mineralogy and major elements in the Cairnsmore of Fleet granite, S.W. Scotland;
Lithos, V.4, pp. 43 - 55.
- PARSONS, A.L. (1912)
Goldfields of Lake of the Woods, Manitou and Dryden;
Ontario Bureau of Mines, Annual Report 21, V.21, Pt. 1.
- PAULUS, G.E. AND TURNOCK, A.C. (1971)
Petrography of the Ross River pluton, Manitoba;
Manitoba Mines Branch, Pub. 71-1 Report 9, pp. 215 - 225.
- PEARCE, T.H. (1968)
A contribution to the theory of variation diagrams;
Contr. Min. Petrol., V.19, pp. 142 - 157.
- PEIKERT, E.W. (1963)
Biotite variation as a guide to petrogenesis of granitic rocks in the Precambrian of N.E. Alberta;
J. Petrol, V.4, No. 3, pp. 432 - 459.
- PEIKERT, E.W. (1965)
Model for three dimensional mineralogical variation in granitic plutons, based on the Glen Alpine stock, Sierra, Nevada, California;
Geol. Soc. Amer., Bull. V.76, pp. 331 - 348.
- PENNER, A.P. AND CLARK, G.S. (1971)
Rb/Sr age determinations from the Bird River Area, S.E. Manitoba;
Geol. Ass. Canada. Sp. Paper 9, pp. 105 - 109.
- PETERMAN, Z.E., GOLDICH, S.S., HEDGE, C.E. AND YARDLEY, D.H. (1972)
Geochronology of the Rainy Lake Region, Minnesota - Ontario;
Geol. Soc. Amer., Memoir 135, p. 193 - 215.
- PETERMAN, Z.E. AND HEDGE, C.E. (1971)
Related Sr isotopic and chemical variations in oceanic basalts;
Geol. Soc. Amer., Bull. V.82, pp. 493 - 500.
- PICHETTE, R.J. (1976)
Petrology and geochemistry of the Taylor Lake stock, Superior Province, Northwest Ontario;
Dept. of Geology, McMaster Univ., B.Sc. thesis.
- PIGEON, R.T. AND HOPGOOD, A.M. (1975)
Geochronology of Archean gneisses and tonalites from north of the Frederickshabs isblink, S.W. Greenland;
Geochim. Cosmochim. Acta, V.39, pp. 1333 - 1346.

- PITCHER, W.S. AND BERGER, A.R. (1972)
The Geology of Donegal: A study of Granite Emplacement and Unroofing;
Wiley Interscience, New York, 435 p.
- PIWINSKII, A.J. (1968)
Studies of batholithic feldspars:
Sierra Nevada, California;
Contr. Min. Petrol., V.17, pp. 204 - 223.
- POLDERVAART, A. AND PARKER, A.B. (1964)
The crystallization index as a parameter of igneous differentiation in binary variation diagrams;
Amer. J. Sci., V.262, pp. 281 - 289.
- POLLOCK, G.D. (1960)
Age determination of granitic rocks from Manitoba and N.W. Ontario by the lead alpha method;
MSc thesis, Dept. of Geology, Univ. Manitoba, Winnipeg.
- PROPÄCH VON, G. AND DOPEL, E. (1972)
Common differentiation of the Bärhalde and Schluchsee granites;
N. Jahrbuch F. Mineral. Monats. pp. 289 - 299.
- PURDY, J. AND YORK, D. (1966)
A geochronometric study of the Superior Province near Red Lake N.W. Ontario;
Can. J. Earth. Sci., V.3, pp. 277 - 286.
- PYE, E.G. (1965)
Geology and lithium deposits of the Georgia Lake area, District of Thunder Bay;
Ontario Department of Mines, Geol. Report 31; 113 p.
- PYÉ, E.G. (1969)
Geology and Scenery, North Shore of Lake Superior;
Ontario Department of Mines, Geol. Guide Book 2, 144 p.
- RAGLAND, P.C., BILLINGS, G.K. AND ADAMS, J.A.S. (1967)
Chemical fractionation and its relationship to the distribution of Th, U in a zoned granite batholith;
Geochim. Cosmochim. Acta, V.31, pp. 17 - 33.
- RAGLAND, P.C. AND BUTLER, J.R. (1972)
Crystallization of the West Farrington pluton, N. Carolina, U.S.A.;
J. Petrol., V.13, No. 3, pp. 381 - 404.

- RAJU, D.R. AND RAO, J.R.K. (1972)
Chemical distinction between replacement and magmatic granitic rocks;
Contr. Min. Petrol., V.35, pp. 169 - 172.
- READ, H.H. (1957)
The Granite Controversy;
Murby, London, 430 p.
- REED, J.C. AND ZAKIMAN, R.E. (1973)
Geochronology of Precambrian rocks of the Teton Range, Wyoming;
Geol. Soc. Amer., Bull. V.84, pp. 561 - 582.
- REILLY, G.A. AND SHAW, D.M. (1967)
An estimate of the composition of part of the Canadian Shield in northwestern Ontario;
Can. Jour. Earth Sci., V.4, pp. 725 - 739.
- RHODES, J.M. (1969)
The application of cluster and discriminatory analysis in mapping granite intrusions;
Lithos, V.2, pp. 223 - 237.
- RILEY, G.H. AND COMPSTON, W. (1962)
Theoretical and technical aspects of Rb-Sr geochronology;
Geochim. Cosmochim. Acta, V.26, pp. 1255 - 1281.
- RINGWOOD, A.E. (1955)a
The principles governing trace element distribution during magmatic crystallization:
Part I, The Influence of Electronegativity;
Geochim. Cosmochim. Acta, V.7, pp. 189 - 202.
- RINGWOOD, A.E. (1955)b
The principles governing trace-element behaviour during magmatic crystallization:
Part II, The Role of Complex Formation;
Geochim. Cosmochim. Acta, V.7, pp. 242 - 254.
- RODDICK, J.C. AND COMPSTON, W. (1977)
Strontium isotopic equilibration:
A solution to a paradox;
Earth, Planet. Sci. Lett., V.34, pp. 238 - 246.

- ROGERS, J.J.W. (1964)
Statistical tests of the homogeneity of the radioactive components of granitic rocks;
In: J.A.S. Adams and W.M. Lowder, editors, The Natural Radiation Environment;
U. Chicago Press, pp. 51 - 62.
- ROGERS, J.J.W. AND ADAMS, J.A.S. (1963)
Lognormality of Th concentrations in the Conway granite;
Geochim. Cosmochim. Acta, V.27, pp. 775 - 783.
- ROSS, J.V. (1957)
Combination twinning in plagioclase feldspars;
Amer. J. Sci., V.255, pp. 650 - 655.
- RYABCHIKOV, I.D. (1962)
The behaviour of trace elements during crystallization in a multicomponent system;
Geochemistry, V.12, pp. 1179 - 1189.
- RYBACH, VON L. AND LABHART, T.P. (1973)
Regelmässigkeiten der Radioaktivitätsverteilung in granitischen Gesteinskörpern;
Schw. Min. u. Petr. Mitt., B.53, H.3, pp. 379 - 384.
- SAGE, R.P., BLACKBURN, C.E., BREAKS, F.W., McWILLIAMS, G.M., SCHWERTNER, W.M. AND STOTT, G.M. (1975)
Internal structure and composition of two granite complexes in Wabigoon Subprovince;
Geotraverse Workshop, Feb. 1975, University of Toronto, pp. 2.1 to 2.15.
- SAHA, A.K. (1959)
Emplacement of three granitic plutons in S.E. Ontario, Canada;
Geol. Soc. Amer., Bull. V.70; pp. 1293 - 1326.
- SAHA, A.K. (1964)
A simple grid deviation technique of study of the areal composition variations in granitic bodies;
Geol. Mag., V.101, No. 2, pp. 145 - 149.
- SANDERS, C.W. (1929)
A composite stock at Snowbank Lake in Northeastern Minnesota;
J. Geol., V.37, pp. 135 - 149.
- SARMA, S.R. AND RAJA, N. (1959)
On myrmekite;
Q.J. Geol. Mining Metal. Soc. India, V.31 (2).

- SCHERMERHORN, L.J.G. (1956)
The granites of Trancoso (Portugal):
A study in microclinization;
Amer. J. Sci., V.254, pp. 329 - 348.
- SCHERMERHORN, L.J.G. (1958)a
Petrogenesis of a porphyritic granite east of Uporto, (Portugal);
Tscherma's min. u. petr. Mitt., Bd.6, H1-2, pp. 73 - 115.
- SCHERMERHORN, L.J.G. (1958)b
The paragenesis of accessory minerals in igneous rocks;
Econ. Geol., V.53, pp. 215 - 218.
- SCHERMERHORN, L.J.G. (1960)
Telescoping of mineral facies in granites;
Bull. Comm. Geol. Finlande, V.188, pp. 121 - 132.
- SCHWERDTNER, W.M. AND GOODWIN, A.M. (1977)
Structural geology of geotraverse region;
Proceedings, 1977 Geotraverse Conf., Univ. Toronto,
pp. 2.1 - 2.29.
- SELIGMAN, G. (1949)
The growth of the glacier crystal;
J. Glaciology, V.1, No. 5, pp. 254 - 267 and V.1, No. 7,
pp. 379 - 381.
- SHAW, D.M. (1967)
U, Th, K in the Canadian Precambrian Shield and possible mantle
compositions;
Geochim. Cosmochim. Acta, V.31, pp. 1111 - 1113.
- SHELLEY, D. (1964)
On myrmekite;
Amer. Min., V.49, pp. 41 - 52.
- SHKLANKA, R. (1972)
Geology of the Steep Rock Lake area, District of Rainy River;
Ontario Division of Mines, Geol. Report 93.
- SHMAKIN, B.M. (1971)
The role of pressure in geochemical differentiation of granites and
pegmatites;
Geochem. Inter., V.8, No. 6; translated from Geokhimiya, V.12,
pp. 1494 - 1500, 1971.

- SIMPSON, E.S.W. (1954)
On the graphical representation of differentiation trends in igneous rocks;
Geol. Mag., V.91, pp. 238 - 244.
- SMITHSON, S.B. (1965)
The nature of the granitic layer of the crust in the southern Norwegian Precambrian;
Norsk. Geol. Tidsskrift, V.45, pp. 114 - 133.
- SMITHSON, S.B. (1966)
Oriented plagioclase grains in K-feldspar porphyroblasts;
Contrib. Geology, V.4, pp. 63 - 68.
- SMITHSON, S.B. AND BROWN, S.K. (1977)
A model for lower continental crust;
Earth, Planet. Sci. Lett., V.35, pp. 134 - 144.
- SÖRGENFREI, T. (1971)
On the granite problem and the similarity of salt and granite structures;
Geol. Fören. Stockholm Förh., V.93, pp. 372 - 435.
- SPEARS, D.A. (1974)
The Rb-Sr age dating of some Carboniferous shales;
Geochim. Cosmochim. Acta, V.38, pp. 235 - 244.
- SPENCER, E. (1938)
The potash-soda feldspars - II Some applications to petrogenesis;
Min. Mag., V.25, No. 162, pp. 87 - 118.
- SPIEGEL, M.R. (1961)
Schaum's Outline of Theory and Problems of Statistics;
Schaum's Outline Series, McGraw-Hill, Toronto, 329 p.
- STACEY, J.S., WILSON, E.E., PETERMAN, Z.E. AND TERRAZAS, R. (1971)
Digital recording of mass spectra in geologic studies I;
Can. J. Earth Sci., V.8, pp. 371 - 377.
- STEPHANSSON, O. (1972)
Theoretical and experimental studies of diapiric structures on Öland;
Bull. Geol. Inst., U. of Uppsala, New series 3, pp. 163 - 200.
- STEPHANSSON, O. (1975)
Polydiapirism of granitic rocks in the Svecofennian of central Sweden; Precambrian Research, V.2, Pt. 2, pp. 189 - 214.

- STOCKWELL, C.H. (1970)
Geology of the Canadian Shield: Introduction;
In: Geology and Economic Minerals of Canada, R.J.W. Douglas
editor,
Geol. Survey of Canada, Econ. Geol. Report No. 1, pp. 44 - 54.
- STOCKWELL, C.H. (1972)
Revised Precambrian time scale for the Canadian Shield;
Geol. Survey Canada, paper 72 - 52, 4 p.
- STONE, M. AND AUSTIN, W.G.C. (1961)
The metasomatic origin of the potash feldspar megacrysts in the
granites of southwest England;
J. Geol., V.69, pp. 464 - 472.
- SUN, S. AND NESBITT, R.W. (1977)
Chemical heterogeneity of the Archean mantle, composition of the
earth and mantle evolution;
Earth, Planet. Sci. Lett., V.35, pp. 429 - 448.
- SUTCLIFFE, R.H. (1977)
Geology and emplacement of the Jackfish Lake pluton, a major
intrusion in the Rainy Lake dome;
Proceedings, 1977 Geotraverse Conference, Feb. 28 - March 1,
University of Toronto, pp. 25.1 - 25.13.
- SUTTON, J. (1973)
Stages in the evolution of the granitic crust;
Spec. Publ. Geol. Soc. S. Africa, V.3; pp. 1-6.
- SYLVESTER, A.G. (1964)
The Precambrian rocks of the Telemark area in south central
Norway:
Part III Geology of the Vradal Granite;
Norsk Geol. Tidsskrift, V.44 pp. 445-482.
- TALBOT, C.J. (1968)
Thermal convection in the Archean crust;
Nature, V.220, No. 5167, pp. 552 - 556.
- TAMMEDI, H.Y. AND SMITH N.L. (1975)
A radiogeologic study of the granites of S.W. England;
J. Geol. Soc. London, V.131, pp. 415 - 427.
- TANTON, T.L. (1936)
Mine Centre area, District of Rainy Lake;
Geol. Survey of Canada,
Map 334A, 1" = 1/2 mile (mapped 1934).

- TAUSDON, L.V. (1967)
Geochemical behaviour of rare elements during crystallization and differentiation of granitic magmas;
Geokhimiya, V.11, pp. 1310 - 1319.
- TAYLOR, H.P. (1964)
The application of trace element data to problems in petrology;
In: L.H. Ahrens, F. Press, S.K. Runcorn, H.C. Urey (editors),
Physics and Chemistry of the Earth, V.6, pp. 133 - 213.
- TERZAGHI, R.D. (1935)
The origin of the K-rich rocks;
Amer. J. Sci., V.172, pp. 369 - 380.
- THOMAS, H.H. AND SMITH W.C. (1932)
Xenoliths of igneous origin in the Tregastel - Ploumanuc'h
Granite, Cotes du Nord, France;
J. Geol. Soc. London, V.88, pp. 274 - 292.
- THOMSON, J.E. (1933)
Geology of the Manitou-Stormy Lakes Area;
Ontario Department of Mines, V.42, pt. 4, pp. 1 - 40 incl. map 42C
1" = 1 mile.
- THOMSON, J.E. (1934)
Geology of the Straw-Manitou Lakes area;
Ontario Department of Mines, V.43, pt. 4, 32 p. incl. map 43a,
1" = 1 mile.
- THORNTON, C.P. AND TUTTLE, O.F. (1960)
Chemistry of igneous rocks: I Differentiation Index;
Amer. J. Sci., V.258, pp. 664 - 684.
- TINKLER, K.J. (1969)
Trend surfaces with low "explanations": The assessment of their
significance;
Amer. J. Sci., V.267, pp. 114 - 123.
- TUOMINEN, H.V. (1964)
The trends of differentiation in percentage diagrams;
J. Geol., V.72, pp. 855 - 860.
- TUREK, A. (1966)
Rubidium - Strontium isotopic studies in the Kalgoorlie - Norseman
area, Western Australia;
Unpublished Ph.D. Thesis, Australian National University, Canberra,
Australia.

- TUREK, A., RIDDLE, C. AND SMITH, F.E. (1977)
Determination of Rb and Sr by x-ray fluorescence in the measurement
of radiometric ages;
Can. J. Spectroscopy, V.22, pp. 20 - 24.
- TYLER, S.A., MARSDEN, R.W., GROOT, F.F. AND THIEL, G.A. (1940)
Studies of the Lake Superior Precambrian by accessory-mineral
methods;
Geol. Soc. Amer., Bull. V.51, pp. 1429 - 1538.
- VAN BREEMEN, O. AND DODSON, M.H. (1972)
Metamorphic chronology of the Limpopo Belt, Southern Africa;
Geol. Soc. Amer., Bull. V.83, pp. 2005 - 2018.
- VAN BREEMEN, O., HUTCHINSON, J. AND BOWDEN, P. (1975)
Age and origin of the Nigerian Mesozoic granites: a Rb-Sr isotopic
study;
Contr. Mineral. Petrol., V.50, pp. 157 - 172.
- VANCE, J.A. (1961)
Zoned granitic intrusions - an alternative hypothesis of origin;
Geol. Soc. Amer., Bull. V.72, pp. 1723 - 1728.
- VANCE, J.A. AND GILREATH, J.P. (1967)
The effect of synneusis on phenocryst distribution patterns in some
porphyritic igneous rocks;
Amer. Min., V.52, pp. 529 - 536.
- VANCE, J.A. (1969)
On synneusis;
Contr. Min. Petrol., V.24, pp. 7 - 29.
- VAN HISE, C.R. (1893)
An historical sketch of the Lake Superior region to Cambrian time;
J. Geol., V.1, pt. 2, pp. 113 - 128.
- VAN SCHMUS, W.R. AND ANDERSON, J.L. (1977)
Gneiss and migmatite of Archean age in the Precambrian basement of
central Wisconsin;
Geology, V.5, pp. 45 - 48.
- VAN SCHMUS, W.R., THURMAN, E.M. AND PETERMAN, Z.E. (1975)
Geology and Rb/Sr chronology of Middle Precambrian rocks in Eastern
and Central Wisconsin;
Geol. Soc. Amer., Bull. V.86, pp. 1255 - 1265.

- VILJOEN, M.J. AND VILJOEN, R.P. (1969)
The geochemical evolution of the granite rocks of the Barberton Region;
Geol. Soc. S. Africa, Special paper 2, pp. 189 - 219.
- VLASOV, K.A. (1966)
Geochemistry and Mineralogy of Rare Elements and Genetic Types of Their Deposits;
Israel Program for Sci. Trans., V.1, Jerusalem.
- WAGER, L.R. (1956)
A chemical definition of fractionation stages as a basis for comparison of Hawaiian, Hebridean and other basic lavas;
Geochim. Cosmochim. Acta, V.9, pp. 217 - 248.
- WALKER, W. (1971)
Time and place in orogeny:
The Precambrian of Manitoba;
Geol. Ass. Canada, Special Paper 9, pp. 61 - 68.
- WANLESS, R.K. AND LOVERIDGE, W.D. (1972)
Rubidium - Strontium isochron age studies, Report 1; Geol. Survey Canada, Paper 72-23.
- WANLESS, R.K., STEVENS, R.D., LACHANCE, G.R. AND DELABIO, R.N.D. (1974)
Age determinations and geologic studies:
K-Ar isotopic ages, Report 12; Geol. Survey Canada, Paper 74-2, 72 p.
- WASSERBURG, G.J., HAYDEN, R.J. AND JENSEN, K.J. (1956)
 A^{40} - K^{40} igneous rocks and sediments;
Geochim. Cosmochim. Acta, V.10, pp. 153 - 165.
- WEARE, J.H., STEPHENS, J.R. AND EUGSTER, H.P. (1976)
Diffusion metasomatism and mineral reaction zones:
General principles and application to feldspar alteration;
Amer. Jour. Sci., V.276, pp. 767 - 816.
- WHITFIELD, J.M., ROGERS, J.J.W. AND McEWEN, M.C. (1959)
Relationships among textural properties and modal compositions of some granitic rocks;
Geochim. Cosmochim. Acta, V.17, pp. 272 - 285.
- WHITTEN, E.H.T. (1960)
Quantitative evidence of palimpsestic ghost - stratigraphy from modal analysis of a granitic complex;
Rep. Int. Geol. Congr. 21, Norden, pt. 14, pp. 182 - 193.

- WHITTEN, E.H.T. (1961)
Quantitative areal modal analysis of granitic complexes;
Geol. Soc. Amer., Bull. V.72, pp. 1331 - 1360.
- WHITTEN, E.H.T. (1962)
A new method for determination of the average composition of a
granite massif;
Geochim. Cosmochim. Acta, V.26, pp. 545 - 560.
- WHITTEN, E.H.T. (1963)
Geological contours and trend surfaces: a discussion;
Jour. Petrol., V.4, pp. 307 - 312.
- WHITTEN, E.H.T. (1975)
Appropriate units for expressing chemical composition of igneous
rocks;
Geol. Soc. Amer., Memoir 142, pp. 283 - 308.
- WILSON, H.D.B. (1971)
The Superior Province in the Precambrian of Manitoba;
Geol. Ass. Canada, Special Paper 9, pp. 41 - 49.
- WILSON, H.D.B., MORRICE, M.G. AND ZIEHLKE, D.V. (1974)
Archean continents;
Geoscience Canada, V.1, No. 3, pp. 12 - 20.
- WOLFF, J.M. (1977)
An operational guide and technical discussion of mass spectrometer
SS-2, McMaster Geochronology Laboratory;
Tech. Memo 77-1, Dept. of Geology McMaster University, Hamilton,
Ontario
- WOLHUTER, L.E. (1973)
Major and trace elements in the Opemisca Lake granite pluton,
Quebec, Canada;
Geol. Soc. S. Africa, Sp. Pub. 3, pp. 387 - 409.
- WRIGHT, J.B. (1969)
A simple alkalinity ratio and its application to questions of
non-orogenic granite genesis;
Geol. Mag., V.106, pp. 370 - 384.
- WRIGHT, T.L. (1974)
Presentation and interpretation of chemical data for igneous
rocks;
Contr. Min. Petrol., V.48, pp. 233 - 248.

YAMAGUCHI, M., YANAGI, T. AND HAMAMOTO, R. (1969)
Some technical aspects of the Rb-Sr geochronology;
Fac. Sci., Kyushu University, Memoir, Series D, Geology, V.19,
pp. 437 - 450.

YANAGI, T., YAMAGUCHI, M. AND NOZAWA, T. (1971)
Rb-Sr whole rock ages of the granites of Minami-osumi and
Amami-oshima, southwest Japan;
Mem. Fac. Sci., Kyushu Univ., Ser. D, Geology, V.21, No. 1,
pp. 163 - 175.

YORK, D. (1966)
Least squares fitting of a straight line;
Can. J. Physics, V.44, pp. 1079 - 1086.

YORK, D. (1969)
Least squares fitting of a straight line with correlated errors;
Earth, Planet. Sci. Lett., V.5, pp. 320 - 324.



APPENDIX



APPENDIX A: PLATES

PLATE 1. METASOMATISM:

PLATE 1.1

FELDSPATHIZED MAFIC ENCLAVE.
NOTE MICROCLINE-PERTHITE MEGACRYSTS
AND CONCENTRIC ZONING OF
FELSIC MINERALS. ARROW SHOWS
MEGACRYST STRADDLING ENCLAVE-
GRANODIORITE INTERFACE.
(LOCATION: RY10, RYCKMAN LAKE STOCK)

PLATE 1.2

FELDSPATHIZED MAFIC ENCLAVE.
(LOCATION: 80, BURDITT LAKE STOCK)

PLATE 1.3

FELDSPATHIZED MAFIC ENCLAVE.
(LOCATION: 49, BURDITT LAKE STOCK)

PLATE 1.4

FELDSPATHIZED AND SILICIFIED
MAFIC ENCLAVE. MEGACRYSTS
INSIDE ENCLAVE INCLUDE FELDSPAR
AND IRRIDESCENT BLUE QUARTZ
IDENTICAL TO BLUE QUARTZ IN
HOST TONALITE.
(LOCATION: F2, FROGHEAD BAY STOCK)

PLATE 1.5

PYRITIZED QUARTZ PORPHYRY:
ANGULAR CHLORITIC XENOLITH OF
META BASALT (BLACK) IN CONTACT
WITH PINK HYPABYSSAL FELSITE (WHITE)
CUBIC PORPHYROBLASTS OF PYRITE
HAVE GROWN ALONG BOTH SIDES
OF INTERFACE (ARROW AND PEN TIP)
XENOLITH WAS LIKELY SOURCE OF
METASOMATIC SULPHIDE.
(LOCATION: EX5, ESUX LAKE)

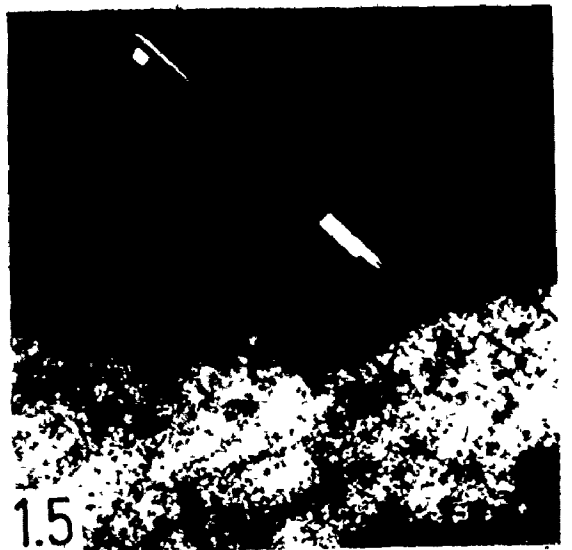
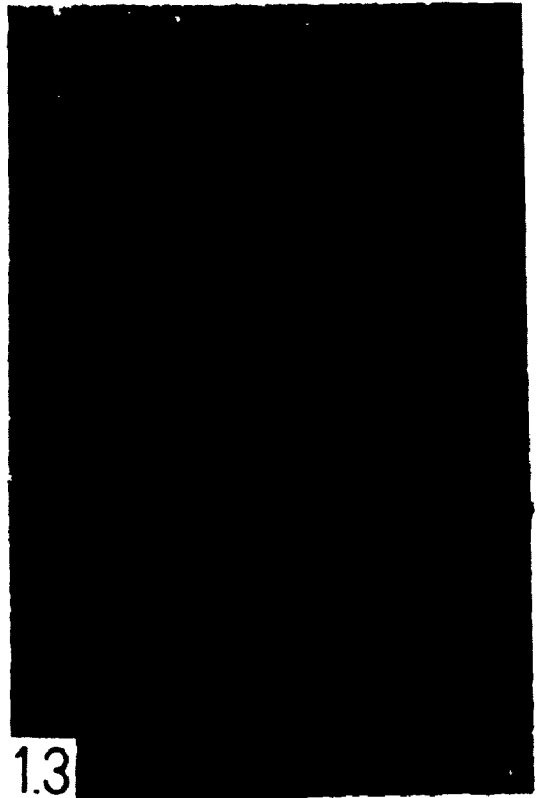


PLATE 2.1

MAFIC SCHLIEREN OF BIOTITE
AND HORNBLende IN ASSOCIATION
WITH CHLORITIC ENCLAVES. TO FORM
PSEUDO-BEDDING AND PSEUDO-SLUMP
STRUCTURES.
(LOCATION: RY93, RYCKMAN LAKE STOCK)

PLATE 2.2

"DOUBLE ENCLAVES" (SENSU STRICTO)
OF INTRUSION BRECCIA.
MONZODIORITIC ENCLAVE IN GRANITE
IS IN TURN HOST TO
GREENSTONE ENCLAVE (ARROW)
(LOCATION: F18, FLORA LAKE STOCK)

PLATE 2. ENCLAVES AND INCLUSIONS:

PLATE 2.3

ALIGNED INCLUSIONS IN MICROCLINE-
PERTHITE MEGACRYST (X25)
M = MICROCLINE-PERTHITE
MY = MYRMEKITE
P = PLAGIOCLASE INCLUSION
(LOCATION: 118, BURDITT LAKE STOCK)
PHOTOMICROGRAPH; X25 CROSSED NICOLS.

PLATE 2.4

PHOTOMICROGRAPH: X160.
INCLUSIONS IN BIOTITE (B) OF MAFIC
ENCLAVE: SECONDARY GROWTH OF
ACCICULAR MINERAL (SILLIMANITE ?)
ALONG CRYSTALLOGRAPHIC AXES.
(LOCATION: S11, SCATTERGOOD LAKE STOCK)



PLATE 3.1

SEVERAL GENERATIONS OF PINK APLITE DYKES (AP) IN GRANODIORITE. NOTE CROSS-CUTTING, DISPLACEMENT AND PLASTIC DEFORMATION.
(LOCATION: 64, BURDITT LAKE STOCK)

PLATE 3.2

GRANODIORITE DYKE IN METAPYROCLASTICS MICROCLINE-PERTHITE MEGACRYSTS AT DYKE-HOST INTERFACE (ARROW) DRILL HOLE CORRESPONDS TO SAMPLE 53412.
(LOCATION: 69, BURDITT LAKE STOCK)

PLATE 3. FELSIC DYKES:**PLATE 3.3**

APLITIC DYKE (AP) WITH FELSIC REACTION RIM; IN GRANODIORITE.
(LOCATION 24, ESOX LAKE)

PLATE 3.4

APLITE VEINLET IN CORROSIVE CONTACT WITH MICROCLINE-PERTHITE GRAIN. NOTE MICROCLINE (M) HAS DIGESTED APLITE, LEAVING QUARTZ (Q) GRAINS AS RELICTS. THUS K METASOMATISM POST DATED DYKES.
PHOTOMICROGRAPH; 63X; CROSSED NICOLS
(LOCATION: 35, BURDITT LAKE STOCK)



PLATE 4.2

ELONGATED QUARTZ "EYES" IN
PINK APLITE DYKE. ELONGATION
IS SUBPARALLEL TO FOLIATION IN
GRANODIORITE HOST.

Q = QUARTZ

AP = APLITE

(LOCATION: 64, BURDITT LAKE STOCK)

PLATE 4.3

EUHEDRAL QUARTZ "EYES" (Q)
MASSIVE PINK APLITE (AP)



PLATE 4. QUARTZ HABIT AND PARAGENESIS:

PLATE 4.1

GLOMEROGANULAR QUARTZ (Q)
SURROUNDED BY PLAGIOCLASE (P)
(LOCATION: 1, BURDITT LAKE STOCK)
PHOTOMICROGRAPH; X25, CROSSED NICOLS.

PLATE 4.4

PHOTOMICROGRAPH; X100; CROSSED NICOLS
EUHEDRAL QUARTZ INCLUSION IN
MICROCLINE-PERTHITE MEGACRYST.
(LOCATION: 118, BURDITT LAKE STOCK)

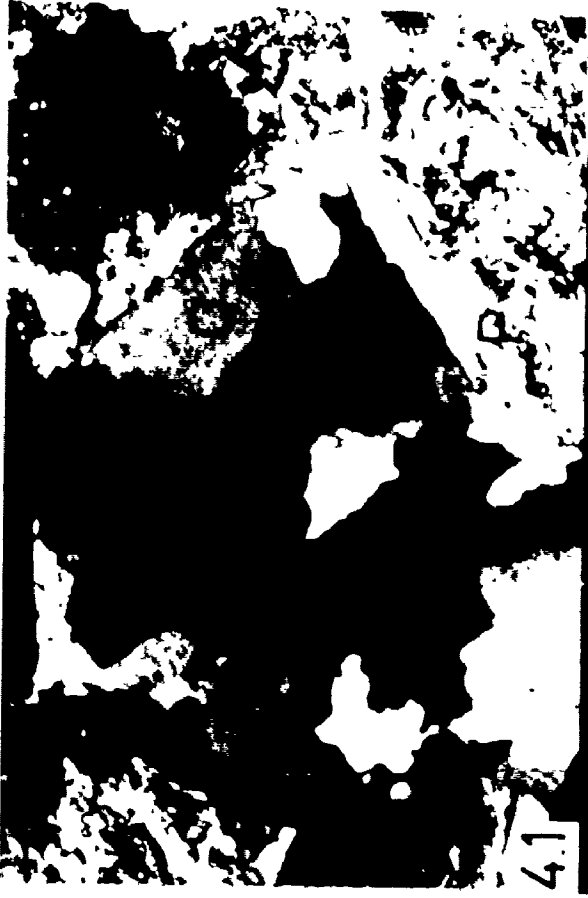
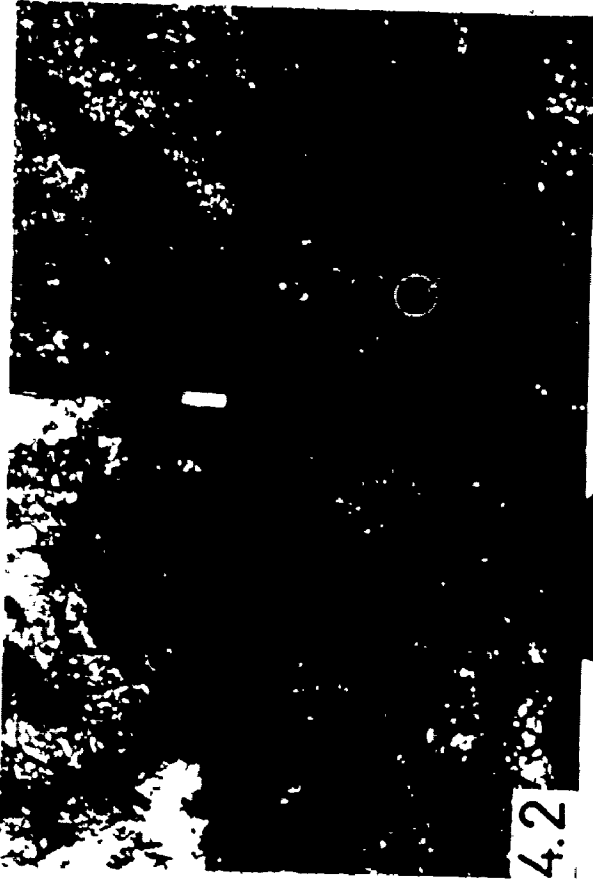


PLATE 5.1

SYNNEUSIS CLUSTER OF PLAGIOCLASE
(P) SHOWN BY COMPOSITE ZONING
AND MISFIT. Q = QUARTZ.
(LOCATION: 27, BURDITT LAKE STOCK)
PHOTOMICROGRAPH, X25, CROSSED NICOLS.

PLATE 5.2

SYNNEUSIS TWINS OF PLAGIOCLASE (P)
PHOTOMICROGRAPH; X25, CROSSED NICOLS.
(LOCATION: S6, SCATTERGOOD LAKE STOCK)

PLATE 5.3

SUBHEDRAL EPIDOTE (E) WITH OPTICAL
ZONING. PHOTOMICROGRAPH; X25; CROSSED
NICOLS.
(LOCATION: 61, BURDITT LAKE STOCK)

PLATE 5.4

EUHEDRAL METAMICT ALLANITE IN
MICROCLINE-PERTHITE (M)
(LOCATION: 60, BURDITT LAKE STOCK)
PHOTOMICROGRAPH; X25; CROSSED NICOLS.

PLATE 5.5

GRANOBLASTIC PLAGIOCLASE (P)
MICROCLINE (M), QUARTZ (Q)
PHOTOMICROGRAPH; X25; CROSSED NICOLS.
(LOCATION RY37, RYCKMAN LAKE STOCK)

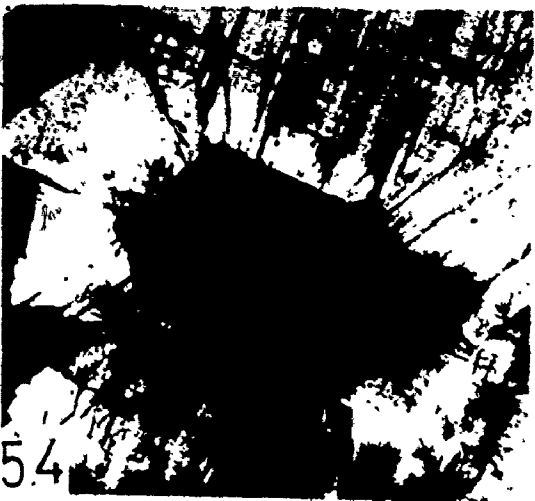
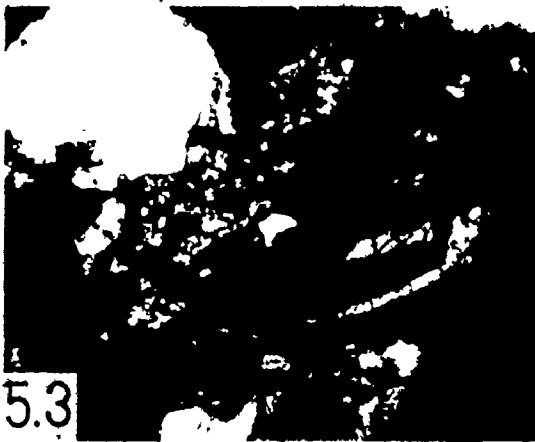


PLATE 6.1

PLAGIOCLASE (P) EMBAYED BY
ALBITE (A). Q = QUARTZ.
PHOTOMICROGRAPH; X63; CROSSED NICOLS.
(LOCATION: 35, BURDITT LAKE STOCK)

PLATE 6.2

SAWTOOTH CONTACT BETWEEN
QUARTZ (Q) AND PLAGIOCLASE (P)
PHOTOMICROGRAPH; X63; CROSSED NICOLS.
(LOCATION: 70, BURDITT LAKE STOCK)

PLATE 6.3

SYNNEUSIS TWINS OF PLAGIOCLASE
WITH SECONDARY EPIDOTE-SERICITE IN
CORES
PHOTOMICROGRAPH; X25; CROSSED NICOLS.
(LOCATION: BURDITT LAKE STOCK)

PLATE 6.4

MYRMEKITIZED PLAGIOCLASE (P)
PARTLY SURROUNDED AND CORRODED
BY MICROCLINE (M). FREED QUARTZ
MYRMEKITIC BODIES (RHABDITES)
LAYING IN MICROCLINE. PARAGENESIS
IS THEREFORE:

1. PLAGIOCLASE
2. MYRMEKITE
3. MICROCLINE

PHOTOMICROGRAPH; X160; CROSSED NICOLS.
(LOCATION: 58, BURDITT LAKE STOCK)

PLATE 6.5

PLAGIOCLASE (P) WITH MYRMEKITIZED
MARGINAL ZONE AGAINST
MICROCLINE (M)
PHOTOMICROGRAPH; X63; CROSSED NICOLS.
(LOCATION: 102, BURDITT LAKE STOCK)



A.C.

6.1



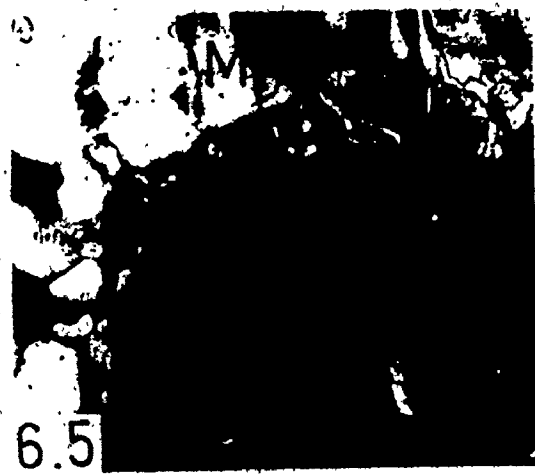
6.2



6.3



6.4



6.5

[Handwritten mark]

APPENDIX B

MODAL ANALYSES:

The following tables of modal analyses were based on point count analyses by the author over 25x 4 cm stained thin sections. Staining was carried out using the apparatus of Dawson and Crawley (1963) and a method similar to Norman (1974) based on HF etching and Na-cobaltinitrite, barium chloride and amaranth baths to stain K-feldspar yellow and plagioclase red.

The need for staining in granitoid modal analysis is well illustrated by the divergent published analyses for the biotite-granodiorite of the Rest Island Stock. Analyses of samples from a homogeneous island outcrop by Cram (1932), Frye (1959) and Harris (1974) plot on the IUGS (1973) Q-A-P ternary as tonalite, granite and quartz monzonite to quartz diorite respectively. Two modes obtained by the author on stained thin sections of the same island outcrop fall near-coincident in the granodiorite field.

For each thin section, 1000 points were analysed with roughly a 0.6 x 0.3 mm grid spacing using a Leitz research binocular microscope. Myrmekite and albite rims were counted with plagioclase while perthite was contributed to the K-feldspar total. The analyses were considered precise to approximately $\pm 5\%$ although the statistics vary with the mineral, grain size, degree of alteration, quality of stain and quality of thin section.

No modal analyses were carried out for the Flora Lake Stock or the Taylor Lake Stock because of available modes in Heimlich (1965)

and Pichette (1976). Pichette's modal analyses are directly comparable to this study because his thin sections were stained with the author's apparatus and he used essentially the same point counting criteria.

The most mafic samples from the Ryckman Lake Stock were tested for the presence of feldspathoids (nepheline, sodalite, analcime) by staining rock slabs using the method of Shand (1939) as quoted in Hutchison (1974). No feldspathoids were detected in RY82, RY35, RY94 or RY93.

APPENDIX B: TABLES

APPENDIX TABLES B:
MODAL MINERALS BASED ON 1000 POINT COUNTS
OVER 4 x 2.5 CM THIN SECTIONS. ALL THIN
SECTIONS WERE STAINED FOR PLAGIOCLASE (RED)
AND K-FELDSPAR (YELLOW) BY THE METHOD OF
DAWSON AND CRAWLEY (1963), NORMAN (1974).

ANALYSES IN % VOLUME.
RECONNAISSANCE MODAL ANALYSES
IDENTIFIED BY PREFIX.
FH = FROGHEAD BAY
REG = REGINA BAY
ST = STORMY LAKE
REST = REST ISLAND
TR = BEARS PASSAGE
OT = OTTERTAIL LAKE
ALL OTHER SAMPLES AS PER FIELD
MAPS PLUS PREFIX EXCEPT BURDITT.
BURDITT SAMPLES AS PER APPENDIX I.

B2

MINERAL

SCATTERGOOD LAKE STOCK - MODES (1000 POINTS)

	S-2	S-4	S-6	S-10B	S-12	S-15	ST-3P	ST-4P
PLAG	50.7	61.4	50.2	57.3	49.8	55.6	52.5	49.4
QTZ	16.8	18.4	19.5	15.0	16.2	13.6	18.1	14.2
KSPAR	21.6	13.9	20.5	13.8	25.7	15.4	19.0	22.4
BIO	0.0	0.0	0.0	0.0	0.0	0.1	0.0	0.0
CHL	0.0	0.0	0.0	0.0	0.0	0.0	0.0	0.0
MUSC	0.0	0.0	0.0	0.0	0.1	0.0	0.0	0.0
EPIIDOTE	2.5	0.7	1.7	1.1	1.1	2.0	1.3	0.0
H9	6.6	4.8	6.1	9.1	5.9	7.7	9.3	9.6
SPHENE	0.8	0.1	0.6	0.0	0.5	0.3	0.3	0.2
OPAQUES	0.5	0.5	1.1	0.5	0.4	0.2	0.4	0.1
APATITE	0.0	0.0	0.2	0.1	0.0	0.1	0.0	0.1
ZIRCON	0.0	0.0	0.0	0.0	0.0	0.0	0.0	0.0
ALLAN.	0.0	0.0	0.0	0.0	0.0	0.0	0.0	0.0
CALCITE	0.0	0.0	0.0	0.0	0.0	0.0	0.0	0.0

	ST-8P	ST-12P						
PLAG	52.9	56.0	0.0	0.0	0.0	0.0	0.0	0.0
QTZ	22.7	17.9	0.0	0.0	0.0	0.0	0.0	0.0
KSPAR	13.6	14.6	0.0	0.0	0.0	0.0	0.0	0.0
BIO	0.0	0.0	0.0	0.0	0.0	0.0	0.0	0.0
CHL	0.0	0.0	0.0	0.0	0.0	0.0	0.0	0.0
MUSC	0.0	0.0	0.0	0.0	0.0	0.0	0.0	0.0
EPIIDOTE	1.9	0.8	0.0	0.0	0.0	0.0	0.0	0.0
H9	8.0	9.9	0.0	0.0	0.0	0.0	0.0	0.0
SPHENE	0.4	0.5	0.0	0.0	0.0	0.0	0.0	0.0
OPAQUES	0.5	0.3	0.0	0.0	0.0	0.0	0.0	0.0
APATITE	0.0	0.0	0.0	0.0	0.0	0.0	0.0	0.0
ZIRCON	0.0	0.0	0.0	0.0	0.0	0.0	0.0	0.0
ALLAN.	0.0	0.0	0.0	0.0	0.0	0.0	0.0	0.0
CALCITE	0.0	0.0	0.0	0.0	0.0	0.0	0.0	0.0

B3

MINERAL

RYCKHAN LAKE STOCK - MODES (1000 POINTS)

	FY-A	RY-5	RY-7	RY-15	RY-21	RY-23	RY-35	RY-37
PLAG	48.1	54.9	41.8	57.1	42.8	42.2	46.0	51.6
QTZ	22.5	24.7	7.3	18.5	9.4	3.6	0.0	0.0
KSPAR	21.4	10.7	15.1	15.6	19.2	20.8	18.4	22.8
BIO	0.1	0.1	5.7	0.1	2.3	0.7	0.0	4.7
CHL	0.0	0.0	0.0	0.0	0.0	0.0	0.6	0.0
PX	0.0	0.0	0.0	0.0	0.0	0.0	0.0	5.8
EPIIDOTE	0.6	2.0	0.3	0.9	0.8	0.4	0.1	1.5
H9	6.9	6.8	28.6	7.7	26.8	32.0	32.3	12.8
SPHENE	0.1	0.4	0.1	0.1	0.6	0.3	0.5	0.9
OPAQUES	0.2	0.4	0.0	0.0	0.1	0.0	0.0	0.2
APATITE	0.1	0.0	0.1	0.0	0.0	0.0	0.0	0.0
ZIRCON	0.0	0.0	0.0	0.0	0.0	0.0	0.0	0.0
ALLAN.	0.0	0.0	0.0	0.0	0.0	0.0	0.0	0.0
SCHOR.	0.0	0.0	0.0	0.0	0.0	0.0	0.0	0.0

	RY-51	RY-54	RY-60	RY-61	RY-71	RY-82	RY-94	
PLAG	48.2	54.8	47.2	52.1	46.4	44.7	44.9	0.0
QTZ	21.1	23.4	7.0	2.6	7.6	0.0	0.0	0.0
KSPAR	20.7	11.1	12.7	17.2	19.3	20.8	9.2	0.0
BIO	0.1	0.0	7.7	0.0	0.0	8.9	18.6	0.0
CHL	0.5	0.1	0.0	0.0	0.0	0.0	0.0	0.0
PX	0.0	0.0	0.0	0.0	0.0	0.0	13.6	0.0
EPIIDOTE	1.1	0.9	0.3	1.8	1.2	1.6	0.7	0.0
H9	7.9	9.6	24.5	25.0	25.1	11.6	9.1	0.0
SPHENE	0.1	0.8	0.1	0.5	0.3	0.5	0.1	0.0
OPAQUES	0.2	0.1	0.1	0.6	0.1	1.0	1.5	0.0
APATITE	0.1	0.0	0.0	0.2	0.0	0.6	1.2	0.0
ZIRCON	0.0	0.0	0.0	0.0	0.0	0.0	0.0	0.0
ALLAN.	0.0	0.0	0.2	0.0	0.0	0.1	0.0	0.0
SCHOR.	0.0	0.0	0.2	0.0	0.0	0.0	0.0	0.0

B4

MINERAL

ESOX LAKE GRANITOIDS - MODAL ANALYSES (1000 POINTS)

	EX-1	EX-2	EX-11	EX-19	EX-20	EX-26	EX-28	EX-29
PLAG	54.3	50.9	55.1	51.8	56.2	51.2	47.7	46.2
QTZ	18.2	18.1	19.4	19.7	20.2	20.4	18.7	13.2
KSPAR	24.6	21.5	21.9	20.6	16.6	20.0	30.7	22.2
BIC	0.0	0.0	0.6	0.6	3.4	4.9	3.3	0.0
CHL	0.0	0.0	0.0	0.0	0.3	0.3	0.0	0.0
MUSC	0.0	0.0	0.0	0.0	0.0	0.0	0.0	0.0
EPIOTOE	1.0	1.1	4.0	3.0	2.3	2.5	2.6	0.0
HB	0.2	0.0	0.2	0.0	0.0	0.0	0.9	1.1
SPHENE	0.1	0.0	0.1	0.4	0.1	0.2	0.1	0.2
OPAQUES	0.0	0.0	0.0	0.0	0.0	0.0	0.0	0.0
APATITE	0.0	0.0	0.0	0.0	0.0	0.0	0.0	0.0
ZIRCON	0.0	0.0	0.0	0.0	0.0	0.0	0.0	0.0
ALLAN.	0.0	0.0	0.0	0.0	0.0	0.0	0.0	0.0
CALCITE	0.0	0.0	0.0	0.0	0.0	0.0	0.0	0.0

EX-30B

PLAG	47.8	0.0	0.0	0.0	0.0	0.0	0.0	0.0
QTZ	15.4	0.0	0.0	0.0	0.0	0.0	0.0	0.0
KSPAR	22.2	0.0	0.0	0.0	0.0	0.0	0.0	0.0
BIC	2.1	0.0	0.0	0.0	0.0	0.0	0.0	0.0
CHL	0.1	0.0	0.0	0.0	0.0	0.0	0.0	0.0
MUSC	0.0	0.0	0.0	0.0	0.0	0.0	0.0	0.0
EPIOTOE	0.0	0.0	0.0	0.0	0.0	0.0	0.0	0.0
HB	0.1	0.0	0.0	0.0	0.0	0.0	0.0	0.0
SPHENE	0.3	0.0	0.0	0.0	0.0	0.0	0.0	0.0
OPAQUES	0.0	0.0	0.0	0.0	0.0	0.0	0.0	0.0
APATITE	0.0	0.0	0.0	0.0	0.0	0.0	0.0	0.0
ZIRCON	0.0	0.0	0.0	0.0	0.0	0.0	0.0	0.0
ALLAN.	0.0	0.0	0.0	0.0	0.0	0.0	0.0	0.0
CALCITE	0.0	0.0	0.0	0.0	0.0	0.0	0.0	0.0

B5

MINERAL

RECONNAISSANCE MODAL ANALYSES (1000 POINTS)

	FH-4	FH-10	FH-8	REG-5	REG-4	ST-4	ST-6	
PLAG	35.8	58.1	55.4	55.8	52.4	53.8	60.5	0.0
QTZ	38.8	33.0	28.2	29.7	28.1	21.3	19.3	0.0
KSPAR	19.1	0.0	4.1	9.0	0.0	13.3	11.7	0.0
BIC	0.0	0.0	11.2	0.0	0.0	7.6	4.2	0.0
CHL	0.0	0.0	0.0	13.9	4.4	0.0	0.0	0.0
MUSC	0.0	0.0	0.0	0.0	0.0	0.0	0.0	0.0
EPIOTOE	0.9	2.0	0.9	0.4	0.7	0.0	0.0	0.0
HB	0.0	0.0	0.0	0.0	0.0	0.0	0.0	0.0
SPHENE	0.0	0.0	0.0	0.0	0.0	0.0	0.0	0.0
OPAQUES	0.0	0.0	0.0	0.0	0.0	0.0	0.0	0.0
APATITE	0.0	0.0	0.0	0.0	0.0	0.0	0.0	0.0
ZIRCON	0.0	0.0	0.0	0.0	0.0	0.0	0.0	0.0
ALLAN.	0.0	0.0	0.0	0.0	0.0	0.0	0.0	0.0
CALCITE	0.0	0.0	0.0	0.4	2.9	0.2	0.1	0.0

	REST-5	REST-2	TR-18	TR-3	TR-4B	OT-5	OT-2	OT-1
PLAG	48.1	47.3	43.1	44.7	45.2	38.6	47.6	42.9
QTZ	31.0	29.0	31.4	30.0	28.3	29.3	22.6	27.9
KSPAR	9.9	11.0	21.7	18.2	18.0	26.6	15.8	9.8
BIC	7.7	0.0	0.0	1.1	0.0	0.0	4.0	9.1
CHL	0.0	0.0	0.6	0.0	0.6	0.5	0.0	2.1
MUSC	0.0	0.0	2.7	5.0	6.8	2.5	0.0	0.0
EPIOTOE	1.0	3.0	0.0	0.0	0.0	0.0	0.0	0.0
HB	0.0	0.0	0.0	0.0	0.0	0.0	0.0	0.0
SPHENE	0.0	0.0	0.0	0.0	0.0	0.0	0.0	0.0
OPAQUES	0.0	0.0	0.0	0.0	0.0	0.0	0.0	0.0
APATITE	0.0	0.0	0.0	0.0	0.0	0.0	0.0	0.0
ZIRCON	0.0	0.0	0.0	0.0	0.0	0.0	0.0	0.0
ALLAN.	0.0	0.0	0.0	0.0	0.0	0.0	0.0	0.0
CALCITE	0.0	0.0	0.0	0.1	0.1	0.3	0.0	0.0

APPENDIX C

MAJOR ELEMENT DETERMINATIONS:

Introduction:

All major element analyses presented in the following appendix tables C1 to C7 were carried out by the author over a two year interval using a PW1450AHP model Philips X-ray fluorescence spectrometer in the Department of Geology, McMaster University. Data reduction was carried out off-line using a CDC6400 computer (McMaster University).

The spectrometer has several features ideal for rapid analysis of large numbers of samples, including: automatic selection of pre-programmed parameters; teletype-read-out and four-sample holders with automatic feed. This allowed all analyses to be carried out in duplicate or replicates with relative ease and results quoted are averages normalized on a water-free basis to 100%.

Two methods of analysis were employed. For samples with SiO_2 greater than 65%, analyses were carried out on pressed whole-rock powder (200 mesh) pellets backed with boric acid. Sample preparation is very rapid and simple, thereby decreasing contamination. Brown et al, (1973) have demonstrated that major elements can be analysed successfully on pressed powder pellets although most laboratories reserve powder pellets for trace element work. Problems have however been reported with sample heterogeneity (Leake et al, 1969) and with water release from the boric acid backing (Fabbi, 1972). Sample heterogeneity was controlled by fine grinding

and by using a 60 rpm sample spinner during measurement. No dehydration of the boric acid was detected during this study although some distortion of intensities may have occurred and are accounted for in precision calculations. Fabbi (1972) reported a 10 to 15% reduction in silica intensities due to boric acid dehydration.

Spectrometer parameters for optimum determination of the major elements were based on recommendations of Leake et al, (1969) and Hutchison (1974) and are listed in Table C.a. Data processing followed Brown et al (1973) using 36 standards with accepted values based on Abbey (1975), Abbey et al (1975) or inhouse atomic absorption determinations (J. Muysson, personal communication).

Some problems were anticipated for low silica, high magnesium rocks because of Mg enhancement by Al, therefore all rocks of less than 65% silica were reanalysed using a fusion technique. Two grams of 200 mesh rock powder were fused with 4 grams of lithium tetraborate. The resultant beads were crushed and pelletized with a boric acid backing. Such fusions have been recommended to eliminate effects of particle size, mineralogy, inter-element absorption and enhancement. In turn this technique suffers from a marked decrease in peak to background ratio, hygroscopic effects, loss of volatiles, residual interelement absorption and enhancement, extra specimen preparation time and additional sources of contamination (Leake et al, 1969). In retrospect the author recommends neither preparation technique used in this study and suggests instead a technique by fusion of 6 parts rock to 1 part phenol formaldehyde as recommended by Leake et al (1969).

Table C.a

OPTIMUM XRF SPECTROMETER PARAMETERS FOR MAJOR ELEMENTS

ELEMENT	PEAK	CRYSTAL	COLLIMATOR	COUNT PEAK	TIME BACKGROUND (Sec.)
Si	K_{α}	PE	C	40	4
Al	K_{α}	TLAP	C	40	10
Fe	K_{α}	LiF200	F	40	4
Mg	K_{α}	TLAP	C	100	20
Na	K_{α}	TLAP	C	100	10
Ca	K_{β}	LiF200	C	20	4
K	K_{α}	PE	C	40	4
P	K_{α}	PE	C	40	20
Mn	K_{α}	LiF200	F	40	20
Ti	K_{α}	LiF200	F	10	4

Chrome tube with generator set at 50 Ma/50 Kv (2.5 Kw).
Gas flow proportional counter and vacuum path throughout.

F = Fine
C = Coarse
LIF = Lithium Fluoride
PE = Penta-Erythritol
Filter in for Mn only.

Data processing for the fusion technique followed a modified version of Gunn (1967) based on single-standard correlations. Since XRF analysis is comparative, the absolute accuracy and compatibility of standards employed is fundamental to meaningful results. The single standard method of Gunn (1967) and to a lesser extent, the multi-standard method of Brown et al (1973) gave results very sensitive to the standards selected. The following discussion on accuracy therefore reflects as much on the data processing as on sample handling. The criteria used in this study to select acceptable analyses for unknowns included:

- Selection of standards as close to unknowns as possible.
- Preference for analyses with major element totals near 100%.
- Confirmation of analyses by duplicates.
- Confirmation of fusion analyses by comparison with powder analyses. No major discrepancies were observed.

Although most of the rocks in this study contain appreciable volatiles and other elements not determined, resultant major element analyses are presented normalized to 100%. The XRF analytical program deals only with the 10 major elements and resultant totals give a measure of the quality of the determinations and not the residuals. To compensate for variations in volatile content in standards, the data processing used standard values also normalized to 100%.

FeO and Fe₂O₃

XRF spectrometry cannot distinguish oxidation states of iron and therefore all iron analyses are reported as Fe₂O₃. Ten wet

chemical determinations of FeO were carried out by the author using a modified version of Method B, in Hutchison (1974, p.357). These analyses have been included in the tabulations.

Hughes and Hussey (1976) have commented on the usefulness of FeO:Fe₂O₃ determinations for norms and indices and pointed out that even reliable analyses may not reflect original rock composition but rather an unknown amount of post-crystallization oxidation.

Several correction procedures for ferric/ferrous iron have been proposed to account for metamorphism and oxidation but no consistency in usage has emerged. Because of these ambiguities the author could not justify carrying out hundreds of FeO determinations for this study. Mesonorms for the rocks of this study are presented in Appendix F. To treat the FeO:Fe₂O₃ ratio the author used an empirical approach. Figure C.a is a compilation of wet chemical ferrous/ferric iron determinations published for granitoid rocks of Northwestern Ontario, Manitoba and Minnesota. Included are ten analyses performed by the author. The linear correlation corresponds approximately to a 1:1 ratio for FeO:Fe₂O₃. This ratio has been used for normative calculations although the effects of post-crystallization oxidation are not accounted for.

Precision:

Table C.b presents a comparison between the precision of this study and published precision of Leake et al (1969). These authors obtained coefficients of variation less than .60% for all oxides in excess of 0.25% except for Na₂O and K₂O, for a wide variety of

FIGURE C.3 COMPILATION OF WET CHEMICAL
FEROUS/FERRIC IRON DETERMINATIONS
FOR GRANITOIDS OF N.W. ONTARIO,
MANITOBA AND MINNESOTA. DATA
SOURCE INCLUDES PREVIOUSLY CITED
REFERENCES (•) PLUS AUTHOR'S
OWN DETERMINATIONS (†):

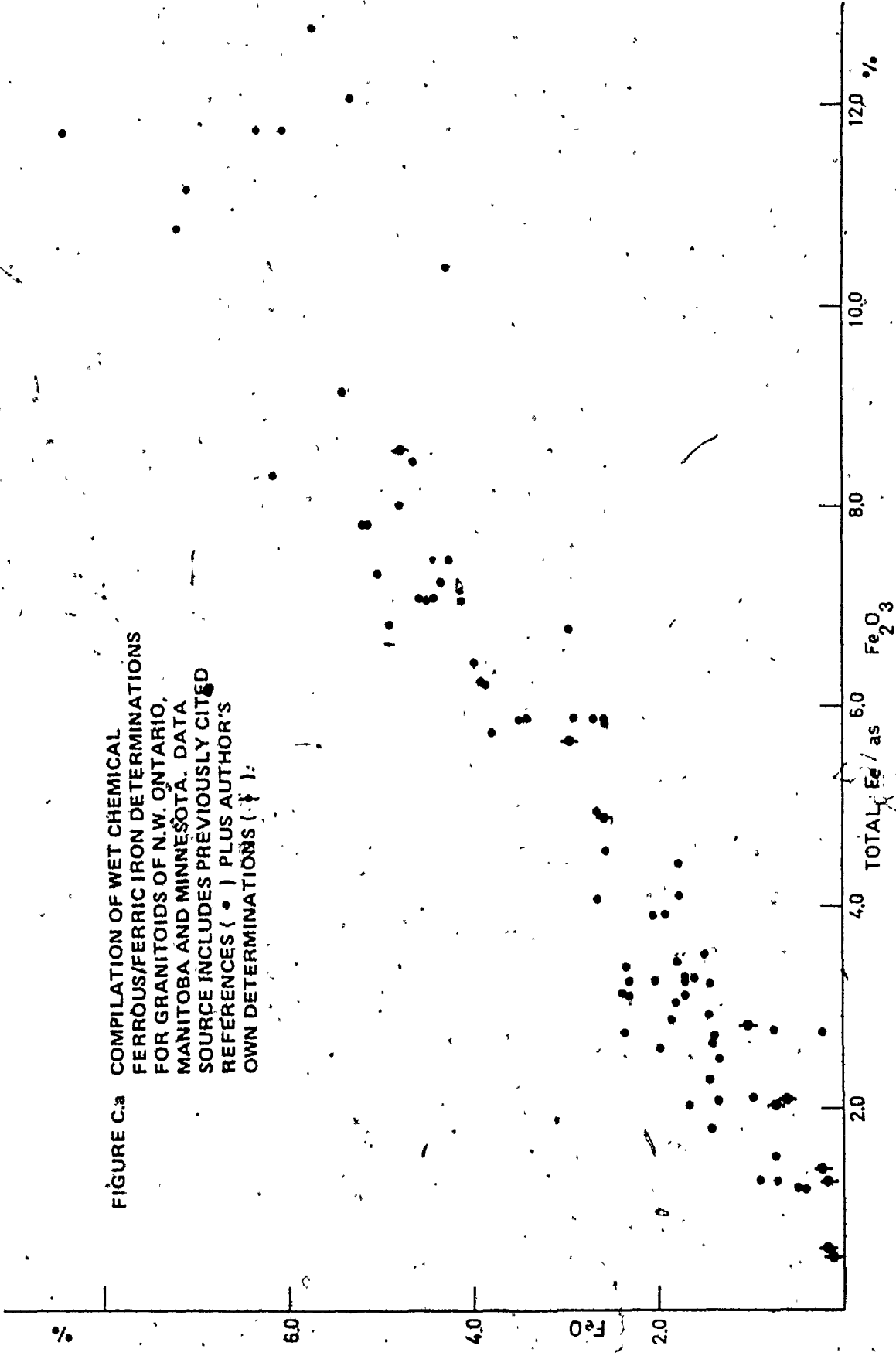


Table C.b

Major Elements: Whole-rock Pressed Powder Method: XRF Precision

a. Precision For Replicate Runs: One machine set-up. Six loadings of sample RY91.

	SiO ₂	Al ₂ O ₃	Fe ₂ O ₃ T	MgO	CaO	Na ₂ O	K ₂ O	TiO ₂	MnO	P ₂ O ₅
Wt.%	59.89	14.47	4.44	5.31	4.81	7.03	3.29	0.41	0.10	0.24
S.D.	.18	.22	.026	.12	.039	.14	.01	.00	.004	.01
C.V.	.30%	1.5%	.59%	2.3%	.81%	2.0%	.30%	.00	4.%	4.2%

b. Published Precision: Leake et al (1969), Table IX. 9 - 45 replicates for 3 pellets of granite JWA6012 averaged:

	SiO ₂	Al ₂ O ₃	Fe ₂ O ₃ T	MgO	CaO	Na ₂ O	K ₂ O	TiO ₂	MnO	P ₂ O ₅
Wt.%	75.89	12.85	0.58	0.11	0.75	3.65	5.05	0.08	0.03	0.01
C.V.	0.14%	0.48%	0.48%	31.4%	0.34%	3.52%	0.21%	2.2%	1.7%	.52%

c. Precision For Long-Term: Separate machine set-ups: (1974 to 1975) sample.

	SiO ₂	Al ₂ O ₃	Fe ₂ O ₃ T	MgO	CaO	Na ₂ O	K ₂ O	TiO ₂	MnO	P ₂ O ₅
Ry5	69.70	15.60	2.10	1.41	2.47	5.39	3.00	0.18	0.04	0.10
	69.67	15.72	2.08	1.32	2.46	5.38	3.06	0.18	0.04	0.08
	69.99	15.63	2.05	0.94	2.46	5.75	2.87	0.17	0.04	0.09
	69.84	15.64	2.05	0.94	2.46	5.88	2.88	0.18	0.04	0.08
S.D.	.15	.05	.024	.25	.006	.25	.093	.006	.00	.01
C.V.	.21%	.32%	1.2%	21.7%	.24%	4.5%	3.2%	3.3%	.00	11.0%
S7	68.37	15.91	2.53	1.40	2.76	5.29	3.21	0.30	0.05	0.18
	68.32	16.14	2.49	1.25	2.77	5.26	3.25	0.29	0.05	0.17
	68.55	16.03	2.52	1.28	2.74	5.14	3.23	0.29	0.05	0.17
	68.57	15.97	2.46	0.94	2.77	5.67	3.11	0.29	0.05	0.18
S.D.	.13	.098	.032	.20	.014	.23	.062	.006	.00	.006
C.V.	.18%	.61%	1.26%	16.1%	.51%	4.3%	1.9%	2.0%	.00	3.3%
Mean										
C.V.	.20%	.47%	1.2%	19.%	.38%	4.4%	2.5%	2.7%	.00	7.2%

S.D. = Standard Deviation

C.V. = Coefficient of Variation

rock types. study pooled analyses obtained during several machine operations over a two year period. Since machine conditions (vacuum, crystal position, sample turret position, room humidity etc.) are never exactly constant, the author was concerned with short-term and long-term precision. Table C.b shows replicate runs at one operating time and replicates for several machine set-ups. Short term precision appears to be better for Fe_2O_3 , MgO , Na_2O and K_2O but worse than long term for SiO_2 , Al_2O_3 and CaO . This statistical evaluation is very limited, therefore no explanations are presented, but the data does confirm the compatibility of the pooled analyses. The coefficients of variation compare favourably with those reported by Leake et al (1969) except for somewhat higher Fe_2O_3 and K_2O variances.

Accuracy:

To check for systematic bias, several international standards were analysed in this study as "unknowns" and are tabulated in Tables C.c (for powder technique) and C.d (for fusion technique). Again this statistical test is limited but for concentrations in excess of 0.5%, the % difference between recommended values and this study is somewhat less for fusion analyses than for powder analyses. No systematic bias is evident for either technique.

Statistical statements of accuracy are difficult to make in view of the uncertainties attached to standard values. Abbey (1975) has commented on the ambiguities implied by the proliferation of terms applied to standard values, including: "proposed", "provisional",

Table C.c

Accuracy of XRF major element power analyses: Standards run as unknowns expressed as normalized weight % compared to normalized proposed values.

Standard	SiO ₂	Al ₂ O ₃	Fe ₂ O ₃ T	MgO	CaO	Na ₂ O	K ₂ O	TiO ₂	MnO	P ₂ O ₅
JG1	1. 72.20	14.75	2.36	0.85	2.17	3.21	3.97	0.30	0.07	0.10
	2. 72.77	14.34	2.22	0.76	2.16	3.39	3.94	0.25	0.06	0.09
% Diff.	.8%	2.9%	6.3%	12%	.5%	5.3%	.8%			
R117	1. 77.64	12.15	1.23	.09	.23	4.03	4.54	.06	.02	.01
	3. 77.12	12.41	1.28	.14	.29	4.04	4.64	.06	.01	.01
% Diff.	.7%	2.1%	3.9%	36%	21%	.25%	2.2%			
GA	1. 71.23	14.62	2.67	.93	2.45	3.54	3.94	.38	.09	.15
	2. 70.74	14.67	2.89	.96	2.48	3.59	4.07	.38	.09	.12
% Diff.	.7%	.34%	7.6%	3.1%	1.2%	1.4%	3.2%			

Mean Difference Omitting Concentrations of <.5%:

.7% 1.8% 5.9% 7.6% .9% 2.3% 2.1%

1. This study
2. Abbey (1975)
3. J. Mysson (personal communication)

Table C.d

Accuracy of XRF major element fusion analyses: Standards run as unknowns expressed as normalized weight % compared to normalized proposed values.

Standard	SiO ₂	Al ₂ O ₃	Fe ₂ O ₃ T	MgO	CaO	Na ₂ O	K ₂ O	TiO ₂	MnO	P ₂ O ₅
<u>GSP-1</u>	1. 68.22	14.97	4.48	0.93	2.08	2.87	5.47	0.69	0.06	0.25
	2. 67.91	15.32	4.37	0.97	2.04	2.82	5.58	0.67	0.04	0.28
% Diff.	.46	2.3	2.5	4.1	2.0	1.8	2.0	3.0		
<u>SY-2</u>	1. 60.38	12.30	6.61	2.67	8.12	4.46	4.56	0.17	0.31	0.44
	3. 60.88	12.16	6.35	2.77	8.04	4.35	4.53	0.14	0.32	0.45
% Diff.	.82	1.2	4.1	3.6	1.0	2.5	.66			
<u>SY-3</u>	1. 60.47	11.96	6.79	2.66	8.52	4.27	4.31	0.18	0.31	0.53
	3. 60.66	11.87	6.73	2.75	8.44	4.20	4.32	0.14	0.33	0.56
% Diff.	.31	.75	.89	3.3	.95	.17	.23			
<u>BCR-1</u>	1. 54.44	13.69	13.17	3.71	7.03	3.34	1.78	2.29	0.19	0.35
	2. 54.72	13.65	13.49	3.48	6.96	3.28	1.68	2.21	0.19	0.33
% Diff.	.51	.29	2.4	6.6	1.0	1.8	6.0	3.5		
<u>DRN</u>	1. 54.29	17.88	10.14	4.28	7.18	3.01	1.66	1.09	0.22	0.24
	2. 53.97	17.92	9.89	4.56	7.24	3.06	1.77	1.12	0.21	0.26
% Diff.	.59	.22	2.5	6.1	.84	1.6	6.2	2.7		
<u>JB-1</u>	1. 52.88	14.67	9.20	7.75	9.71	2.72	1.40	1.30	0.16	0.20
	2. 52.83	14.76	9.14	7.85	9.37	2.82	1.43	1.38	0.16	0.26
% Diff.	.09	.61	.66	1.3	3.6	3.5	2.0	5.8		
<u>W1</u>	1. 52.49	14.91	11.00	6.69	10.56	2.22	0.65	1.13	0.17	0.18
	2. 52.47	14.80	11.06	6.60	10.93	2.14	0.64	1.06	0.17	0.14
% Diff.	.04	.74	.55	1.4	3.4	3.7	1.6	6.6		

Mean Difference Omitting Concentrations less than 0.5%:
 .40% .87% 1.9% 4.9% 1.8% 2.4% 2.7% 4.3%

1. This Study
2. Abbey (1975)
3. Abbey et al (1975)

"tentative", "usable", "recommended", "certified" and "guaranteed". Other authors have suggested that heterogeneities exist in the internationally distributed standard specimens. Leake et al (1969) have based the overall accuracy of their XRF determinations on the linear fit of XRF standard determinations plotted against wet chemical determinations. For this study the author considers SiO_2 and Al_2O_3 to be the most accurate and MgO the least accurate but all major element determinations are considered suitable for the application. Systematic errors introduced by the selected standard values and by omission of volatiles do not alter conclusions for rock suites and are partially overcome by the large number of samples.

APPENDIX C: TABLES

APPENDIX C TABLES:
MAJOR AND MINOR ELEMENTS EXPRESSED
AS WEIGHT PERCENT OXIDES NORMALIZED TO 100%
FeO DETERMINED BY WET CHEMISTRY
MODIFIED AFTER HUTCHISON (1974);
OTHERS BY X-RAY FLUORESCENCE
SPECTROMETRY. TOTAL Fe EXPRESSED
AS Fe₂O₃

SAMPLE LOCATIONS ARE OBTAINED FROM
FIELD MAPS AS FOLLOWS:

BEARS:	FIGURE 2.91
BURDITT:	FIGURE 2.2*
ESOX:	FIGURE 2.87
FLORA:	FIGURE 2.67
FROGHEAD:	FIGURE 2.93
OTTERTAIL:	FIGURE 2.92
REGINA:	FIGURE 2.94
REST:	FIGURE 2.90
RYCKMAN:	FIGURE 2.46
SCATTERGOOD:	FIGURE 2.42
STORMY	FIGURE 2.95
TAYLOR:	FIGURE 2.96

* SEE APPENDIX I

BURDITT LAKE STOCK

SAMPLE	SiO2	AL2O3	TiO2	Fe2O3T	FeO	MnO	MgO	CaO	Na2O	K2O	P2O5
MEDIUM GRAINED GRANODIORITE (MUSC.- BI.)											
44223	74.71	14.76	.08	.90		.02	.32	1.27	5.44	2.46	.04
G42	74.78	14.70	.07	.74		.02	.29	1.25	5.33	2.47	.04
4311	74.19	14.92	.09	.84		.02	.43	1.35	5.22	2.48	.04
G43	73.60	15.07	.10	1.02		.02	.39	1.60	5.56	2.48	.05
43114	73.43	15.22	.10	1.03		.02	.57	1.21	5.53	2.48	.04
53431	73.41	15.30	.10	.96		.02	.34	1.67	5.76	2.48	.05
G48	73.20	15.30	.11	.96		.03	.53	1.80	5.56	2.48	.05
4345	72.94	15.32	.11	1.00		.02	.53	1.72	5.53	2.48	.05
44222	72.86	15.59	.12	.96		.02	.47	1.44	5.52	2.48	.05
53448	72.78	15.45	.12	1.06		.03	.60	1.72	5.51	2.48	.06
43112	72.55	15.55	.12	1.04		.03	.53	1.74	5.73	2.48	.07
43213	72.63	15.49	.11	1.07		.03	.66	1.53	5.58	2.48	.05
53435	72.60	15.54	.11	1.00		.02	.58	1.53	5.61	2.48	.05
G53	72.58	15.25	.11	1.30		.03	.60	1.55	5.53	2.48	.05
G56	72.57	15.33	.12	1.24		.03	.60	1.79	5.66	2.48	.06
4411	72.57	15.33	.11	1.04		.02	.56	1.82	5.53	2.48	.06
4416	72.54	15.73	.12	1.04		.02	.56	1.74	5.74	2.48	.06
43119	72.44	15.79	.11	1.00		.03	.58	1.63	5.65	2.48	.05
43113	71.94	15.90	.12	1.08		.02	.61	1.63	5.60	2.48	.05
43410	71.82	15.92	.13	1.20		.02	.61	1.83	5.96	2.48	.07
43310	71.73	16.03	.14	1.36		.03	.73	1.91	5.73	2.48	.07
FINE GRAINED GRANODIORITE (MUSC.- BI.)											
43216	73.29	15.19	.10	1.02		.02	.41	1.71	5.51	2.71	.05
G51	73.11	15.31	.10	1.04		.02	.40	1.72	5.76	2.49	.05
43116	73.00	15.35	.11	1.04		.02	.43	1.77	5.75	2.47	.06
FOLIATED GRANODIORITE (MUSC.- BI.)											
G318	74.51	14.64	.06	.70		.02	.26	1.27	5.46	3.02	.03
G308	74.06	14.72	.10	.82		.03	.39	1.27	5.46	3.02	.04
44240	73.76	15.24	.09	.80		.02	.27	1.73	5.43	3.02	.05
G41	73.57	15.06	.10	1.02		.02	.40	1.40	5.55	2.75	.05
G52	73.56	15.82	.11	1.04		.03	.43	1.73	5.64	2.75	.05
5347	73.52	15.11	.09	.92		.03	.37	1.73	5.77	2.71	.05
53430	72.75	15.63	.12	1.00		.02	.54	1.67	5.84	2.57	.06
GA-B	72.60	15.97	.11	1.04		.03	.60	1.38	5.64	2.52	.05
G67	72.43	15.63	.13	1.29	.17	.02	.56	1.64	5.33	2.52	.06
GAA	72.43	15.77	.13	1.12		.02	.51	1.64	5.33	2.52	.06
43251	72.29	15.71	.11	1.04		.03	.51	1.63	5.33	2.52	.06
4411	72.28	15.59	.11	1.12		.03	.51	1.77	5.33	2.52	.06
4412	72.25	15.66	.11	1.18		.02	.55	1.80	5.75	2.50	.06
MASSIVE APLITE PATCHES IN FOLIATED GRANODIORITE											
G78	75.48	14.06	.03	.53	.14	.03	.10	.73	5.11	3.92	.01
51144P	75.48	14.12	.03	.56		.02	.20	.62	5.58	3.40	.04
G62A	74.94	14.45	.03	.48		.02	.09	.66	5.40	3.93	.01
GAC	73.70	15.04	.09	.62		.02	.44	1.10	5.52	3.15	.04
NORTH RIM GRANODIORITE (MUSC.- BI.)											
53350	72.74	15.35	.11	1.06		.02	.42	1.74	5.57	2.93	.06
53310	72.47	14.88	.13	1.54		.03	.72	1.68	5.07	3.40	.07
53312	72.34	15.36	.13	1.34		.03	.74	1.54	5.46	2.98	.05
BI.- H9. GRANODIORITE (MICROCLINE MEGACRYSTS)											
G22	71.83	14.99	.15	1.84		.04	.91	1.35	5.23	3.03	.08
G28	71.66	14.89	.15	2.04	.75	.03	.95	1.91	5.19	3.03	.09
G79	71.63	15.03	.14	1.72		.04	.82	2.01	5.49	3.03	.09
G15	71.57	15.13	.15	1.76		.03	.80	2.01	5.56	3.03	.09
G4	71.50	15.11	.15	1.88		.03	.91	2.10	5.67	3.03	.09
5428	71.32	15.14	.17	1.68		.04	.93	2.13	5.51	3.03	.10
5332	71.32	15.27	.16	1.92		.03	.95	2.03	5.41	3.03	.09
44210	71.25	15.58	.17	1.84		.04	.97	2.01	5.53	3.03	.09
G74	71.25	15.05	.16	1.86		.04	.90	2.29	5.39	3.03	.10
G4	70.23	15.16	.15	1.80		.04	.88	2.19	5.55	3.03	.09
5474	71.18	15.19	.17	1.88		.04	.93	2.13	5.44	3.03	.09
G27A	71.09	15.18	.16	1.86		.04	.94	2.17	5.44	3.03	.10
G7	71.08	15.46	.15	1.78		.04	.98	2.04	5.24	3.03	.09
G77	71.02	15.22	.16	1.88		.04	.92	2.27	5.24	3.03	.09
5412	71.00	15.49	.17	1.96		.04	.98	2.20	5.24	3.03	.10
G44	70.95	15.42	.18	2.04		.05	.91	2.20	5.24	3.03	.10
53322	70.81	15.44	.16	1.80		.04	.93	2.16	5.24	3.03	.09
51414	70.74	15.62	.15	1.72		.04	.89	2.11	5.11	3.03	.09
G9	70.72	15.44	.15	2.09		.04	.97	2.12	5.24	3.03	.11
G70*2	70.68	15.33	.14	1.74		.03	.95	2.14	5.24	3.03	.09
G21	70.62	15.58	.17	1.86		.04	.95	2.06	5.24	3.03	.09
53424	70.60	15.52	.15	1.84		.04	.96	2.09	5.24	3.03	.10
G26	70.54	15.37	.16	1.83		.03	.95	2.08	5.24	3.03	.09
53320	70.10	15.74	.17	2.02		.03	1.10	2.08	5.24	3.03	.10

SAMPLE	SiO2	AL2O3	TiO2	Fe2O3T	FeO	MnO	MgO	CaO	Na2O	K2O	P2O5
FELSIC DYKES WITHIN STOCK											
RED SPOTTED APLITE (APPROX. 2 INCH DYKES)											
G31	76.58	13.43	.81	.56		.03	.09	.71	4.87	3.78	.01
4343	75.66	14.05	.83	.55		.03	.06	.90	5.31	3.35	.02
WHITE APLITE (APPROX. 2 INCH DYKES)											
G30A	72.69	14.02	.83	.58		.02	.10	.87	5.36	3.59	.01
4272BA	75.48	13.91	.85	.54		.03	.23	.76	4.81	4.12	.01
APLITE-PEGMATITE (1 IN.)											
4342AP	76.42	13.76	.83	.54		.01	.08	.87	5.12	3.21	.02
FELSIC DYKES CUTTING MOST FELSIC PYROCLASTICS											
APLITE-PEGMATITE (1 IN.)											
53313	76.13	13.65	.83	.60		.01	.07	.86	4.99	3.65	.01
APLITE-PEGMATITE (ZONED, 3 IN., R=PEGMATITE RIM, C=APLITE CORE)											
53318R	75.53	14.02	.83	.54		.02	.11	.76	4.49	4.69	.01
53318C	75.34	12.13	.83	.53		.04	.11	.59	4.46	5.19	.01
GRANODIORITE (+ MICROCLINE MEGACRYSTS) DYKE (2 IN.)											
53412	73.45	15.54	.87	.80		.02	.36	1.82	6.24	1.55	.06
INTRUSION BRECCIA G=GRANODIORITE, X=ENCLAVE, F=METAVOLCANIC											
53413G	71.58	15.16	.14	1.54		.03	.90	2.11	5.69	2.77	.03
53413X	56.61	16.56	.60	7.35		.12	.39	6.48	5.11	3.91	.11
53413F	56.80	13.19	.64	7.60		.16	.99	6.85	5.29	2.16	.03
LENSOID MAFIC ENCLAVES (LESS THAN 4 X 8 IN.)											
53413X	61.20	15.32	.43	5.42		.03	3.83	3.97	3.88	5.58	.01
53413X	56.76	16.67	.61	7.71		.14	6.08	6.00	5.34	3.28	.02
53413X	55.85	14.93	.53	8.42		.21	4.99	6.08	4.61	3.28	.02
53413X	55.45	14.41	.63	8.49		.21	7.99	7.64	5.61	3.28	.02
53413X	52.69	12.52	.63	11.08		.26	9.28	7.58	2.63	2.64	.02
FELSIC TO INTERMEDIATE METAVOLCANICS											
G61T	75.36	14.78	.26	.85		.02	.98	1.29	5.65	1.78	.08
6126T	78.54	16.05	.31	2.33		.04	2.68	2.18	5.95	1.30	.08
6127T	78.15	15.22	.31	2.32		.03	1.08	2.27	5.95	1.30	.08
6128T	69.67	16.25	.31	2.42		.03	1.06	2.07	5.77	1.74	.07
6129T	69.45	16.37	.31	2.03		.02	1.98	2.84	5.15	1.16	.07
6130T	69.37	16.53	.31	2.24		.04	1.24	2.56	5.33	1.16	.07
6131T	68.84	16.44	.31	2.04		.05	1.14	2.15	5.33	1.16	.07
6132T	67.99	16.34	.31	2.02		.03	.98	2.01	5.72	1.16	.07

C2

SCATTERGOOD LAKE STOCK

SAMPLE	SiO2	AL2O3	TiO2	Fe2O3T	FeO	MnO	MgO	CaO	Na2O	K2O	P2O5
HB GRANODIORITE (+ MICROCLINE MEGACRYSTS)											
6006A	69.22	13.23	.22	2.78		.03	2.09	2.52	5.65	1.78	.05
6006B	68.49	14.66	.22	2.62		.03	1.12	2.79	5.28	1.78	.05
6006C	68.63	14.31	.22	2.62		.03	1.06	2.72	5.28	1.78	.05
6006D	68.60	14.47	.22	2.62		.03	1.06	2.72	5.28	1.78	.05
6006E	68.60	14.61	.22	2.62		.03	1.06	2.72	5.28	1.78	.05
6006F	68.54	14.72	.22	2.62		.03	1.06	2.72	5.28	1.78	.05
6006G	68.52	14.77	.22	2.62		.03	1.06	2.72	5.28	1.78	.05
6006H	68.50	14.70	.22	2.62		.03	1.06	2.72	5.28	1.78	.05
6006I	68.49	14.70	.22	2.62		.03	1.06	2.72	5.28	1.78	.05
6006J	68.46	14.73	.22	2.62		.03	1.06	2.72	5.28	1.78	.05
6006K	68.45	14.73	.22	2.62		.03	1.06	2.72	5.28	1.78	.05
6006L	68.45	14.73	.22	2.62		.03	1.06	2.72	5.28	1.78	.05
6006M	68.45	14.73	.22	2.62		.03	1.06	2.72	5.28	1.78	.05
6006N	68.45	14.73	.22	2.62		.03	1.06	2.72	5.28	1.78	.05
6006O	68.45	14.73	.22	2.62		.03	1.06	2.72	5.28	1.78	.05
6006P	68.45	14.73	.22	2.62		.03	1.06	2.72	5.28	1.78	.05
6006Q	68.45	14.73	.22	2.62		.03	1.06	2.72	5.28	1.78	.05
6006R	68.45	14.73	.22	2.62		.03	1.06	2.72	5.28	1.78	.05
6006S	68.45	14.73	.22	2.62		.03	1.06	2.72	5.28	1.78	.05
6006T	68.45	14.73	.22	2.62		.03	1.06	2.72	5.28	1.78	.05
6006U	68.45	14.73	.22	2.62		.03	1.06	2.72	5.28	1.78	.05
6006V	68.45	14.73	.22	2.62		.03	1.06	2.72	5.28	1.78	.05
6006W	68.45	14.73	.22	2.62		.03	1.06	2.72	5.28	1.78	.05
6006X	68.45	14.73	.22	2.62		.03	1.06	2.72	5.28	1.78	.05
6006Y	68.45	14.73	.22	2.62		.03	1.06	2.72	5.28	1.78	.05
6006Z	68.45	14.73	.22	2.62		.03	1.06	2.72	5.28	1.78	.05
6007A	68.45	14.73	.22	2.62		.03	1.06	2.72	5.28	1.78	.05
6007B	68.45	14.73	.22	2.62		.03	1.06	2.72	5.28	1.78	.05
6007C	68.45	14.73	.22	2.62		.03	1.06	2.72	5.28	1.78	.05
6007D	68.45	14.73	.22	2.62		.03	1.06	2.72	5.28	1.78	.05
6007E	68.45	14.73	.22	2.62		.03	1.06	2.72	5.28	1.78	.05
6007F	68.45	14.73	.22	2.62		.03	1.06	2.72	5.28	1.78	.05
6007G	68.45	14.73	.22	2.62		.03	1.06	2.72	5.28	1.78	.05
6007H	68.45	14.73	.22	2.62		.03	1.06	2.72	5.28	1.78	.05
6007I	68.45	14.73	.22	2.62		.03	1.06	2.72	5.28	1.78	.05
6007J	68.45	14.73	.22	2.62		.03	1.06	2.72	5.28	1.78	.05
6007K	68.45	14.73	.22	2.62		.03	1.06	2.72	5.28	1.78	.05
6007L	68.45	14.73	.22	2.62		.03	1.06	2.72	5.28	1.78	.05
6007M	68.45	14.73	.22	2.62		.03	1.06	2.72	5.28	1.78	.05
6007N	68.45	14.73	.22	2.62		.03	1.06	2.72	5.28	1.78	.05
6007O	68.45	14.73	.22	2.62		.03	1.06	2.72	5.28	1.78	.05
6007P	68.45	14.73	.22	2.62		.03	1.06	2.72	5.28	1.78	.05
6007Q	68.45	14.73	.22	2.62		.03	1.06	2.72	5.28	1.78	.05
6007R	68.45	14.73	.22	2.62		.03	1.06	2.72	5.28	1.78	.05
6007S	68.45	14.73	.22	2.62		.03	1.06	2.72	5.28	1.78	.05
6007T	68.45	14.73	.22	2.62		.03	1.06	2.72	5.28	1.78	.05
6007U	68.45	14.73	.22	2.62		.03	1.06	2.72	5.28	1.78	.05
6007V	68.45	14.73	.22	2.62		.03	1.06	2.72	5.28	1.78	.05
6007W	68.45	14.73	.22	2.62		.03	1.06	2.72	5.28	1.78	.05
6007X	68.45	14.73	.22	2.62		.03	1.06	2.72	5.28	1.78	.05
6007Y	68.45	14.73	.22	2.62		.03	1.06	2.72	5.28	1.78	.05
6007Z	68.45	14.73	.22	2.62		.03	1.06	2.72	5.28	1.78	.05
6008A	68.45	14.73	.22	2.62		.03	1.06	2.72	5.28	1.78	.05
6008B	68.45	14.73	.22	2.62		.03	1.06	2.72	5.28	1.78	.05
6008C	68.45	14.73	.22	2.62		.03	1.06	2.72	5.28	1.78	.05
6008D	68.45	14.73	.22	2.62		.03	1.06	2.72	5.28	1.78	.05
6008E	68.45	14.73	.22	2.62		.03	1.06	2.72	5.28	1.78	.05
6008F	68.45	14.73	.22	2.62		.03	1.06	2.72	5.28	1.78	.05
6008G	68.45	14.73	.22	2.62		.03	1.06	2.72	5.28	1.78	.05
6008H	68.45	14.73	.22	2.62		.03	1.06	2.72	5.28	1.78	.05
6008I	68.45	14.73	.22	2.62		.03	1.06	2.72	5.28	1.78	.05
6008J	68.45	14.73	.22	2.62		.03	1.06	2.72	5.28	1.78	.05
6008K	68.45	14.73	.22	2.62		.03	1.06	2.72	5.28	1.78	.05
6008L	68.45	14.73	.22	2.62		.03	1.06	2.72	5.28	1.78	.05
6008M	68.45	14.73	.22	2.62		.03	1.06	2.72	5.28	1.78	.05
6008N	68.45	14.73	.22	2.62		.03	1.06	2.72	5.28	1.78	.05
6008O	68.45	14.73	.22	2.62		.03	1.06	2.72	5.28	1.78	.05
6008P	68.45	14.73	.22	2.62		.03	1.06	2.72	5.28	1.78	.05
6008Q	68.45	14.73	.22	2.62		.03	1.06	2.72	5.28	1.78	.05
6008R	68.45	14.73	.22	2.62		.03	1.06	2.72	5.28	1.78	.05
6008S	68.45	14.73	.22	2.62		.03	1.06	2.72	5.28	1.78	.05
6008T	68.45	14.73	.22	2.62		.03	1.06	2.72	5.28	1.78	.05
6008U	68.45	14.73	.22	2.62		.03	1.06				

C3

ESOX LAKE GRANITOIDS

SAMPLE SiO2 AL2O3 TiO2 Fe2O3T FeO MnO MgO CaO Na2O K2O P2O5

ESOX EAST STOCK

91 GRANODIORITE

(CORE)

SAMPLE	SiO2	AL2O3	TiO2	Fe2O3T	FeO	MnO	MgO	CaO	Na2O	K2O	P2O5
EX25	71.91	15.53	.14	1.13		.03	.56	1.00	5.80	4.46	.06
EX25	71.85	15.55	.14	1.21		.05	.56	1.00	5.80	4.42	.06
EX20	71.33	15.32	.13	1.64		.04	.77	1.76	5.03	3.58	.06
EX21	70.67	15.36	.13	1.80		.04	.85	2.11	5.11	3.58	.06
EX19	69.97	16.09	.22	2.03		.04	.79	2.11	5.00	3.83	.10
EX27	69.88	16.13	.22	2.44		.05	.92	2.21	4.84	3.84	.10
EX26	66.83	15.39	.23	2.27		.06	1.20	3.24	4.79	3.73	.17

BI - HB MONZODIORITE

(RIM)

SAMPLE	SiO2	AL2O3	TiO2	Fe2O3T	FeO	MnO	MgO	CaO	Na2O	K2O	P2O5
EX30A	67.99	15.71	.24	2.02	1.02	.06	1.44	2.41	4.88	4.17	.17
EX30B	66.27	16.10	.32	3.36		.07	1.74	2.81	4.86	4.24	.21
EX29	66.15	16.17	.33	3.37		.07	1.67	2.93	4.92	4.13	.21
EX24	65.98	16.28	.35	3.56		.08	1.46	2.53	4.79	4.71	.25
EX28	64.44	16.33	.39	4.22		.09	2.09	3.14	5.12	4.54	.25

ESOX WEST STOCK

LEUCO - QUARTZ MONZODIORITE

SAMPLE	SiO2	AL2O3	TiO2	Fe2O3T	FeO	MnO	MgO	CaO	Na2O	K2O	P2O5
EX2	71.62	15.58	.14	1.24		.33	.55	1.62	5.40	3.64	.35
EX1	70.74	16.09	.14	1.43	.24	.04	.49	1.44	5.91	3.71	.06
EX11	70.43	16.36	.18	1.50		.04	.43	1.44	5.57	3.98	.05

HYPABYSSAL SYNVOLCANIC FELSITE

PINK FELSITE (QUARTZ - FELSPAR PORPHYRY)

SAMPLE	SiO2	AL2O3	TiO2	Fe2O3T	FeO	MnO	MgO	CaO	Na2O	K2O	P2O5
EX5	74.51	13.65	.10	1.02		.02	.09	1.97	3.49	5.99	.05
EX31	72.24	13.33	.09	1.04		.09	.33	3.11	1.83	7.79	.08

GREY FELSITE (QUARTZ - FELSPAR PORPHYRY)

SAMPLE	SiO2	AL2O3	TiO2	Fe2O3T	FeO	MnO	MgO	CaO	Na2O	K2O	P2O5
EX7	68.33	16.81	.31	3.26		.07	1.07	3.53	4.81	2.42	.18
EX8	67.41	15.34	.31	3.04		.09	.61	4.27	3.77	5.03	.13

C4

FLORA LAKE STOCK

SAMPLE SiO2 AL2O3 TiO2 Fe2O3T FeO MnO MgO CaO Na2O K2O P2O5

SIOTITE GRANITE (CORE)

SAMPLE	SiO2	AL2O3	TiO2	Fe2O3T	FeO	MnO	MgO	CaO	Na2O	K2O	P2O5
FL24	73.49	15.14	.11	.92		.03	.50	1.00	5.50	3.28	.06
FL15	73.48	15.82	.09	.92		.03	.50	1.00	5.50	3.28	.06
FLOP6	72.72	15.47	.13	.90		.03	.50	1.00	5.50	3.28	.06
FLR17	72.51	15.28	.14	1.22		.03	.50	1.00	5.50	3.28	.06
FLOR3	72.50	15.49	.09	.90		.03	.50	1.00	5.50	3.28	.06
FL13	72.40	15.24	.13	.90		.03	.50	1.00	5.50	3.28	.06
FL28	72.07	15.68	.11	.90		.03	.50	1.00	5.50	3.28	.06
FLOP5	70.59	16.04	.13	1.30		.03	.53	1.27	5.48	4.62	.05

HB - BI MONZONITE (MANTLE)

SAMPLE	SiO2	AL2O3	TiO2	Fe2O3T	FeO	MnO	MgO	CaO	Na2O	K2O	P2O5
FLP21	63.34	17.94	.37	3.64		.08	1.48	2.41	5.64	5.09	.18
FLR2	63.33	18.27	.37	3.73		.08	1.48	2.41	5.64	5.09	.18
FLR24	63.14	18.82	.37	3.73		.08	1.48	2.41	5.64	5.09	.18
FLR23	62.33	19.33	.31	3.24		.08	1.48	2.41	5.64	5.09	.18
FLOR4	61.80	19.33	.31	3.24		.08	1.48	2.41	5.64	5.09	.18
FLR14	61.70	19.34	.31	3.24		.08	1.48	2.41	5.64	5.09	.18
FLR20	61.16	19.94	.33	3.45		.08	1.48	2.41	5.64	5.09	.18

HB - BI MONZODIORITE (RIM)

SAMPLE	SiO2	AL2O3	TiO2	Fe2O3T	FeO	MnO	MgO	CaO	Na2O	K2O	P2O5
FL11	57.09	18.10	.41	5.96		.13	2.70	4.30	6.14	4.72	.46
FL17	56.30	18.72	.43	7.80		.16	3.20	4.11	5.33	4.41	.44
FL1	54.81	17.44	.39	7.80		.16	3.20	4.11	5.33	4.41	.44
FL20	53.24	18.14	1.06	8.30		.14	3.00	3.80	4.80	4.18	.42
FL26	52.35	17.85	1.00	8.45		.14	3.00	3.80	4.80	4.18	.42

MONZODIORITE - METAVOLCANIC CONTACT

SAMPLE	SiO2	AL2O3	TiO2	Fe2O3T	FeO	MnO	MgO	CaO	Na2O	K2O	P2O5
FL9	60.68	20.36	.35	2.96		.03	.98	3.45	5.92	4.98	.29

GRANITE DYKE IN MONZONITE

SAMPLE	SiO2	AL2O3	TiO2	Fe2O3T	FeO	MnO	MgO	CaO	Na2O	K2O	P2O5
FLR18	73.35	14.66	.11	1.80		.02	.48	1.10	5.22	3.91	.03

GRANITE DYKE IN MONZODIORITE

SAMPLE	SiO2	AL2O3	TiO2	Fe2O3T	FeO	MnO	MgO	CaO	Na2O	K2O	P2O5
FLOP8	67.30	17.94	.23	2.06		.04	.75	2.52	5.61	3.47	.08

APLITE DYKE IN METAVOLCANICS

SAMPLE	SiO2	AL2O3	TiO2	Fe2O3T	FeO	MnO	MgO	CaO	Na2O	K2O	P2O5
FLR27	76.04	13.72	.04	.46		.02	.12	.59	4.80	6.21	.01

MONZODIORITE ENCLAVE IN GRANITE

SAMPLE	SiO2	AL2O3	TiO2	Fe2O3T	FeO	MnO	MgO	CaO	Na2O	K2O	P2O5
FLR29	56.40	16.24	.73	6.86		.13	6.73	6.29	4.85	3.33	.44

MONZODIORITE ENCLAVE IN MONZONITE

SAMPLE	SiO2	AL2O3	TiO2	Fe2O3T	FeO	MnO	MgO	CaO	Na2O	K2O	P2O5
FLR19	52.86	14.67	1.15	11.48		.19	3.24	5.75	3.91	4.37	.46

SAMPLE	SiO2	Al2O3	TiO2	Fe2O3T	FeO	H2O	MgO	CaO	Na2O	K2O	P2O5
BI - HB GRANODIORITE (+ MICROCLINE MEGACRYSTS) (CORE)											
RY85	70.01	15.16	.15	1.99		.03	1.08	2.23	5.90	2.84	.09
RY15	70.48	15.16	.16	2.00		.04	1.14	2.15	5.79	2.99	.09
RY90	70.43	15.60	.21	2.32		.09	1.17	2.35	5.19	3.19	.10
RY14	70.17	15.37	.16	2.02		.05	1.10	2.29	6.06	2.69	.09
RY55	70.07	15.44	.15	2.62		.05	1.18	2.21	5.94	2.83	.10
RY32	59.36	15.21	.17	2.22		.04	1.21	2.29	5.92	2.91	.10
RY33	69.84	15.27	.19	2.20		.05	1.36	2.30	5.50	3.06	.11
RY5	69.79	15.65	.18	2.09	.62	.04	1.22	2.40	5.51	2.98	.09
RY54	69.77	15.41	.20	2.14		.04	1.60	2.33	5.18	3.18	.09
RY10	69.75	15.37	.20	2.22		.04	1.46	2.44	5.34	3.02	.11
RY75	69.62	15.57	.16	2.08		.04	1.41	2.42	5.31	3.10	.09
RY13	69.58	15.33	.19	2.28		.05	1.61	2.50	5.30	3.04	.11
RYA	69.53	15.44	.19	2.28		.04	1.51	2.62	5.36	2.91	.11
RY74	69.53	15.61	.19	2.12		.14	1.43	2.43	5.26	3.29	.10
RY1	69.31	15.37	.21	2.46		.05	1.61	2.76	5.21	2.91	.12
RY51	68.80	15.20	.22	2.66		.05	1.90	2.77	5.07	3.19	.12
RY6	67.14	15.85	.26	3.04		.05	2.08	3.31	5.34	2.78	.15
MYLONITE											
RY 70	58.67	15.72	.35	5.06		.10	5.19	5.40	5.96	3.24	.31
BI - HB QUARTZ MONZODIORITE (MANTLE)											
RY50	66.13	15.73	.24	3.24		.06	2.83	3.28	4.86	3.49	.14
RY 76	65.27	15.27	.31	3.52		.04	3.33	3.19	5.69	3.21	.18
RY 77	63.66	15.69	.30	3.62		.04	4.12	3.66	5.65	3.23	.22
RY 73	62.66	14.73	.37	4.34		.05	5.31	4.00	5.12	3.18	.25
RY 3	62.51	14.61	.33	4.42		.10	3.90	4.63	5.64	3.42	.20
RY 72	62.05	15.11	.23	4.60		.03	4.35	4.47	5.49	3.31	.23
RY 21	61.29	14.10	.32	5.12		.09	5.53	5.14	4.84	3.21	.27
RY 7	60.84	14.09	.32	5.36		.12	5.77	5.25	4.75	3.28	.23
RY61	60.35	14.42	.33	4.34		.11	4.62	5.03	7.19	3.46	.14
RY 60	59.76	13.97	.33	5.52		.09	6.90	3.18	4.66	3.32	.27
RY 23	59.54	14.69	.34	5.52		.16	5.65	5.76	4.76	3.40	.31
BI - HB MONZODIORITE (RIM)											
RY 4	60.47	15.49	.30	4.84		.12	4.28	4.77	6.01	3.50	.22
RY 91	59.90	15.39	.41	4.50		.05	5.86	4.53	5.83	3.24	.30
RY 63	59.44	14.69	.35	5.34		.10	5.48	5.65	5.56	3.09	.31
RY 62	58.16	14.60	.33	5.60		.11	6.31	5.98	5.57	2.97	.33
RY 35	57.47	13.75	.35	5.96		.11	8.19	5.76	4.70	3.36	.32
PX - HB MONZODIORITE (RIM)											
RY 37	58.62	16.24	.35	5.28	2.63	.10	4.01	5.01	6.13	3.93	.32
RY 81	57.32	15.64	.47	5.40		.06	6.00	4.89	5.28	4.04	.39
RY 80	57.41	15.14	.42	5.66		.11	6.13	6.24	5.87	2.88	.35
RY 93	56.95	15.42	.50	5.56		.06	6.77	5.34	5.45	3.54	.42
RY 92	55.92	14.59	.43	6.48		.12	7.40	6.83	4.97	2.87	.42
RY 82	55.36	14.94	.45	7.22		.13	6.04	6.54	4.85	3.98	.46
RY 94	52.16	15.29	.60	6.48	4.51	.14	7.10	7.44	4.47	3.70	.61
APLITE DYKE IN MAFIC METAVOLCANICS											
RY22	74.56	14.27	.07	.60		.02	.21	1.15	4.45	4.63	.03
APLITE - PEGMATITE DYKE FROM DYKE SWARM WITHIN STOCK											
RY91A	75.63	13.43	.05	.32		.01	.13	.38	4.03	6.01	.01
MAFIC ENCLAVES											
RY 71	61.65	15.20	.32	4.44		.09	4.13	4.57	5.64	3.47	.25
RY 60X	58.86	14.01	.34	5.76		.10	7.55	5.49	5.11	2.50	.29
RY61X	55.61	12.37	.59	6.66		.14	11.09	7.50	4.84	.82	.35
METAVOLCANICS											
RY84TP	72.08	15.63	.20	1.84		.03	1.08	2.79	5.42	.89	.11
RY 84	56.74	16.40	.38	5.73		.11	3.49	4.73	5.63	4.48	.34

C6 RAINY LAKE GRANITOID PLUTONS (ALGMAN OF LAWSON 1913)

BEARS PASSAGE STOCK

SAMPLE	SI02	AL2O3	TIO2	FE2O3T	FE0	MNO	MGO	CAO	NA2O	K2O	P2O5
BI - MUSC GRANODIORITE											
TR4B	74.24	14.90	.08	.66		.03	.47	1.08	4.74	3.55	.03
TR3	74.1A	14.83	.07	.79		.07	.36	1.13	5.12	3.42	.02
TR1B	74.07	14.76	.12	.63		.02	.54	1.29	5.03	3.46	.04
TR5	74.06	14.95	.07	.77		.03	.38	1.00	4.58	4.13	.03
TP4A	73.91	14.88	.03	.83		.03	.40	1.18	4.93	3.63	.03
TR2	73.66	14.97	.11	.89		.03	.50	1.36	5.03	3.41	.03

PEST ISLAND STOCK

SAMPLE	SI02	AL2O3	TIO2	FE2O3T	FE0	MNO	MGO	CAO	NA2O	K2O	P2O5
MUSC - BI GRANODIORITE (WITHIN BLUE QUARTZ ZONE OF HARRIS 1974)											
REST2	70.49	15.37	.30	2.42		.03	.94	2.64	4.91	2.78	.11
REST1	69.45	15.24	.32	2.60		.04	1.86	2.76	4.44	2.99	.11
REST3	68.63	15.31	.43	3.46		.05	2.09	3.02	4.28	2.58	.14
(OUTSIDE BLUE QUARTZ ZONE OF HARRIS 1974)											
REST5	71.45	15.36	.24	2.03		.03	.92	2.37	5.07	2.47	.09
REST6	68.93	15.20	.36	3.36		.05	1.82	3.16	4.33	2.66	.13
SYENITIC BORDER											
REST4	66.51	14.21	.75	9.12		.14	4.64	7.32	2.58	2.43	.27
GRANITIC DYKE IN SYENITIC BORDER (AGMATITE)											
PEST40	67.75	15.55	.42	3.64		.06	2.23	3.17	4.17	2.88	.13

OTTERTAIL LAKE STOCK

SAMPLE	SI02	AL2O3	TIO2	FE2O3T	FE0	MNO	MGO	CAO	NA2O	K2O	P2O5
MUSCOVITE GRANITE											
OT3	74.39	14.31	.09	.82		.03	.58	1.00	4.41	4.33	.03
OT5	73.18	14.97	.11	.91		.03	.42	1.24	4.48	4.62	.03
BI GRANODIORITE (+ MICHCLINE MEGACRYSTS)											
OT4	71.99	14.98	.18	1.62		.04	.85	1.85	4.79	3.58	.10
OT6	71.12	14.86	.25	2.15		.04	.93	1.93	4.76	3.69	.13
OT7	69.23	14.92	.37	2.66		.06	2.23	1.69	4.29	4.36	.19
OT2	68.39	14.85	.41	3.03		.06	1.62	2.64	4.31	4.04	.19
BI - HB QUARTZ MONZONIORITE											
OT1	68.04	13.46	.75	7.26		.11	7.76	5.79	3.91	2.60	.32

C7 WAPITON GRANITOID PLUTONS

FROGHEAD BAY STOCK

SAMPLE	SiO2	AL2O3	TiO2	Fe2O3*	FeO	MnO	MgO	CaO	Na2O	K2O	P2O5
BI TONALITE											
FH9	70.53	15.50	.31	3.12		.05	.93	3.11	4.30	2.05	.10
FH10	73.47	15.40	.34	3.26		.04	.93	2.92	4.70	1.01	.10
FH11	69.81	15.41	.31	3.64		.05	1.30	3.20	4.33	2.11	.11
FH5	69.64	15.62	.35	3.34		.05	1.20	3.10	4.33	2.10	.10
FH6	69.17	15.05	.30	4.22		.06	1.44	3.44	4.33	1.91	.10
FH7	68.64	15.34	.34	4.13		.05	1.50	3.50	4.33	1.90	.10
FH2	68.62	14.93	.31	4.02		.05	1.61	3.31	4.00	2.06	.10
FH1	68.06	15.24	.33	4.00		.05	1.55	3.50	4.30	1.90	.10
FH4	68.04	15.74	.36	4.10		.05	1.47	3.43	4.24	2.24	.13
BI GRANODIORITE											
FH4	74.43	11.96	.10	1.00		.02	.66	1.54	4.16	3.29	.05

REGINA BAY STOCK

SAMPLE	SiO2	AL2O3	TiO2	Fe2O3*	FeO	MnO	MgO	CaO	Na2O	K2O	P2O5
TONALITE (SERICITIZED, CARBONATIZED, CHLORITIZED)											
REG1	67.76	15.85	.44	4.38		.03	2.46	4.53	4.03	.77	.24
REG2	66.59	15.85	.40	4.55		.08	2.60	4.64	4.15	.72	.19
REG5	66.39	15.03	.44	4.64		.07	2.60	4.43	4.33	.69	.17
REG-2	66.24	15.46	.46	5.19		.07	2.93	4.30	3.07	1.17	.19
REG3	67.17	15.12	.45	4.82		.06	2.60	4.75	4.33	1.24	.17
REG4	65.12	16.00	.41	4.74		.05	2.55	4.30	4.30	1.24	.18
REG-1	63.64	17.36	.49	4.76		.07	2.72	5.23	4.24	1.31	.16
SHEAR ZONE											
REG5	64.02	15.00	.52	5.14		.05	2.82	5.06	3.92	1.51	.16

STONY LAKE STOCK

SAMPLE	SiO2	AL2O3	TiO2	Fe2O3*	FeO	MnO	MgO	CaO	Na2O	K2O	P2O5
BI GRANODIORITE											
ST4	69.64	15.88	.34	2.69		.04	1.22	2.43	5.13	2.69	.14
ST7	68.75	16.13	.40	2.76		.04	1.11	2.62	5.12	2.84	.21
ST2	68.68	16.00	.33	2.92		.04	1.30	2.47	4.90	3.08	.17
ST5	68.12	16.00	.33	2.76		.04	1.35	2.39	5.05	3.15	.15
ST1	65.95	16.21	.42	3.02		.04	1.48	2.71	5.33	2.83	.19

TAYLOR LAKE STOCK (SAMPLES AFTER PICHETTE 1976)

SAMPLE	SiO2	AL2O3	TiO2	Fe2O3*	FeO	MnO	MgO	CaO	Na2O	K2O	P2O5
BI - HB GRANODIORITE											
T54	69.99	15.86	.24	2.02		.04	.93	2.04	5.22	3.85	.11
T10	69.21	15.33	.33	2.33		.06	1.44	2.44	4.77	3.75	.16
T11	68.75	15.33	.33	2.33		.06	1.44	2.44	4.77	3.75	.16
T13	68.25	15.74	.33	2.33		.05	1.33	2.71	4.03	3.64	.16
T15	67.76	16.05	.33	2.71		.05	1.33	2.65	4.03	3.84	.17
T17	66.85	16.25	.33	2.03		.07	1.44	2.56	4.99	3.47	.17
T18	66.85	16.25	.33	2.03		.07	1.44	2.56	4.93	4.62	.18
BI - HB - PX MONZONITE / TC QUARTZ MONZONITE											
T65	67.72	16.01	.33	2.77		.06	1.61	2.82	5.07	3.44	.17
T16	65.98	16.28	.35	3.24		.07	1.61	2.61	5.26	4.26	.18
T72	63.4	17.23	.56	3.15		.07	1.41	2.56	6.23	4.65	.21
T37	61.27	16.39	.53	4.63		.13	2.73	4.43	5.98	3.56	.20
T-2	58.39	14.42	.63	6.15		.13	3.44	7.15	5.26	3.74	.71
T-1	57.23	14.49	.79	6.85		.14	4.93	5.99	4.30	4.02	.46
HB - BI GRANODIORITE (FINE GRAINED)											
T25	71.93	15.72	.13	1.34		.02	.73	1.80	5.33	2.77	.07
T46	71.90	15.45	.13	1.37		.03	.73	1.79	5.27	3.21	.07
HB - PX MONZONITE											
T16	65.46	15.47	.63	6.48		.14	4.25	8.31	5.45	1.03	.57
HB - PX MONZONITE (MEDIUM GRAINED)											
T69	61.41	16.92	.55	4.35		.11	1.93	3.94	6.16	4.32	.35
BI - PX - HB MONZONITE (COURSE GRAINED)											
T75	60.84	16.73	.56	4.66		.11	1.85	4.70	5.99	3.68	.40
MUSC - BI LEUCO MICROGRANITE											
T60	72.86	15.57	.14	1.09		.03	.35	.40	5.02	5.31	.03
APLITE											
T47	78.64	16.27	.25	1.79		.03	.85	1.99	5.57	2.53	.10
MAFIC ENCLAVE											
T24X	61.18	13.97	.45	5.31		.20	5.68	6.88	2.96	5.72	.18
MAFIC VOLCANIC											
T49	49.53	12.02	1.23	14.66		.33	8.08	10.07	2.94	.94	.16

APPENDIX D

TRACE ELEMENT DETERMINATIONS

Introduction:

Trace element determinations were carried out by the author on the PW1450AHP (Philips) X-ray fluorescence spectrometer using the same boric acid backed powder pellets of the major element study. Determinations for Rb and Sr were carried out in duplicate or replicate whereas Nb, Zr, Y, Ba and Ce represent mainly singlicate runs. U and Th were determined by in situ portable gamma ray spectrometry and are discussed in Appendix G.

Nb, Zr, Y

These three elements were analyzed together using a tungsten tube and operating conditions as set out in Table D.a. Peak interference corrections were made for Rb and Sr by analysing for these elements as well but the concentration results for Rb and Sr were not retained since molybdenum tube determinations were considered superior. Matrix effects were corrected by using the reciprocal of the Compton scatter peak intensity. SY2 was used as a standard based on the values of Abbey et al (1975) and background intensities were read from a synthetic "spec-pure" andesite pellet.

Ba and Ce

Ba was analysed with a tungsten tube and conditions as set out

Table D.a

OPTIMUM XRF SPECTROMETER PARAMETERS FOR TRACE ELEMENTS:

<u>ELEMENT</u>	<u>PEAK</u>	<u>COUNTER</u>	<u>COLLIMATOR</u>	<u>TIME PEAK (Sec.)</u>	<u>VACUUM</u>	<u>TUBE</u>	<u>KV</u>	<u>Ma</u>
Nb	K _α	S	F	100	no	W	50	25
Zr	K _α	S	F	100	no	W	50	25
Y	K _α	S	F	100	no	W	50	25
Rb	K _α	S	F	40	yes	Mo	90	25
Sr	K _α	S	F	40	yes	Mo	90	25
Ba	L _β	FP	C	100	yes	Mo	50	50
Ce	L _β	FP	C	100	yes	Mo	50	50

LiF200 crystal, no filter and 10 second backgrounds used throughout.

S = Scintillation Counter,
 FP = Gas Flow Proportional Counter,
 F = Fine (15 mm.)
 C = Coarse (.48 mm.).

by Table D.a. Readings on $Ba_{L\beta}$, were corrected for overlap from $Ce_{L\alpha}$ by simultaneously running $Ce_{L\beta 1}$. This technique is best applied to rocks of low rare-earth content (Gunn, 1969) such as basalts but was considered suitable for this study because of the very high barium concentrations encountered. Mass absorption coefficients were calculated from known major element compositions as described by Hutchison (1974). Concentrations were determined from calibration curves based on six standards reported by Abbey (1975).

Rb and Sr

Rb and Sr determinations were made using the procedure of Marchand (1973) except that the spectrometer employed by the author allowed for automatic pulse height selection. Mass absorption coefficients were calculated from the reciprocal of the Mo-compton peak, and concentrations were derived by linear least squares regression of six standards against unknowns. The standards used were: NBS70, G2, GSP1, AGV1, W1, BCR1 with values accepted from Delaeter et al (1970). The background profile was determined on a spec-pure silica powder pellet.

Doering (1968) demonstrated that better precision for the ratio Rb/Sr is achieved if the ratio is derived directly from XRF counts rather than from elemental determinations. Since Rb and Sr are consecutive elements with K lines close together (.87660 A° for Sr; .92688 A° for Rb) matrix effects are virtually identical and therefore are self-cancelling for the ratio Rb/Sr. Ratio determinations for geochronological application were therefore obtained by a modified

version of Doering (1968) as described by Marchand (1973) using raw background-corrected counts related to the above mentioned six standards by linear least squares regression. Turek et al (1977) have shown that isochron uncertainties based on XRF data are not significantly greater than for corresponding isotope dilution data. They, however, propose the use of a LiF220 crystal in place of LiF200 and make mass absorption corrections using the intensity of the Compton scatter. No comparative data is available at present to determine whether their approach is superior to the method of Marchand (1973) adopted in this thesis.

Precision:

Trace element analyses were performed at several intermittent times over six months for Nb, Zr, Y, Rb and Sr but at one sitting for Ba and Ce. For the former elements both short-term (one machine set-up) and long-term (intermittent runs with several machine resettings) precision must be accounted for. Tables D.b and D.c present the coefficients of variation for replications and compare them with reported precision of Leake et al (1969). These authors report less precise Ba, Ce, Nb, Sr and similar precision for Zr, Y and Rb. Much of this difference reflects concentration differences in replicates. Marchand (1973) pointed out that Rb and Sr have a constant coefficient of variation at high concentrations while a constant standard error at low concentrations. The poorest precision in this study was recorded for Nb, Y and Ce which also showed the lowest concentrations. Long term precision was poorer than short term precision for all elements.

Table D.b

Short-term precision for trace element XRF determinations; one machine set-up, one pellet:

Element	Ba	Ce	Nb	Zr	Y	Rb	Sr
Standard	GA	GA	BR	BR	BR	GA	GA
This Study X	844.6	61.6	82.0	241.1	27.5	169.0	292.8
Replicates #	41	41	17	17	17	44	44
Coef. Var.	0.81%	3.3%	2.9%	1.1%	6.7%	0.39%	0.33%

Published coefficients of variation: Leake et al (1969) Table IX: "Granite"

JWAG012	X	122.1	28.6	19.6	77.6	30.4	20.6
(3 Pellets)	#	9	9	10	30	11	11
C.V.		7.6%	20.3%	9.5%	4.2%	5.4%	3.4%

Table D.c

Long-term precision: Trace element XRF determinations; Several machine set-ups, one pellet:

Standard:	Nb	Zr	Y	Rd		Sr	
				G8	RY22	G8	RY94
Jan./76	76.5	245.4	25.9%	102.0	295.8	969.4	626.4
Feb./76	86.2	250.3	29.1	102.1	292.8	944.3	610.0
Mar./76	83.3	227.6	27.4	100.6	292.2	953.0	613.2
				103.5	297.1	978.7	623.2
Coef. Var.	6.1%	5.0%	5.8%	1.2%	0.8%	1.6%	1.3%

Average Coefficient of Variation: Rb: 1.1% Sr: 1.5%

except Y which demonstrates that replicate runs under one set of machine conditions do not provide an accurate estimate of XRF precision if analyses are made intermittently.

The precision for Rb and Sr is the best achievable for any of these elements (Leake et al, 1969) because of freedom from line interference, optimum excitation by the MoK α line and large critical depth. This reflects favourably on the geochronological application. The coefficient of variation on the Rb/Sr ratio is similar to that for elemental Rb and Sr for a single machine operation and is lower for intermittent runs (Table D.d). This confirms that ratios by the methods of Doering (1968) and Marchand (1973) are superior to ratios obtained from elemental abundances. The "blanket" coefficient of variation for Rb/Sr adopted for the isochron calculations is 1.0%. Since the error on Rb⁸⁷/Sr⁸⁶ is largely controlled by the error on Rb/Sr (Gibbins, 1973) the blanket error for ⁸⁷Rb/⁸⁶Sr is also 1.0% for regression treatments. This coincides with the 1% (1 sigma) adopted by Gibbins and McNutt (1975).

Accuracy:

Accuracy estimates for trace element determinations by XRF are greatly hampered by uncertainties in standard values. Gunn (1969) recognized 10 to 20% variations in proposed Ba values for silicate standards. Leake et al (1969) pointed out that for many trace elements only the standards G1 and W1 have reliable published results. Abbey (1975) indicated by question marks the uncertainties in his tables; these have been included here.

Table D.d

Rb/Sr ratio based on method of Marchand (1973):

Precision: Long-Term (One pellet):

Sample: G8 RY22

Oct./74 .10519 .47137
 Apr./75 .10750 .47228
 Jul./75 .10484 .46827
 Nov./75 .10478 .47242

Coef. Var. 1.2% 0.41%

Average Coefficient of Variation: 0.89%

Accuracy: Standards Run as Unknowns

Standard

This Study

De Laeter et al
(1970)*

Pankhurst et al
(1973)*

Pankhurst & O'Nions
(1973)*

Abbey (1975)
(Elemental)

NBS70 8.1934 7.955 8.105 0.0333
 G2 0.35649 0.3558 0.355 1.00
 GSP1 1.0833 1.091 1.093 0.583
 AGV1 0.10290 0.1020 0.1014 0.0909
 W1 0.11551 0.1158 0.1158 7.37
 BCR1 0.14407 0.1446
 BR 0.03564
 JGI 0.96300
 GA 0.57518
 JBI 0.09092
 NIMS 8.7757

Precision: Short-Term (One pellet)
 Sample: GA

X: .57115
 Replicates: 44
 Standard Deviation: .00207

Coef. Var: 0.36%

* By Isotope Dilution

A comparison of the deviations of standard values of this study (Table D.e) with deviations experienced by Leake et al (1969, Table XIV) shows results for this study to be more accurate (relative to recommended values) for Zr, Rb, Sr and Ba and of similar accuracy for Ce, Nb and Y. Ba results for this study deviate less than 6% for concentrations in excess of 30 ppm (most of our samples). A very sharp rise in error occurs for samples with Ba <100 ppm, reflecting interference from rare earths and/or contamination of standard GH. Ce values in excess of 100 ppm appear to be systematically too low by about 20%. Nb values show large deviations partially attributable to uncertainty in the standard value for SY2 (Abbey et al, 1975). Zr values show close agreement illustrating the improved accuracy with higher concentrations.

Sr error increase sharply for concentrations < 100 ppm. Only one sample (F1-27: Sr = 73 ppm) in this study falls in that range. Sr shows values consistently lower than recommended while Rb values are lower for concentrations > 50 ppm. These observations do not reflect on the ratio determination and therefore do not discredit the chronological application.

Ratios for standards run as unknowns (Table D.d) compare favourably with isotope dilution values of Delaeter et al (1970) and Pankhurst and O'Nions (1973). Unfortunately not all standards have corresponding isotope dilution values, therefore some comparisons must rely on Abbey's (1975) elemental values. This scant survey suggests that high Rb/Sr ratios (see NBS70; NIMS) are overestimated by the method of Marchand (1973) which may explain the "dropping off" effect

Table D.e

Accuracy of Trace Element XRF Determinations: Standards, as Unknowns in ppm.

Standard	Ce			Ba			Nb			Zr			Y			
	1	2	3	1	2	3	1	2	3	1	2	3	1	2	3	
GA	61.6	55	12%	844.2	850	0.7%	10.2	13?	22%	148.6	140	6.1%	21.8	18?	21%	
GSPI	254.8	390?	35	1307.6	1300	0.6	21.5	29	26	501.3.	500	.26	25.9	32	19	
NIMS	15.9	12?	33	2604.1	2400	8.5	-	-	-	-	-	-	-	-	-	
GH	49.1	52*	5.6	73.8	22	235.	-	-	-	-	-	-	-	-	-	
NIMG	169.3	200?	15	182.1	210	13.3	49.7	?	?	281.5	260	8.2	152.6	120?	27	
NIMN	10.4	15?	31	131.5	110	19.5	-	-	-	-	-	-	-	-	-	
W1	17.8	23?	23	196.4	160	22.8	3.5	9.5	63	84.6	105	19.	21.1	25	16	
BCRI	60.4	54	12	642.7	680	5.5	-	-	-	-	-	-	-	-	-	
AGWI	66.0	63?	5	1144.4	1200	4.6	7.9	15	47	222.3	220	1.0	18.2	26	30	
G2	131.6	150?	12	1885.7	1850	1.9	7.1	14	49	304.1	300	1.3	8.1	12	33	
NIML	274.6	280?	2	459.0	450	2.0	658.9	850?	22	8126.2	?	?	13.2	?	?	
Br	-	-	-	-	-	-	82.0	90?	9	241.1	240	.5	27.5	27	2	
SY3	-	-	-	-	-	-	192.2	145.†	33	324.7	320+	1.5	678.1	750+	9	
Mean %			17%						34%							19
									Omitting GH							4.7%

1. Values from this study, using standards as unknowns, expressed in parts per million.

2. Values recommended by Abbey (1975) or as otherwise marked: *Leake et al (1969)
+Abbey et al (1975)

3. Difference between this study and recommended value, as a percentage.

? Uncertain value (Abbey, 1975) or unknown value.

Table D.e (Continued)

Accuracy of Trace Element XRF Determinations in ppm: Rb and Sr

Standard	Sr			Rb		
	1	2	3	1	2	3
Br	1342.2	1350	.58	48.4	45	7.6
GA	291.8	300	2.7	170.5	175	2.5
NIMS	61.9	76	18.6	546.9	560	2.3
GH	7.5	10	25	370.8	390	4.9
JG1	183.3	185	0.91	177.1	185	4.3
JB1	437.3	440	0.63	40.8	40	1.9
Mean %			1.2%			3.9%
			for > 100 ppm			

1, 2, 3 = previous legend

experienced by the aplite of the Flora Lake Stock isochron (Fl-27: Rb/Sr = 2.091) although Doering (1968) recommended the XRF method for ratios from 0.2 to 5.0.

Detection Limits:

Detection limits appropriate for the instrumentation and data processing of this study were previously reported by Marchand (1976) as:

Nb	Zr	Y	Sr	Rb
2.0 ppm	1.7 ppm	1.2 ppm	1.2 ppm	1.5 ppm

The detection limit for Ba is estimated at lower than 15 ppm (Murad, 1975), but was not calculated.

APPENDIX D: TABLES

APPENDIX D TABLES:
TRACE ELEMENTS AND RADIOELEMENTS
EXPRESSED IN PARTS PER MILLION.
Rb, Sr, Y, Zr, Nb, Ba AND Ce BY XRF
SPECTROMETRY; Th and U BY IN SITU
PORTABLE GAMMA-RAY SPECTROMETRY,
ASSUMING PARENT-DAUGHTER EQUILIBRIUM,
AND CORRELATION OF DETECTOR STATIONS
WITH HAND SPECIMENS. SAMPLE LOCATIONS
AS FOR APPENDIX C TABLES.

NOTE:
(0.0) = NOT DETECTED
(.0) = NOT DETERMINED

BURDITT LAKE STOCK

SAMPLE	RB	SR	Y	ZR	NB	BA	GE	TH	U
MEIUM GRAINED GRANODIORITE (MUSC.- BI.)									
4223	181.1	637.4	3.2	54.4	1.5	777.7	20.4	.0	.0
G42	76.1	648.8	2.0	51.2	.6	1170.7	16.4	.0	.0
4311	53.3	711.9	.0	92.9	0.0	1328.0	18.5	.0	.0
G43	76.6	791.8	2.0	92.0	3.4	1882.0	19.0	.0	.0
43114	76.6	685.1	.2	75.4	.5	939.0	16.5	.0	.0
431431	50.2	810.3	.0	72.1	0.0	1050.4	16.8	.0	.0
G48	72.8	829.9	.0	82.0	2.8	1087.1	17.7	.0	.0
4345	67.8	794.8	.0	59.9	0.0	1035.8	19.9	.0	.0
4222	70.5	714.2	3.9	56.8	.9	1048.3	18.7	.0	.0
53448	81.2	773.8	3.5	68.2	1.5	1022.9	19.1	.0	.0
43112	72.5	842.6	3.6	62.6	0.0	1833.6	18.4	.0	.0
43213	58.4	791.4	3.0	75.0	2.1	1062.0	21.2	.0	.0
53145	80.2	776.8	3.1	57.1	0.0	996.8	13.1	.0	.0
G53	71.3	897.2	3.1	82.6	.2	1158.0	18.6	1.0	.9
G56	72.0	869.0	3.0	87.2	2.2	1084.9	17.4	2.0	.9
43111	64.6	869.5	3.0	83.0	1.2	1040.3	17.1	.0	.0
4316	58.1	921.1	3.9	95.2	1.3	1201.8	21.4	.0	.0
43119	84.5	789.4	3.0	78.7	3.8	1042.5	16.8	.0	.0
43113	74.1	896.1	3.0	61.7	0.0	1013.7	19.3	.0	.0
43110	57.1	928.6	2.8	62.6	0.0	1071.2	19.4	.0	.0
43310	72.0	875.0	4.0	53.1	0.0	1188.8	19.1	.0	.0
FINE GRAINED GRANODIORITE (MUSC.- BI.)									
43216	79.0	721.0	2.5	59.1	2.0	1113.7	14.9	.0	.0
G51	75.9	828.0	2.6	78.4	1.4	1157.1	16.3	1.7	.8
43116	63.1	833.9	3.4	84.8	4.5	1066.0	19.7	.0	.0
FOLIATED GRANODIORITE (MUSC.- BI.)									
G318	106.4	498.5	2.0	46.9	1.5	672.4	15.8	.0	.0
G18	124.2	532.5	0.0	56.6	.1	2016.4	13.0	.0	.0
4224C	71.6	843.3	3.3	51.3	0.0	1730.2	15.9	.0	.0
G31	80.6	756.4	3.9	75.7	2.4	951.1	19.5	1.3	.7
G27	79.0	841.3	3.7	66.8	2.6	945.8	23.1	2.0	.7
5347	92.0	771.8	2.2	54.0	1.5	926.6	18.6	.0	.0
53430	71.1	896.8	2.2	61.1	0.0	1566.0	19.8	.0	.0
GA-8	66.5	673.7	2.5	76.0	.8	1895.7	18.4	1.9	.8
G87	61.5	961.1	1.8	98.7	1.6	1125.4	23.6	1.6	.5
GAA	76.1	818.3	1.1	74.7	0.0	1065.1	14.0	1.0	.0
43251	72.9	850.4	1.0	76.8	0.0	1855.8	14.0	.0	.0
4411	62.4	873.9	1.3	85.5	1.8	965.3	15.6	.0	.0
4412	61.2	890.6	1.4	86.2	0.0	952.8	16.5	2.8	.8
MASSIVE APLITE PATCHES IN FOLIATED GRANODIORITE									
G78	149.7	117.5	1.7	57.4	5.3	239.4	19.7	2.8	1.3
5344P	140.2	152.9	1.2	46.9	3.5	270.8	9.6	.0	.0
G62A	124.1	195.3	1.2	42.8	4.6	312.6	14.1	.0	.0
GAC	67.6	512.8	3.5	70.8	3.4	1001.5	14.9	.0	.0
NORTH FIN GRANODIORITE (MUSC. - BI.)									
53350	77.8	823.0	3.3	67.4	0.0	928.1	24.5	.0	.0
53310	189.2	769.3	3.3	76.7	2.2	1045.5	29.8	.0	.0
53312	76.7	777.7	.0	.0	.0	943.8	25.6	.0	.0
BI.- NB. GRANODIORITE (MICROCLINE MEGACRYSTS)									
G22	102.8	878.4	4.2	93.3	2.9	1079.1	34.5	3.8	.8
G22	101.8	899.0	4.9	96.7	2.9	1156.7	29.2	3.8	.8
G20	101.4	938.8	4.6	75.3	2.2	1166.4	29.0	3.8	.8
G21	105.4	882.7	3.0	98.8	2.0	1108.8	26.0	3.8	.8
G24	80.6	901.0	3.7	99.7	2.7	1168.8	29.4	3.8	.8
5322	58.6	988.0	3.3	93.9	1.1	1103.9	28.0	3.8	.8
43132	64.1	988.0	3.3	93.9	1.1	1103.9	28.0	3.8	.8
43110	64.1	988.0	3.3	93.9	1.1	1103.9	28.0	3.8	.8
G24	77.2	936.0	3.7	96.0	1.1	1179.6	25.6	3.8	.8
G24	102.1	961.1	3.0	96.5	2.0	1298.8	33.0	3.8	.8
G22	89.0	913.0	3.2	100.4	3.0	1149.1	32.7	3.8	.8
G27A	81.0	925.0	3.0	93.7	3.3	1285.9	27.8	3.8	.8
G27	81.6	905.5	3.4	78.1	4.7	1242.6	27.1	3.8	.8
G27	83.8	926.0	3.3	90.1	4.6	1278.6	30.0	3.8	.8
43412	57.4	807.7	3.0	93.1	1.1	1111.1	27.9	3.8	.8
G44	84.0	901.1	3.0	93.1	1.1	1111.1	27.9	3.8	.8
53322	83.0	941.1	3.0	93.1	1.1	1111.1	27.9	3.8	.8
G21	102.1	913.0	3.2	100.4	3.0	1149.1	32.7	3.8	.8
43414	102.1	913.0	3.2	100.4	3.0	1149.1	32.7	3.8	.8
G21	86.4	933.0	3.5	72.2	0.0	1111.1	28.0	3.8	.8
53624	63.3	991.0	3.9	73.6	0.0	1281.6	31.5	3.8	.8
G26	87.1	932.0	3.6	98.8	1.0	1188.8	27.0	3.8	.8
53320	79.9	968.8	3.8	93.1	1.4	1200.4	27.0	3.8	.8
FELSIC DYKES WITHIN STOCK									
RED SPOTTED APLITE									
G31	146.2	116.5	5.0	70.6	5.0	228.4	13.7	1.6	1.0
4343	140.6	302.8	1.0	82.2	4.3	368.9	9.6	.8	.0
WHITE APLITE									
G30A	144.8	128.3	2.3	51.8	6.4	170.6	9.5	.8	.8
4232BA	114.1	134.8	3.2	51.3	4.8	344.2	9.6	.8	.8
APLITE-PEGMATITE									
4342AP	115.9	386.1	8.8	78.8	4.9	348.8	8.3	.8	.0

FELSIC DYKES CUTTING HOST METAVOLCANICS

APLITE-PEGMATITE

53313 90.1 212.6 2.5 73.9 6.0 267.7 18.2 .0 .0

APLITE-PEGMATITE (ZONEO)

53318R 133.3 107.5 0.0 39.9 4.3 155.3 7.7 .0 .0
53318C 152.4 88.7 4.8 57.1 8.3 146.7 17.1 .0 .0

GRANODIORITE (+ MICROCLINE MEGACRYSTS) DYKE

53412 22.8 907.8 2.9 60.1 .2 871.0 21.7 .0 .0

INTRUSION BRECCIA

53413G 73.4 946.6 5.0 92.6 2.4 1465.5 20.0 .0 .0
53413X 79.9 662.3 16.2 127.9 6.1 1099.4 63.8 .0 .0
53413T 49.1 660.9 16.2 78.4 5.6 752.0 38.2 .0 .0

LENSOID MAFIC ENCLAVES

541 JX 181.2 615.5 14.2 148.7 7.5 1650.5 70.7 .0 .0
54228X 83.2 634.3 14.3 133.2 7.9 687.6 51.3 .0 .0
53322X 140.8 623.9 12.9 136.9 5.0 1056.0 80.0 .0 .0
G 3X 46.0 563.9 23.9 178.9 3.9 361.7 114.4 .0 .0
533 2X 53.9 373.5 15.4 116.2 6.7 851.9 48.5 .0 .0

FELSIC TO INTERMEDIATE METAVOLCANICS

G61T 13.3 295.3 2.8 93.8 2.4 225.1 16.1 .0 .3
5426T 39.9 345.2 3.5 85.3 3.0 463.9 17.0 .0 .0
53412T 34.2 491.3 3.9 96.3 0.0 355.4 17.1 .0 .0
4242T 30.8 663.6 3.2 99.1 1.8 615.1 20.7 .0 .0
53150T 51.8 605.8 2.8 97.7 1.8 739.6 22.7 .0 .0
4341T 36.3 521.3 2.2 96.2 0.0 553.0 24.4 .0 .0
3321T 46.9 410.5 7.4 102.2 1.7 646.0 30.0 .0 .0
G59T 29.8 231.6 5.0 93.8 2.9 400.0 22.3 2.6 .4

D2

SCATTERGOOD LAKE STOCK

SAMPLE RB SR Y ZR NB BA CE TH U

MS. GRANODIORITE (+ MICROCLINE MEGACRYSTS)

ST6-P 106.1 832.1 7.5 114.0 2.2 1319.8 45.4 .0 .0
ST13P 92.4 823.0 8.8 121.2 1.5 1248.3 45.2 .0 .0
ST12P 69.0 843.2 8.9 126.2 3.5 1170.9 49.0 .0 .0
ST8-P 90.6 791.7 9.3 127.4 1.5 1263.4 43.9 .0 .0
ST5-P 87.9 825.1 10.0 125.8 2.6 1269.9 46.0 .0 .0
S109 96.4 804.6 9.6 111.3 2.3 1323.2 54.2 .0 .0
S1 85.9 862.5 9.9 136.0 5.0 1140.6 58.8 .0 .0
S5 100.1 865.1 10.8 126.0 4.2 1231.9 50.3 .0 .0
ST2-P 95.5 841.7 10.9 126.0 2.1 1298.5 54.1 .0 .0
ST3-P 99.4 854.1 6.3 123.1 2.9 1320.1 46.3 .0 .0
S14 100.0 870.3 8.3 116.0 1.3 1226.1 46.0 .0 .0
S5 96.1 908.6 8.3 124.7 1.6 1260.6 49.8 .0 .0
S6 90.7 958.4 10.3 139.6 2.8 1401.9 57.3 .0 .0
S11A 114.2 860.5 10.6 119.4 2.3 1221.2 45.6 .0 .0
ST7-P 92.4 869.0 9.6 133.6 3.3 1216.4 51.1 .0 .0
S7 89.1 881.5 9.4 124.2 1.1 1277.3 55.0 .0 .0
ST4-P 92.2 877.6 9.2 126.1 1.5 1251.4 42.6 .0 .0
S13B 107.2 828.2 6.4 113.3 1.9 1255.0 38.3 .0 .0
ST-1P 92.8 854.7 7.6 124.3 1.0 1205.4 54.9 .0 .0
ST18P 108.4 839.3 11.4 133.6 3.2 1127.9 60.2 .0 .0
S2 82.4 815.5 9.8 134.8 3.5 1155.6 36.1 .0 .0
ST11P 88.4 836.2 10.0 123.9 2.1 1268.9 41.5 .0 .0
S15 94.7 926.5 7.4 115.8 1.6 1462.0 42.1 .0 .0
S12 89.2 894.6 10.5 119.1 3.3 1261.4 48.9 .0 .0
ST9-P 107.8 932.0 11.1 140.8 2.6 1416.8 60.5 .0 .0

LENSOID MAFIC ENCLAVE (SXTM) AND HOST (SXTMG)

SXTM 125.9 463.1 11.3 116.5 5.5 1454.7 51.8 .0 .0
SXTMG 99.6 886.2 9.3 124.0 4.0 1406.3 45.5 .0 .0

INTRUSION BRECCIA - FELDSPATHIZED ENCLAVE

S17 61.2 1276.9 12.7 160.8 4.6 1485.7 77.3 .0 .0

INTRUSION BRECCIA - METAVOLCANIC BLOCK

S16 71.3 795.6 10.6 133.2 2.1 1079.5 68.0 .0 .0

D3

ESOX LAKE GRANITOIDS

SAMPLE	RB	SF	Y	ZR	NB	BA	CE	TM	U
BI GRANODIORITE									
EX25	119.0	779.6	5.4	97.1	3.2	1405.9	34.4	.0	.0
EX20	139.3	819.5	9.4	122.2	6.0	1184.6	55.3	.0	.0
EX21	116.6	834.4	5.6	111.0	.1	1470.6	43.2	.0	.0
EX19	103.1	995.5	3.2	132.7	1.9	1409.9	65.5	.0	.0
EX27	115.1	1123.4	9.3	144.3	2.6	1549.4	79.4	.0	.0
EX26	116.0	1072.1	10.3	134.5	5.8	1564.7	66.1	.0	.0
BI. - HB. MONZODIORITE									
EX10A	144.9	951.5	14.6	175.1	5.5	1156.5	75.0	.0	.0
EX30B	154.3	1073.3	14.0	191.3	5.2	1278.5	91.3	.0	.0
EX29	144.1	1169.3	14.6	194.9	4.1	1319.9	103.9	.0	.0
EX24	153.2	1200.8	19.2	224.7	7.7	1311.9	120.5	.0	.0
EX28	104.1	1197.4	15.9	220.9	7.7	1472.4	105.3	.0	.0
LEUCO QUARTZ MONZODIORITE									
EX2	100.1	1019.4	6.2	91.4	2.3	1600.8	39.3	.0	.0
EX1	102.6	1222.2	7.4	115.6	1.7	1830.9	50.5	.0	.0
EX11	96.2	1356.2	8.4	126.6	.1	1961.6	61.6	.0	.0
PINK FELSITE (QUARTZ-FELDSPAR PORPHYRY)									
EX5	71.7	224.7	5.3	61.5	4.7	1436.5	26.4	.0	.0
EX31	107.7	149.9	8.0	56.5	3.2	1422.4	29.8	.0	.0
GREY FELSITE (QUARTZ-FELDSPAR PORPHYRY)									
EX7	34.4	964.0	4.9	86.1	0.0	1021.8	61.0	.0	.0
EX8	73.3	539.9	4.8	82.0	0.0	1267.7	62.1	.0	.0

D4

FLORA LAKE STOCK

SAMPLE	RB	SF	Y	ZR	NB	BA	CE	TM	U
BIOTITE GRANITE (COPE)									
FLR25	93.7	652.0	3.7	35.1	3.8	1300.7	26.7	.0	.0
FLR15	139.9	340.5	1.0	136.7	6.0	1128.7	21.2	.0	.0
FLOR6	88.2	615.4	3.7	96.7	1.1	1297.6	20.2	.0	.0
FLR17	129.2	620.6	3.4	13.0	.7	1248.6	55.2	.0	.0
FLOR3	151.4	577.5	0.0	195.3	3.7	1358.9	37.0	.0	.0
FLR13	141.9	449.7	3.0	129.0	5.6	1135.1	37.4	.0	.0
FLR28	85.0	618.4	5.1	104.6	3.6	1268.7	29.6	.0	.0
FLOR5	125.1	569.7	8.9	141.9	5.3	1157.3	49.6	.0	.0
HB. - BI. MONZODIORITE (MANTLE)									
FLR21	210.3	775.5	12.2	353.3	12.4	1160.2	66.5	.0	.0
FLOR2	222.2	762.4	17.3	417.7	13.6	1174.9	73.6	.0	.0
FLR24	262.9	674.7	18.1	448.3	17.6	890.2	92.8	.0	.0
FLR22	211.4	778.6	15.0	417.5	12.2	1012.7	88.3	.0	.0
FLOR4	222.7	777.9	16.4	465.9	11.5	1020.4	112.1	.0	.0
FLR14	192.0	802.7	14.5	512.9	9.0	1066.3	84.5	.0	.0
FLR20	164.0	986.5	11.8	197.2	8.4	1351.5	91.4	.0	.0
HB. - BI. MONZODIORITE (RIM)									
FL 11	177.0	1432.1	14.6	223.0	6.1	1404.7	154.6	.0	.0
FL 12	174.0	865.3	14.7	135.5	9.9	1396.5	85.0	.0	.0
FL 1	197.2	734.7	22.2	212.3	10.8	1413.4	113.8	.0	.0
FL 16	121.1	1178.8	23.3	131.8	3.3	1555.7	117.3	.0	.0
FL 26	178.1	1133.9	20.5	130.4	7.2	2121.8	98.8	.0	.0
MONZODIORITE - METAVOLCANIC CONTACT									
FL 9	203.4	1071.6	9.8	211.1	.9	1755.0	63.1	.0	.0
GRANITE DYKE IN MONZONITE									
FLOR10	112.1	526.8	4.1	116.3	6.3	1130.1	38.3	.0	.0
GRANITE DYKE IN MONZODIORITE									
FLOR8	106.9	1053.9	11.9	169.6	5.6	1259.2	56.7	.0	.0
APLITE DYKE IN METAVOLCANICS									
FLR27	153.6	73.0	0.0	31.6	6.1	212.7	12.0	.0	.0
MONZODIORITE ENCLAVE IN GRANITE									
FLP29	88.3	1300.2	17.0	113.8	1.3	1289.8	114.0	.0	.0
MONZODIORITE ENCLAVE IN MONZONITE									
FLR19	181.3	693.6	33.4	276.3	11.8	1083.1	151.7	.0	.0

D5

PYCKMAN LAKE STOCK

SAMPLE	RB	SR	Y	ZR	NB	BA	CE	TH	U
BI.-HB. GRANODIORITE (+MICROCLINE MEGACRYSTS)									
PY65	83.4	990.0	2.6	82.0	.7	1099.1	24.1	.0	.0
RY15	90.6	948.1	4.7	79.5	0.0	1219.0	25.2	2.5	1.3
RY90	98.6	967.1	4.4	98.2	2.2	1163.3	25.5	2.0	1.0
RY14	81.3	1007.8	1.9	85.2	.9	1233.4	27.2	2.4	1.0
RY55	82.1	1028.0	3.7	77.7	0.0	1222.6	28.4	.0	.0
RY32	79.5	946.0	2.8	91.6	1.7	1178.6	30.2	3.1	1.2
RY33	90.9	978.1	10.3	172.7	1.9	1177.7	33.9	2.9	1.1
RY5	67.8	1102.1	7.7	83.8	1.3	1327.1	32.5	2.8	1.3
RY54	76.9	958.7	4.2	85.9	0.0	1263.8	28.3	.0	.0
RY10	84.4	1020.7	4.9	97.8	0.0	1221.1	30.9	2.4	1.4
RY75	86.3	981.5	3.3	79.5	0.0	1273.3	22.6	2.0	.0
RY13	84.4	1014.1	1.8	91.5	0.0	1316.1	34.3	2.3	1.2
RY4	67.5	1110.8	4.8	94.9	2.3	1275.9	29.9	3.1	1.3
RY74	82.5	961.1	3.4	80.7	0.0	1211.9	29.6	.0	.0
PY1	76.9	1102.0	4.7	89.9	1.3	1221.2	35.5	4.1	1.1
RY51	89.3	1038.4	4.2	97.0	.4	1253.2	33.3	.0	.0
RY6	58.9	1307.9	2.3	101.6	0.0	1511.8	33.3	3.1	.9
MYLONITE									
RY 70	63.7	1547.7	9.0	135.4	0.0	1836.2	83.3	.0	.0
BI.- HB. QUARTZ MONZODIORITE									
RY50	87.3	1016.8	5.7	100.6	1.1	1236.2	41.5	.0	.0
RY 76	87.9	1021.6	5.7	108.2	.2	1343.1	37.9	.0	.0
PY 77	90.1	1183.5	5.5	112.5	0.0	1334.4	42.3	.0	.0
RY 73	88.8	1087.0	3.1	113.2	0.0	1357.4	51.1	.0	.0
RY 3	87.4	1316.5	8.7	136.3	2.0	1553.5	63.8	6.2	1.5
RY 72	80.5	1223.2	7.5	119.5	1.1	1617.8	58.6	.0	.0
RY 21	97.1	1069.3	9.1	112.0	1.9	1259.8	55.2	4.4	1.4
RY 7	97.0	1097.5	8.3	101.6	0.0	1431.7	60.7	7.1	1.7
RY61	86.0	1402.5	8.4	118.6	0.0	1661.5	73.6	.0	.0
RY 60	102.9	910.1	6.9	130.3	0.9	1269.8	63.0	.0	.0
RY 23	98.1	1142.1	11.2	146.9	1.3	1622.9	81.8	5.1	2.0
BI.- HB. MONZODIORITE									
RY 4	86.8	1373.5	6.9	238.8	0.0	1718.1	67.4	7.0	1.7
RY 01	82.5	1449.4	6.7	153.7	.5	1666.8	81.1	.0	.0
RY 63	71.9	1359.9	11.4	115.6	0.0	1657.7	80.5	.0	.0
RY 62	78.0	1356.0	8.5	153.5	0.0	1666.7	72.5	.0	.0
RY 35	83.6	791.5	10.9	119.8	1.4	1637.8	61.4	4.3	1.9
PX - HB MONZODIORITE									
RY 37	107.1	1655.2	11.8	174.5	1.9	1648.7	92.8	6.3	1.7
RY 81	78.2	1460.8	10.6	105.9	0.0	1837.5	82.8	.0	.0
RY 80	56.2	1664.1	10.2	121.9	0.0	1793.7	74.6	.0	.0
RY 93	84.4	1688.5	12.2	135.7	0.0	1697.8	95.8	.0	.0
PY 92	67.0	1687.6	14.2	122.3	1.8	1832.7	90.2	.0	.0
PY 82	99.4	1598.6	15.1	205.3	1.7	1662.9	104.7	.0	.0
PY 94	119.6	1863.4	14.2	97.3	3.3	1665.9	115.5	.0	.0
APLITE DYKE IN MAFIC METAVOLCANICS									
RY22	294.5	618.2	0.0	62.7	2.6	1353.8	27.3	4.1	1.5
APLITE - PEGMATITE DYKE FROM DYKE SWARM WITHIN STOCK									
RY91A.	172.2	296.1	0.0	9.9	0.0	433.6	9.6	.0	.0
MAFIC ENCLAVES									
PY 71	93.1	1251.0	7.2	143.9	2.7	1530.5	72.3	.0	.0
RY 60X	97.4	968.5	7.4	95.4	0.0	830.1	62.3	.0	.0
RY61X	41.4	1406.2	12.7	174.2	1.5	438.2	105.9	.0	.0
METAVOLCANICS									
RY84TP	40.0	993.4	1.0	84.7	1.5	1280.8	31.5	.0	.0
RY 84	114.3	1416.7	11.7	269.4	2.1	1515.0	83.5	.0	.0

D6 RAINY LAKE GRANULOID FLUIONS (ALGOMAN OF LAWSON 1913)

SAMPLE	R8	SF	Y	ZP	NB	BA	CE	TH	U
	<u>BEARS PASSAGE STOCK</u>								
	<u>BI.- MUSC. GFANODIOPHYTE</u>								
TR39	100.4	365.4	14.9	72.0	8.8	900.8	26.7	3.7	0
TR3	97.5	401.7	14.9	63.9	5.8	861.7	25.0	3.7	1.9
TR18	82.8	467.1	15.7	63.5	7.2	831.7	28.7	3.5	1.9
TR35	111.8	256.1	19.1	58.8	9.2	848.9	27.7	3.9	1.7
TR4A	195.3	431.9	13.0	59.5	3.8	977.5	29.5	3.6	1.7
TR2	79.2	496.1	14.4	68.2	3.8	919.5	23.4	4.0	1.2

REST ISLAND STOCK

	<u>MUSC.- BI. GFANODIOPHYTE (WITHIN BLUE QUARTZ ZONE)</u>								
REST2	62.1	491.0	16.0	112.0	5.2	827.0	35.5	0.0	0.0
REST1	68.7	472.0	15.6	119.6	4.4	728.3	40.3	0.0	0.0
REST3	62.9	474.1	16.1	131.7	4.4	696.4	61.2	0.0	0.0
	(OUTSIDE BLUE QUARTZ ZONE)								
REST5	55.9	477.5	14.3	99.3	4.3	778.5	38.8	0.0	0.0
REST6	64.7	458.9	14.4	122.0	5.6	738.5	52.6	0.0	0.0
	<u>SYENITIC BORDER</u>								
REST4	65.6	569.2	27.6	148.1	5.6	888.1	71.4	0.0	0.0
	<u>GRANITIC DYKE IN SYENITIC BORDER (AGMATITE)</u>								
REST4D	57.7	456.9	20.6	122.7	4.7	736.2	50.5	0.0	0.0

OTTERTAIL LAKE STOCK

	<u>MUSCOVITE GRANITE</u>								
O13	128.0	438.3	8.8	98.3	6.7	1232.8	23.2	0.0	0.0
O15	142.6	469.3	8.2	93.1	5.0	893.1	25.7	0.0	0.0
	<u>BI. GRANODIOPHYTE (+ MICROCLINE MEGACRYSTS)</u>								
O14	102.3	652.8	9.2	88.9	7.5	1194.6	37.5	0.0	0.0
O15	114.3	751.7	12.5	113.7	3.1	1164.1	44.1	0.0	0.0
O17	127.7	657.3	12.4	150.4	6.0	1401.1	66.5	0.0	0.0
O12	104.5	898.4	14.6	132.6	5.0	1315.3	71.4	0.0	0.0
	<u>BI.- MB. QUARTZ MONZONICRITE</u>								
O11	60.6	1014.3	18.3	109.5	1.3	1244.9	66.5	0.0	0.0

D7

WABIGOON GRANITOID PLUTONS

SAMPLE	RB	SR	Y	ZR	NB	BA	CE	TH	U
<u>FRCGHEAD BAY STOCK</u>									
BI. TONALITE									
FH9	49.9	245.3	12.6	112.7	5.5	475.7	32.2	.0	.0
FH10	46.5	246.0	8.5	114.7	3.8	463.2	25.2	.0	.0
FH1	51.7	249.1	18.0	123.0	7.2	438.0	31.7	.0	.0
FH8	42.7	251.8	9.3	113.2	5.0	459.2	26.7	.0	.0
FH5	37.0	233.6	10.8	123.4	5.0	437.5	28.0	.0	.0
FH7	41.7	241.8	11.4	126.4	5.7	394.9	35.2	.0	.0
FH2	36.6	224.6	12.0	127.7	5.1	418.4	32.1	.0	.0
FH3	41.2	248.5	14.6	128.9	5.4	438.1	30.7	.0	.0
FH5	44.6	254.6	11.2	128.0	2.0	441.1	33.2	.0	.0
91. GRANODIORITE									
FH4	66.3	119.3	18.1	80.3	7.7	477.4	35.6	.0	.0
<u>REGINA BAY STOCK</u>									
TONALITE (SERICITIZED, CARBONATIZED, CHLORITIZED)									
REG1	17.7	534.5	10.3	103.4	3.9	325.9	35.1	.0	.0
REG2	18.6	522.9	9.7	100.8	1.0	308.7	34.2	.0	.0
REG5	16.5	554.8	7.6	99.3	1.3	330.5	37.8	.0	.0
REG6-2	23.3	422.2	7.7	44.0	.7	392.0	38.1	.0	.0
REG3	23.6	530.8	7.8	36.4	0.8	349.1	34.4	.0	.0
REG6	19.0	726.1	8.0	31.2	0.0	313.6	40.5	.0	.0
REG4-2	23.8	407.2	6.8	40.4	.2	373.2	34.6	.0	.0
SHEAR ZONE									
REG4S	26.5	491.5	8.0	95.5	1.2	376.6	36.2	.0	.0
<u>STORMY LAKE STOCK</u>									
BIOTITE GRANODIORITE									
ST4	73.6	746.8	7.7	134.2	0.8	1139.6	49.6	.0	.0
ST7	73.4	825.2	6.2	150.7	3.8	1194.7	59.9	.0	.0
ST2	79.8	739.1	9.0	138.7	1.5	1114.6	57.2	.0	.0
ST3	84.4	781.4	9.0	134.0	1.5	1027.0	57.1	.0	.0
ST1	76.4	775.6	7.6	140.7	1.1	1072.5	64.9	.0	.0
<u>TAYLOR LAKE STOCK (SAMPLES AFTER PICHETTE 1976)</u>									
91.- HB. GRANODIORITE									
T54	173.1	739.0	8.2	156.5	7.0	1197.0	65.1	.0	.0
T12	133.2	959.7	9.2	152.9	5.2	1408.2	78.7	.0	.0
T13	126.8	979.7	9.3	160.1	2.0	1430.0	69.8	.0	.0
T14	140.9	948.9	7.0	148.4	4.0	1430.9	69.2	.0	.0
T15	102.7	1066.7	9.0	169.0	3.2	1627.1	67.6	.0	.0
T37	242.3	237.7	10.5	165.8	6.9	1870.1	85.9	.0	.0
91.- HB.-PX MONZONITE TO QUARTZ MONZONITE									
T65	106.4	1044.7	9.0	166.3	1.9	1378.6	76.3	.0	.0
T16	129.8	821.1	10.2	177.0	3.3	1297.0	65.1	.0	.0
T17	122.6	1304.8	10.2	227.4	1.0	1673.8	100.0	.0	.0
T37	83.3	1231.5	10.2	100.9	13.0	1583.8	131.0	.0	.0
T42	67.2	2831.4	10.2	139.3	3.0	2287.0	173.2	.0	.0
T41	135.5	1192.2	23.5	182.4	1.8	1874.6	87.4	.0	.0
91.- BI. GRANODIORITE (FINE GRAINED)									
T28	73.9	477.0	2.3	106.0	2.3	734.7	25.6	.0	.0
T49	98.4	415.8	5.1	113.7	7.0	587.2	29.4	.0	.0
91.- PX. MONZONIORITE									
T30	19.4	3470.3	19.9	60.5	3.8	2769.6	120.5	.0	.0
91.- PX. MONZONITE (MEDIUM GRAINED)									
T69	99.5	1848.1	17.3	119.9	10.1	2114.2	126.4	.0	.0
91 - PX - HB MONZONITE (COURSE GRAINED)									
T70	78.7	1559.4	21.6	169.3	2.3	1716.4	116.3	.0	.0
MUSC.- BI. LEUCO MICROGRANITE									
T60	299.8	402.1	.6	162.7	6.6	780.8	52.5	.0	.0
APLITE									
T47	70.7	514.9	5.0	115.7	3.9	705.2	25.8	.0	.0
MAFIC ENCLAVE									
T24X	299.9	555.2	12.4	144.2	5.2	1584.4	73.0	.0	.0
MAFIC METAVOLCANIC									
T49	18.8	353.7	25.3	44.3	.9	235.6	14.4	.0	.0

APPENDIX E: TABLES

**APPENDIX E TABLES:
ELEMENT RATIOS BASED ON PPM
AND APPENDIX C AND D TABLES.
NOTE: (0.000) = NOT DETERMINED.
SAMPLE LOCATIONS AS FOR APPENDIX
C TABLES.**

ELEMENT RATIOS BASED ON PPM

SAMPLE	NA/K	K/RP	SR/9A	PB/SR	CA/SR	CA/Y	TI/7R	TH/U
<u>BUFOITT LAKE STOCK</u>								
MEDIUM GRAINED GRANODIORITE (MISC - BI)								
44221	1.780	276.982	.820	.159	14.240	28.165	8.416	0.000
442	1.169	384.653	.551	.117	13.769	44.669	8.196	0.000
4311	1.534	415.875	.472	.074	15.441	107.205	8.352	0.000
441	1.326	274.888	.793	.096	14.384	40.840	7.501	0.000
43154	1.861	281.979	.730	.111	12.623	432.374	7.951	0.000
43431	2.083	166.843	.771	.043	14.718	112.617	4.115	0.000
G4	2.078	282.435	.761	.043	15.502	11.377	4.047	0.000
4345	1.784	277.104	.767	.045	15.443	29.171	11.002	0.000
44222	1.611	147.719	.641	.049	14.411	76.149	11.665	0.000
51440	1.854	241.270	.756	.105	15.907	15.122	10.467	0.000
43112	2.024	281.519	.792	.046	15.211	15.119	10.534	0.000
43213	1.997	234.459	.747	.074	13.775	52.071	8.445	0.000
4345	1.751	298.651	.740	.104	15.647	16.118	11.509	0.000
G53	1.901	293.571	.783	.049	16.379	37.777	9.415	2.084
G56	1.977	288.729	.777	.046	15.207	42.644	5.250	2.127
43411	1.977	318.729	.764	.074	14.954	18.257	7.945	0.000
4315	2.178	174.334	.764	.041	11.817	141.152	8.444	0.000
43119	1.854	254.467	.757	.117	14.757	18.837	7.179	0.000
43111	1.946	285.467	.764	.041	14.815	47.892	11.660	0.000
43410	2.229	339.716	.755	.062	14.114	56.852	13.487	0.000
43310	1.847	305.671	.741	.082	15.602	34.127	12.351	0.000
FINE GRAINED GRANODIORITE (MISC - BI)								
43216	1.817	266.217	.701	.141	15.644	48.845	10.144	0.000
G51	2.067	263.904	.715	.097	14.947	47.240	7.647	2.156
43116	2.080	312.096	.782	.075	15.170	37.206	7.777	0.000
FOLIATED GRANODIORITE (MISC - BI)								
G318	1.622	238.855	.741	.213	14.201	45.333	6.322	0.000
G30B	1.708	236.174	.731	.175	14.741	40.000	10.592	0.000
4424C	2.357	252.520	.638	.045	14.654	95.110	8.340	0.000
G81	1.831	276.714	.745	.107	13.224	75.656	7.919	1.881
G62	2.277	239.751	.913	.044	14.697	13.417	3.481	0.000
4347	1.837	239.818	.873	.140	15.157	46.894	8.872	0.000
43439	1.961	287.513	.873	.090	13.310	56.252	11.773	0.000
G1-B	1.834	332.532	.854	.044	14.639	19.465	8.479	0.000
G67	2.584	291.377	.854	.041	12.195	65.117	0.786	2.922
44A	2.092	262.652	.854	.041	14.111	10.000	0.000	0.000
43251	1.898	107.714	.808	.085	14.872	78.864	8.547	1.884
4411	1.888	339.604	.808	.071	14.124	440.732	5.115	0.000
4612	2.055	344.747	.935	.069	15.247	96.995	9.041	2.545
MASSIVE APLITE PATCHES IN FOLIATED GRANODIORITE								
G78	1.165	204.409	.492	1.274	44.290	10.690	3.133	2.239
4314P	1.467	184.167	.545	.517	28.383	13.847	3.415	0.000
G62A	1.276	245.971	.614	.737	23.822	24.826	4.202	0.000
G4C	1.666	177.486	.512	.132	15.310	22.462	7.621	0.000
(NORTH FIM GRANODIORITE (MISC - BI)								
51359	1.699	305.571	.887	.095	15.110	37.684	3.784	0.000
51310	1.111	272.443	.725	.133	15.814	31.597	10.161	0.000
51112?	1.617	222.000	.824	.093	14.383	0.000	0.000	0.000
BI - MB GRANODIORITE (MICROCLINE MEGACRYSTS)								
G22	1.557	233.769	.807	.118	15.190	31.481	9.678	4.844
G28	1.216	247.107	.751	.113	15.188	47.872	11.159	2.794
G70	1.474	244.782	.793	.139	16.205	32.743	11.146	2.294
G15	1.710	218.899	.802	.119	16.437	37.291	4.102	2.442
G4	1.970	255.124	.780	.090	16.657	27.794	9.020	2.442
512P	1.774	226.626	.815	.051	15.903	28.723	10.154	0.000
533P	1.714	249.731	.757	.084	15.605	34.544	12.441	0.000
44210	1.686	310.711	.766	.074	15.424	33.235	10.888	0.000
G24	1.721	308.826	.794	.083	17.482	21.052	9.785	5.063
G4	1.613	241.861	.748	.136	19.292	41.149	9.319	4.167
5424	1.727	251.181	.795	.094	17.604	38.925	10.151	0.000
G27	1.497	273.762	.746	.047	16.778	19.611	11.975	2.294
G27A	1.765	295.305	.720	.084	16.757	20.407	9.798	0.000
G7	1.519	307.805	.729	.090	16.126	11.917	7.287	1.931
541-2	2.067	345.427	.807	.054	17.516	19.350	10.830	0.000
G44	1.493	263.813	.744	.095	17.129	41.250	11.591	0.000
53327	1.493	328.059	.698	.089	15.830	28.826	12.621	0.000
53414	1.507	253.111	.700	.119	16.916	25.560	11.663	0.000
G9	1.576	267.904	.743	.181	16.532	23.674	10.963	5.260
G70*2	1.718	244.547	.740	.107	16.380	33.988	11.545	0.000
G21	1.571	243.777	.782	.093	15.800	24.538	10.442	4.858
53424	1.794	367.656	.792	.054	17.160	43.615	12.235	0.000
G26	1.633	278.252	.793	.091	16.468	29.878	9.784	2.549
53320	1.644	311.434	.750	.081	15.476	25.631	10.947	4.915
FELSIC DYKES WITHIN STOCK								
RED SPOTTED APLITE								
G31	1.164	282.528	.510	1.255	44.785	10.435	2.547	1.568
4343	1.416	181.529	.819	.492	21.382	64.323	2.188	0.000
WHITE APLITE								
G30A	1.334	191.841	.785	1.283	19.800	20.820	3.526	0.000
42728A	1.838	288.324	.789	.851	49.526	16.974	9.577	0.000
APLITE-PEGMATITE								
4342AP	1.425	225.066	.980	.379	20.310	0.000	2.548	0.000

SAMPLE	NA/K	K/RB	SR/BA	RB/SR	CA/SR	CA/Y	TI/ZR	TM/U
FELSIC DYKES CUTTING METAVOLCANICS								
APLITE-PEGMATITE								
5331J	1.222	320.640	.794	.424	28.914	24.586	2.634	0.000
APLITE-PEGMATITE (ZONED)								
5311BR	.856	271.507	.692	1.240	50.527	0.080	4.582	0.000
5311BC	.768	263.354	.604	1.719	47.543	8.785	1.150	0.000
GRANODIORITE DYKE WITH MEGACRYSTS								
5341Z	3.621	528.944	1.042	.025	14.329	44.454	6.983	0.000
INTRUSION BRECCIA								
5341JG	1.816	307.422	.646	.071	15.931	30.160	9.064	0.000
5341IX	1.569	306.955	.607	.121	69.063	28.235	28.724	0.000
5341IT	2.189	344.832	.879	.074	74.888	38.220	46.939	0.000
LENSOID MAFIC ENCLAVES								
541 IX	.609	250.655	.373	.295	46.101	19.981	17.336	0.000
54220X	1.988	240.914	.923	.131	67.602	29.987	27.455	0.000
53122X	1.184	212.890	.591	.276	60.651	33.685	21.896	0.000
541X	1.991	217.810	1.969	.082	96.126	22.846	22.117	0.000
533 2X	.975	442.747	.438	.144	145.046	15.178	35.599	0.000
FELSIC TO INTERMEDIATE METAVOLCANICS								
661T	6.485	412.431	1.312	.045	31.222	32.927	18.760	3.196
5426T	3.925	271.508	.455	.116	45.135	41.001	21.787	0.000
53412T	3.271	364.456	1.275	.070	31.022	41.599	18.053	0.000
4242T	2.961	440.384	1.079	.046	28.758	59.633	10.148	0.000
53150T	1.689	421.247	.819	.085	21.700	46.966	17.181	0.000
4341T	2.823	466.499	.943	.070	19.194	43.165	18.595	0.000
3321T	1.794	417.521	.636	.114	37.803	20.862	21.744	0.000
669T	1.967	448.224	.579	.129	151.542	70.184	17.896	6.941

SAMPLE	NA/K	K/RB	SR/BA	RB/SR	CA/SR	CA/Y	TI/ZR	TM/U
E2								
SCATTERGOOD LAKE STOCK								
HR GRANODIORITE (+ - MICROCLINE MEGACRYSTS)								
ST6-P	1.209	279.325	.633	.128	21.645	24.814	13.147	0.000
ST13P	1.359	295.719	.559	.112	24.228	24.925	15.334	0.000
ST12P	1.415	279.102	.720	.176	24.667	24.469	13.301	0.000
ST8-P	1.251	317.871	.627	.114	24.555	20.983	13.176	0.000
ST5-P	1.384	299.871	.650	.107	24.339	20.813	13.343	0.000
ST10B	1.416	283.865	.484	.107	22.201	20.920	15.914	0.000
S1	1.458	308.287	.704	.177	24.225	19.016	12.783	0.000
S6	1.488	250.289	.702	.116	22.637	19.132	13.794	0.000
ST2-P	1.286	277.545	.648	.117	34.115	18.622	15.225	0.000
ST3-P	1.301	277.539	.647	.116	22.844	28.693	15.097	0.000
S14	1.442	263.318	.710	.115	23.835	28.693	15.097	0.000
S5	1.479	263.326	.721	.106	22.419	23.127	13.954	0.000
S4	1.538	294.326	.712	.106	22.419	23.147	14.823	0.000
ST11A	1.398	237.393	.705	.133	19.614	19.812	12.883	0.000
ST7-P	1.424	275.846	.731	.184	24.336	19.755	14.561	0.000
ST4-P	1.443	295.895	.690	.181	23.877	22.111	11.096	0.000
ST13B	1.374	276.425	.701	.181	22.376	20.985	11.994	0.000
ST10P	1.467	272.613	.709	.189	25.652	24.471	13.747	0.000
S2	1.499	310.354	.706	.121	22.771	31.603	14.286	0.000
ST11P	1.369	300.805	.559	.186	23.761	19.869	13.545	0.000
S15	1.354	293.920	.634	.107	22.524	28.202	13.974	0.000
S12	1.404	298.371	.709	.180	23.568	20.080	15.229	0.000
ST9-P	1.201	282.637	.658	.115	24.999	28.990	14.982	0.000
LENSOID MAFIC ENCLAVE (SXTM) AND HOST (SXTMG)								
SXTM	.782	269.592	.318	.272	91.680	37.569	30.361	0.000
SXTMG	1.376	271.139	.630	.182	22.419	21.354	15.471	0.000
INTRUSION BRECCIA - FELDSPATHIZED ENCLAVE								
S17	1.871	413.810	.859	.048	21.940	22.060	19.387	0.000
INTRUSION BRECCIA - METAVOLCANIC BLOCK								
S16	1.558	295.996	.737	.090	28.750	15.575	24.754	0.000

SAMPLE	NA/K	K/RB	SR/BA	RB/SR	CA/SR	CA/Y	TI/ZR	TH/U
E3								
ESOX LAKE GRANITIOIS								
BI GRANODIORITE								
EX25	1.014	310.349	.581	.153	9.717	14.829	8.644	0.000
EX20	1.159	224.459	.692	.170	15.349	13.382	9.321	0.000
EX21	1.283	250.664	.713	.140	18.873	26.929	10.882	0.000
EX19	1.164	392.231	.706	.184	14.143	17.170	9.939	0.000
EX27	1.173	278.652	.725	.183	14.859	16.984	18.386	0.000
EX26	1.148	257.609	.664	.188	35.191	16.637	12.926	0.000
BI - MB MONZODIORITE								
EX10A	.982	252.278	.923	.152	18.103	11.797	8.217	0.000
EX10B	1.029	230.205	.839	.144	18.712	14.345	10.020	0.000
EX29	1.063	246.302	.866	.123	17.989	14.343	10.766	0.000
EX24	.909	256.394	.915	.128	15.158	9.418	9.338	0.000
EX28	1.088	368.855	.773	.092	19.738	14.114	10.313	0.000
LEUCO - QUARTZ MONZODIORITE								
EX2	1.348	299.776	.656	.095	11.633	18.674	9.183	0.000
EX1	1.424	299.306	.700	.088	7.913	13.715	7.268	0.000
EX11	1.251	348.267	.691	.071	7.641	12.337	8.524	0.000
PINK FELSITE (QUARTZ-FELDSPAR PORPHYRY)								
EX5	.613	567.176	.156	.319	49.933	21.171	9.748	0.000
EX31	.210	596.025	.182	.719	148.317	27.784	9.550	0.000
GREY FELSITE (QUARTZ-FELDSPAR PORPHYRY)								
EX7	1.774	554.962	.885	.838	28.382	52.363	21.585	0.000
EX8	.670	575.952	.426	.136	56.526	63.579	22.664	0.000

SAMPLE	NA/K	K/RB	SR/BA	RB/SR	CA/SR	CA/Y	TI/ZR	TH/U
E4								
FLORA LAKE STCK								
BIOTITE GRANITE (CORE)								
FLR25	1.430	281.581	.501	.139	13.702	24.145	6.934	0.000
FLR15	.879	269.702	.838	.353	15.209	30.469	5.057	0.000
FLR26	1.338	317.939	.474	.143	15.338	25.497	6.200	0.000
FLR17	1.104	259.500	.442	.202	12.453	21.640	6.263	0.000
FLOP1	1.020	226.380	.425	.283	12.994	8.000	6.263	0.000
FLR13	.499	267.790	.396	.316	15.735	23.585	5.124	0.000
FLR24	1.258	348.447	.486	.138	15.422	18.638	4.647	0.000
FLOR5	1.050	248.002	.492	.320	15.934	10.678	6.304	0.000
MB - BI MONZONITE (MANTLE)								
FLOR21	.990	195.352	.668	.271	21.472	12.616	6.174	0.000
FLOR2	.912	193.906	.449	.292	21.468	9.195	4.880	0.000
FLR24	.998	171.238	.758	.390	23.514	8.766	3.875	0.000
FLR22	.924	209.326	.769	.272	21.622	10.911	4.451	0.000
FLOP4	.932	206.847	.762	.286	21.958	10.352	4.114	0.000
FLR14	.978	238.876	.753	.239	23.240	12.604	3.712	0.000
FLR20	.989	232.859	.730	.166	21.590	16.049	13.680	0.000
MB - BI MONZODIORITE (RIM)								
FL 11	1.162	221.123	1.017	.124	21.459	21.049	11.022	0.000
FL 12	.943	241.713	.620	.203	33.951	19.982	30.970	0.000
FL 1	.991	282.218	.520	.268	51.560	17.063	27.674	0.000
FL 16	1.202	252.859	.739	.183	41.836	21.185	47.594	0.000
FL 26	1.052	200.812	.534	.157	39.269	21.720	45.974	0.000
MONZODIORITE - METAVOLCANIC CONTACT								
FL 9	1.062	202.754	.611	.190	23.810	25.160	9.940	0.000
GRANITE DYKE IN MONZONITE								
FLOR18	1.193	275.875	.466	.213	14.924	19.175	5.670	0.000
GRANITE DYKE IN MONZODIORITE								
FLOP8	1.445	261.162	.043	1.984	334.400	15.135	8.130	0.000
APLITE DYKE IN METAVOLCANICS								
FLR27	1.019	206.191	.343	2.183	57.744	0.000	2.939	0.000
MONZODIORITE ENCLAVE IN GRANITE								
FLR29	1.382	328.324	1.089	.058	34.576	26.444	38.457	0.000
MONZODIORITE ENCLAVE IN MONZONITE								
FLR19	.800	284.958	.640	.262	59.253	12.304	24.952	0.000

SAMPLE	NA/K	K/RB	SR/BA	RB/SR	CA/SR	CA/Y	TI/7R	TH/U
E5								
RYCKMAN LAKE STOCK								
BI - HB GRANODIORITE (MICROCLINE MEGACRYSTS)								
RYA5	1.057	274.467	.901	.094	16.098	61.299	10.966	0.000
RY15	1.731	269.799	.778	.096	16.207	219.515	12.050	1.866
RY90	1.454	257.105	.780	.109	13.516	38.171	12.320	0.000
RY14	2.017	271.337	.817	.091	15.239	46.140	11.259	2.430
RY55	1.976	282.032	.841	.090	15.165	42.689	11.573	0.000
RY32	1.818	294.962	.803	.094	16.998	57.431	11.126	2.524
RY11	1.596	246.801	.831	.093	17.464	16.584	6.592	2.599
RY5	1.652	354.419	.830	.067	15.951	22.833	12.152	2.091
RY54	1.458	328.343	.759	.080	17.118	40.670	13.958	0.000
RY10	1.580	294.255	.836	.093	17.365	36.173	13.656	1.732
RY75	1.438	316.705	.771	.098	17.622	52.411	12.865	0.000
RY13	1.558	295.164	.771	.083	17.618	94.039	12.449	1.905
RYA	1.646	364.613	.871	.051	16.157	38.215	12.003	2.456
RY74	1.429	327.481	.791	.086	18.071	51.040	14.115	0.000
RY1	1.600	312.111	.907	.070	17.901	41.970	14.004	3.560
RY51	1.420	290.689	.909	.096	14.584	45.945	13.597	0.000
RY6	1.717	397.215	.865	.045	18.088	102.855	15.342	3.549
MYLONITE								
RY 70	1.644	415.075	.816	.041	24.936	42.882	15.497	0.000
BI - HB QUARTZ MONZODIORITE								
RY50	1.244	318.027	.823	.096	23.056	41.127	14.302	0.000
RY 76	1.581	312.401	.761	.091	22.319	39.938	17.176	0.000
RY 77	1.563	290.823	.987	.076	22.107	47.560	15.987	0.000
RY 73	1.439	305.541	.801	.092	26.300	97.219	19.595	0.000
RY 3	1.474	328.100	.848	.066	24.970	37.789	16.714	4.020
RY 72	1.482	335.916	.756	.066	25.118	42.596	14.047	0.000
RY 21	1.347	277.871	.802	.096	36.374	40.369	17.129	3.167
RY 7	1.294	281.209	.767	.088	34.359	42.638	19.582	4.241
RY61	1.257	331.677	.844	.061	25.833	42.797	19.714	0.000
RY 60	1.254	269.413	.717	.113	40.680	53.654	15.183	0.000
RY 23	1.251	292.791	.784	.096	35.669	36.373	13.875	2.507
BI - HB MONZODIORITE								
RY 4	1.535	337.064	.799	.063	24.821	49.498	8.614	4.263
RY 91	1.609	338.325	.870	.057	22.319	48.322	15.992	0.000
RY 63	1.608	346.644	.820	.053	29.693	35.422	18.151	0.000
RY 62	1.676	304.013	.814	.058	31.518	50.291	14.841	0.000
RY 35	1.250	328.153	.483	.106	52.014	41.167	19.016	2.265
DX - HB MONZODIORITE								
RY 37	1.394	310.713	1.009	.065	21.633	30.344	12.024	3.653
RY 81	1.168	427.781	.822	.054	23.924	32.971	26.607	0.000
RY 80	1.759	426.173	.928	.034	25.799	43.723	20.655	0.000
RY 93	1.376	357.945	.995	.050	27.603	31.283	22.089	0.000
RY 92	1.544	364.301	.921	.040	29.010	34.477	21.078	0.000
RY 82	1.089	347.789	.961	.052	29.239	30.955	13.141	0.000
RY 94	1.080	278.979	1.105	.064	24.536	37.446	16.968	0.000
APLITE IN MAFIC METAVOLCANICS								
RY22	.861	125.280	.457	.476	13.295	0.000	5.693	2.789
APLITE-PEGMATITE DYKE FROM DYKE SWAMP WITHIN STOCK								
RY91A	.599	271.005	.683	.582	-9.173	0.000	10.278	0.000
MAFIC ENCLAVES								
RY 71	1.517	292.746	.817	.074	26.109	45.364	13.331	0.000
RY 60X	1.827	215.288	1.094	.107	43.191	53.023	21.366	0.000
RY61X	5.275	163.243	1.224	.029	34.120	42.207	20.305	0.000
METAVOLCANICS								
RY84TP	5.442	167.157	.776	.040	20.072	199.401	14.156	0.000
RY 84	1.123	344.359	.935	.081	23.862	28.893	10.879	0.000

SAMPLE NA/K K/RB SR/BA RB/SR CA/SR CA/Y TI/ZR TH/Y

E6 RAINY LAKE GRANITOID PLUTONS (ALGOMAN OF LAWSON 1913)

BEARS PASSAGE STOCK

BI - MUSC GRANODIORITE	
TR4B	1.193 279.340 .406 .275 21.127 5.190 6.561 0.000
TR3	1.334 297.289 .409 .243 21.173 5.708 6.598 1.954
TR1B	1.312 351.569 .562 .177 19.737 5.872 17.329 2.039
TR5	1.091 300.747 .302 .437 27.903 3.742 9.161 2.073
TR4A	1.214 310.985 .442 .221 19.524 6.487 9.061 2.098
TR2	1.314 345.221 .540 .160 19.5291 6.750 9.559 3.267

REST ISLAND STOCK

MUSC - PT GRANODIORITE (WITHIN BLUE QUARTZ ZONE OF HARRIS 1974)	
REST2	1.574 355.049 .594 .127 38.427 11.793 15.058 0.000
REST1	1.327 351.570 .648 .146 41.792 12.645 16.060 0.000
REST3	1.482 313.565 .681 .133 42.530 13.406 19.574 0.000
(OUTSIDE BLUE QUARTZ ZONE OF HARRIS 1974)	
REST5	1.834 352.315 .613 .117 35.470 11.845 14.489 0.000
REST6	1.455 321.895 .621 .141 45.209 15.634 17.693 0.000
SYENITIC BORDER	
REST4	.949 304.723 .641 .115 92.291 19.033 30.360 0.000
GRANITIC DYKE IN SYENITIC BORDER (AGMATITE)	
REST40	1.294 406.604 .621 .126 49.592 10.998 20.521 0.000

OTTERTAIL LAKE STOCK

MUSCOVITE GRANITE	
OT3	.910 274.216 .358 .232 16.287 9.122 9.119 0.000
OT5	.867 256.986 .458 .345 21.619 10.808 9.093 0.000
BI GRANODIORITE (MICROCLINE MEGACRYSTS)	
OT4	1.196 286.590 .546 .157 20.364 14.449 12.138 0.000
OT6	1.158 269.396 .646 .152 18.827 11.321 13.102 0.000
OT7	.878 280.260 .469 .192 18.376 9.741 14.745 0.000
OT2	.953 324.667 .682 .116 21.001 12.923 18.537 0.000
BI - HB QUARTZ MONZONIORITE	
OT1	1.344 349.820 .815 .050 40.797 22.613 41.062 0.000

SAMPLE	NAME	K/RD	W/OA	R/OA	CA/P	CA/Y	TE/2R	TH/1
E7	<u>MARICOPA GRANITOID SOLUTION</u>							
	<u>FOOTHEAD BAY STOCK</u>							
	BI TONALITE							
F49	1.474	174.777	.515	.203	97.630	17.641	16.490	0.000
F410	2.171	207.519	.579	.190	45.154	34.532	17.771	0.000
F41	1.464	174.251	.567	.207	93.234	15.645	13.007	0.000
F48	1.443	174.987	.548	.183	90.531	14.615	10.065	0.000
F46	1.017	109.197	.734	.154	104.750	27.795	22.144	0.000
F47	1.997	146.656	.601	.123	101.335	21.947	20.463	0.000
F42	1.770	137.374	.587	.141	107.849	20.140	21.942	0.000
F43	1.975	174.544	.601	.153	97.117	17.231	24.793	0.000
F45	1.708	190.657	.577	.175	97.357	21.771	21.177	0.000
	BI GRANODIORITE							
F44	1.130	177.758	.242	.575	97.377	11.180	11.945	0.000
	<u>REGINA BAY STOCK</u>							
	TONALITE (SERICITIZED, CARBONATIZED, CHLORITIZED)							
0501	4.677	341.426	1.440	.033	41.243	11.788	25.511	0.000
0502	4.141	371.247	1.791	.014	40.970	14.118	27.158	0.000
0505	4.344	308.917	1.473	.030	47.065	11.649	29.533	0.000
0506-2	2.056	483.019	1.501	.034	50.182	10.466	12.473	0.000
0507	3.121	394.411	1.521	.044	44.982	13.523	11.226	0.000
0508	1.157	443.687	1.245	.025	44.373	14.413	11.747	0.000
0509-2	2.920	472.824	0.980	.034	0.007	45.539	15.537	0.000
	SHEAR ZONE							
0545	2.329	419.740	1.395	.054	45.205	42.152	12.643	0.000
	<u>STORMY LAKE STOCK</u>							
	BI GRANODIORITE							
ST4	1.704	108.864	.745	.039	27.255	22.555	19.189	0.000
ST7	1.611	126.069	.674	.031	27.254	10.202	15.501	0.000
ST2	1.441	107.453	.661	.044	27.884	19.615	16.457	0.000
ST5	1.433	104.067	.641	.076	32.410	10.524	16.553	0.000
ST1	1.495	100.425	.771	.039	24.974	25.415	17.996	0.000
	<u>TAYLOR LAKE STOCK (SAMPLES AFTER FICHETTE 1975)</u>							
	BI - NO GRANODIORITE							
T54	1.717	170.353	.617	.234	19.729	21.516	9.194	0.000
T19	1.117	274.076	.481	.139	14.467	19.246	11.763	0.000
T13	1.144	240.545	.524	.123	10.777	23.826	11.953	0.000
T15	1.138	226.565	.544	.144	10.959	27.057	12.927	0.000
T56	1.248	251.034	.612	.035	18.434	20.142	11.706	0.000
T57	.944	160.473	.777	.269	21.170	17.017	11.468	0.000
	BI - HR - PY MONZONITE (PT) QUARTZ MONZONITE							
T64	1.317	267.891	.772	.130	14.330	22.334	11.490	0.000
T16	1.103	226.443	.634	.121	22.714	34.293	15.191	0.000
T77	1.197	223.909	.741	.137	13.643	11.555	14.763	0.000
T17	1.401	353.509	.819	.054	25.710	20.427	10.553	0.000
T42	1.257	472.566	.938	.033	24.826	23.613	25.422	0.000
T41	.797	300.403	.616	.114	35.939	19.140	26.965	0.000
	HR - BI GRANODIORITE (FINE GRAINED)							
T24	1.739	107.011	.663	.152	25.413	45.945	12.180	0.000
T40	1.467	244.624	.704	.234	30.750	25.045	13.010	0.000
	HR - PY MONZONITE							
T30	2.441	644.313	1.753	.096	17.114	29.045	52.427	0.000
	HR - PY MONZONITE (MEDIUM GRAINED)							
T69	1.274	377.508	.874	.054	14.002	15.112	22.501	0.000
	BI - PY - HR MONZONITE (COARSE GRAINED)							
T70	1.455	398.299	.909	.051	21.908	15.916	19.839	0.000
	MUSC - BI LEUCO MICROGRANITE							
T60	.844	140.834	.515	.744	7.110	47.647	5.159	0.000
	TAPLITE							
T47	1.967	300.469	.733	.137	27.422	24.445	12.954	0.000
	MAFIC ENCLAVE							
T24X	.466	181.183	.350	.534	62.314	29.127	18.708	0.000
	MAFIC VOLCANIC							
T49	2.795	431.124	1.501	.051	203.450	24.447	173.219	0.000

APPENDIX F

MESONORM CALCULATIONS:

Introduction

Modal analyses were not performed on all rocks analysed in this study, therefore to provide an approximation of mineral modes the author carried out normative calculations from major element analyses, based on the method of Hutchison and Jeacocké (1971).

For normative minerals based on the CIPW classification, a large discrepancy between norms and modes occurs with granitoids due to modal micas and hornblende being unaccounted for. The error introduced is a function of the modal percentages of non-felsic K:Na:Ca minerals (Parslow, 1969). For a granite with 10% biotite, the CIPW norm gives an Or value 5% too high.

Parslow (1969) suggested a modified CIPW norm to account for biotite and muscovite. His method requires the determination of modal primary and secondary muscovite which defeats the purpose of the present application.

The Barth Mesonorm as developed by Barth (1959, 1962) and as modified by Hutchison and Jeacocke (1971) provides normative minerals more appropriate to granitoids. Granitoids generally display mineral assemblages compatible with amphibolite facies metamorphism assigned by Barth to the "mesozone". Furthermore, Barth mesonorms are calculated from cation percentages which are more compatible with the volume units of modal minerals than are the weight percentage units of the CIPW norm.

The following mesonorm tables are considered appropriate for plotting petrogenetic phase diagrams (i.e., Qtz-Ab-Or-An) after these normative minerals are recalculated to weight proportions.

APPENDIX F: TABLES

APPENDIX F TABLES:
 BARTH MESONORMS IN VOLUME % BY
 CALCULATION METHOD OF HUTCHISON
 AND JEACOCKE (1971). ONLY MAJOR
 AND MINOR ELEMENTS CONSIDERED
 (APPENDIX C). FeO/Fe_2O_3 RATIO ASSUMED
 AS 1:1. NORMATIVE MINERALS CALCULATED
 BY HUTCHISON AND JEACOCKE (1971) BUT
 NOT SHOWN DID NOT APPEAR.
 NORMATIVE MINERALS AS FOLLOWS:

MINERAL	ABBREVIATION
QUARTZ	QTZ
ORTHOCLASE	OR
ALBITE	AB
ANORTHITE	AN
CORUNDUM	COR
NEPHELINE	NE
ACTINOLITE	ACT
EDENITE	ED
RIEBECKITE	RI
BIOTITE	BI
HYPERSTHENE	HY
WOLLASTONITE	WO
HEMATITE	HE
MAGNETITE	MT
TITANITE	TN
APATITE	AP

F1

BURDITT LAKE STOCK

SAMPLE	QTZ	OR	AB	AN	COR	NE	ACT	ED	RI	BI	HY	WO	HM	MT	IN	AP
MEDIUM GRAINED GRANODIORITE (MUSC - BI)																
44223	26.9	15.7	42.6	5.7	.7	0.0	0.0	0.0	0.0	1.7	0.0	0.0	0.0	0.5	.2	.1
G42	26.9	21.0	43.7	5.7	.6	0.0	0.0	0.0	0.0	1.5	0.0	0.0	0.0	.5	.2	.1
4311	22.7	15.3	46.6	6.1	1.1	0.0	0.0	0.0	0.0	2.3	0.0	0.0	0.0	.4	.2	.1
G43	25.9	13.9	46.6	7.2	.5	0.0	0.0	0.0	0.0	2.0	0.0	0.0	0.0	.5	.2	.1
43114	26.0	14.0	49.4	5.4	1.3	0.0	0.0	0.0	0.0	2.7	0.0	0.0	0.0	.6	.2	.1
53431	25.3	12.6	51.3	7.6	.5	0.0	0.0	0.0	0.0	2.9	0.0	0.0	0.0	.5	.2	.1
G48	25.6	12.8	49.6	3.2	.9	0.0	0.0	0.0	0.0	2.5	0.0	0.0	0.0	.5	.2	.1
4345	24.6	16.7	45.2	7.7	.4	0.0	0.0	0.0	0.0	2.5	0.0	0.0	0.0	.5	.2	.1
44222	24.4	16.4	45.2	6.4	1.0	0.0	0.0	0.0	0.0	2.1	0.0	0.0	0.0	.5	.2	.1
53448	25.0	13.7	46.0	7.7	.5	0.0	0.0	0.0	0.0	2.9	0.0	0.0	0.0	.6	.2	.1
43112	25.0	13.2	49.7	7.9	.5	0.0	0.0	0.0	0.0	2.6	0.0	0.0	0.0	.5	.2	.1
43213	25.1	12.2	49.7	6.8	1.6	0.0	0.0	0.0	0.0	3.0	0.0	0.0	0.0	.5	.2	.1
5345	23.3	15.2	49.6	7.6	.2	0.0	0.0	0.0	0.0	2.6	0.0	0.0	0.0	.5	.2	.1
G53	23.4	13.5	49.6	8.3	.4	0.0	0.0	0.0	0.0	3.0	0.0	0.0	0.0	.5	.2	.1
G56	24.3	13.0	50.2	8.0	.4	0.0	0.0	0.0	0.0	3.1	0.0	0.0	0.0	.7	.3	.1
43411	23.7	13.7	48.2	8.2	.4	0.0	0.0	0.0	0.0	2.7	0.0	0.0	0.0	.5	.2	.1
441F	24.2	12.5	51.0	7.9	.8	0.0	0.0	0.0	0.0	2.7	0.0	0.0	0.0	.5	.2	.1
43119	23.1	14.2	50.2	7.3	.9	0.0	0.0	0.0	0.0	2.7	0.0	0.0	0.0	.5	.2	.1
43113	22.2	13.5	50.2	8.3	.5	0.0	0.0	0.0	0.0	3.3	0.0	0.0	0.0	.6	.2	.1
43410	22.3	12.1	50.9	8.0	.6	0.0	0.0	0.0	0.0	3.0	0.0	0.0	0.0	.6	.3	.1
43310	21.5	14.1	50.9	8.5	.5	0.0	0.0	0.0	0.0	3.5	0.0	0.0	0.0	.7	.3	.1
FINE GRAINED GRANODIORITE (MUSC - BI)																
43216	25.2	14.6	49.1	7.8	.4	0.0	0.0	0.0	0.0	2.1	0.0	0.0	0.0	.5	.2	.1
G51	24.4	13.3	51.3	7.8	.3	0.0	0.0	0.0	0.0	2.1	0.0	0.0	0.0	.5	.2	.1
43115	24.4	13.1	51.2	7.9	.3	0.0	0.0	0.0	0.0	2.2	0.0	0.0	0.0	.5	.2	.1
FOLIATED GRANODIORITE (MUSC - BI)																
G318	26.2	16.9	48.9	5.9	.2	0.0	0.0	0.0	0.0	1.4	0.0	0.0	0.0	.4	.1	.1
G10P	26.6	20.4	44.1	5.7	.6	0.0	0.0	0.0	0.0	1.9	0.0	0.0	0.0	.4	.2	.1
4424C	25.6	12.0	51.9	7.9	.4	0.0	0.0	0.0	0.0	1.5	0.0	0.0	0.0	.4	.2	.1
G41	25.2	14.8	50.3	6.2	.6	0.0	0.0	0.0	0.0	2.1	0.0	0.0	0.0	.5	.2	.1
G62	25.6	11.9	51.4	7.8	.2	0.0	0.0	0.0	0.0	2.2	0.0	0.0	0.0	.5	.2	.1
5347	24.2	14.7	49.7	7.4	.3	0.0	0.0	0.0	0.0	1.9	0.0	0.0	0.0	.5	.2	.1
53430	24.6	13.4	50.2	7.4	.9	0.0	0.0	0.0	0.0	2.6	0.0	0.0	0.0	.5	.2	.1
GA-8	23.2	14.7	51.5	6.1	.8	0.0	0.0	0.0	0.0	2.8	0.0	0.0	0.0	.5	.2	.1
G67	23.3	11.1	44.4	7.2	.6	0.0	0.0	0.0	0.0	2.8	0.0	0.0	0.0	.5	.2	.1
GAA	23.6	13.0	51.8	7.3	.9	0.0	0.0	0.0	0.0	2.5	0.0	0.0	0.5	.6	.3	.1
43251	22.7	14.3	51.3	7.9	.4	0.0	0.0	0.0	0.0	2.5	0.0	0.0	0.0	.6	.2	.1
4411	23.4	13.6	51.6	8.3	.2	0.0	0.0	0.0	0.0	2.7	0.0	0.0	0.0	.6	.2	.1
4412	23.3	12.9	51.1	8.5	.4	0.0	0.0	0.0	0.0	2.7	0.0	0.0	0.0	.6	.3	.1
MASSIVE APLITE PATCHES IN FOLIATED GRANODIORITE																
G78	27.0	22.8	45.7	3.4	.2	0.0	0.0	0.0	0.0	.4	0.0	0.0	0.0	.4	.1	.0
5314AP	26.5	19.3	49.8	2.7	.3	0.0	0.0	0.0	0.0	1.1	0.0	0.0	0.0	.3	.1	.1
G62A	25.0	22.7	45.1	4.1	.2	0.0	0.0	0.0	0.0	.5	0.0	0.0	0.0	.3	.1	.0
GAC	25.2	17.1	45.2	4.8	.8	0.0	0.0	0.0	0.0	2.1	0.0	0.0	0.0	.4	.2	.1
NORTH PIN GRANODIORITE (MUSC - BI)																
53350	23.6	15.8	49.6	7.8	.2	0.0	0.0	0.0	0.0	2.2	0.0	0.0	0.0	.6	.2	.1
53310	24.6	17.8	45.3	7.4	.2	0.0	0.0	0.0	0.0	3.6	0.0	0.0	0.0	.8	.3	.2
533122	24.0	15.3	48.6	6.4	.7	0.0	0.0	0.0	0.0	3.5	0.0	0.0	0.0	.7	.3	.1
BI - HB GRANODIORITE (MICROCLINE MEGACRYSTS)																
G22	23.9	15.0	47.1	6.1	.1	0.0	0.0	0.0	0.0	4.5	0.0	0.0	0.0	1.0	.3	.2
G28	24.0	15.6	46.4	6.2	.0	0.0	0.0	0.0	0.0	3.9	0.0	0.0	0.0	1.0	.3	.2
G70	22.7	14.7	48.9	7.7	.0	0.0	0.0	0.0	0.0	4.1	0.0	0.0	0.0	.9	.3	.2
G19	22.5	14.5	49.0	7.7	.0	0.0	0.0	0.0	0.0	4.1	0.0	0.0	0.0	.9	.3	.2
G4	22.7	12.2	50.1	8.2	.0	0.0	0.0	0.0	0.0	4.4	0.0	0.0	0.0	.9	.3	.2
5428	22.7	13.4	46.1	8.3	.0	0.0	0.0	0.0	0.0	4.4	0.0	0.0	0.0	.9	.3	.2
5332	23.1	13.7	48.2	8.9	.1	0.0	0.0	0.0	0.0	4.5	0.0	0.0	0.0	.9	.3	.2
44210	23.3	12.4	48.0	8.0	.7	0.0	0.0	0.0	0.0	4.4	0.0	0.0	0.0	.9	.3	.2
G24	22.4	14.0	48.9	8.2	.0	0.0	0.0	0.0	0.0	4.4	0.0	0.0	0.0	.9	.3	.2
G4	22.1	15.0	47.6	7.9	.0	0.0	0.0	0.0	0.0	4.4	0.0	0.0	0.0	.9	.3	.2
5424	22.6	13.7	48.6	8.6	.0	0.0	0.0	0.0	0.0	4.3	0.0	0.0	0.0	.9	.3	.2
G27A	21.6	13.8	50.1	7.7	.0	0.0	0.0	0.0	0.0	4.6	0.0	0.0	0.0	.9	.3	.2
G7	22.0	15.3	47.0	8.9	.2	0.0	0.0	0.0	0.0	4.4	0.0	0.0	0.0	.9	.3	.2
G27	21.0	13.5	50.0	8.0	.0	0.0	0.0	0.0	0.0	4.4	0.0	0.0	0.0	.9	.3	.2
5412	22.7	11.3	50.0	9.6	.1	0.0	0.0	0.0	0.0	4.3	0.0	0.0	0.0	.9	.3	.2
544	23.0	14.4	46.8	9.4	.2	0.0	0.0	0.0	0.0	4.4	0.0	0.0	0.0	.9	.3	.2
53322	20.8	16.4	48.8	7.8	.0	0.0	0.0	0.0	0.0	4.5	0.0	0.0	0.0	.9	.3	.2
53414	21.9	16.2	48.3	8.7	.0	0.0	0.0	0.0	0.0	4.4	0.0	0.0	0.0	.9	.3	.2
G9	21.9	14.9	47.5	9.1	.0	0.0	0.0	0.0	0.0	4.4	0.0	0.0	0.0	.9	.3	.2
G70*2	20.6	14.7	48.8	7.8	.0	0.0	0.0	0.0	0.0	4.5	0.0	0.0	0.0	.9	.3	.2
G21	21.4	15.0	48.4	8.9	.0	0.0	0.0	0.0	0.0	4.5	0.0	0.0	0.0	.9	.3	.2
53424	20.0	13.7	49.5	8.1	.0	0.0	0.0	0.0	0.0	4.6	0.0	0.0	0.0	.9	.3	.2
G26	20.9	14.6	49.0	8.6	.0	0.0	0.0	0.0	0.0	4.6	0.0	0.0	0.0	.9	.3	.2
53320	20.0	14.6	49.8	8.7	.0	0.0	0.0	0.0	0.0	4.6	0.0	0.0	0.0	.9	.3	.2

FELSIC DYKES WITHIN STOCK

RED SPOTTED APLITE

531	32.0	21.7	43.7	3.5	.1	0.0	0.0	0.0	0.0	0.0	.7	0.3	0.0	0.0	.1	.1	.0
4343	27.4	19.3	47.5	4.7	.2	0.0	0.0	0.0	0.0	0.0	.5	0.0	0.0	0.0	.3	.1	.0

WHITE APLITE

630A	27.1	20.7	47.9	3.1	.2	0.0	0.0	0.0	0.0	0.0	.7	0.3	0.0	0.0	.3	.1	.0
4232BA	27.8	23.6	43.1	3.5	.2	0.0	0.0	0.0	0.0	0.0	1.2	0.0	0.0	0.0	.3	.1	.0

APLITE-PEGMATITE

4342AP	30.1	18.6	45.9	4.1	.3	0.0	0.0	0.0	0.0	0.0	.6	0.3	0.0	0.0	.3	.1	.0
--------	------	------	------	-----	----	-----	-----	-----	-----	-----	----	-----	-----	-----	----	----	----

FELSIC DYKES CUTTING HOST FELSIC PYROCLASTICS

APLITE-PEGMATITE

53311	29.0	21.2	44.8	4.1	0.0	0.0	0.0	0.0	0.0	0.0	.0	0.0	0.0	0.0	.3	.1	.0
-------	------	------	------	-----	-----	-----	-----	-----	-----	-----	----	-----	-----	-----	----	----	----

APLITE-PEGMATITE (ZONED)

53318P	27.7	27.1	40.3	3.6	.1	0.0	0.0	0.0	0.0	0.0	.6	0.0	0.0	0.0	.2	.1	.0
53318C	25.9	30.2	40.0	2.8	.2	0.0	0.0	0.0	0.0	0.0	.7	0.0	0.0	0.0	.2	.1	.0

GRANODIOPITE DYKE (+ MICROCLINE MEGACRYSTS)

53412	25.0	7.9	55.7	8.3	.5	0.0	0.0	0.0	0.0	0.0	1.8	0.0	0.0	0.0	.4	.1	.1
-------	------	-----	------	-----	----	-----	-----	-----	-----	-----	-----	-----	-----	-----	----	----	----

INTRUSION BRECCIA

53413G	22.1	13.6	50.6	7.6	0.0	0.0	0.0	0.0	0.0	0.0	4.2	0.0	.7	0.0	.8	.3	.2
53413X	6.9	.6	45.1	8.1	0.0	0.0	0.0	0.0	0.0	0.0	26.1	0.0	7.6	0.0	3.8	1.2	.6
53413T	4.3	0.0	46.6	5.8	0.0	0.0	11.0	0.0	0.0	0.0	20.0	0.0	6.4	0.0	1.9	1.3	.7

LENSOID MAFIC ENGLAVES

5413Y	11.1	22.0	33.9	8.4	0.0	0.0	0.0	0.0	0.0	0.0	17.2	0.0	3.1	0.0	2.8	.3	.6
5422BX	5.8	0.0	47.1	8.3	0.0	0.0	4.9	0.0	0.0	0.0	22.3	0.0	5.3	0.0	4.0	1.3	.6
53322X	7.0	4.6	41.0	9.7	0.0	0.0	0.0	0.0	0.0	0.0	25.2	0.0	6.3	0.0	4.4	1.8	.9
53322X	1.8	0.0	49.8	10.2	0.0	0.0	16.2	0.0	0.0	0.0	11.7	0.3	4.2	0.0	4.3	1.4	1.1
53322X	7.0	0.0	25.8	13.4	0.0	0.0	18.0	0.0	0.0	0.0	24.9	0.0	2.9	0.0	5.6	1.4	.8

FELSIC TO INTERMEDIATE METAVOLCANICS

G61T	34.2	2.0	50.6	5.0	3.0	0.0	0.0	0.0	0.0	0.0	4.1	0.0	0.0	0.0	.5	.5	.2
5426T	24.4	5.2	53.0	9.1	1.5	0.0	0.0	0.0	0.0	0.0	4.7	0.0	0.0	0.0	1.3	.6	.2
53412T	23.0	6.1	52.7	9.6	1.3	0.0	0.0	0.0	0.0	0.0	5.1	0.0	0.0	0.0	1.2	.6	.2
4242T	22.2	5.9	51.4	11.5	2.7	0.0	0.0	0.0	0.0	0.0	5.3	0.3	0.0	0.0	1.3	.6	.2
53450T	21.3	10.7	45.9	7.6	2.3	0.0	0.0	0.0	0.0	0.0	8.4	0.0	0.0	0.0	1.1	.6	.1
4341T	21.5	9.3	47.5	11.0	1.6	0.0	0.0	0.0	0.0	0.0	6.0	0.0	0.0	0.0	1.3	.6	.2
3321T	23.0	10.6	45.9	8.8	2.1	0.0	0.0	0.0	0.0	0.0	7.0	0.0	0.0	0.0	1.5	.6	.2
G89T	35.4	5.0	34.0	22.8	.2	0.0	0.0	0.0	0.0	0.0	8.2	0.3	0.0	0.0	3.5	.6	.3

F2

SCATTERGOOD LAKE STOCK

SAMPLE	QTZ	OR	AB	AN	COR	NE	ACT	EQ	RI	BI	MY	MO	MM	MI	TN	AP
--------	-----	----	----	----	-----	----	-----	----	----	----	----	----	----	----	----	----

HB GRANODIOPITE (+ - MICROCLINE MEGACRYSTS)

ST6-P	21.0	17.1	43.2	10.1	0.0	0.0	0.0	0.0	0.0	0.0	6.3	0.0	0.0	0.0	.5	.3
ST13P	20.5	15.0	45.1	8.6	0.0	0.0	0.0	0.0	0.0	0.0	7.2	1.0	0.0	0.0	.6	.4
ST12P	21.1	13.9	46.1	10.7	0.0	0.0	0.0	0.0	0.0	0.0	7.1	0.0	0.0	0.0	.6	.4
ST8-P	20.7	15.5	43.1	10.0	0.0	0.0	0.0	0.0	0.0	0.0	7.7	0.3	0.0	0.0	.5	.4
ST5-P	20.9	14.0	43.4	10.7	0.0	0.0	0.0	0.0	0.0	0.0	7.8	0.0	0.0	0.0	.6	.4
S10B	19.4	14.7	46.1	9.6	0.0	0.0	0.0	0.0	0.0	0.0	7.1	0.0	0.0	0.0	.5	.4
S1	19.1	14.4	46.9	9.6	0.0	0.0	0.0	0.0	0.0	0.0	7.1	0.0	0.0	0.0	.6	.4
S6	19.1	14.5	47.0	10.2	0.0	0.0	0.0	0.0	0.0	0.0	6.0	0.0	0.0	0.0	.6	.4
ST2-P	20.5	15.0	43.1	10.3	0.0	0.0	0.0	0.0	0.0	0.0	6.3	0.0	0.0	0.0	.5	.4
ST3-P	20.2	15.4	43.9	10.7	0.0	0.0	0.0	0.0	0.0	0.0	7.1	0.0	0.0	0.0	.7	.4
S14	19.8	14.3	46.1	9.8	0.0	0.0	0.0	0.0	0.0	0.0	7.2	0.0	0.0	0.0	.6	.4
S5	19.2	14.3	46.6	10.4	0.0	0.0	0.0	0.0	0.0	0.0	6.7	0.0	0.0	0.0	.6	.4
S9	18.7	14.3	47.8	10.1	0.0	0.0	0.0	0.0	0.0	0.0	6.3	0.0	0.0	0.0	.6	.4
S11A	19.5	14.6	45.4	9.7	0.0	0.0	0.0	0.0	0.0	0.0	7.5	0.0	0.0	0.0	.6	.4
S17-P	19.9	14.3	45.1	10.8	0.0	0.0	0.0	0.0	0.0	0.0	6.9	0.0	0.0	0.0	.6	.4
S17	18.9	15.0	46.6	10.6	0.0	0.0	0.0	0.0	0.0	0.0	6.3	0.0	0.0	0.0	.6	.4
S14-P	20.7	17.8	43.4	11.0	0.0	0.0	0.0	0.0	0.0	0.0	7.7	0.0	0.0	0.0	.6	.4
S13B	18.7	15.2	46.5	9.6	0.0	0.0	0.0	0.0	0.0	0.0	6.9	0.0	0.0	0.0	.6	.4
S11-P	19.9	13.6	45.4	10.3	0.0	0.0	0.0	0.0	0.0	0.0	7.4	0.0	0.0	0.0	.6	.4
ST10P	20.3	13.4	44.7	10.4	0.0	0.0	0.0	0.0	0.0	0.0	7.5	0.0	0.0	0.0	.6	.4
S2	17.7	15.0	46.6	9.2	0.0	0.0	0.0	0.0	0.0	0.0	6.5	0.0	0.0	0.0	.6	.4
ST11P	19.2	14.9	45.5	9.3	0.0	0.0	0.0	0.0	0.0	0.0	7.4	0.0	0.0	0.0	.6	.4
S15	18.9	15.2	45.3	10.3	0.0	0.0	0.0	0.0	0.0	0.0	7.1	0.0	0.0	0.0	.6	.4
S12	18.4	14.1	45.6	10.3	0.0	0.0	0.0	0.0	0.0	0.0	8.1	0.0	0.0	0.0	.6	.4
S19-P	17.2	16.2	43.9	9.8	0.0	0.0	0.0	0.0	0.0	0.0	8.5	0.0	1.4	0.0	.7	.5

LENSOID MAFIC ENCLAVE (SXTM) AND HOST (SXTMG)

SXTM	14.7	3.6	30.6	5.7	0.0	0.0	0.0	0.0	0.0	0.0	31.0	0.0	8.1	0.0	4.5	1.2	.4
SXTMG	21.2	14.8	44.6	9.3	0.0	0.0	0.0	0.0	0.0	0.0	6.9	0.0	.9	0.0	1.5	.7	.4

INTRUSION BRECCIA - FELDSPATHIZED ENCLAVE

S17	8.6	10.3	55.3	7.2	0.0	0.0	0.0	0.0	0.0	0.0	11.4	0.0	3.4	0.0	2.2	1.1	.5
-----	-----	------	------	-----	-----	-----	-----	-----	-----	-----	------	-----	-----	-----	-----	-----	----

INTRUSION BRECCIA (METAVOLCANIC BLOCK)

S16	24.7	7.5	41.0	8.1	1.5	0.0	0.0	0.0	0.0	0.0	12.8	0.0	0.0	0.0	2.9	1.2	.5
-----	------	-----	------	-----	-----	-----	-----	-----	-----	-----	------	-----	-----	-----	-----	-----	----

F3

ISOX LAKE GRANITOIDS

SAMPLE	QTZ	OR	AB	AN	COR	NE	ACT	ED	RI	BI	HY	MO	HM	HT	TH	AP
BI GRANODIORITE																
EX25	21.5	24.4	45.1	4.4	.8	0.0	0.0	0.0	0.0	2.8	0.0	0.0	0.0	.6	.3	.1
EX25	21.1	24.2	45.6	4.4	.8	0.0	0.0	0.0	0.0	2.8	0.0	0.0	0.0	.6	.3	.1
EX20	27.0	28.5	44.9	7.4	.1	0.0	0.0	0.0	0.0	3.6	0.0	0.0	0.0	.9	.4	.2
EX21	21.4	18.3	45.6	9.0	0.0	0.0	0.0	0.0	0.0	4.2	0.0	0.0	0.0	.9	.4	.2
EX19	20.7	19.9	44.5	8.3	.7	0.0	0.0	0.0	0.0	4.1	0.0	0.0	0.0	1.0	.5	.2
EX27	19.1	19.5	47.0	9.7	.1	0.0	0.0	0.0	0.0	4.9	0.0	0.0	0.0	1.3	.5	.3
EX26	15.9	18.1	47.7	9.4	0.0	0.0	0.0	0.0	0.0	5.8	0.0	5.8	0.0	1.7	.6	.4
BI - HR MONZODIORITE																
EX10A	27.7	22.0	42.6	8.4	0.0	0.0	0.0	0.0	0.0	5.3	0.0	.6	0.0	1.9	.5	.4
EX10B	15.5	19.6	43.5	9.4	0.0	0.0	0.0	0.0	0.0	4.4	0.0	.8	0.0	1.7	.7	.4
EX29	15.4	19.1	43.8	9.8	0.0	0.0	0.0	0.0	0.0	6.2	0.0	.6	0.0	1.8	.7	.5
EX24	14.5	22.9	42.7	9.0	0.0	0.0	0.0	0.0	0.0	7.5	0.0	.3	0.0	1.9	.7	.5
EX2A	11.8	20.5	45.4	8.1	0.0	0.0	0.0	0.0	0.0	9.6	0.0	1.8	0.0	1.7	.8	.5
LEUCO - QUARTZ MONZODIORITE																
EX2	20.7	19.5	48.8	7.1	0.0	0.0	0.0	0.0	0.0	2.9	0.0	.0	0.0	.6	.3	.1
EX1	17.7	20.5	52.4	6.1	.1	0.0	0.0	0.0	0.0	1.3	0.0	0.0	0.0	.4	.3	.1
EX11	18.3	21.7	49.5	6.2	.7	0.0	0.0	0.0	0.0	2.5	0.0	0.0	0.0	.8	.4	.1
PINK FELSITE																
EX5	29.6	28.8	31.6	6.6	0.0	0.0	0.0	0.0	0.0	2.4	0.0	.2	0.0	.5	.2	.1
EX11	25.3	45.1	16.7	5.2	0.0	0.0	0.0	0.0	0.0	2.1	0.0	3.8	0.0	.6	.2	.2
GREY FELSITE																
EX7	22.4	10.6	41.7	14.9	0.0	0.0	0.0	0.0	0.0	5.9	0.0	.4	0.0	1.7	.7	.3
EX8	18.3	27.2	34.0	18.1	0.0	0.0	0.0	0.0	0.0	4.2	0.0	1.7	0.0	1.6	.7	.3

F4

FLOPA LAKE STOCK

SAMPLE	QTZ	OR	AB	AN	COR	NE	ACT	ED	RI	BI	HY	MO	HM	HT	TH	AP
BIOTITE GRANITE																
FLR25	25.7	17.8	46.8	5.5	1.0	0.0	0.0	0.0	0.0	2.4	0.0	0.0	0.0	.5	.2	.1
FLR15	24.4	27.8	42.8	3.5	.4	0.0	0.0	0.0	0.0	1.4	0.0	0.0	0.0	.5	.2	.1
FLOPE	22.9	19.7	44.0	6.0	.6	0.0	0.0	0.0	0.0	2.2	0.0	0.0	0.0	.5	.2	.1
FLP17	27.6	21.2	45.9	4.7	.6	0.0	0.0	0.0	0.0	2.1	0.0	0.0	0.0	.6	.3	.1
FLOP3	21.2	25.8	45.9	4.7	.4	0.0	0.0	0.0	0.0	1.5	0.0	0.0	0.0	.5	.2	.1
FLP13	21.3	27.7	44.0	4.1	.2	0.0	0.0	0.0	0.0	1.7	0.0	0.0	0.0	.5	.2	.1
FLP28	21.7	21.2	48.4	6.9	.4	0.0	0.0	0.0	0.0	2.3	0.0	0.0	0.0	.5	.2	.1
FLOP5	17.3	25.3	48.7	5.5	.1	0.0	0.0	0.0	0.0	2.7	0.0	0.0	0.0	.7	.3	.1
HR - BI MONZONITE																
FLP21	6.3	25.0	40.8	8.5	0.0	0.0	0.0	0.0	0.0	7.3	0.0	.2	0.0	1.9	.8	.4
FLOP2	6.2	27.1	42.6	8.3	.2	0.0	0.0	0.0	0.0	6.6	0.0	0.0	0.0	1.6	.7	.4
FLR24	4.5	24.2	40.5	8.9	.2	0.0	0.0	0.0	0.0	5.1	0.0	0.0	0.0	1.6	.6	.3
FLP22	3.0	24.6	50.6	9.0	.5	0.0	0.0	0.0	0.0	5.7	0.0	0.0	0.0	1.7	.6	.4
FLOP4	7.5	24.2	50.7	9.4	.6	0.0	0.0	0.0	0.0	6.0	0.0	0.0	0.0	1.7	.7	.4
FLP16	1.9	27.6	51.7	10.3	.6	0.0	0.0	0.0	0.0	5.5	0.0	0.0	0.0	1.8	.7	.4
FLP20	5.5	22.9	47.3	11.1	1.5	0.0	0.0	0.0	0.0	8.4	0.0	0.0	0.0	1.8	.9	.5
HR - BI MONZODIORITE																
FL 11	0.0	19.0	48.6	7.7	0.0	3.2	0.0	0.0	0.0	11.3	0.0	3.5	0.0	3.0	.3	.9
FL 12	0.0	20.0	45.1	11.6	0.0	1.1	0.0	0.0	0.0	15.1	0.0	1.3	0.0	1.0	1.4	.9
FL 1	0.0	16.5	42.0	9.6	0.0	2.4	0.0	0.0	0.0	18.1	0.0	3.9	0.0	4.1	2.3	1.1
FL 15	1.2	6.8	43.8	10.8	0.0	0.0	0.0	0.0	0.0	23.4	0.0	5.4	0.0	4.3	2.1	1.1
FL 26	0.0	11.4	40.8	14.1	0.0	1.7	0.3	0.0	0.0	29.7	0.0	3.8	0.0	4.4	2.1	1.2
MONZODIORITE - METAVOLCANIC CONTACT																
FL 9	.8	25.5	51.0	13.7	.1	0.0	0.0	0.0	0.0	5.2	0.0	0.0	0.0	1.5	.7	.4
GRANITE DYKE IN MONZONITE																
FLOP19	23.3	21.7	46.6	4.9	.3	0.0	0.0	0.0	0.0	2.1	0.0	0.0	0.0	.5	.2	.1
GRANITE DYKE IN MONZODIORITE																
FLOP8	15.0	17.7	49.7	11.0	.9	0.0	0.0	0.0	0.0	4.0	0.0	0.0	0.0	1.1	.5	.2
APLITE DYKE IN METAVOLCANICS																
FLR27	28.5	24.4	43.0	2.7	.3	0.0	0.0	0.0	0.0	.7	0.0	0.0	0.0	.2	.1	.0
MONZODIORITE ENCLAVE IN GRANITE																
FLR29	6.0	6.1	43.0	12.5	0.0	0.0	0.0	0.0	0.0	21.3	0.0	5.2	0.0	3.5	1.5	.9
MONZODIORITE ENCLAVE IN MONZONITE																
FLR19	5.4	9.5	35.2	9.6	0.0	0.0	0.0	0.0	0.0	26.2	0.0	4.8	0.0	6.0	2.4	1.0

F5

RYCKMAN LAKE STOCK

SAMPLE QTZ OP AB AN COR NE ACT ED RI BI HY HO HM HT TN AP

BI - HB GRANODIORITE (+ MICROCLINE MEGACRYSTS)

RY85	19.9	13.4	52.3	6.4	0.0	0.0	0.0	0.0	0.0	5.1	0.0	1.4	0.0	1.0	.3	.2
RY15	19.9	14.1	51.4	6.5	0.0	0.0	0.0	0.0	0.0	5.4	0.0	1.2	0.0	1.0	.3	.2
RY90	22.0	15.7	46.1	6.7	0.0	0.0	0.0	0.0	0.0	5.7	0.0	1.8	0.0	1.2	.3	.2
RY14	19.1	12.4	53.7	6.7	0.0	0.0	0.0	0.0	0.0	5.7	0.0	1.4	0.0	1.0	.3	.2
RY55	12.2	11.1	52.6	7.0	0.0	0.0	0.0	0.0	0.0	5.5	0.0	1.1	0.0	1.0	.3	.2
RY32	19.0	13.4	52.5	6.1	0.0	0.0	0.0	0.0	0.0	5.7	0.0	1.4	0.0	1.2	.4	.3
RY33	20.1	14.1	48.9	7.8	0.0	0.0	0.0	0.0	0.0	6.1	0.0	1.0	0.0	1.1	.4	.2
RY5	10.7	13.0	52.2	7.7	0.0	0.0	0.0	0.0	0.0	4.5	0.0	1.3	0.0	1.1	.4	.2
RY5	20.0	14.7	49.0	9.1	0.0	0.0	0.0	0.0	0.0	4.5	0.0	.7	0.0	1.5	.4	.2
RY54	21.1	14.2	46.1	9.3	0.0	0.0	0.0	0.0	0.0	7.1	0.0	.5	0.0	1.1	.4	.2
RY10	20.8	13.5	47.5	9.0	0.0	0.0	0.0	0.0	0.0	0.7	0.0	.7	0.0	1.2	.4	.2
RY7F	14.9	15.1	47.2	8.8	0.0	0.0	0.0	0.0	0.0	0.4	0.0	.8	0.0	1.1	.4	.2
RY11	20.5	11.3	47.1	9.0	0.0	0.0	0.0	0.0	0.0	7.1	0.0	.8	0.0	1.2	.4	.2
RYA	20.7	12.7	47.7	9.4	0.0	0.0	0.0	0.0	0.0	6.9	0.0	.9	0.0	1.2	.4	.3
RY74	20.1	15.2	46.6	9.2	0.0	0.0	0.0	0.0	0.0	6.5	0.0	.6	0.0	1.1	.4	.2
RY1	21.1	12.5	46.6	9.0	0.0	0.0	0.0	0.0	0.0	7.4	0.0	.9	0.0	1.3	.4	.3
RY51	20.5	13.4	45.1	9.5	0.0	0.0	0.0	0.0	0.0	8.5	0.0	.9	0.0	1.4	.5	.3
RY6	18.1	10.4	47.4	11.0	0.0	0.0	0.0	0.0	0.0	9.4	0.0	1.4	0.0	1.6	.5	.3

MYLONITE

RY 70	4.4	5.1	52.0	6.4	0.0	0.0	0.0	0.0	0.0	21.6	0.0	6.6	0.0	2.6	.7	.6
-------	-----	-----	------	-----	-----	-----	-----	-----	-----	------	-----	-----	-----	-----	----	----

BI - HB QUARTZ MONZODIORITE

RY50	17.3	12.7	43.1	10.7	0.0	0.0	0.0	0.0	0.0	12.2	0.0	1.5	0.0	1.7	.5	.3
RY 76	14.0	9.8	50.1	6.6	0.0	0.0	0.0	0.0	0.0	14.1	0.0	2.7	0.0	1.8	.6	.4
RY 77	12.0	8.1	40.6	7.2	0.0	0.0	0.0	0.0	0.0	16.9	0.0	1.3	0.0	1.9	.6	.5
RY 73	13.7	4.9	45.1	7.7	0.0	0.0	0.0	0.0	0.0	21.7	0.0	3.6	0.0	2.2	.8	.5
RY 3-	9.9	9.4	49.7	5.0	0.0	0.0	0.0	0.0	0.0	16.3	0.0	5.9	0.0	2.3	.8	.5
RY 72	10.5	7.6	46.3	6.7	0.0	0.0	0.0	0.0	0.0	18.4	0.0	5.1	0.0	2.4	.6	.5
RY 21	12.8	4.2	42.7	7.4	0.0	0.0	0.0	0.0	0.0	23.1	0.0	5.9	0.0	2.6	.7	.5
RY 7	12.5	4.0	41.9	7.3	0.0	0.0	0.0	0.0	0.0	24.1	0.0	6.3	0.0	2.8	.7	.5
RY61	0.0	9.5	54.2	0.0	0.0	1.2	0.0	0.0	8.5	16.4	0.0	8.6	.3	0.0	.8	.4
RY 60	12.0	1.6	41.0	7.2	0.0	0.0	0.0	0.0	0.0	28.1	0.0	5.0	0.0	2.8	.7	.6
RY 23	10.3	4.9	42.0	9.5	0.0	0.0	0.0	0.0	0.0	21.7	0.0	6.4	0.0	2.8	.7	.6

BI - HB MONZODIORITE

RY 4	5.7	8.7	52.6	4.8	0.0	0.0	0.0	0.0	0.0	18.3	0.0	5.3	0.0	2.5	.6	.5
RY 01	7.0	3.9	50.8	6.1	0.0	0.0	0.0	0.0	0.0	23.5	0.0	5.0	0.0	2.3	.6	.6
RY91	10.2	6.8	46.2	7.4	0.0	0.0	0.0	0.0	0.0	20.2	0.0	5.7	0.0	2.3	.9	.6
RY 83	7.6	3.5	48.8	5.9	0.0	0.0	0.0	0.0	0.0	22.9	0.0	7.3	0.0	2.7	.7	.6
RY F2	6.5	0.0	46.7	5.9	0.0	0.0	0.0	0.0	0.0	25.3	0.0	7.9	0.0	2.9	.8	.7
RY 35	9.3	0.0	41.1	6.3	0.0	0.0	2.2	0.0	0.0	30.9	0.0	6.7	0.0	3.0	.8	.7

PX - HB MONZODIORITE

RY 37	1.7	11.8	53.6	5.1	0.0	0.0	0.0	0.0	0.0	17.4	0.0	6.4	0.0	2.7	.7	.7
RY A1	4.3	7.9	46.2	6.9	0.0	0.0	0.0	0.0	0.0	24.6	0.0	5.1	0.0	2.8	1.0	.8
RY A0	5.1	.7	49.5	7.2	0.0	0.0	0.0	0.0	0.0	25.3	0.0	7.7	0.0	2.9	.9	.7
RY 93	4.4	3.2	47.5	7.1	0.0	0.0	0.0	0.0	0.0	27.4	0.0	5.7	0.0	2.8	1.0	.9
RY 92	4.3	0.0	43.5	8.7	0.0	0.0	4.4	0.0	0.0	26.5	0.0	5.9	0.0	3.3	.9	.9
RY F2	3.7	6.8	42.7	7.1	0.0	0.0	0.0	0.0	0.0	26.1	0.0	6.1	0.0	3.7	.9	1.0
RY 94	2.4	1.3	39.4	10.5	0.0	0.0	0.0	0.0	0.0	32.3	0.0	7.9	0.0	3.8	1.2	1.3

APLITE DYKE IN MAFIC METAVOLCANICS

RY22	26.5	26.6	40.0	5.2	0.0	0.0	0.0	0.0	0.0	1.2	0.0	.0	0.0	.3	.2	.1
------	------	------	------	-----	-----	-----	-----	-----	-----	-----	-----	----	-----	----	----	----

APLITE - PEGMATITE DYKE FROM DYKE SHAPED WITHIN STOCK

RY91A	26.5	35.1	36.2	.8	0.0	0.0	0.0	0.0	0.0	.7	0.0	.3	0.0	.2	.1	.0
-------	------	------	------	----	-----	-----	-----	-----	-----	----	-----	----	-----	----	----	----

MAFIC ENCLAVES

RY 71	7.7	9.1	51.7	4.7	0.0	0.0	0.0	0.0	0.0	17.5	0.0	5.9	0.0	2.3	.7	.5
RY 60X	7.8	0.0	44.7	7.7	0.0	0.0	3.4	0.0	0.0	23.3	0.0	4.1	0.0	2.9	.7	.6
RY 61X	0.0	0.0	38.9	9.3	0.0	0.0	24.2	10.2	0.0	7.5	4.5	0.0	0.0	3.4	1.2	.7

METAVOLCANICS

RY44TP	29.2	2.3	46.5	12.4	1.3	0.0	0.0	0.0	0.0	4.8	0.0	3.0	0.0	1.0	.4	.2
RY 84	2.7	15.9	49.5	6.1	0.0	0.0	0.0	0.0	0.0	16.0	3.0	5.4	0.0	2.9	.8	.7

F7

WABIGOON GRANITOID PLUTONS

SAMPLE QTZ OR AB AN COR NE ACT ED RI BI HY MO HM HT TN AP

FROGHEAD BAY STOCK

BI TONALITE

FH9	29.4	8.9	32.8	13.8	1.3	0.0	0.0	0.0	0.0	5.3	0.0	0.0	0.0	1.6	.7	.2
FH10	28.4	7.4	32.9	12.7	1.2	0.0	0.0	0.0	0.0	5.4	0.0	0.0	0.0	1.7	.7	.2
FH1	30.4	8.2	35.6	14.2	1.7	0.0	0.0	0.0	0.0	7.0	0.0	0.0	0.0	1.9	.9	.3
FH8	28.0	8.3	39.1	14.0	1.2	0.0	0.0	0.0	0.0	6.7	0.0	0.0	0.0	1.8	.8	.3
FH6	29.1	9.5	37.4	14.8	.9	0.0	0.0	0.0	0.0	7.9	0.0	0.0	0.0	2.2	.9	.3
FH7	27.1	6.1	35.4	15.1	.9	0.0	0.0	0.0	0.0	3.4	0.0	0.0	0.0	2.2	1.1	.1
FH2	28.6	6.2	35.8	14.4	.8	0.0	0.0	0.0	0.0	3.6	0.0	0.0	0.0	2.4	1.1	.1
FH1	27.6	4.0	34.0	15.1	1.2	0.0	0.0	0.0	0.0	3.5	0.0	0.0	0.0	2.4	1.1	.1
FH5	25.9	8.4	38.6	14.9	.9	0.0	0.0	0.0	0.0	7.9	0.0	0.0	0.0	2.7	1.0	.3

BI GRANODIORITE

FH4	32.2	17.4	37.6	7.0	1.0	0.0	0.0	0.0	0.0	3.5	0.0	0.0	0.0	1.0	.3	.1
-----	------	------	------	-----	-----	-----	-----	-----	-----	-----	-----	-----	-----	-----	----	----

REGINA BAY STOCK

TONALITE (SERPENTINIZED, CARBONATIZED, CHLORITIZED)

REG1	28.3	0.0	36.4	19.7	1.3	0.0	0.0	0.0	0.0	7.3	1.3	0.0	0.0	2.2	.9	.5
REG2	26.6	0.0	37.5	28.3	.7	0.0	0.0	0.0	0.0	6.1	4.3	0.0	0.0	2.4	1.0	.4
REG5	25.5	0.0	39.0	19.4	.8	0.0	0.0	0.0	0.0	8.4	1.2	0.0	0.0	2.3	.9	.4
REG5-2	27.7	0.0	35.0	16.9	1.1	0.0	0.0	0.0	0.0	11.1	2.1	0.0	0.0	2.7	1.0	.4
REG1	24.0	0.0	38.9	20.9	0.8	0.0	0.0	0.0	0.0	11.7	.7	0.0	0.0	2.4	.9	.4
REG6	24.6	0.0	39.4	18.7	1.5	0.0	0.0	0.0	0.0	11.7	.4	0.0	0.0	2.5	.9	.4
RFG4-2	21.3	0.0	38.4	21.6	.2	0.0	0.0	0.0	0.0	12.4	.4	0.0	0.0	2.5	1.0	.3

SHEEP POPE

REG4S	21.0	.5	35.3	21.6	0.0	0.0	0.0	0.0	0.0	13.5	0.0	1.9	0.0	2.7	1.1	.3
-------	------	----	------	------	-----	-----	-----	-----	-----	------	-----	-----	-----	-----	-----	----

STORMY LAKE STOCK

BI GRANODIORITE

ST4	21.0	12.0	45.9	9.9	.7	0.0	0.0	0.0	0.0	6.1	0.0	0.0	0.0	1.4	.7	.3
ST7	21.6	13.1	45.7	18.2	1.0	0.0	0.0	0.0	0.0	5.7	0.0	0.0	0.0	1.4	.8	.4
ST2	21.4	13.4	44.5	9.7	1.1	0.0	0.0	0.0	0.0	6.4	0.0	0.0	0.0	1.5	.9	.4
ST5	19.5	14.4	45.1	11.6	0.0	0.0	0.0	0.0	0.0	6.6	0.0	.3	0.0	1.4	.8	.4
ST1	21.1	12.1	45.1	18.7	1.0	0.0	0.0	0.0	0.0	7.2	0.0	0.0	0.0	1.6	.9	.4

TAYLOR LAKE STOCK (SAMPLES AFTER PICHETTE 1976)

SAMPLE QTZ OF AB AN COR NE ACT ED RI BI HY MO HM HT TN AP

BI - HB GRANODIORITE

T54	19.5	19.7	46.5	7.6	0.0	0.0	0.0	0.0	0.0	4.6	0.0	.4	0.0	1.1	.5	.2
T12	20.5	19.8	42.6	3.8	0.0	0.0	0.0	0.0	0.0	6.7	0.0	.2	0.0	1.2	.6	.3
T13	20.1	17.0	43.1	9.9	0.0	0.0	0.0	0.0	0.0	7.1	0.0	.3	0.0	1.3	.7	.3
T32	14.8	17.9	43.8	9.6	0.0	0.0	0.0	0.0	0.0	7.1	0.0	.3	0.0	1.3	.7	.3
T51	18.7	15.5	44.4	11.1	0.0	0.0	0.0	0.0	0.0	7.7	0.0	.2	0.0	1.4	.7	.4
T57	14.9	22.7	43.9	8.5	0.0	0.0	0.0	0.0	0.0	7.0	0.0	.6	0.0	1.5	.7	.4

BI - HB - PX MONZONITE TO QUARTZ MONZONITE

T65	16.3	15.4	45.1	18.7	0.0	0.0	0.0	0.0	0.0	7.6	0.0	.4	0.0	1.4	.7	.4
T35	13.5	19.8	44.7	8.1	0.0	0.0	0.0	0.0	0.0	6.1	0.0	.4	0.0	1.7	.9	.4
T72	5.8	27.8	54.8	7.2	0.0	0.0	0.0	0.0	0.0	7.0	0.0	1.3	0.0	1.6	1.2	.4
T37	6.3	12.6	52.7	7.2	0.0	0.0	0.0	0.0	0.0	12.9	0.0	4.3	0.0	2.4	1.1	.6
T42	6.4	11.7	45.7	4.6	0.0	0.0	0.0	0.0	0.0	15.2	0.0	9.5	0.0	3.2	1.2	1.5
T41	6.2	14.4	38.2	5.9	0.0	0.0	0.0	0.0	0.0	22.1	0.0	7.1	0.0	3.6	1.6	1.0

HB - BI GRANODIORITE (FINE GRAINED)

T28	24.3	14.0	48.0	7.3	1.1	0.0	0.0	0.0	0.0	3.7	0.3	0.0	0.0	.7	.4	.2
T40	23.4	16.6	47.0	7.7	.5	0.0	0.0	0.0	0.0	3.5	0.3	0.0	0.0	.7	.4	.2

HB - PX MONZODIORITE

T30	3.2	0.0	48.1	12.1	0.0	0.0	6.6	0.0	0.0	17.0	0.0	7.3	0.0	3.3	1.3	1.2
-----	-----	-----	------	------	-----	-----	-----	-----	-----	------	-----	-----	-----	-----	-----	-----

HB - PX MONZONITE (MEDIUM GRAINED)

T69	3.7	19.0	54.2	5.7	0.0	0.0	0.0	0.0	0.0	9.6	0.0	3.7	0.0	2.2	1.1	.7
-----	-----	------	------	-----	-----	-----	-----	-----	-----	-----	-----	-----	-----	-----	-----	----

BI - PX - HB MONZONITE (COARSE GRAINED)

T78	4.4	12.7	52.7	7.7	0.0	0.0	0.0	0.0	0.0	13.8	0.0	4.4	0.0	2.4	1.2	.8
-----	-----	------	------	-----	-----	-----	-----	-----	-----	------	-----	-----	-----	-----	-----	----

MUSC - BI LEUCO MICROGRANITE

T60	28.1	29.9	44.7	1.3	1.2	0.0	0.0	3.0	0.0	2.0	0.0	0.0	0.0	.6	.3	.1
-----	------	------	------	-----	-----	-----	-----	-----	-----	-----	-----	-----	-----	----	----	----

APLITE

T47	22.7	12.2	49.6	8.3	1.4	0.0	0.0	0.0	0.0	4.2	0.0	0.0	0.0	.9	.5	.2
-----	------	------	------	-----	-----	-----	-----	-----	-----	-----	-----	-----	-----	----	----	----

MAFIC ENCLAVE

T24X	14.2	18.6	26.6	6.7	0.0	0.0	0.0	0.0	0.0	23.9	0.0	5.9	0.0	2.8	.9	.4
------	------	------	------	-----	-----	-----	-----	-----	-----	------	-----	-----	-----	-----	----	----

MAFIC METAVOLCANIC

T49	.1	0.0	26.0	17.1	0.0	0.0	34.1	0.0	0.0	9.0	0.0	2.1	0.0	7.8	2.7	.3
-----	----	-----	------	------	-----	-----	------	-----	-----	-----	-----	-----	-----	-----	-----	----

APPENDIX G

RADIOELEMENT DETERMINATIONS:

Introduction:

U and Th analyses were performed in the field (in situ) using a four channel differential gamma ray spectrometer, model DISA400A loaned by Geometrics Services (Canada) Ltd. Exploranium Division, Downsview, Ontario). The unit consisted of an electronics console connected by cable to a detector housing a 3" x 3" NaI(Tl) crystal (347.47 cm³).

The energy window settings were identical to those reported by Grasty and Darnley (1971). Machine calibration was carried out using an external Cesium 137 pellet (1 micro curie) with peak setting at 0.662 Mev. The window widths were sufficient that effects from instrument drift should have been minimal ($\pm 3\%$, Lovborg et al, 1971). Intensity calibrations were carried out by the method of Grasty and Darnley (1971) using concrete calibration pads at Uplands Airport, Ottawa. In Table G.1 the Compton scattering coefficients (stripping ratios) and sensitivities for this instrument are compared with those reported by Grasty and Darnley (1971) and average values obtained on three other Exploranium DISA400 units calibrated on the same pads.

The three other DISA400 units give average sensitivities compatible with this instrument for U and Th but show a large discrepancy for K sensitivity. This can be partially attributed to the narrow variation in K content of the pads which were designed

primarily for U and Th calibration (B.W. Charbonneau, personal communication). Field tests of the unit used in this thesis project have revealed serious temperature dependent fluctuations in K counts giving precisions as bad as 22% (Birk, 1974). Other workers report problems with in situ K determinations (Lovborg et al, 1971). Because of these considerations, the author rejected all in situ K analyses.

In situ measurements of U and Th are evaluated with the assumption that the parent elements of the decay series are in secular equilibrium with their decay products. Therefore the concentrations obtained in this thesis are expressed as eU and eTh respectively.

Field Procedures:

At every field station, four readings of two minute duration were taken with the spectrometer detector relocated on the outcrop each time. All locations were selected to ensure a dose approximation to a 180° solid angle of detection. Lovborg et al (1971) recommended a lead collimator but any improvement in geometry would have been off-set by loss in sensitivity, especially for U (Balykin et al, 1971). The author also didn't feel like carrying a lead weight through bush terrain. Background readings were obtained daily in replicate by counting over the centers of lakes adjacent to the granitic stocks.

Precision and Accuracy:

Ten replicate readings over a one week time span taken on a "standard" outcrop gave the precision for a single measurement of:

8.5% for uranium and 13.5% for thorium. This compares with 12% for U and 8% for Th reported by Lovborg et al (1971) for rocks of much higher radioelement content. The major source of fluctuation is felt to be the temperature sensitivity of the photo multiplier tube.

An estimate of accuracy of the field data was provided by 15 powdered specimens (200 gram at 200 mesh) analysed by the Geological Survey of Canada by laboratory gamma ray spectrometry. Field gamma ray spectrometry analyses several times larger volumes of rock than laboratory techniques - furthermore, in situ readings selectively sample the flat regions of outcrops whereas hand sampling must take advantage of outcrop perturbations. Therefore direct correlation cannot be expected. The comparison between lab analyses and in situ analyses do, however, suggest that field values for Th are systematically too low by 1.4 ppm (Figure G.a, Table G.b). Lovborg et al (1971) reported accuracies of 2.5% for Th and 7.5% for U. This study encountered much lower radioelement contents than Lovborg et al (1971) and therefore accuracy was likely not as good.

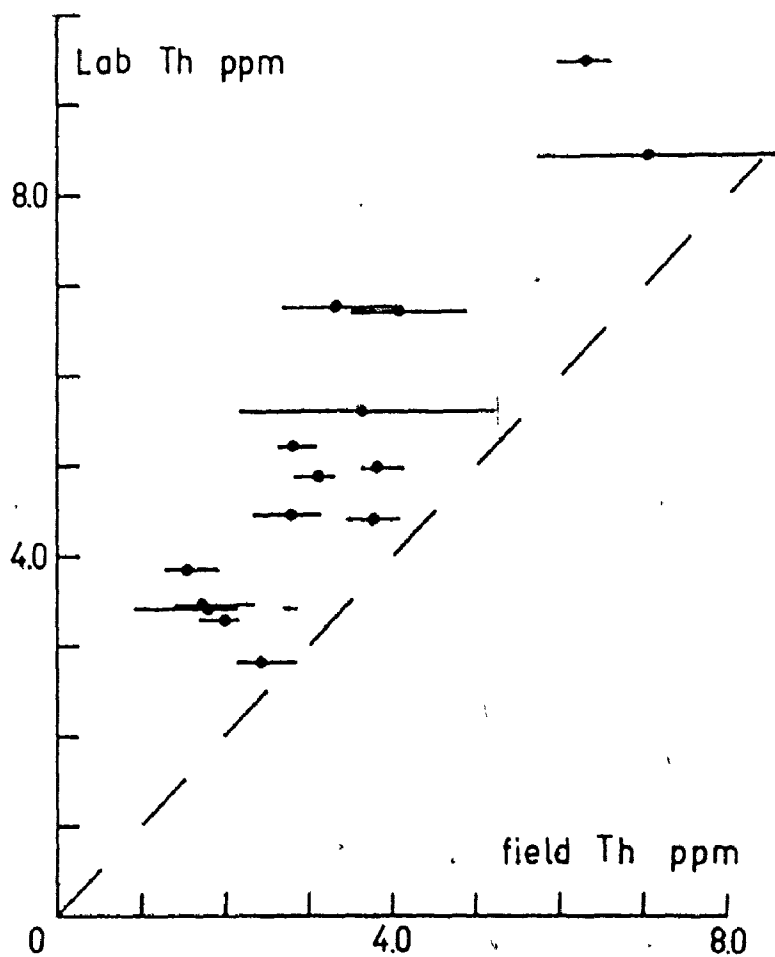


FIGURE G.8 IN SITU ANALYSES VERSUS LAB ANALYSES FOR ^{232}Th . DOTS REPRESENT MEAN VALUE OF 4 STATION READINGS. ERROR BARS SHOW RANGE OF FIELD STATION READINGS. DASHED LINE SHOWS 1:1 RATIO, EXPECTED IF LAB AND FIELD ANALYSES COINCIDENT.

Table G.a

Calibration at Uplands Airport, Ottawa

Reference	#	Sensitivities (Cts/min./ppm)			Stripping Ratios		
		U	Th	K	α	β	γ
Grasty & Darnley (1971)	3	22.	7.1	198	0.710	0.878	1.03
Charbonneau*	3	18.6	8.1	163.3	0.592	0.693	0.952
This Study	1	19.4	7.5	245.2	0.592	0.693	0.952

* B.W. Charbonneau, personal communication: 3 DISA400 units tested 1975.

Number of spectrometer units.

Table G.b

Accuracy of in situ eU, eTh outcrop analyses by comparison with Geological Survey of Canada laboratory gamma ray analyses of near equivalent hand specimens (200 gm, 200 mesh).
(B.W. Charbonneau, personal communication, 1975)

Sample	ppm eU Lab	ppm eU Field	ppm eTh Lab	ppm eTh Field
G8	0.91	0.95	4.96	3.86
G22	0.80	0.77	4.40	3.79
G27	1.57	1.70	5.62	5.19
G51	0.70	0.81	3.47	1.74
G53	0.57	0.86	3.43	1.79
G56	0.59	0.94	3.27	2.01
G62	0.79	0.71	2.84	2.45
G67	0.38	0.53	3.82	1.56
G70	1.29	1.45	6.75	3.32
G78	0.94	1.07	4.45	2.93
RY4	1.22	1.51	8.42	7.41
RY5	0.64	1.35	5.20	2.81
RY6	0.58	0.96	4.88	2.96
RY22	0.68	0.57	6.70	3.02
RY37	1.32	1.72	9.45	6.31

Samples G = Burditt Lake stock stations (Appendix I)
RY = Ryckman Lake stock stations (Figure 2.46)

APPENDIX H.

ISOTOPIC DETERMINATIONS:

Introduction:

Chemical and mass spectrometric techniques for determination of $^{87}\text{Sr}/^{86}\text{Sr}$ are well established in published literature (Allsopp et al, 1968; Yamaguchi et al, 1969; Wanless and Loveridge, 1972; Gibbins, 1972, 1973, Marchand, 1976; Wolff, 1977; etc.). Procedures followed in this thesis included the wet chemistry of Wanless and Loveridge (1972) and the machine operation of Marchand (1976) with the following modifications.

Wet Chemistry:

Powdered rock at 200 mesh and 100 mg was dissolved in HNO_3 and HF without need for HClO_4 . Ion exchange columns identical to those of Marchand (1976) were calibrated for cation extraction by sequential analyses on a Perkin-Elmer 303 Atomic Absorption Spectrophotometer, thereby eliminating the need for a radioactive Sr^{89} tracer. No Rb extracts were necessary since $^{87}\text{Rb}/^{86}\text{Sr}$ was calculated from the XRF determined Rb/Sr ratio by the method described in Gibbins (1973) and Turek et al (1977).

Contamination Levels:

Several new precautions were introduced to the laboratory procedures of Gibbins (1972, 1973) and Marchand (1976) to reduce contaminant levels in the determination of $^{87}\text{Sr}/^{86}\text{Sr}$:

1. HF was distilled in a sub-boiling teflon (FEP) apparatus (Mattinson, 1969).
2. Plastic fume hoods surrounded the ion exchange columns and were ventilated through a connection to a laboratory chemical fume hood.
3. HCl was distilled by sub-boiling in a pyrex still, using heat lamps.
4. All concentrated distillates (6 N or 12 N HCl; 8 N nitric acid; concentrated HF) were stored in teflon bottles to avoid possible chemical leaching (suspected for previously used polyethylene bottles).
5. Sample evaporations were carried out under teflon jackets using filtered air and infra-red heat lamps.
6. Sample transfers were made with disposable pipettes.

These precautions should have resulted in considerably lower blank levels than those experienced by previous workers. To determine Sr contamination, samples of pure Sr⁸⁴ spike were processed through the wet chemical procedure and run on the spectrometer. The spike was the National Bureau of Standards SRM 988 (⁸⁴Sr:.99892; ⁸⁶Sr:.00059; ⁸⁷Sr:.0001; ⁸⁸Sr:.00039) prepared as a 1.84 μgm/gm solution in 2.5 N HCl. Accurate mass spectrometer measurements were not possible with the present running method because of uncertainties of machine fractionation. A rough fractionation correction was made using the equation of Faure and Powell (1972, page 21) and a typical ⁸⁶Sr/⁸⁸Sr value for this machine of 0.122 and allowing for the 4 mass unit difference between ⁸⁴Sr and ⁸⁸Sr. The maximum Sr contamination was then

calculated from the relationship:

$$\left(\frac{^{84}\text{Sr}}{^{88}\text{Sr}}\right)_{m^*} = \frac{^{84}\text{Sr}_s \quad ^{84}\text{Sr}_c}{^{88}\text{Sr}_s \quad ^{88}\text{Sr}_c}$$

c - contaminant
s - spike
m* - measured (normalized)

Assuming normal Sr to contain 82.6% ^{88}Sr and 0.56% ^{84}Sr .

Table H.a Sr laboratory contamination

	m	m*	w	c/s	c (contaminant)
1	34.98	36.48	0.54157	.033	.033 x 10 ⁻⁶ gm/100 mg
2	69.57		0.28224	.0169	.0088 x 10 ⁻⁶ gm/100 mg

w = weight of spike solution

1 = based on one spike solution run twice by the author (35.109; 34.850)

2 = based on a second spike solution run once on a different mass spectrometer, (M. Wolff, personal communication).

The amount of Sr contaminant per 100 mg sample picked up from reagents, containers and machinery is therefore estimated at less than 33 nanograms. This compares with a value of $0.26 \mu\text{gms}/100 \text{ mg}$ reported by Mitchell (1969) and $.0016 \mu\text{gms}/100 \text{ mg}$ reported by Gibbins (1973) and is considered high in view of the additional precautions. Nevertheless, contamination levels for Sr were considered low enough not to require ratio corrections.

Filament Preparation:

Sr column extracts were mounted on the same baked ceramic "button" and tantalum filament (.02" x .001") holders described by Gibbins (1973). Filament surfaces were prepared with a centered drop of 1.0 N orthophosphoric acid rather than the Ta-Ta₂O₅ metal slurry technique of Gibbins (1973). This produced more uniform mounts and consequently steadier Sr emissions. Sr was loaded as a 1N nitrate after the filament was oxidized with a 1 amp. current.

Mass Spectrometry:

Isotopic ratios of Sr were measured on the same 10" single sector solid source mass spectrometer described by Gibbins (1973) with operating conditions similar to Wolff (1977). Peak hopping was accomplished by manually adjusting the $\sim 5.0 \text{ Kv}$. accelerating voltage and recording beam intensities in a Faraday cup coupled to a Cary 401 vibrating reed electrometer and a Hewlett-Packard digital recorder.

In contrast to Gibbins (1973) and Marchand (1976) the author preferred to collect data on the 1 V scale of the Cary 401 unit with

one second peak readings and six second switch-delay intervals. The faster switching and shorter peak readings allowed for more data collection per sample life and gave better statistics because of less beam variation between peak readings. Longer 10 second readings tended to mask spurious electronic signals (such as an IBM time signal for the hall clock) which were easily filtered out of the one second data tapes.

Each run consisted of 10 to 15 scans across the Sr^{86} - Sr^{87} - Sr^{88} peak and background spectrum after steady Sr emission was achieved. Acceptable analyses were based on the mean of at least three runs displaying low standard deviations and steady beam growth.

Data Processing:

The data processing technique used, required extreme labor and perserverence: for every useful isotopic ratio obtained, some 700 six digit numbers were manually transposed from the digital recorder tape to computer cards. The author strongly recommends some form of teletype or on-line computer hook-up for future projects.

The computer program of Stacey et al (1971) as modified by Terrazas and Stacey (1972, personal communication) and Marchand (1976) was adopted in part but rewritten by the author to account for certain machine peculiarities including: a sloping base line and "tailing" from the ^{88}Sr peak.

A tail overlap on the ^{87}Sr peak from the stronger ^{88}Sr peak is a problem common to many machines and reflects geometrical and/or vacuum imperfections. Allsopp et al (1968) compensated by

visually estimating a correction from magnetic spectra scans. The author introduced a correction factor into the data processing based on background readings on either side of the ^{87}Sr peak taken at the beginning and end of each run. After the tail contribution to the baseline at mass 87.5 was determined, a straight-line extrapolation to the ^{87}Sr position gave the correction factor. This correction procedure assumes a constant slope tail which is likely only a crude approximation for the spectrum range in question. Only during the early stages of sample life did the tail corrections contribute more than $\pm 0.2\%$ to peak intensities and these readings were generally discarded. The assumption of constant-slope tails is therefore acceptable.

The second major modification in data processing compensated for a sloping baseline. Grant (1970) reported baseline variations throughout the peak spectrum and compensated by reading the baseline at mass units 84.5, 85.5, 86.5, 87.5 and 88.5. The baseline was monitored in a similar fashion in this study to give straight-line extrapolated background estimates for each peak. Again the assumption of a linear baseline is only a first approximation but yields satisfactory precision and accuracy.

The author's modified version of the Stacey et al (1971) program also calculated a "beam growth factor" for each peak reading based on the percentage growth since the preceding reading. The best runs were obtained when all three peaks recorded similar positive "beam growth factors".

Precision and Accuracy:

Precision of the solid source mass spectrometer was determined from multiple sets of Sr peak scans for 14 samples. This precision relates to machine stability only since single filament loads were involved. The mean coefficient of variation for the 14 single load replications was 0.062%, (Table H.b).

Five replicate dissolutions to test the precision of the entire chemical and spectrometric procedure were carried out (Table H.b) and yielded a mean coefficient of variation of 0.045%. This compares with reported precision of .039% for 24 duplicates (Marchand, 1976) and .08% for 12 duplicates (Gibbins and McNutt 1975). The better precision of Marchand (1976) correlates with higher Sr content in the rocks and is more comparable to this study.

Accuracy of the $^{87}\text{Sr}/^{86}\text{Sr}$ determinations was based on 7 replicate runs (separate loadings) of the Eimer and Amend SrCO_3 isotope standard (lot 492327) prepared as a $56\ \mu\text{gm/ml}$ solution in 2 M HCl. Table H.c gives the individual determinations which averaged to: $0.70805 \pm .00039$ (1 sigma).

The coefficient of variation decreased steadily during the term of operation from 0.065% in March 1976 (5 replicates) to 0.060% in October 1976 (6 replicates) to 0.056% by January 1977. A conservative estimate of error in $^{87}\text{Sr}/^{86}\text{Sr}$ for all isotopic determinations is therefore 0.065% and this value was chosen as the "blanket error" for regression treatments.

This compares with a value of 0.05% reported by Gibbins and McNutt (1975) on E & A (12 replicates) and 0.046% reported by Marchand

Table H.b

Precision of $^{87}\text{Sr}/^{86}\text{Sr}$ Determinations:1. Machine Precision: Replicate Runs From Single Filament Load.

Sample	G8	G62A	T13	FL5	G70	FL13	GAC
\bar{x}	0.71220	0.76773	0.71410	0.72552	0.71183	0.73546	0.71546
1σ	.00085	.00050	.00031	.00067	.00037	.00013	.00043
C.V.	.119%	.065%	.043%	.092%	.052%	.018%	.060%
#	3	2	3	4	2	2	5
Sample	G78	T57	FL24	4343	FL22	T40	FL8
\bar{x}	0.83826	0.73136	0.74293	0.75489	0.73107	0.72792	0.71236
1σ	.00034	.00042	.00047	.00035	.00117	.00018	.00018
C.V.	.041%	.057%	.063%	.047%	.16%	.025%	.025%
#	5	6	5	3	3	3	3

Mean coefficient of variation (1 sigma) for 14 replications: 0.062%

2. Analytical precision: replicate samples, multiple filament loads.

Sample	#1	#2	\bar{x}	1σ	C.V.
RY22	.75126	.75073	.75100	.00037	0.049
EX5	.73445	.73503	.73474	.00065	0.088
TR5	.74765	.74805	.74785	.00028	0.037
TR1B	.71893	.71927	.71910	.00024	0.033
OT1	.70727	.70746	.70737	.00013	0.018

Mean coefficient of variation, 5 duplicates: 0.045%

(1976) for the NBS standard SRM-987 (15 replications) using the same machine.

A comparison of the E & A value and one determination of NBS SRM-987 obtained in this study with published values shows these results to be free of systematic bias (Table H.c).

Isochron Calculation and Compatibility:

Meaningful comparisons between published isochrons can only be made between compatible data. Brooks et al (1972) made available computer soft-ware allowing isochron calculation simultaneously by four commonly used two-error linear regression techniques. A total of eight sets of "ages", intercepts and error parameters can be generated from a single data block, dependent on the regression technique and "model" chosen. If that is not enough confusion, the isochron parameters are dependent on other variables, including:

1. Decay constant used for ^{87}Rb : $1.39 \times 10^{-11} \text{y}^{-1}$;
 $1.42 \times 10^{-11} \text{y}^{-1}$; $1.47 \times 10^{-11} \text{y}^{-1}$
2. Blanket errors assigned to $^{87}\text{Rb}/^{86}\text{Sr}$ and $^{87}\text{Sr}/^{86}\text{Sr}$.
3. Whether data is introduced at the 1σ or 2σ error confidence level.
4. Whether resultant isochron parameters are quoted at 1σ or 2σ .
5. Whether errors on $^{87}\text{Rb}/^{86}\text{Sr}$ correlate analytically to $^{87}\text{Sr}/^{86}\text{Sr}$ errors.
6. Number of points regressed; their distribution.

Table H.c

Eimer & Amend Replicates:

Date	⁸⁶ Sr/ ⁸⁶ Sr*
May/75	0.70879
Jan./76	0.70774
Feb./76	0.70784
Feb./76	0.70792
Mar./76	0.70763
Oct./76	0.70817
Jan./77	0.70824
	Mean
	0.70805
	1σ
	0.00039
	C.V.
	0.056%

NBS 987 Sr CO₃: singlicate

Feb./76 0.070946

Published Values[†]

Reference	Standard	⁸⁷ Sr/ ⁸⁶ Sr*	1σ	Coef. Var.
Pankhurst & O'Nions (1973)	E&A	0.70815	.00004	.0056%
"	NBS 987	0.71039	.00002	.0028%
Gibbins & McNutt (1975)	E&A	0.7079	.0004	.057%
Marchand (1976)	NBS 987	0.70995	.0003	.046%

[†] see also Table 2.4 of Gibbins (1973) and Table A-2 of Marchand (1976).

* Normalized



A 6

7. Whether small sampling theory (Students-T) is applied to errors.

These variables allow for an almost infinite number of isochrons and isochron parameters to be generated from one set of data. This variability is still confined to one computer package and assumes the analyst's ability to reproduce international standard values and calculate experimental error satisfactorily.

Comparisons between published isochrons can best be made if the data is recalculated to standardize treatments as much as feasible. The author's approach has been to recompute published data through the Brooks et al (1972) package using the same constants and error treatments of this study.

The adoption of one regression treatment over others available in the Brooks et al (1972) package was based primarily on the error treatment in each. Since $^{87}\text{Rb}/^{86}\text{Sr}$ and $^{87}\text{Sr}/^{86}\text{Sr}$ were obtained by two unrelated analytical techniques (XRF versus mass spectrometry) no correlation of errors could be expected. Brooks et al (1972) furthermore have pointed out that correlation of experimental errors in X and Y has not been found to apply to total-rock isochrons. Since the Wendt I regression model assumes a -1.0 correlation coefficient and the York II model is designed to treat correlation, these two regression techniques were rejected. The McIntyre models assume a constant absolute error in Y which has been disproven by Brooks et al (1972). For this reason, the author settled on the York I regression model as the most appropriate for this study. The York I treatment has the following advantages:

1. York I calculates isochron errors from actual data scatter. This is geologically more appropriate than error estimates based on experimental error in a much larger analytical sample population.
2. The York I method is the only regression technique in the Brooks et al (1972) package that gives expected large error estimates if data results in an errorchron. Outliers are easily recognized.
3. Analytical procedures in our laboratory are being continuously modified, therefore the number of comparable replicate runs for each study is limited. In the York I Model, an uncertainty in the experimental error is not reflected in the isochron error as long as any likely changes in error estimates are proportional for x and y (Brooks et al, 1972).
4. The majority of published isochrons from Northwestern Ontario and vicinity were derived by the near-identical York (1966) method thereby eliminating many recalculations.

The isochron errors calculated directly from data scatter carry a major disadvantage because of the possibility of generating "pseudoisochrons" due to fortuitous alignment of points better than anticipated from known analytical error estimates (see section 4.5.2). For this reason the distinction between errorchrons, pseudoisochrons and isochrons was made from consideration of all four regression techniques. For isochrons sensu stricto the plots in this thesis were

L	#	L	#	L	#
46	G21	47	G22	48	G24
49	G26	50	G27 (A)	51	G28
52	G44	53	44210	54	G71, 5332(X)
55	53320, G20	56	53322 (AX)	57	53414
58	5412	59	5424	60	5428
61	53310, G73	62	53312, G74	63	53350
64	G2, 5314AP	65	4342 (AP)	66	5341
67	53313	68	G3, 5331 (BC, BR)	69	53412
70	53413 (G, X, T)	71	5413	72	5422
73	G61(T)	74	G89T	75	3321T
76	4242T	77	4341T	78	53150(T)
79	5426T	80	G12	81	43115
82	43117	83	4321	84	4324
85	4326	86	43210	87	43212
88	43214	89	43215	90	43217
91	G52, 43219	92	G1, 43250	93	4335
94	4336	95	4339	96	4344
97	43412	98	4413, G63	99	4422 (C, D)
100	4423	101	4425	102	4426

APPENDIX I

Sample numbers corresponding to field locations of Figure 2.2, Burditt Lake Stock. L = Location, # = Sample numbers:

L	#	L	#	L	#
1	53424	2	G8 (X)	3	G70, G17
4	GA (A,B,C)	5	44223	6	4343
7	G62 (A), 4414	8	G31 (B)	9	G78
10	G30 (A,B), 4232BA	11	G42	12	G43
13	G48	14	G51	15	G53
16	G56	17	G67	18	G81
19	4311	20	43112	21	43113
22	43114	23	43116	24	43119
25	43213	26	43216	27	43251, G50
28	43310	29	4345	30	43410
31	43411	32	4411, G65, G66	33	4412, G64
34	4416	35	4424C	36	44222
37	5344 (B)	38	5345	39	5347
40	53430	41	53431	42	G4, G5
43	G7	44	G9	45	G15

L	#	L	#	L	#
103	4427	104	44221	105	44224
106	5313, G77	107	5338	108	5339
109	5343	110	5349	111	53410
112	5411	113	5414	114	5421
115	5423	116	5427	117	5429, G10
118	54210	119	54211	120	54212
121	54213	122	G6	123	G11
124	G13	125	G14	126	G16
127	G25	128	G29	129	G40
130	G70	131	G68	132	G72
133	G75	134	G76	135	G79
136	G80	137	G82	138	G83
139	G85	140	G86	141	G87
142	G88	143	53316		